

## 2.9 Fuel Rod Buckling Assessment

The bounding condition for the assessment of the evaluation of the fuel rod buckling is the end drop orientation. This orientation maximizes not only the axial force component that would buckle the fuel rod, but it is also the orientation, which has the maximum axial acceleration. As the cask orientation shifts from the axial end drop condition, the cask body accelerations decrease. Two fuel rod configurations are evaluated: 1) 17 x 17 PWR fuel for the directly loaded fuel case; and 2) Yankee-Class fuel for the canistered fuel case.

### 2.9.1 Fuel Rod Buckling Assessment for Directly Loaded 17 x 17 PWR Fuel

For this fuel configuration, the fuel rods are laterally restrained by the grids and may come into contact with the fuel assembly base. The only vertical constraint for the fuel rod is the base of the assembly. This is considered to be the bounding condition. Additionally, the weight of the fuel pellets is also included in this evaluation, as it is considered to be vertically supported by the cladding. Use of the fuel pellet weight in the evaluation is considered to be the bounding condition (as opposed to an evaluation that considers the cladding only). Fuel rod buckling is evaluated using the finite element beam model shown in Figure 2.9.1-1.

During the end drop, the fuel rod is expected to impact the fuel assembly base. The fuel rod itself will respond as an elastic bar under a sudden compression load at its bottom end. The duration of this impact is bounded by the first extentional mode shape of the fuel rod. Contribution of higher frequency extentional modes of the rod would tend to shorten the duration of impact of the fuel rod with the fuel assembly base. The fuel rod, upon initiation of impact, corresponds to an undeformed state. In the process of the impact, the compression of the fuel rod will increase to a maximum and then return to a near uncompressed state, at which point the time of impact has been completed. This actually represents half of a cycle of the lowest frequency mode shape of the fuel rod. The frequency of this mode shape is evaluated to be 214.5 Hz using ANSYS Revision 5.2. The shape of the time dependence of the deformation is sinusoidal. The single extentional mode shape can also be considered to be a single degree of freedom (SDOF) with a corresponding mass and stiffness. In viewing such an event as a spring mass system, the time variation of the deformation during the impact is expected to be sinusoidal.

The buckling mode for the fuel rod is governed by the boundary conditions. For this configuration, the eight grids provide a lateral support, but no vertical support. The only vertical restraint is considered to be at the point of contact of the fuel rod and the base of the assembly.

The weight of the fuel rod pellets and cladding is assumed to be uniformly distributed along the length of the fuel rod. In the end drop, this results in the maximum compressive load occurring at the base of the fuel rod. The first buckling mode shape corresponding to these conditions is computed using ANSYS Revision 5.2 and is shown in Figure 2.9.1-2.

Typically eigenvalue buckling is applied for static environments. For dynamic loading, it is assumed that the duration of the loading is sufficiently long to allow the system to experience the complete load, even as the deformation associated with the buckling is commenced. For dynamic loading, the lateral motion, which would correspond to the buckled shape, will correspond to the lowest mode shape. This lowest frequency mode shape is shown in Figure 2.9.1-2 and corresponds to a frequency of 31.31 Hz. The similarity of the two shapes shown in Figure 2.9.1-2 is expected, since both have the same displacement boundary conditions, the same stiffness matrix, and the same governing finite element equations, i.e.,

$$[K] \{\phi_i\} = \lambda_i [A] \{\phi_i\}$$

where:

$[K]$  = structure stiffness matrix

$\{\phi_i\}$  = eigenvector

$\lambda_i$  = eigenvalue

$[A]$  = mass matrix for the mode shape calculation or stress stiffening  
matrix for the buckling evaluation

Based on the time duration of the impact and the inherent inability of the fuel rod to rapidly displace in the lateral direction, the effect of the actual lateral motion of buckling can be computed with a dynamic load factor (DLF) (Clough). The expression for the DLF for a half-sine loading for an SDOF is given by

$$DLF = \frac{2\beta \cos(\pi/2\beta)}{1 - \beta^2}$$

where:

$\beta$  = ratio of the first extentional mode frequency to the first lateral mode frequency

These values, computed as described below, are  $\beta = 6.85$  and  $DLF = .2905$ .



This DLF is applied to the end drop acceleration of 56.1 g for the 30-foot end drop (see Table 2.6.7.4.2-2), which is the driving force to potentially result in the buckling of the fuel rod. The product of  $56.1 \times \text{DLF} = 16.3\text{g}$  is compared to the vertical acceleration corresponding to the first buckling mode shape, computed in Section 2.9.1.2, 28.9g. This indicates that the time duration of the impact of the fuel onto the fuel assembly base is of sufficiently short nature that buckling of the fuel rod cannot occur. The calculational methodology used to determine the acceleration corresponding to the first buckling shape for the PWR 17 by 17 fuel assembly will also be applied to the Yankee-Class fuel assembly using the same vertical restraint location. This calculation is performed in Section 2.9.2, which results in a value of 78g. The increase in this value is primarily due to the difference in the distance between the grids.

#### Numerical Evaluation of the Fuel Rod Mode Shapes and Buckling Acceleration

The condition is evaluated for the fuel pellet weight being combined with the cladding. To be consistent with this approach, an effective cross-sectional property is used in the evaluation, which incorporates the properties of the fuel pellet and the fuel cladding. The model used in this evaluation is comprised of two-dimensional beam elements in ANSYS Revision 5.2 as shown in Figure 2.9.1-1. In this model, the beam elements considered the weight of the fuel pellet, as well as the cladding. The modulus of elasticity (EX) for the fuel pellet is listed in Rust as having a nominal value of  $26.0 \times 10^6$  psi. To be conservative, only 50 percent of this value was employed in this evaluation. The EX for the fuel pellet was, therefore, taken to be  $13.0 \times 10^6$  psi. The EX for the fuel cladding used in the evaluation was also  $13.0 \times 10^6$  psi, which bounds the EX for the Zircaloy cladding at the end of the fuel assembly. The dimensions and physical data for the fuel rod used in the evaluation are:

Outer diameter of cladding (inches)	.36
Cladding thickness (inches)	.0225
Cladding density (lb/in <sup>3</sup> )	.237
Fuel pellet density (lb/in <sup>3</sup> )	.396

The elevations of grids are 6.18, 31.08, 51.63, 72.18, 92.73, 113.83, and 153.96 inches as measured from bottom of fuel assembly.

The effective cross-sectional properties ( $Ei_{\text{eff}}$ ) for the beam are computed by adding the value of EI for the cladding and the pellet, where:

- E = modulus of elasticity (lb/in<sup>2</sup>)  
I = cross-sectional moment of inertia (in<sup>4</sup>)

The model and the associated displacement boundary conditions for the fuel rod is shown in Figure 2.9.1-1. Using this model, the lowest frequency for the extentional mode shape was computed to be 214.5 Hz. The first mode shape corresponds to a frequency of 31.31 Hz. Using the expression for the DLF in Section 2.9.1.1, the DLF is computed to be  $\beta = 6.85$  and  $DLF = 0.2905$ .

The buckling calculation used the same model employed for the mode shape calculation. The load that would potentially buckle the fuel rod in the end drop is due to the deceleration of the rod. This loading was implemented by applying a 1g acceleration in the direction that would result in the compressive stress of the fuel rod. The first buckling shape based on the applied boundary conditions is shown in Figure 2.9.1-2. The acceleration corresponding to the first buckling mode for the combined cladding and fuel pellet was computed to be 28.9 g.

Figure 2.9.1-1 Two-dimensional Beam Finite Element Model of the PWR 17 by 17 Fuel Rod

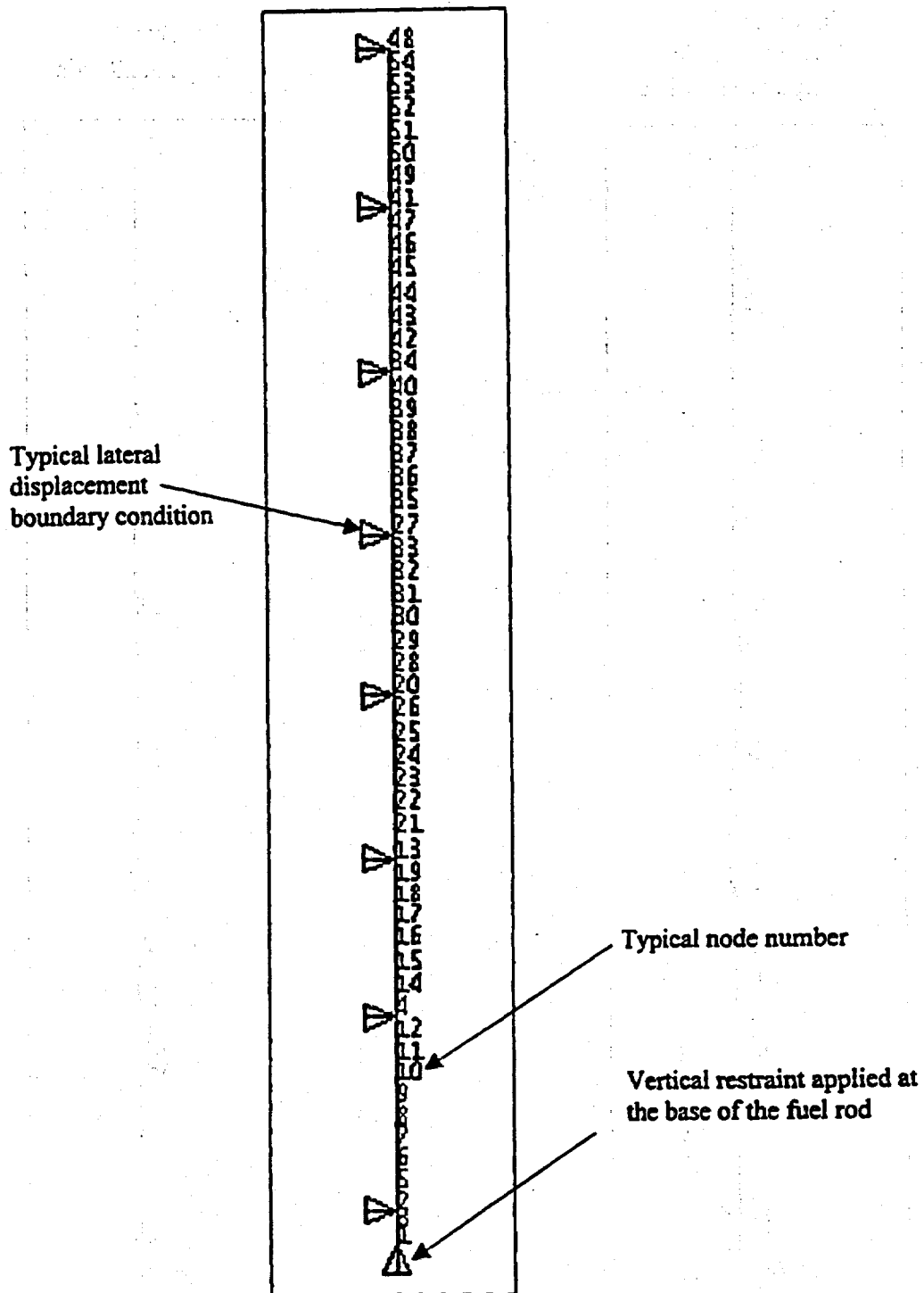
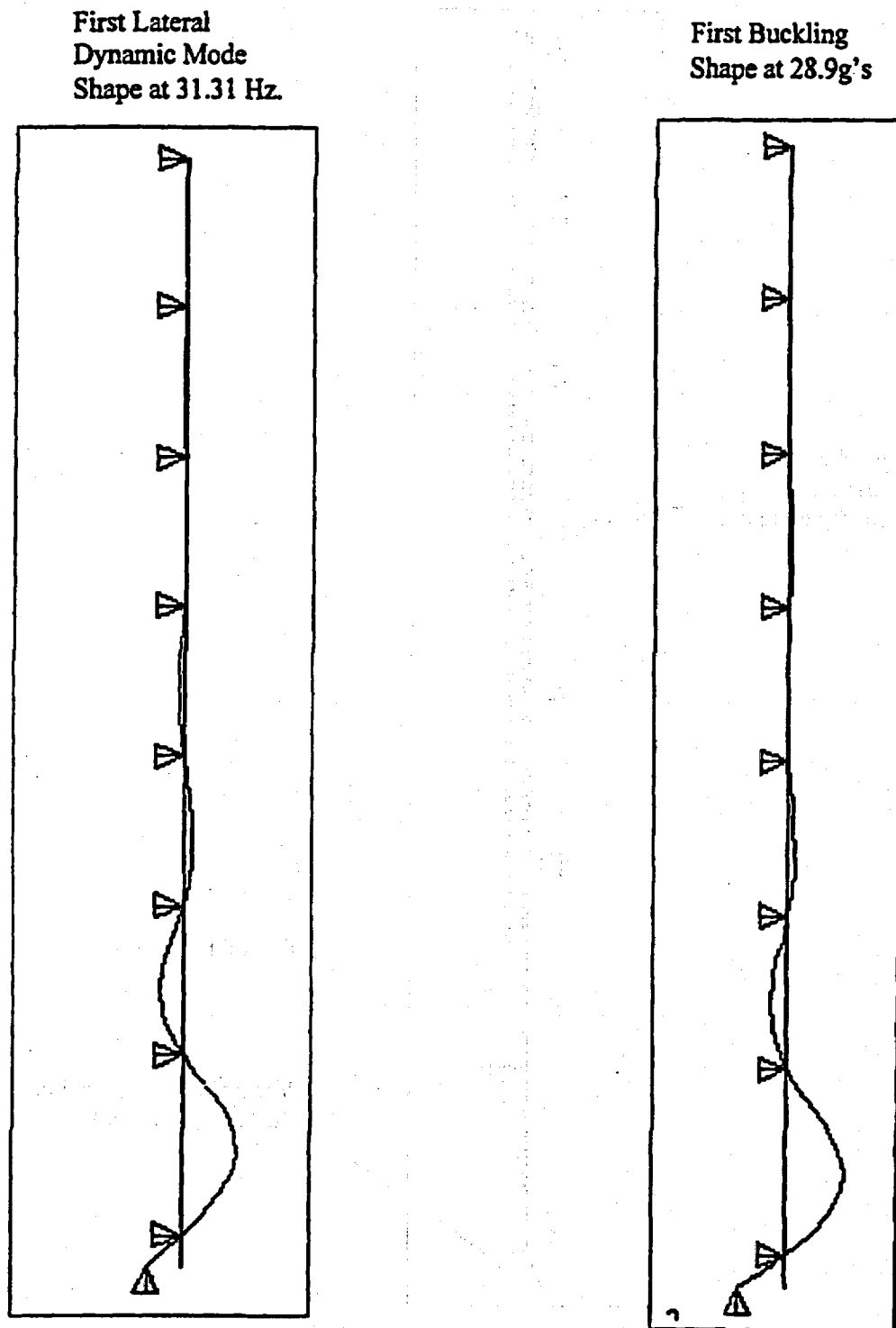


Figure 2.9.1-2 Mode Shape and First Buckling Shape for the PWR 17 by 17 Fuel Rod



## 2.9.2 Fuel Rod Buckling Assessment for Yankee-Class Canistered Fuel

For the Yankee-Class fuel, two materials are available for the fuel rod cladding: Zircaloy and stainless steel. For this fuel configuration, the fuel rods are restrained by the grids and are in contact with the fuel assembly base. In the vertical orientation, the weight of the fuel rods is transferred to the base of the fuel assembly. Each of the six grids restraining the fuel rods is considered to provide lateral support, but no rotational resistance to buckling. The calculation of the first buckling mode is performed using ANSYS Revision 5.2. Two models are constructed using beam elements. In the first model, the beam elements use effective cross-sectional properties, which combined the cross-sectional properties of the fuel pellet and the fuel rod cladding. To be consistent with this approach, the beam element considers the weight of the fuel pellet and the cladding. The modulus of elasticity (EX) for the fuel pellet is listed in Rust as having a nominal value of  $26 \times 10^6$  psi. Conservatively, only 50% of this value is used. The EX for the fuel pellet is therefore taken to be  $13 \times 10^6$  psi. The EX for zircaloy fuel cladding used in the evaluation is also  $13 \times 10^6$  psi. The EX for the stainless steel cladding is conservatively taken to be  $13 \times 10^6$  psi, even though the minimum EX for stainless steels at 600°F is  $25.2 \times 10^6$  psi. The fuel rod dimensions and physical data used in the evaluation are:

Fuel Rod Parameters	Stainless Steel Cladding	Zircaloy Cladding
Outer diameter of cladding (inches)	.34	.365
Cladding thickness (inches)	.042	.048
Cladding density (lb/in <sup>3</sup> )	.291	.237
Fuel pellet density (lb/in <sup>3</sup> )	.396	.396

The elevations of the grids are 2.86, 20.5975, 38.8975, 57.1975, 75.49 and 75.93 inches as measured from bottom of fuel assembly.

The effective cross-sectional properties ( $EI_{eff}$ ) for the beam are computed by adding the value of EI for the cladding and for the pellet.

where:

$E$  = modulus of elasticity (lb/in<sup>2</sup>)

$I$  = cross-sectional moment of inertia (in<sup>4</sup>)

For each material, two configurations are evaluated:

- with the weight and the contribution of the cross-section properties of the fuel pellet and cladding, and
- with out the contribution of the fuel pellet (cladding only).

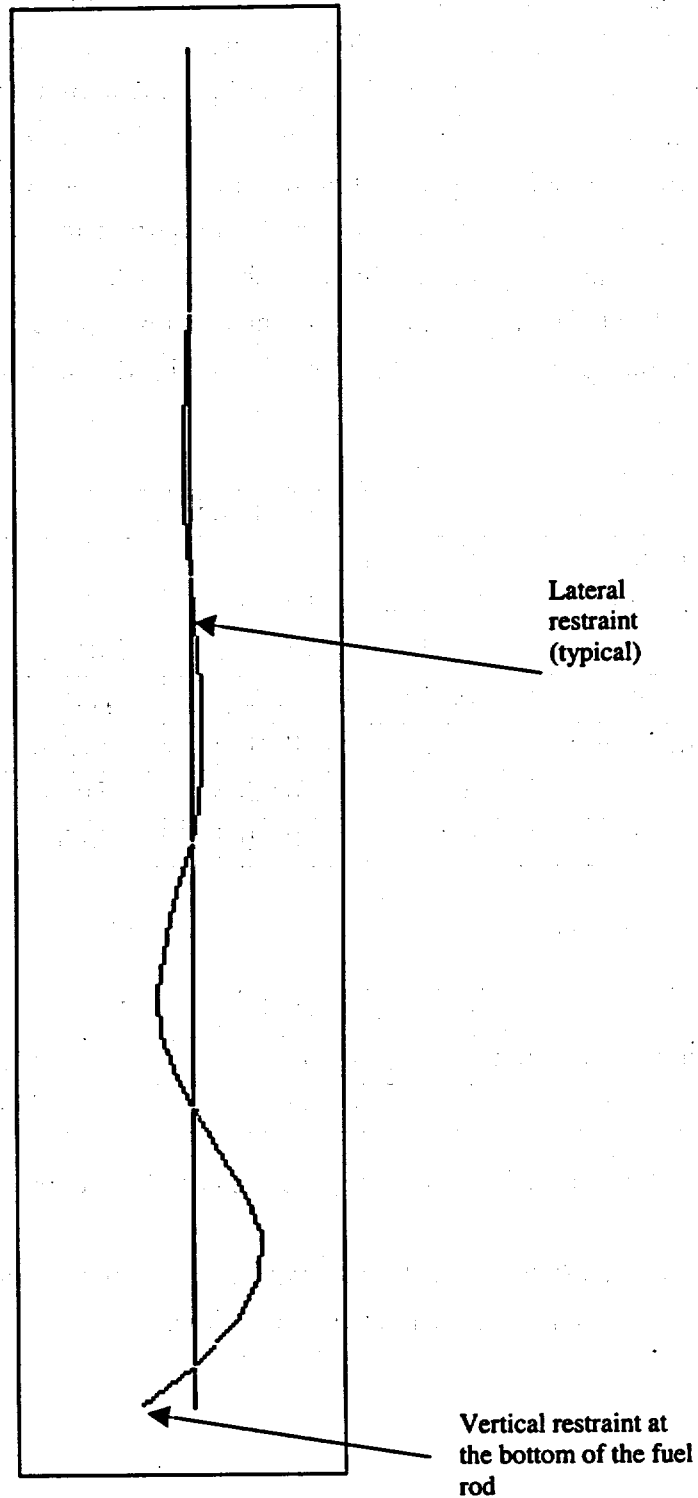
The buckling shapes for each material for the case using the combined cross-sectional properties of the fuel pellet and the cladding, along with the applied boundary conditions are shown in Figure 2.9.2-1. The acceleration corresponding to the first buckling mode for the combined cladding and fuel pellet for both materials are:

Cladding Material	With the cross-sectional properties and weight of the fuel pellet	With the cladding cross-sectional and weight of the fuel cladding only
Zircaloy	94 g	248 g
Stainless Steel	78 g	177 g

This analysis is considered to be conservative. For undamaged fuel the pressure inside the fuel rod actually provides a significant tensile stress in the cladding. For this evaluation, this stress is not considered to stiffen the cladding. Additionally, rotational resistance from each grid is not considered, which would increase the acceleration corresponding to the first buckling mode. Since the impact limiters for the NAC-STC limit the maximum accelerations in the end drop to less than 60g's, based on this evaluation, the fuel rods do not buckle.

Figure 2.9.2-1 First Buckling Mode for the Yankee Class Canistered Fuel

Combined properties for the fuel pellet and for the cladding.



### 2.9.3 Fuel Rod Buckling Assessment for CY-MPC Canistered Fuel

For the Yankee-Class fuel, two materials are available for the fuel rod cladding: Zircaloy and stainless steel. For this fuel configuration, the fuel rods are restrained by the grids and are in contact with the fuel assembly base. In the vertical orientation, the weight of the fuel rods is transferred to the base of the fuel assembly. Each of the grids restraining the fuel rods is considered to provide lateral support, but no rotational resistance to buckling. The calculation of the first buckling mode is performed using ANSYS Revision 5.5. The beam elements use effective cross-sectional properties, which combined the cross-sectional properties of the fuel pellet and the fuel rod cladding. To be consistent with this approach, the beam element considers the weight of the fuel pellet and the cladding. The fuel rod dimensions and physical data used in the evaluation are:

Case	Fuel Assembly Vendor	Cladding			Pellet Diameter (inch)	Rod Length (inch)
		Outer Diameter (inch)	Thickness (inch)	Material		
1	Westinghouse	0.422	0.0242	Zirc-4	0.3659	151.85
2	Westinghouse	0.422	0.0165	SS304	0.3895	126.52
3	B&W	0.43	0.0265	Zirc-4	0.3686	153.68
4	B&W	0.422	0.0165	SS304	0.3825	126.68

The material properties are:

	Density (lb/in <sup>3</sup> )	Young's Modulus (psi)
Zircaloy-2 Cladding	0.237	$11.5 \times 10^6$
UO <sub>2</sub> Fuel	0.396	$27.5 \times 10^6$

The Young's Modulus used for fuel in the analysis is  $13.0 \times 10^6$  psi.

The elevations of grids (lateral constraints) vary for each fuel assembly type. The locations of the constraints considered are shown in the table below:



Case	Rod Length (inch)	Lateral Constraints (inch)							
1	151.85	2.93	27.14	53.33	79.52	105.71	131.90	150.57	
2	126.52	1.24	20.12	41.20	62.28	83.36	104.44	125.52	
3	153.68	3.45	25.57	46.70	67.79	88.88	109.98	131.07	153.15
4	126.68	1.84	20.21	41.29	62.27	83.45	104.53	125.51	

The vertical constraint is located at the 0.00-inch location. The lateral constraint locations are adjusted to correspond to a 0.00-inch base location.

The effective cross-sectional properties ( $EI_{eff}$ ) for the beam is computed by adding the value of  $EI$  for the cladding and for the pellet, where:

$E$  = modulus of elasticity ( $lb/in^2$ )

$I$  = cross-sectional moment of inertia ( $in^4$ )

The acceleration corresponding to the first buckling mode for the combined cladding and fuel pellet for both materials are:

Case	First Extensional Frequency (Hz)	First Lateral Frequency (Hz)	Frequency Ratio ( $\beta$ )	Dynamic Load Factor (DLF)	Dynamic Acceleration	First Buckling Mode Acceleration
1	211.5	29.1	7.3	0.279	15.3	41.0
2	231.2	37.1	6.2	0.331	18.2	64.3
3	209.5	41.3	5.1	0.408	22.4	48.2
4	230.4	38.1	6.0	0.343	18.9	60.2

The dynamic acceleration is less than the first buckling mode acceleration for all four cases. Therefore, the fuel assembly will not buckle during a 30-foot end impact.

**THIS PAGE INTENTIONALLY LEFT BLANK**

## 2.10 Appendices

### 2.10.1 Computer Program Descriptions

The structural evaluation of the NAC-STC body, closure lids, canister, baskets, and impact limiters is accomplished using three computer codes, ANSYS, RBCUBED, and LS-DYNA. Each program is described in the following sections.

#### 2.10.1.1 ANSYS

The structural analysis of the main body, the closure lids, the canister, and the baskets of the NAC-STC is performed by the finite element analysis method using the ANSYS structural analysis computer program. The ANSYS computer program is a large-scale, general purpose computer program for the solution of several classes of engineering analyses that include: static and dynamic; elastic, plastic, creep and swelling; buckling; and small and large deflections. The matrix displacement method of analysis based on finite element idealization is employed throughout the program. The large variety of element types available gives ANSYS the capability of analyzing two-dimensional and three-dimensional frame structures, piping systems, two-dimensional plane and axisymmetric solids, three-dimensional solids, flat plates, axisymmetric and three-dimensional shells, and nonlinear problems, including gap element interfaces. A two-dimensional axisymmetric model and two three-dimensional models, a top fine model and a bottom fine model, are used in the analysis of the NAC-STC. The interface gap elements provide the capability of realistic modeling and evaluation of the interactions between the lead layer and the surrounding stainless steel shells; between the top forging, inner lid, and outer lid; and between the neutron shield material and the steel in the inner lid and in the bottom of the cask.

The ANSYS preprocessing routine (PREP7) is used to construct the finite element mesh, describe each cask component material (temperature-dependent) property, assign unique identifiers for cask components, model displacement boundary conditions and prescribe temperature, point loads, or surface tractions of appropriate element faces or nodes. The PREP7 graphics option is a valuable tool that permits the user to check the model for completeness. The ANSYS analysis option uses the PREP7 file to generate a solution file and to provide a user-oriented printout of the solution phase. In general, each solution provides a complete echo of the

model input data, model displacement solution, element stresses, nodal forces, reaction forces, and any warnings or errors related to the analysis.

A variety of ANSYS post-processors (for example, Post1) utilize the solution file to sort, print, or plot selected results from the ANSYS analysis. The post-processors can provide many useful features including a maximum set of variables (such as stress components or displacements) or sectional stresses along a designated path. Additionally, the structural behavior can be viewed by model displacement and stress contour plots.

#### 2.10.1.2 RBCUBED - A Program to Calculate Impact Limiter Dynamics

RBCUBED is an impact limiter analysis computer program developed by NAC (Hardeman) and used in the NAC-STC impact limiter analyses. RBCUBED utilizes quasi-static methodology; that is, each iteration freezes an instant in time during which all calculations are performed, and then, proceeds to the next time increment. The methodology employed in the program sizes the impact limiter and calculates the deceleration forces used to calculate the stresses imposed on the cask structure, but does not implement any load factor. There are several assumptions that are attendant to this methodology:

1. Gravity is the only force that acts on the cask during free fall. While falling, the cask is translating vertically and continues to do so until the initial (first) impacting end has been brought to rest. In oblique and side drop cases, after the first end has been stopped, the cask rotates until the second limiter strikes the unyielding surface and absorbs the remaining kinetic energy.
2. There is no sliding or lateral motion of the cask at any time during the impact(s).
3. The cask weight includes the impact limiters, but the length of the cask does not.
4. The deceleration force generated during crushing of the isotropic energy absorption material acts at the centroid of the area engaged in crushing for that increment in time.
5. Crushing of the energy absorption material occurs from the outside toward the cask body.

6. The component of the cask weight acting downward and the crush force acting upward are assumed to act colinearly. The magnitude of the weight component is very small compared to the crush force.
7. The impact limiter material that is not between the cask and the unyielding surface does not absorb any kinetic energy. The extraneous limiter material is ineffective for the purposes of this impact limiter analysis.

RBCUBED is capable of analyzing any cask impact orientation from vertical ( $0^\circ$ ) to horizontal ( $90^\circ$ ).

The input data for RBCUBED includes the following: (1) height of drop; (2) weight of cask system; (3) cask length; (4) impact orientation angle; (5) deflection increment; (6) material crush properties (stress-strain curve or force deflection curve); and (7) impact limiter geometry. Geometric modeling of the impact limiter is performed using combinatorial geometry based on the MORSE-CG computer program.

The output data from RBCUBED includes the following: (1) a verbatim input return; (2) a processed input of general problem parameters and material properties; (3) the results of the RBCUBED execution--deflection; (4) resultant force; (5) remaining kinetic energy; (6) velocity; (7) elapsed time since the beginning of impact; (8) area currently involved in crushing; and (9) a series of crush "footprints" at crush intervals of one inch.

The computer program, RBCUBED--A Program to Calculate Impact Limiter Dynamics, was benchmarked for validity by comparison of analysis results to manual calculations using crush areas determined by drafting methods.

#### 2.10.1.3 LS-DYNA

The structural analysis of balsa impact limiters is performed by the finite element analysis method using the LS-DYNA. LS-DYNA is an explicit general-purpose finite element program for the nonlinear dynamic analysis of three-dimensional structures. It was originally used to simulate permanent deformations of metallic objects impacting hard surfaces at high velocities whose accuracy has been proven through correlation with experimental data. LS-DYNA features include the ability to handle large deformations, sophisticated material models (for steel and

aluminum, rubbers, foams, plastics, and composites), complex contact conditions among multiple components, and short-duration impact dynamics.

Pre- and post-processing is accomplished with FEMB (Finite Element Model Builder). FEMB is a general-purpose finite element pre- and post-processor compatible with most major finite analysis codes and CAD software. FEMB post-processes result data including the real-time animation of stresses, strain energy, displacements, and time history curves.

## 2.10.2 Finite Element Analysis

### 2.10.2.1 Model Descriptions

The finite element models of the NAC-STC body are generated utilizing the ANSYS PREP7 routine. The aspect ratio of finite elements and the density of the geometric mesh is carefully arranged, especially at the locations of geometric discontinuities and force boundaries, to minimize the possibility of numerical inaccuracies in the finite element method.

The cask components considered in the finite element models include the cask inner lid and outer lids; the top forging; the NS-4-FR neutron shield layer in the inner lid; the inner shell, transition sections, and outer shell; the lead layer; the bottom forging; the bottom plate; and the NS-4-FR neutron shield layer in the bottom.

Due to the complexity of the cask geometry and the loading conditions, it is apparent that one model is not sufficiently accurate to characterize all loading conditions and still be of a manageable size for available computer resources; therefore, three separate models are used to perform the analysis of the NAC-STC.

A two-dimensional axisymmetric model is used for the axisymmetric loading cases, which include internal pressure, thermal heat load, end drop on top, and end drop on the bottom. The two-dimensional axisymmetric model is described in Section 2.10.2.1.1.

The other two models are three-dimensional, so that they can properly analyze non-axisymmetric loading conditions, which include gravity (with the cask in the horizontal position), the side drop impact, the corner drop impacts, and the oblique drop impacts. The three-dimensional models are described in Section 2.10.2.1.2.

#### 2.10.2.1.1 Two-Dimensional Axisymmetric Model

The ANSYS PREP7 routine is used to generate the finite element model of the NAC-STC. Because of the axisymmetric geometry of the cask, several of the loading conditions can be effectively analyzed using a two-dimensional axisymmetric model. These conditions include bolt preload, internal pressure, thermal expansion, and drops on both the bottom and the top ends of the cask. The model is also described in Section 2.7.1.6.1.

The two-dimensional finite element model of the NAC-STC is constructed of 3083 nodes and 2842 elements. Care is taken when developing the model to maintain adequate mesh density and aspect ratio for the elements in order to minimize any numerical inaccuracies that might result from the finite element method.

The cask components that are considered in the ANSYS model include the inner lid, the outer lid, the bolting for each of the lids, the top forging, the inner shell, the transition sections, and the outer shell, the lead shell, the bottom forging, the bottom plate, and the BISCO NS-4-FR material in the bottom and in the inner lid.

ANSYS STIF3, STIF12, and STIF42 elements are used to construct the two-dimensional finite element model of the NAC-STC. The overall view of the model is shown in Figure 2.10.2-1. Detailed plots showing node numbering patterns and the mesh arrangements in the different regions of the model are included in Figures 2.10.2-2 through 2.10.2-7.

ANSYS STIF42 elements, which are two-dimensional, axisymmetric, isoparametric solid elements, are used to model all of the cask components except the bolts, the interfaces between the lead and the steel, and the interfaces between the neutron shield material and the steel. The bolts are modeled using ANSYS STIF3 elements, which are two-dimensional beam elements. The section properties of the bolts are entered on a "per radian" basis. The bolt preload is included in the model by applying an initial strain to the bolt shaft, which connects the bolt head to the threaded portions of the cask. For a detailed description of how the bolts are modeled, and how the initial strain is determined, see Section 2.10.2.2.3.



The "gap" element, STIF12, represents two surfaces that may maintain or break physical contact and may slide relative to each other. Such surfaces exist between: (1) the lead shell and the inner and outer stainless steel shells, (2) the neutron shield and the cask bottom, (3) the neutron shield and the inner lid, (4) the inner lid, and the outer lid, (5) the inner lid and the cask, and (6) the outer lid and the cask. Note that the gap element is only capable of supporting compression in the direction normal to the surfaces and friction in the tangential direction.

Gap elements completely surround the lead shell in the cask wall. If there is contact between the lead and the stainless steel surfaces, the gap elements transmit compressive load, but permit no tensile load between the lead and the stainless steel. This means that the gap elements allow the lead to move freely inside the space surrounded by the stainless steel. When a deceleration is imposed on the entire mass of the cask model to simulate the inertial effect of a drop impact condition, the deceleration causes the lead to slump and, consequently, creates a lateral pressure on the inner and the outer shells along the lead/shell interfaces.

Similarly, since the lead has a higher coefficient of thermal expansion than the stainless steel, the lead will incur larger thermal expansions and contractions than the stainless steel inner and outer shells; and thus, may be restrained by those shells. The gap element again allows the lead to move freely inside the annulus between the inner and the outer shells. Pressures resulting from the thermal expansion restraints develop wherever the lead contacts the stainless steel shells.

Thus, accurate modeling is achieved for the lead slump during an impact load condition and for the differential thermal expansions and contractions during temperature excursions.

In Figure 2.10.2-1, the elements representing the lead shell and the neutron shield layers are intentionally not shown, in order to improve the clarity of the mesh in the stainless steel components.

A gap element stiffness of  $3.0 \times 10^8$  psi, approximately 10 times greater than the cask stiffness, is specified to maintain the boundaries between the lead/steel and neutron shield/steel surfaces.

Similar gap elements are used to model the interfaces between the lids and the top forging. The initial radial gap between the lead shell and the outer shell is calculated to be 0.0428 inch.

The neutron shield that is located around the outer shell of the cask along the length of the cask cavity is not modeled because its structural rigidity is conservatively ignored in the structural analyses of the cask. However, its weight effects are included in the model by using an increased effective density in the region of the cask between the top of the bottom forging and the bottom of the inner lid. Modification of the density of this portion of the cask allows the overall weight of the empty cask to be adjusted to the proper value. Minor density changes are also made to the bottom end forging and bottom plate to allow for proper center of gravity location. The mass of the upper impact limiter is distributed to the top end of the cask by increasing the density of the lids and top forging. The mass of the lower impact limiter is distributed to the cask bottom by increasing the density of the bottom forging and bottom plate. The resulting cask total weight (including impact limiters) and center of gravity are then verified by an ANSYS check run.

The material properties used in the stress analyses include the elastic modulus, the Poisson's ratio, the density and the coefficient of thermal expansion. The elastic moduli and coefficients of thermal expansion are functions of temperature. They are represented by a table of material property values at various temperatures. The material property evaluation for each element is performed by linear interpolation of the tabular data at the element average or integration point temperatures. Thermal expansion is computed relative to a reference temperature (assumed to be 70°F for this analysis). The material property values used are given in Section 2.3.

The nodal temperatures in the structural model are determined from the results of the thermal analysis, which is performed using the HEATING5 computer program. The temperature distribution is considered to be constant around the circumference.

Stability of the finite element analysis requires that one node on the model be restrained in the cask longitudinal (axial) direction to prevent any vertical rigid body motion. Node 7332, located at the top outside corner, is axially restrained for the pressure, thermal, and bottom end impact cases (see Figure 2.10.2-6). Node 360, located at the bottom outside corner, is axially restrained for the top end impact case (see Figure 2.10.2-2).

#### 2.10.2.1.2 Three-Dimensional Finite Element Models (Directly Loaded Fuel Configuration)

There are a number of loading conditions that can only be characterized by a three-dimensional finite element analysis. In order to reduce the overall problem size, two three-dimensional models are developed: (1) the top fine mesh model, to be used in the stress evaluations for the top half of the cask; and (2) the bottom fine mesh model, to be used in the stress evaluations for the bottom half of the cask. In fact, both models are complete representations of the cask, since the entire cask is modeled. The top fine mesh model contains a very detailed representation of the top end of the cask, while the bottom end of the cask is modeled using a coarser mesh density. The top fine mesh model is used in those analyses that are expected to produce larger stresses in the top half of the cask. Similarly, the bottom fine mesh model contains a very detailed representation of the bottom end region of the cask, while the upper end of the cask is modeled with a coarser mesh density. The bottom fine mesh model is used in those analyses that are expected to produce larger stresses in the bottom half of the cask.

For the side drop analysis, both the top and bottom fine mesh models are used separately to obtain the detailed stresses in the upper and lower portions of the NAC-STC, respectively. The stress summary for the entire cask combines the results of the two runs. The oblique drop analyses use the fine mesh model for the impacting end of the cask.

The two three-dimensional models are constructed by first creating a mesh representing a two-dimensional plane of the cask, and then revolving that mesh 180 degrees around the axis of symmetry of the cask to create a model of one-half of the cask. This half-model of the cask is adequate for the drop analyses, because the cask geometry and the imposed loads are also symmetric about the midplane

of the cask. The plane of symmetry is chosen to pass through the line of impact in the side, corner, and oblique drop cases. Symmetry boundary conditions (i.e., no translations normal to the plane of symmetry), are imposed on all nodes on the plane of symmetry.

Mesh adequacy in the circumferential direction is ensured by first reviewing the ANSYS reference manual for a recommended mesh size, then adapting a non-uniform circumferential element size to accurately capture the high stresses in the impact region. Finally, a parametric study of mesh density is performed to verify the validity of the chosen mesh arrangement.

The ANSYS reference manual recommends a 15-degree circumferential mesh increment for shell structures. A minimum of twelve (180/15) circumferential elements would be required to model a 180-degree surface, according to this criteria. Since the region of impact will have much higher stresses than the region of the cask remote from the impact, a non-uniform circumferential element spacing is chosen. A very fine mesh near the region of impact varies to a coarse mesh on the side of the cask opposite the impact region. The largest circumferential element size was chosen to be twice that of the smallest, with the element size varying linearly in between. Figure 2.10.2-8 illustrates the resulting non-uniform angular locations of each row of nodes. Table 2.10.2-1 documents the angular location of each plane of nodes, and the circumferential element size for each row of elements. The arc length of the smallest elements, those along the line of impact, is 8.3 degrees. The arc length increases to 16.6 degrees for the elements farthest away from the impact.

A series of parametric studies were performed, which considered a thick-walled cylinder subject to a gravity loading in the lateral direction, in order to examine the results of using different mesh densities. Circumferential mesh densities of 28 uniformly spaced elements and of 15 uniformly spaced elements were considered. The results of the parametric study indicated that maximum stresses as determined by the mesh with 28 circumferential elements were within 1 percent of those determined by the mesh with 15 elements. Therefore, it is concluded that the 15 element non-uniform mesh is adequate to model the structural behavior of the

cask. The parametric studies also considered the effects of varying the number of elements through the wall thickness and of varying the element aspect ratio.

Three-dimensional beam elements (STIF4), solid elements (STIF45), and gap elements (STIF52) are used in the construction of the two three-dimensional finite element models. All cask components (forgings, lids, lead shell, shielding, inner and outer shells, etc.) are modeled using the STIF45 element. The STIF45 element is an eight-node, three-dimensional, parametric solid element having three degrees of freedom at each node (translations in X, Y, and Z directions).

Connections and interfaces between the components of the cask are modeled using the ANSYS STIF52 gap element. The STIF52 gap element is a three-dimensional interface element that represents two surfaces that may maintain or break physical contact, and may slide relative to each other. The use of this element is required in areas where contact between adjacent surfaces is not guaranteed by the geometry or loading. Such locations include the lead/steel shell interfaces and lid top forging interfaces. The cask lid bolts are modeled using the ANSYS beam element (STIF4). The STIF4 is a three-dimensional, uniaxial element with tension, compression, torsion, and bending capabilities. The element has six degrees of freedom at each node (translations in the nodal X, Y and Z directions and rotations about the nodal X, Y, and Z axes).

The material properties required by ANSYS for the three-dimensional analyses are those identified in Section 2.10.2.1.1.

#### 2.10.2.1.2.1 Bottom Fine Mesh Model

The complete bottom fine mesh model is shown in Figure 2.10.2-9. A two-dimensional view of the model is shown in Figure 2.10.2-10. The node numbering patterns and mesh arrangement in different regions of the model are provided in Figures 2.10.2-11 through 2.10.2-19. The node numbers shown in these figures are for the 0-degree circumferential plane. A circumferential node number increment of 2000 is used to determine the node numbers on the remaining circumferential planes. The bottom half of the cask contains the finer mesh density. The structural components have a mesh density of at least three elements through their

thicknesses in areas of structural discontinuities to ensure detection of stress gradients in those regions. The lead shell and the neutron shield end layers are modeled with one element through their thickness, which is sufficient to distribute their loads to the surrounding structure. In Figure 2.10.2-10, the elements representing the lead layer and the neutron shield layers are intentionally not shown in order to improve the clarity of the mesh used in modeling the stainless steel components.

The bottom fine mesh model is constructed by first building a two-dimensional mesh of the cask, and then revolving that mesh 180 degrees around the longitudinal axis of the cask to get a three-dimensional model of one-half of the cask.

All of the cask components - cask body, lead, shielding, lids, etc. - are modeled with the three-dimensional solid elements (STIF45). Interaction between the components is modeled by the use of three-dimensional gap elements (STIF52). The cask components which are enclosed by stainless steel, including the lead and the end neutron shields, are surrounded radially and axially by gap elements. Just as for the two-dimensional model, a gap element stiffness of  $3.0 \times 10^8$  psi is specified to maintain the boundaries between the surfaces. The initial radial gap between the lead layer and the outer shell is set to 0.0428 inches.

The mass densities of some of the cask components are modified to distribute the impact limiter masses onto the cask ends and to distribute the mass of the external neutron shield material to the region between the top of the bottom forging and the bottom of the inner lid, as described in Section 2.10.2.1.1.

#### 2.10.2.1.2.2 Top Fine Mesh Model

The top fine mesh model of the NAC-STC is comprised of 12,601 elements and 15,261 nodes. The maximum in-core wavefront size is 1338, as compared to the maximum permissible wavefront size of 1439, which is based on ANSYS program limitations. The maximum in-core wavefront size is used as a measurement of the ANSYS analysis size. The RMS wavefront size is 664. The three-dimensional model is generated by first creating a mesh for a two-dimensional plane and then

revolving the mesh 180 degrees around the longitudinal axis of the cask to create a half model, as described in Section 2.10.2.1.2.

The complete top fine mesh model is shown in Figure 2.10.2-20. The upper half of the model is shown at a larger scale in Figure 2.10.2-21. Figure 2.10.2-22 is a view of the 0-degree circumferential plane of the top fine mesh model. Figures 2.10.2-23 through 2.10.2-31 show in detail the node numbering patterns and the mesh arrangement at different regions of the cask. The node numbers shown in these figures are for the 0-degree circumferential plane. The node numbers on the remaining circumferential planes can be determined by adding 2000 (unless otherwise noted on each plot) to the node numbers on each succeeding circumferential plane. In Figure 2.10.2-22, the elements representing the lead layer and the neutron shield layers are intentionally not shown, in order to improve the clarity of the mesh used in the stainless steel components.

All cask components (cask body, lead, shielding, lids, etc.) are modeled using the ANSYS STIF45 solid elements, as in the bottom fine mesh model. The structural components have a mesh density of at least three elements through their thickness near areas of structural discontinuities to ensure the detection of stress gradients in those regions. The lead shell and the neutron shield end layers are modeled with one element through their thicknesses, which is adequate to distribute their loads to the surrounding structure. The lids are modeled with two or more elements through their thickness near the center of the cask, where stresses are low, and with a finer mesh density near the outer radius of the cask, where the stresses are higher as a result of the bolt loads and the impact loads.

Interaction between the cask components is modeled by use of three-dimensional gap elements (STIF52). The cask components that are enclosed by stainless steel, including the lead and the end neutron shields, are surrounded radially and axially by gap elements. The interface between the inner lid and the cask top forging is modeled using STIF52 gap elements in the axial and radial directions. The outer lid interfaces also use STIF52 gap elements in the radial direction (between the outer lid and the cask top forging) and in the axial direction (between the outer lid and the inner lid and between the outer lid and the top forging). There are 0.03-inch radial gaps between the top forging and the inner lid outside diameter.

There is a 0.06-inch axial gap between the inner lid and the outer lid. Just as for the two-dimensional model, a gap element stiffness of  $3.0 \times 10^8$  psi is used to maintain the boundaries between the surfaces.

The cask lead shielding is modeled using ANSYS STIF45 elements. The interface between the lead and the cask body is modeled using gap elements in the radial direction along its entire length. All runs are made with an initial gap specification of 0.00 inches at the inside diameter of the lead and 0.0428 inch at the outside diameter of the lead. At locations where the lead surface is angled, the gaps are oriented in such a way that they close in the direction perpendicular to the surface. This allows these gaps to support some axial load, as would be the case in the actual cask. The shielding at the bottom end of the cask is far enough removed from the area of interest for this model, that any gap element effects would be negligible. For this reason, the bottom end shielding is modeled using ANSYS STIF45 brick elements having common nodes with the cask body. The neutron shielding between the lids is also connected to the inner lid with common nodes. Since its modulus of elasticity is small compared to that of steel, the lid stresses are not significantly affected.

The mass densities of some of the cask components are modified to distribute the impact limiter masses onto the cask ends, and to distribute the external neutron shield mass to the region between the top of the bottom forging and the bottom of the inner lid, as described in Section 2.10.2.1.1.

The bolts are modeled using ANSYS STIF4 beam elements and are located on their appropriate radii (connecting the outer lid and the inner lid to the cask top forging), on each circumferential plane location. Since there are 16 circumferential planes contained in the finite element model, this results in 16 equivalent bolts per lid. Each bolt consists of four elements--one element as the bolt shaft, one as the bolt thread, and two as the bolt head.

The effective properties of each bolt are determined by calculating the percentage of the 180-degree arc that each bolt affects, and multiplying that by an overall sum of the actual properties. Table 2.10.2-2 shows the calculated percentages of the 180-degree arc, determined by summing one-half of the angles of the arc of the



two elements adjacent to a given node. Tables 2.10.2-3 and 2.10.2-4 document the calculated effective properties for all of the bolts in both lids, including the associated real constant numbers. Following are example calculations for the inner and outer lid bolt properties:

Inner Lid Bolts (42, 1 1/2 - 8 UN)

$$\text{Tensile area of one bolt} = 1.492 \text{ in}^2$$

$$\text{Total tensile area} = (42)(1.492) = 62.66 \text{ in}^2$$

$$\text{Bolt minor radius (R)} = 1.3444/2 = 0.6722 \text{ in}$$

$$\text{Moment of inertia (I) of one bolt} = \pi R^4/4 = 0.1604 \text{ in}^4$$

$$\text{Total moment of inertia} = (42)(0.1604) = 6.7368 \text{ in}^4$$

Referring to Table 2.10.2-3, the inner lid bolt properties for circumferential plane location 4, real constant number 17, are:

$$\text{Tensile area} = (0.0522)(62.66)(0.5) = 1.6354 \text{ in}^2$$

$$I = (0.0522)(6.7368)(0.5) = 0.1758 \text{ in}^4$$

$$\text{Diameter for stress recovery} = [(1.492)(4)/\pi]^{0.5} = 1.378 \text{ in}$$

Additionally, to determine the shear area of the bolt, a shear factor of 10/9 is applied to the bolt tensile area, as recommended by the ANSYS User's Manual, Section 4.0.5. In the ANSYS model, bolt head properties are taken to be 10 times the associated bolt shaft properties.

Outer Lid Bolts (36, 1 - 8 UNC)

$$\text{Tensile area of one bolt} = 0.606 \text{ in}^2$$

$$\text{Total tensile area} = (36)(0.606) = 21.816 \text{ in}^2$$

$$\text{Bolt minor radius (R)} = 0.8446/2 = 0.4223 \text{ in}$$

$$\text{Moment of inertia (I) of one bolt} = \pi R^4/4 = 0.0250 \text{ in}^4$$

$$\text{Total moment of inertia} = (36)(0.0250) = 0.900 \text{ in}^4$$

Referring to Table 2.10.2-4, the outer lid bolt properties for circumferential plane location 8, real constant number 38, are:

$$\text{Tensile area} = (0.0639)(21.816)(0.5) = 0.697 \text{ in}^2$$

$$I = (0.0639)(0.900)(0.5) = 0.02876 \text{ in}$$

$$\text{Diameter for stress recovery} = [(0.606)(4)/\pi]^{0.5} = 0.878 \text{ in}$$

Additionally, to determine the shear area of the bolt, a shear factor of 10/9 is applied to the bolt tensile area, as recommended by the ANSYS User's Manual, Section 4.0.5. In the ANSYS model, bolt head properties are taken to be 10 times the associated bolt shaft properties.

The bolt preload is calculated as shown in Section 2.6.7.5. The preload on the inner lid bolts is calculated to be  $4.51 \times 10^6$  pounds for 42 bolts. The preload on the outer lid bolts is calculated to be  $6.02 \times 10^5$  pounds for 36 bolts.

Section 2.10.2.2.3 contains a detailed description of the bolt preload strain calculation for both the inner and outer lids.

#### 2.10.2.1.3 Transport Cask Body Finite Element Model for the Canistered Fuel Configurations

The cask body model used for the Yankee-MPC and CY-MPC analyses is represented using ANSYS SOLID45, BEAM4, CONTACT52, and spring/damper COMBIN14 elements. Gap elements are used to model contact interfaces between components. Friction effects are ignored in the model. Lump mass elements (MASS21) are used to model components such as the impact limiters and NS-4-FR gamma shield.

The loaded canister is represented by a surface pressure load as described in Section 2.10.2.2.1. An acceleration of 20g's is applied to the cask and canister for the 1-ft drop. The pressure load for the canister lid and canister body loaded with fuel is applied to the cask body using a cosine-shaped pressure distribution, where the total pressure applied to the cask body is equal to the total impact load of the contents. The weight of the spacers is included in the weight of the canister and contents. Gap elements are defined at both ends of the cask to simulate the pressure applied by the impact limiters during drop conditions (based on a cosine distribution). The stiffness of the gap elements is varied from a maximum value ( $1 \times 10^6$  lb/in) at the line of impact to a lower

value ( $2.4 \times 10^5$  lb/in) at an angle of  $75^\circ$  from the line of impact, and a minimal value (100 lb/in) from  $82.5^\circ$  to  $180^\circ$ ). Element types with ANSYS key options are:

Element Type Number	Description	K1	K2	K3	K4	K5	K6	K7	K8	K9	K10	K11	K12
2	SOLID45	0	0	0	0	0	0	0	0	0	0	0	0
3	BEAM4	0	0	0	0	0	0	0	0	0	0	0	0
4	CONTAC52	0	0	0	0	0	0	0	0	0	0	0	0
5	MASS21	0	0	2	0	0	0	0	0	0	0	0	0
6	COMBIN14	0	0	0	0	0	0	0	0	0	0	0	0

The model consists of the following major regions with appropriate model data.

Region	Material	Mat Num	Type Num	Real Num
Inner Shell	SS304 SA240	1	2	20
Outer Shell	SS304 SA240	1	2	21
Bottom Ring	SS304 SA240	3	2	3
Neutron Shield	NS-4-FR	5	2	5
Bottom Exterior	SS304 SA240	6	2	6
Bottom Forging	SS304 SA336	6	2	6
Gamma Shield	PB ASTM B29	8	2	8
Upper Forging	SS304 SA336	9	2	9
Lid	SS304 SA336	10	2	10
B.C. Hole Annulus	Reduced Modulus	11	2	11

Solid 45 elements have real property numbers assigned but the values are ignored since real properties are not used by this element type. A small hole is modeled in the center of the lid and bottom section to eliminate the need for the generation of prisms or tetrahedrons at these locations. A small stress raiser results in this region but is not significant. The bolt circle annulus region is included in the model to restrain the lids. Since this evaluation is not concerned with bolt preload, the actual bolts are not modeled. Instead, nodes in this region are joined to corresponding nodes in the top forging. Real Property Data for Contact (Gap) elements is as follows:

Real Number	Normal Stiffness	Gap	Start	Tangential Stiffness
2	1.00E+06	0.00E+00	1	0.00E+00
3	1.00E+06	1.00E-05	1	0.00E+00
5	1.00E+06	0.00E+00	1	0.00E+00
6	100	0.00E+00	0.00E+00	0.00E+00
7	100	0.00E+00	0.00E+00	0.00E+00
8	1.00E+06	0.00E+00	0.00E+00	0.00E+00
9	1.00E+06	0.5	0.00E+00	0.00E+00
100	5.00E+05	0.00E+00	0.00E+00	0.00E+00
101	9.89E+05	0.00E+00	0.00E+00	0.00E+00
102	9.57E+05	0.00E+00	0.00E+00	0.00E+00
103	9.04E+05	0.00E+00	0.00E+00	0.00E+00
104	8.32E+05	0.00E+00	0.00E+00	0.00E+00
105	7.41E+05	0.00E+00	0.00E+00	0.00E+00
106	6.34E+05	0.00E+00	0.00E+00	0.00E+00
107	5.14E+05	0.00E+00	0.00E+00	0.00E+00
108	3.83E+05	0.00E+00	0.00E+00	0.00E+00
109	2.43E+05	0.00E+00	0.00E+00	0.00E+00
110	100	0.00E+00	0.00E+00	0.00E+00

Friction is ignored in these analyses. For Start=1, the gap element is initially closed, irrespective of the gap constant or its graphical configuration. For Start=0, the initial condition is based on the Gap constant value. Mass elements are used to model components, which are of little stress interest, yet contribute to the mass and loading of the assembly. This includes items such as the outer neutron shield and the impact limiters. Real property data for this element type is as follows:

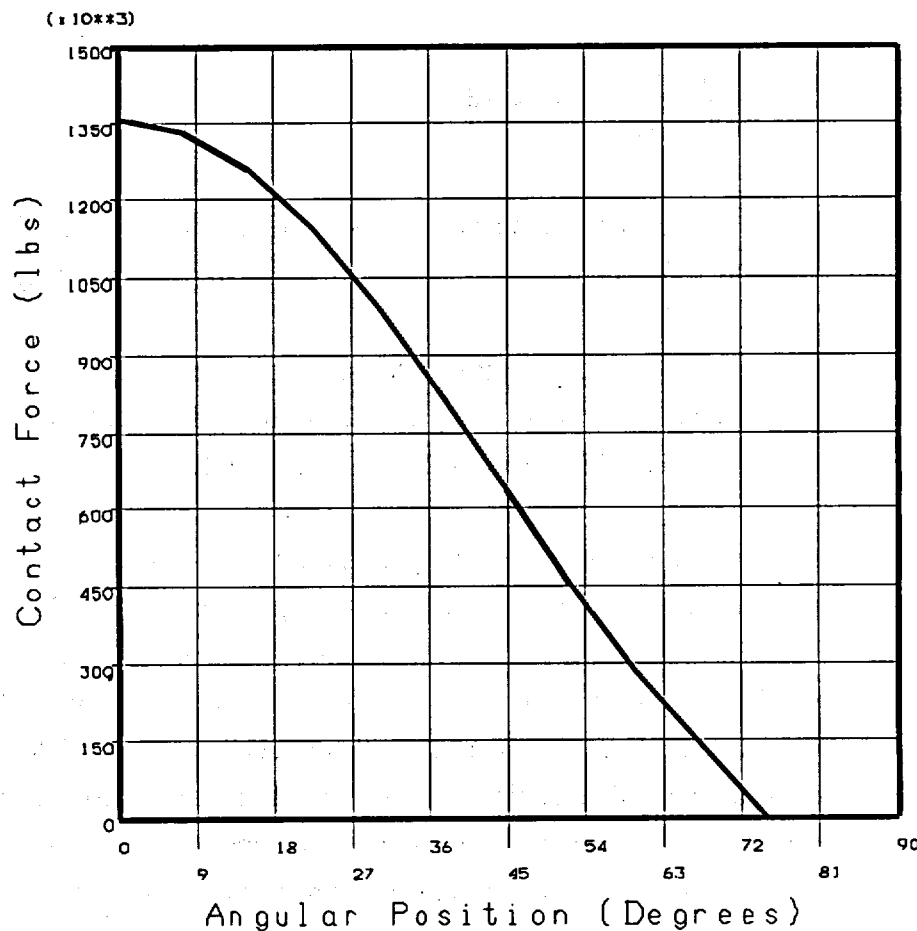
Real Number	MASS X	MASS Y	MASS Z	IXX	IYY	IZZ	Region
10	15.032	0.00E+00	0.00E+00	0.00E+00	0.00E+00	0.00E+00	Outer Shell
11	10.051	0.00E+00	0.00E+00	0.00E+00	0.00E+00	0.00E+00	Top
12	9.5942	0.00E+00	0.00E+00	0.00E+00	0.00E+00	0.00E+00	Bottom

These elements are distributed over nodes on the exterior surface of the cask.

The three-dimensional model is similar to the model shown in Fig. 2.10.2-9 and Fig. 2.10.2-20. The mesh is refined to increase element density in the loading area. The canistered fuel configuration model has a higher mesh density at both the top and bottom of the cask body model (as compared to the cask model for directly loaded fuel), eliminating the need for a separate top and bottom model as presented for directly loaded fuel. In the bottom forging (Fig.2.10.2-12), the mesh density of the model for directly loaded fuel transitions from a five element layer to a two

element layer. To avoid triangular and trapezoidal shaped elements, a uniform 3 element layer is used in the canistered fuel model. While the directly loaded fuel model is more conservative, the canistered fuel model is considered to behave accurately in the shell region.

To ensure that the gap elements close properly and apply the total load to the cask outer shell, the gap forces were reviewed at the angular positions to show that the impact limiter loads represent a cosine distribution. The plot below shows the gap forces as a function of angle for the Yankee-MPC configuration 30-ft drop. The angular position of zero corresponds to the point of impact. The value of the gap force represents the sum of all the gap elements at that angle. The CY-MPC configuration evaluation employs the same method of representing the impact limiter, which would, therefore, result in the same contact force distribution shown below.



#### 2.10.2.2 Loading Conditions

This section documents the methods of calculating contents pressure loads and impact pressure loads for the end drop, side drop, corner drop, and oblique drop scenarios. Additionally, the use of bolt initial strain to represent the bolt preload and the determination of the bolt initial strain are explained.

##### 2.10.2.2.1 Contents Pressure Calculation for the Directly Loaded and Yankee-MPC Configurations

For the end drop analyses, the contents weight is assumed to be uniformly distributed on the cask end, over an area determined by the inside diameter of the cask. Therefore, the contents weight of 56,000 pounds, and the cask cavity inside radius of 35.5 inches are used to calculate a contact pressure of:

$$p = \frac{56,000}{(\pi)(35.5)^2} = 14.14 \text{ psi}$$

The contents weight of the canistered Yankee class fuel configuration is 55,590 pounds. Therefore, the directly loaded fuel configuration bounds the canistered fuel configuration.

This pressure applies to a 1 g loading condition. Pressure values for the 1-foot and 30-foot end drop analyses are determined by ratioing this pressure by the g-load values applicable to the specific case, which are documented in Sections 2.6.7.1 and 2.7.1.1.

For the side drop condition, the basket stress analysis performed in Section 2.7.8 indicates that the contact area between the basket and the cask cavity is approximately 180 degrees (90 degrees on each side of the drop centerline), therefore, for the side drop analyses, the cask contents are conservatively assumed to contact the inner cask diameter on an arc of only 79.4 degrees on either side of the impact centerline. The inertial load produced by the 56,000-pound contents weight is represented as an equivalent static pressure applied on the interior surface of the cask. The pressure is uniformly distributed along the cavity length, and is varied in the circumferential direction as a cosine distribution. The maximum pressure occurs at the impact centerline; the pressure decreases to zero at locations that are 79.4 degrees either side of the impact centerline, as illustrated in Figure 2.10.2-32. The method used to determine the varying pressures on the elements within the 79.4-degree arc is presented in the following paragraphs.

Eight sectors of elements in the ANSYS model are defined within the 79.4-degree arc. The first sector of elements subtends the arc from the 0-degree circumferential plane to the 8.3-degree circumferential plane. The second sector subtends the arc from the 8.3-degree circumferential plane to the 17-degree circumferential plane. The remaining five sectors are defined in the same manner, by the 26.2-, 35.8-, 45.9-, 56.5-, and 67.7-degree circumferential planes, which are shown in Figure 2.10.2-8.

The following formula is used to determine the contents pressures for the side drop analyses, which vary around the circumference. This method uses a summation scheme to approximate the integration of the cosine-shaped pressure distribution:

$$F_{\text{total}} = \sum_{i=1}^8 P_{\text{max}} A_i \cos(\theta_i) \cos(\theta_i)$$

where

$F_{\text{total}} = 28,000 \text{ lb}$  (cask contents weight is 56,000 lb:  
therefore, 28,000 lb for a half model)

$P_{\text{max}} = \text{maximum pressure (at impact centerline)}$

$\theta_i = \text{average angle of subtended arc}$

$i = i^{\text{th}}$  circumferential sector

$\theta = \text{normalized angle to peak at } 0^\circ \text{ and to be zero at } 79.4^\circ$

$$= \theta_i \left( \frac{90}{79.4} \right) = 1.1335(\theta_i)$$

$A_i = i^{\text{th}}$  circumferential area over which the pressure is applied

$$= R (\Delta\theta_i)(\pi/180) L$$

$R = \text{inner radius of cask} = 35.5 \text{ in}$

$L = \text{cask cavity length} = 165 \text{ in}$

Therefore,  $A_i = (35.5)(\Delta\theta_i)(\pi/180)(165) = 102.23 (\Delta\theta_i)$

$$\Delta\theta_1 = 8.3 - 0 = 8.3^\circ$$

$$\Delta\theta_2 = 17.0 - 8.3 = 8.7^\circ$$

$$\Delta\theta_3 = 26.2 - 17.0 = 9.2^\circ$$

$$\Delta\theta_4 = 35.8 - 26.2 = 9.6^\circ$$

$$\Delta\theta_5 = 45.9 - 35.8 = 10.1^\circ$$

$$\Delta\theta_6 = 56.5 - 45.9 = 10.6^\circ$$

$$\Delta\theta_7 = 67.7 - 56.5 = 11.2^\circ$$

$$\Delta\theta_8 = 79.4 - 67.7 = 11.7^\circ$$

$$\theta_1 = \frac{0 + 8.3}{2} = 4.15^\circ; \theta_1 = 4.15^\circ(1.1335) = 4.70^\circ$$

$$\theta_2 = \frac{8.3 + 17.0}{2} = 12.65^\circ; \theta_2 = 12.65^\circ(1.1335) = 14.34^\circ$$

$$\theta_3 = \frac{17.0 + 26.2}{2} = 21.6^\circ; \theta_3 = 21.6^\circ(1.1335) = 24.48^\circ$$

$$\theta_4 = \frac{26.2 + 35.8}{2} = 31^\circ; \theta_4 = 31^\circ(1.1335) = 35.14^\circ$$

$$\theta_5 = \frac{35.8 + 45.9}{2} = 40.85^\circ; \theta_5 = 40.85^\circ(1.1335) = 46.30^\circ$$

$$\theta_6 = \frac{45.9 + 56.5}{2} = 51.20^\circ; \theta_6 = 51.20^\circ(1.1335) = 58.04^\circ$$

$$\theta_7 = \frac{56.5 + 67.7}{2} = 62.10^\circ; \theta_7 = 62.10^\circ(1.1335) = 70.39^\circ$$

$$\theta_8 = \frac{67.7 + 79.4}{2} = 73.55^\circ; \theta_8 = 73.55^\circ(1.1335) = 83.37^\circ$$

$$\text{Define: } F_i = P_{\max} A_i \cos(\theta_i) \cos(\theta_i)$$

where  $i = 1$  through 8

$$\begin{aligned} F_1 &= P_{\max}(102.23)(8.3^\circ) \cos(4.15^\circ) \cos(4.70^\circ) \\ &= 843.4 (P_{\max}) \end{aligned}$$

$$\begin{aligned} F_2 &= P_{\max}(102.23)(8.7^\circ) \cos(12.65^\circ) \cos(14.34^\circ) \\ &= 840.8 (P_{\max}) \end{aligned}$$

$$\begin{aligned} F_3 &= P_{\max}(102.23)(9.2^\circ) \cos(21.6^\circ) \cos(24.48^\circ) \\ &= 795.9 (P_{\max}) \end{aligned}$$

$$\begin{aligned} F_4 &= P_{\max}(102.23)(9.6^\circ) \cos(31^\circ) \cos(35.14^\circ) \\ &= 687.9 (P_{\max}) \end{aligned}$$



$$\begin{aligned}F_5 &= P_{\max}(102.23)(10.1^\circ) \cos(40.85^\circ) \cos(46.30^\circ) \\&= 539.6 (P_{\max})\end{aligned}$$

$$\begin{aligned}F_6 &= P_{\max}(102.23)(10.6^\circ) \cos(51.20^\circ) \cos(58.04^\circ) \\&= 359.4 (P_{\max})\end{aligned}$$

$$\begin{aligned}F_7 &= P_{\max}(102.23)(11.2^\circ) \cos(62.10^\circ) \cos(70.39^\circ) \\&= 179.8 (P_{\max})\end{aligned}$$

$$\begin{aligned}F_8 &= P_{\max}(102.23)(11.7^\circ) \cos(73.55^\circ) \cos(83.37^\circ) \\&= 39.11 (P_{\max})\end{aligned}$$

$$F_{\text{total}} = 4286(P_{\max})$$

Setting the total load ( $F_{\text{total}}$ ) to 28,000 lb

$$4286(P_{\max}) = 28,000$$

$$(P_{\max}) = 6.533 \text{ psi}$$

$P_{\max}$  represents the contents pressure load which would occur along the drop centerline. Given  $P_{\max}$ , the contents pressure loadings, which are applied to the eight sectors of elements, are calculated as follows:

$$P_1 = P_{\max} \cos \theta_1 = 6.533 \cos(4.70^\circ) = 6.51 \text{ psi}$$

$$P_2 = P_{\max} \cos \theta_2 = 6.533 \cos(14.34^\circ) = 6.33 \text{ psi}$$

$$P_3 = P_{\max} \cos \theta_3 = 6.533 \cos(24.48^\circ) = 5.95 \text{ psi}$$

$$P_4 = P_{\max} \cos \theta_4 = 6.533 \cos(35.14^\circ) = 5.34 \text{ psi}$$

$$P_5 = P_{\max} \cos \theta_5 = 6.533 \cos(46.30^\circ) = 4.51 \text{ psi}$$

$$P_6 = P_{\max} \cos \theta_6 = 6.533 \cos(58.04^\circ) = 3.46 \text{ psi}$$

$$P_7 = P_{\max} \cos \theta_7 = 6.533 \cos(70.39^\circ) = 2.19 \text{ psi}$$

$$P_8 = P_{\max} \cos \theta_8 = 6.533 \cos(83.37^\circ) = 0.76 \text{ psi}$$

The following is a summary of the side drop contents pressures applied to the finite element model in the eight circumferential sectors:

<u>ARC (deg)</u>	<u>PRESSURE (psi)</u>
0 - 8.3	6.51
8.3 - 17.0	6.33
17.0 - 26.2	5.95
26.2 - 35.8	5.34
35.8 - 45.9	4.51
45.9 - 56.5	3.46
56.5 - 67.7	2.19
67.7 - 79.4	0.76

The pressures are applied to the cask inner shell, over the length of the cask cavity for the side drop analyses. It should be noted that these pressures consider a 1 g deceleration condition. Pressures for the 1-foot and 30-foot side drop analyses are calculated by ratioing these pressure values by the appropriate deceleration g-loads, which are documented in Sections 2.6.7.2 and 2.7.1.2.

For the corner and oblique drop analyses, the contents pressure loading is a combination of the end drop pressure load and the side drop pressure load. The corner and oblique drop pressure loadings are determined by breaking up the contents pressure load into longitudinal and lateral components, based on the drop angle. The longitudinal component is applied to the cask end, and the lateral component is applied to the cask inner shell as described previously for the side drop case.

Adequacy of this modeling technique has been evaluated by performing a finite element analysis of the cask wall subjected to both a distributed pressure load and a line load along the center line of the support disk contact surface. Analyses results identified a 22 percent more conservative stress value for the distributed pressure load than the results for the discrete line loads. This conservative result is due to higher load being carried over the modeled contact area by piece wise linear pressure. Since the only difference between the corner impact cases and the side impact configuration is the component distribution relative to the angle of impact similarly conservative results are included in the current analysis documentation for all stress combinations using the pressure distribution results.

#### 2.10.2.2.2 Impact Pressure Calculation

For the end drop analysis, the impact pressure is assumed to uniformly contact the cask end over an area determined by the outside diameter of the cask. Therefore, the cask weight (including

contents) of 250,000 pounds and the cask outside radius of 43.35 inches are used to calculate an end drop impact pressure of:

$$P = \frac{250,000}{(\pi)(43.35)^2} = 42.35 \text{ psi}$$

For cases when no contents are present, the weight of the empty cask plus basket is 211,000 pounds, therefore the end drop impact pressure is:

$$P = \frac{211,000}{(\pi)(43.35)^2} = 35.74 \text{ psi}$$

These pressures apply to a 1 g loading condition. Pressure values for the 1-foot and 30-foot end drop analyses are determined by ratioing these pressure values by the g-loads applicable to the specific case, which are documented in Sections 2.6.7.1 and 2.7.1.1.

For the side drop analyses, the impact pressure load is applied to the finite element model as a distributed pressure over the contact area between the impact limiters and the cask. Since the center of gravity of the loaded cask is located within 1 inch of the cask middle plane, the impact load is assumed to be evenly divided between the two limiters.

The distribution of impact pressure is assumed to be uniform, in the longitudinal direction, over the two 12.0-inch impact limiter contact areas. The distribution of impact limiter pressure is assumed to vary sinusoidally in the circumferential direction. A cosine-shaped pressure distribution is selected, which is "peaked" at the impact centerline, and is spread over a 79.4-degree arc on each side of the impact centerline, as shown in Figure 2.10.2-32. The region of applied pressure (a 158.8° arc) is defined based on the "crush" geometry of the impact limiter. The assumption of a peaked pressure distribution is a conservative, classical, stress analysis procedure since the applied pressure actually is spread over a 180-degree arc (90-degree half-cask arc).

The following calculation is performed to determine the pressure ( $P_i$ ) to be applied to elements within the eight circumferential sectors defined in Section 2.10.2.2.1. The calculation is based on the weight of a half-model of the cask at 1 g. Pressure forces for the 1-foot and 30-foot side drop analyses are determined by ratioing these pressure forces by the g-load applicable to the specific case.

The following formula can be used to compute the maximum impact pressure. This method uses a summation scheme to approximate the integration of the cosine-shaped pressure distribution:

$$F_{\text{total}} = \sum_{i=1}^8 P_{\text{max}} A_i \cos(\theta_i) \cos(\theta_i)$$

where

$F_{\text{total}} = 125,000$  lb (the cask design weight for a half model)

$P_{\text{max}}$  = maximum impact pressure occurring at the impact centerline

$\theta_i$  = average angle of subtended arc

$i = i^{\text{th}}$  circumferential sector

$\Delta\theta_i$  = arc length, in degrees, of sector  $i$

$\theta_i$  = Normalized angle to peak at  $0^\circ$  and to be zero at  $79.4^\circ$

$= \theta_i (90/79.4) = 1.1335 \theta_i$

$A_i = i^{\text{th}}$  circumferential area over which the pressure is applied

$= R(\Delta\theta_i)(\pi/180)L = 0.01745(\Delta\theta_i)(R)(L)$

$R$  = outer radius of the cask at impact limiter contact points

$= 43.35$  in

$L$  = Impact limiter contact length = 24.03 in (for two limiters, one on each end of the cask)

$\Delta\theta_1 = 8.3 - 0 = 8.3^\circ$

$\Delta\theta_2 = 17.0 - 8.3 = 8.7^\circ$

$\Delta\theta_3 = 26.2 - 17.0 = 9.2^\circ$

$\Delta\theta_4 = 35.8 - 26.2 = 9.6^\circ$

$\Delta\theta_5 = 45.9 - 35.8 = 10.1^\circ$

$\Delta\theta_6 = 56.5 - 45.9 = 10.6^\circ$

$\Delta\theta_7 = 67.7 - 56.5 = 11.2^\circ$

$\Delta\theta_8 = 79.4 - 67.7 = 11.7^\circ$

$\theta_1 = \frac{0 + 8.3}{2} = 4.15^\circ; \theta_1 = 4.15^\circ(1.1335) = 4.70^\circ$

$\theta_2 = \frac{8.3 + 17.0}{2} = 12.65^\circ; \theta_2 = 12.65^\circ(1.1335) = 14.34^\circ$

$$\theta_3 = \frac{17.0 + 26.2}{2} = 21.6^\circ; \theta_3 = 21.6^\circ(1.1335) = 24.48^\circ$$

$$\theta_4 = \frac{26.2 + 35.8}{2} = 31^\circ; \theta_4 = 31^\circ(1.1335) = 35.14^\circ$$

$$\theta_5 = \frac{35.8 + 45.9}{2} = 40.85^\circ; \theta_5 = 40.85^\circ(1.1335) = 46.30^\circ$$

$$\theta_6 = \frac{45.9 + 56.5}{2} = 51.20^\circ; \theta_6 = 51.20^\circ(1.1335) = 58.04^\circ$$

$$\theta_7 = \frac{56.5 + 67.7}{2} = 62.10^\circ; \theta_7 = 62.10^\circ(1.1335) = 70.39^\circ$$

$$\theta_8 = \frac{67.7 + 79.4}{2} = 73.55^\circ; \theta_8 = 73.55^\circ(1.1335) = 83.37^\circ$$

$$F_i = P_{\max} A_i \cos(q_i) \cos(q)$$

i = 1 through 8

$$\begin{aligned} F_1 &= P_{\max}(0.01745)(R)(8.3^\circ)(L) \cos(4.15^\circ) \cos(4.70^\circ) \\ &= 0.1440 (P_{\max})(L)(R) \end{aligned}$$

$$\begin{aligned} F_2 &= P_{\max}(0.01745)(R)(8.7^\circ)(L) \cos(12.65^\circ) \cos(14.34^\circ) \\ &= 0.1435 (P_{\max})(L)(R) \end{aligned}$$

$$\begin{aligned} F_3 &= P_{\max}(0.01745)(R)(9.2^\circ)(L) \cos(21.6^\circ) \cos(24.48^\circ) \\ &= 0.1359 (P_{\max})(L)(R) \end{aligned}$$

$$\begin{aligned} F_4 &= P_{\max}(0.01745)(R)(9.6^\circ)(L) \cos(31^\circ) \cos(35.14^\circ) \\ &= 0.1174 (P_{\max})(L)(R) \end{aligned}$$

$$\begin{aligned} F_5 &= P_{\max}(0.01745)(R)(10.1^\circ)(L) \cos(40.85^\circ) \cos(46.30^\circ) \\ &= 0.0921 (P_{\max})(L)(R) \end{aligned}$$

$$\begin{aligned} F_6 &= P_{\max}(0.01745)(R)(10.6^\circ)(L) \cos(51.20^\circ) \cos(58.04^\circ) \\ &= 0.0614 (P_{\max})(L)(R) \end{aligned}$$

$$\begin{aligned} F_7 &= P_{\max}(0.01745)(R)(11.2^\circ)(L) \cos(62.10^\circ) \cos(70.39^\circ) \\ &= 0.0307 (P_{\max})(L)(R) \end{aligned}$$

$$\begin{aligned} F_8 &= P_{\max}(0.01745)(R)(11.7^\circ)(L) \cos(73.55^\circ) \cos(83.37^\circ) \\ &= 0.0067 (P_{\max})(L)(R) \end{aligned}$$

$$F_{\text{total}} = 0.7317 (P_{\max})(L)(R)$$

$$P_{\max} = \frac{F_{\text{total}}}{(0.7317)(L)(R)}$$

The pressures to be applied to the finite element analysis can then be computed as follows:

$$P_i = \frac{F_{\text{Total}} \cos(\theta_i)}{(0.7317)(L)(R)}$$

where  $F_{\text{total}} = 125,000 \text{ lb (for half model)}$

$$L = 24.06 \text{ in}$$

$$R = 43.35 \text{ in}$$

$$P_i = 163.7918 \cos(\theta)$$

$$P_1 = 163.7918 \cos(4.70^\circ) = 163.22 \text{ psi}$$

$$P_2 = 163.7918 \cos(14.34^\circ) = 158.67 \text{ psi}$$

$$P_3 = 163.7918 \cos(24.48^\circ) = 149.06 \text{ psi}$$

$$P_4 = 163.7918 \cos(35.14^\circ) = 133.98 \text{ psi}$$

$$P_5 = 163.7918 \cos(46.30^\circ) = 113.17 \text{ psi}$$

$$P_6 = 163.7918 \cos(58.04^\circ) = 86.96 \text{ psi}$$

$$P_7 = 163.7918 \cos(70.39^\circ) = 54.99 \text{ psi}$$

$$P_8 = 163.7918 \cos(83.37^\circ) = 18.96 \text{ psi}$$

The following is a summary of the side drop impact pressures applied to the finite element model in the eight circumferential sectors:

<u>ARC (deg)</u>	<u>PRESSURE (psi)</u>
0 - 8.3	163.22
8.3 - 17.0	158.67
17.0 - 26.2	149.06
26.2 - 35.8	133.98
35.8 - 45.9	113.17
45.9 - 56.5	86.69
56.5 - 67.7	54.99
67.7 - 79.4	18.96

It should be noted that these pressures consider a 1 g deceleration condition. Pressures for the 1-foot and 30-foot side drop analyses are calculated by ratioing these pressure values by the appropriate deceleration or g values, which are documented in Sections 2.6.7.2 and 2.7.1.2.

For the corner and oblique drop analyses, the impact pressure loading is a combination of the end drop impact pressure load and the side drop impact pressure load. The corner and oblique drop impact pressure loadings are determined by breaking up the impact pressure load into longitudinal and lateral components, based on the drop angle. The longitudinal component is applied to the cask end, and the lateral component is applied to the cask inner shell as previously described for the side drop case.

#### 2.10.2.2.3 Bolt Initial Strain Determination

The standard technique for applying bolt preload to a finite element model is employed. The bolts are modeled using beam elements, ANSYS STIF3 elements for the two-dimensional model and ANSYS STIF4 elements for the three-dimensional top fine mesh model. Each bolt is modeled by four beam elements, two that represent the bolt head and two that represent the bolt shaft. The two bolt head elements are defined by three nodes that are an integral part of the non-threaded plate. The bolt head elements are assigned a stiffness of 10 times the actual bolt stiffness. The first bolt shaft element connects the center node of the bolt head with a node located at the top of the threaded hole. This element represents the portion of the bolt that is not engaged in the threaded hole. This portion of the bolt will be in tension due to the bolt preload. The second bolt shaft element connects the node at the top of the threaded hole with a node at the bottom of the threaded hole. This element represents the portion of the bolt that is engaged in the threaded hole. The two bolt shaft elements are assigned material property values (area and stiffness) equal to the actual bolt properties.

The effect of bolt preload is imposed on the model by applying an initial strain to the bolt shaft. The initial strain is applied only to the beam element representing the portion of the bolt shaft not engaged in threads. The initial strain values, which result in the required preload values, are determined by first running ANSYS analyses of both the two- and three-dimensional models with a "trial" initial strain, applied to the bolt shaft element, as the only loading condition. The resulting beam element force (from the element representing the portion of the bolt shaft not engaged in threads), is then used to ratio the trial initial strain to a value that will result in a beam element force closer to the actual bolt preload. This procedure is performed iteratively until the beam element force is effectively equal to the actual bolt preload.

The trial initial strain values are first determined by performing hand calculations of the value of  $P/nAE$  for the inner and the outer lid bolts. For the inner lid bolts, the calculation considers a required total bolt preload of  $4.51 \times 10^6$  pounds, a quantity (n) of 42 bolts, a bolt cross-sectional area (A) of 1.492 square inches per bolt, and a Young's modulus (E) of  $31.0 \times 10^6$  psi.

For the outer lid bolts, the calculation considers a required total bolt preload (P) of  $6.02 \times 10^5$  pounds, a quantity (n) of 36 bolts, a bolt cross-sectional area (A) of 0.606 square inches per bolt, and a Young's modulus (E) of  $28.3 \times 10^6$  psi.

#### 2.10.2.2.4 Contents Pressure Calculation—CY-MPC Configuration

For the end drop analyses, the contents weight is assumed to be uniformly distributed on the cask end, over an area determined by the inside diameter of the cask. Therefore, the conservatively assumed CY-MPC contents weight of 67,621 pounds (Fuel + Fuel Basket + Canister with lids + Spacer = 35,100 + 14,055 + 16,666 + 1,800), and the cask cavity inside radius of 35.5 inches are used to calculate a contact pressure of:

$$p = \frac{67,621}{(\pi)(35.5)^2} = 17.08 \text{ psi}$$

Note a spacer heavier than the weight reported in Table 2.2-4 is conservatively used in this evaluation.

This pressure applies to a 1 g loading condition. Pressure values for the 1-foot and 30-foot end drop analyses are determined by ratioing this pressure by the g-load values applicable to the specific case, which are documented in Sections 2.6.7.1 and 2.7.1.1.

For the side drop condition, the cask contents are conservatively assumed to contact the inner cask diameter on an arc of only 30 degrees during the 1-foot drop and 45 degrees during the 30-foot drop on either side of the impact centerline. The inertial load produced by each component (Lids + Canister body and fuel + Spacer) are represented as equivalent static pressures applied on the interior surface of the cask. The pressures are uniformly distributed along the cavity length, and are varied in the circumferential direction as a cosine distribution. The maximum pressure occurs along the impact centerline and decreases to zero at 30 degrees (1-foot drop) or 45 degrees (30-foot drop) either side of the impact centerline. The method used to determine the varying pressures on the elements within the contact arc is presented in Section 2.10.2.2.1.



### 2.10.2.3 Finite Element Analysis Procedures

The structural evaluation of the NAC-STC is performed by ANSYS analyses using three finite element models. A two-dimensional axisymmetric model is used for the axisymmetric loading cases, including bolt preload, internal pressure (high and low), thermal hot and cold, thermal fire transient, top end drop, and bottom end drop. A three-dimensional top fine mesh model is used in the non-axisymmetric loading conditions that result in high stresses on the top end of the cask, including the top corner drop and top oblique drops. The three-dimensional bottom fine mesh model is used for the non-axisymmetric loading conditions that result in high stresses on the bottom end of the cask, including the bottom corner drop, and bottom oblique drops. For the side drop analysis, both the top fine mesh model and the bottom fine mesh model are analyzed separately, in order to obtain the detailed stresses for both ends of the cask.

A number of individual and combined loading conditions are evaluated using separate ANSYS analyses. The ANSYS analyses performed for each individual loading condition are for the purpose of studying the structural effects of each individual type of load applied to the cask. The stress results of the ANSYS analysis of each individual load case are documented by nodal stress summaries (for details about finite element stress documentation procedures, see Section 2.10.2.4). The individual loading conditions considered are:

1. Bolt preload plus maximum internal pressure, 50 psig.
2. Bolt preload plus minimum internal pressure, 12 psig.
3. Gravity with 100°F ambient temperature, maximum decay heat load, and maximum insolation.
4. Gravity with -40°F ambient temperature, no decay heat load, and no insolation.
5. Thermal heat with 100°F ambient temperature, maximum decay heat load, and maximum insolation.
6. Thermal cold with -20°F ambient temperature, maximum decay heat load, and no insolation.
7. Thermal cold with -40°F ambient temperature, no decay heat load, and no insolation.
8. Thermal fire transient with 1475°F surrounding environment, 30-minute period.

9. Impact and inertial loads, 1-foot top end drop, 20 g impact load,  $\phi = 0$  degrees.
10. Impact and inertial loads, 1-foot bottom end drop, 20 g impact load,  $\phi = 0$  degrees.
11. Impact and inertial loads, 1-foot side drop, 20 g impact load,  $\phi = 90$  degrees.
12. Impact and inertial loads, 1-foot top corner drop, 20 g impact load,  $\phi = 24$  degrees.
13. Impact and inertial loads, 1-foot bottom corner drop, 20 g impact load,  $\phi = 24$  degrees.
14. Impact and inertial loads, 30-foot top end drop, 56.1 g impact load,  $\phi = 0$  degrees.
15. Impact and inertial loads, 30-foot bottom end drop, 56.1 g impact load,  $\phi = 0$  degrees.
16. Impact and inertial loads, 30-foot side drop, 55 g impact load,  $\phi = 90$  degrees.
17. Impact and inertial loads, 30-foot top corner drop, 55 g impact load,  $\phi = 24$  degrees.
18. Impact and inertial loads, 30-foot bottom corner drop, 55 g impact load,  $\phi = 24$  degrees.
19. Impact and inertial loads, 30-foot bottom oblique drop, 55 g impact load,  $\phi = 15$  degrees.
20. Impact and inertial loads, 30-foot top critical oblique drop, 55 g impact load,  $\phi = 75$  Degrees. ( $\phi = 75$  degrees is the angle that results in the most critical stresses for the 30-foot top oblique drops).
21. Impact and inertial loads, 30-foot bottom critical oblique drop, 55 g impact load,  $\phi = 75$  degrees. ( $\phi = 75$  degrees is the angle that results in the most critical stresses for the 30-foot bottom oblique drops).

Combined load cases are then evaluated by running ANSYS analyses of the combined loading conditions. For example, the 30-foot top corner drop accident condition is evaluated by a single ANSYS analysis with the following loads applied simultaneously:

55 g impact and inertial loads ( $\phi = 24$  degrees), 100°F ambient temperature, maximum decay heat load, maximum solar insolation, bolt preload, and 50 psig internal pressure.

A single analysis with multiple loads is used in contrast to the method of superimposing the stress results from the individual analyses, in order to more accurately evaluate the effect of the simultaneous loads on the cask structure. For combined load cases, the stresses are documented by nodal, sectional, and critical stress summaries. The following combined load cases are considered:

1. Thermal Heat (normal condition), with bolt preload, maximum internal pressure of 50 psig, 100°F ambient temperature, maximum solar insolation, maximum decay heat, 1 g gravity load, still air, loaded and ready for shipment in the horizontal position.
2. Thermal Cold (normal condition) with bolt preload, minimum internal pressure of 12 psig, -40°F ambient temperature, no solar insolation, no decay heat load, 1 g gravity load, still air, loaded and ready for shipment in the horizontal position.
3. Thermal Fire Transient (hypothetical accident condition) with a surrounding environment of 1475°F for a 30-minute period, with bolt preload, internal pressure of 125 psig (conservative; actual internal pressure is 65.5 psig), maximum solar insolation, maximum decay heat load, and 1 g gravity load in the vertical direction.
4. 1-foot Top End Drop (normal condition) with bolt preload, maximum internal pressure of 50 psig, 100°F ambient temperature, maximum solar insolation, maximum decay heat load, 20 g impact and inertial load ( $\phi = 0$  degrees), still air.
5. 1-foot Top End Drop (normal condition) with bolt preload, minimum internal pressure of 12 psig, -20°F ambient temperature, no solar insolation, maximum decay heat load, 20 g impact and inertial load ( $\phi = 0$  degrees), still air.

6. 1-foot Top End Drop (normal condition) with bolt preload, minimum internal pressure of 12 psig, -20°F ambient temperature, no solar insolation, no decay heat load, 20 g impact and inertial load ( $\phi = 0$  degrees), still air.
7. 1-foot Bottom End Drop (normal condition) with bolt preload, maximum internal pressure of 50 psig, 100°F ambient temperature, maximum solar insolation, maximum decay heat load, 20 g impact and inertial load ( $\phi = 0$  degrees), still air.
8. 1-foot Bottom End Drop (normal condition) with bolt preload, minimum internal pressure of 12 psig, -20°F ambient temperature, no solar insolation, maximum decay heat load, 20 g impact and inertial load ( $\phi = 0$  degrees), still air.
9. 1-foot Bottom End Drop (normal condition) with bolt preload, minimum internal pressure of 12 psig, -20°F ambient temperature, no solar insolation, no decay heat load, 20 g impact and inertial load ( $\phi = 0$  degrees), still air.
10. 1-foot Side Drop (normal condition) with bolt preload, maximum internal pressure of 50 psig, 100°F ambient temperature, maximum solar insolation, maximum decay heat load, 20 g impact and inertial load ( $\phi = 90$  degrees), still air.
11. 1-foot Top Corner Drop (normal condition) with bolt preload, maximum internal pressure of 50 psig, 100°F ambient temperature, maximum solar insolation, maximum decay heat load, 20 g impact and inertial load ( $\phi = 24$  degrees), still air.
12. 1-foot Bottom Corner Drop (normal condition) with bolt preload, maximum internal pressure of 50 psig, 100°F ambient temperature, maximum solar insolation, 20 g impact and inertial load ( $\phi = 24$  degrees), still air.
13. 30-foot Top End Drop (hypothetical accident condition) with bolt preload, maximum internal pressure of 50 psig, 100°F ambient temperature, maximum solar insolation, maximum decay heat load, 56.1 g impact and inertial load ( $\phi = 0$  degrees), still air.

14. 30-foot Top End Drop (hypothetical accident condition) with bolt preload, minimum internal pressure of 12 psig, -20°F ambient temperature, no solar insolation, maximum decay heat load, 56.1 g impact and inertial load ( $\phi = 0$  degrees), still air.
15. 30-foot Top End Drop (hypothetical accident condition) with bolt preload, minimum internal pressure of 12 psig, -20°F ambient temperature, no solar insolation, no decay heat load, 56.1 g impact and inertial load ( $\phi = 0$  degrees), still air.
16. 30-foot Bottom End Drop (hypothetical accident condition) with bolt preload, maximum internal pressure of 50 psig, 100°F ambient temperature, maximum solar insolation, maximum decay heat load, 56.1 g impact and inertial load ( $\phi = 0$  degrees), still air.
17. 30-foot Bottom End Drop (hypothetical accident condition) with bolt preload, minimum internal pressure of 12 psig, -20°F ambient temperature, no solar insolation, maximum decay heat load, 56.1 g impact and inertial load ( $\phi = 0$  degrees), still air.
18. 30-foot Bottom End Drop (hypothetical accident condition) with bolt preload, minimum internal pressure of 12 psig, -20°F ambient temperature, no solar insolation, no decay heat load, 56.1 g impact and inertial load ( $\phi = 0$  degrees), still air.
19. 30-foot Side Drop (hypothetical accident condition) with bolt preload, maximum internal pressure of 50 psig, 100°F ambient temperature, maximum solar insolation, maximum decay heat load, 55 g impact and inertial load ( $\phi = 90$  degrees), still air.
20. 30-foot Top Corner Drop (hypothetical accident condition) with bolt preload, maximum internal pressure of 50 psig, 100°F ambient temperature, maximum solar insolation, maximum decay heat load, 55 g impact and inertial load ( $\phi = 24$  degrees), still air.

21. 30-foot Bottom Corner Drop (hypothetical accident condition) with bolt preload, maximum internal pressure of 50 psig, 100°F ambient temperature, maximum solar insolation, maximum decay heat load, 55 g impact and inertial load ( $\phi = 24$  degrees), still air.
22. 30-foot Bottom Oblique Drop (hypothetical accident condition) with bolt preload, maximum internal pressure of 50 psig, 100°F ambient temperature, maximum solar insolation, maximum decay heat load, 55 g impact and inertial load ( $\phi = 15$  degrees), still air.
23. 30-foot Top Oblique Drop (hypothetical accident condition) with bolt preload, maximum internal pressure of 50 psi, 100°F ambient temperature, maximum solar insolation, maximum decay heat load, 55 g impact and inertial load ( $\phi = 75$  degrees), still air. ( $\phi = 75$  degrees is the angle which results in the most critical stresses for 30-foot top oblique drops).
24. 30-foot Bottom Oblique Drop (hypothetical accident condition) with bolt preload, maximum internal pressure of 50 psig, 100°F ambient temperature, maximum solar insolation, maximum decay heat load, 55 g impact and inertial load ( $\phi = 75$  degrees), still air. ( $\phi = 75$  degrees is the angle which results in the most critical stresses for 30-foot top oblique drops).

#### 2.10.2.4 Finite Element Documentation Procedures

Documentation of the finite element stress calculations is performed according to the following procedure:

1. A sketch of the cask is prepared showing the points on each shell for which stresses are calculated and tabulated. At given axial locations on the cask, separate points are designated on the inside and outside of each shell. At given radial locations on the end and closure plates, separate points are designated on the inside and outside of each plate. In addition, for thick sections or thin sections at structural discontinuities, the stresses are presented for several points through the thickness in order to adequately define the stress distribution for the stress linearization calculations. Furthermore, for three-dimensional

models, the stress variations around the circumference are documented at several selected circumferential locations.

2. For each stress point identified in step 1, a nodal stress summary, including stress components and principal stresses, is prepared for each individual normal and accident condition loading (e.g., internal pressure, hot and cold temperature, impact, etc.).
3. Summaries are prepared for the combined stresses at each stress point per the load combinations specified in Regulatory Guide 7.8. The combined stresses are classified in the categories of primary, and primary plus secondary stress intensities, as specified in Regulatory Guide 7.6.
4. Stress intensity summaries are prepared for the primary membrane ( $P_m$ ), primary membrane plus primary bending ( $P_m + P_b$ ), and primary plus secondary ( $S_n$ ) stress categories. These stress intensity values are obtained by performing stress linearization calculations using the nodal stresses obtained from step 2. This calculation is performed on all of the selected sections.

In order to perform steps 1 through 4, representative section cut locations were chosen based on the critical stress locations. The nodes representing the stress points used in steps 1 through 4 are located on these representative section cuts. The section locations are described in detail in Section 2.10.2.4.2.

5. Stress evaluations are then performed at every feasible cross-section of the cask. Then, the most critical cross-section within each component is determined by searching, on a component basis, for the cross section where the maximum stress intensity is located. Since the stress evaluations and the search are performed by a computer algorithm, every feasible cross-section is identified and evaluated, insuring that the maximum stress location within each component is found. Stress tables are then prepared to summarize the critical primary membrane, primary membrane plus primary bending, primary plus secondary stresses, and the margin of safety, of each cask component, for each loading condition.

In order to perform step 5, the cask is divided into components based on the physical geometry of the cask, such that each component consists of a single material. The details of the cask component identification are given in Section 2.10.2.4.1.

#### 2.10.2.4.1     Structural Component Identification

Cask components are defined so that the qualification of the cask can be performed on a component basis. Stress evaluations are performed at every feasible cask cross-section, and then a computer search is performed to identify the section within each component which has the maximum stress intensity. Critical stress summaries are then prepared on a component basis.

The determination of critical stresses considers the stress results at a total of 3877 cross-sections on the three-dimensional top fine mesh model, and at a total of 3188 cross-sections on the three-dimensional bottom fine mesh model. For the two-dimensional axisymmetric model, stress evaluations are performed for a total of 487 cross-sections. These evaluations cover all of the feasible cross-sections of the cask.

Preparation of the critical stress summaries also requires the calculation of allowable stress values. Since allowable stress is a function of material properties (design stress intensity, yield strength and ultimate tensile strength), it is convenient that the components be defined such that each component consists of a single material. This is accomplished by designating the components in a manner consistent with the actual physical construction of the cask, i.e., the components are defined as the unique physical entities which exist prior to the final assembly of the cask.

The material properties used to determine allowable stresses are functions of temperature. If the allowable stresses for all components were determined using the maximum cask temperature, the allowable stresses will be overly conservative in those components which never experience the maximum cask temperature. Maximum temperatures determined on a component basis, rather than on a cask basis, permit the determination of more reasonable, but still conservative, allowable stresses. Therefore, the maximum component temperature is used in calculating the allowable stresses for that component.

The finite element cask components are uniquely designated as shown in Figure 2.10.2.33. Table 2.10.2-5 documents the name of each component, the material of which it is constructed, and an



arbitrary material identification number (used in the ANSYS model). The fifth column of the table documents the maximum temperature which occurs in each individual component, as determined by the 100°F ambient thermal analysis condition.

The sixth and eighth columns of Table 2.10.2-5 documents the design stress intensity ( $S_m$ ), and the ultimate tensile strength ( $S_u$ ), for the component material at the maximum component temperature. The values of  $1.5(S_m)$  and  $0.7(S_u)$  are also provided. These component allowables are conservatively used for the -20°F and -40°F ambient condition load cases.

#### 2.10.2.4.2 Representative Section Locations

The entire NAC-STC body and closure lids are analyzed for structural adequacy. Representative section cut locations are defined, based on the critical stress locations, in order to illustrate the overall structural behavior of the cask. The selected section locations are identified by letters on Figure 2.10.2-34.

Each load case--pressure, thermal, and mechanical--is evaluated separately. The stress components are documented for each of the selected sections and for the nodes on the sections. The individual load cases are then combined to obtain total principal stresses and stress intensities for the primary membrane, primary membrane plus primary bending, and primary plus secondary stress categories.

Figures 2.10.2-35 and 2.10.2-36 show the distribution of nodes and elements in the circumferential direction for the three-dimensional top fine mesh model, and for the three-dimensional bottom fine mesh model, respectively. For the three-dimensional models, stress results are documented for several of the 16 circumferential planes.

The coordinates of the nodes which define the ends of the section cuts for the two-dimensional axisymmetric, three-dimensional bottom fine mesh, and three-dimensional top fine mesh models are provided in Tables 2.10.2-8 through 2.10.2-10, respectively. Tables 2.10.2-11 through 2.10.2-13 contain the node numbers and coordinates of all stress point locations on each section cut, for the three models.

Figure 2.10.2-1 ANSYS Two-Dimensional Finite Element Model - NAC-STC

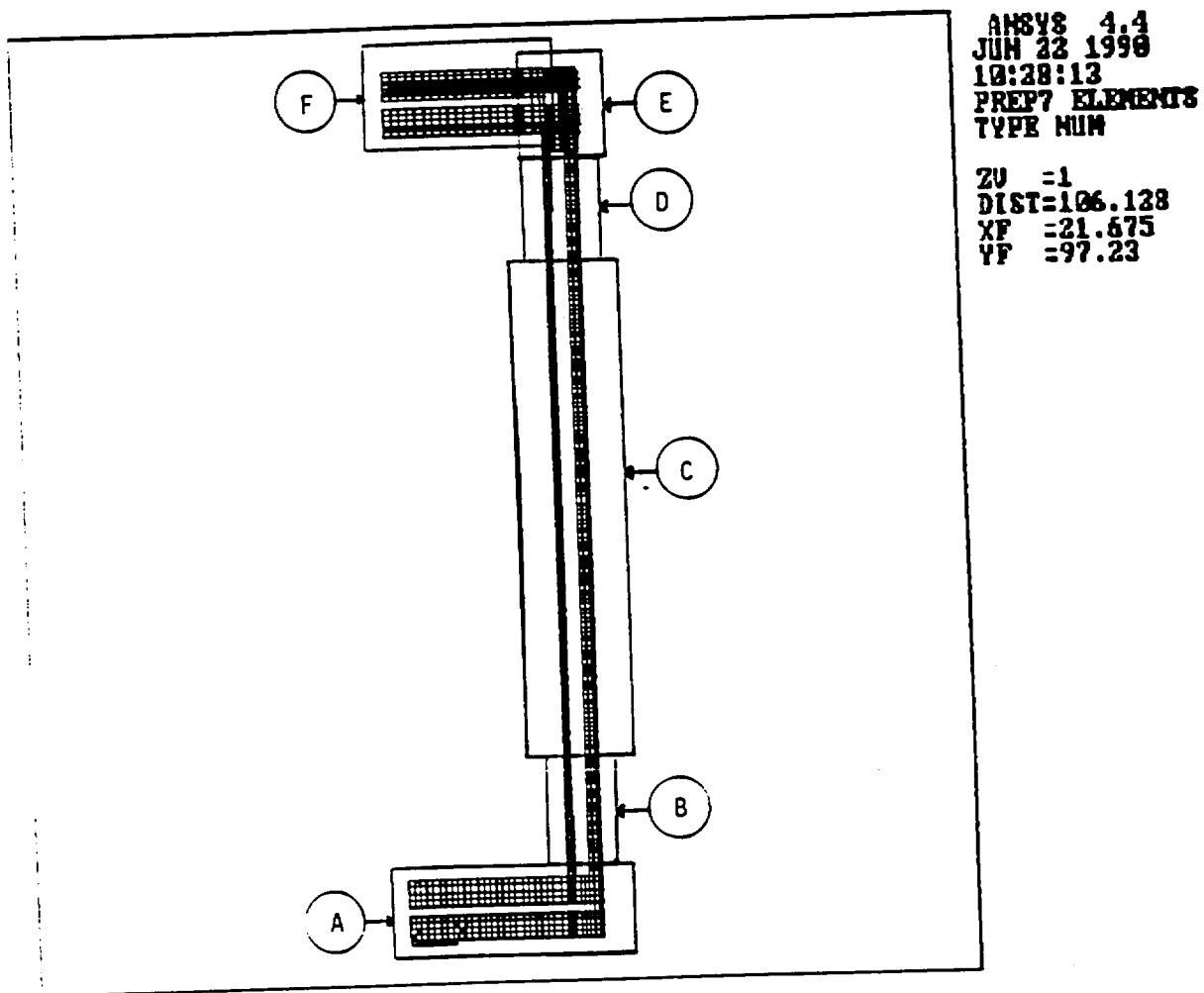


Figure 2.10.2-2 Cask Bottom (Region A) - NAC-STC ANSYS Two-Dimensional Model

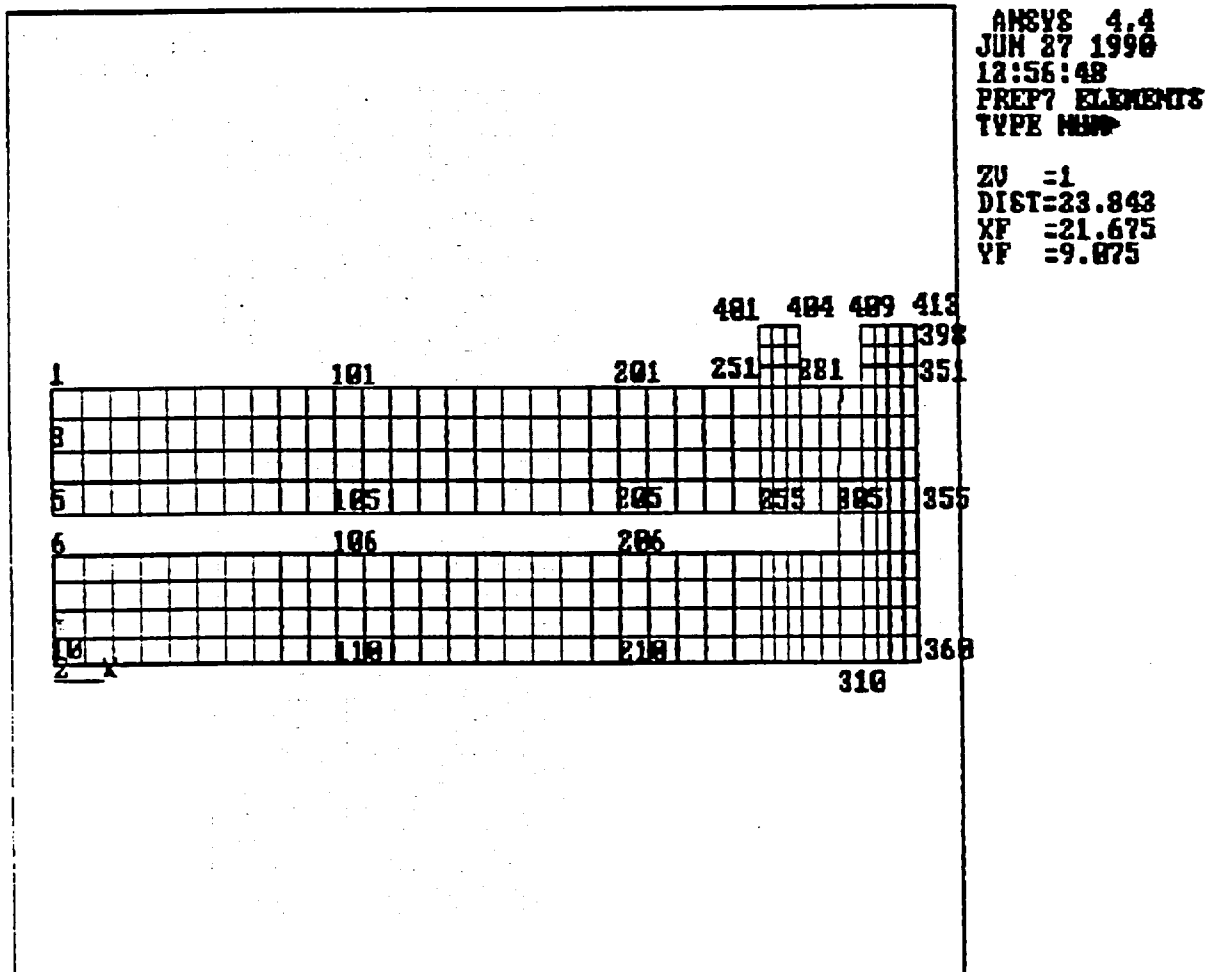


Figure 2.10.2-3 Cask Lower Transition (Region B) - NAC-STC ANSYS Two-Dimensional Model

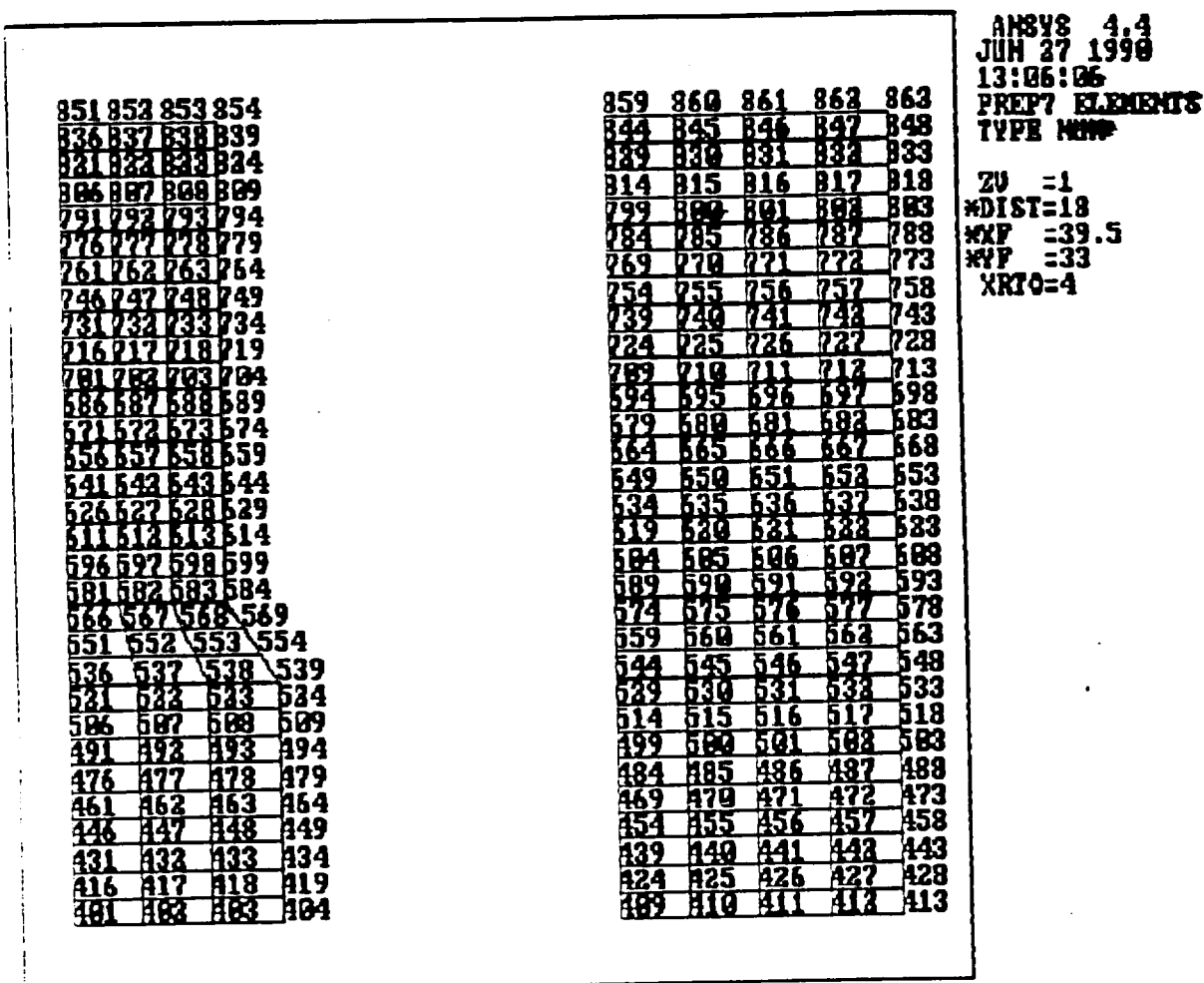


Figure 2.10.2-4 Cask Shells (Region C) - NAC-STC ANSYS Two-Dimensional Model

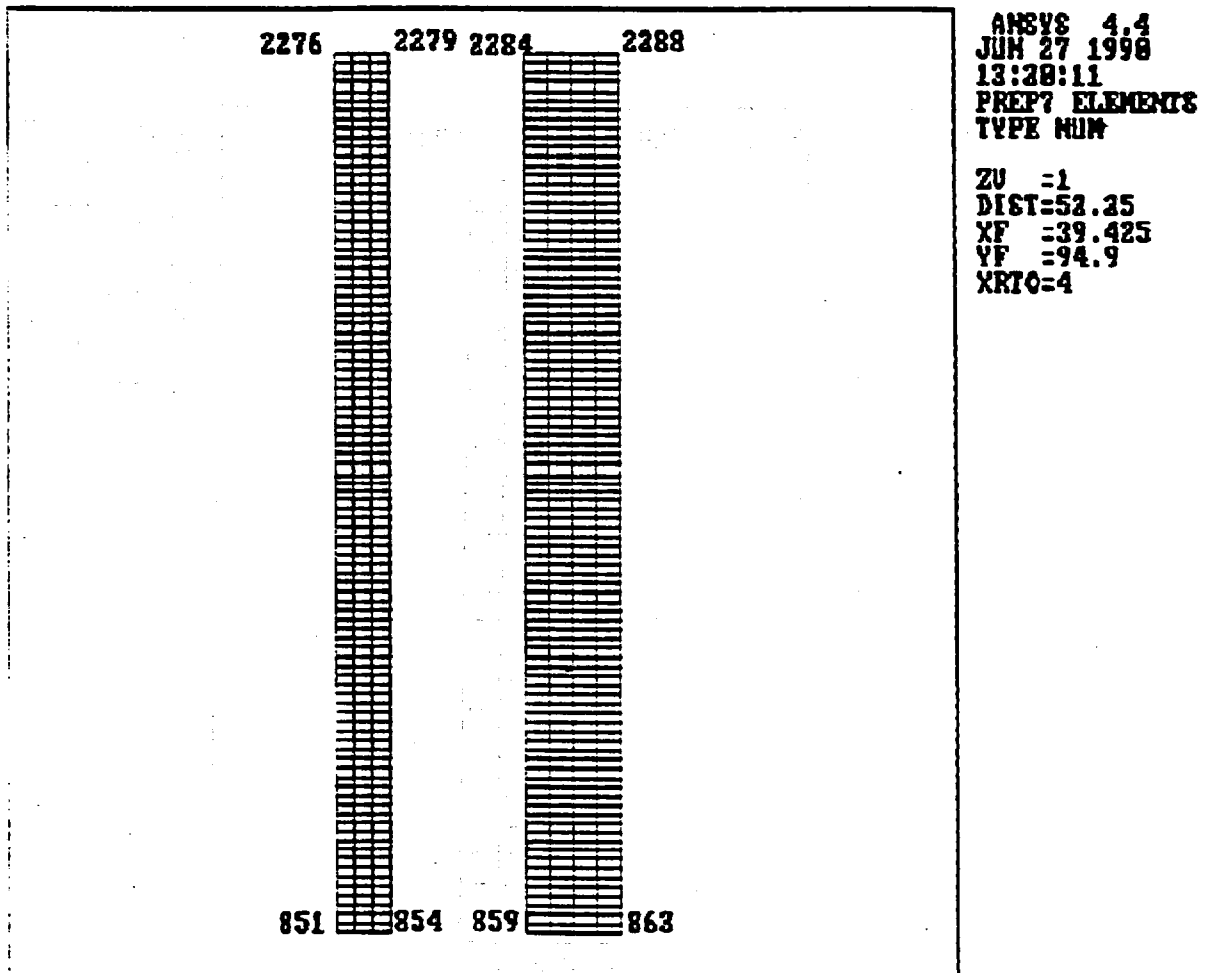


Figure 2.10.2-5 Cask Upper Transition (Region D) - NAC-STC ANSYS Two-Dimensional Model

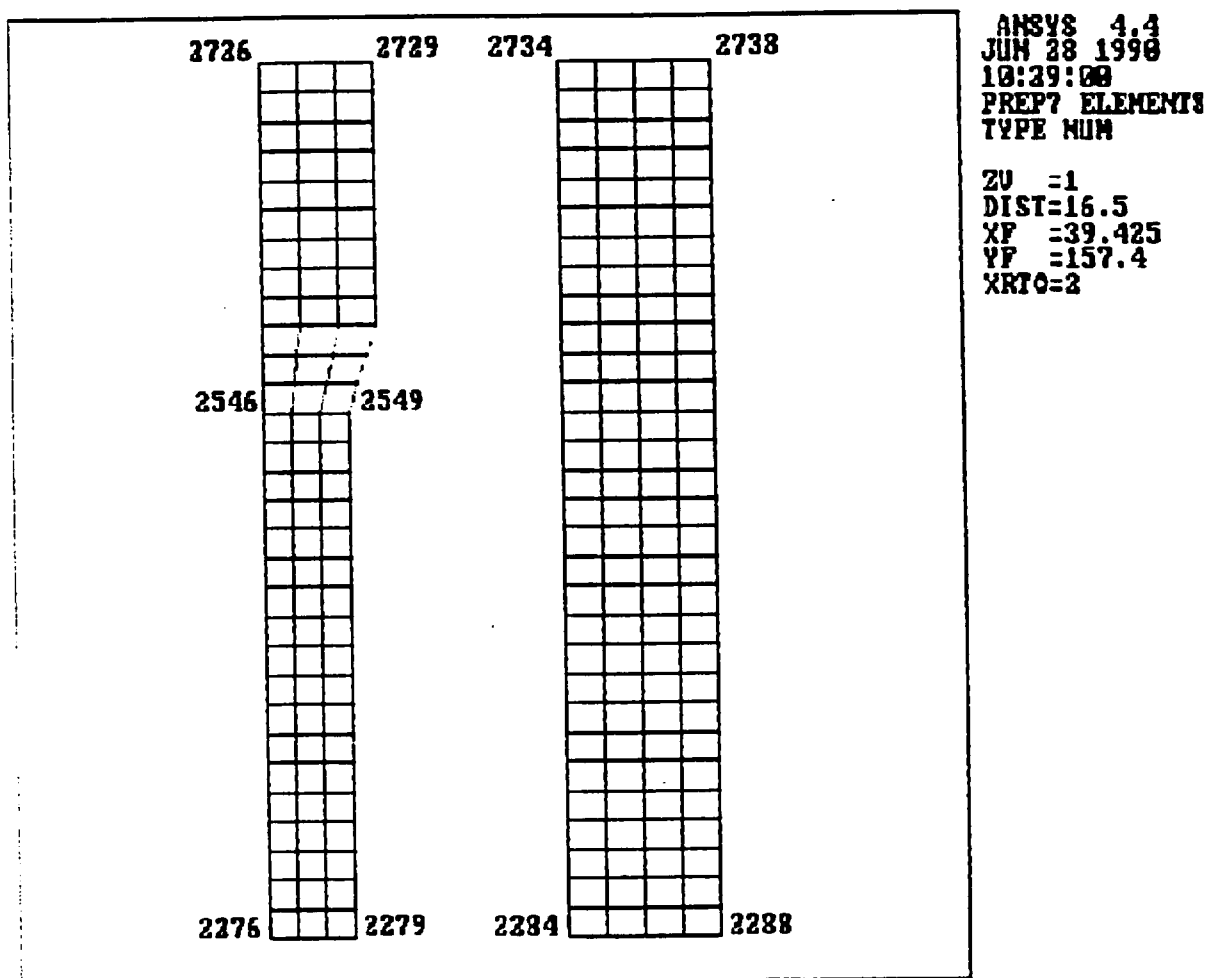


Figure 2.10.2-6 Cask Top Forging (Region E) - NAC-STC ANSYS Two-Dimensional Model

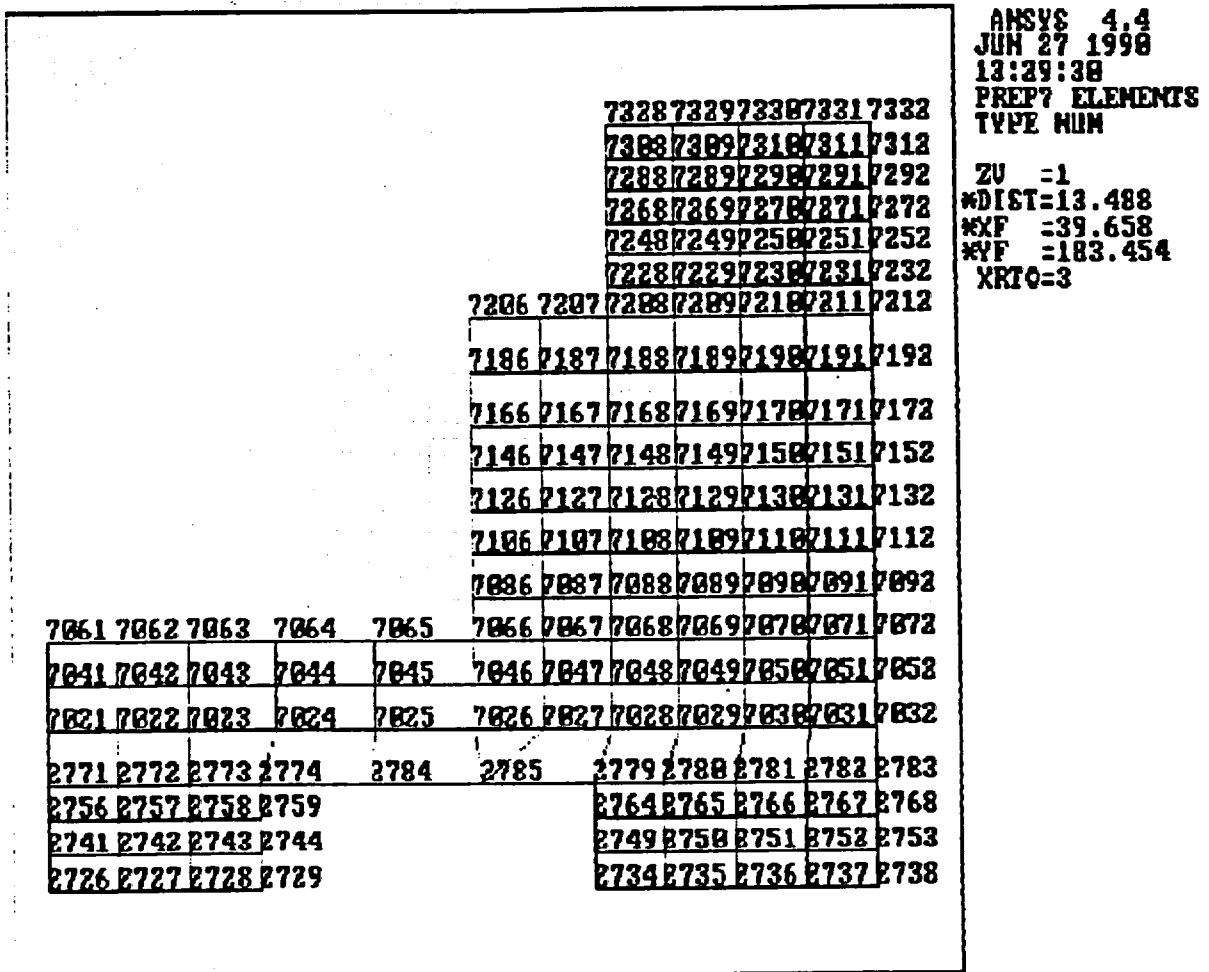


Figure 2.10.2-7 Cask Lids (Region F) - NAC-STC ANSYS Two-Dimensional Model

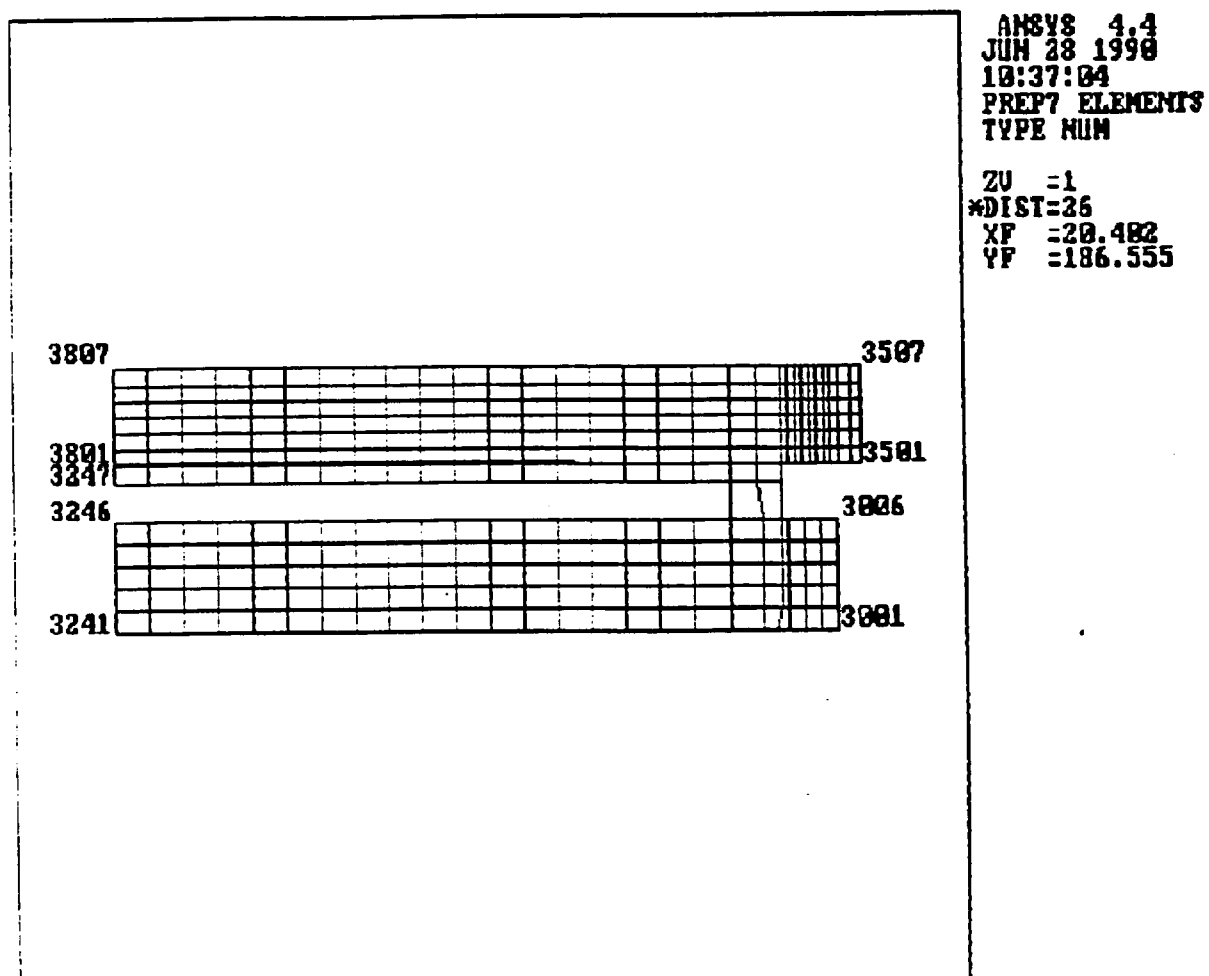




Figure 2.10.2-8      Circumferential Mesh Spacing (End View) - ANSYS Three-Dimensional  
Top and Bottom Fine Mesh Models

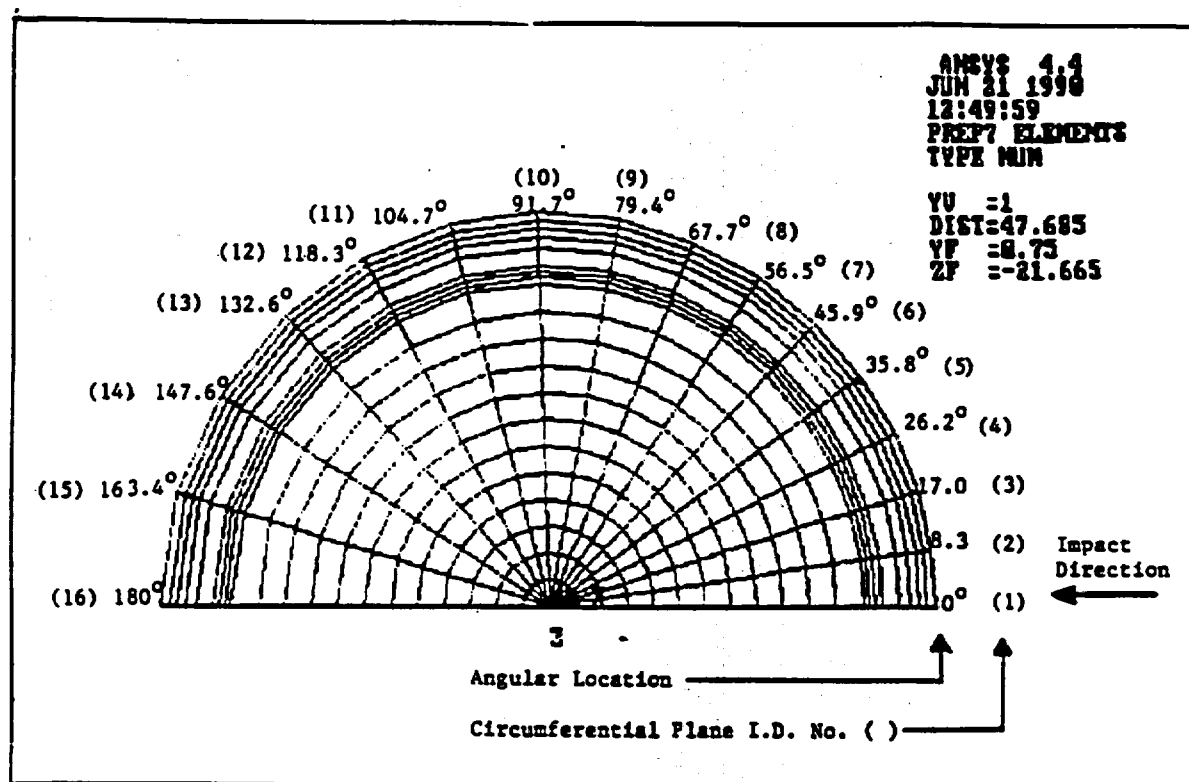


Figure 2.10.2-9 ANSYS Three-Dimensional Bottom Fine Mesh Finite Element Model -  
NAC-STC

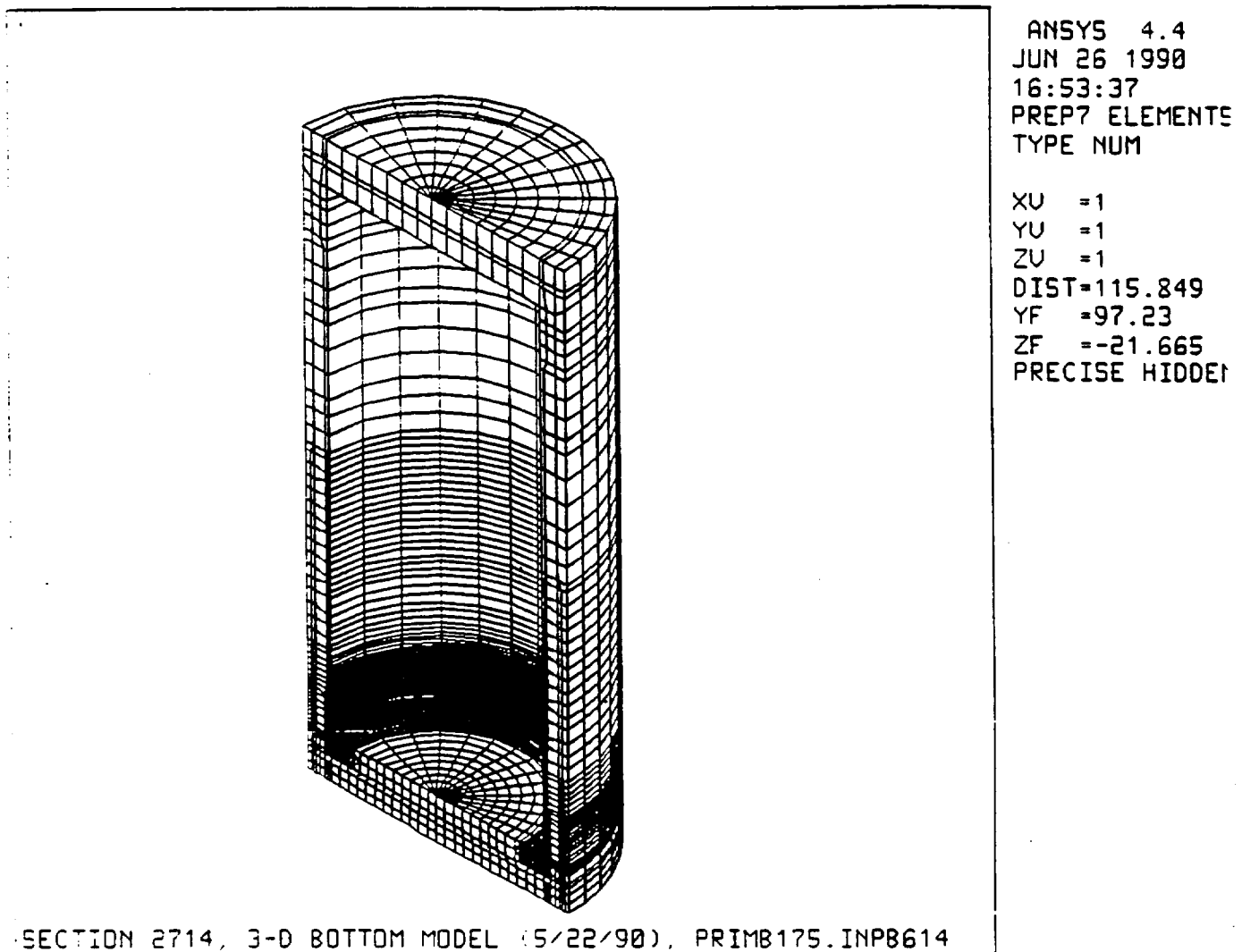
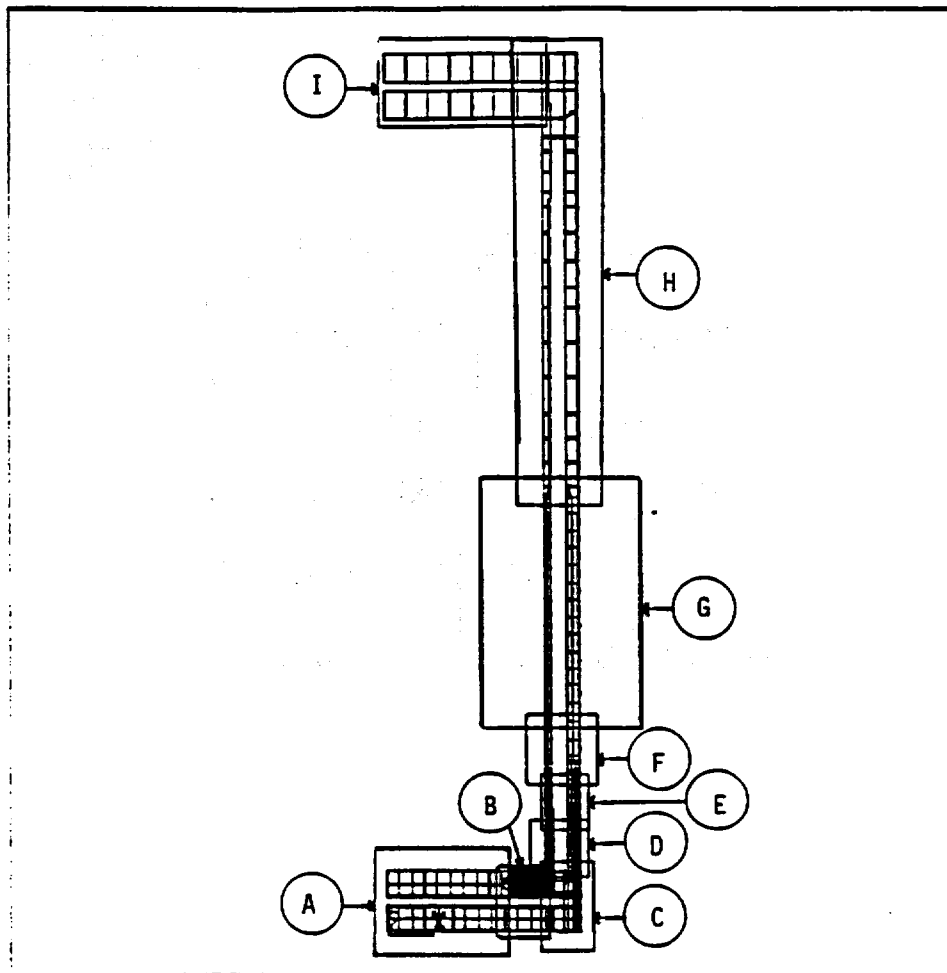


Figure 2.10.2-10 Details - NAC-STC ANSYS Three-Dimensional Bottom Fine Mesh Model



ANSYS 4.4  
JUN 21 1998  
12:16:08  
PREP7 ELEMENTS  
TYPE NUM  
  
ZU =1  
DIST=106.128  
XF =21.675  
YF =97.23

Figure 2.10.2-11 Cask Bottom (Region A) - NAC-STC ANSYS Bottom Fine Mesh Three-Dimensional Model

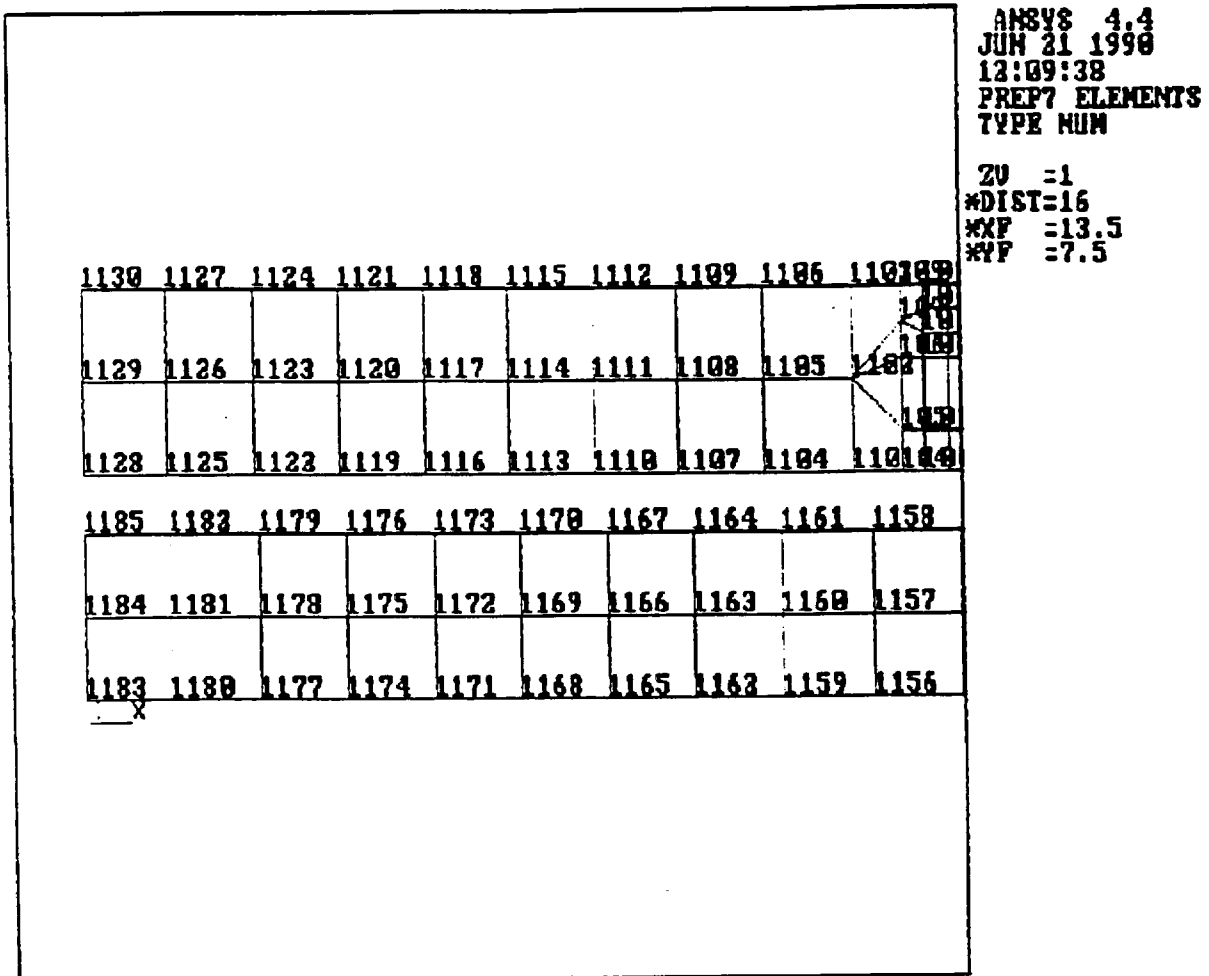


Figure 2.10.2-12 Cask Bottom (Region B) - NAC-STC ANSYS Bottom Fine Mesh Three-Dimensional Model

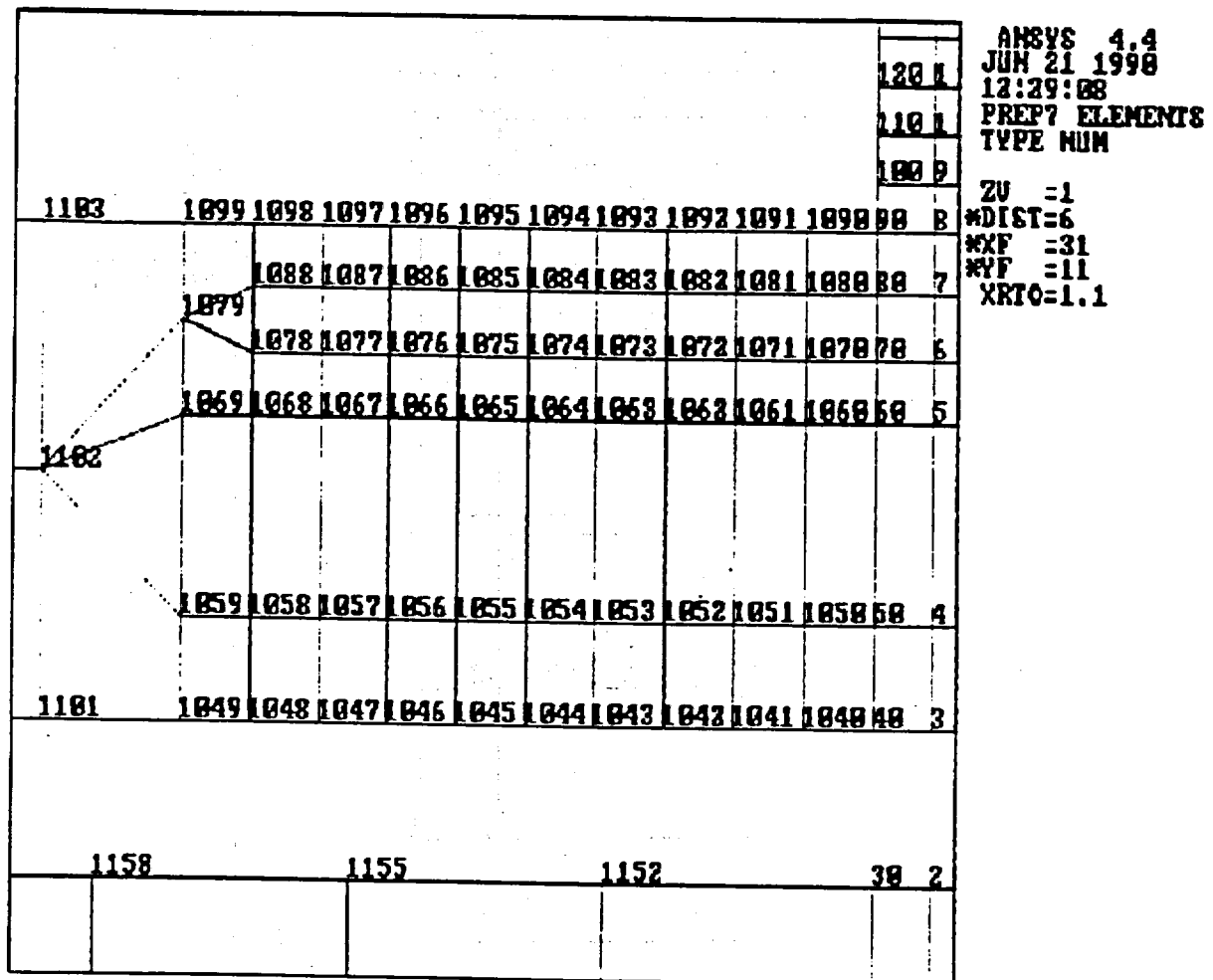


Figure 2.10.2-13 Cask Bottom (Region C) - NAC-STC ANSYS Bottom Fine Mesh Three-Dimensional Model

110	109	108	107					
100	99	98	97		84	83	82	81
109080	89	88	87	85	84	83	82	81
108080	79	78	77	75	74	73	72	71
107080	69	68	67	65	64	63	62	61
106080	59	58	57	55	54	53	52	51
105050	49	48	47	45	44	43	42	41
104040	39	38	37	35	34	33	32	31
30	29	28	27	25	24	23	22	21
20	19	18	17	15	14	13	12	11
10	9	8	7	5	4	3	2	1

ANSYS 4.4  
JUN 27 1990  
12:16:34  
PREP7 ELEMENTS  
TYPE NUM  
  
ZU =1  
\*DIST=6  
\*XF =40  
\*YF =7.5  
XRT0=1.1  
YRT0=8.7

Figure 2.10.2-14 Cask Lower Transition (Region D) - NAC-STC ANSYS Bottom Fine Mesh Three-Dimensional Model

210	209	208	207			154	153	152	151
200	199	198	197						
190	189	188	187			144	143	142	141
180	179	178	177						
170	169	168	167			134	133	132	131
160	159	158	157						
150	149	148	147						
140	139	138	137			114	113	112	111
130	129	128	127						
120	119	118	117			104	103	102	101
110	109	108	107						
100	99	98	97			94	93	92	91
1091	1090	89	88	87	85	84	83	82	81
1081	1080	79	78	77	75	74	73	72	71
1071	1070	69	68	67	65	64	63	62	61
1061	1060	59	58	57	55	54	53	52	51

ANSYS 4.4  
JUN 21 1990  
12:36:20  
PREP7 ELEMENTS  
TYPE NUM  
  
ZU =1  
\*DIST=6  
\*XF =39  
\*YF =17  
\*RT0=1.1

Figure 2.10.2-15 Cask Lower Transition (Region E) - NAC-STC ANSYS Bottom Fine Mesh Three-Dimensional Model

410009100107								ANSYS 4.4
400099098397								JUN 21 1990
390089088087	264	263	262	261				12:43:31
380079078377								PREP7 ELEMENTS
370069068067								TYPE NUM
360059058357	254	253	252	251				ZU =1
350049048047								*DIST=6
340039038337								*XF =39
330029028027	244	243	242	241				*YF =28
320019018317	234	233	232	231				XRT0=1.2
310009008007								
300009000007	224	223	222	221				
290009000007	214	213	212	211				
280009000007	204	203	202	201				
270009000007	194	193	192	191				
260009000007	184	183	182	181				
250009000007	174	173	172	171				
240009000007	164	163	162	161				
230009000007	154	153	152	151				



Figure 2.10.2-16 Cask Lower Shell (Region F) - NAC-STC ANSYS Bottom Fine Mesh Three-Dimensional Model

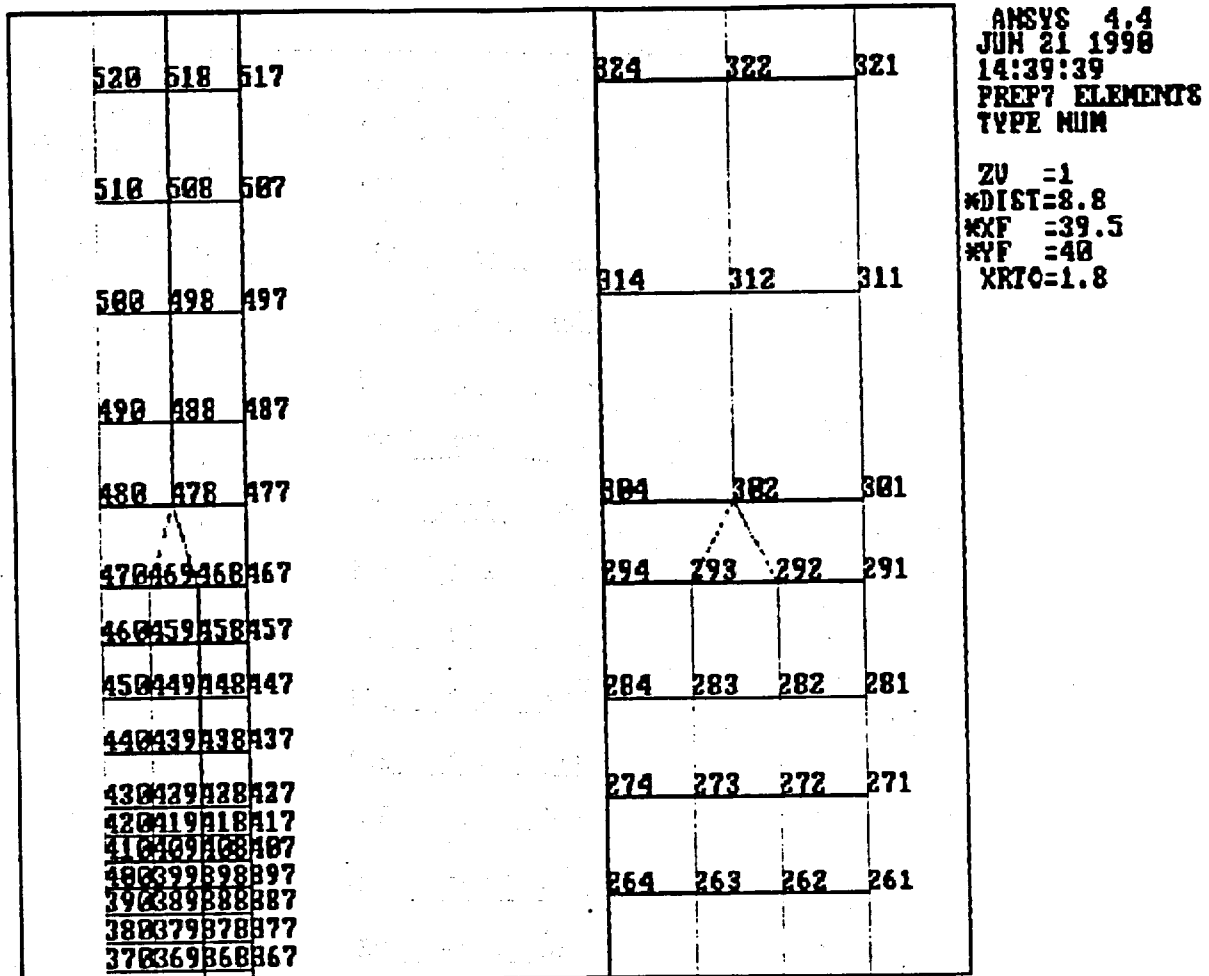


Figure 2.10.2-17 Cask Lower Shell (Region G) - NAC-STC ANSYS Bottom Fine Mesh  
Three-Dimensional Model

750	747	464	461	ANSYS 4.4 JUN 21 1990 14:45:33 PREP7 ELEMENTS TYPE NUM  ZU =1 *DIST=29 *XP =39.5 *YP =73 XRT0=4.5
740	738	454	452	
730	728			
720	718	444	442	
710	708			
700	698	434	432	
690	688			
680	678	424	422	
670	668			
660	658	414	412	
650	648			
640	638	404	402	
630	628			
620	618	394	392	
610	608			
600	598	384	382	
590	588			
580	578	374	372	
570	568			
560	558	364	362	
550	548			
540	538	354	352	
530	528			
520	518	344	342	
510	508			
		334	332	
		324	322	

Figure 2.10.2-18 Cask Upper Shell (Region H) - NAC-STC ANSYS Bottom Fine Mesh  
Three-Dimensional Model

1240	930	927	644	641
1230	820	817	534	531
1220	810	807	524	521
1210	800	897	514	511
	890	887	504	501
	880	877	594	591
	870	867	584	581
	860	857	574	571
	850	847	564	561
	840	837	554	551
	830	827	544	541
	820	817	534	531
	810	807	524	521
	800	797	514	511
	790	787	504	501
	780	777	494	491
	770	767	484	481
	760	757	474	471
	750	747	464	461
	740	737	454	451

ANSYS 4.4  
JUN 21 1998  
14:53:49  
PREP7 ELEMENTS  
TYPE NUM

ZU =1  
WDIST=51  
MXF =38.8  
MYF =146.5  
XR10=4.5

Figure 2.10.2-19 Cask Lids (Region I) - NAC-STC ANSYS Bottom Fine Mesh Three-Dimensional Model

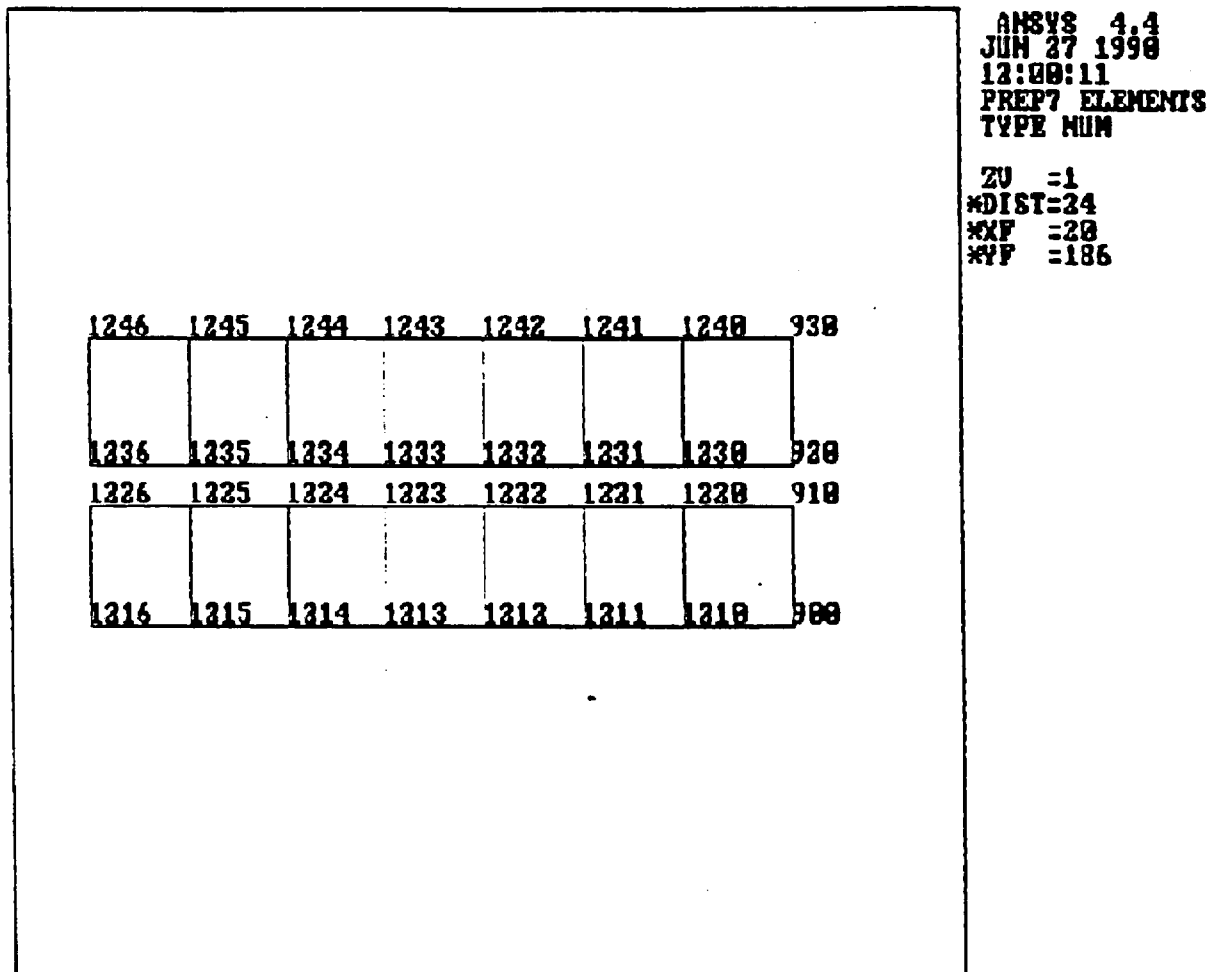


Figure 2.10.2-20 ANSYS Three-Dimensional Top Fine Mesh Finite Element Model - NAC-STC

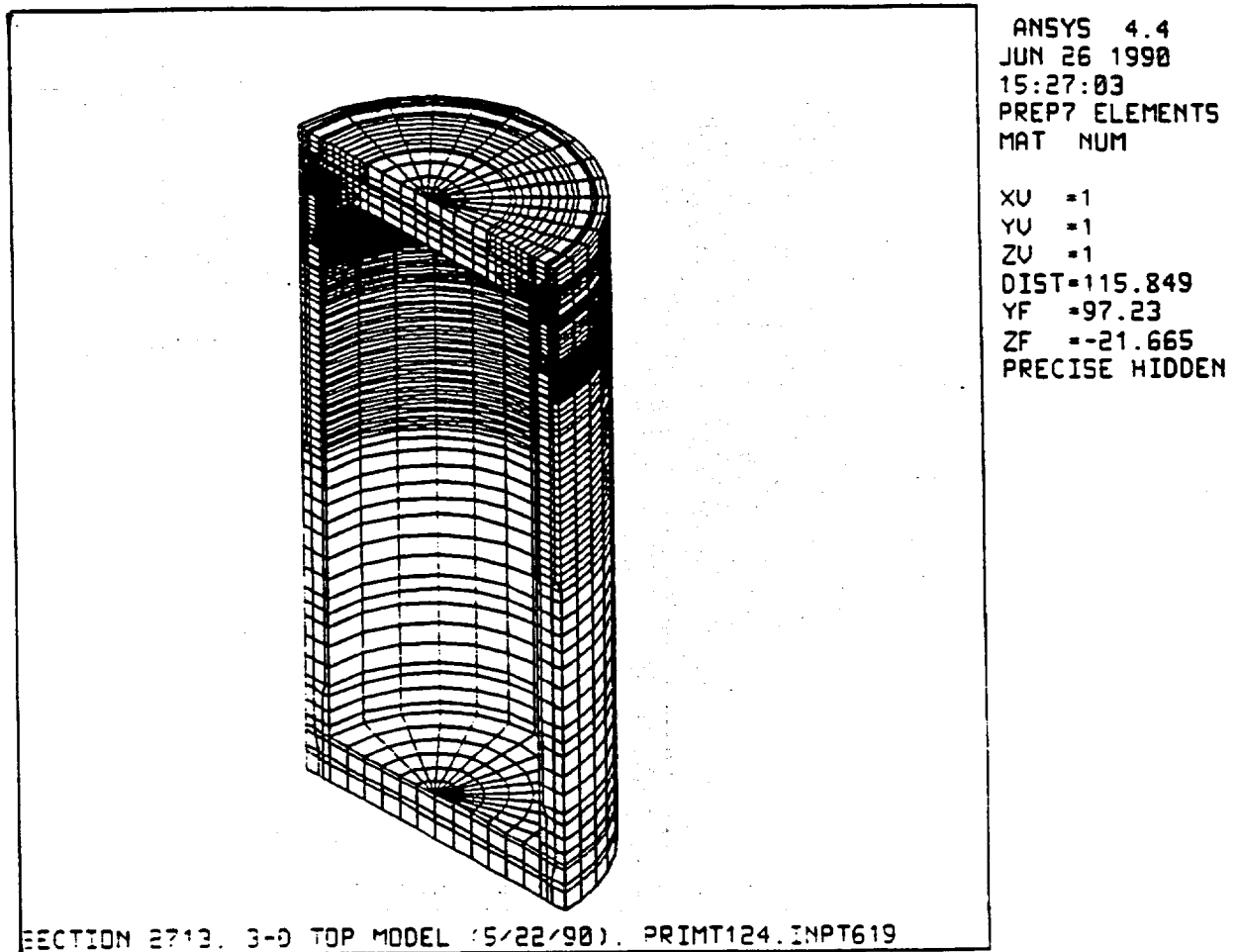


Figure 2.10.2-21 Upper Half of NAC-STC ANSYS Three-Dimensional Top Fine Mesh  
Finite Element Model

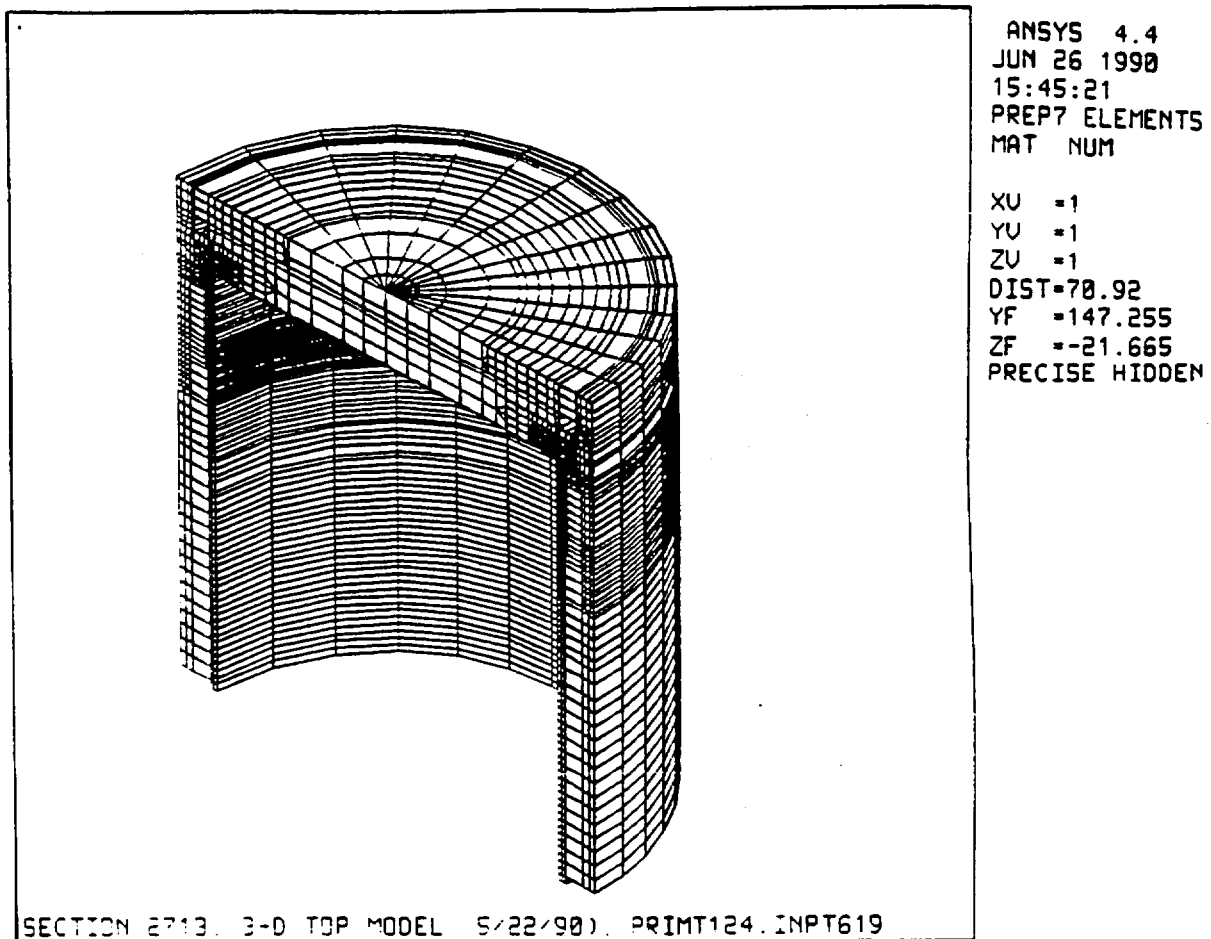


Figure 2.10.2-22 Details - NAC-STC ANSYS Three-Dimensional Top Fine Mesh Model

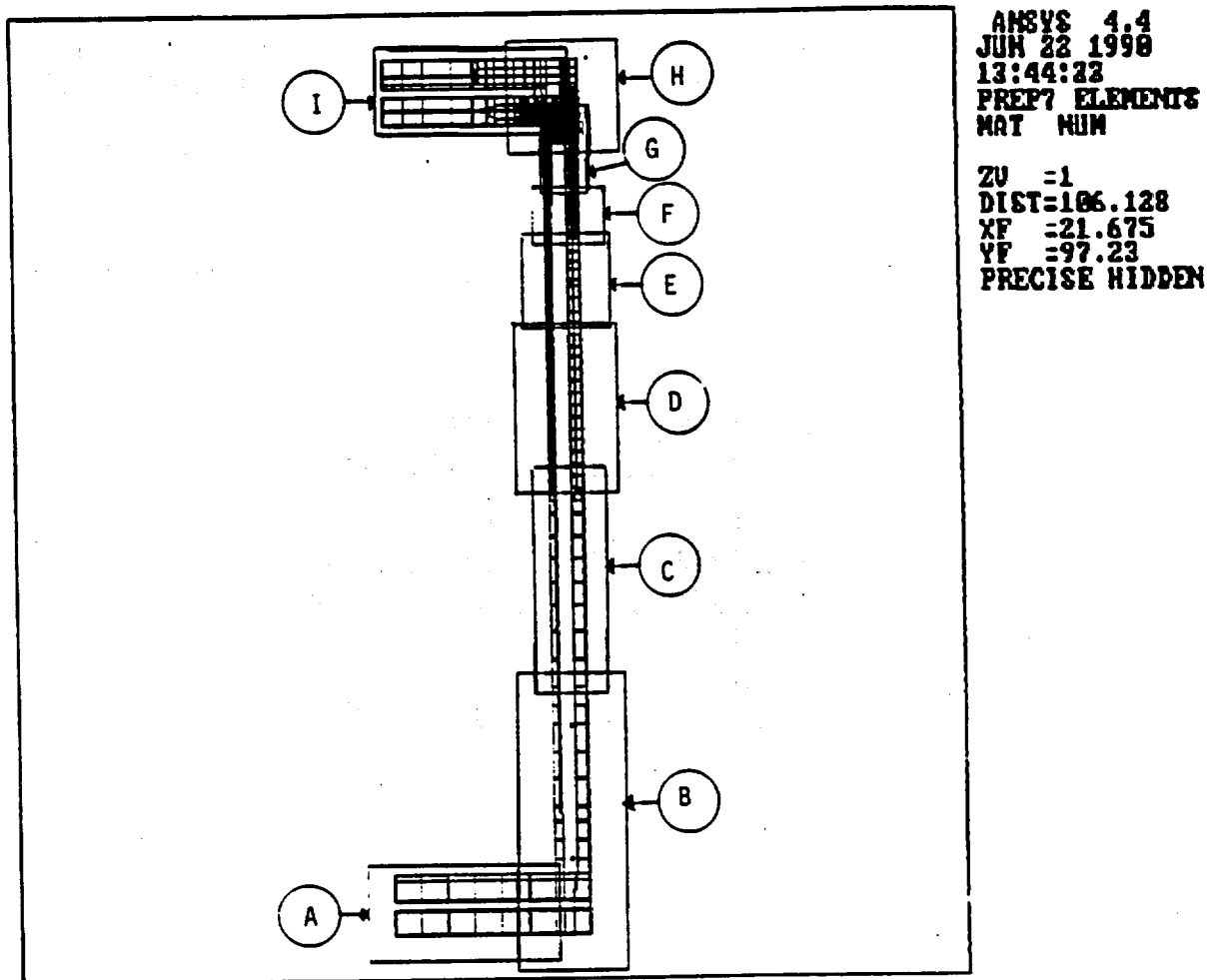


Figure 2.10.2-23 Cask Bottom (Region A) - NAC-STC ANSYS Top Fine Mesh Three-Dimensional Model

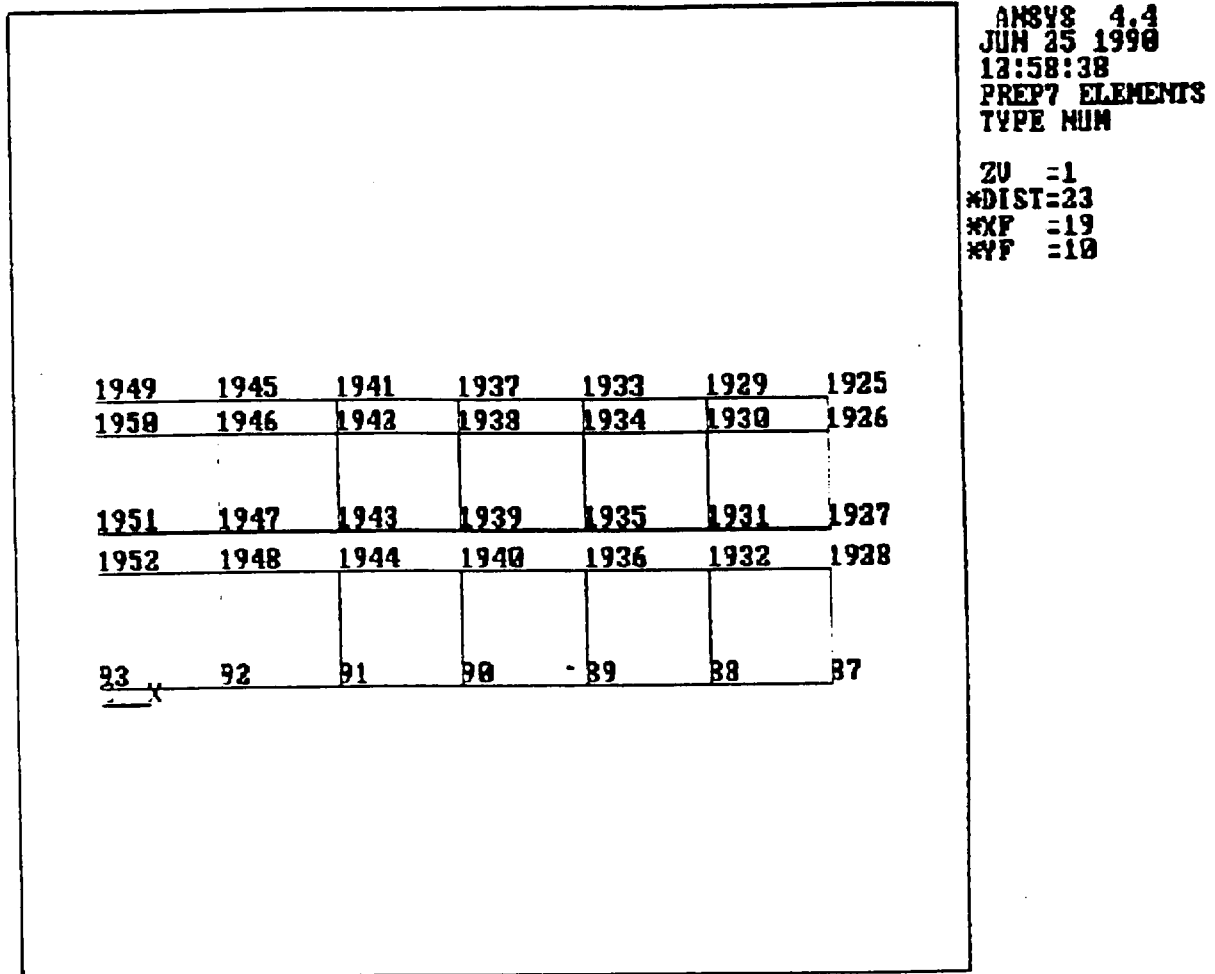




Figure 2.10.2-24 Cask Lower Transition (Region B) - NAC-STC ANSYS Top Fine Mesh  
Three-Dimensional Model

					ANSYS 4.4
					JUN 23 1998
					12:07:32
					PREP7 ELEMENTS
					TYPE NUM
					ZU =1
					*DIST=30
					*XF =38
					*YF =29
					XRT0=3
	1916	1316	671	71	
	1917	1317	672	72	
	1918	1318	673	73	
	1919	1319	674	74	
	1920	1320	675	75	
	1921	1321	676	76	
	1922	1322	677	77	
	1923	1323	678	78	
	1924	1324	679	79	
1929	1925	1325	680	80	
1930	1926	1326	681	81	
1931	1927	1327	682	82	
1932	1928	1328	683	83	
88	87	86	85	84	

Figure 2.10.2-25 Cask Lower Shell (Region C) - NAC-STC ANSYS Top Fine Mesh Three-Dimensional Model

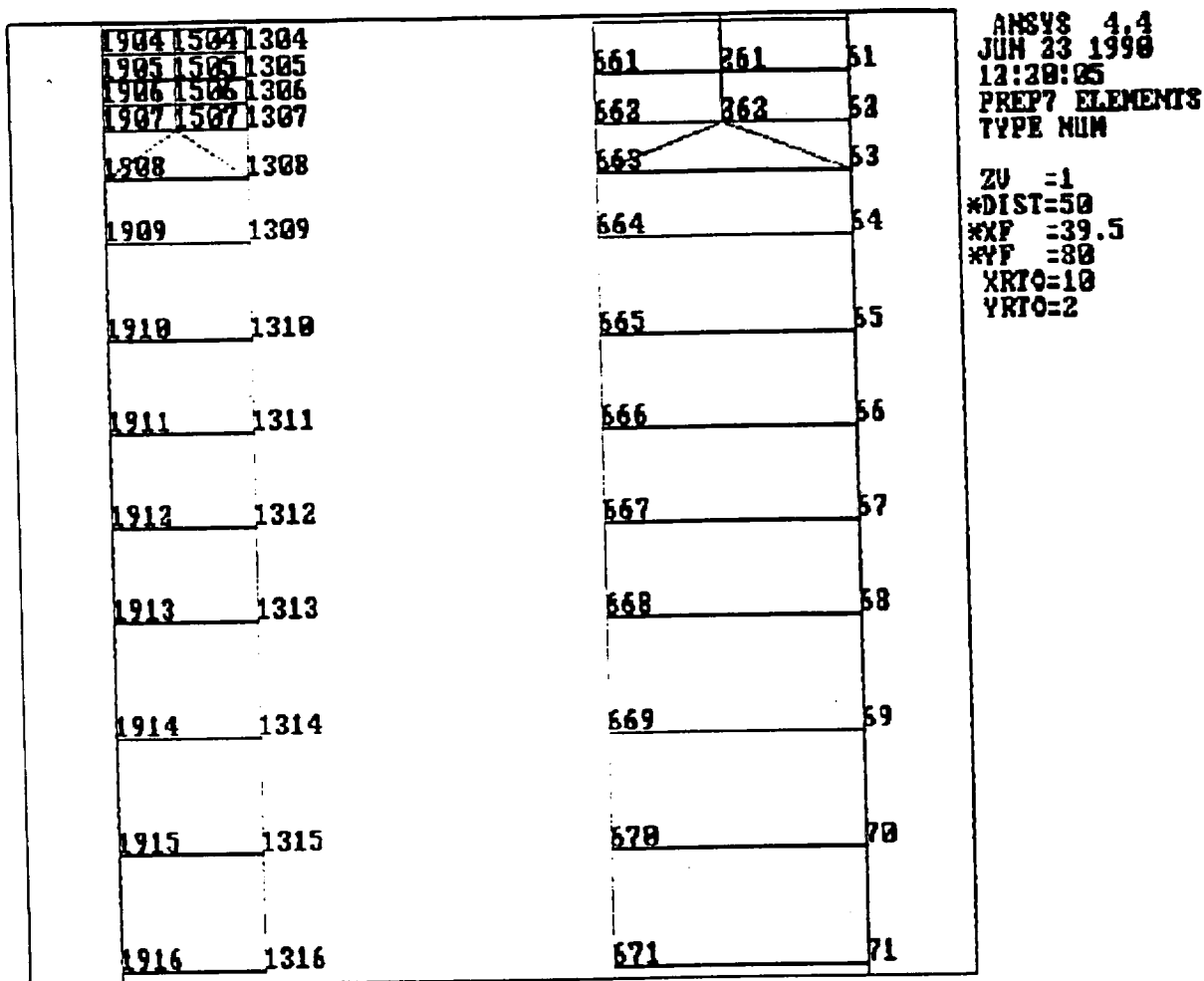


Figure 2.10.2-26 Cask Middle Shell (Region D) - NAC-STC ANSYS Top Fine Mesh  
Three-Dimensional Model

1876 1476 1276	647	247	47	ANSYS 4.4 JUN 23 1998 12:26:52 PREP7 ELEMENTS TYPE NUM  ZU =1 *DIST=50 *XF =39.5 *YF =120 XRT0=10 YRT0=2.4
1877 1477 1277	648	248	48	
1878 1478 1278	649	249	49	
1879 1479 1279	650	250	50	
1880 1480 1280	651	251	51	
1881 1481 1281	652	252	52	
1882 1482 1282	653	253	53	
1883 1483 1283	654	254	54	
1884 1484 1284	655	255	55	
1885 1485 1285	656	256	56	
1886 1486 1286	657	257	57	
1887 1487 1287	658	258	58	
1888 1488 1288	659	259	59	
1889 1489 1289	660	260	60	
1890 1490 1290	661	261	61	
1891 1491 1291	662	262	62	
1892 1492 1292				
1893 1493 1293				
1894 1494 1294				
1895 1495 1295				
1896 1496 1296				
1897 1497 1297				
1898 1498 1298				
1899 1499 1299				
1900 1500 1300				
1901 1501 1301				
1902 1502 1302				
1903 1503 1303				
1904 1504 1304				
1905 1505 1305				
1906 1506 1306				
1907 1507 1307				

Figure 2.10.2-27 Cask Upper Shell (Region E) - NAC-STC ANSYS Top Fine Mesh Three-Dimensional Model

1851 1651 1451 1251	534	334	234	34	ANSYS 4.4 JUN 25 1990 13:03:07 PREP7 ELEMENTS TYPE NUM  ZU =1 *DIST=47 *XF =39.5 *YF =146 XRT0=10 YRT0=5
1852 1652 1452 1252	535	335		35	
1854 1454 1254					
1856 1456 1256					
1858 1458 1258	537	237		37	
1860 1460 1260					
1862 1462 1262	539	239		39	
1864 1464 1264					
1866 1466 1266	541	241		41	
1868 1468 1268					
1870 1470 1270	543	243		43	
1872 1472 1272					
1873 1473 1273	545	245		45	
1874 1474 1274					
1875 1475 1275	546	246		46	
1876 1476 1276					
1877 1477 1277	547	247		47	
1878 1478 1278					

Figure 2.10.2-28 Cask Upper Transition (Region F) - NAC-STC ANSYS Top Fine Mesh Three-Dimensional Model

1828	1628	1428	1228	522	422	322	22	ANSYS 4.4 JUN 23 1998 12:44:01 PREP7 ELEMENTS TYPE NUM  ZU =1 *DIST=50 *XF =39.5 *YF =168 XRT0=12.1 YRT0=7
1829	1629	1429	1229	523	423	323	23	
1830	1630	1430	1230	524	424	224	24	
1831	1631	1431	1231	525	425	225	25	
1832	1632	1432	1232	526	426	226	26	
1833	1633	1433	1233	527	427	227	27	
1834	1634	1434	1234	528	428	228	28	
1835	1635	1435	1235	529	429	229	29	
1836	1636	1436	1236	530	430	230	30	
1837	1637	1437	1237	531	431	231	31	
1838	1638	1438	1238	532	432	232	32	
1839	1639	1439	1239	533	433	233	33	
1840	1640	1440	1240	534	434	234	34	
1841	1641	1441	1241	535	435	235	35	
1842	1642	1442	1242					
1843	1643	1443	1243					
1844	1644	1444	1244					
1845	1645	1445	1245					
1846	1646	1446	1246					
1847	1647	1447	1247					
1848	1648	1448	1248					
1849	1649	1449	1249					
1850	1650	1450	1250					
1851	1651	1451	1251					
1852	1652	1452	1252					
1853	1653	1453	1253					
1854	1654	1454	1254					

Figure 2.10.2-29 Cask Upper Transition (Region G) - NAC-STC ANSYS Top Fine Mesh Three-Dimensional Model

										ANSYS 4.4
										JUN 23 1990
										12:57:01
										PREP7 ELEMENTS
										TYPE NUM
										ZU =1
										*DIST=50
										*XF =39.5
										*YF =175
										XRT0=11
										YRT0=5
					808	608	408	208	8	
					809	609	409	209	9	
					810	610	410	210	10	
1811	1611	1411	1211	1011	811	611	411	211	11	
1812	1612	1412	1212	1012	812	612	412	212	12	
1813	1613	1413	1213	1013	813	613	413	213	13	
1814	1614	1414	1214	1014	814	614	414	214	14	
1815	1615	1415	1215	1015	815	615	415	215	15	
1816	1616	1416	1216	1016	816	616	416	216	16	
1817	1617	1417	1217							
1818	1618	1418	1218			617	417	217	17	
1819	1619	1419	1219							
1820	1620	1420	1220			618	418	218	18	
1821	1621	1421	1221							
1822	1622	1422	1222			619	419	219	19	
1823	1623	1423	1223							
1824	1624	1424	1224			620	420	220	20	
1825	1625	1425	1225							
1826	1626	1426	1226			621	421	221	21	
1827	1627	1427	1227							
1828	1628	1428	1228			622	422	222	22	
1829	1629	1429	1229							
1830	1630	1430	1230			623	423	223	23	

Figure 2.10.2-30 Cask Top Forging (Region H) - NAC-STC ANSYS Top Fine Mesh Three-Dimensional Model

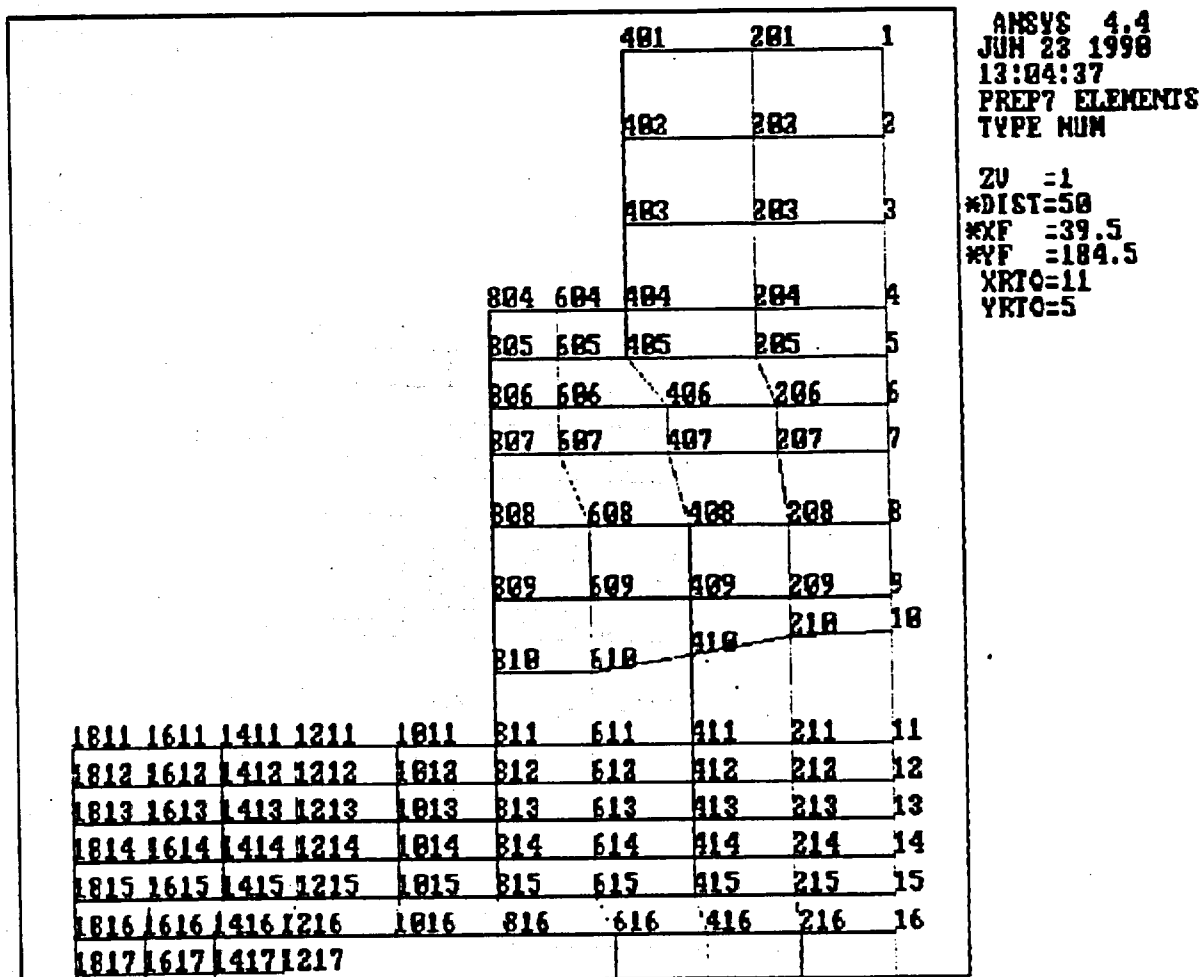


Figure 2.10.2-31 Cask Lids (Region I) - NAC-STC ANSYS Top Fine Mesh Three-Dimensional Model

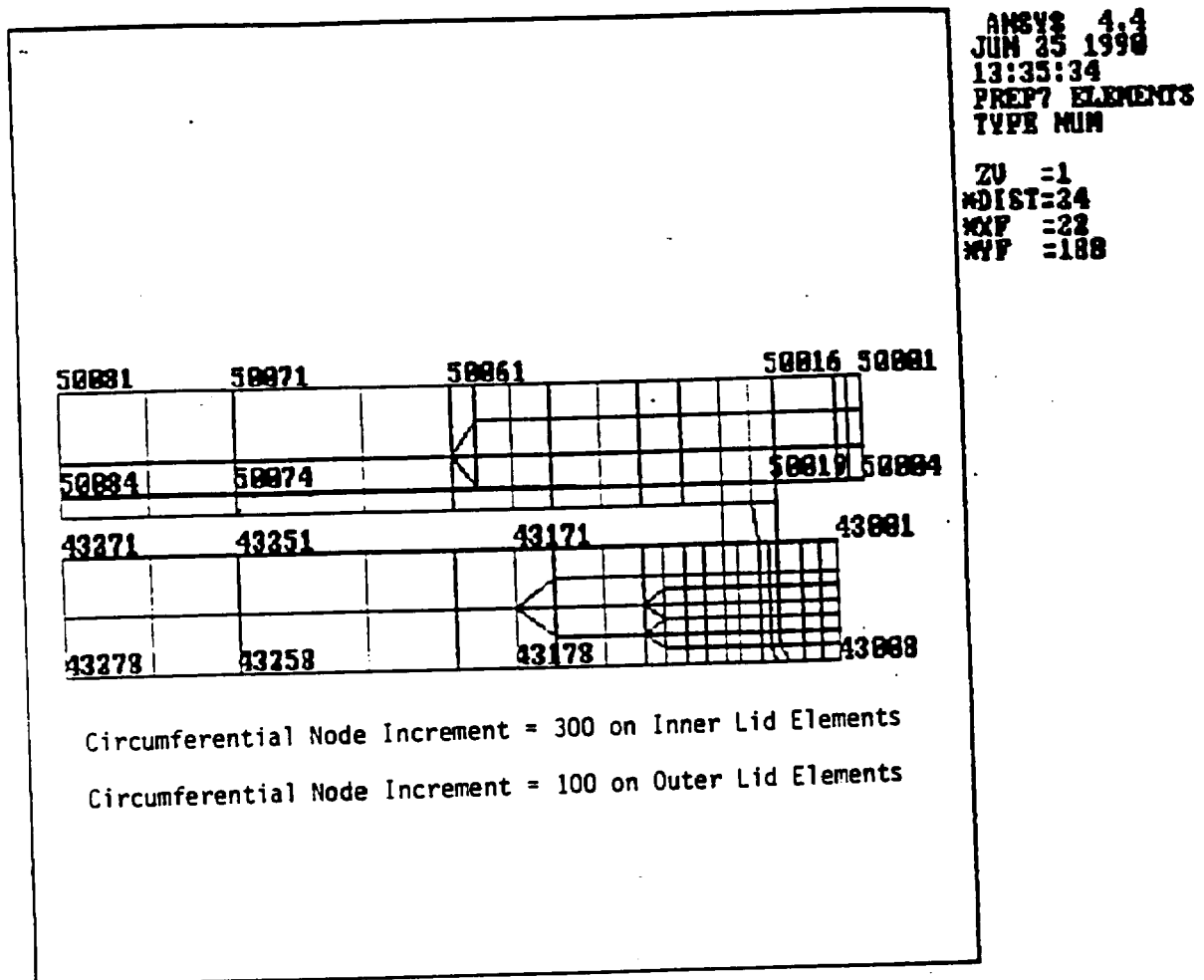




Figure 2.10.2-32 Load Distribution for Cask Side Drop Impact

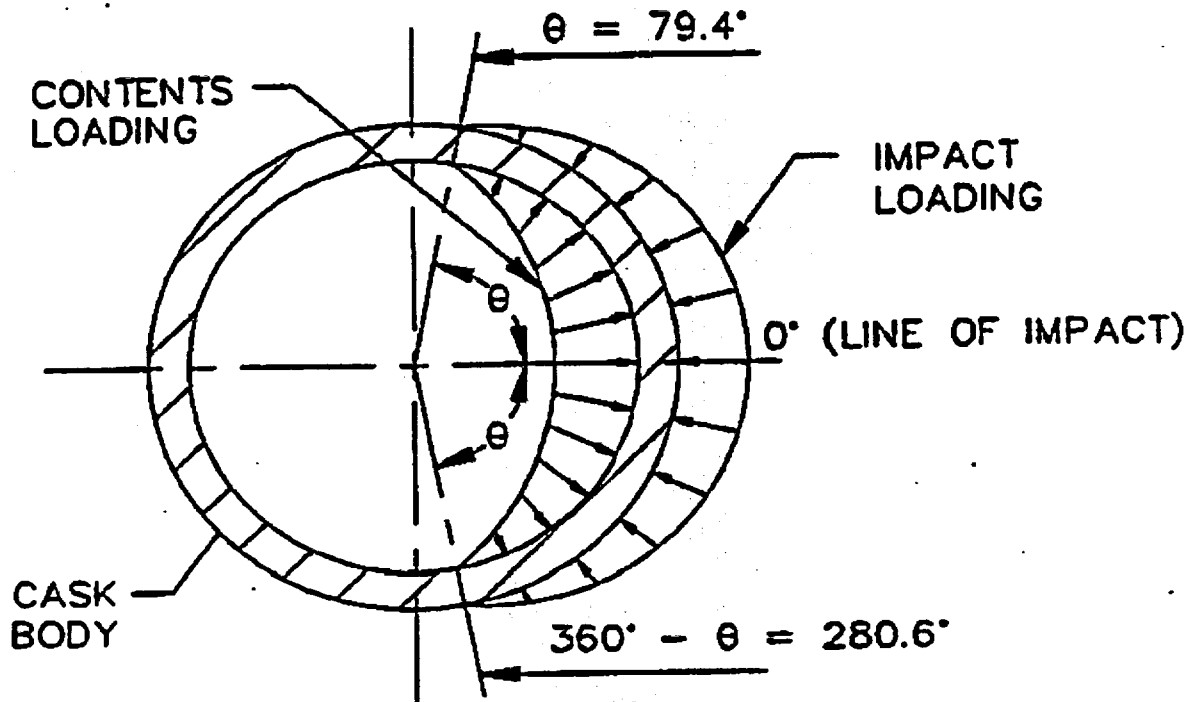
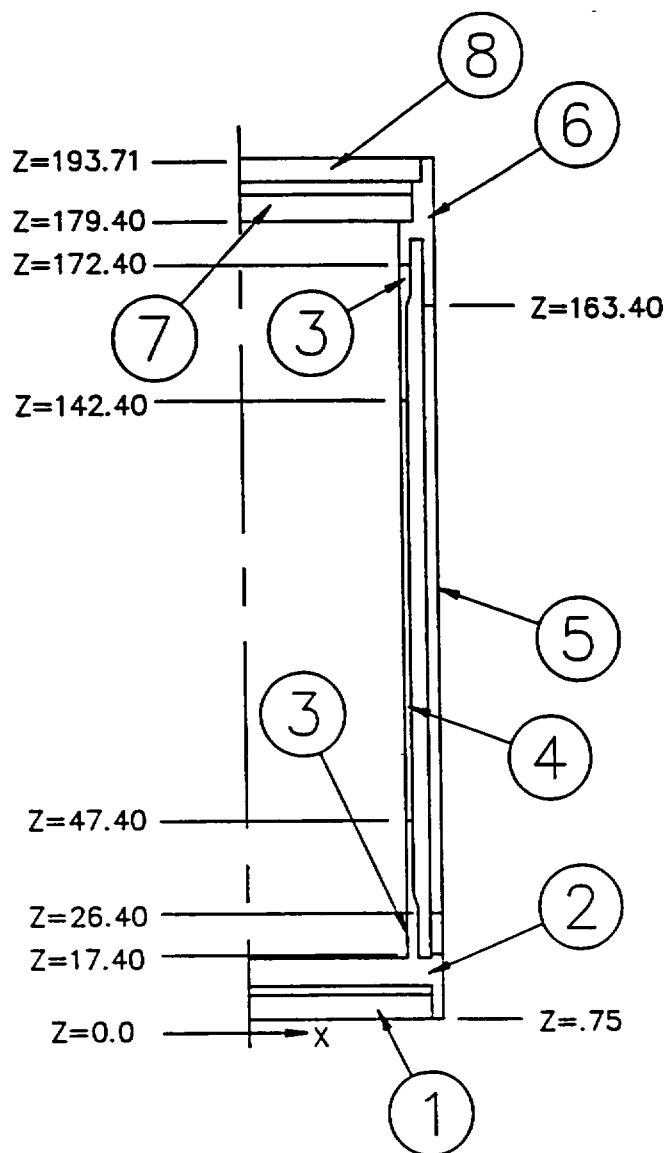


Figure 2.10.2-33 ANSYS Finite Element Model - Structural Component Identification



- 1 - Bottom Plate
- 2 - Bottom Forging and  
Bottom Ring Forging
- 3 - Transition Shell
- 4 - Inner Shell
- 5 - Outer Shell
- 6 - Top Forging
- 7 - Inner Lid
- 8 - Outer Lid

Figure 2.10.2-34 ANSYS Finite Element Model - Representative Section Locations

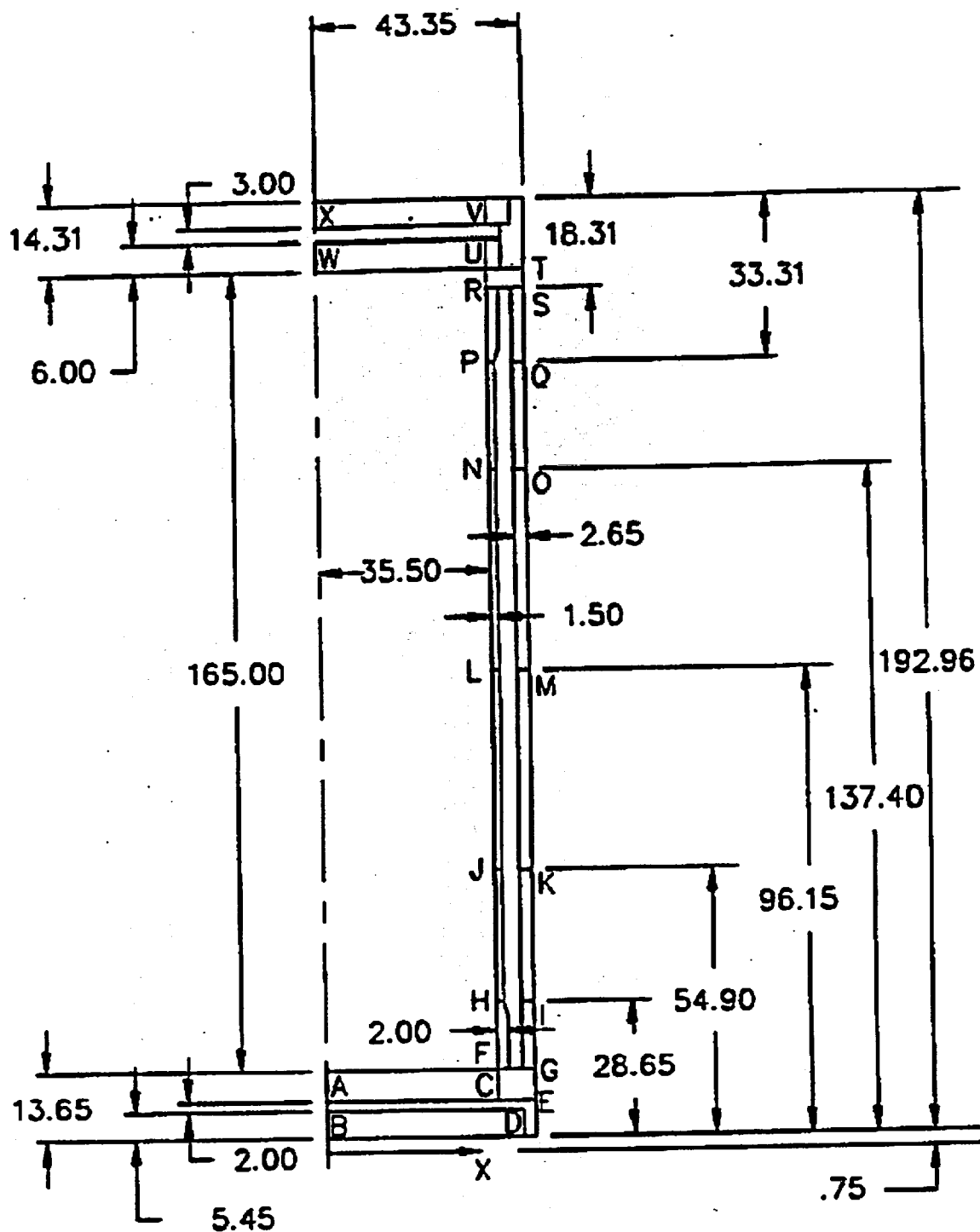
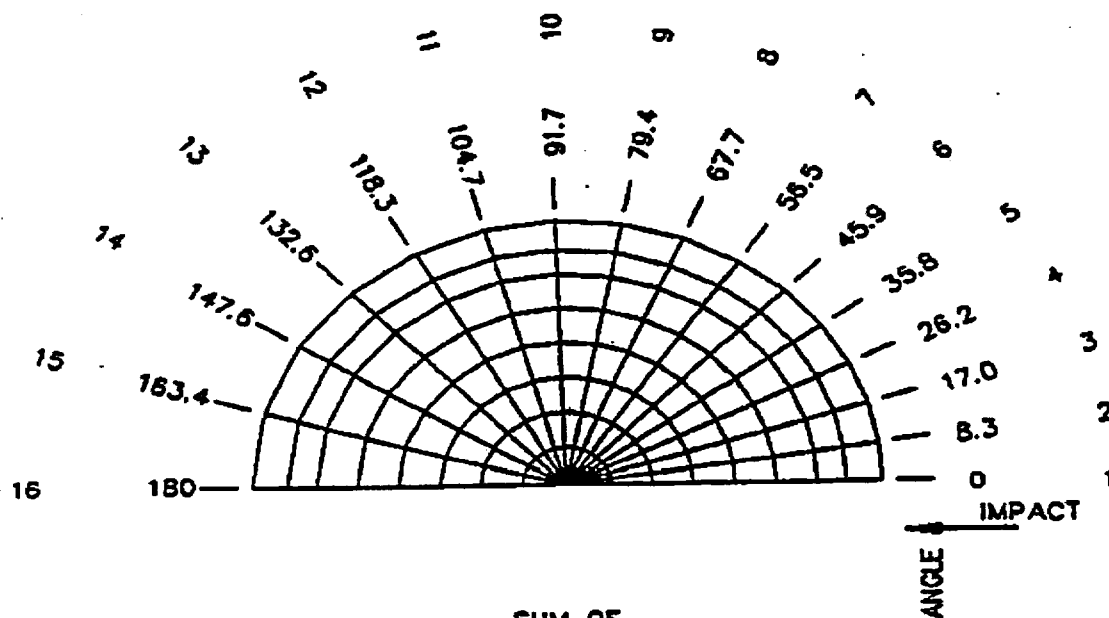
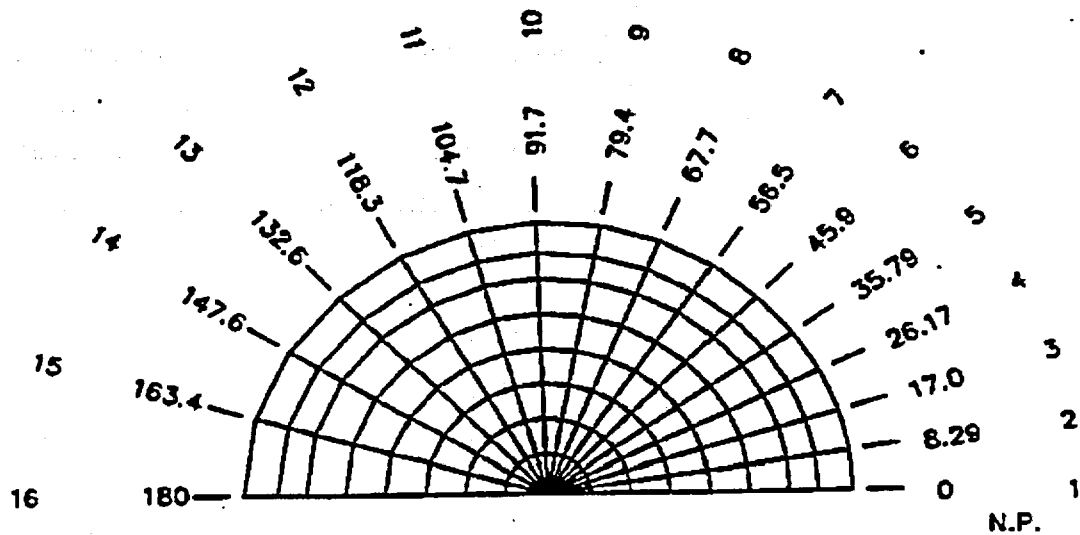


Figure 2.10.2-35 Circular Nodal Locations - NAC-STC ANSYS Three-Dimensional Model



<u>NODE LOCATION</u>	<u>SUM OF ADJACENT HALF ANGLES</u>	<u>CIRCUMFERENCE %</u>
1	4.2	2.33
2	8.5	4.72
3	9.0	5.00
4	9.4	5.22
5	9.9	5.50
6	10.4	5.77
7	10.9	6.05
8	11.5	6.39
9	12.0	6.67
10	12.7	7.06
11	13.3	7.38
12	14.0	7.78
13	14.7	8.17
14	15.4	8.56
15	16.2	9.00
16	8.3	4.61

Figure 2.10.2-36 Nodal Identification - NAC-STC ANSYS Three-Dimensional Model



<u>NODE LOCATION</u>	<u>ANGLE</u>	<u>NODES</u>
1	0	1-2000
2	8.29	2001-4000
3	17.0	4001-6000
4	26.17	6001-8000
5	35.79	8001-10000
6	45.9	10001-12000
7	56.5	12001-14000
8	67.7	14001-16000
9	79.4	16001-18000
10	91.7	18001-20000
11	104.7	20001-22000
12	118.3	22001-24000
13	132.6	24001-26000
14	147.6	26001-28000
15	163.4	28001-30000
16	180.0	30001-32000

Table 2.10.2-1      Tabulation of Circumferential Mesh Spacing - ANSYS Three-Dimensional Top and Bottom Fine Mesh Models

Circumferential Plane Identification Number	Angular Location $\theta$ (degrees)	Angular Spacing Increment (degrees)
1	0.0	---
2	8.3	8.3
3	17.0	8.7
4	26.2	9.2
5	35.8	9.6
6	45.9	10.1
7	56.5	10.6
8	67.7	11.2
9	79.4	11.7
10	91.7	12.3
11	104.7	13.0
12	118.3	13.6
13	132.6	14.3
14	147.6	15.0
15	163.4	15.8
16	180.0	16.6

Table 2.10.2-2 Circumferential Plane - Percentage of 180° Arc

Circumferential Plane Identification No.	Real Constant Numbers		Sum of Adjacent Half-Angles	Percentage of 180° Arc
	Inner <u>Bolts</u>	Outer <u>Bolts</u>		
1	14	31	$(1/2)(8.3) = 4.2$	0.0233
2	15	32	$(1/2)(8.3 + 8.7) = 8.5$	0.0472
3	16	33	$(1/2)(8.7 + 9.2) = 9.0$	0.0500
4	17	34	$(1/2)(9.2 + 9.6) = 9.4$	0.0522
5	18	35	$(1/2)(9.6 + 10.1) = 9.9$	0.0550
6	19	36	$(1/2)(10.1 + 10.6) = 10.4$	0.0577
7	20	37	$(1/2)(10.6 + 11.2) = 10.9$	0.0605
8	21	38	$(1/2)(11.2 + 11.7) = 11.5$	0.0639
9	22	39	$(1/2)(11.7 + 12.3) = 12.0$	0.0667
10	23	40	$(1/2)(12.3 + 13.0) = 12.7$	0.0706
11	24	41	$(1/2)(13.0 + 13.6) = 13.3$	0.0738
12	25	42	$(1/2)(13.6 + 14.3) = 14.0$	0.0778
13	26	43	$(1/2)(14.3 + 15.0) = 14.7$	0.0817
14	27	44	$(1/2)(15.0 + 15.8) = 15.4$	0.0856
15	28	45	$(1/2)(15.8 + 16.6) = 16.2$	0.0900
16	29	46	$(1/2)(16.6) = 8.3$	0.0461

Table 2.10.2-3 Effective Inner Lid Bolt Properties

Circumferential Plane	Real Constant				
Identification No.	Numbers	Area	$I_{zz}/I_{yy}$	$T_{kz}/T_{ky}$	$\left( \frac{\text{Shear } z}{\text{Shear } y} \right)$
1	14	0.7300	0.0785	1.378	1.11
2	15	1.4790	0.1590	1.378	1.11
3	16	1.5665	0.1684	1.378	1.11
4	17	1.6354	0.1758	1.378	1.11
5	18	1.723	0.1852	1.378	1.11
6	19	1.8077	0.1943	1.378	1.11
7	20	1.8955	0.2037	1.378	1.11
8	21	2.0020	0.2152	1.378	1.11
9	22	2.0897	0.2246	1.378	1.11
10	23	2.2119	0.2377	1.378	1.11
11	24	2.3122	0.2485	1.378	1.11
12	25	2.4375	0.2620	1.378	1.11
13	26	2.5500	0.2751	1.378	1.11
14	27	2.6818	0.2883	1.378	1.11
15	28	2.8197	0.3031	1.378	1.11
16	29	1.4443	0.1552	1.378	1.11



Table 2.10.2-4 Outer Lid Effective Bolt Properties

Circumferential Plane		Real Constant			
Identification No.	Numbers	Area	$I_{zz}/I_{yy}$	$T_{kz}/T_{ky}$	$\left( \frac{\text{Shear } z}{\text{Shear } y} \right)$
1	31	0.2342	0.0105	0.879	1.11
2	32	0.5149	0.2124	0.879	1.11
3	33	0.5454	0.0225	0.879	1.11
4	34	0.5694	0.0235	0.879	1.11
5	35	0.5999	0.0248	0.879	1.11
6	36	0.6294	0.0260	0.879	1.11
7	37	0.6599	0.0272	0.879	1.11
8	38	0.6970	0.0288	0.879	1.11
9	39	0.7276	0.0300	0.879	1.11
10	40	0.7701	0.0318	0.879	1.11
11	41	0.8050	0.0332	0.879	1.11
12	42	0.8486	0.0350	0.879	1.11
13	43	0.8912	0.0378	0.879	1.11
14	44	0.9337	0.0385	0.879	1.11
15	45	0.9817	0.0405	0.879	1.11
16	46	0.5029	0.0207	0.879	1.11

Table 2.10.2-5 Identification of ANSYS Model Structural Components, Material and Allowables; Condition 1

Condition 1: 100°F Ambient with Contents

Comp ID.	Description	Material	Mat ID	Max Temp.	Allowable Stress (ksi)			
					Normal		Accident	
					$P_m$ ( $S_m$ )	$P_m+P_b$ ( $1.5S_m$ )	$P_m$ ( $0.7S_u$ )	$P_m+P_b$ ( $S_u$ )
1	Bottom Plate	304SS	5	350	19.2	28.7	45.6	65.2
2	Bottom Forging	304SS	6	417	18.5	27.7	44.9	64.2
3	Transition Shell	XM-19SS	15	300	31.4	47.1	66.0	94.3
4	Inner Shell	304SS	7	331	19.6	29.4	45.8	65.5
5	Outer Shell	304SS	8	292	20.0	30.0	46.4	66.4
6	Top Forging	304SS	9	211	20.0	30.0	49.3	70.9
7	Inner Lid	304SS	10	223	20.0	30.0	48.0 <sup>1</sup>	69.8
8	Outer Lid	17-4 PH SS	11	178	45.0	67.5	94.5	135.0
9	Inner Lid Bolt	SB-637 Ni	13	190		144.4 <sup>2</sup>		144.4 <sup>2</sup>
10	Outer Lid Bolt	17-4 PH SS	12	178		98.8 <sup>2</sup>		98.8 <sup>2</sup>

<sup>1</sup> 2.4  $S_m$  governs.

<sup>2</sup> Bolt allowables based on material yield strength.

Table 2.10.2-6 Deleted

Table 2.10.2-7 Deleted

Table 2.10.2-8 Section Cut Identification - (2-D Model)

Section <sup>1</sup>	Inside Node		Outside Node	
	Radial (in)	Axial (in)	Radial (in)	Axial (in)
A	0.00	14.40	0.00	8.20
B	0.00	6.20	0.00	0.75
C	35.50	14.40	35.50	8.20
D	39.44	6.20	39.44	0.75
E	39.44	8.20	43.35	8.20
F	35.50	14.40	37.50	14.40
G	40.70	14.40	43.35	14.40
H	35.50	29.40	37.00	29.40
I	40.70	29.40	43.35	29.40
J	35.50	55.65	37.00	55.65
K	40.70	55.65	43.35	55.65
L	35.50	96.90	37.00	96.90
M	40.70	96.90	43.35	96.90
N	35.50	138.15	37.00	138.15
O	40.70	138.15	43.35	138.15
P	35.50	160.40	37.00	160.40
Q	40.70	160.40	43.35	160.40
R	35.50	175.40	37.00	175.40
S	40.70	175.40	43.35	175.40
T	39.56	179.40	43.35	179.40
U	35.50	179.40	35.50	185.40
V	35.21	188.40	35.21	193.71
W	0.00	179.40	0.00	185.40
X	0.00	188.46	0.00	193.71

<sup>1</sup> Refer to Figure 2.10.2-34 for the section cut locations.

Table 2.10.2-9 Section Cut Identification - (3-D Bottom Fine Mesh Model)

Section <sup>1</sup>	Inside Node		Outside Node	
	Radial (in)	Axial (in)	Radial (in)	Axial (in)
A	0.00	14.40	0.00	8.20
B	0.00	6.20	0.00	0.75
C	35.50	14.40	35.50	8.20
D	39.44	6.20	39.44	0.75
E	39.44	8.20	43.35	8.20
F	35.50	15.00 <sup>2</sup>	37.50	15.00 <sup>2</sup>
G	40.70	15.00 <sup>2</sup>	43.35	15.00 <sup>2</sup>
H	35.50	29.40	37.00	29.40
I	40.70	29.40	43.35	29.40
J	35.50	55.65	37.00	55.65
K	40.70	55.65	43.35	55.65
L	35.50	96.90	37.00	96.90
M	40.70	96.90	43.35	96.90
N	35.50	138.15	37.00	138.15
O	40.70	138.15	43.35	138.15
P	35.50	160.40	37.00	160.40
Q	40.70	160.40	43.35	160.40
R	35.50	175.40	37.50	175.40
S	40.70	175.40	43.35	175.40
T	40.70	179.40	43.35	181.68 <sup>3</sup>
U	35.50	179.40	35.50	185.40
V	35.50 <sup>4</sup>	187.40	35.50 <sup>4</sup>	193.71
W	0.00	179.40	0.00	185.40
X	0.00	187.40	0.00	193.71

<sup>1</sup> Refer to Figure 2.10.2-34 for the section cut locations

<sup>2</sup> Moved one section up from the root (Y = 14.40") to pick up higher stresses

<sup>3</sup> Moved up for impact pressure specification

<sup>4</sup> No nodes at outer lid bolt circle for three-dimensional bottom model

Table 2.10.2-10 Section Cut Identification - (3-D Top Fine Mesh Model)

Section <sup>1</sup>	Inside Node		Outside Node	
	Radial (in)	Axial (in)	Radial (in)	Axial (in)
A	0.00	14.40	0.00	8.20
B	0.00	6.20	0.00	0.75
C	35.50	14.40	35.50	8.20
D	39.44	6.20	39.44	0.75
E	39.44	8.20	43.35	8.20
F	35.50	14.40	37.50	14.40
G	40.70	14.40	43.35	14.40
H	35.50	29.40	37.00	29.40
I	40.70	29.40	43.35	29.40
J	35.50	55.65	37.00	55.65
K	40.70	55.65	43.35	55.65
L	35.50	96.90	37.00	96.90
M	40.70	96.90	43.35	96.90
N	35.50	138.15	37.00	138.15
O	40.70	138.15	43.35	138.15
P	35.50	160.40	37.00	160.40
Q	40.70	160.40	43.35	160.40
R	35.50	175.40	37.50	175.40
S	40.70	175.40	43.35	175.40
T	39.56	179.40	43.35	179.40
U	35.50	179.41	35.50	185.40
V	35.21	188.40	35.21	193.71
W	0.00	179.40	0.00	185.40
X	0.00	188.46	0.00	193.71

<sup>1</sup> Refer to Figure 2.10.2-34 for the section cut locations

Table 2.10.2-11 Stress Point Locations - 2-D Model

ID	Stress Point Node	Location	
		Radial (in)	Axial (in)
A-1	1	0.00	14.40
A-2	2	0.00	12.95
A-3	3	0.00	11.30
A-4	4	0.00	9.75
A-5	5	0.00	8.20
B-1	6	0.00	6.20
B-2	7	0.00	4.84
B-3	8	0.00	3.48
B-4	9	0.00	2.11
B-5	10	0.00	0.75
C-1	251	35.50	14.40
C-2	252	35.50	12.85
C-3	253	35.50	11.30
C-4	254	35.50	9.75
C-5	255	35.50	8.20
D-1	306	39.44	6.20
D-2	307	39.44	4.84
D-3	308	39.44	3.48
D-4	309	39.44	2.11
D-5	310	39.44	0.75
E-1	305	39.44	8.20
E-2	315	40.70	8.20
E-3	325	41.36	8.20
E-4	335	42.03	8.20
E-5	345	42.69	8.20
E-6	355	43.35	8.20



Table 2.10.2-11 Stress Point Locations - 2-D Model (continued)

ID	Stress Point Node	Location	
		Radial (in)	Axial (in)
F-1	251	35.50	14.40
F-2	261	36.17	14.40
F-3	271	36.83	14.40
F-4	281	37.50	14.40
G-1	311	40.70	14.40
G-2	321	41.36	14.40
G-3	331	42.03	14.40
G-4	341	42.69	14.40
G-5	351	43.35	14.40
H-1	581	35.50	29.40
H-2	582	36.00	29.40
H-3	583	36.50	29.40
H-4	584	37.00	29.40
I-1	589	40.70	29.40
I-2	590	41.36	29.40
I-3	591	42.03	29.40
I-4	592	42.69	29.40
I-5	593	43.35	29.40
J-1	971	35.50	55.65
J-2	972	36.00	55.65
J-3	973	36.50	55.65
J-4	974	37.00	55.65
K-1	979	40.70	55.65
K-2	980	41.36	55.65
K-3	981	42.03	55.65

Table 2.10.2-11 Stress Point Locations - 2-D Model (continued)

ID	Stress Point Node	Location	
		Radial (in)	Axial (in)
K-4	982	42.69	55.65
K-5	983	43.35	55.65
L-1	1601	35.50	96.90
L-2	1602	36.00	96.90
L-3	1603	36.50	96.90
L-4	1604	37.00	96.90
M-1	1609	40.70	96.90
M-2	1610	41.36	96.90
M-3	1611	42.03	96.90
M-4	1612	42.69	96.90
M-5	1613	43.35	96.90
N-1	2216	35.50	138.15
N-2	2217	36.00	138.15
N-3	2218	36.50	138.15
N-4	2219	37.00	138.15
O-1	2224	40.70	138.15
O-2	2225	41.36	138.15
O-3	2226	42.03	138.15
O-4	2227	42.69	138.15
O-5	2228	43.35	138.15
P-1	2546	35.50	160.40
P-2	2547	36.00	160.40
P-3	2548	36.50	160.40
P-4	2549	37.00	160.40

Table 2.10.2-11 Stress Point Locations - 2-D Model (continued)

ID	Stress Point Node	Location	
		Radial (in)	Axial (in)
Q-1	2554	40.70	160.40
Q-2	2555	41.36	160.40
Q-3	2556	42.03	160.40
Q-4	2557	42.69	160.40
Q-5	2558	43.35	160.40
R-1	2771	35.50	175.40
R-2	2772	36.17	175.40
R-3	2773	36.83	175.40
R-4	2774	37.50	175.40
S-1	2779	40.70	175.40
S-2	2780	41.36	175.40
S-3	2781	42.03	175.40
S-4	2782	42.69	175.40
S-5	2783	43.35	175.40
T-1	7066	39.56	179.40
T-2	7067	40.22	179.40
T-3	7068	40.88	179.40
T-4	7069	41.50	179.40
T-5	7070	42.11	179.40
T-6	7071	42.73	179.40
T-7	7072	43.35	179.40
U-1	3051	35.50	179.40
U-2	3052	35.50	180.60
U-3	3053	35.50	181.80
U-4	3054	35.50	183.00
U-5	3055	35.50	184.20
U-6	3056	35.50	185.40

Table 2.10.2-11 Stress Point Locations - 2-D Model (continued)

ID	Stress Point Node	Location	
		Radial (in)	Axial (in)
V-1	3611	35.21	188.40
V-2	3612	35.21	189.28
V-3	3613	35.21	190.15
V-4	3614	35.21	191.03
V-5	3615	35.21	191.90
V-6	3616	35.21	192.78
V-7	3617	35.21	193.71
W-1	3241	0.00	179.40
W-2	3242	0.00	180.60
W-3	3243	0.00	181.80
W-4	3244	0.00	183.00
W-5	3245	0.00	184.20
W-6	3246	0.00	185.40
X-1	3801	0.00	188.46
X-2	3802	0.00	189.28
X-3	3803	0.00	190.15
X-4	3804	0.00	191.03
X-5	3805	0.00	191.90
X-6	3806	0.00	192.78
X-7	3807	0.00	193.71

Table 2.10.2-12 Stress Point Locations - 3-D Bottom Fine Mesh Model

ID	Stress Point Node	Location	
		Radial (in)	Axial (in)
A-1	1130	0.00	14.40
A-2	1129	0.00	11.35
A-3	1128	0.00	8.20
B-1	1185	0.00	6.20
B-2	1184	0.00	3.48
B-3	1183	0.00	0.75
C-1	90	35.50	14.40
C-2	80	35.50	13.60
C-3	70	35.50	12.80
C-4	60	35.50	12.00
C-5	50	35.50	9.50
C-6	40	35.50	8.20
D-1	25	39.44	6.20
D-2	15	39.44	3.48
D-3	5	39.44	0.75
E-1	35	39.44	8.20
E-2	34	40.70	8.20
E-3	33	41.58	8.20
E-4	32	42.47	8.20
E-5	31	43.35	8.20
F-1	100	35.50	15.07
F-2	99	36.17	15.07
F-3	98	36.83	15.07
F-4	97	37.50	15.07

Table 2.10.2-12 Stress Point Locations - 3-D Bottom Fine Mesh Model (continued)

ID	Stress Point Node	Location	
		Radial (in)	Axial (in)
G-1	94	40.70	15.52
G-2	93	41.58	15.52
G-3	92	42.47	15.52
G-4	91	43.35	15.52
H-1	330	35.50	29.40
H-2	329	36.00	29.40
H-3	328	36.50	29.40
H-4	327	37.00	29.40
I-1	244	40.70	29.40
I-2	243	41.58	29.40
I-3	242	42.47	29.40
I-4	241	43.35	29.40
J-1	550	35.50	55.65
J-2	548	36.25	55.65
J-3	547	37.00	55.65
K-1	344	40.70	55.65
K-2	342	42.03	55.65
K-3	341	43.35	55.65
L-1	740	35.50	96.90
L-2	738	36.25	96.90
L-3	737	37.00	96.90
M-1	454	40.70	96.90
M-2	452	42.03	96.90

Table 2.10.2-12 Stress Point Locations - 3-D Bottom Fine Mesh Model (continued)

ID	Stress Point Node	Location	
		Radial (in)	Axial (in)
M-3	451	43.35	96.90
N-1	810	35.50	138.15
N-2	807	37.00	138.15
O-1	524	40.70	138.15
O-2	521	43.35	138.15
P-1	850	35.50	160.40
P-2	847	37.00	160.40
Q-1	564	40.70	160.40
Q-2	561	43.35	160.40
R-1	890	35.50	175.40
R-2	887	37.50	175.40
S-1	604	40.70	175.40
S-2	601	43.35	175.40
T-1	614	40.70	179.40
T-2	611	43.35	179.40
U-1	900	35.50	179.40
U-2	910	35.50	185.40
V-1	920	35.50	187.40
V-2	930	35.50	193.71

Table 2.10.2-12 Stress Point Locations - 3-D Bottom Fine Mesh Model (continued)

ID	Stress Point Node	Location	
		Radial (in)	Axial (in)
W-1	1216	0.00	179.40
W-2	1226	0.00	185.40
X-1	1236	0.00	187.40
X-2	1246	0.00	193.71



Table 2.10.2-13 Stress Point Locations - 3-D Top Fine Mesh Model

ID	Stress Point Node	Location	
		Radial (in)	Axial (in)
A-1	1949	0.00	14.40
A-2	1950	0.00	12.78
A-3	1951	0.00	8.20
B-1	1952	0.00	6.20
B-2	93	0.00	0.75
C-1	1925	35.50	14.40
C-2	1926	35.50	12.78
C-3	1927	35.50	8.20
D-1	683	39.44	6.20
D-2	85	39.44	0.75
E-1	682	39.44	8.20
E-2	82	43.35	8.20
F-1	1925	35.50	14.40
F-2	1325	37.50	14.40
G-1	680	40.70	14.40
G-2	80	43.35	14.40
H-1	1921	35.50	29.40
H-2	1321	37.00	29.40
I-1	676	40.70	29.40
I-2	76	43.35	29.40

Table 2.10.2-13 Stress Point Locations - 3-D Top Fine Mesh Model (continued)

ID	Stress Point Node	Location	
		Radial (in)	Axial (in)
J-1	1916	35.50	55.65
J-2	1316	37.00	55.65
K-1	671	40.70	55.65
K-2	71	43.50	55.65
L-1	1908	35.50	96.90
L-2	1308	37.00	96.90
M-1	663	40.70	96.90
M-2	63	43.50	96.90
N-1	1877	35.50	138.15
N-2	1477	36.25	138.15
N-3	1277	37.00	138.15
O-1	647	40.70	138.15
O-2	247	42.03	138.15
O-3	47	43.35	138.15
P-1	1840	35.50	160.40
P-2	1640	36.00	160.40
P-3	1440	36.50	160.40
P-4	1240	37.00	160.40
Q-1	628	40.70	160.40
Q-2	428	41.58	160.40
Q-3	228	42.47	160.40
Q-4	28	43.35	160.40

Table 2.10.2-13 Stress Point Locations - 3-D Top Fine Mesh Model (continued)

ID	Stress Point Node	Location	
		Radial (in)	Axial (in)
R-1	1816	35.50	175.40
R-2	1616	36.17	175.40
R-3	1416	36.83	175.40
R-4	1216	37.50	175.40
S-1	616	40.70	175.40
S-2	416	41.58	175.40
S-3	216	42.47	175.40
S-4	16	43.35	175.40
T-1	811	39.56	179.40
T-2	611	40.51	179.40
T-3	411	41.46	179.40
T-4	211	42.40	179.40
T-5	11	43.35	179.40
U-1	43058	35.50	179.40
U-2	43057	35.50	180.15
U-3	43056	35.50	180.90
U-4	43055	35.50	181.65
U-5	43054	35.50	182.40
U-6	43053	35.50	183.15
U-7	43052	35.50	183.90
U-8	43051	35.50	185.40
V-1	50024	35.21	188.40
V-2	50023	35.21	190.15
V-3	50022	35.21	191.90
V-4	50021	35.21	193.71

Table 2.10.2-13 Stress Point Locations - 3-D Top Fine Mesh Model (continued)

ID	Stress Point Node	Location	
		Radial (in)	Axial (in)
W-1	43278	0.00	179.40
W-2	43274	0.00	182.40
W-3	43271	0.00	185.40
X-1	50084	0.00	188.46
X-2	50083	0.00	190.15
X-3	50081	0.00	193.71

### 2.10.3 LS-DYNA Computer Code

The validation of the use of LS-DYNA to represent the behavior of the balsa impact limiters was accomplished by using the balsa stress strain curve for a simple geometry for which the crushing and acceleration could be determined. The geometry used is shown in Figure 2.10.3.2-1, which corresponds to a right circular cylinder 50 inches in diameter and 50 inches in length. The model employed symmetry boundary conditions for the quarter symmetry model. The stress strain curve representative of balsa material is shown in Figure 2.10.3.2-2. The material model used in this evaluation is the FU\_CHANG\_FOAM (material 83), which is the material model employed in the balsa impact limiter evaluation. The impacting object is a quarter symmetry circular plate of the same diameter with an assigned weight of 257 kips. The interface between the balsa cylinder and the plate is modeled using automatic surface to surface, while the unyielding surface was modeled using the RIGIDWALL\_GEOMETRIC\_FLAT option. The system has an initial velocity of 150 in/sec. To compute the crush, an energy balance is used.

$$\frac{mv_o^2}{2} = AL \int_0^{\epsilon_i} \sigma_i d\epsilon$$

where

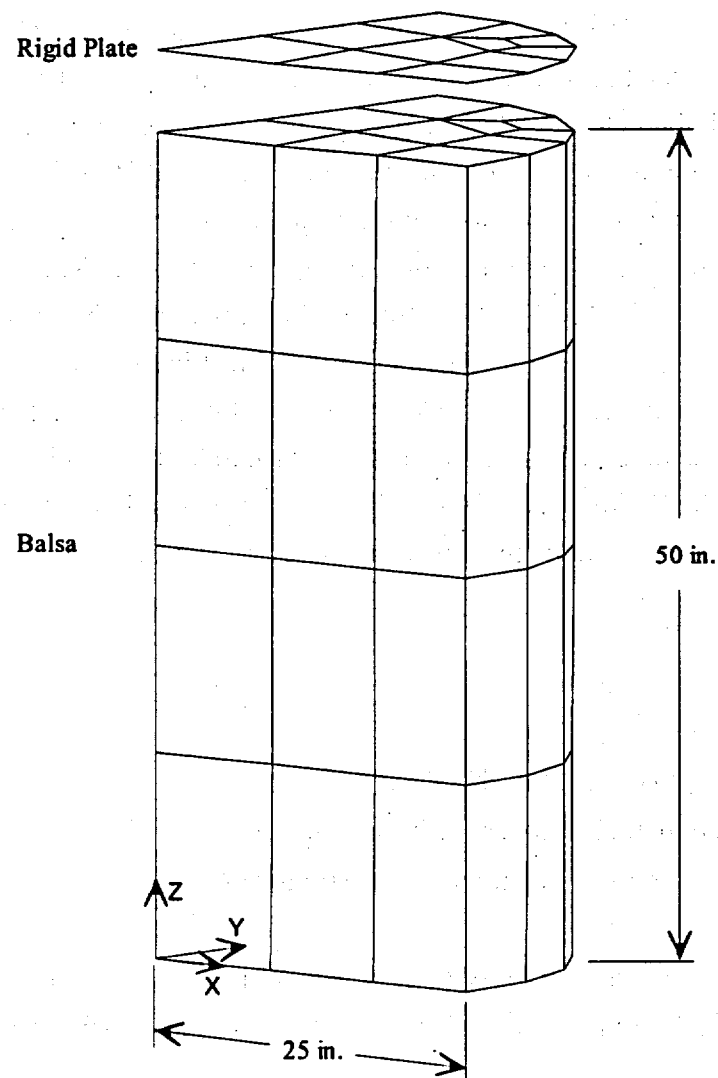
- A = area of the block being crushed
- L = total original height of the block
- $d\epsilon_i$  = the incremental strain as the block crushes
- $\sigma_i$  = the stress at the given incremental strain value

The acceleration is computed by  $\sigma A/W$  (g's), where W is the weight of the modeled plate. The peak crush strength is 2,090 psi obtained from Figure 2.10.3.2-2. The results of the calculation are:

Item	LS-DYNA	Calculation	% Difference
Crush (in)	12.9	12.6	2
Acceleration (maximum) (g's)	4.04	3.99	1

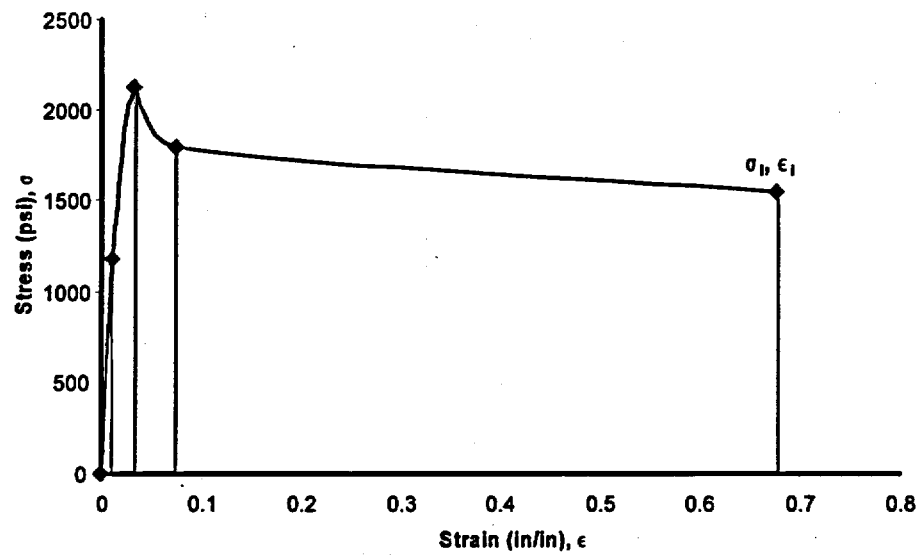
This demonstrates that the material model and numerical methodology employed in LS-DYNA for the balsa impact limiters is acceptable.

Figure 2.10.3.2-1 LS-DYNA Model used to Verify the Material Model



Note: XZ and YZ planes are planes of symmetry.

Figure 2.10.3.2-2 Balsa Stress-Strain Curve used for the Balsa Material



**THIS PAGE INTENTIONALLY LEFT BLANK**



#### 2.10.4 Detailed Finite Element Stress Summaries - Directly Loaded Fuel Configuration

This section documents the finite element stress results from the different loading cases for the normal condition of transport and hypothetical accident conditions for the directly loaded fuel configuration of the NAC-STC. Nodal and sectional stress summaries are presented for the representative sections as defined in Section 2.10.2.4.2. Critical stress summaries are presented for the critical component sections determined as described in Section 2.10.2.4.1. The maximum stress intensity is the maximum value of  $(S1-S3)$ , where  $S1$  and  $S3$  are the maximum and minimum principle stresses, respectively.

A summary of the individual and combined loading conditions is provided, followed by the stress summary tables. The values for  $S_x$ ,  $S_y$ , and  $S_z$  shown in the tables are normal stresses corresponding to radial, longitudinal and circumferential stresses, respectively. Allowable stresses, in tables where these data items appear, are based on maximum component temperature for normal conditions.

## SUMMARY OF INDIVIDUAL LOADING ANALYSES

(The following are individual loading analyses, nodal stress summaries are prepared for each)

<u>ANALYSIS</u> <u>NO.</u>	<u>LOADING DESCRIPTION</u>	<u>SAR</u> <u>SECTION</u>	<u>TABLE</u> <u>NO.</u>
1.	50 psi Maximum Internal Pressure plus Bolt Preload, 100°F		2.10.4-1
2.	12 psi Minimum Internal Pressure plus Bolt Preload, -40°F		2.10.4-2
3.	Gravity, 100°F, Decay Heat, Solar Insolation	2.6.1	2.10.4-3
4.	Gravity, -40°F, no Decay Heat, No Solar Insolation	2.6.2	2.10.4-4
5.	Thermal Heat, 100°F, Decay Heat, Solar Insolation	2.6.1	2.10.4-5
6.	Thermal Cold, -20°F, Decay Heat		2.10.4-6
7.	Thermal Cold, -40°F, No Decay Heat	2.6.2	2.10.4-7
8.	Impact, 1 Ft Top End Drop, 20 g, $\phi = 0^\circ$	2.6.7.1	2.10.4-8
9.	Impact, 1 Ft Bottom End Drop, 20 g, $\phi = 0^\circ$	2.6.7.1	2.10.4-9
10.	Impact, 1 Ft Side Drop, 20 g, $\phi = 90^\circ$	2.6.7-2	2.10.4-10
11.	Impact, 1 Ft Top Corner Drop, 20 g, $\phi = 24^\circ$	2.6.7.3	2.10.4-11
12.	Impact, 1 Ft Bottom Corner Drop, 20 g, $\phi = 24^\circ$	2.6.7.3	2.10.4-12
13.	Impact, 30 Ft Top End Drop, 56.1 g, $\phi = 0^\circ$	2.7.1.1	2.10.4-13
14.	Impact, 30 Ft Bottom End Drop, 56.1 g, $\phi = 0^\circ$	2.7.1.1	2.10.4-14
15.	Impact, 30 Ft Side Drop, 55 g, $\phi = 90^\circ$	2.7.1.2	2.10.4-15
16.	Impact, 30 Ft Top Corner Drop, 55 g, $\phi = 24^\circ$	2.7.1.3	2.10.4-16
17.	Impact, 30 Ft Bottom Corner Drop, 55 g, $\phi = 24^\circ$	2.7.1.3	2.10.4-17
18.	Impact, 30 Ft Bottom Oblique Drop, 55 g, $\phi = 15^\circ$	2.7.1.4	2.10.4-18
19.	Impact, 30 Ft Top Oblique Drop, 55 g, $\phi = 75^\circ$	2.7.1.4	2.10.4-19
20.	Impact, 30 Ft Bottom Oblique Drop, 55 g, $\phi = 75^\circ$	2.7.1.4	2.10.4-20
21.	Thermal Fire Transient, 1475°F, 30 Minutes	2.7.3	2.10.4-178 through 2.10.4-180

SUMMARY OF COMBINED LOADING ANALYSES

ANALYSIS NO.	LOADING DESCRIPTION	SAR SECTION	TABLE NO.
22.	Thermal Heat 50 psi Internal Pressure, Bolt Preload 1 g Gravity with Cask in Horizontal Position 100°F, Solar Insolation, Decay Heat	2.6.1	2.10.4-21 through 2.10.4-28
23.	Thermal Cold 12 psi Internal Pressure, Bolt Preload 1 g Gravity with Cask in Horizontal Position -40°F, no Solar Insolation, no Decay Heat	2.6.2	2.10.4-29 through 2.10.4-36
24.	1 Ft Top End Drop 50 psi Internal Pressure, Bolt Preload Impact (20 g, $f = 0^\circ$ ) 100°F, Solar Insolation, Decay Heat	2.6.7.1	2.10.4-37 through 2.10.4-44
25.	1 Ft Top End Drop 12 psi Internal Pressure, Bolt Preload Impact (20 g, $f = 0^\circ$ ) -20°F, no Solar Insolation, Decay Heat	2.6.7.1	2.10.4-45 through 2.10.4-47
26.	1 Ft Top End Drop 12 psi Internal Pressure, Bolt Preload Impact (20 g, $f = 0^\circ$ ) -20°F, no Solar Insolation, no Contents	2.6.7.1	2.10.4-48 through 2.10.4-50
27.	1 Ft Bottom End Drop 50 psi Internal Pressure, Bolt Preload Impact (20 g, $f = 0^\circ$ ) 100°F, Solar Insolation, Decay Heat	2.6.7.1	2.10.4-51 through 2.10.4-58

SUMMARY OF COMBINED LOADING ANALYSES (Continued)

ANALYSIS NO.	LOADING DESCRIPTION	SAR SECTION	TABLE NO.
28.	1 Ft Bottom End Drop 12 psi Internal Pressure, Bolt Preload Impact (20 g, f = 0°) -20°F, no Solar Insolation, Decay Heat	2.6.7.1	2.10.4-59 through 2.10.4-61
29.	1 Ft Bottom End Drop 12 psi Internal Pressure, Bolt Preload Impact (20 g, f = 0°) -20°F, no Solar Insolation, no Contents	2.6.7.1	2.10.4-62 through 2.10.4-64
30.	1 Ft Side Drop 50 psi Internal Pressure, Bolt Preload Impact (20 g, f = 90°) 100°F, Solar Insolation, Decay Heat	2.6.7.2	2.10.4-65 through 2.10.4-83
31.	1 Ft Top Corner Drop 50 psi Internal Pressure, Bolt Preload Impact (20 g, f = 24°) 100°F, Solar Insolation, Decay Heat	2.6.7.3	2.10.4-84 through 2.10.4-97
32.	1 Ft Bottom Corner Drop 50 psi Internal Pressure, Bolt Preload Impact (20 g, f = 24°) 100°F, Solar Insolation, Decay Heat	2.6.7.3	2.10.4-98 through 2.10.4-111
33.	30 Ft Top End Drop 50 psi Internal Pressure, Bolt Preload Impact (56.1 g, f = 0°) 100°F, Solar Insolation, Decay Heat	2.7.7.1	2.10.4-112 through 2.10.4-116

SUMMARY OF COMBINED LOADING ANALYSES (Continued)

ANALYSIS NO.	LOADING DESCRIPTION	SAR SECTION	TABLE NO.
34.	30 Ft Top End Drop 12 psi Internal Pressure, Bolt Preload Impact (56.1 g, $f = 0^\circ$ ) -20°F, no Solar Insolation, Decay Heat	2.7.1.1	2.10.4-117 through 2.10.4-118
35.	30 Ft Top End Drop 12 psi Internal Pressure, Bolt Preload Impact (56.1 g, $f = 0^\circ$ ) -20°F, no Solar Insolation, no Contents	2.7.1.1	2.10.4-119 through 2.10.4-120
36.	30 Ft Bottom End Drop 50 psi Internal Pressure, Bolt Preload Impact (56.1 g, $f = 0^\circ$ ) 100°F, Solar Insolation, Decay Heat	2.7.1.1	2.10.4-121 through 2.10.4-125
37.	30 Ft Bottom End Drop 12 psi Internal Pressure, Bolt Preload Impact (56.1 g, $f = 0^\circ$ ) -20°F, no Solar Insolation, Decay Heat	2.7.1.1	2.10.4-126 through 2.10.4-127
38.	30 Ft Bottom End Drop 12 psi Internal Pressure, Bolt Preload Impact (56.1 g, $f = 0^\circ$ ) -20°F, no Solar Insolation, no Contents	2.7.1.1	2.10.4-128 through 2.10.4-129
39.	30 Ft Side Drop 50 psi Internal Pressure, Bolt Preload Impact, (55 g, $f = 90^\circ$ ) 100°F, Solar Insolation, Decay Heat	2.7.1.2	2.10.4-130 through 2.10.4-140

SUMMARY OF COMBINED LOADING ANALYSES (Continued)

ANALYSIS NO.	LOADING DESCRIPTION	SAR SECTION	TABLE NO.
40.	30 Ft Top Corner Drop 50 psi Internal Pressure, Bolt Preload Impact, (55 g, $f = 24^\circ$ ) 100°F, Solar Insolation, Decay Heat	2.7.1.3	2.10.4-141 through 2.10.4-151
41.	30 Ft Bottom Corner Drop 50 psi Internal Pressure, Bolt Preload Impact, (55 g, $f = 24^\circ$ ) 100°F, Solar Insolation, Decay Heat	2.7.1.3	2.10.4-152 through 2.10.4-162
42.	30 Ft Bottom Critical Oblique Drop 50 psi Internal Pressure, Bolt Preload Impact (55 g, $f = 15^\circ$ ) 100°F, Solar Insolation, Decay Heat	2.7.1.4	2.10.4-163 through 2.10.4-167
43.	30 Ft Top Critical Oblique Drop 50 psi Internal Pressure, Bolt Preload Impact (55 g, $f = 75^\circ$ ) 100°F, Solar Insolation, Decay Heat	2.7.1.4	2.10.4-168 through 2.10.4-172
44.	30 Ft Bottom Critical Oblique Drop 50 psi Internal Pressure, Bolt Preload Impact (55 g, $f = 75^\circ$ ) 100°F, Solar Insolation, Decay Heat	2.7.1.4	2.10.4-173 through 2.10.4-177
45.	Thermal Fire Transient 125 psi Internal Pressure, Bolt Preload 1 g Gravity with Cask in Vertical Position 1475°F, 30 Minute Period, Decay Heat	2.7.3	2.10.4-178 through 2.10.4-180

Table 2.10.4-1 Stress Components – 50 psig Internal Pressure + Bolt Preload; 2-D Model;  
Condition 1

Condition 1: 100°F Ambient with Contents

Stress Points		Stress Components (ksi)						Principal Stresses (ksi)		
Section <sup>1</sup>	Node	S <sub>x</sub>	S <sub>y</sub>	S <sub>z</sub>	S <sub>xy</sub>	S <sub>xz</sub>	S <sub>yz</sub>	S1	S2	S3
A1	1	-0.7	0.0	-0.7	0.0	0.0	0.0	0.0	-0.7	-0.7
A2	2	-0.4	0.0	-0.4	0.0	0.0	0.0	0.0	-0.4	-0.4
A3	3	0.0	0.0	0.0	0.0	0.0	0.0	0.0	0.0	0.0
A4	4	0.3	0.0	0.3	0.0	0.0	0.0	0.3	0.3	0.0
A5	5	0.6	0.0	0.6	0.0	0.0	0.0	0.6	0.6	0.0
B1	6	-0.5	0.0	-0.5	0.0	0.0	0.0	0.0	-0.5	-0.5
B2	7	-0.2	0.0	-0.2	0.0	0.0	0.0	0.0	-0.2	-0.2
B3	8	0.1	0.0	0.1	0.0	0.0	0.0	0.1	0.1	0.0
B4	9	0.4	0.0	0.4	0.0	0.0	0.0	0.4	0.4	0.0
B5	10	0.7	0.0	0.7	0.0	0.0	0.0	0.7	0.7	0.0
C1	251	0.7	1.1	0.3	0.2	0.0	0.0	1.2	0.6	0.3
C2	252	0.1	0.4	0.0	0.1	0.0	0.0	0.4	0.1	0.0
C3	253	-0.1	0.1	0.0	0.0	0.0	0.0	0.1	0.0	-0.1
C4	254	-0.3	0.0	0.0	0.0	0.0	0.0	0.0	0.0	-0.3
C5	255	-0.6	0.0	-0.1	0.0	0.0	0.0	0.0	-0.1	-0.6
D1	306	0.5	0.2	0.2	0.1	0.0	0.0	0.0	0.2	0.2
D2	307	0.2	0.2	0.1	0.0	0.0	0.0	0.2	0.1	0.1
D3	308	0.0	0.1	0.1	0.0	0.0	0.0	0.1	0.1	0.0
D4	309	-0.1	0.0	0.1	0.0	0.0	0.0	0.1	0.0	-0.1
D5	310	-0.2	0.0	0.1	0.0	0.0	0.0	0.1	0.0	-0.2
E1	305	-0.5	-0.1	-0.1	0.1	0.0	0.0	-0.1	-0.1	-0.5
E2	315	-0.3	0.1	0.0	0.1	0.0	0.0	0.1	0.0	-0.3
E3	325	-0.1	0.1	0.0	0.1	0.0	0.0	0.1	0.0	-0.2
E4	335	-0.1	0.1	0.0	0.1	0.0	0.0	0.1	0.0	-0.1
E5	345	0.0	0.1	0.0	0.1	0.0	0.0	0.1	0.0	0.0
E6	355	0.0	0.1	0.0	0.0	0.0	0.0	0.1	0.0	0.0
F1	251	0.7	1.1	0.3	0.2	0.0	0.0	1.2	0.6	0.3
F2	261	0.5	0.4	0.1	0.0	0.0	0.0	0.5	0.4	0.1
F3	271	0.2	-0.1	-0.1	0.0	0.0	0.0	0.2	-0.1	-0.1
F4	281	0.1	-0.6	-0.3	0.0	0.0	0.0	0.1	-0.3	-0.6
G1	311	0.2	0.3	0.0	0.0	0.0	0.0	0.3	0.2	0.0

Table 2.10.4-1 Stress Components – 50 psig Internal Pressure + Bolt Preload; 2-D Model;  
Condition 1 (continued)

Stress Points Section <sup>1</sup> Node	Stress Components (ksi)						Principal Stresses (ksi)		
	S <sub>x</sub>	S <sub>y</sub>	S <sub>z</sub>	S <sub>xy</sub>	S <sub>yz</sub>	S <sub>xz</sub>	S1	S2	S3
G2	321	0.1	0.2	0.0	0.0	0.0	0.2	0.1	0.0
G3	331	0.1	0.1	0.0	0.0	0.0	0.1	0.0	0.0
G4	341	0.0	0.0	-0.1	0.0	0.0	0.0	0.0	-0.1
G5	351	0.0	-0.1	-0.0	0.0	0.0	0.0	-0.1	-0.1
H1	581	0.0	0.1	0.9	0.0	0.0	0.9	0.1	0.0
H2	582	0.0	0.3	0.9	0.0	0.0	0.9	0.3	0.0
H3	583	0.0	0.5	1.0	0.0	0.0	1.0	0.5	0.0
H4	584	0.0	0.7	1.0	0.0	0.0	1.0	0.7	0.0
I1	589	0.0	0.1	0.0	0.0	0.0	0.1	0.0	0.0
I2	590	0.0	0.1	0.0	0.0	0.0	0.1	0.0	0.0
I3	591	0.0	0.1	0.0	0.0	0.0	0.1	0.0	0.0
I4	592	0.0	0.1	0.0	0.0	0.0	0.1	0.0	0.0
I5	593	0.0	0.1	0.0	0.0	0.0	0.1	0.0	0.0
J1	971	-0.1	0.4	1.1	0.0	0.0	1.1	0.4	-0.1
J2	972	0.0	0.4	1.0	0.0	0.0	1.0	0.4	0.0
J3	973	0.0	0.4	1.0	0.0	0.0	1.0	0.4	0.0
J4	974	0.0	0.4	1.0	0.0	0.0	1.0	0.4	0.0
K1	979	0.0	0.1	0.0	0.0	0.0	0.1	0.0	0.0
K2	980	0.0	0.1	0.0	0.0	0.0	0.1	0.0	0.0
K3	981	0.0	0.1	0.0	0.0	0.0	0.1	0.0	0.0
K4	982	0.0	0.1	0.0	0.0	0.0	0.1	0.0	0.0
K5	983	0.0	0.1	0.0	0.0	0.0	0.1	0.0	0.0
L1	160	-0.1	0.4	1.1	0.0	0.0	1.1	0.0	-0.1
L2	1602	0.0	0.4	1.0	0.0	0.0	1.0	0.4	0.0
L3	1603	0.0	0.4	1.0	0.0	0.0	1.0	0.4	0.0
L4	1604	0.0	0.4	1.0	0.0	0.0	1.0	0.4	0.0
M1	1609	0.0	0.1	0.0	0.0	0.0	0.1	0.0	0.0
M2	1610	0.0	0.1	0.0	0.0	0.0	0.1	0.0	0.0
M3	1611	0.0	0.1	0.0	0.0	0.0	0.1	0.0	0.0
M4	1612	0.0	0.1	0.0	0.0	0.0	0.1	0.0	0.0
M5	1613	0.0	0.1	0.0	0.0	0.0	0.1	0.0	0.0
N1	2216	-0.1	0.4	1.1	0.0	0.0	1.1	0.4	-0.1
N2	2217	0.0	0.4	1.0	0.0	0.0	1.0	0.4	0.0



Table 2.10.4-1 Stress Components – 50 psig Internal Pressure + Bolt Preload; 2-D Model;  
Condition 1 (continued)

Stress Points		Stress Components (ksi)						Principal Stresses (ksi)		
Section <sup>1</sup>	Node	S <sub>x</sub>	S <sub>y</sub>	S <sub>z</sub>	S <sub>xy</sub>	S <sub>yz</sub>	S <sub>xz</sub>	S1	S2	S3
N3	2218	0.0	0.4	1.0	0.0	0.0	0.0	1.0	0.4	0.0
N4	2219	0.0	0.4	1.0	0.0	0.0	0.0	1.0	0.4	0.0
O1	2224	0.0	0.1	0.0	0.0	0.0	0.0	0.1	0.0	0.0
O2	2225	0.0	0.1	0.0	0.0	0.0	0.0	0.1	0.0	0.0
O3	2226	0.0	0.1	0.0	0.0	0.0	0.0	0.1	0.0	0.0
O4	2227	0.0	0.1	0.0	0.0	0.0	0.0	0.1	0.0	0.0
O5	2228	0.0	0.1	0.0	0.0	0.0	0.0	0.1	0.0	0.0
P1	2546	0.0	0.2	1.0	0.0	0.0	0.0	1.0	0.2	0.0
P2	2547	0.0	0.3	1.0	0.0	0.0	0.0	1.0	0.3	0.0
P3	2548	0.0	0.4	1.0	0.0	0.0	0.0	1.0	0.4	0.0
P4	2549	0.0	0.6	1.0	0.0	0.0	0.0	1.0	0.6	0.0
Q1	2554	0.0	0.1	0.0	0.0	0.0	0.0	0.1	0.0	0.0
Q2	2555	0.0	0.1	0.0	0.0	0.0	0.0	0.1	0.0	0.0
Q3	2556	0.0	0.1	0.0	0.0	0.0	0.0	0.1	0.0	0.0
Q4	2557	0.0	0.1	0.0	0.0	0.0	0.0	0.1	0.0	0.0
Q5	2558	0.0	0.0	0.0	0.0	0.0	0.0	0.0	0.0	0.0
R1	2771	-0.3	0.1	0.3	0.1	0.0	0.0	0.3	0.2	-0.3
R2	2772	-0.3	0.2	0.3	0.2	0.0	0.0	0.3	0.2	-0.3
R3	2773	-0.5	0.2	0.2	0.2	0.0	0.0	0.3	0.2	-0.6
R4	2774	-1.1	0.7	0.2	0.1	0.0	0.0	0.7	0.2	-1.1
S1	2775	-0.3	0.0	0.1	-0.1	0.0	0.0	0.1	0.0	-0.3
S2	2780	-0.1	0.0	0.2	0.0	0.0	0.0	0.2	0.0	-0.1
S3	2781	0.0	0.1	0.2	0.0	0.0	0.0	0.2	0.1	0.0
S4	2782	0.0	0.1	0.2	0.0	0.0	0.0	0.2	0.1	0.0
S5	2783	0.0	0.1	0.2	0.0	0.0	0.0	0.2	0.1	0.0
T1	7066	-0.3	-0.2	0.1	0.1	0.0	0.0	0.1	-0.2	-0.3
T2	7067	0.1	-0.6	0.1	-0.1	0.0	0.0	0.1	0.1	-0.6
T3	7068	0.1	-0.4	0.1	0.0	0.0	0.0	0.1	0.1	-0.4
T4	7069	0.0	-0.2	0.2	0.0	0.0	0.0	0.2	0.0	-0.2
T5	7070	0.0	-0.1	0.2	0.0	0.0	0.0	0.2	0.0	-0.1
T6	7071	0.0	0.1	0.2	0.0	0.0	0.0	0.2	0.1	0.0
T7	7072	0.0	0.2	0.3	0.0	0.0	0.0	0.3	0.2	0.0
U1	3051	0.3	-1.4	-0.6	0.4	0.0	0.0	0.4	-0.6	-1.5

Table 2.10.4-1 Stress Components – 50 psig Internal Pressure + Bolt Preload; 2-D Model;  
Condition 1 (continued)

Stress Points Section <sup>1</sup> Node	Stress Components (ksi)						Principal Stresses (ksi)		
	S <sub>x</sub>	S <sub>y</sub>	S <sub>z</sub>	S <sub>xy</sub>	S <sub>yz</sub>	S <sub>xz</sub>	S1	S2	S3
U2 3052	-0.4	-1.8	-0.9	0.4	0.0	0.0	-0.3	-0.9	-1.9
U3 3053	-0.1	-2.0	-0.7	0.1	0.0	0.0	-0.1	-0.7	-2.0
U4 3054	0.0	-1.5	-0.4	-0.4	0.0	0.0	0.1	-0.4	-1.7
U5 3055	-0.5	-0.7	-0.1	-0.5	0.0	0.0	0.0	-0.1	-1.2
U6 3056	0.9	0.2	0.7	-0.4	0.0	0.0	1.1	0.7	0.0
V1 3611	1.2	0.0	0.3	0.0	0.0	0.0	1.2	0.3	0.0
V2 3612	0.7	-0.1	0.2	0.0	0.0	0.0	0.7	0.2	-0.1
V3 3613	0.3	-0.2	0.0	0.0	0.0	0.0	0.4	0.0	-0.2
V4 3614	0.1	-0.5	-0.1	0.0	0.0	0.0	0.1	-0.1	-0.5
V5 3615	-0.2	-1.0	-0.3	0.0	0.0	0.0	-0.2	-0.3	-1.0
V6 3616	-0.4	-0.5	-0.2	0.0	0.0	0.0	-0.2	-0.4	-0.5
V7 3617	-1.4	0.4	-0.2	0.0	0.0	0.0	0.4	-0.2	-1.4
W1 3241	-1.2	0.0	-1.2	0.0	0.0	0.0	0.0	-1.2	-1.2
W2 3242	-0.8	0.0	-0.8	0.0	0.0	0.0	0.0	-0.8	-0.8
W3 3243	-0.3	0.0	-0.3	0.0	0.0	0.0	0.0	-0.3	-0.3
W4 3244	0.2	0.0	0.2	0.0	0.0	0.0	0.2	0.2	0.0
W5 3245	0.7	0.0	0.7	0.0	0.0	0.0	0.7	0.7	0.0
W6 3246	1.1	0.0	1.1	0.0	0.0	0.0	1.1	1.1	0.0
X1 3801	-0.3	0.0	-0.3	0.0	0.0	0.0	0.0	-0.3	-0.3
X2 3802	-0.2	0.0	-0.2	0.0	0.0	0.0	0.0	-0.2	-0.2
X3 3803	-0.1	0.0	-0.1	0.0	0.0	0.0	0.0	-0.1	-0.1
X4 3804	0.0	0.0	0.0	0.0	0.0	0.0	0.0	0.0	0.0
X5 3805	0.1	0.0	0.1	0.0	0.0	0.0	0.1	0.1	0.0
X6 3806	0.2	0.0	0.2	0.0	0.0	0.0	0.2	0.2	0.0
X7 3807	0.3	0.0	0.3	0.0	0.0	0.0	0.3	0.3	0.0

<sup>1</sup> Refer to Figure 2.10.2-34 for the identification of the representative section.

Table 2.10.4-2 Stress Components - 12 psig Internal Pressure + Bolt Preload; 2-D Model;  
Condition 4

Condition 4: -40°F Ambient, No Decay Heat

Stress Points Section <sup>1</sup> Node	Stress Components (ksi)						Principal Stresses (ksi)		
	$S_x$	$S_y$	$S_z$	$S_{xy}$	$S_{yz}$	$S_{xz}$	S1	S2	S3
A1	1	-0.2	0.0	-0.2	0.0	0.0	0.0	-0.2	-0.2
A2	2	-0.1	0.0	-0.1	0.0	0.0	0.0	-0.1	-0.1
A3	3	0.0	0.0	0.0	0.0	0.0	0.0	0.0	0.0
A4	4	0.1	0.0	0.1	0.0	0.0	0.1	0.1	0.0
A5	5	0.1	0.0	0.1	0.0	0.0	0.1	0.1	0.0
B1	6	-0.1	0.0	-0.1	0.0	0.0	0.0	-0.1	-0.1
B2	7	0.0	0.0	0.0	0.0	0.0	0.0	0.0	0.0
B3	8	0.0	0.0	0.0	0.0	0.0	0.0	0.0	0.0
B4	9	0.1	0.0	0.1	0.0	0.0	0.1	0.1	0.0
B5	10	0.2	0.0	0.2	0.0	0.0	0.2	0.2	0.0
C1	251	0.2	0.3	0.1	0.0	0.0	0.3	0.1	0.1
C2	252	0.0	0.1	0.0	0.0	0.0	0.1	0.0	0.0
C3	253	0.0	0.0	0.0	0.0	0.0	0.0	0.0	0.0
C4	254	-0.1	0.0	0.0	0.0	0.0	0.0	0.0	-0.1
C5	255	-0.1	0.0	0.0	0.0	0.0	0.0	0.0	-0.1
D1	306	0.1	0.1	0.1	0.0	0.0	0.1	0.1	0.0
D2	307	0.0	0.0	0.0	0.0	0.0	0.1	0.0	0.0
D3	308	0.0	0.0	0.0	0.0	0.0	0.0	0.0	0.0
D4	309	0.0	0.0	0.0	0.0	0.0	0.0	0.0	0.0
D5	310	-0.1	0.0	0.0	0.0	0.0	0.0	0.0	-0.1
E1	305	-0.1	0.0	0.0	0.0	0.0	0.0	0.0	-0.1
E2	315	-0.1	0.0	0.0	0.0	0.0	0.0	0.0	-0.1
E3	325	0.0	0.0	0.0	0.0	0.0	0.0	0.0	0.0
B4	335	0.0	0.0	0.0	0.0	0.0	0.0	0.0	0.0
E5	345	0.0	0.0	0.0	0.0	0.0	0.0	0.0	0.0
E6	355	0.0	0.0	0.0	0.0	0.0	0.0	0.0	0.0
F1	251	0.2	0.3	0.1	0.0	0.0	0.3	0.1	0.1
F2	261	0.1	0.1	0.0	0.0	0.0	0.1	0.1	0.0
F3	271	0.0	0.0	0.0	0.0	0.0	0.0	0.0	0.0
F4	281	0.0	-0.2	-0.1	0.0	0.0	0.0	-0.1	-0.2
G1	311	0.1	0.1	0.0	0.0	0.0	0.1	0.0	0.0

Table 2.10.4-2 Stress Components - 12 psig Internal Pressure + Bolt Preload; 2-D Model;  
Condition 4 (continued)

Stress Points Section <sup>1</sup> Node	Stress Components (ksi)						Principal Stresses (ksi)		
	S <sub>x</sub>	S <sub>y</sub>	S <sub>z</sub>	S <sub>xy</sub>	S <sub>yz</sub>	S <sub>xz</sub>	S1	S2	S3
G2 321	0.0	0.0	0.0	0.0	0.0	0.0	0.0	0.0	0.0
G3 331	0.0	0.0	0.0	0.0	0.0	0.0	0.0	0.0	0.0
G4 341	0.0	0.0	0.0	0.0	0.0	0.0	0.0	0.0	0.0
G5 351	0.0	0.0	0.0	0.0	0.0	0.0	0.0	0.0	0.0
H1 581	0.0	0.0	0.2	0.0	0.0	0.0	0.2	0.0	0.0
H2 582	0.0	0.1	0.2	0.0	0.0	0.0	0.2	0.1	0.0
H3 583	0.0	0.1	0.2	0.0	0.0	0.0	0.2	0.1	0.0
H4 584	0.0	0.2	0.2	0.0	0.0	0.0	0.2	0.2	0.0
I1 589	0.0	0.0	0.0	0.0	0.0	0.0	0.0	0.0	0.0
I2 590	0.0	0.0	0.0	0.0	0.0	0.0	0.0	0.0	0.0
I3 591	0.0	0.0	0.0	0.0	0.0	0.0	0.0	0.0	0.0
I4 592	0.0	0.0	0.0	0.0	0.0	0.0	0.0	0.0	0.0
I5 593	0.0	0.0	0.0	0.0	0.0	0.0	0.0	0.0	0.0
J1 971	0.0	0.1	0.2	0.0	0.0	0.0	0.2	0.1	0.0
J2 972	0.0	0.1	0.2	0.0	0.0	0.0	0.2	0.1	0.0
J3 973	0.0	0.1	0.2	0.0	0.0	0.0	0.2	0.1	0.0
J4 974	0.0	0.1	0.2	0.0	0.0	0.0	0.2	0.1	0.0
K1 979	0.0	0.0	0.0	0.0	0.0	0.0	0.0	0.0	0.0
K2 980	0.0	0.0	0.0	0.0	0.0	0.0	0.0	0.0	0.0
K3 981	0.0	0.0	0.0	0.0	0.0	0.0	0.0	0.0	0.0
K4 982	0.0	0.0	0.0	0.0	0.0	0.0	0.0	0.0	0.0
K5 983	0.0	0.0	0.0	0.0	0.0	0.0	0.0	0.0	0.0
L1 1601	0.0	0.1	0.2	0.0	0.0	0.0	0.2	0.1	0.0
L2 1602	0.0	0.1	0.2	0.0	0.0	0.0	0.2	0.1	0.0
L3 1603	0.0	0.1	0.2	0.0	0.0	0.0	0.2	0.1	0.0
L4 1604	0.0	0.1	0.2	0.0	0.0	0.0	0.2	0.1	0.0
M1 1609	0.0	0.0	0.0	0.0	0.0	0.0	0.0	0.0	0.0
M2 1610	0.0	0.0	0.0	0.0	0.0	0.0	0.0	0.0	0.0
M3 1611	0.0	0.0	0.0	0.0	0.0	0.0	0.0	0.0	0.0
M4 1612	0.0	0.0	0.0	0.0	0.0	0.0	0.0	0.0	0.0
M5 1613	0.0	0.0	0.0	0.0	0.0	0.0	0.0	0.0	0.0
N1 2216	0.0	0.1	0.2	0.0	0.0	0.0	0.2	0.1	0.0
N2 2217	0.0	0.1	0.2	0.0	0.0	0.0	0.2	0.1	0.0

Table 2.10.4-2 Stress Components – 12 psig Internal Pressure + Bolt Preload; 2-D Model;  
Condition 4 (continued)

Stress Points Section <sup>1</sup> Node		Stress Components (ksi)						Principal Stresses (ksi)		
		S <sub>x</sub>	S <sub>y</sub>	S <sub>z</sub>	S <sub>xy</sub>	S <sub>xz</sub>	S <sub>yz</sub>	S1	S2	S3
N3	2218	0.0	0.1	0.2	0.0	0.0	0.0	0.2	0.1	0.0
N4	2219	0.0	0.1	0.2	0.0	0.0	0.0	0.2	0.1	0.0
O1	2224	0.0	0.0	0.0	0.0	0.0	0.0	0.0	0.0	0.0
O2	2225	0.0	0.0	0.0	0.0	0.0	0.0	0.0	0.0	0.0
O3	2226	0.0	0.0	0.0	0.0	0.0	0.0	0.0	0.0	0.0
O4	2227	0.0	0.0	0.0	0.0	0.0	0.0	0.0	0.0	0.0
O5	2228	0.0	0.0	0.0	0.0	0.0	0.0	0.0	0.0	0.0
P1	2546	0.0	0.1	0.3	0.0	0.0	0.0	0.3	0.1	0.0
P2	2547	0.0	0.1	0.3	0.0	0.0	0.0	0.3	0.1	0.0
P3	2548	0.0	0.1	0.2	0.0	0.0	0.0	0.2	0.1	0.0
P4	2549	0.0	0.1	0.2	0.0	0.0	0.0	0.2	0.1	0.0
Q1	2554	0.0	0.1	0.0	0.0	0.0	0.0	0.1	0.0	0.0
Q2	2555	0.0	0.0	0.0	0.0	0.0	0.0	0.0	0.0	0.0
Q3	2556	0.0	0.0	0.0	0.0	0.0	0.0	0.0	0.0	0.0
Q4	2557	0.0	0.0	0.0	0.0	0.0	0.0	0.0	0.0	0.0
Q5	2558	0.0	0.0	0.0	0.0	0.0	0.0	0.0	0.0	0.0
R1	2771	-0.2	-0.8	0.0	0.2	0.0	0.0	0.0	-0.2	-0.8
R2	2772	-0.2	-0.3	0.1	0.2	0.0	0.0	0.1	0.0	-0.5
R3	2773	-0.4	0.1	0.1	0.3	0.0	0.0	0.2	0.1	-0.5
R4	2774	-0.9	1.1	0.2	0.2	0.0	0.0	1.1	0.2	-1.0
S1	2779	-0.4	0.0	0.0	-0.1	0.0	0.0	0.0	0.0	-0.4
S2	2780	-0.1	0.0	0.0	0.0	0.0	0.0	0.0	0.0	-0.2
S3	2781	-0.1	0.0	0.1	0.0	0.0	0.0	0.1	0.0	-0.1
S4	2782	0.0	0.0	0.1	0.0	0.0	0.0	0.1	0.0	0.0
S5	2783	0.0	0.1	0.1	0.0	0.0	0.0	0.1	0.1	0.0
T1	7066	0.0	0.0	0.1	0.1	0.0	0.0	0.1	0.1	-0.1
T2	7067	0.2	-0.5	0.0	0.0	0.0	0.0	0.2	0.0	-0.5
T3	7068	0.2	-0.4	0.0	0.0	0.0	0.0	0.2	0.0	-0.4
T4	7069	0.1	-0.3	0.1	0.0	0.0	0.0	0.1	0.1	-0.3
T5	7070	0.0	-0.2	0.1	0.0	0.0	0.0	0.1	0.0	-0.2
T6	7071	0.0	-0.1	0.1	0.0	0.0	0.0	0.1	0.0	-0.1
T7	7072	0.0	0.0	0.1	0.0	0.0	0.0	0.1	0.0	0.0
U1	3051	-0.1	-1.8	-0.6	0.5	0.0	0.0	0.0	-0.6	-1.9

Table 2.10.4-2 Stress Components – 12 psig Internal Pressure + Bolt Preload; 2-D Model;  
Condition 4 (continued)

Stress Points Section <sup>1</sup> Node	Stress Components (ksi)						Principal Stresses (ksi)		
	S <sub>x</sub>	S <sub>y</sub>	S <sub>z</sub>	S <sub>xy</sub>	S <sub>yz</sub>	S <sub>xz</sub>	S1	S2	S3
U2 3052	-0.4	-2.1	-0.8	0.4	0.0	0.0	-0.3	-0.8	-2.2
U3 3053	-0.1	-2.3	-0.7	0.1	0.0	0.0	-0.1	-0.7	-2.3
U4 3054	0.1	-1.7	-0.5	-0.5	0.0	0.0	0.2	-0.5	-1.9
U5 3055	-0.4	-0.9	-0.2	-0.6	0.0	0.0	0.0	-0.2	-1.3
U6 3056	1.0	0.1	0.6	-0.4	0.0	0.0	1.1	0.6	-0.1
V1 3611	1.2	0.0	0.5	0.0	0.0	0.0	1.2	0.5	0.0
V2 3612	0.7	-0.1	0.3	0.0	0.0	0.0	0.7	0.3	-0.1
V3 3613	0.4	-0.3	0.1	0.0	0.0	0.0	0.4	0.1	-0.3
V4 3614	0.1	-0.5	-0.1	0.0	0.0	0.0	0.1	-0.1	-0.5
V5 3615	-0.2	-1.1	-0.4	0.1	0.0	0.0	-0.2	-0.4	-1.1
V6 3616	-0.4	-0.5	-0.3	0.0	0.0	0.0	-0.3	-0.4	-0.5
V7 3617	-1.4	0.4	-0.4	0.0	0.0	0.0	0.4	-0.4	-1.4
W1 3241	-0.3	0.0	-0.3	0.0	0.0	0.0	0.0	-0.3	-0.3
W2 3242	-0.2	0.0	-0.2	0.0	0.0	0.0	0.0	-0.2	-0.2
W3 3243	0.0	0.0	0.0	0.0	0.0	0.0	0.0	0.0	0.0
W4 3244	0.1	0.0	0.1	0.0	0.0	0.0	0.1	0.1	0.0
W5 3245	0.2	0.0	0.2	0.0	0.0	0.0	0.2	0.2	0.0
W6 3246	0.3	0.0	0.3	0.0	0.0	0.0	0.3	0.3	0.0
X1 3801	0.0	0.0	0.0	0.0	0.0	0.0	0.0	0.0	0.0
X2 3802	0.0	0.0	0.0	0.0	0.0	0.0	0.0	0.0	0.0
X3 3803	0.0	0.0	0.0	0.0	0.0	0.0	0.0	0.0	0.0
X4 3804	0.0	0.0	0.0	0.0	0.0	0.0	0.0	0.0	0.0
X5 3805	0.0	0.0	0.0	0.0	0.0	0.0	0.0	0.0	0.0
X6 3806	0.0	0.0	0.0	0.0	0.0	0.0	0.0	0.0	0.0
X7 3807	0.0	0.0	0.0	0.0	0.0	0.0	0.0	0.0	0.0

<sup>1</sup> Refer to Figure 2.10.2-34 for the identification of the representative sections.

Table 2.10.4-3 Stress Components – Gravity; 1 g; 3-D Top Model; 0-Degree  
Circumferential Location; Condition 1

Condition 1: 100°F Ambient with Contents

Stress Points		Stress Components (ksi)						Principal Stresses (ksi)		
Section <sup>1</sup>	Node	S <sub>x</sub>	S <sub>y</sub>	S <sub>z</sub>	S <sub>xy</sub>	S <sub>yz</sub>	S <sub>xz</sub>	S1	S2	S3
A1	1949	0.0	0.0	0.0	0.0	0.0	0.0	0.0	0.0	0.0
A2	1950	0.0	0.0	0.0	0.0	0.0	0.0	0.0	0.0	0.0
A3	1951	0.0	0.0	0.0	0.0	0.0	0.0	0.0	0.0	0.0
B1	1952	0.0	0.0	0.0	0.0	0.0	0.0	0.0	0.0	0.0
B2	93	0.0	0.0	0.0	0.0	0.0	0.0	0.0	0.0	0.0
C1	1925	0.0	0.0	0.1	0.0	0.0	0.0	0.1	0.0	0.0
C2	1926	0.0	0.0	0.0	0.0	0.0	0.0	0.0	0.0	0.0
C3	1927	0.0	0.0	0.0	0.0	0.0	0.0	0.0	0.0	0.0
D1	683	0.0	0.0	0.0	0.0	0.0	0.0	0.0	0.0	0.0
D2	85	0.0	0.1	0.0	0.0	0.0	0.0	0.1	0.0	0.0
E1	682	0.0	0.0	0.0	0.0	0.0	0.0	0.0	0.0	0.0
E2	82	0.0	0.1	0.1	0.0	0.0	0.0	0.1	0.1	0.0
F1	1925	0.0	0.0	0.1	0.0	0.0	0.0	0.1	0.0	0.0
F2	1325	-0.1	-0.1	-0.3	0.0	0.0	0.0	-0.1	-0.1	-0.3
G1	680	0.0	0.0	0.1	0.0	0.0	0.0	0.1	0.0	0.0
G2	80	0.0	0.0	0.1	0.0	0.0	0.0	0.1	0.0	0.0
H1	1921	0.0	0.1	-0.1	0.0	0.0	0.0	0.1	0.0	-0.1
H2	1321	0.0	0.2	0.0	0.0	0.0	0.0	0.2	0.0	0.0
I1	676	0.0	0.0	0.1	0.0	0.0	0.0	0.1	0.0	0.0
I2	76	0.0	0.0	0.2	0.0	0.0	0.0	0.2	0.0	0.0
J1	1916	0.0	0.1	0.2	0.0	0.0	0.0	0.2	0.1	0.0
J2	1316	0.0	0.2	0.3	0.0	0.0	0.0	0.3	0.2	0.0
K1	671	0.0	0.0	0.1	0.0	0.0	0.0	0.1	0.0	0.0
K2	71	0.0	0.1	0.1	0.0	0.0	0.0	0.1	0.1	0.0
L1	1908	0.0	0.1	0.4	0.0	0.0	0.0	0.4	0.1	0.0
L2	1308	0.0	0.2	0.5	0.0	0.0	0.0	0.5	0.3	0.0
M1	663	0.0	0.0	0.1	0.0	0.0	0.0	0.1	0.0	0.0
M2	63	0.0	0.0	0.1	0.0	0.0	0.0	0.1	0.0	0.0
N1	1877	0.0	0.2	0.2	0.0	0.0	0.0	0.3	0.1	0.0

Table 2.10.4-3 Stress Components – Gravity; 1 g; 3-D Top Model; 0-Degree  
Circumferential Location; Condition 1 (continued)

Stress Points Section <sup>1</sup> Node	Stress Components (ksi)						Principal Stresses (ksi)		
	S <sub>x</sub>	S <sub>y</sub>	S <sub>z</sub>	S <sub>xy</sub>	S <sub>yz</sub>	S <sub>xz</sub>	S1	S2	S3
N2 1477	0.0	0.2	0.3	0.0	0.0	0.0	0.3	0.2	0.0
N3 1277	0.0	0.2	0.3	0.0	0.0	0.0	0.3	0.2	0.0
O1 647	0.0	0.1	0.0	0.0	0.0	0.0	0.1	0.0	0.0
O2 247	0.0	0.0	0.0	0.0	0.0	0.0	0.0	0.0	0.0
O3 47	0.0	0.0	0.0	0.0	0.0	0.0	0.0	0.0	0.0
P1 1840	0.0	0.1	-0.2	0.0	0.0	0.0	0.1	0.0	-0.2
P2 1640	0.0	0.1	-0.1	0.0	0.0	0.0	0.1	0.0	-0.1
P3 1440	0.0	0.2	0.1	0.0	0.0	0.0	0.2	0.1	0.0
P4 1240	0.0	0.2	0.3	0.0	0.0	0.0	0.3	0.2	0.0
Q1 628	0.0	-0.3	-0.3	0.0	0.0	0.0	0.0	-0.3	-0.3
Q2 428	0.0	-0.2	-0.1	0.0	0.0	0.0	0.0	-0.1	-0.2
Q3 228	0.0	-0.2	0.0	0.0	0.0	0.0	0.0	0.0	-0.2
Q4 28	0.0	-0.1	0.2	0.0	0.0	0.0	0.2	0.0	-0.1
R1 1816	-0.1	-0.2	1.6	0.0	0.0	0.1	1.6	-0.1	-0.2
R2 1616	-0.2	-0.5	0.5	0.0	0.0	0.1	0.5	-0.2	-0.5
R3 1416	-0.6	-0.9	-0.4	0.0	0.0	0.0	-0.4	-0.6	-0.9
R4 1216	-1.1	-1.3	-1.5	0.0	0.0	-0.3	-1.0	-1.3	-1.6
S1 616	-0.8	-0.7	0.4	0.0	0.0	0.3	0.5	-0.7	-0.9
S2 416	-0.5	-0.6	0.3	0.0	0.0	0.5	0.6	-0.6	-0.7
S3 216	0.0	-0.7	-0.3	0.0	0.0	0.5	0.4	-0.7	-0.7
S4 16	0.3	-0.7	-0.8	0.0	0.0	0.4	0.4	-0.7	-0.9
T1 811	0.1	-0.2	-0.5	0.0	0.0	0.1	0.1	-0.2	-0.5
T2 611	-0.3	-0.3	-0.2	0.0	0.0	0.1	-0.2	-0.3	-0.3
T3 411	-0.1	-0.2	-0.1	0.0	0.0	0.0	0.0	-0.1	-0.2
T4 211	0.0	-0.1	0.2	0.0	0.0	0.0	0.2	0.0	-0.1
T5 11	0.0	0.0	0.5	0.0	0.0	0.0	0.5	0.0	0.0
U1 43058	-0.7	-0.5	-0.4	0.0	0.0	0.0	-0.4	-0.5	-0.7
U2 43057	-0.4	-0.4	-0.3	0.0	0.0	0.0	-0.3	-0.4	-0.5
U3 43056	-0.3	-0.3	-0.2	0.0	0.0	0.1	-0.2	-0.3	-0.3
U4 43055	-0.2	-0.2	-0.1	0.0	0.0	0.0	-0.1	-0.2	-0.2
U5 43054	-0.1	-0.2	-0.1	0.0	0.0	0.0	-0.1	-0.1	-0.2



Table 2.10.4-3 Stress Components – Gravity; 1 g; 3-D Top Model; 0-Degree Circumferential Location; Condition 1 (continued)

Stress Points Section <sup>1</sup> Node	Stress Components (ksi)						Principal Stresses (ksi)		
	S <sub>x</sub>	S <sub>y</sub>	S <sub>z</sub>	S <sub>xy</sub>	S <sub>yz</sub>	S <sub>xz</sub>	S1	S2	S3
U6 43053	0.0	-0.1	-0.1	0.0	0.0	0.0	0.0	-0.1	-0.1
U7 43052	0.0	0.0	-0.1	0.0	0.0	0.0	0.0	0.0	-0.1
U8 43051	0.1	0.1	0.0	0.0	0.0	0.0	0.1	0.1	0.0
V1 50024	-0.1	-0.1	0.0	0.0	0.0	0.0	0.0	-0.1	-0.1
V2 50023	-0.1	-0.1	0.0	0.0	0.0	0.0	0.0	-0.1	-0.1
V3 50022	0.0	0.0	0.0	0.0	0.0	0.0	0.0	0.0	0.0
V4 50021	0.1	0.1	0.0	0.0	0.0	0.0	0.1	0.1	0.0
W1 43278	-0.1	-0.1	0.0	0.0	0.0	0.0	0.0	-0.1	-0.1
W2 43274	0.0	-0.1	0.0	0.0	0.0	0.0	0.0	0.0	-0.1
W3 43271	0.0	-0.1	0.0	0.0	0.0	0.0	0.0	0.0	-0.1
X1 50084	-0.1	0.0	0.0	0.0	0.0	0.0	0.0	0.0	-0.1
X2 50083	0.0	0.0	0.0	0.0	0.0	0.0	0.0	0.0	0.0
X3 50081	0.1	0.0	0.0	0.0	0.0	0.0	0.1	0.0	0.0

<sup>1</sup> Refer to Figure 2.10.2-34 for the identification of the representative sections.

Table 2.10.4-4 Stress Components – Gravity; 1 g; 3-D Top Model; 0-Degree  
Circumferential Location; Condition 4

Condition 4: -40°F Ambient, No Decay Heat

Stress Points		Stress Components (ksi)						Principal Stresses (ksi)		
Section <sup>1</sup>	Node	S <sub>x</sub>	S <sub>y</sub>	S <sub>z</sub>	S <sub>xy</sub>	S <sub>yz</sub>	S <sub>xz</sub>	S1	S2	S3
A1	1949	0.0	0.0	0.0	0.0	0.0	0.0	0.0	0.0	0.0
A2	1950	0.0	0.0	0.0	0.0	0.0	0.0	0.0	0.0	0.0
A3	1951	0.0	0.0	0.0	0.0	0.0	0.0	0.0	0.0	0.0
B1	1952	0.0	0.0	0.0	0.0	0.0	0.0	0.0	0.0	0.0
B2	93	0.0	0.0	0.0	0.0	0.0	0.0	0.0	0.0	0.0
C1	1925	0.0	0.0	0.1	0.0	0.0	0.0	0.1	0.0	0.0
C2	1926	0.0	0.0	0.0	0.0	0.0	0.0	0.0	0.0	0.0
C3	1927	0.0	0.0	0.0	0.0	0.0	0.0	0.0	0.0	0.0
D1	683	0.0	0.0	0.0	0.0	0.0	0.0	0.0	0.0	0.0
D2	85	0.0	0.1	0.0	0.0	0.0	0.0	0.1	0.0	0.0
E1	682	0.0	0.0	0.0	0.0	0.0	0.0	0.0	0.0	0.0
E2	82	0.0	0.1	0.1	0.0	0.0	0.0	0.1	0.1	0.0
F1	1925	0.0	0.0	0.1	0.0	0.0	0.0	0.1	0.0	0.0
F2	1325	-0.1	-0.1	-0.3	0.0	0.0	0.0	-0.1	-0.1	-0.3
G1	680	0.0	0.0	0.1	0.0	0.0	0.0	0.1	0.0	0.0
G2	80	0.0	0.0	0.1	0.0	0.0	0.0	0.1	0.0	0.0
H1	1921	0.0	0.1	-0.1	0.0	0.0	0.0	0.1	0.0	-0.1
H2	1321	0.0	0.2	0.1	0.0	0.0	0.0	0.2	0.0	0.0
I1	676	0.0	0.0	0.1	0.0	0.0	0.0	0.1	0.0	0.0
I2	76	0.0	0.0	0.2	0.0	0.0	0.0	0.2	0.0	0.0
J1	1916	0.0	0.1	0.2	0.0	0.0	0.0	0.2	0.1	0.0
J2	1316	0.0	0.2	0.3	0.0	0.0	0.0	0.3	0.2	0.0
K1	671	0.0	0.0	0.1	0.0	0.0	0.0	0.1	0.0	0.0
K2	71	0.0	0.1	0.1	0.0	0.0	0.0	0.1	0.1	0.0
L1	1908	0.0	0.1	0.4	0.0	0.0	0.0	0.4	0.1	0.0
L2	1308	0.0	0.2	0.5	0.0	0.0	0.0	0.5	0.3	0.0
M1	663	0.0	0.0	0.1	0.0	0.0	0.0	0.1	0.0	0.0
M2	63	0.0	0.0	0.1	0.0	0.0	0.0	0.1	0.0	0.0
N1	1877	0.0	0.1	0.2	0.0	0.0	0.0	0.3	0.1	0.0

Table 2.10.4-4 Stress Components – Gravity; 1 g; 3-D Top Model; 0-Degree  
Circumferential Location; Condition 4 (continued)

Stress Points		Stress Components (ksi)						Principal Stresses (ksi)		
Section <sup>1</sup>	Node	S <sub>x</sub>	S <sub>y</sub>	S <sub>z</sub>	S <sub>xy</sub>	S <sub>yz</sub>	S <sub>xz</sub>	S1	S2	S3
N2	1477	0.0	0.2	0.3	0.0	0.0	0.0	0.3	0.2	0.0
N3	1277	0.0	0.2	0.3	0.0	0.0	0.0	0.3	0.2	0.0
O1	647	0.0	0.1	0.0	0.0	0.0	0.0	0.1	0.0	0.0
O2	247	0.0	0.0	0.0	0.0	0.0	0.0	0.0	0.0	0.0
O3	47	0.0	0.0	0.0	0.0	0.0	0.0	0.0	0.0	0.0
P1	1840	0.0	0.1	-0.2	0.0	0.0	0.0	0.1	0.0	-0.2
P2	1640	0.0	0.1	-0.1	0.0	0.0	0.0	0.1	0.0	-0.1
P3	1440	0.0	0.2	0.1	0.0	0.0	0.0	0.2	0.1	0.0
P4	1240	0.0	0.2	0.3	0.0	0.0	0.0	0.3	0.2	0.0
Q1	628	0.0	-0.3	-0.3	0.0	0.0	0.0	0.0	-0.3	-0.3
Q2	428	0.0	-0.2	-0.1	0.0	0.0	0.0	0.0	-0.1	-0.2
Q3	228	0.0	-0.2	0.0	0.0	0.0	0.0	0.0	0.0	-0.2
Q4	28	0.0	-0.1	0.2	0.0	0.0	0.0	0.2	0.0	-0.1
R1	1816	-0.1	-0.2	1.6	0.0	0.0	0.1	1.6	-0.1	-0.2
R2	1616	-0.2	-0.5	0.5	0.0	0.0	0.1	0.5	-0.2	-0.5
R3	1416	-0.6	-0.9	-0.4	0.0	0.0	0.0	-0.4	-0.6	-0.9
R4	1216	-1.1	-1.3	-1.5	0.0	0.0	-0.3	-1.0	-1.3	-1.6
S1	616	-0.8	-0.7	0.4	0.0	0.0	0.3	0.5	-0.7	-0.9
S2	416	-0.5	-0.6	0.3	0.0	0.0	0.5	0.5	-0.6	-0.7
S3	216	0.0	-0.7	-0.3	0.0	0.0	0.5	0.4	-0.7	-0.7
S4	16	0.3	-0.7	-0.8	0.0	0.0	0.4	0.4	-0.7	-0.9
T1	811	0.1	-0.2	-0.5	0.0	0.0	0.1	0.1	-0.2	-0.5
T2	611	-0.3	-0.3	-0.2	0.0	0.0	0.1	-0.2	-0.3	-0.3
T3	411	-0.1	-0.2	-0.1	0.0	0.0	0.0	0.0	-0.1	-0.2
T4	211	0.0	-0.1	0.2	0.0	0.0	0.0	0.2	0.0	-0.1
T5	11	0.0	0.0	0.5	0.0	0.0	0.0	0.5	0.0	0.0
U1	43058	-0.7	-0.5	-0.4	0.0	0.0	0.0	-0.4	-0.5	-0.7
U2	43057	-0.4	-0.4	-0.3	0.0	0.0	0.0	-0.3	-0.4	-0.5
U3	43056	-0.3	-0.3	-0.2	0.0	0.0	0.1	-0.2	-0.3	-0.3
U4	43055	-0.2	-0.2	-0.1	0.0	0.0	0.0	-0.1	-0.2	-0.2
U5	43054	-0.1	-0.2	-0.1	0.0	0.0	0.0	-0.1	-0.1	-0.2

Table 2.10.4-4 Stress Components – Gravity; 1 g; 3-D Top Model; 0-Degree Circumferential Location; Condition 4 (continued)

Stress Points Section <sup>1</sup> Node	Stress Components (ksi)						Principal Stresses (ksi)		
	S <sub>x</sub>	S <sub>y</sub>	S <sub>z</sub>	S <sub>xy</sub>	S <sub>yz</sub>	S <sub>xz</sub>	S1	S2	S3
U6 43053	0.0	-0.1	-0.1	0.0	0.0	0.0	0.0	-0.1	-0.1
U7 43052	0.0	0.0	-0.1	0.0	0.0	0.0	0.0	0.0	-0.1
U8 43051	0.1	0.1	0.0	0.0	0.0	0.0	0.1	0.1	0.0
V1 50024	-0.1	-0.1	0.0	0.0	0.0	0.0	0.0	-0.1	-0.1
V2 50023	-0.1	-0.1	0.0	0.0	0.0	0.0	0.0	-0.1	-0.1
V3 50022	0.0	0.0	0.0	0.0	0.0	0.0	0.0	0.0	0.0
V4 50021	0.1	0.1	0.0	0.0	0.0	0.0	0.1	0.1	0.0
W1 43278	-0.1	-0.1	0.0	0.0	0.0	0.0	0.0	-0.1	-0.1
W2 43274	0.0	-0.1	0.0	0.0	0.0	0.0	0.0	0.0	-0.1
W3 43271	0.0	-0.1	0.0	0.0	0.0	0.0	0.0	0.0	-0.1
X1 50084	-0.1	0.0	0.0	0.0	0.0	0.0	0.0	0.0	-0.1
X2 50083	0.0	0.0	0.0	0.0	0.0	0.0	0.0	0.0	0.0
X3 50081	0.1	0.0	0.0	0.0	0.0	0.0	0.1	0.0	0.0

<sup>1</sup> Refer to Figure 2.10.2-34 for the identification of the representative sections.

Table 2.10.4-5 Stress Components – Thermal Heat, 100°F; 2-D Model; Condition 1

Condition 1: 100°F Ambient with Contents

Stress Points		Stress Components (ksi)						Principal Stresses (ksi)		
Section <sup>1</sup>	Node	S <sub>x</sub>	S <sub>y</sub>	S <sub>z</sub>	S <sub>xy</sub>	S <sub>yz</sub>	S <sub>xz</sub>	S1	S2	S3
A1	1	0.8	0.0	0.8	0.0	0.0	0.0	0.8	0.8	0.0
A2	2	0.1	0.0	0.1	0.0	0.0	0.0	0.1	0.1	0.0
A3	3	-0.5	0.0	-0.5	0.0	0.0	0.0	0.0	-0.5	-0.5
A4	4	-1.2	0.0	-1.2	0.0	0.0	0.0	0.0	-1.2	-1.2
A5	5	-1.8	0.0	-1.8	0.0	0.0	0.0	0.0	-1.8	-1.8
B1	6	0.8	0.0	0.8	0.0	0.0	0.0	0.8	0.8	0.0
B2	7	1.1	0.0	1.1	0.0	0.0	0.0	1.1	1.1	0.0
B3	8	1.3	0.0	1.3	0.0	0.0	0.0	1.3	1.3	0.0
B4	9	1.6	0.0	1.6	0.0	0.0	0.0	1.6	1.6	0.0
B5	10	1.8	0.0	1.8	0.0	0.0	0.0	1.8	1.8	0.0
C1	251	-0.7	-2.7	-0.5	-0.5	0.0	0.0	-0.5	-0.5	-2.8
C2	252	0.1	-1.2	-0.3	-0.4	0.0	0.0	0.3	-0.3	-1.4
C3	253	-0.3	-0.9	-0.8	-0.4	0.0	0.0	-0.1	-0.8	-1.1
C4	254	-0.6	-1.0	-1.3	-0.3	0.0	0.0	-0.5	-1.1	-1.3
C5	255	-1.2	-1.0	-1.9	-0.1	0.0	0.0	-1.0	-1.2	-1.9
D1	306	5.7	6.6	3.5	2.0	0.0	0.0	8.2	4.1	3.5
D2	307	1.0	3.7	1.5	1.3	0.0	0.0	4.3	1.5	0.5
D3	308	0.3	1.4	0.9	0.4	0.0	0.0	1.5	0.9	0.2
D4	309	-0.5	0.5	0.6	0.1	0.0	0.0	0.6	0.5	-0.5
D5	310	-1.7	0.2	0.4	0.0	0.0	0.0	0.4	0.2	-1.7
E1	305	-1.0	3.6	0.3	0.6	0.0	0.0	3.7	0.3	-1.1
E2	315	-0.7	2.4	0.2	1.5	0.0	0.0	3.1	0.2	-1.3
E3	325	0.0	1.5	0.2	1.7	0.0	0.0	2.6	0.2	-1.1
E4	335	0.1	0.8	0.1	1.4	0.0	0.0	1.8	0.1	-1.0
E5	345	0.1	0.0	-0.1	0.8	0.0	0.0	0.8	-0.1	-0.8
E6	355	0.1	-1.0	-0.3	0.5	0.0	0.0	0.3	-0.3	-1.1
F1	251	-0.7	-2.7	-0.5	-0.5	0.0	0.0	-0.5	-0.5	-2.8
F2	261	-0.2	-0.9	0.1	-0.4	0.0	0.0	0.1	0.0	-1.1
F3	271	0.7	0.5	0.6	-0.6	0.0	0.0	1.2	0.6	-0.1
F4	281	1.0	2.5	1.0	-1.2	0.0	0.0	3.1	1.0	0.4
G1	311	-3.5	0.5	-0.8	1.5	0.0	0.0	1.1	-0.8	-4.1
G2	321	-3.2	3.4	0.1	1.1	0.0	0.0	3.6	0.1	-3.4

Table 2.10.4-5 Stress Components - Thermal Heat, 100°F; 2-D Model; Condition 1  
(continued)

Stress Points Section <sup>1</sup> Node		Stress Components (ksi)						Principal Stresses (ksi)		
		S <sub>x</sub>	S <sub>y</sub>	S <sub>z</sub>	S <sub>xy</sub>	S <sub>xz</sub>	S <sub>yz</sub>	S1	S2	S3
G3	331	-1.6	4.7	0.9	0.2	0.0	0.0	4.7	0.9	-1.6
G4	341	-0.6	6.0	1.5	-0.1	0.0	0.0	6.0	1.5	-0.6
G5	351	-0.2	7.9	2.2	-0.1	0.0	0.0	7.9	2.2	-0.2
H1	581	0.0	1.1	-0.2	0.1	0.0	0.0	1.1	0.0	-0.2
H2	582	0.0	0.4	-0.3	0.1	0.0	0.0	0.4	0.0	-0.3
H3	583	0.0	-0.2	-0.3	0.1	0.0	0.0	0.1	-0.3	-0.3
H4	584	-0.1	-1.0	-0.4	0.1	0.0	0.0	-0.1	-0.4	-1.0
I1	589	-0.3	5.7	2.1	0.1	0.0	0.0	5.7	2.1	-0.3
I2	590	-0.2	5.8	2.3	0.1	0.0	0.0	5.8	2.3	-0.2
I3	591	-0.1	5.8	2.4	0.1	0.0	0.0	5.9	2.4	-0.2
I4	592	-0.1	5.9	2.5	0.1	0.0	0.0	5.9	2.5	-0.1
I5	593	0.0	5.9	2.7	0.1	0.0	0.0	5.9	2.7	0.0
J1	971	0.0	-1.8	-1.1	0.0	0.0	0.0	0.0	-1.1	-1.8
J2	972	0.0	-0.6	-0.4	0.0	0.0	0.0	0.0	-0.4	-0.6
J3	973	0.0	0.7	0.4	0.0	0.0	0.0	0.7	0.4	0.0
J4	974	0.0	1.9	1.1	0.0	0.0	0.0	1.9	1.1	0.0
K1	979	-0.3	3.6	3.7	0.0	0.0	0.0	3.7	3.6	-0.3
K2	980	-0.2	4.7	4.3	0.0	0.0	0.0	4.7	4.3	-0.2
K3	981	-0.2	5.8	4.9	0.0	0.0	0.0	5.8	4.9	-0.2
K4	982	-0.1	6.9	5.5	0.0	0.0	0.0	6.9	5.5	-0.1
K5	983	0.0	7.9	6.0	0.0	0.0	0.0	7.9	6.0	0.0
L1	1601	0.0	-1.3	-1.1	0.0	0.0	0.0	0.0	-1.1	-1.3
L2	1602	0.0	-0.4	-0.3	0.0	0.0	0.0	0.0	-0.3	-0.4
L3	1603	0.0	0.5	0.4	0.0	0.0	0.0	0.5	0.4	0.0
L4	1604	0.0	1.4	1.1	0.0	0.0	0.0	1.4	1.1	0.0
M1	1609	-0.4	3.8	4.6	0.0	0.0	0.0	4.6	3.8	-0.4
M2	1610	-0.3	4.8	5.3	0.0	0.0	0.0	5.3	4.8	-0.3
M3	1611	-0.2	5.8	5.9	0.0	0.0	0.0	5.9	5.8	-0.2
M4	1612	-0.1	6.9	6.6	0.0	0.0	0.0	6.9	6.6	-0.1
M5	1613	0.0	7.9	7.2	0.0	0.0	0.0	7.9	7.2	0.0
N1	2216	0.0	-1.6	-1.4	0.0	0.0	0.0	0.0	-1.4	-1.6
N2	2217	0.0	-0.5	-0.7	0.0	0.0	0.0	0.0	-0.5	-0.7
N3	2218	0.0	0.6	-0.1	0.0	0.0	0.0	0.6	0.0	-0.1

Table 2.10.4-5 Stress Components – Thermal Heat, 100°F; 2-D Model; Condition 1  
(continued)

Stress Points		Stress Components (ksi)						Principal Stresses (ksi)		
Section <sup>1</sup>	Node	S <sub>x</sub>	S <sub>y</sub>	S <sub>z</sub>	S <sub>xy</sub>	S <sub>yz</sub>	S <sub>xz</sub>	S1	S2	S3
N4	2219	0.0	1.7	0.6	0.0	0.0	0.0	1.7	0.6	0.0
O1	2224	-0.3	4.2	3.7	0.0	0.0	0.0	4.2	3.7	-0.3
O2	2225	-0.2	5.0	4.2	0.0	0.0	0.0	5.0	4.2	-0.2
O3	2226	-0.2	5.8	4.8	0.0	0.0	0.0	5.8	4.8	-0.2
O4	2227	-0.1	6.6	5.3	0.0	0.0	0.0	6.6	5.3	-0.1
O5	2228	0.0	7.4	5.7	0.0	0.0	0.0	7.4	5.7	0.0
P1	2546	0.0	-0.3	-0.5	0.0	0.0	0.0	0.0	-0.4	-0.5
P2	2547	0.0	-0.1	-0.2	0.0	0.0	0.0	0.0	-0.1	-0.2
P3	2548	0.1	0.2	0.0	0.0	0.0	0.0	0.2	0.1	0.0
P4	2549	-0.2	0.4	0.2	0.1	0.0	0.0	0.5	0.2	-0.2
Q1	2554	-0.1	5.1	2.3	0.0	0.0	0.0	5.1	2.3	-0.1
Q2	2555	-0.1	5.4	2.6	0.1	0.0	0.0	5.4	2.6	-0.1
Q3	2556	-0.1	5.8	2.9	0.1	0.0	0.0	5.8	2.9	-0.1
Q4	2557	0.0	6.2	3.2	0.1	0.0	0.0	6.2	3.2	0.0
Q5	2558	0.0	6.6	3.4	0.0	0.0	0.0	6.6	3.4	0.0
R1	2771	-0.3	3.4	-3.0	0.1	0.0	0.0	3.4	-0.3	-3.0
R2	2772	-0.7	0.9	-3.2	0.1	0.0	0.0	0.9	-0.7	-3.2
R3	2773	-1.6	-1.0	-3.5	0.2	0.0	0.0	-1.0	-1.7	-3.5
R4	2774	-3.0	-3.4	-3.9	0.0	0.0	0.0	-3.0	-3.4	-3.9
S1	2779	2.5	8.3	2.0	-2.2	0.0	0.0	9.1	2.0	1.8
S2	2780	2.3	6.2	1.7	-0.9	0.0	0.0	6.4	2.1	1.7
S3	2781	1.2	4.4	1.2	0.3	0.0	0.0	4.5	1.2	1.2
S4	2782	0.5	2.7	0.8	0.4	0.0	0.0	2.8	0.8	0.4
S5	2783	0.3	0.7	0.5	0.3	0.0	0.0	0.8	0.5	0.1
T1	7066	-1.8	-5.8	-0.7	-1.8	0.0	0.0	-0.7	-1.1	-6.5
T2	7067	-1.6	-3.1	0.2	-1.1	0.0	0.0	0.2	-1.1	-3.6
T3	7068	-1.2	-0.9	1.0	-0.6	0.0	0.0	1.0	-0.4	-1.7
T4	7069	-0.7	0.7	1.6	-0.3	0.0	0.0	1.6	0.8	-0.8
T5	7070	-0.4	2.2	2.2	-0.2	0.0	0.0	2.2	2.2	-0.4
T6	7071	-0.2	3.8	2.8	0.0	0.0	0.0	3.8	2.8	-0.2
T7	7072	-0.1	5.6	3.4	0.0	0.0	0.0	5.6	3.4	-0.1
U1	3051	-0.7	-1.2	-2.1	0.0	0.0	0.0	-0.7	-1.2	-2.1
U2	3052	0.2	-0.8	-1.6	-0.1	0.0	0.0	0.2	-0.9	-1.6

Table 2.10.4-5 Stress Components – Thermal Heat, 100°F; 2-D Model; Condition 1  
(continued)

Stress Points Section <sup>1</sup> Node	Stress Components (ksi)						Principal Stresses (ksi)		
	S <sub>x</sub>	S <sub>y</sub>	S <sub>z</sub>	S <sub>xy</sub>	S <sub>yz</sub>	S <sub>xz</sub>	S1	S2	S3
U3 3053	0.2	-0.4	-1.3	-0.2	0.0	0.0	0.2	-0.4	-1.3
U4 3054	0.2	-0.1	-1.2	-0.3	0.0	0.0	0.3	-0.3	-1.2
U5 3055	0.1	0.3	-1.0	-0.2	0.0	0.0	0.4	-0.1	-1.0
U6 3056	0.5	0.0	-0.8	0.0	0.0	0.0	0.5	-0.1	-0.8
V1 3611	0.1	0.0	-2.1	0.0	0.0	0.0	0.2	-0.1	-2.1
V2 3612	0.2	-0.1	-1.5	-0.1	0.0	0.0	0.2	-0.1	-1.5
V3 3613	0.1	-0.2	-1.0	-0.2	0.0	0.0	0.2	-0.3	-1.0
V4 3614	0.1	-0.4	-0.6	-0.2	0.0	0.0	0.2	-0.4	-0.6
V5 3615	0.1	-0.7	-0.2	-0.1	0.0	0.0	0.2	-0.2	-0.7
V6 3616	0.1	-0.3	0.3	-0.1	0.0	0.0	0.3	0.1	-0.3
V7 3617	-0.2	0.3	0.9	0.0	0.0	0.0	0.9	0.3	-0.2
W1 3241	1.9	0.0	1.9	0.0	0.0	0.0	1.9	1.9	0.0
W2 3242	1.7	0.0	1.7	0.0	0.0	0.0	1.7	1.7	0.0
W3 3243	1.4	0.0	1.4	0.0	0.0	0.0	1.4	1.4	0.0
W4 3244	1.2	0.0	1.2	0.0	0.0	0.0	1.2	1.2	0.0
W5 3245	1.0	0.0	1.0	0.0	0.0	0.0	1.0	1.0	0.0
W6 3246	0.7	0.0	0.7	0.0	0.0	0.0	0.7	0.7	0.0
X1 3801	-1.8	0.0	-1.8	0.0	0.0	0.0	0.0	-1.8	-1.8
X2 3802	-1.1	0.0	-1.1	0.0	0.0	0.0	0.0	-1.1	-1.1
X3 3803	-0.3	0.0	-0.3	0.0	0.0	0.0	0.0	-0.3	-0.3
X4 3804	0.4	0.0	0.4	0.0	0.0	0.0	0.4	0.4	0.0
X5 3805	1.2	0.0	1.2	0.0	0.0	0.0	1.2	1.2	0.0
X6 3806	2.0	0.0	2.0	0.0	0.0	0.0	2.0	2.0	0.0
X7 3807	2.8	-0.1	2.8	0.0	0.0	0.0	2.8	2.8	-0.1

<sup>1</sup> Refer to Figure 2.10.2-34 for the identification of the representative sections.



Table 2.10.4-6 Stress Components – Thermal Cold, -20°F; 2-D Model; Condition 2

Condition 2: -20°F Ambient with Contents

Stress Points		Stress Components (ksi)						Principal Stresses (ksi)		
Section <sup>1</sup>	Node	S <sub>x</sub>	S <sub>y</sub>	S <sub>z</sub>	S <sub>xy</sub>	S <sub>yz</sub>	S <sub>xz</sub>	S1	S2	S3
A1	1	0.0	0.0	0.0	0.0	0.0	0.0	0.0	0.0	0.0
A2	2	-0.3	0.0	-0.3	0.0	0.0	0.0	0.0	-0.3	-0.3
A3	3	-0.6	0.0	-0.6	0.0	0.0	0.0	0.0	-0.6	-0.6
A4	4	-0.9	0.0	-0.9	0.0	0.0	0.0	0.0	-0.9	-0.9
A5	5	-1.2	0.0	-1.2	0.0	0.0	0.0	0.0	-1.2	-1.2
B1	6	1.6	0.0	1.6	0.0	0.0	0.0	1.6	1.6	0.0
B2	7	1.3	0.0	1.3	0.0	0.0	0.0	1.3	1.3	0.0
B3	8	0.9	0.0	0.9	0.0	0.0	0.0	0.9	0.9	0.0
B4	9	0.6	0.0	0.6	0.0	0.0	0.0	0.6	0.6	0.0
B5	10	0.2	0.0	0.2	0.0	0.0	0.0	0.2	0.2	0.0
C1	251	-0.4	-0.1	-0.6	-0.1	0.0	0.0	-0.1	-0.5	-0.6
C2	252	-0.6	-0.3	-0.8	-0.1	0.0	0.0	-0.3	-0.6	-0.8
C3	253	-0.6	-0.3	-0.9	0.0	0.0	0.0	-0.3	-0.6	-0.9
C4	254	-0.7	-0.2	-0.9	0.0	0.0	0.0	-0.2	-0.7	-0.9
C5	255	-0.3	-0.1	-0.9	0.0	0.0	0.0	-0.1	-0.4	-0.9
D1	306	2.2	-1.1	0.9	0.7	0.0	0.0	2.4	0.9	-1.3
D2	307	1.1	0.0	0.8	0.1	0.0	0.0	1.2	0.8	0.0
D3	308	0.9	0.0	0.6	-0.1	0.0	0.0	0.9	0.6	0.0
D4	309	-1.0	-0.5	-1.4	-0.1	0.0	0.0	-0.5	-1.0	-1.4
D5	310	0.6	0.2	0.2	0.0	0.0	0.0	0.6	0.2	0.2
E1	305	-3.0	-3.3	-1.7	1.2	0.0	0.0	-1.7	-1.9	-4.4
E2	315	-1.7	-0.3	-0.3	0.9	0.0	0.0	0.2	-0.3	-2.2
E3	325	-1.0	0.4	0.1	0.8	0.0	0.0	0.8	0.1	-1.3
E4	335	-0.5	1.2	0.5	0.6	0.0	0.0	1.4	0.5	-0.7
E5	345	-0.2	2.0	0.8	0.4	0.0	0.0	2.1	0.8	-0.3
E6	355	-0.1	3.0	1.1	0.2	0.0	0.0	3.0	1.1	-0.1
F1	251	-0.4	-0.1	-0.6	-0.1	0.0	0.0	-0.1	-0.5	-0.6
F2	261	-0.4	-0.7	-0.8	-0.1	0.0	0.0	-0.4	-0.8	-0.8
F3	271	-0.7	-1.6	-1.3	0.0	0.0	0.0	-0.7	-1.3	-1.6
F4	281	-1.0	-2.3	-1.8	0.1	0.0	0.0	-1.0	-1.8	-2.4
G1	311	-0.6	1.9	-0.5	0.7	0.0	0.0	2.0	-0.5	-0.8
G2	321	-0.3	2.5	-0.1	0.3	0.0	0.0	2.5	-0.1	-0.3

Table 2.10.4-6 Stress Components - Thermal Cold, -20°F; 2-D Model; Condition 2  
(continued)

Stress Points		Stress Components (ksi)						Principal Stresses (ksi)		
Section <sup>1</sup>	Node	S <sub>x</sub>	S <sub>y</sub>	S <sub>z</sub>	S <sub>xy</sub>	S <sub>yz</sub>	S <sub>xz</sub>	S1	S2	S3
G3	331	-0.1	2.7	0.1	-0.1	0.0	0.0	2.7	0.1	-0.1
G4	341	-0.1	3.0	0.2	-0.2	0.0	0.0	3.0	0.2	-0.1
G5	351	0.0	3.3	0.3	-0.1	0.0	0.0	3.3	0.3	0.0
H1	581	0.0	-1.1	-0.4	0.0	0.0	0.0	0.0	-0.4	-1.1
H2	582	0.0	-1.6	-0.5	0.1	0.0	0.0	0.0	-0.5	-1.6
H3	583	0.0	-2.0	-0.4	0.1	0.0	0.0	0.0	-0.4	-2.0
H4	584	-0.1	-2.7	-0.6	0.2	0.0	0.0	-0.1	-0.6	-2.7
I1	589	0.0	3.3	-0.2	0.0	0.0	0.0	3.3	0.0	-0.2
I2	590	0.0	3.3	-0.1	0.1	0.0	0.0	3.3	0.0	-0.1
I3	591	0.0	3.2	0.0	0.1	0.0	0.0	3.2	0.0	0.0
I4	592	0.0	3.2	0.2	0.1	0.0	0.0	3.2	0.2	0.0
I5	593	0.0	3.1	0.3	0.0	0.0	0.0	3.1	0.3	0.0
J1	971	0.0	-3.5	-1.0	0.0	0.0	0.0	0.0	-1.0	-3.5
J2	972	0.0	-2.4	-0.3	0.0	0.0	0.0	0.0	-0.3	-2.4
J3	973	0.0	-1.4	0.4	0.0	0.0	0.0	0.4	0.0	-1.4
J4	974	0.0	-0.4	1.1	0.0	0.0	0.0	1.1	0.0	-0.4
K1	979	-0.1	1.0	-0.7	0.0	0.0	0.0	1.0	-0.1	-0.7
K2	980	-0.1	2.1	0.0	0.0	0.0	0.0	2.1	0.0	-0.1
K3	981	-0.1	3.2	0.7	0.1	0.0	0.0	3.2	0.7	-0.1
K4	982	0.0	4.3	1.3	0.0	0.0	0.0	4.3	1.3	0.0
K5	983	0.0	5.3	1.9	0.0	0.0	0.0	5.3	1.9	0.0
L1	1601	0.0	-3.3	-1.1	0.0	0.0	0.0	0.0	-1.1	-3.3
L2	1602	0.0	-2.4	-0.3	0.0	0.0	0.0	0.0	-0.3	-2.4
L3	1603	0.0	-1.5	0.4	0.0	0.0	0.0	0.4	0.0	-1.5
L4	1604	0.0	-0.6	1.1	0.0	0.0	0.0	1.1	0.0	-0.6
M1	1609	-0.1	1.1	0.3	0.0	0.0	0.0	1.1	0.3	-0.1
M2	1610	-0.1	2.2	1.1	0.0	0.0	0.0	2.2	1.1	-0.1
M3	1611	-0.1	3.2	1.8	0.0	0.0	0.0	3.2	1.8	-0.1
M4	1612	0.0	4.2	2.5	0.0	0.0	0.0	4.2	2.5	0.0
M5	1613	0.0	5.3	3.2	0.0	0.0	0.0	5.3	3.2	0.0
N1	2216	0.0	-3.2	-1.1	0.0	0.0	0.0	0.0	-1.1	-3.2
N2	2217	0.0	-2.3	-0.5	0.0	0.0	0.0	0.0	-0.5	-2.3
N3	2218	0.0	-1.5	0.1	0.0	0.0	0.0	0.1	0.0	-1.5

Table 2.10.4-6 Stress Components - Thermal Cold, -20°F; 2-D Model; Condition 2  
(continued)

Stress Points		Stress Components (ksi)						Principal Stresses (ksi)		
Section <sup>1</sup>	Node	S <sub>x</sub>	S <sub>y</sub>	S <sub>z</sub>	S <sub>xy</sub>	S <sub>yz</sub>	S <sub>xz</sub>	S1	S2	S3
N4	2219	0.0	-0.7	0.7	0.0	0.0	0.0	0.7	0.0	-0.7
O1	2224	-0.1	1.6	-0.5	0.0	0.0	0.0	1.6	-0.1	-0.5
O2	2225	-0.1	2.4	0.0	0.0	0.0	0.0	2.4	0.0	-0.1
O3	2226	-0.1	3.2	0.6	0.0	0.0	0.0	3.2	0.6	-0.1
O4	2227	0.0	4.0	1.2	0.0	0.0	0.0	4.0	1.2	0.0
O5	2228	0.0	4.8	1.7	0.0	0.0	0.0	4.8	1.7	0.0
P1	2546	0.0	-2.4	-0.6	0.0	0.0	0.0	0.0	-0.6	-2.4
P2	2547	0.0	-2.1	-0.3	0.0	0.0	0.0	0.0	-0.3	-2.1
P3	2548	0.1	-1.6	0.0	0.0	0.0	0.0	0.1	0.0	-1.6
P4	2549	-0.2	-1.4	0.1	0.0	0.0	0.0	0.1	-0.2	-1.4
Q1	2554	0.0	2.8	-0.8	0.0	0.0	0.0	2.8	0.0	-0.8
Q2	2555	0.0	3.0	-0.5	0.0	0.0	0.0	3.0	0.0	-0.5
Q3	2556	0.0	3.2	-0.2	0.0	0.0	0.0	3.2	0.0	-0.2
Q4	2557	0.0	3.4	0.0	0.0	0.0	0.0	3.4	0.0	0.0
Q5	2558	0.0	3.6	0.3	0.0	0.0	0.0	3.6	0.3	0.0
R1	2771	-0.3	3.8	-3.2	0.1	0.0	0.0	3.8	-0.3	-3.2
R2	2772	-0.8	0.4	-3.7	0.1	0.0	0.0	0.5	-0.8	-3.7
R3	2773	-1.7	-2.2	-4.2	-0.2	0.0	0.0	-1.6	-2.2	-4.2
R4	2774	-2.7	-5.3	-4.7	-0.7	0.0	0.0	-2.5	-4.7	-5.5
S1	2779	1.2	4.0	0.1	-0.9	0.0	0.0	4.3	0.9	0.1
S2	2780	1.1	3.3	0.2	-0.2	0.0	0.0	3.3	1.0	0.2
S3	2781	0.6	2.6	0.2	0.3	0.0	0.0	2.7	0.5	0.2
S4	2782	0.2	1.9	0.2	0.3	0.0	0.0	2.0	0.2	0.2
S5	2783	0.1	1.2	0.2	0.2	0.0	0.0	1.2	0.2	0.1
T1	7066	-1.9	-4.5	-0.9	-1.3	0.0	0.0	-0.9	-1.3	-5.0
T2	7067	-1.5	-2.3	-0.2	-0.8	0.0	0.0	-0.2	-1.1	-2.8
T3	7068	-1.1	-0.7	0.5	-0.4	0.0	0.0	0.5	-0.5	-1.3
T4	7069	-0.6	0.5	1.0	-0.2	0.0	0.0	1.0	0.6	-0.7
T5	7070	-0.3	1.7	1.5	-0.1	0.0	0.0	1.7	1.5	-0.3
T6	7071	-0.2	2.9	2.0	0.0	0.0	0.0	2.9	2.0	-0.2
T7	7072	-0.1	4.2	2.5	0.0	0.0	0.0	4.2	2.5	-0.1
U1	3051	0.1	-0.6	-2.0	0.0	0.0	0.0	0.1	-0.6	-2.0
U2	3052	0.3	-0.4	-1.7	0.0	0.0	0.0	0.3	-0.4	-1.7

Table 2.10.4-6 Stress Components - Thermal Cold, -20°F; 2-D Model; Condition 2  
(continued)

Stress Points Section <sup>1</sup> Node		Stress Components (ksi)						Principal Stresses (ksi)		
		S <sub>x</sub>	S <sub>y</sub>	S <sub>z</sub>	S <sub>xy</sub>	S <sub>yz</sub>	S <sub>xz</sub>	S1	S2	S3
U3	3053	0.2	-0.2	-1.5	0.0	0.0	0.0	0.2	-0.2	-1.5
U4	3054	0.1	-0.2	-1.4	0.0	0.0	0.0	0.1	-0.2	-1.4
U5	3055	0.0	-0.1	-1.3	0.0	0.0	0.0	0.0	-0.1	-1.3
U6	3056	0.0	-0.1	-1.2	-0.1	0.0	0.0	0.1	-0.2	-1.2
V1	3611	0.0	0.0	-0.7	0.0	0.0	0.0	0.0	0.0	-0.7
V2	3612	0.1	0.0	-0.6	0.0	0.0	0.0	0.1	0.0	-0.6
V3	3613	0.1	0.0	-0.6	0.0	0.0	0.0	0.1	0.0	-0.6
V4	3614	0.1	0.0	-0.6	0.0	0.0	0.0	0.1	-0.1	-0.6
V5	3615	0.0	-0.1	-0.6	0.0	0.0	0.0	0.0	-0.1	-0.6
V6	3616	0.0	0.0	-0.6	0.0	0.0	0.0	0.0	0.0	-0.6
V7	3617	0.0	0.0	-0.6	0.0	0.0	0.0	0.0	0.0	-0.6
W1	3241	1.1	0.0	1.1	0.0	0.0	0.0	1.1	1.1	0.0
W2	3242	1.0	0.0	1.0	0.0	0.0	0.0	1.0	1.0	0.0
W3	3243	0.9	0.0	0.9	0.0	0.0	0.0	0.9	0.9	0.0
W4	3244	0.8	0.0	0.8	0.0	0.0	0.0	0.8	0.8	0.0
W5	3245	0.6	0.0	0.6	0.0	0.0	0.0	0.6	0.6	0.0
W6	3246	0.5	0.0	0.5	0.0	0.0	0.0	0.5	0.5	0.0
X1	3801	0.5	0.0	0.5	0.0	0.0	0.0	0.5	0.5	0.0
X2	3802	0.5	0.0	0.5	0.0	0.0	0.0	0.5	0.5	0.0
X3	3803	0.5	0.0	0.5	0.0	0.0	0.0	0.5	0.5	0.0
X4	3804	0.4	0.0	0.4	0.0	0.0	0.0	0.4	0.4	0.0
X5	3805	0.4	0.0	0.4	0.0	0.0	0.0	0.4	0.4	0.0
X6	3806	0.4	0.0	0.4	0.0	0.0	0.0	0.4	0.4	0.0
X7	3807	0.4	0.0	0.4	0.0	0.0	0.0	0.4	0.4	0.0

<sup>1</sup> Refer to Figure 2.10.2-34 for the identification of the representative sections.

Table 2.10.4-7 Stress Components – Thermal Cold, -40°F; 2-D Model; Condition 4

Condition 4: -40°F Ambient, No Decay Heat

Stress Points		Stress Components (ksi)						Principal Stresses (ksi)		
Section <sup>1</sup>	Node	S <sub>x</sub>	S <sub>y</sub>	S <sub>z</sub>	S <sub>xy</sub>	S <sub>yz</sub>	S <sub>xz</sub>	S1	S2	S3
A1	1	-0.5	0.0	-0.5	0.0	0.0	0.0	0.0	-0.5	-0.5
A2	2	-0.3	0.0	-0.3	0.0	0.0	0.0	0.0	-0.3	-0.3
A3	3	-0.2	0.0	-0.2	0.0	0.0	0.0	0.0	-0.2	-0.2
A4	4	0.0	0.0	0.0	0.0	0.0	0.0	0.0	0.0	0.0
A5	5	0.1	0.0	0.1	0.0	0.0	0.0	0.1	0.1	0.0
B1	6	0.1	0.0	0.1	0.0	0.0	0.0	0.1	0.1	0.0
B2	7	0.1	0.0	0.1	0.0	0.0	0.0	0.1	0.1	0.0
B3	8	0.1	0.0	0.1	0.0	0.0	0.0	0.1	0.1	0.0
B4	9	0.1	0.0	0.1	0.0	0.0	0.0	0.1	0.1	0.0
B5	10	0.1	0.0	0.1	0.0	0.0	0.0	0.1	0.1	0.0
C1	251	-0.7	-1.7	-1.0	-0.2	0.0	0.0	-0.7	-1.0	-1.7
C2	252	0.0	-0.6	-0.4	0.0	0.0	0.0	0.0	-0.4	-0.6
C3	253	-0.1	-0.2	-0.2	0.2	0.0	0.0	0.0	-0.2	-0.3
C4	254	-0.1	-0.1	0.0	0.1	0.0	0.0	0.0	0.0	-0.2
C5	255	0.0	0.0	0.1	0.1	0.0	0.0	0.1	0.1	-0.1
D1	306	0.1	-0.5	0.0	0.1	0.0	0.0	0.1	0.0	-0.5
D2	307	0.1	-0.1	0.1	0.0	0.0	0.0	0.1	0.1	-0.1
D3	308	0.1	-0.1	0.1	0.0	0.0	0.0	0.1	0.1	-0.1
D4	309	0.1	0.0	0.1	0.0	0.0	0.0	0.1	0.1	0.0
D5	310	0.1	0.0	0.1	0.0	0.0	0.0	0.1	0.1	0.0
E1	305	-0.6	-0.7	-0.3	0.2	0.0	0.0	-0.3	-0.5	-0.8
E2	315	-0.4	-0.1	-0.1	0.1	0.0	0.0	-0.1	-0.1	-0.4
E3	325	-0.2	0.1	0.0	0.0	0.0	0.0	0.1	0.0	-0.2
E4	335	-0.1	0.2	0.1	0.0	0.0	0.0	0.2	0.1	-0.1
E5	345	-0.1	0.4	0.1	0.0	0.0	0.0	0.4	0.1	-0.1
E6	355	0.0	0.7	0.2	0.0	0.0	0.0	0.7	0.2	0.0
F1	251	-0.7	-1.7	-1.0	-0.2	0.0	0.0	-0.7	-1.0	-1.7
F2	261	-0.3	-0.7	-0.6	-0.1	0.0	0.0	-0.3	-0.6	-0.7
F3	271	0.2	0.1	-0.2	0.0	0.0	0.0	0.2	0.1	-0.2
F4	281	0.5	1.1	0.1	-0.1	0.0	0.0	1.1	0.5	0.1
G1	311	0.4	0.7	0.1	0.1	0.0	0.0	0.7	0.4	0.1
G2	321	0.3	0.4	-0.1	0.0	0.0	0.0	0.4	0.3	-0.1

Table 2.10.4-7 Stress Components – Thermal Cold, -40°F; 2-D Model; Condition 4  
(continued)

Stress Points Section <sup>1</sup> Node	Stress Components (ksi)						Principal Stresses (ksi)		
	S <sub>x</sub>	S <sub>y</sub>	S <sub>z</sub>	S <sub>xy</sub>	S <sub>yz</sub>	S <sub>xz</sub>	S1	S2	S3
G3	331	0.1	0.2	-0.1	0.0	0.0	0.2	0.1	-0.1
G4	341	0.1	0.0	-0.2	0.0	0.0	0.1	-0.1	-0.2
G5	351	0.0	-0.3	-0.3	0.0	0.0	0.0	-0.3	-0.3
H1	581	0.0	-0.2	-3.4	0.0	0.0	0.0	-0.2	-3.4
H2	582	0.0	-0.4	-3.3	0.0	0.0	0.0	-0.4	-3.3
H3	583	0.0	-0.6	-3.3	0.1	0.0	0.0	-0.6	-3.3
H4	584	0.0	-0.8	-3.4	0.1	0.0	0.0	-0.8	-3.4
I1	589	0.0	0.2	-0.1	0.0	0.0	0.2	0.0	-0.1
I2	590	0.0	0.2	-0.1	0.0	0.0	0.2	0.0	-0.1
I3	591	0.0	0.2	-0.1	0.0	0.0	0.2	0.0	-0.1
I4	592	0.0	0.3	0.0	0.0	0.0	0.3	0.0	0.0
I5	593	0.0	0.3	0.0	0.0	0.0	0.3	0.0	0.0
J1	971	0.0	-0.5	-3.9	0.0	0.0	0.0	-0.5	-3.9
J2	972	-0.1	-0.5	-3.9	0.0	0.0	-0.1	-0.5	-3.9
J3	973	-0.1	-0.5	-3.8	0.0	0.0	-0.1	-0.5	-3.8
J4	974	-0.2	-0.5	-3.8	0.0	0.0	-0.2	-0.5	-3.8
K1	979	0.0	0.2	0.0	0.0	0.0	0.2	0.0	0.0
K2	980	0.0	0.2	0.0	0.0	0.0	0.2	0.0	0.0
K3	981	0.0	0.2	0.0	0.0	0.0	0.2	0.0	0.0
K4	982	0.0	0.2	0.0	0.0	0.0	0.2	0.0	0.0
K5	983	0.0	0.2	0.0	0.0	0.0	0.2	0.0	0.0
L1	1601	0.0	-0.5	-3.9	0.0	0.0	0.0	-0.5	-3.9
L2	1602	-0.1	-0.5	-3.9	0.0	0.0	-0.1	-0.5	-3.9
L3	1603	-0.1	-0.5	-3.8	0.0	0.0	-0.1	-0.5	-3.8
L4	1604	-0.2	-0.5	-3.8	0.0	0.0	-0.2	-0.5	-3.8
M1	1609	0.0	0.2	0.0	0.0	0.0	0.2	0.0	0.0
M2	1610	0.0	0.2	0.0	0.0	0.0	0.2	0.0	0.0
M3	1611	0.0	0.2	0.0	0.0	0.0	0.2	0.0	0.0
M4	1612	0.0	0.2	0.0	0.0	0.0	0.2	0.0	0.0
M5	1613	0.0	0.2	0.0	0.0	0.0	0.2	0.0	0.0
N1	2216	0.0	-0.5	-4.0	0.0	0.0	0.0	-0.5	-4.0
N2	2217	-0.1	-0.5	-3.9	0.0	0.0	-0.1	-0.5	-3.9
N3	2218	-0.1	-0.5	-3.8	0.0	0.0	-0.1	-0.5	-3.8

Table 2.10.4-7 Stress Components – Thermal Cold, -40°F; 2-D Model; Condition 4  
(continued)

Stress Points Section <sup>1</sup> Node	S <sub>x</sub>	Stress Components (ksi)					Principal Stresses (ksi)		
		S <sub>y</sub>	S <sub>z</sub>	S <sub>xy</sub>	S <sub>yz</sub>	S <sub>xz</sub>	S1	S2	S3
N4 2219	-0.2	-0.5	-3.8	0.0	0.0	0.0	-0.2	-0.5	-3.8
O1 2224	0.0	0.2	0.0	0.0	0.0	0.0	0.2	0.0	0.0
O2 2225	0.0	0.2	0.0	0.0	0.0	0.0	0.2	0.0	0.0
O3 2226	0.0	0.2	0.0	0.0	0.0	0.0	0.2	0.0	0.0
O4 2227	0.0	0.2	0.0	0.0	0.0	0.0	0.2	0.0	0.0
O5 2228	0.0	0.2	0.0	0.0	0.0	0.0	0.2	0.0	0.0
P1 2546	0.0	-0.3	-3.4	0.0	0.0	0.0	0.0	-0.3	-3.4
P2 2547	0.0	-0.4	-3.4	0.0	0.0	0.0	0.0	-0.4	-3.4
P3 2548	0.0	-0.5	-3.4	-0.1	0.0	0.0	0.0	-0.5	-3.4
P4 2549	0.0	-0.7	-3.4	-0.1	0.0	0.0	0.0	-0.7	-3.4
Q1 2554	0.0	0.1	-0.2	0.0	0.0	0.0	0.1	0.0	-0.2
Q2 2555	0.0	0.1	-0.1	0.0	0.0	0.0	0.1	0.0	-0.1
Q3 2556	0.0	0.2	-0.1	0.0	0.0	0.0	0.2	0.0	-0.1
Q4 2557	0.0	0.3	-0.1	0.0	0.0	0.0	0.3	0.0	-0.1
Q5 2558	0.0	0.4	-0.1	0.0	0.0	0.0	0.4	0.0	-0.1
R1 2771	0.1	-1.1	-1.0	0.0	0.0	0.0	0.1	-1.0	-1.1
R2 2772	0.2	-0.6	-0.8	0.0	0.0	0.0	0.2	-0.6	-0.8
R3 2773	0.5	-0.2	-0.6	0.0	0.0	0.0	0.5	-0.2	-0.6
R4 2774	1.0	0.2	-0.4	0.0	0.0	0.0	1.0	0.1	-0.4
S1 2779	1.1	1.2	0.1	-0.1	0.0	0.0	1.3	1.0	0.1
S2 2780	0.7	0.6	-0.2	0.0	0.0	0.0	0.7	0.6	-0.2
S3 2781	0.3	0.1	-0.4	0.1	0.0	0.0	0.4	0.1	-0.4
S4 2782	0.1	-0.3	-0.5	0.1	0.0	0.0	0.2	-0.4	-0.5
S5 2783	0.1	-0.9	-0.7	0.1	0.0	0.0	0.1	-0.7	-0.9
T1 7066	-1.0	-0.7	-0.6	-0.2	0.0	0.0	-0.6	-0.6	-1.1
T2 7067	-0.7	-0.3	-0.4	0.0	0.0	0.0	-0.3	-0.4	-0.7
T3 7068	-0.4	0.0	-0.3	0.1	0.0	0.0	0.0	-0.3	-0.5
T4 7069	-0.3	0.1	-0.2	0.1	0.0	0.0	0.1	-0.2	-0.3
T5 7070	-0.1	0.2	-0.1	0.1	0.0	0.0	0.3	-0.1	-0.2
T6 7071	-0.1	0.4	-0.1	0.1	0.0	0.0	0.4	-0.1	-0.1
T7 7072	0.0	0.6	0.0	0.0	0.0	0.0	0.6	0.0	0.0
U1 3051	-0.1	0.0	-0.1	0.0	0.0	0.0	0.0	-0.1	-0.1
U2 3052	-0.1	0.0	0.0	0.0	0.0	0.0	0.0	0.0	-0.1

Table 2.10.4-7 Stress Components – Thermal Cold, -40°F; 2-D Model; Condition 4  
(continued)

Stress Points		Stress Components (ksi)						Principal Stresses (ksi)		
Section <sup>1</sup>	Node	S <sub>x</sub>	S <sub>y</sub>	S <sub>z</sub>	S <sub>xy</sub>	S <sub>xz</sub>	S <sub>yz</sub>	S1	S2	S3
U3	3053	0.0	0.0	0.0	0.0	0.0	0.0	0.0	0.0	0.0
U4	3054	0.1	-0.1	0.0	0.0	0.0	0.0	0.1	0.0	-0.1
U5	3055	0.3	-0.1	0.1	-0.1	0.0	0.0	0.3	0.1	-0.1
U6	3056	-0.3	-0.1	-0.1	-0.1	0.0	0.0	0.0	-0.1	-0.3
V1	3611	0.0	0.0	-0.1	0.0	0.0	0.0	0.0	0.0	-0.1
V2	3612	0.0	0.0	0.0	0.0	0.0	0.0	0.0	0.0	0.0
V3	3613	0.0	0.0	0.0	0.0	0.0	0.0	0.0	0.0	0.0
V4	3614	0.0	0.0	0.0	0.0	0.0	0.0	0.0	0.0	0.0
V5	3615	0.0	0.0	0.0	-0.1	0.0	0.0	0.1	0.0	-0.1
V6	3616	0.0	0.0	0.0	0.0	0.0	0.0	0.0	0.0	0.0
V7	3617	0.0	0.0	0.0	0.0	0.0	0.0	0.0	0.0	0.0
W1	3241	-0.1	0.0	-0.1	0.0	0.0	0.0	0.0	-0.1	-0.1
W2	3242	0.0	0.0	0.0	0.0	0.0	0.0	0.0	0.0	0.0
W3	3243	0.0	0.0	0.0	0.0	0.0	0.0	0.0	0.0	0.0
W4	3244	0.0	0.0	0.0	0.0	0.0	0.0	0.0	0.0	0.0
W5	3245	0.0	0.0	0.0	0.0	0.0	0.0	0.0	0.0	0.0
W6	3246	0.1	0.0	0.1	0.0	0.0	0.0	0.1	0.1	0.0
X1	3801	-0.1	0.0	-0.1	0.0	0.0	0.0	0.0	-0.1	-0.1
X2	3802	-0.1	0.0	-0.1	0.0	0.0	0.0	0.0	-0.1	-0.1
X3	3803	0.0	0.0	0.0	0.0	0.0	0.0	0.0	0.0	0.0
X4	3804	0.0	0.0	0.0	0.0	0.0	0.0	0.0	0.0	0.0
X5	3805	0.0	0.0	0.0	0.0	0.0	0.0	0.0	0.0	0.0
X6	3806	0.0	0.0	0.0	0.0	0.0	0.0	0.0	0.0	0.0
X7	3807	0.0	0.0	0.0	0.0	0.0	0.0	0.0	0.0	0.0

<sup>1</sup> Refer to Figure 2.10.2-34 for the identification of the representative sections.



Table 2.10.4-8 Stress Components – Impact; 1-Foot Top End Drop; Drop Orientation = 0 Degrees; 2-D Model; Condition 1

Condition 1: 100°F Ambient with Contents

Stress Points		Stress Components (ksi)						Principal Stresses (ksi)		
Section <sup>1</sup>	Node	S <sub>x</sub>	S <sub>y</sub>	S <sub>z</sub>	S <sub>xy</sub>	S <sub>yz</sub>	S <sub>xz</sub>	S1	S2	S3
A1	1	1.6	0.0	1.6	0.0	0.0	0.0	1.6	1.6	0.0
A2	2	0.9	0.0	0.9	0.0	0.0	0.0	0.9	0.9	0.0
A3	3	0.2	0.0	0.2	0.0	0.0	0.0	0.2	0.2	0.0
A4	4	-0.5	0.0	-0.5	0.0	0.0	0.0	0.0	-0.5	-0.5
A5	5	-1.2	0.0	-1.2	0.0	0.0	0.0	0.0	-1.2	-1.2
B1	6	1.0	0.0	1.0	0.0	0.0	0.0	1.0	1.0	0.0
B2	7	0.4	0.0	0.4	0.0	0.0	0.0	0.4	0.4	0.0
B3	8	-0.3	0.0	-0.3	0.0	0.0	0.0	0.0	-0.3	-0.3
B4	9	-0.9	0.0	-0.9	0.0	0.0	0.0	0.0	-0.9	-0.9
B5	10	-1.5	0.0	-1.5	0.0	0.0	0.0	0.0	-1.5	-1.5
C1	251	-1.0	-1.2	-0.2	-0.2	0.0	0.0	-0.2	-0.8	-1.4
C2	252	-0.2	-0.5	0.1	-0.2	0.0	0.0	0.1	-0.1	-0.6
C3	253	0.2	-0.2	0.1	-0.2	0.0	0.0	0.3	0.1	-0.3
C4	254	0.7	-0.1	0.2	-0.1	0.0	0.0	0.7	0.2	-0.1
C5	255	1.2	-0.1	0.1	-0.1	0.0	0.0	1.2	0.1	-0.1
D1	306	-1.2	-0.7	-0.5	-0.3	0.0	0.0	-0.5	-0.5	-1.4
D2	307	-0.4	-0.5	-0.3	-0.1	0.0	0.0	-0.3	-0.3	-0.6
D3	308	-0.1	-0.2	-0.3	0.0	0.0	0.0	-0.1	-0.2	-0.3
D4	309	0.2	-0.1	-0.2	0.1	0.0	0.0	0.2	-0.1	-0.2
D5	310	0.5	0.0	-0.2	0.1	0.0	0.0	0.5	0.0	-0.2
E1	305	1.1	0.0	0.3	-0.3	0.0	0.0	1.2	0.3	0.0
E2	315	0.6	-0.3	0.1	-0.3	0.0	0.0	0.7	0.1	-0.4
E3	325	0.3	-0.2	0.0	-0.3	0.0	0.0	0.4	0.0	-0.3
E4	335	0.1	-0.2	0.0	-0.2	0.0	0.0	0.2	0.0	-0.3
E5	345	0.1	-0.2	0.0	-0.1	0.0	0.0	0.1	0.0	-0.3
E6	355	0.0	-0.3	-0.1	-0.1	0.0	0.0	0.0	-0.1	-0.3
F1	251	-1.0	-1.2	-0.2	-0.2	0.0	0.0	-0.2	-0.8	-1.4
F2	261	-0.8	-0.7	0.0	-0.1	0.0	0.0	0.0	-0.6	-0.8
F3	271	-0.6	-0.3	0.2	0.1	0.0	0.0	0.2	-0.3	-0.6
F4	281	-0.6	0.0	0.2	0.1	0.0	0.0	0.2	0.0	-0.6
G1	311	-0.5	-0.8	-0.1	-0.1	0.0	0.0	-0.1	-0.5	-0.8

Table 2.10.4-8 Stress Components – Impact; 1-Foot Top End Drop; Drop Orientation = 0 Degrees; 2-D Model; Condition 1 (continued)

Stress Points Section <sup>1</sup> Node		Stress Components (ksi)						Principal Stresses (ksi)		
		S <sub>x</sub>	S <sub>y</sub>	S <sub>z</sub>	S <sub>xy</sub>	S <sub>yz</sub>	S <sub>xz</sub>	S1	S2	S3
G2	321	-0.3	-0.5	0.1	0.0	0.0	0.0	0.1	-0.3	-0.5
G3	331	-0.2	-0.3	0.2	0.1	0.0	0.0	0.2	-0.2	-0.3
G4	341	-0.1	-0.1	0.3	0.1	0.0	0.0	0.3	0.0	-0.1
G5	351	0.0	0.2	0.3	0.0	0.0	0.0	0.3	0.2	0.0
H1	581	0.0	-0.8	0.0	0.0	0.0	0.0	0.0	0.0	-0.8
H2	582	0.0	-1.0	0.0	0.0	0.0	0.0	0.0	0.0	-1.0
H3	583	0.0	-1.2	-0.1	0.0	0.0	0.0	0.0	-0.1	-1.2
H4	584	0.0	-1.6	-0.2	0.1	0.0	0.0	0.0	-0.2	-1.6
I1	589	0.0	-0.4	0.1	0.0	0.0	0.0	0.1	0.0	-0.4
I2	590	0.0	-0.4	0.1	0.0	0.0	0.0	0.1	0.0	-0.4
I3	591	0.0	-0.5	0.1	0.0	0.0	0.0	0.1	0.0	-0.5
I4	592	0.0	-0.5	0.0	0.0	0.0	0.0	0.0	0.0	-0.5
I5	593	0.0	-0.6	0.0	0.0	0.0	0.0	0.0	0.0	-0.6
J1	971	0.0	-1.4	0.0	0.0	0.0	0.0	0.0	0.0	-1.4
J2	972	0.0	-1.4	0.0	0.0	0.0	0.0	0.0	0.0	-1.4
J3	973	0.0	-1.4	0.0	0.0	0.0	0.0	0.0	0.0	-1.4
J4	974	0.0	-1.4	0.0	0.0	0.0	0.0	0.0	0.0	-1.4
K1	979	0.0	-0.7	0.0	0.0	0.0	0.0	0.0	0.0	-0.7
K2	980	0.0	-0.7	0.0	0.0	0.0	0.0	0.0	0.0	-0.7
K3	981	0.0	-0.7	0.0	0.0	0.0	0.0	0.0	0.0	-0.7
K4	982	0.0	-0.7	0.0	0.0	0.0	0.0	0.0	0.0	-0.7
K5	983	0.0	-0.7	0.0	0.0	0.0	0.0	0.0	0.0	-0.7
L1	1601	0.0	-1.8	0.0	0.0	0.0	0.0	0.0	0.0	-1.8
L2	1602	0.0	-1.8	0.0	0.0	0.0	0.0	0.0	0.0	-1.8
L3	1603	0.0	-1.8	0.0	0.0	0.0	0.0	0.0	0.0	-1.8
L4	1604	0.0	-1.8	0.0	0.0	0.0	0.0	0.0	0.0	-1.8
M1	1609	0.0	-1.0	0.0	0.0	0.0	0.0	0.0	0.0	-1.0
M2	1610	0.0	-1.0	0.0	0.0	0.0	0.0	0.0	0.0	-1.0
M3	1611	0.0	-1.0	0.0	0.0	0.0	0.0	0.0	0.0	-1.0
M4	1612	0.0	-1.0	0.0	0.0	0.0	0.0	0.0	0.0	-1.0
M5	1613	0.0	-1.0	0.0	0.0	0.0	0.0	0.0	0.0	-1.0
N1	2216	0.0	-2.1	0.0	0.0	0.0	0.0	0.0	0.0	-2.1
N2	2217	0.0	-2.1	0.0	0.0	0.0	0.0	0.0	0.0	-2.1

Table 2.10.4-8 Stress Components – Impact; 1-Foot Top End Drop; Drop Orientation = 0 Degrees; 2-D Model; Condition 1 (continued)

Stress Points Section <sup>1</sup> Node	Stress Components (ksi)						Principal Stresses (ksi)		
	S <sub>x</sub>	S <sub>y</sub>	S <sub>z</sub>	S <sub>xy</sub>	S <sub>yz</sub>	S <sub>xz</sub>	S1	S2	S3
N3	2218	0.0	-2.1	0.0	0.0	0.0	0.0	0.0	-2.1
N4	2219	0.0	-2.1	0.0	0.0	0.0	0.0	0.0	-2.1
O1	2224	0.0	-1.4	0.0	0.0	0.0	0.0	0.0	-1.4
O2	2225	0.0	-1.4	0.0	0.0	0.0	0.0	0.0	-1.4
O3	2226	0.0	-1.4	0.0	0.0	0.0	0.0	0.0	-1.4
O4	2227	0.0	-1.4	0.0	0.0	0.0	0.0	0.0	-1.4
O5	2228	0.0	-1.4	0.0	0.0	0.0	0.0	0.0	-1.4
P1	2546	0.0	-1.2	0.3	0.0	0.0	0.3	0.0	-1.2
P2	2547	0.0	-1.9	0.1	0.0	0.0	0.1	0.0	-1.9
P3	2548	0.0	-2.5	-0.1	-0.1	0.0	0.0	-0.1	-2.5
P4	2549	0.0	-3.4	-0.3	-0.2	0.0	0.0	-0.3	-3.4
Q1	2554	0.0	-1.3	0.5	0.0	0.0	0.5	0.0	-1.3
Q2	2555	0.0	-1.4	0.4	0.0	0.0	0.4	0.0	-1.4
Q3	2556	0.0	-1.6	0.4	0.0	0.0	0.4	0.0	-1.6
Q4	2557	0.0	-1.7	0.3	0.0	0.0	0.3	0.0	-1.7
Q5	2558	0.0	-1.9	0.3	0.0	0.0	0.3	0.0	-1.9
R1	2771	0.1	-6.5	-0.3	0.0	0.0	0.1	-0.3	-6.5
R2	2772	0.2	-3.8	0.4	0.0	0.0	0.4	0.2	-3.8
R3	2773	0.6	-1.3	1.2	0.4	0.0	1.2	0.7	-1.4
R4	2774	0.6	1.7	2.0	1.0	0.0	2.3	2.0	-0.1
S1	2779	-3.3	-4.5	-1.0	0.3	0.0	-1.0	-3.3	-4.6
S2	2780	-2.1	-2.7	-0.2	-0.1	0.0	-0.2	-2.1	-2.7
S3	2781	-1.1	-1.4	0.4	-0.4	0.0	0.4	-0.8	-1.7
S4	2782	-0.4	-0.1	0.9	-0.3	0.0	0.9	0.1	-0.6
S5	2783	-0.2	1.6	1.4	-0.2	0.0	1.6	1.4	-0.2
T1	7066	4.1	3.6	1.7	1.1	0.0	5.0	2.8	1.7
T2	7067	2.8	1.3	0.8	0.4	0.0	2.9	1.2	0.8
T3	7068	1.9	-0.1	0.2	-0.1	0.0	1.9	0.2	-0.1
T4	7069	1.1	-1.0	-0.3	-0.3	0.0	1.2	-0.3	-1.0
T5	7070	0.6	-1.8	-0.6	-0.4	0.0	0.7	-0.6	-1.8
T6	7071	0.3	-2.7	-0.9	-0.3	0.0	0.3	-0.9	-2.7
T7	7072	0.1	-3.8	-1.2	-0.2	0.0	0.1	-1.2	-3.8
U1	3051	0.0	-3.1	2.3	0.7	0.0	2.3	0.1	-3.3

Table 2.10.4-8 Stress Components -- Impact; 1-Foot Top End Drop; Drop Orientation = 0 Degrees; 2-D Model; Condition 1 (continued)

Stress Points Section <sup>1</sup> Node	Stress Components (ksi)						Principal Stresses (ksi)		
	S <sub>x</sub>	S <sub>y</sub>	S <sub>z</sub>	S <sub>xy</sub>	S <sub>yz</sub>	S <sub>xz</sub>	S1	S2	S3
U2 3052	1.1	-2.9	1.7	1.0	0.0	0.0	1.7	1.3	-3.1
U3 3053	0.9	-2.4	0.9	1.2	0.0	0.0	1.3	0.9	-2.8
U4 3054	0.6	-2.3	-0.1	1.1	0.0	0.0	1.0	-0.1	-2.7
U5 3055	0.4	-2.8	-1.2	1.2	0.0	0.0	0.8	-1.2	-3.2
U6 3056	-0.8	-2.0	-2.1	1.6	0.0	0.0	0.3	-2.1	-3.1
V1 3611	-3.4	-0.9	2.3	-0.6	0.0	0.0	2.3	-0.7	-3.5
V2 3612	-2.3	-1.0	1.6	-0.8	0.0	0.0	1.6	-0.6	-2.7
V3 3613	-1.2	-1.1	0.8	-1.1	0.0	0.0	0.8	-0.1	-2.2
V4 3614	-0.2	-1.1	-0.1	-1.0	0.0	0.0	0.5	-0.1	-1.8
V5 3615	0.7	-0.9	-0.9	-0.9	0.0	0.0	1.1	-0.9	-1.3
V6 3616	0.9	-0.7	-1.9	-0.6	0.0	0.0	1.0	-0.8	-1.9
V7 3617	3.0	-0.6	-2.4	-0.3	0.0	0.0	3.0	-0.6	-2.4
W1 3241	1.1	-0.2	1.1	0.0	0.0	0.0	1.1	1.1	-0.2
W2 3242	1.1	-0.2	1.1	0.0	0.0	0.0	1.1	1.1	-0.2
W3 3243	1.1	-0.2	1.1	0.0	0.0	0.0	1.1	1.1	-0.2
W4 3244	1.0	-0.1	1.0	0.0	0.0	0.0	1.0	1.0	-0.1
W5 3245	1.0	-0.1	1.0	0.0	0.0	0.0	1.0	1.0	-0.1
W6 3246	1.0	0.0	1.0	0.0	0.0	0.0	1.0	1.0	0.0
X1 3801	18.9	-0.6	18.9	0.0	0.0	0.0	18.9	18.9	-0.6
X2 3802	12.8	-0.5	12.8	0.0	0.0	0.0	12.8	12.8	-0.5
X3 3803	6.6	-0.3	6.6	0.0	0.0	0.0	6.6	6.6	-0.3
X4 3804	0.4	-0.4	0.4	0.0	0.0	0.0	0.4	0.4	-0.4
X5 3805	-5.8	-0.5	-5.8	0.0	0.0	0.0	-0.5	-5.8	-5.8
X6 3806	-12.0	-0.4	-12.0	0.0	0.0	0.0	-0.4	-12.0	-12.0
X7 3807	-18.8	-0.3	-18.8	0.0	0.0	0.0	-0.3	-18.8	-18.8

<sup>1</sup> Refer to Figure 2.10.2-34 for the identification of the representative sections.

Table 2.10.4-9 Stress Components – Impact; 1-Foot Bottom End Drop; Drop Orientation = 0 Degrees; 2-D Model; Condition 1

Condition 1: 100°F Ambient with Contents

Stress Points		Stress Components (ksi)						Principal Stresses (ksi)		
Section <sup>1</sup>	Node	S <sub>x</sub>	S <sub>y</sub>	S <sub>z</sub>	S <sub>xy</sub>	S <sub>yz</sub>	S <sub>xz</sub>	S1	S2	S3
A1	1	7.7	-0.3	7.7	0.0	0.0	0.0	7.7	7.7	-0.3
A2	2	4.4	-0.4	4.4	0.0	0.0	0.0	4.4	4.4	-0.4
A3	3	1.1	-0.5	1.1	0.0	0.0	0.0	1.1	1.1	-0.5
A4	4	-2.3	-0.5	-2.3	0.0	0.0	0.0	-0.5	-2.3	-2.3
A5	5	-5.6	-0.6	-5.6	0.0	0.0	0.0	-0.6	-5.6	-5.6
B1	6	4.5	-0.6	4.5	0.0	0.0	0.0	4.5	4.5	-0.6
B2	7	1.6	-0.7	1.6	0.0	0.0	0.0	1.6	1.6	-0.7
B3	8	-1.3	-0.7	-1.3	0.0	0.0	0.0	-0.7	-1.3	-1.3
B4	9	-4.3	-0.8	-4.3	0.0	0.0	0.0	-0.8	-4.3	-4.3
B5	10	-7.1	-0.8	-7.1	0.0	0.0	0.0	-0.8	-7.1	-7.1
C1	251	-4.2	-5.2	-0.3	-0.9	0.0	0.0	-0.3	-3.7	-5.7
C2	252	-0.7	-2.1	0.8	-0.6	0.0	0.0	0.8	-0.4	-2.4
C3	253	1.1	-0.9	1.0	-0.7	0.0	0.0	1.3	1.0	-1.1
C4	254	3.4	-0.6	1.0	-0.5	0.0	0.0	3.5	1.0	-0.6
C5	255	5.9	-0.5	0.9	-0.4	0.0	0.0	6.0	0.9	-0.5
D1	306	-6.6	-5.5	-3.1	-1.9	0.0	0.0	-3.1	-4.0	-8.1
D2	307	-1.7	-4.0	-1.7	-0.8	0.0	0.0	-1.5	-1.7	-4.2
D3	308	-0.4	-2.0	-1.4	0.0	0.0	0.0	-0.4	-1.4	-2.0
D4	309	0.8	-1.3	-1.4	0.2	0.0	0.0	0.8	-1.3	-1.4
D5	310	2.4	-1.0	-1.4	0.2	0.0	0.0	2.4	-1.0	-1.4
E1	305	5.6	-1.6	1.3	-1.3	0.0	0.0	5.8	1.3	-1.9
E2	315	2.7	-2.5	0.4	-1.7	0.0	0.0	3.2	0.4	-3.0
E3	325	1.1	-2.0	0.1	-1.6	0.0	0.0	1.8	0.1	-2.6
E4	335	0.6	-1.6	0.1	-1.3	0.0	0.0	1.1	0.1	-2.2
E5	345	0.2	-1.3	0.1	-0.7	0.0	0.0	0.5	0.1	-1.6
E6	355	0.1	-1.3	0.0	-0.4	0.0	0.0	0.2	0.0	-1.4
F1	251	-4.2	-5.2	-0.3	-0.9	0.0	0.0	-0.3	-3.7	-5.7
F2	261	-3.1	-2.3	0.7	-0.3	0.0	0.0	0.7	-2.2	-3.2
F3	271	-2.0	-0.2	1.5	0.1	0.0	0.0	1.5	-0.2	-2.0
F4	281	-2.0	1.6	2.0	-0.1	0.0	0.0	2.0	1.6	-2.0
G1	311	-2.9	-4.6	-0.4	-0.1	0.0	0.0	-0.4	-2.8	-4.6

Table 2.10.4-9 Stress Components – Impact; 1-Foot Bottom End Drop; Drop Orientation = 0 Degrees; 2-D Model; Condition 1 (continued)

Stress Points Section <sup>1</sup> Node		Stress Components (ksi)						Principal Stresses (ksi)		
		S <sub>x</sub>	S <sub>y</sub>	S <sub>z</sub>	S <sub>xy</sub>	S <sub>xz</sub>	S <sub>yz</sub>	S1	S2	S3
G2	321	-2.0	-2.9	0.3	0.1	0.0	0.0	0.3	-2.0	-2.9
G3	331	-1.0	-1.7	0.8	0.3	0.0	0.0	0.8	-0.9	-1.8
G4	341	-0.4	-0.5	1.3	0.2	0.0	0.0	1.3	-0.2	-0.7
G5	351	-0.2	1.0	1.7	0.2	0.0	0.0	1.7	1.0	-0.2
H1	581	0.0	-1.1	0.3	0.0	0.0	0.0	0.3	0.0	-1.1
H2	582	0.0	-1.8	0.0	0.0	0.0	0.0	0.0	0.0	-1.8
H3	583	-0.1	-2.5	-0.2	0.1	0.0	0.0	0.0	-0.2	-2.5
H4	584	0.0	-3.5	-0.4	0.2	0.0	0.0	0.0	-0.4	-3.6
I1	589	0.0	-1.3	0.4	0.0	0.0	0.0	0.4	0.0	-1.3
I2	590	0.0	-1.5	0.3	0.0	0.0	0.0	0.3	0.0	-1.5
I3	591	0.0	-1.7	0.3	0.0	0.0	0.0	0.3	0.0	-1.7
I4	592	0.0	-1.9	0.2	0.0	0.0	0.0	0.2	0.0	-1.9
I5	593	0.0	-2.1	0.2	0.0	0.0	0.0	0.2	0.0	-2.1
J1	971	0.0	-2.1	0.0	0.0	0.0	0.0	0.0	0.0	-2.1
J2	972	0.0	-2.1	0.0	0.0	0.0	0.0	0.0	0.0	-2.1
J3	973	0.0	-2.1	0.0	0.0	0.0	0.0	0.0	0.0	-2.1
J4	974	0.0	-2.1	0.0	0.0	0.0	0.0	0.0	0.0	-2.1
K1	979	0.0	-1.5	0.0	0.0	0.0	0.0	0.0	0.0	-1.5
K2	980	0.0	-1.5	0.0	0.0	0.0	0.0	0.0	0.0	-1.5
K3	981	0.0	-1.5	0.0	0.0	0.0	0.0	0.0	0.0	-1.5
K4	982	0.0	-1.5	0.0	0.0	0.0	0.0	0.0	0.0	-1.5
K5	983	0.0	-1.5	0.0	0.0	0.0	0.0	0.0	0.0	-1.5
L1	1601	0.0	-1.7	0.0	0.0	0.0	0.0	0.0	0.0	-1.7
L2	1602	0.0	-1.7	0.0	0.0	0.0	0.0	0.0	0.0	-1.7
L3	1603	0.0	-1.7	0.0	0.0	0.0	0.0	0.0	0.0	-1.7
L4	1604	0.0	-1.7	0.0	0.0	0.0	0.0	0.0	0.0	-1.7
M1	1609	0.0	-1.2	0.0	0.0	0.0	0.0	0.0	0.0	-1.2
M2	1610	0.0	-1.2	0.0	0.0	0.0	0.0	0.0	0.0	-1.2
M3	1611	0.0	-1.2	0.0	0.0	0.0	0.0	0.0	0.0	-1.2
M4	1612	0.0	-1.2	0.0	0.0	0.0	0.0	0.0	0.0	-1.2
M5	1613	0.0	-1.2	0.0	0.0	0.0	0.0	0.0	0.0	-1.2
N1	2216	0.0	-1.4	0.0	0.0	0.0	0.0	0.0	0.0	-1.4
N2	2217	0.0	-1.4	0.0	0.0	0.0	0.0	0.0	0.0	-1.4

Table 2.10.4-9 Stress Components – Impact; 1-Foot Bottom End Drop; Drop Orientation = 0 Degrees; 2-D Model; Condition 1 (continued)

Stress Points Section <sup>1</sup> Node	Stress Components (ksi)						Principal Stresses (ksi)		
	S <sub>x</sub>	S <sub>y</sub>	S <sub>z</sub>	S <sub>xy</sub>	S <sub>yz</sub>	S <sub>xz</sub>	S1	S2	S3
N3	2218	0.0	-1.4	0.0	0.0	0.0	0.0	0.0	-1.4
N4	2219	0.0	-1.4	0.0	0.0	0.0	0.0	0.0	-1.4
O1	2224	0.0	-0.8	0.0	0.0	0.0	0.0	0.0	-0.8
O2	2225	0.0	-0.8	0.0	0.0	0.0	0.0	0.0	-0.8
O3	2226	0.0	-0.8	0.0	0.0	0.0	0.0	0.0	-0.8
O4	2227	0.0	-0.8	0.0	0.0	0.0	0.0	0.0	-0.8
O5	2228	0.0	-0.8	0.0	0.0	0.0	0.0	0.0	-0.8
P1	2546	0.0	-0.8	0.0	0.0	0.0	0.0	0.0	-0.8
P2	2547	0.0	-1.0	0.0	0.0	0.0	0.0	0.0	-1.0
P3	2548	0.0	-1.2	-0.1	0.0	0.0	0.0	-0.1	-1.2
P4	2549	0.0	-1.5	-0.2	-0.1	0.0	0.0	-0.2	-1.5
Q1	2554	0.0	-0.6	0.1	0.0	0.0	0.1	0.0	-0.6
Q2	2555	0.0	-0.6	0.1	0.0	0.0	0.1	0.0	-0.6
Q3	2556	0.0	-0.6	0.1	0.0	0.0	0.1	0.0	-0.6
Q4	2557	0.0	-0.7	0.1	0.0	0.0	0.1	0.0	-0.7
Q5	2558	0.0	-0.7	0.1	0.0	0.0	0.1	0.0	-0.7
R1	2771	0.0	-1.6	-0.1	0.0	0.0	0.0	-0.1	-1.6
R2	2772	0.0	-1.1	0.0	0.0	0.0	0.0	0.0	-1.1
R3	2773	0.1	-0.6	0.2	0.1	0.0	0.2	0.1	-0.6
R4	2774	0.1	0.1	0.4	0.1	0.0	0.4	0.2	0.0
S1	2779	-0.6	-1.0	-0.2	0.1	0.0	-0.2	-0.6	-1.0
S2	2780	-0.4	-0.7	0.0	0.0	0.0	0.0	-0.4	-0.7
S3	2781	-0.2	-0.4	0.1	-0.1	0.0	0.1	-0.2	-0.4
S4	2782	-0.1	-0.1	0.2	-0.1	0.0	0.2	0.0	-0.2
S5	2783	0.0	0.2	0.3	0.0	0.0	0.3	0.2	0.0
T1	7066	0.7	0.6	0.3	0.2	0.0	0.9	0.5	0.3
T2	7067	0.5	0.2	0.2	0.1	0.0	0.5	0.2	0.2
T3	7068	0.3	0.0	0.0	0.0	0.0	0.3	0.0	0.0
T4	7069	0.2	-0.2	0.0	0.0	0.0	0.2	0.0	-0.2
T5	7070	0.1	-0.4	-0.1	-0.1	0.0	0.1	-0.1	-0.4
T6	7071	0.0	-0.5	-0.2	0.0	0.0	0.0	-0.2	-0.5
T7	7072	0.0	-0.8	-0.2	0.0	0.0	0.0	-0.2	-0.8
U1	3051	-0.5	-0.8	0.4	0.1	0.0	0.4	-0.5	-0.8

Table 2.10.4-9 Stress Components -- Impact; 1-Foot Bottom End Drop; Drop Orientation = 0 Degrees; 2-D Model; Condition 1 (continued)

Stress Points Section <sup>1</sup> Node	Stress Components (ksi)						Principal Stresses (ksi)		
	S <sub>x</sub>	S <sub>y</sub>	S <sub>z</sub>	S <sub>xy</sub>	S <sub>yz</sub>	S <sub>xz</sub>	S1	S2	S3
U2 3052	0.0	-0.7	0.4	0.1	0.0	0.0	0.4	0.0	-0.7
U3 3053	0.1	-0.5	0.2	0.1	0.0	0.0	0.2	0.2	-0.5
U4 3054	0.2	-0.5	0.0	0.0	0.0	0.0	0.2	0.0	-0.5
U5 3055	0.3	-0.6	-0.3	0.1	0.0	0.0	0.3	-0.3	-0.6
U6 3056	0.1	-0.4	-0.5	0.3	0.0	0.0	0.2	-0.5	-0.5
V1 3611	-0.2	0.0	0.5	0.0	0.0	0.0	0.5	0.0	-0.2
V2 3612	-0.1	0.0	0.4	0.0	0.0	0.0	0.4	0.0	-0.2
V3 3613	-0.1	-0.1	0.2	0.0	0.0	0.0	0.2	0.0	-0.1
V4 3614	0.0	-0.1	0.0	0.0	0.0	0.0	0.0	0.0	-0.1
V5 3615	0.0	0.0	-0.2	0.0	0.0	0.0	0.0	0.0	-0.2
V6 3616	0.0	0.0	-0.4	0.0	0.0	0.0	0.0	0.0	-0.4
V7 3617	0.2	0.0	-0.5	0.0	0.0	0.0	0.2	0.0	-0.5
W1 3241	2.1	0.0	2.1	0.0	0.0	0.0	2.1	2.1	0.0
W2 3242	1.4	0.0	1.4	0.0	0.0	0.0	1.4	1.4	0.0
W3 3243	0.6	0.0	0.6	0.0	0.0	0.0	0.6	0.6	0.0
W4 3244	-0.1	0.0	-0.1	0.0	0.0	0.0	0.0	-0.1	-0.1
W5 3245	-0.9	0.0	-0.9	0.0	0.0	0.0	0.0	-0.9	-0.9
W6 3246	-1.7	0.0	-1.7	0.0	0.0	0.0	0.0	-1.7	-1.7
X1 3801	1.7	0.0	1.7	0.0	0.0	0.0	1.7	1.7	0.0
X2 3802	1.2	0.0	1.2	0.0	0.0	0.0	1.2	1.2	0.0
X3 3803	0.6	0.0	0.6	0.0	0.0	0.0	0.6	0.6	0.0
X4 3804	0.0	0.0	0.0	0.0	0.0	0.0	0.0	0.0	0.0
X5 3805	-0.5	0.0	-0.5	0.0	0.0	0.0	0.0	-0.5	-0.5
X6 3806	-1.1	0.0	-1.1	0.0	0.0	0.0	0.0	-1.1	-1.1
X7 3807	-1.8	0.0	-1.8	0.0	0.0	0.0	0.0	-1.8	-1.8

<sup>1</sup> Refer to Figure 2.10.2-34 for the identification of the representative sections.



Table 2.10.4-10 Stress Components -- Impact; 1-Foot Side Drop; Drop Orientation = 90 Degrees; 3-D Model; 0-Degree Circumferential Location; Condition 1

Condition 1: 100°F Ambient with Contents

Stress Points Section <sup>1</sup> Node		Stress Components (ksi)						Principal Stresses (ksi)		
		S <sub>x</sub>	S <sub>y</sub>	S <sub>z</sub>	S <sub>xy</sub>	S <sub>xz</sub>	S <sub>yz</sub>	S1	S2	S3
A1	1130	-0.4	-0.7	-0.1	0.0	0.0	0.0	-0.1	-0.4	-0.7
A2	1129	-0.4	-1.2	0.0	0.0	0.0	0.0	0.0	-0.4	-1.2
A3	1128	-0.4	-1.7	0.1	0.0	0.0	0.0	0.1	-0.4	-1.7
B1	1185	-0.4	-1.9	0.0	0.0	0.0	-0.1	0.0	-0.4	-1.9
B2	1184	-0.2	-2.1	0.0	0.0	0.0	-0.1	0.0	-0.2	-2.1
B3	1183	0.1	-2.3	0.0	0.0	0.0	-0.1	0.1	0.0	-2.3
C1	90	1.6	-1.3	5.6	0.0	-0.3	0.4	5.6	1.6	-1.3
C2	80	-1.3	-2.9	2.3	0.0	-0.2	-0.1	2.3	-1.3	-2.9
C3	70	-1.6	-3.4	0.6	0.0	-0.1	-0.3	0.6	-1.7	-3.4
C4	60	-1.8	-3.6	0.0	0.1	-0.1	-0.2	0.0	-1.9	-3.6
C5	50	-3.3	-4.1	-0.1	0.1	0.0	0.0	-0.1	-3.3	-4.1
C6	40	-3.8	-4.2	-0.1	0.1	0.0	0.0	-0.1	-3.8	-4.2
D1	25	-1.8	-3.5	1.5	0.1	0.0	0.1	1.5	-1.8	-3.5
D2	15	-3.5	-4.0	0.6	0.1	0.0	-0.2	0.6	-3.5	-4.0
D3	5	-3.9	-4.1	0.1	0.1	0.0	-0.1	0.1	-3.9	-4.1
E1	35	-4.1	-4.3	1.0	0.1	0.0	0.8	1.1	-4.1	-4.3
E2	34	-2.9	-4.1	0.6	0.1	0.0	0.8	0.8	-3.1	-4.1
E3	33	-3.0	-4.4	0.0	0.1	0.0	0.7	0.2	-3.1	-4.4
E4	32	-3.2	-4.6	-0.6	0.1	0.0	0.4	-0.5	-3.2	-4.6
E5	31	-3.2	-4.9	-1.2	0.1	0.0	0.2	-1.2	-3.2	-4.9
F1	100	-0.5	-1.1	8.7	0.0	-0.5	0.8	8.8	-0.6	-1.1
F2	99	-0.7	-3.4	0.3	0.2	-0.4	0.9	0.8	-1.2	-3.5
F3	98	-0.3	-4.8	-5.2	0.3	-0.3	1.4	0.0	-4.6	-5.7
F4	97	0.2	-7.5	-16.1	0.6	-0.3	1.7	0.4	-7.5	-16.3
G1	94	0.3	-0.8	8.2	0.1	-0.1	1.2	8.4	0.1	-0.8
G2	93	0.5	-2.1	3.1	0.2	-0.1	0.8	3.3	0.3	-2.1
G3	92	0.5	-2.5	1.4	0.2	-0.1	0.3	1.5	0.5	-2.5
G4	91	0.3	-3.1	-0.5	0.2	0.0	0.1	0.3	-0.5	-3.1
H1	330	-0.1	2.3	-2.3	-0.2	-0.7	0.0	2.4	-0.1	-2.4
H2	329	0.0	2.9	-1.1	-0.2	-0.6	0.0	3.0	-0.1	-1.2

Table 2.10.4-10 Stress Components – Impact; 1-Foot Side Drop; Drop Orientation = 90 Degrees; 3-D Model; 0-Degree Circumferential Location; Condition 1  
(continued)

Stress Points Section <sup>1</sup> Node		Stress Components (ksi)						Principal Stresses (ksi)		
		S <sub>x</sub>	S <sub>y</sub>	S <sub>z</sub>	S <sub>xy</sub>	S <sub>yz</sub>	S <sub>xz</sub>	S1	S2	S3
H3	328	0.0	3.5	0.1	-0.2	-0.6	0.0	3.6	0.1	-0.1
H4	327	0.1	4.1	1.5	-0.3	-0.6	-0.1	4.3	1.4	0.0
I1	244	-0.1	-0.6	2.1	0.0	-0.3	0.0	2.1	-0.1	-0.6
I2	243	-0.1	0.1	3.0	0.0	-0.2	0.0	3.0	0.1	-0.1
I3	242	0.0	0.7	3.9	0.0	-0.1	0.0	3.9	0.7	0.0
I4	241	0.0	1.4	4.9	-0.1	-0.1	0.0	4.9	1.4	0.0
J1	550	-0.1	2.3	4.1	-0.2	-0.4	0.0	4.2	2.2	-0.1
J2	548	-0.1	3.3	4.8	-0.3	-0.4	0.0	4.9	3.2	-0.1
J3	547	0.0	4.3	5.4	-0.3	-0.4	0.0	5.5	4.2	0.0
K1	344	-0.1	-0.9	3.8	0.1	-0.1	0.0	3.8	-0.1	-0.9
K2	342	0.0	0.6	4.6	-0.1	-0.1	0.0	4.6	0.6	0.0
K3	341	0.0	2.1	5.3	-0.2	-0.1	0.0	5.3	2.1	0.0
L1	740	0.0	1.9	7.0	0.2	0.0	-0.1	7.1	1.9	0.0
L2	738	-0.2	3.3	8.0	-0.5	0.0	0.0	8.0	3.3	-0.3
L3	737	0.2	4.7	8.8	-1.2	0.0	0.0	8.8	5.0	-0.1
M1	663	-0.4	-1.5	4.6	0.1	0.0	0.0	4.6	-0.4	-1.5
M2	63	0.2	2.7	6.4	0.8	0.0	0.0	6.4	2.9	-0.1
N1	1877	-0.1	2.1	3.3	-0.2	0.5	0.0	3.5	2.0	-0.1
N2	1477	-0.1	3.3	3.9	-0.3	0.4	0.0	4.2	3.1	-0.1
N3	1277	0.0	4.5	4.6	-0.3	0.4	0.0	4.9	4.1	0.0
O1	647	-0.1	-1.1	4.5	0.1	0.1	0.0	4.5	-0.1	-1.1
O2	247	0.0	0.5	5.3	0.0	0.1	0.0	5.3	0.5	0.0
O3	47	0.0	2.0	6.0	-0.2	0.0	0.0	6.0	2.0	0.0
P1	1840	-0.1	2.3	-2.1	-0.2	0.7	0.0	2.4	-0.1	-2.2
P2	1640	-0.1	3.0	-1.1	-0.2	0.7	0.0	3.1	-0.1	-1.2
P3	1440	0.0	3.7	-0.2	-0.2	0.6	0.0	3.8	0.0	-0.3
P4	1240	0.0	4.4	0.9	-0.3	0.6	0.1	4.5	0.8	0.0
Q1	628	0.0	-0.3	3.9	0.0	0.2	0.0	3.9	0.0	-0.3
Q2	428	0.0	0.4	4.4	0.0	0.2	0.0	4.4	0.4	0.0
Q3	228	0.0	1.0	4.8	-0.1	0.1	0.0	4.8	1.0	0.0
Q4	28	0.0	1.6	5.3	-0.1	0.0	0.0	5.3	1.6	0.0
R1	1816	-0.4	-2.8	2.1	0.2	0.4	0.0	2.1	-0.4	-2.8

Table 2.10.4-10 Stress Components – Impact; 1-Foot Side Drop; Drop Orientation = 90 Degrees; 3-D Model; 0-Degree Circumferential Location; Condition 1 (continued)

Stress Points Section <sup>1</sup> Node		Stress Components (ksi)						Principal Stresses (ksi)		
		S <sub>x</sub>	S <sub>y</sub>	S <sub>z</sub>	S <sub>xy</sub>	S <sub>xz</sub>	S <sub>yz</sub>	S1	S2	S3
R2	1616	-0.8	-3.5	-1.0	0.3	0.4	-0.1	-0.7	-0.9	-3.6
R3	1416	-1.9	-4.4	-3.6	0.3	0.3	-0.8	-1.6	-3.7	-4.6
R4	1216	-2.6	-5.3	-7.3	0.4	0.2	-1.8	-2.0	-5.3	-7.9
S1	616	0.5	-1.7	0.2	0.1	0.2	-0.1	0.5	0.2	-1.7
S2	416	-0.2	-1.1	2.7	0.0	0.1	-0.1	2.7	-0.2	-1.1
S3	216	0.0	-0.3	4.8	0.0	0.1	0.1	4.8	0.0	-0.3
S4	16	0.0	0.4	7.0	0.0	0.0	0.1	7.0	0.4	0.0
T1	811	-6.5	-7.8	-8.0	0.4	0.1	-2.5	-4.7	-7.8	-9.9
T2	611	-3.6	-5.2	-2.0	0.2	0.1	-1.7	-0.9	-4.6	-5.3
T3	411	-1.7	-3.7	1.1	0.2	0.1	-1.3	1.6	-2.1	-3.7
T4	211	-0.4	-2.4	3.9	0.1	0.0	-0.7	4.1	-0.5	-2.4
T5	11	0.1	-1.1	8.0	0.1	0.0	-0.4	8.0	0.1	-1.1
U1	43058	1.4	-0.2	0.0	0.1	0.0	0.0	1.4	0.0	-0.2
U2	43057	0.8	-0.5	-0.1	0.1	0.0	0.0	0.8	-0.1	-0.5
U3	43056	0.3	-0.7	-0.2	0.1	0.0	0.0	0.3	-0.2	-0.7
U4	43055	-0.2	-1.0	-0.4	0.0	0.0	-0.2	0.0	-0.5	-1.0
U5	43054	-0.7	-1.3	-0.5	0.0	0.0	-0.4	-0.2	-1.1	-1.3
U6	43053	-1.3	-1.6	-0.7	0.0	-0.1	-0.9	-0.1	-1.6	-1.9
U7	43052	-2.3	-1.9	-0.4	0.0	-0.1	-1.1	0.2	-1.9	-2.8
U8	43051	-5.0	-2.8	0.0	-0.1	0.0	0.0	0.0	-2.8	-5.0
V1	50024	0.5	-0.6	0.1	0.0	0.0	0.0	0.5	0.1	-0.6
V2	50023	-1.5	-1.5	-0.1	0.0	0.0	0.0	-0.1	-1.5	-1.5
V3	50022	-2.4	-2.1	-0.2	0.0	0.0	-0.1	-0.1	-2.1	-2.4
V4	50021	-5.6	-3.3	0.0	0.0	0.0	0.0	0.0	-3.3	-5.6
W1	43278	-0.8	-1.1	0.0	0.0	0.0	0.1	0.0	-0.8	-1.1
W2	43274	-0.5	-1.2	0.0	0.0	-0.1	0.1	0.0	-0.6	-1.2
W3	43271	-0.1	-0.7	0.0	0.0	-0.1	0.0	0.0	-0.2	-0.7
X1	50084	-0.4	-2.0	0.0	0.0	0.0	0.1	0.1	-0.4	-2.0
X2	50083	-0.2	-2.1	0.0	0.0	0.0	0.1	0.1	-0.2	-2.1
X3	50081	0.2	-2.3	-0.1	0.0	0.0	0.1	0.3	-0.1	-2.3

<sup>1</sup> Refer to Figure 2.10.2-34 for the identification of the representative sections.

Table 2.10.4-11 Stress Components - Impact; 1-Foot Top Corner Drop; Drop Orientation = 24 Degrees; 3-D Top Model; 0-Degree Circumferential Location; Condition 1

Condition 1: 100°F Ambient with Contents

Stress Points		Stress Components (ksi)						Principal Stresses (ksi)		
Section <sup>1</sup>	Node	S <sub>x</sub>	S <sub>y</sub>	S <sub>z</sub>	S <sub>xy</sub>	S <sub>xz</sub>	S <sub>yz</sub>	S1	S2	S3
A1	1949	0.8	1.1	-0.1	0.0	0.0	0.1	1.1	0.8	-0.1
A2	1950	0.4	0.7	-0.1	0.0	0.0	0.1	0.7	0.5	-0.1
A3	1951	-0.2	-0.1	0.2	0.0	0.0	0.1	0.2	-0.1	-0.2
B1	1952	0.0	0.0	-0.2	0.0	0.0	0.1	0.0	0.0	-0.2
B2	93	-0.7	-1.0	0.4	0.0	0.0	0.1	0.5	-0.8	-1.0
C1	1925	-0.3	-0.1	0.2	0.0	-0.1	0.0	0.2	-0.1	-0.3
C2	1926	-0.1	-0.1	-0.1	0.0	0.0	-0.1	0.1	-0.1	-0.2
C3	1927	0.3	-0.1	-0.1	0.0	0.0	-0.1	0.3	-0.1	-0.1
D1	683	0.0	-0.2	-0.2	0.0	0.0	0.0	0.0	-0.2	-0.2
D2	85	0.0	-0.4	-0.2	0.1	0.0	0.0	0.0	-0.2	-0.4
E1	682	0.2	-0.1	-0.3	0.0	0.0	0.1	0.2	-0.1	-0.3
E2	82	0.2	0.1	0.5	0.0	0.0	0.1	0.5	0.1	0.1
F1	1925	-0.3	-0.1	0.2	0.0	-0.1	0.0	0.2	-0.1	-0.3
F2	1325	-0.7	-0.9	-2.2	0.0	-0.1	0.1	-0.7	-0.9	-2.2
G1	680	-0.4	0.0	0.2	0.0	0.0	0.2	0.3	0.0	-0.5
G2	80	0.0	0.2	0.6	0.0	0.0	0.0	0.6	0.2	0.0
H1	1921	0.0	1.1	-1.6	-0.1	-0.2	0.0	1.1	0.0	-1.6
H2	1321	0.0	1.4	-0.8	-0.1	-0.1	0.0	1.4	0.0	-0.8
I1	676	0.0	0.0	0.1	0.0	0.0	0.0	0.1	0.0	0.0
I2	76	0.0	0.3	0.3	0.0	0.0	0.0	0.3	0.2	0.0
J1	1916	0.0	1.1	-0.5	-0.1	-0.1	0.0	1.1	0.0	-0.5
J2	1316	0.0	1.7	-0.1	-0.1	-0.1	0.0	1.7	0.0	-0.1
K1	671	0.0	-0.2	-0.4	0.0	0.0	0.0	0.0	-0.2	-0.4
K2	71	0.0	0.4	-0.1	0.0	0.0	0.0	0.4	0.0	-0.1
L1	1908	-0.2	0.6	-1.3	-0.1	0.1	0.0	0.6	-0.2	-1.3
L2	1308	0.0	2.1	-0.7	0.4	0.1	0.0	2.2	0.0	-0.7
M1	663	-0.2	-0.5	-1.4	0.0	0.0	0.0	-0.2	-0.5	-1.4
M2	63	0.1	0.9	-0.9	0.3	0.1	0.0	1.0	0.0	-0.9
N1	1877	0.0	0.7	-4.6	-0.1	0.3	0.0	0.7	0.0	-4.6
N2	1477	0.0	1.4	-4.3	-0.1	0.3	0.0	1.4	0.0	-4.3

Table 2.10.4-11 Stress Components – Impact; 1-Foot Top Corner Drop; Drop Orientation = 24 Degrees; 3-D Top Model; 0-Degree Circumferential Location; Condition 1 (continued)

Stress Points Section <sup>1</sup> Node		Stress Components (ksi)						Principal Stresses (ksi)		
		S <sub>x</sub>	S <sub>y</sub>	S <sub>z</sub>	S <sub>xy</sub>	S <sub>yz</sub>	S <sub>xz</sub>	S1	S2	S3
N3	1277	0.0	2.0	-4.0	-0.2	0.2	0.0	2.1	0.0	-4.0
O1	647	0.0	-0.5	-2.5	0.0	0.1	0.0	0.0	-0.5	-2.5
O2	247	0.0	0.1	-2.3	0.0	0.1	0.0	0.1	0.0	-2.3
O3	47	0.0	0.6	-2.1	-0.1	0.1	0.0	0.6	0.0	-2.1
P1	1840	-0.1	1.1	-5.2	-0.1	0.4	0.0	1.1	-0.1	-5.2
P2	1640	-0.2	1.0	-6.3	-0.1	0.4	0.0	1.0	-0.2	-6.3
P3	1440	-0.2	1.0	-7.3	-0.1	0.3	-0.2	1.0	-0.2	-7.3
P4	1240	-0.2	0.6	-9.4	0.0	0.3	-0.5	0.6	-0.2	-9.5
Q1	628	0.0	0.8	-2.5	-0.1	0.1	0.0	0.9	0.0	-2.5
Q2	428	0.0	0.9	-2.9	-0.1	0.1	0.0	0.9	0.0	-2.9
Q3	228	0.0	1.0	-3.2	-0.1	0.1	0.0	1.0	0.0	-3.2
Q4	28	0.0	1.0	-3.5	-0.1	0.0	0.0	1.0	0.0	-3.5
R1	1816	0.1	-1.2	-11.4	0.1	0.2	0.0	0.1	-1.2	-11.5
R2	1616	0.2	-0.3	-8.4	0.1	-0.2	0.1	0.2	-0.3	-8.5
R3	1416	0.2	0.5	-5.7	0.0	0.2	0.3	0.5	0.2	-5.7
R4	1216	2.8	2.0	-3.1	0.1	0.1	0.3	2.8	1.9	-3.1
S1	616	-3.6	-2.1	-11.8	-0.1	0.2	1.5	-2.1	-3.3	-12.1
S2	416	-3.6	-0.4	-5.3	-0.2	0.0	-0.3	-0.4	-3.5	-5.4
S3	216	-1.3	1.4	-0.8	-0.2	0.0	-0.5	1.4	-0.5	-1.6
S4	16	-0.5	3.0	4.5	-0.3	0.0	-0.4	4.5	3.0	-0.5
T1	811	0.1	-1.6	-1.4	0.2	0.2	0.3	0.2	-1.4	-1.7
T2	611	0.4	-1.8	-2.6	0.2	0.1	-0.1	0.4	-1.8	-2.6
T3	411	0.3	-1.8	-2.6	0.2	0.1	-0.2	0.3	-1.8	-2.6
T4	211	0.3	-1.7	-2.3	0.1	0.1	-0.2	0.3	-1.7	-2.3
T5	11	0.3	-1.5	-1.7	0.1	0.0	-0.1	0.3	-1.5	-1.7
U1	43058	0.5	3.0	-5.0	-0.3	0.2	1.1	3.0	0.7	-5.2
U2	43057	1.5	2.5	-4.4	-0.2	0.1	1.6	2.5	1.8	-4.8
U3	43056	1.2	1.7	-3.7	-0.1	0.1	2.1	2.0	1.7	-4.5
U4	43055	0.8	0.8	-3.4	0.0	0.1	2.2	1.7	0.8	-4.4
U5	43054	0.3	-0.1	-3.4	0.0	0.1	2.1	1.3	-0.1	-4.4
U6	43053	-0.3	-0.9	-2.7	0.1	0.1	1.7	0.6	-0.9	-3.5
U7	43052	-0.5	-2.4	-4.7	0.2	0.1	1.7	0.2	-2.4	-5.3

Table 2.10.4-11 Stress Components – Impact; 1-Foot Top Corner Drop; Drop Orientation = 24 Degrees; 3-D Top Model; 0-Degree Circumferential Location; Condition 1 (continued)

Stress Points Section <sup>1</sup> Node	Stress Components (ksi)						Principal Stresses (ksi)		
	S <sub>x</sub>	S <sub>y</sub>	S <sub>z</sub>	S <sub>xy</sub>	S <sub>yz</sub>	S <sub>xz</sub>	S1	S2	S3
UB 43051	-3.5	-4.8	-4.6	0.2	0.2	2.8	-1.1	-4.8	-6.9
V1 50024	-6.9	0.2	-1.8	-0.6	-0.1	-0.9	0.2	-1.7	-7.1
V2 50023	-4.4	-1.6	-1.9	-0.3	-0.1	-0.7	-1.5	-1.7	-4.6
V3 50022	-1.6	-3.3	-1.9	0.1	0.0	-0.3	-1.4	-2.0	-3.3
V4 50021	1.4	-5.0	-1.8	0.4	0.0	-0.1	1.4	-1.8	-5.1
W1 43278	1.0	0.2	-0.3	-0.1	-0.3	-0.1	1.0	0.3	-0.5
W2 43274	0.4	-0.2	-0.1	0.0	-0.3	-0.1	0.4	0.1	-0.5
W3 43271	-0.1	-0.3	0.1	0.0	-0.4	0.0	0.3	-0.1	-0.6
X1 50084	13.8	11.1	-3.4	-0.4	0.2	-3.3	14.5	11.1	-4.0
X2 50083	4.3	2.2	-2.2	-0.1	0.2	-3.3	5.7	2.2	-3.6
X3 50081	-13.0	-13.8	6.9	0.4	-0.2	-3.3	7.4	-13.3	-14.0

<sup>1</sup> Refer to Figure 2.10.2-33 for the identification of the representative sections.

Table 2.10.4-12 Stress Components – Impact; 1-Foot Bottom Corner Drop; Drop Orientation = 24 Degrees; 3-D Bottom Model; 0-Degree Circumferential Location; Condition 1

Condition 1: 100°F Ambient with Contents

Stress Points		Stress Components (ksi)						Principal Stresses (ksi)		
Section <sup>1</sup>	Node	S <sub>x</sub>	S <sub>y</sub>	S <sub>z</sub>	S <sub>xy</sub>	S <sub>xz</sub>	S <sub>yz</sub>	S1	S2	S3
A1	1130	6.6	5.0	-2.4	-0.2	0.8	0.8	6.7	5.1	-2.6
A2	1129	0.9	0.1	-0.5	0.0	0.6	0.8	1.3	0.3	-1.1
A3	1128	-4.8	-4.9	1.5	0.2	0.8	0.8	1.7	-4.9	-5.1
B1	1185	3.8	1.5	-2.5	-0.2	0.8	0.8	3.9	1.7	-2.8
B2	1184	-1.4	-2.9	-0.7	0.0	0.6	0.9	-0.1	-1.9	-3.1
B3	1183	-6.7	-7.3	1.1	0.1	0.6	0.8	1.2	-6.8	-7.3
C1	90	-7.0	-2.1	-8.5	-0.4	-0.3	-1.7	-2.0	-5.9	-9.7
C2	80	-3.3	-0.6	-5.0	-0.4	-0.2	-1.3	-0.6	-2.7	-5.7
C3	70	-2.1	-0.4	-3.1	-0.2	-0.1	-1.0	-0.4	-1.6	-3.7
C4	60	-1.1	-0.3	-1.8	0.0	-0.1	-0.9	-0.3	-0.5	-2.4
C5	50	2.5	-0.9	-0.6	0.3	-0.1	-0.6	2.7	-0.7	-1.0
C6	40	5.8	-0.9	-0.1	0.6	0.0	-0.4	5.9	-0.1	-1.0
D1	25	-12.4	-9.3	-15.2	-0.1	-0.3	-3.3	-9.3	-10.2	-17.4
D2	15	-2.0	-7.0	-6.5	0.2	-0.1	-1.6	-1.5	-7.0	-7.0
D3	5	0.9	-8.6	-3.0	0.6	0.0	-0.5	1.0	-3.1	-8.7
E1	35	2.9	-3.8	-11.7	0.5	-0.1	-1.2	3.1	-3.9	-11.8
E2	34	0.0	-3.4	-7.8	0.2	-0.3	-3.0	1.0	-3.4	-8.8
E3	33	-2.4	-3.0	-4.0	0.0	-0.3	-3.3	0.2	-3.0	-6.6
E4	32	-2.7	-2.4	-1.1	0.0	-0.2	-2.0	0.3	-2.4	-4.1
E5	31	-2.8	-1.6	1.9	-0.1	-0.1	-1.2	2.2	-1.6	-3.1
F1	100	0.0	-0.8	-11.1	0.0	-0.4	-1.1	0.1	-0.8	-11.2
F2	99	-1.0	0.1	-6.7	-0.1	-0.3	-0.5	0.2	-1.0	-6.8
F3	98	-1.1	0.5	-5.2	-0.1	-0.2	0.4	0.5	-1.0	-5.3
F4	97	0.0	0.9	-4.6	-0.1	-0.2	0.8	1.0	0.1	-4.7
G1	94	0.1	-0.8	-8.1	0.0	-0.1	-0.3	0.1	-0.8	-8.1
G2	93	-0.2	-0.1	-5.3	0.0	-0.1	-0.2	-0.1	-0.2	-5.3
G3	92	-0.3	0.4	-3.2	-0.1	-0.1	0.0	0.4	-0.4	-3.2
G4	91	-0.2	1.1	-0.6	-0.1	0.0	0.0	1.1	-0.2	-0.6

Table 2.10.4-12 Stress Components - Impact; 1-Foot Bottom Corner Drop; Drop Orientation = 24 Degrees; 3-D Bottom Model; 0-Degree Circumferential Location; Condition 1 (continued)

Stress Points		Stress Components (ksi)						Principal Stresses (ksi)		
Section <sup>1</sup>	Node	S <sub>x</sub>	S <sub>y</sub>	S <sub>z</sub>	S <sub>xy</sub>	S <sub>yz</sub>	S <sub>xz</sub>	S1	S2	S3
H1	330	-0.1	1.1	-5.0	-0.1	-0.4	0.0	1.2	-0.1	-5.0
H2	329	-0.2	1.0	-6.0	-0.1	-0.3	0.0	1.0	-0.2	-6.1
H3	328	-0.2	0.9	-7.0	-0.1	-0.3	0.2	0.9	-0.2	-7.0
H4	327	-0.2	0.6	-9.0	0.0	-0.3	0.5	0.6	-0.2	-9.1
I1	244	0.0	0.1	-3.6	0.0	-0.2	0.0	0.1	0.0	-3.7
I2	243	0.0	0.4	-3.7	0.0	-0.1	0.0	0.4	0.0	-3.7
I3	242	0.0	0.6	-3.7	0.0	-0.1	0.0	0.6	0.0	-3.7
I4	241	0.0	0.8	-3.7	-0.1	0.0	0.0	0.8	0.0	-3.7
J1	550	0.0	0.8	-3.9	-0.1	-0.3	0.0	0.9	0.0	-3.9
J2	548	0.0	1.4	-3.7	-0.1	-0.2	0.0	1.4	0.0	-3.7
J3	547	0.0	1.9	-3.5	-0.1	-0.2	0.0	1.9	0.0	-3.5
K1	344	0.0	-0.7	-3.1	0.0	-0.1	0.0	0.0	-0.7	-3.1
K2	342	0.0	0.2	-2.7	0.0	-0.1	0.0	0.0	0.0	-2.7
K3	341	0.0	1.1	-2.4	-0.1	-0.1	0.0	1.1	0.0	-2.4
L1	740	0.0	0.9	-0.9	0.0	-0.1	0.0	0.9	0.0	-0.9
L2	738	-0.1	1.3	-0.6	-0.2	-0.1	0.0	1.4	-0.1	-0.6
L3	737	0.0	1.8	-0.3	-0.4	-0.1	0.0	1.9	0.0	-0.3
M1	454	0.0	-0.7	-1.8	-0.3	0.0	0.0	0.1	-0.9	-1.8
M2	452	0.1	0.2	-1.4	-0.1	-0.1	0.0	0.3	0.0	-1.4
M3	451	-0.1	0.9	-1.2	0.0	-0.1	0.0	0.9	-0.1	-1.2
N1	810	0.0	1.2	-0.5	-0.1	0.1	0.0	1.2	0.0	-0.5
N2	807	0.0	1.6	-0.1	-0.1	0.1	0.0	1.6	0.0	-0.1
O1	524	0.0	-0.2	-0.6	0.0	0.0	0.0	0.0	-0.2	-0.6
O2	521	0.0	0.4	-0.3	0.0	-0.1	0.0	0.4	0.0	-0.3
P1	850	0.0	1.0	-1.6	-0.1	0.2	0.0	1.1	0.0	-1.6
P2	847	0.0	1.4	-0.7	-0.1	0.2	0.0	1.5	0.0	-0.8
Q1	564	0.0	0.1	0.0	0.0	0.0	0.0	0.1	0.0	0.0
Q2	561	0.0	0.3	0.1	0.0	0.0	0.0	0.3	0.1	0.0
R1	890	-0.3	-0.1	0.2	0.0	0.1	0.0	0.2	-0.2	-0.3
R2	887	-0.4	-0.7	-2.1	0.0	0.1	-0.1	-0.4	-0.7	-2.1



Table 2.10.4-12 Stress Components – Impact; 1-Foot Bottom Corner Drop; Drop Orientation = 24 Degrees; 3-D Bottom Model; 0-Degree Circumferential Location; Condition 1 (continued)

Stress Points Section <sup>1</sup> Node	Stress Components (ksi)						Principal Stresses (ksi)		
	S <sub>x</sub>	S <sub>y</sub>	S <sub>z</sub>	S <sub>xy</sub>	S <sub>yz</sub>	S <sub>xz</sub>	S1	S2	S3
S1 604	-0.2	0.1	0.0	0.0	0.0	-0.1	0.2	0.1	-0.2
S2 601	0.0	0.4	0.7	0.0	0.0	0.0	0.7	0.4	0.0
T1 897	0.1	-0.1	-0.7	0.0	0.0	-0.1	0.1	-0.1	-0.7
T2 614	0.1	0.1	0.0	0.0	0.0	-0.2	0.2	0.1	-0.1
T3 611	0.0	0.1	0.3	0.0	0.0	-0.1	0.3	0.1	0.0
U1 900	0.1	0.0	-0.4	0.0	0.0	0.1	0.1	0.0	-0.4
U2 910	0.3	-0.1	-0.3	0.0	0.0	0.1	0.3	-0.1	-0.3
V1 920	-0.1	-0.2	-0.2	0.0	0.0	0.1	-0.1	-0.2	-0.2
V2 930	-0.1	-0.4	-0.1	0.1	0.0	0.0	0.0	-0.1	-0.4
W1 1216	0.5	0.9	-0.4	0.0	0.0	-0.1	0.9	0.5	-0.4
W2 1226	-0.1	-0.1	0.2	0.0	0.0	-0.1	0.2	-0.1	-0.1
X1 1236	0.0	0.0	-0.2	0.0	0.0	-0.1	0.1	0.0	-0.3
X2 1246	-0.7	-1.0	0.5	0.0	0.0	-0.1	0.5	-0.7	-1.0

<sup>1</sup> Refer to Figure 2.10.2-34 for the identification of the representative sections.

Table 2.10.4-13 Stress Components – Impact; 30-Foot Top End Drop; Drop Orientation = 0 Degrees; 2-D Model; Condition 1

Condition 1: 100°F Ambient with Contents

Stress Points		Stress Components (ksi)						Principal Stresses (ksi)		
Section <sup>1</sup>	Node	S <sub>x</sub>	S <sub>y</sub>	S <sub>z</sub>	S <sub>xy</sub>	S <sub>yz</sub>	S <sub>xz</sub>	S1	S2	S3
A1	1	4.4	0.0	4.4	0.0	0.0	0.0	4.4	4.4	0.0
A2	2	2.4	0.0	2.4	0.0	0.0	0.0	2.4	2.4	0.0
A3	3	0.5	0.0	0.5	0.0	0.0	0.0	0.5	0.5	0.0
A4	4	-1.4	0.0	-1.4	0.0	0.0	0.0	0.0	-1.4	-1.4
A5	5	-3.3	0.0	-3.3	0.0	0.0	0.0	0.0	-3.3	-3.3
B1	6	2.7	0.0	2.7	0.0	0.0	0.0	2.7	2.7	0.0
B2	7	1.0	0.0	1.0	0.0	0.0	0.0	1.0	1.0	0.0
B3	8	-0.7	0.0	-0.7	0.0	0.0	0.0	0.0	-0.7	-0.7
B4	9	-2.4	0.0	-2.4	0.0	0.0	0.0	0.0	-2.4	-2.4
B5	10	-4.1	0.0	-4.1	0.0	0.0	0.0	0.0	-4.1	-4.1
C1	251	-2.8	-3.5	-0.5	-0.7	0.0	0.0	-0.5	-2.4	-3.9
C2	252	-0.5	-1.4	0.3	-0.5	0.0	0.0	0.3	-0.3	-1.6
C3	253	0.6	-0.6	0.4	-0.4	0.0	0.0	0.8	0.4	-0.7
C4	254	1.9	-0.2	0.4	-0.3	0.0	0.0	2.0	0.4	-0.3
C5	255	3.4	-0.2	0.4	-0.2	0.0	0.0	3.4	0.4	-0.2
D1	306	-3.4	-1.9	-1.5	-0.9	0.0	0.0	-1.4	-1.5	-3.8
D2	307	-1.0	-1.5	-0.9	-0.3	0.0	0.0	-0.9	-0.9	-1.6
D3	308	-0.3	-0.6	-0.7	0.1	0.0	0.0	-0.3	-0.6	-0.7
D4	309	0.4	-0.2	-0.7	0.2	0.0	0.0	0.5	-0.3	-0.7
D5	310	1.3	-0.1	-0.7	0.1	0.0	0.0	1.3	-0.1	-0.7
E1	305	3.2	0.1	0.9	-0.7	0.0	0.0	3.4	0.9	0.0
E2	315	1.6	-0.7	0.3	-0.8	0.0	0.0	1.9	0.3	-1.0
E3	325	0.8	-0.6	0.1	-0.8	0.0	0.0	1.1	0.1	-1.0
E4	335	0.4	-0.6	0.0	-0.6	0.0	0.0	0.7	0.0	-0.9
E5	345	0.2	-0.6	-0.1	-0.4	0.0	0.0	0.3	-0.1	-0.8
E6	355	0.1	-0.8	-0.2	-0.2	0.0	0.0	0.1	-0.2	-0.9
F1	251	-2.8	-3.5	-0.5	-0.7	0.0	0.0	-0.5	-2.4	-3.9
F2	261	-2.1	-1.9	0.1	-0.2	0.0	0.0	0.1	-1.8	-2.3
F3	271	-1.6	-0.9	0.5	0.2	0.0	0.0	0.5	-0.8	-1.7
F4	281	-1.7	-0.1	0.6	0.3	0.0	0.0	0.6	0.0	-1.7
G1	311	-1.5	-2.3	-0.2	-0.2	0.0	0.0	-0.2	-1.4	-2.4

Table 2.10.4-13 Stress Components – Impact; 30-Foot Top End Drop; Drop Orientation = 0 Degrees; 2-D Model; Condition 1 (continued)

Stress Points Section <sup>1</sup> Node	Stress Components (ksi)						Principal Stresses (ksi)		
	S <sub>x</sub>	S <sub>y</sub>	S <sub>z</sub>	S <sub>w</sub>	S <sub>xy</sub>	S <sub>xz</sub>	S1	S2	S3
G2	321	-1.0	-1.5	0.2	0.0	0.0	0.2	-1.0	-1.5
G3	331	-0.5	-0.8	0.5	0.2	0.0	0.5	-0.4	-0.9
G4	341	-0.2	-0.2	0.7	0.1	0.0	0.7	-0.1	-0.3
G5	351	-0.1	0.7	1.0	0.1	0.0	1.0	0.7	-0.1
H1	581	0.0	-2.3	0.1	0.0	0.0	0.1	0.0	-2.3
H2	582	-0.1	-2.9	-0.1	0.0	0.0	-0.1	-0.1	-2.9
H3	583	-0.1	-3.5	-0.3	0.1	0.0	-0.1	-0.3	-3.5
H4	584	0.0	-4.4	-0.5	0.2	0.0	0.0	-0.5	-4.4
I1	589	0.0	-1.1	0.2	0.0	0.0	0.2	0.0	-1.1
I2	590	0.0	-1.2	0.2	0.0	0.0	0.2	0.0	-1.2
I3	591	0.0	-1.4	0.2	0.0	0.0	0.2	0.0	-1.4
I4	592	0.0	-1.5	0.1	0.0	0.0	0.1	0.0	-1.5
I5	593	0.0	-1.6	0.1	0.0	0.0	0.1	0.0	-1.6
J1	971	0.0	-3.9	0.0	0.0	0.0	0.0	0.0	-3.9
J2	972	0.0	-3.9	0.0	0.0	0.0	0.0	0.0	-3.9
J3	973	0.0	-3.9	0.0	0.0	0.0	0.0	0.0	-3.9
J4	974	0.0	-3.9	0.0	0.0	0.0	0.0	0.0	-3.9
K1	979	0.0	-2.0	0.0	0.0	0.0	0.0	0.0	-2.0
K2	980	0.0	-2.0	0.0	0.0	0.0	0.0	0.0	-2.0
K3	981	0.0	-2.0	0.0	0.0	0.0	0.0	0.0	-2.0
K4	982	0.0	-2.0	0.0	0.0	0.0	0.0	0.0	-2.0
K5	983	0.0	-2.0	0.0	0.0	0.0	0.0	0.0	-2.0
L1	1601	0.0	-4.9	0.0	0.0	0.0	0.0	0.0	-4.9
L2	1602	0.0	-4.9	0.0	0.0	0.0	0.0	0.0	-4.9
L3	1603	0.0	-4.9	0.0	0.0	0.0	0.0	0.0	-4.9
L4	1604	0.0	-4.9	0.0	0.0	0.0	0.0	0.0	-4.9
M1	1609	0.0	-3.0	0.0	0.0	0.0	0.0	0.0	-3.0
M2	1610	0.0	-3.0	0.0	0.0	0.0	0.0	0.0	-3.0
M3	1611	0.0	-3.0	0.0	0.0	0.0	0.0	0.0	-3.0
M4	1612	0.0	-3.0	0.0	0.0	0.0	0.0	0.0	-3.0
M5	1613	0.0	-3.0	0.0	0.0	0.0	0.0	0.0	-3.0
N1	2216	0.0	-6.0	0.0	0.0	0.0	0.0	0.0	-6.0
N2	2217	0.0	-5.9	0.0	0.0	0.0	0.0	0.0	-5.9

Table 2.10.4-13 Stress Components – Impact; 30-Foot Top End Drop; Drop Orientation = 0 Degrees; 2-D Model; Condition 1 (continued)

Stress Points Section <sup>1</sup> Node	Stress Components (ksi)						Principal Stresses (ksi)		
	S <sub>x</sub>	S <sub>y</sub>	S <sub>z</sub>	S <sub>xy</sub>	S <sub>yz</sub>	S <sub>xz</sub>	S1	S2	S3
N3	2218	0.0	-5.9	0.0	0.0	0.0	0.0	0.0	-5.9
N4	2219	0.0	-5.9	0.0	0.0	0.0	0.0	0.0	-5.9
O1	2224	0.0	-3.9	-0.1	0.0	0.0	0.0	-0.1	-3.9
O2	2225	0.0	-3.9	-0.1	0.0	0.0	0.0	-0.1	-3.9
O3	2226	0.0	-3.9	-0.1	0.0	0.0	0.0	-0.1	-3.9
O4	2227	0.0	-3.9	-0.1	0.0	0.0	0.0	-0.1	-3.9
O5	2228	0.0	-3.9	-0.1	0.0	0.0	0.0	-0.1	-3.9
P1	2546	-0.1	-3.5	0.7	0.0	0.0	0.7	-0.1	-3.5
P2	2547	-0.1	-5.3	0.2	0.0	0.0	0.2	-0.1	-5.3
P3	2548	-0.1	-7.0	-0.3	-0.2	0.0	-0.1	-0.3	-7.0
P4	2549	-0.1	-9.5	-0.9	-0.5	0.0	-0.1	-0.9	-9.5
Q1	2554	0.0	-3.6	1.3	0.0	0.0	1.3	0.0	-3.6
Q2	2555	0.0	-4.0	1.1	0.0	0.0	1.1	0.0	-4.0
Q3	2556	0.0	-4.4	1.0	0.1	0.0	1.0	0.0	-4.4
Q4	2557	0.0	-4.9	0.9	0.0	0.0	0.9	0.0	-4.9
Q5	2558	0.0	-5.3	0.7	0.0	0.0	0.7	0.0	-5.3
R1	2771	0.2	-18.3	-0.9	-0.1	0.0	0.2	-0.9	-18.3
R2	2772	0.6	-10.8	1.3	0.1	0.0	1.3	0.6	-10.8
R3	2773	1.7	-3.7	3.5	1.2	0.0	3.5	1.9	-3.9
R4	2774	1.4	4.6	5.6	2.9	0.0	6.4	5.6	-0.3
S1	2779	-9.2	-12.6	-2.8	0.8	0.0	-2.8	-9.1	-12.7
S2	2780	-5.9	-7.5	-0.6	-0.3	0.0	-0.6	-5.8	-7.6
S3	2781	-3.0	-4.0	1.1	-1.1	0.0	1.1	-2.3	-4.8
S4	2782	-1.2	-0.4	2.5	-0.9	0.0	2.5	0.2	-1.8
S5	2783	-0.5	4.2	3.8	-0.6	0.0	4.3	3.8	-0.6
T1	7066	11.5	9.1	4.7	2.7	0.0	13.3	7.3	4.7
T2	7067	7.7	2.8	2.0	1.0	0.0	7.9	2.6	2.0
T3	7068	5.1	-0.7	0.5	-0.2	0.0	5.1	0.5	-0.7
T4	7069	3.0	-3.0	-0.6	-0.9	0.0	3.2	-0.6	-3.1
T5	7070	1.6	-5.1	-1.5	-1.0	0.0	1.8	-1.5	-5.2
T6	7071	0.7	-7.4	-2.4	-0.7	0.0	0.8	-2.4	-7.4
T7	7072	0.4	-10.5	-3.3	-0.4	0.0	0.4	-3.3	-10.5
U1	3051	-1.9	-9.3	6.3	1.8	0.0	6.3	-1.5	-9.7

Table 2.10.4-13 Stress Components – Impact; 30-Foot Top End Drop; Drop Orientation = 0 Degrees; 2-D Model; Condition 1 (continued)

Stress Points		Stress Components (ksi)						Principal Stresses (ksi)		
Section <sup>1</sup>	Node	S <sub>x</sub>	S <sub>y</sub>	S <sub>z</sub>	S <sub>xy</sub>	S <sub>yz</sub>	S <sub>xz</sub>	S1	S2	S3
U2	3052	2.1	-8.6	4.7	2.2	0.0	0.0	4.7	2.5	-9.0
U3	3053	2.5	-7.2	2.4	2.5	0.0	0.0	3.1	2.4	-7.8
U4	3054	2.2	-7.1	-0.3	2.3	0.0	0.0	2.8	-0.3	-7.7
U5	3055	2.1	-8.6	-3.5	2.7	0.0	0.0	2.7	-3.5	-9.3
U6	3056	-1.6	-6.8	-6.4	4.4	0.0	0.0	0.9	-6.4	-9.2
V1	3611	-8.4	-4.6	5.3	-1.5	0.0	0.0	5.3	-4.2	-8.9
V2	3612	-5.0	-4.5	3.7	-1.8	0.0	0.0	3.7	-2.9	-6.6
V3	3613	-2.4	-4.0	1.8	-2.3	0.0	0.0	1.8	-0.9	-5.6
V4	3614	-0.3	-3.6	-0.3	-2.1	0.0	0.0	0.7	-0.3	-4.6
V5	3615	1.6	-2.7	-2.3	-1.8	0.0	0.0	2.3	-2.3	-3.4
V6	3616	1.7	-2.0	-4.9	-1.1	0.0	0.0	2.0	-2.3	-4.9
V7	3617	6.9	-1.9	-6.3	-0.7	0.0	0.0	6.9	-1.9	-6.3
W1	3241	21.5	-1.0	21.5	0.0	0.0	0.0	21.5	21.5	-1.0
W2	3242	13.9	-1.3	13.9	0.0	0.0	0.0	13.9	13.9	-1.3
W3	3243	6.5	-1.8	6.5	0.0	0.0	0.0	6.5	6.5	-1.8
W4	3244	-0.8	-2.3	-0.8	0.0	0.0	0.0	-0.8	-0.8	-2.3
W5	3245	-8.3	-2.8	-8.3	0.0	0.0	0.0	-2.8	-8.3	-8.3
W6	3246	-16.2	-3.0	-16.2	0.0	0.0	0.0	-3.0	-16.2	-16.2
X1	3801	27.5	-3.5	27.5	0.0	0.0	0.0	27.5	27.5	-3.5
X2	3802	19.0	-3.3	19.0	0.0	0.0	0.0	19.0	19.0	-3.3
X3	3803	9.8	-3.0	9.8	0.0	0.0	0.0	9.8	9.8	-3.0
X4	3804	0.5	-2.8	0.5	0.0	0.0	0.0	0.5	0.5	-2.8
X5	3805	-8.9	-2.6	-8.9	0.0	0.0	0.0	-2.6	-8.9	-8.9
X6	3806	-18.2	-2.1	-18.2	0.0	0.0	0.0	-2.1	-18.2	-18.2
X7	3807	-28.0	-1.8	-28.0	0.0	0.0	0.0	-1.8	-28.0	-28.0

<sup>1</sup> Refer to Figure 2.10.2-34 for the identification of the representative sections.

Table 2.10.4-14 Stress Components – Impact; 30-Foot Bottom End Drop; Drop Orientation = 0 Degrees; 2-D Model; Condition 1

Condition 1: 100°F Ambient with Contents

Stress Points		Stress Components (ksi)						Principal Stresses (ksi)		
Section <sup>1</sup>	Node	S <sub>x</sub>	S <sub>y</sub>	S <sub>z</sub>	S <sub>xy</sub>	S <sub>yz</sub>	S <sub>xz</sub>	S1	S2	S3
A1	1	21.7	-0.9	21.7	0.0	0.0	0.0	21.7	21.7	-0.9
A2	2	12.3	-1.0	12.3	0.0	0.0	0.0	12.3	12.3	-1.0
A3	3	3.0	-1.3	3.0	0.0	0.0	0.0	3.0	3.0	-1.3
A4	4	-6.3	-1.5	-6.3	0.0	0.0	0.0	-1.5	-6.3	-6.3
A5	5	-15.9	-1.6	-15.9	0.0	0.0	0.0	-1.6	-15.9	-15.9
B1	6	12.7	-1.8	12.7	0.0	0.0	0.0	12.7	12.7	-1.8
B2	7	4.5	-1.9	4.5	0.0	0.0	0.0	4.5	4.5	-1.9
B3	8	-3.7	-2.1	-3.7	0.0	0.0	0.0	-2.1	-3.7	-3.7
B4	9	-11.9	-2.2	-11.9	0.0	0.0	0.0	-2.2	-11.9	-11.9
B5	10	-20.0	-2.4	-20.0	0.0	0.0	0.0	-2.4	-20.0	-20.0
C1	251	-11.9	-14.6	-0.8	-2.5	0.0	0.0	-0.8	-10.4	-16.1
C2	252	-1.9	-6.0	2.4	-1.8	0.0	0.0	2.4	-1.2	-6.6
C3	253	3.1	-2.6	2.7	-1.8	0.0	0.0	3.7	2.7	-3.1
C4	254	9.6	-1.6	2.7	-1.5	0.0	0.0	9.8	2.7	-1.8
C5	255	16.7	-1.5	2.6	-1.0	0.0	0.0	16.7	2.6	-1.5
D1	306	-18.4	-15.6	-8.6	-5.5	0.0	0.0	-8.6	-11.3	-22.6
D2	307	-4.9	-11.2	-4.9	-2.3	0.0	0.0	-4.1	-4.9	-11.9
D3	308	-1.2	-5.7	-3.8	0.0	0.0	0.0	-1.2	-3.8	-5.7
D4	309	2.3	-3.7	-3.9	0.5	0.0	0.0	2.4	-3.7	-3.9
D5	310	6.8	-2.9	-4.0	0.6	0.0	0.0	6.8	-2.9	-4.0
E1	305	15.7	-4.6	3.6	-3.6	0.0	0.0	16.3	3.6	-5.2
E2	315	7.6	-6.9	1.1	-4.7	0.0	0.0	8.9	1.1	-8.3
E3	325	3.2	-5.5	0.3	-4.6	0.0	0.0	5.1	0.3	-7.4
E4	335	1.6	-4.5	0.2	-3.5	0.0	0.0	3.2	0.2	-6.1
E5	345	0.6	-3.8	0.2	-2.1	0.0	0.0	1.4	0.2	-4.6
E6	355	0.3	-3.7	0.1	-1.2	0.0	0.0	0.6	0.1	-4.0
F1	251	-11.9	-14.6	-0.8	-2.5	0.0	0.0	-0.8	-10.4	-16.1
F2	261	-8.6	-6.5	2.1	-0.8	0.0	0.0	2.1	-6.2	-8.9
F3	271	-5.6	-0.5	4.3	0.2	0.0	0.0	4.3	-0.5	-5.6
F4	281	-5.6	4.6	5.5	-0.2	0.0	0.0	5.5	4.6	-5.6
G1	311	-8.0	-12.9	-1.1	-0.4	0.0	0.0	-1.1	-8.0	-12.9

Table 2.10.4-14 Stress Components – Impact; 30-Foot Bottom End Drop; Drop Orientation = 0 Degrees; 2-D Model; Condition 1 (continued)

Stress Points Section <sup>1</sup> Node	Stress Components (ksi)						Principal Stresses (ksi)		
	S <sub>x</sub>	S <sub>y</sub>	S <sub>z</sub>	S <sub>xy</sub>	S <sub>xz</sub>	S <sub>yz</sub>	S1	S2	S3
G2	321	-5.6	-8.0	0.8	0.3	0.0	0.8	-5.6	-8.1
G3	331	-2.9	-4.8	2.3	0.9	0.0	2.3	-2.5	-5.2
G4	341	-1.2	-1.5	3.6	0.7	0.0	3.6	-0.6	-2.1
G5	351	-0.5	2.8	4.9	0.4	0.0	4.9	2.8	-0.6
H1	581	-0.1	-3.0	0.7	0.0	0.0	0.7	-0.1	-3.0
H2	582	-0.1	-5.1	0.1	0.0	0.0	0.1	-0.1	-5.1
H3	583	-0.1	-7.1	-0.5	0.3	0.0	-0.1	-0.5	-7.1
H4	584	-0.1	-9.9	-1.2	0.6	0.0	-0.1	-1.2	-10.0
I1	589	0.0	-3.6	1.1	0.0	0.0	1.1	0.0	-3.6
I2	590	0.0	-4.2	1.0	0.0	0.0	1.0	0.0	-4.2
I3	591	0.0	-4.8	0.8	0.0	0.0	0.8	0.0	-4.8
I4	592	0.0	-5.4	0.6	0.0	0.0	0.6	0.0	-5.4
I5	593	0.0	-6.0	0.4	0.0	0.0	0.4	0.0	-6.0
J1	971	0.0	-5.8	0.0	0.0	0.0	0.0	0.0	-5.8
J2	972	0.0	-5.8	0.0	0.0	0.0	0.0	0.0	-5.8
J3	973	0.0	-5.8	0.0	0.0	0.0	0.0	0.0	-5.8
J4	974	0.0	-5.8	0.0	0.0	0.0	0.0	0.0	-5.8
K1	979	0.0	-4.3	0.0	0.0	0.0	0.0	0.0	-4.3
K2	980	0.0	-4.2	0.0	0.0	0.0	0.0	0.0	-4.2
K3	981	0.0	-4.2	0.0	0.0	0.0	0.0	0.0	-4.2
K4	982	0.0	-4.2	0.0	0.0	0.0	0.0	0.0	-4.2
K5	983	0.0	-4.2	0.0	0.0	0.0	0.0	0.0	-4.2
L1	1601	0.0	-4.8	0.0	0.0	0.0	0.0	0.0	-4.8
L2	1602	0.0	-4.8	0.0	0.0	0.0	0.0	0.0	-4.8
L3	1603	0.0	-4.8	0.0	0.0	0.0	0.0	0.0	-4.8
L4	1604	0.0	-4.8	0.0	0.0	0.0	0.0	0.0	-4.8
M1	1609	0.0	-3.2	0.0	0.0	0.0	0.0	0.0	-3.2
M2	1610	0.0	-3.2	0.0	0.0	0.0	0.0	0.0	-3.2
M3	1611	0.0	-3.2	0.0	0.0	0.0	0.0	0.0	-3.2
M4	1612	0.0	-3.2	0.0	0.0	0.0	0.0	0.0	-3.2
M5	1613	0.0	-3.2	0.0	0.0	0.0	0.0	0.0	-3.2
N1	2216	0.0	-3.8	0.0	0.0	0.0	0.0	0.0	-3.8
N2	2217	0.0	-3.8	0.0	0.0	0.0	0.0	0.0	-3.8

Table 2.10.4-14 Stress Components – Impact; 30-Foot Bottom End Drop; Drop Orientation = 0 Degrees; 2-D Model; Condition 1 (continued)

Stress Points Section <sup>1</sup> Node	Stress Components (ksi)						Principal Stresses (ksi)		
	S <sub>x</sub>	S <sub>y</sub>	S <sub>z</sub>	S <sub>xy</sub>	S <sub>yz</sub>	S <sub>xz</sub>	S1	S2	S3
N3	2218	0.0	-3.8	0.0	0.0	0.0	0.0	0.0	-3.8
N4	2219	0.0	-3.8	0.0	0.0	0.0	0.0	0.0	-3.8
O1	2224	0.0	-2.3	0.0	0.0	0.0	0.0	0.0	-2.3
O2	2225	0.0	-2.3	0.0	0.0	0.0	0.0	0.0	-2.3
O3	2226	0.0	-2.3	0.0	0.0	0.0	0.0	0.0	-2.3
O4	2227	0.0	-2.3	0.0	0.0	0.0	0.0	0.0	-2.3
O5	2228	0.0	-2.3	0.0	0.0	0.0	0.0	0.0	-2.3
P1	2546	0.0	-2.3	0.1	0.0	0.0	0.1	0.0	-2.3
P2	2547	-0.1	-2.9	-0.1	0.0	0.0	-0.1	-0.1	-2.9
P3	2548	-0.1	-3.4	-0.2	-0.1	0.0	-0.1	-0.2	-3.4
P4	2549	0.0	-4.3	-0.5	-0.2	0.0	0.0	-0.5	-4.3
Q1	2554	0.0	-1.6	0.3	0.0	0.0	0.3	0.0	-1.6
Q2	2555	0.0	-1.6	0.3	0.0	0.0	0.3	0.0	-1.6
Q3	2556	0.0	-1.7	0.2	0.0	0.0	0.2	0.0	-1.7
Q4	2557	0.0	-1.8	0.2	0.0	0.0	0.2	0.0	-1.8
Q5	2558	0.0	-1.9	0.2	0.0	0.0	0.2	0.0	-1.9
R1	2771	0.0	-4.4	-0.3	0.0	0.0	0.0	-0.3	-4.4
R2	2772	0.1	-3.0	0.1	0.1	0.0	0.1	0.1	-3.0
R3	2773	0.3	-1.6	0.6	0.2	0.0	0.6	0.3	-1.6
R4	2774	0.4	0.2	1.1	0.3	0.0	1.1	0.7	-0.1
S1	2779	-1.7	-2.8	-0.5	0.3	0.0	-0.5	-1.6	-2.9
S2	2780	-1.1	-1.9	-0.1	0.0	0.0	-0.1	-1.1	-1.9
S3	2781	-0.6	-1.1	0.2	-0.2	0.0	0.2	-0.5	-1.2
S4	2782	-0.2	-0.4	0.5	-0.2	0.0	0.5	-0.1	-0.5
S5	2783	-0.1	0.5	0.8	-0.1	0.0	0.8	0.6	-0.1
T1	7066	2.1	1.8	0.9	0.5	0.0	2.4	1.5	0.9
T2	7067	1.3	0.6	0.4	0.2	0.0	1.4	0.6	0.4
T3	7068	0.9	-0.1	0.1	0.0	0.0	0.9	0.1	-0.1
T4	7069	0.5	-0.6	-0.1	-0.1	0.0	0.5	-0.1	-0.6
T5	7070	0.3	-1.0	-0.3	-0.1	0.0	0.3	-0.3	-1.0
T6	7071	0.1	-1.5	-0.4	-0.1	0.0	0.1	-0.4	-1.5
T7	7072	0.1	-2.1	-0.6	-0.1	0.0	0.1	-0.6	-2.1
U1	3051	-1.4	-2.3	1.3	0.3	0.0	1.3	-1.3	-2.3



Table 2.10.4-14 Stress Components – Impact; 30-Foot Bottom End Drop; Drop Orientation = 0 Degrees; 2-D Model; Condition 1 (continued)

Stress Points		Stress Components (ksi)						Principal Stresses (ksi)		
Section <sup>1</sup>	Node	S <sub>x</sub>	S <sub>y</sub>	S <sub>z</sub>	S <sub>xy</sub>	S <sub>xz</sub>	S <sub>yz</sub>	S1	S2	S3
U2	3052	0.1	-2.0	1.0	0.3	0.0	0.0	1.0	0.1	-2.0
U3	3053	0.4	-1.5	0.5	0.2	0.0	0.0	0.5	0.4	-1.5
U4	3054	0.6	-1.3	-0.1	0.1	0.0	0.0	0.6	-0.1	-1.3
U5	3055	0.9	-1.5	-0.8	0.2	0.0	0.0	0.9	-0.8	-1.6
U6	3056	0.2	-1.1	-1.5	0.8	0.0	0.0	0.6	-1.5	-1.5
V1	3611	-0.5	-0.1	1.5	-0.1	0.0	0.0	1.5	0.0	-0.5
V2	3612	-0.4	-0.1	1.0	-0.1	0.0	0.0	1.0	-0.1	-0.4
V3	3613	-0.2	-0.2	0.5	-0.1	0.0	0.0	0.5	0.0	-0.3
V4	3614	0.0	-0.2	0.0	-0.1	0.0	0.0	0.0	0.0	-0.2
V5	3615	0.1	-0.1	-0.5	-0.1	0.0	0.0	0.1	-0.1	-0.5
V6	3616	0.0	0.0	-1.1	-0.1	0.0	0.0	0.1	0.0	-1.1
V7	3617	0.5	0.0	-1.5	0.0	0.0	0.0	0.5	0.0	-1.5
W1	3241	6.0	0.0	6.0	0.0	0.0	0.0	6.0	6.0	0.0
W2	3242	3.8	0.0	3.8	0.0	0.0	0.0	3.8	3.8	0.0
W3	3243	1.7	0.0	1.7	0.0	0.0	0.0	1.7	1.7	0.0
W4	3244	-0.4	0.0	-0.4	0.0	0.0	0.0	0.0	-0.4	-0.4
W5	3245	-2.5	0.0	-2.5	0.0	0.0	0.0	0.0	-2.5	-2.5
W6	3246	-4.7	0.0	-4.7	0.0	0.0	0.0	0.0	-4.7	-4.7
X1	3801	4.9	-0.1	4.9	0.0	0.0	0.0	4.9	4.9	-0.1
X2	3802	3.3	-0.1	3.3	0.0	0.0	0.0	3.3	3.3	-0.1
X3	3803	1.7	0.0	1.7	0.0	0.0	0.0	1.7	1.7	0.0
X4	3804	0.1	0.0	0.1	0.0	0.0	0.0	0.1	0.1	0.0
X5	3805	-1.5	0.0	-1.5	0.0	0.0	0.0	0.0	-1.5	-1.5
X6	3806	-3.2	0.1	-3.2	0.0	0.0	0.0	0.1	-3.2	-3.2
X7	3807	-4.9	0.1	-4.9	0.0	0.0	0.0	0.1	-4.9	-4.9

<sup>1</sup> Refer to Figure 2.10.2-34 for the identification of the representative sections.

Table 2.10.4-15 Stress Components -- Impact; 30-Foot Side Drop; Drop Orientation = 90 Degrees; 3-D Model; 0-Degree Circumferential Location; Condition 1

Condition 1: 100°F Ambient with Contents

Stress Points Section <sup>1</sup> Node		Stress Components (ksi)						Principal Stresses (ksi)		
		S <sub>x</sub>	S <sub>y</sub>	S <sub>z</sub>	S <sub>xy</sub>	S <sub>yz</sub>	S <sub>xz</sub>	S1	S2	S3
A1	1130	-0.9	-2.0	-0.3	-0.1	0.1	0.0	-0.3	-0.9	-2.0
A2	1129	-1.1	-3.2	0.0	-0.1	0.1	0.0	0.0	-1.1	-3.2
A3	1128	-1.3	-4.4	0.2	0.0	0.1	0.0	0.2	-1.3	-4.4
B1	1185	-1.1	-5.3	0.0	-0.1	0.0	-0.2	0.0	-1.1	-5.3
B2	1184	-0.3	-6.0	0.0	-0.1	0.0	-0.2	0.1	-0.4	-6.0
B3	1183	0.5	-6.7	0.0	-0.1	0.1	-0.2	0.5	-0.1	-6.7
C1	90	5.6	-2.8	14.7	0.0	-0.8	1.4	14.9	5.4	-2.8
C2	80	-2.4	-7.2	6.3	-0.1	-0.5	0.0	6.3	-2.4	-7.2
C3	70	-3.6	-8.7	2.0	0.1	-0.4	-0.8	2.1	-3.7	-8.7
C4	60	-4.7	-9.5	0.2	0.2	-0.2	-0.5	0.3	-4.7	-9.6
C5	50	-9.8	-11.5	-0.1	0.2	-0.1	0.0	-0.1	-9.8	-11.6
C6	40	-12.0	-12.5	-0.1	0.2	0.0	0.0	-0.1	-11.9	-12.5
D1	25	-4.9	-9.6	5.4	0.3	-0.1	0.1	5.4	-4.9	-9.6
D2	15	-9.7	-11.3	1.8	0.1	-0.1	-0.5	1.8	-9.8	-11.3
D3	5	-10.8	-11.6	0.4	0.2	0.0	-0.4	0.4	-10.8	-11.6
E1	35	-10.7	-11.5	4.6	0.2	-0.1	1.6	4.8	-10.8	-11.6
E2	34	-7.6	-11.5	2.1	0.3	0.0	1.8	2.4	-7.9	-11.5
E3	33	-8.0	-12.4	-0.3	0.3	0.0	1.6	0.0	-8.3	-12.4
E4	32	-8.6	-13.3	-2.7	0.4	0.0	0.9	-2.6	-8.7	-13.4
E5	31	-8.8	-14.2	-5.2	0.4	0.0	0.5	-5.1	-8.8	-14.2
F1	100	-1.2	-2.7	22.2	0.0	-1.2	2.2	22.5	-1.4	-2.8
F2	99	-1.5	-8.3	1.9	0.4	-0.9	2.4	3.2	-2.6	-8.5
F3	98	-0.5	-11.5	-11.1	0.8	-0.7	3.2	0.4	-10.9	-12.6
F4	97	0.6	-17.8	-36.4	1.3	-0.7	3.8	1.0	-17.9	-36.8
G1	94	0.8	-2.2	21.7	0.2	-0.5	3.3	22.2	0.3	-2.3
G2	93	1.5	-6.0	7.2	0.5	-0.3	2.5	8.2	0.6	-6.0
G3	92	1.5	-7.1	2.5	0.6	-0.3	1.0	3.2	0.9	-7.2
G4	91	0.7	-8.7	-3.1	0.7	-0.2	0.4	0.8	-3.1	-8.8
H1	330	-0.2	6.2	-4.5	-0.4	-1.6	0.1	6.5	-0.3	-4.8
H2	329	-0.1	8.0	-0.9	-0.5	-1.6	0.0	8.3	-0.1	-1.2

Table 2.10.4-15 Stress Components – Impact; 30-Foot Side Drop; Drop Orientation = 90 Degrees; 3-D Model; 0-Degree Circumferential Location; Condition 1  
(continued)

Stress Points		Stress Components (ksi)						Principal Stresses (ksi)		
Section <sup>1</sup>	Node	S <sub>x</sub>	S <sub>y</sub>	S <sub>z</sub>	S <sub>xy</sub>	S <sub>xz</sub>	S <sub>yz</sub>	S1	S2	S3
H3	328	0.1	9.7	2.6	-0.6	-1.5	-0.1	10.0	2.3	0.0
H4	327	0.2	11.6	6.9	-0.7	-1.4	-0.5	12.0	6.6	0.1
I1	244	-0.2	-0.4	4.9	0.0	-0.8	0.0	5.0	-0.2	-0.5
I2	243	-0.1	1.2	7.5	-0.1	-0.7	0.0	7.6	1.2	-0.1
I3	242	-0.1	2.8	10.1	-0.2	-0.5	0.0	10.1	2.8	-0.1
I4	241	0.0	4.2	12.7	-0.3	-0.4	0.0	12.7	4.3	0.0
J1	550	-0.3	6.7	10.7	-0.5	-0.8	0.0	10.8	6.6	-0.3
J2	548	-0.2	9.2	12.6	-0.7	-0.8	0.0	12.8	9.1	-0.2
J3	547	-0.1	11.6	14.4	-0.9	-0.7	0.0	14.6	11.4	-0.1
K1	344	-0.1	-1.2	11.3	0.0	-0.5	0.0	11.3	-0.1	-1.2
K2	342	-0.1	2.5	13.1	-0.2	-0.4	0.0	13.1	2.5	-0.1
K3	341	0.0	6.0	14.8	-0.5	-0.3	0.0	14.8	6.0	-0.1
L1	740	-0.1	3.8	16.6	0.3	0.0	-0.2	16.6	3.8	-0.1
L2	738	-0.6	6.6	18.2	-1.1	0.0	0.0	18.2	6.8	-0.7
L3	737	0.2	9.6	19.9	-2.5	0.0	0.0	19.9	10.2	-0.4
M1	663	-1.3	-2.6	14.1	0.1	0.0	0.0	14.1	-1.3	-2.6
M2	63	0.5	9.3	19.4	2.2	0.0	0.0	19.4	9.8	0.0
N1	1877	-0.3	6.2	8.7	-0.5	1.0	0.0	9.1	5.9	-0.3
N1	1877	-0.3	6.2	8.7	-0.5	1.0	0.0	9.1	5.9	-0.3
N2	1477	-0.2	9.2	10.6	-0.7	0.9	0.0	11.1	8.7	-0.2
N3	1277	-0.1	12.0	12.4	-0.9	0.9	0.0	13.1	11.3	-0.1
O1	647	-0.1	-1.7	12.9	0.1	0.4	0.0	12.9	-0.1	-1.7
O2	247	-0.1	2.4	14.9	-0.2	0.3	0.0	14.9	2.4	-0.1
O3	47	0.0	6.1	16.8	-0.5	0.2	0.0	16.8	6.2	-0.1
P1	1840	-0.3	6.5	-4.5	-0.5	1.7	0.0	6.8	-0.3	-4.7
P2	1640	-0.1	8.5	-1.6	-0.6	1.6	0.0	8.7	-0.2	-1.9
P3	1440	0.0	10.4	1.2	-0.7	1.5	0.1	10.6	1.0	-0.1
P4	1240	0.1	12.4	4.5	-0.8	1.5	0.3	12.7	4.3	0.0
Q1	628	-0.3	0.5	8.8	-0.1	0.6	0.1	8.8	0.5	-0.3
Q2	428	-0.2	2.4	11.0	-0.2	0.5	0.1	11.1	2.4	-0.2
Q3	228	-0.1	4.3	13.3	-0.3	0.4	0.1	13.3	4.3	-0.1
Q4	28	0.0	6.0	15.5	-0.4	0.3	0.1	15.5	6.1	-0.1
R1	1816	-0.9	-8.3	3.0	0.6	1.2	-0.2	3.1	-0.9	-8.4

Table 2.10.4-15 Stress Components – Impact; 30-Foot Side Drop; Drop Orientation = 90 Degrees; 3-D Model; 0-Degree Circumferential Location; Condition 1 (continued)

Stress Points Section <sup>1</sup> Node		Stress Components (ksi)						Principal Stresses (ksi)		
		S <sub>x</sub>	S <sub>y</sub>	S <sub>z</sub>	S <sub>xy</sub>	S <sub>xz</sub>	S <sub>yz</sub>	S1	S2	S3
R2	1616	-1.8	-9.5	-2.6	0.7	1.0	-0.6	-1.5	-2.7	-9.7
R3	1416	-4.1	-10.8	-7.4	0.8	0.7	-2.0	-3.2	-8.0	-11.2
R4	1216	-5.5	-12.4	-14.5	0.8	0.4	-3.8	-4.0	-12.4	-16.0
S1	616	1.3	-4.9	0.6	0.1	0.6	-0.1	1.3	0.7	-4.9
S2	416	-0.2	-3.4	6.5	0.1	0.5	-0.2	6.6	-0.3	-3.5
S3	216	0.1	-1.6	11.8	0.1	0.3	0.2	11.8	0.1	-1.6
S4	16	0.1	0.2	17.0	0.0	0.2	0.1	17.0	0.2	0.1
T1	811	-16.0	-21.2	-18.8	1.1	0.5	-6.0	-11.2	-20.8	-24.0
T2	611	-8.9	-14.6	-4.4	0.7	0.4	-4.4	-1.7	-11.4	-14.8
T3	411	-4.1	-11.0	2.8	0.6	0.3	-3.4	4.2	-5.4	-11.0
T4	211	-0.9	-8.0	9.3	0.5	0.2	-1.9	9.7	-1.2	-8.0
T5	11	0.3	-4.7	19.0	0.3	0.1	-1.0	19.1	0.3	-4.8
U1	43058	3.9	-0.7	-0.1	0.2	0.0	0.1	3.9	-0.1	-0.7
U2	43057	2.2	-1.4	-0.2	0.1	0.0	0.1	2.2	-0.2	-1.4
U3	43056	0.8	-2.1	-0.6	0.1	0.0	-0.1	0.8	-0.6	-2.1
U4	43055	-0.5	-2.8	-1.0	0.1	0.0	-0.5	-0.1	-1.3	-2.8
U5	43054	-2.1	-3.6	-1.4	0.1	-0.1	-1.2	-0.5	-3.0	-3.6
U6	43053	-3.6	-4.5	-1.9	0.1	-0.2	-2.4	-0.2	-4.5	-5.3
U7	43052	-6.2	-5.2	-0.9	0.0	-0.2	-3.1	0.5	-5.2	-7.6
U8	43051	-13.6	-7.5	0.2	-0.2	0.0	0.0	0.2	-7.5	-13.6
V1	50024	1.5	-1.8	0.2	0.1	0.0	-0.1	1.5	0.2	-1.8
V2	50023	-4.0	-4.2	-0.3	0.1	0.0	0.0	-0.3	-4.0	-4.3
V3	50022	-6.7	-5.7	-0.4	0.1	0.0	0.0	-0.4	-5.7	-6.7
V4	50021	-15.8	-9.0	0.0	-0.1	0.0	-0.1	0.0	-9.0	-15.8
W1	43278	-2.2	-3.1	0.1	-0.1	-0.1	0.2	0.1	-2.2	-3.1
W2	43274	-1.5	-3.4	0.0	0.0	-0.2	0.2	0.0	-1.5	-3.4
W3	43271	-0.4	-1.9	0.0	0.0	-0.2	0.1	0.0	-0.4	-1.9
X1	50084	-1.0	-5.6	0.1	-0.1	0.0	0.3	0.1	-1.0	-5.6
X2	50083	-0.4	-5.8	0.0	-0.1	0.0	0.3	0.2	-0.6	-5.8
X3	50081	0.7	-6.4	-0.1	0.0	-0.1	0.3	0.7	-0.2	-6.4

<sup>1</sup> Refer to Figure 2.10.2-34 for the identification of the representative sections.

Table 2.10.4-16 Stress Components – Impact; 30-Foot Top Corner Drop; Drop Orientation = 24 Degrees; 3-D Top Model; 0-Degree Circumferential Location; Condition 1

Condition 1: 100°F Ambient with Contents

Stress Points		Stress Components (ksi)						Principal Stresses (ksi)		
Section <sup>1</sup>	Node	S <sub>x</sub>	S <sub>y</sub>	S <sub>z</sub>	S <sub>xy</sub>	S <sub>yz</sub>	S <sub>xz</sub>	S1	S2	S3
A1	1949	2.2	3.2	-0.4	0.0	-0.1	0.4	3.2	2.2	-0.4
A2	1950	1.2	2.0	-0.3	0.0	-0.1	0.4	2.0	1.3	-0.4
A3	1951	-0.4	-0.4	0.5	0.0	0.1	0.2	0.6	-0.4	-0.5
B1	1952	0.1	0.0	-0.6	0.0	0.0	0.2	0.1	0.0	-0.7
B2	93	-2.0	-2.9	1.2	-0.1	-0.1	0.4	1.3	-2.1	-3.0
C1	1925	-0.4	-0.1	0.7	-0.1	-0.1	0.0	0.7	-0.1	-0.4
C2	1926	0.2	-0.3	-0.2	0.0	-0.1	-0.3	0.4	-0.2	-0.4
C3	1927	0.7	-0.2	-0.2	0.1	0.0	-0.2	0.7	-0.2	-0.2
D1	683	-0.3	-0.6	-0.6	0.1	0.0	0.0	-0.3	-0.6	-0.6
D2	85	0.0	-1.1	-0.5	0.2	0.0	0.0	0.0	-0.5	-1.1
E1	682	0.6	-0.3	-0.6	0.1	0.0	0.2	0.6	-0.3	-0.6
E2	82	0.5	-0.1	0.5	0.1	0.1	0.1	0.7	0.4	-0.1
F1	1925	-0.4	-0.1	0.7	-0.1	-0.1	0.0	0.7	-0.1	-0.4
F2	1325	-1.3	-2.0	-5.2	0.1	-0.1	0.4	-1.3	-1.9	-5.2
G1	680	-0.4	0.0	1.0	0.0	0.0	0.6	1.2	0.0	-0.6
G2	80	0.2	0.0	-0.1	0.0	0.0	0.0	0.2	0.0	-0.1
H1	1921	0.0	2.5	-3.9	-0.1	-0.4	0.1	2.5	0.0	-3.9
H2	1321	-0.1	4.2	-1.8	-0.2	-0.3	0.0	4.2	-0.1	-1.8
I1	676	0.0	-0.2	-0.2	0.0	-0.1	0.0	0.0	-0.1	-0.3
I2	76	0.0	1.4	1.0	-0.1	0.0	0.0	1.4	1.0	0.0
J1	1916	-0.1	2.1	-1.8	-0.1	-0.2	0.0	2.1	-0.1	-1.8
J2	1316	-0.1	5.3	-0.3	-0.4	-0.1	0.0	5.3	-0.1	-0.3
K1	671	0.0	-0.6	-1.0	0.0	0.0	0.0	0.0	-0.6	-1.0
K2	71	0.0	2.1	0.4	-0.2	0.1	0.0	2.1	0.4	0.0
L1	1908	-0.7	0.5	-4.4	-0.1	0.3	0.0	0.5	-0.7	-4.4
L2	1308	0.1	6.9	-2.1	1.8	0.3	0.0	7.4	-0.3	-2.1
M1	663	-0.4	-0.8	-3.2	0.0	0.2	0.0	-0.4	-0.8	-3.2
M2	63	0.2	2.6	-1.9	0.6	0.2	0.0	2.8	0.0	-1.9

Table 2.10.4-16 Stress Components – Impact; 30-Foot Top Corner Drop; Drop Orientation = 24 Degrees; 3-D Top Model; 0-Degree Circumferential Location; Condition 1 (continued)

Stress Points		Stress Components (ksi)						Principal Stresses (ksi)		
Section <sup>1</sup>	Node	S <sub>x</sub>	S <sub>y</sub>	S <sub>z</sub>	S <sub>xy</sub>	S <sub>xz</sub>	S <sub>yz</sub>	S1	S2	S3
N1	1877	-0.1	1.2	-12.8	-0.1	0.8	0.0	1.3	-0.1	-12.8
N2	1477	-0.1	3.7	-11.8	-0.3	0.7	0.0	3.8	-0.1	-11.8
N3	1277	0.0	6.1	-10.9	-0.5	0.6	0.0	6.1	-0.1	-10.9
O1	647	-0.1	-0.2	-6.5	0.0	0.3	0.0	-0.1	-0.2	-6.5
O2	247	0.0	1.0	-6.1	-0.1	0.2	0.0	1.1	0.0	-6.1
O3	47	0.0	2.2	-5.7	-0.2	0.2	0.0	2.3	0.0	-5.7
P1	1840	-0.3	2.8	-13.9	-0.2	1.0	0.1	2.9	-0.3	-14.0
P2	1640	-0.5	2.7	-16.9	-0.2	0.9	0.0	2.8	-0.5	-17.0
P3	1440	-0.5	2.7	-19.7	-0.2	0.8	-0.6	2.7	-0.5	-19.8
P4	1240	-0.5	1.9	-25.4	-0.1	0.7	-1.3	1.9	-0.5	-25.5
Q1	628	-0.2	2.9	-7.9	-0.2	0.4	0.1	2.9	-0.2	-8.0
Q2	428	-0.1	3.2	-8.3	-0.2	0.3	0.1	3.2	-0.1	-8.3
Q3	228	0.0	3.5	-8.7	-0.3	0.3	0.1	3.5	-0.1	-8.7
Q4	28	0.0	3.7	-9.0	-0.3	0.2	0.1	3.7	0.0	-9.0
R1	1816	0.1	-3.5	-30.8	0.3	0.6	0.0	0.1	-3.5	-30.8
R2	1616	0.3	-1.1	-22.7	0.2	0.6	0.1	0.3	-1.1	-22.7
R3	1416	0.2	1.0	-15.2	0.1	0.5	0.7	1.0	0.2	-15.3
R4	1216	7.2	4.9	-8.4	0.3	0.4	0.9	7.2	4.9	-8.4
S1	616	-8.8	-5.4	-30.7	-0.3	0.7	4.1	-5.4	-8.1	-31.5
S2	416	-8.8	-1.4	-14.7	-0.5	0.2	-0.7	-1.3	-8.8	-14.8
S3	216	-3.2	3.1	-3.3	-0.5	0.1	-1.2	3.1	-2.1	-4.4
S4	16	-1.2	7.1	10.0	-0.6	0.0	-0.9	10.1	7.1	-1.3
T1	811	0.2	-5.1	-4.5	0.7	0.5	0.7	0.4	-4.4	-5.4
T2	611	0.9	-5.5	-7.5	0.6	0.3	-0.2	1.0	-5.5	-7.6
T3	411	0.6	-5.4	-7.4	0.5	0.3	-0.3	0.7	-5.4	-7.4
T4	211	0.8	-5.1	-6.6	0.4	0.2	-0.3	0.8	-5.1	-6.7
T5	11	0.8	-4.6	-4.9	0.4	0.1	-0.2	0.8	-4.6	-5.0
U1	43058	0.5	8.1	-13.5	-0.8	0.6	3.0	8.2	1.0	-14.1
U2	43057	3.3	6.7	-12.1	-0.6	0.1	4.1	6.8	4.2	-13.1
U3	43056	2.7	4.6	-10.2	-0.3	0.4	5.4	4.8	4.4	-12.2

Table 2.10.4-16 Stress Components -- Impact; 30-Foot Top Corner Drop; Drop Orientation = 24 Degrees; 3-D Top Model; 0-Degree Circumferential Location; Condition 1 (continued)

Stress Points		Stress Components (ksi)						Principal Stresses (ksi)		
Section <sup>1</sup>	Node	S <sub>x</sub>	S <sub>y</sub>	S <sub>z</sub>	S <sub>xy</sub>	S <sub>yz</sub>	S <sub>xz</sub>	S1	S2	S3
U4	43055	1.8	2.2	-9.4	-0.1	0.4	5.6	4.1	2.2	-11.8
U5	43054	0.8	-0.4	-9.3	0.1	0.4	5.4	3.1	-0.4	-11.7
U6	43053	-0.7	-2.6	-7.3	0.2	0.3	4.2	1.4	-2.6	-9.4
U7	43052	-1.0	-6.6	-13.0	0.5	0.2	4.3	0.5	-6.6	-14.3
U8	43051	-9.0	-13.2	-13.1	0.5	0.5	7.5	-3.2	-13.3	-18.9
V1	50024	-16.7	0.7	-5.9	-1.4	-0.2	-2.1	0.8	-5.5	-17.2
V2	50023	-11.0	-4.2	-5.8	-0.7	-0.2	-1.3	-4.2	-5.5	-11.4
V3	50022	-4.9	-9.2	-5.4	0.4	0.0	-0.1	-4.9	-5.4	-9.2
V4	50021	1.3	-14.3	-5.0	1.1	0.0	0.3	1.3	-5.0	-14.4
W1	43278	10.5	7.2	-3.9	-0.6	-1.3	-2.1	10.9	7.3	-4.4
W2	43274	1.7	-0.1	-1.2	-0.1	-1.3	-2.1	3.0	0.4	-2.8
W3	43271	-4.0	-4.2	-0.1	0.2	-1.7	-1.1	0.7	-4.2	-4.8
X1	50084	23.6	17.8	-8.5	-0.5	0.2	-5.3	24.5	17.7	-9.3
X2	50083	7.0	1.6	-6.0	-0.2	0.3	-5.4	9.0	1.6	-8.0
X3	50081	-23.8	-27.6	11.0	0.5	-0.1	-5.3	11.8	-24.5	-27.7

<sup>1</sup> Refer to Figure 2.10.2-34 for the identification of the representative sections.

Table 2.10.4-17 Stress Components - Impact; 30-Foot Bottom Corner Drop; Drop Orientation = 24 Degrees; 3-D Bottom Model; 0-Degree Circumferential Location; Condition 1

Condition 1: 100°F Ambient with Contents

Stress Points		Stress Components (ksi)						Principal Stresses (ksi)		
Section <sup>1</sup>	Node	S <sub>x</sub>	S <sub>y</sub>	S <sub>z</sub>	S <sub>xy</sub>	S <sub>xz</sub>	S <sub>yz</sub>	S1	S2	S3
A1	1130	18.0	13.9	-6.7	-0.5	2.0	2.1	18.2	14.1	-7.1
A2	1129	2.3	-0.1	-1.2	0.0	1.5	2.1	3.4	0.5	-2.8
A3	1128	-13.5	-14.1	4.4	0.5	2.0	2.1	4.8	-13.7	-14.4
B1	1185	10.5	3.7	-6.6	-0.5	2.4	2.3	10.8	4.3	-7.5
B2	1184	-3.7	-7.9	-1.9	0.0	1.8	2.3	0.0	-5.0	-8.5
B3	1183	-18.1	-19.4	2.9	0.4	1.9	2.3	3.3	-18.4	-19.5
C1	90	-20.6	-6.2	-26.3	-1.3	-0.8	-5.4	-6.1	-17.4	-29.6
C2	80	-9.1	-1.7	-15.1	-1.0	-0.5	-4.3	-1.6	-6.9	-17.4
C3	70	-5.8	-1.2	-9.4	-0.5	-0.4	-3.8	-1.1	-3.4	-11.9
C4	60	-3.0	-1.2	-5.6	-0.1	-0.4	-3.7	-0.3	-1.2	-8.2
C5	50	6.9	-4.1	-3.6	1.0	-0.2	-2.5	7.5	-4.2	-4.2
C6	40	14.3	-5.4	-3.6	1.7	-0.1	-1.5	14.5	-3.7	-5.6
D1	25	-30.8	-23.1	-32.0	-0.4	-0.7	-8.5	-22.8	-23.2	-39.9
D2	15	-6.7	-18.6	-14.9	0.6	-0.3	-3.8	-5.2	-16.4	-18.6
D3	5	0.7	-22.4	-7.5	1.4	-0.1	-1.2	0.9	-7.7	-22.5
E1	35	11.0	-8.2	-21.9	1.3	-0.4	-3.9	11.5	-8.3	-22.3
E2	34	2.0	-8.9	-17.6	0.7	-0.8	-7.5	4.6	-8.9	-20.1
E3	33	-5.1	-9.1	-11.2	0.3	-0.7	-7.9	0.4	-9.1	-16.6
E4	32	-6.7	-8.4	-6.8	0.1	-0.4	-4.9	-1.8	-8.4	-11.6
E5	31	-7.2	-7.6	-2.6	0.0	-0.3	-2.9	-1.1	-7.6	-8.7
F1	100	0.0	-2.5	-34.8	-0.1	-0.9	-3.4	0.3	-2.5	-35.1
F2	99	-2.8	0.9	-19.5	-0.4	-0.8	-1.7	1.0	-2.7	-19.7
F3	98	-2.8	2.5	-13.4	-0.5	-0.4	0.9	2.5	-2.8	-13.5
F4	97	0.1	5.0	-6.8	-0.5	-0.4	1.9	5.1	0.5	-7.3
G1	94	0.3	-2.6	-24.6	0.1	-0.4	-1.2	0.4	-2.6	-24.7
G2	93	-0.7	-0.2	-15.0	-0.1	-0.4	-0.6	-0.2	-0.7	-15.0
G3	92	-1.1	1.4	-8.4	-0.2	-0.2	0.1	1.4	-1.1	-8.4
G4	91	-0.5	3.6	-0.5	-0.3	-0.1	0.1	3.6	-0.4	-0.7
H1	330	-0.3	3.0	-13.1	-0.2	-1.0	-0.1	3.1	-0.3	-13.2
H2	329	-0.4	2.8	-16.3	-0.2	-0.9	0.0	2.8	-0.5	-16.4



Table 2.10.4-17 Stress Components - Impact; 30-Foot Bottom Corner Drop; Drop Orientation = 24 Degrees; 3-D Bottom Model; 0-Degree Circumferential Location; Condition 1 (continued)

Stress Points Section <sup>1</sup> Node		S <sub>x</sub>	Stress Components (ksi)					Principal Stresses (ksi)		
			S <sub>y</sub>	S <sub>z</sub>	S <sub>xy</sub>	S <sub>yz</sub>	S <sub>xz</sub>	S1	S2	S3
H3	328	-0.5	2.6	-19.3	-0.2	-0.8	0.6	2.7	-0.5	-19.4
H4	327	-0.5	1.7	-25.2	-0.1	-0.7	1.3	1.8	-0.5	-25.3
I1	244	0.0	1.9	-10.2	-0.1	-0.4	-0.1	1.9	0.0	-10.2
I2	243	0.0	2.3	-10.1	-0.2	-0.4	-0.1	2.4	0.0	-10.2
I3	242	0.0	2.8	-10.0	-0.2	-0.3	-0.1	2.8	0.0	-10.0
I4	241	0.0	3.2	-10.0	-0.2	-0.2	-0.1	3.2	0.0	-10.0
J1	550	-0.1	1.2	-11.2	-0.1	-0.7	0.0	1.3	-0.1	-11.2
J2	548	-0.1	3.7	-10.3	-0.3	-0.6	0.0	3.7	-0.1	-10.3
J3	547	0.0	6.0	-9.4	-0.5	-0.6	0.0	6.1	-0.1	-9.4
K1	344	-0.1	-0.3	-7.7	0.0	-0.3	0.0	-0.1	-0.3	-7.7
K2	342	0.0	1.2	-7.1	-0.1	-0.3	0.0	1.2	0.0	-7.1
K3	341	0.0	2.6	-6.5	-0.2	-0.2	0.0	2.6	0.0	-6.5
L1	740	0.1	1.1	-3.3	0.5	-0.2	-0.1	1.3	-0.1	-3.3
L2	738	-0.3	3.5	-2.4	-0.8	-0.2	0.0	3.7	-0.5	-2.4
L3	737	0.3	6.1	-1.2	-2.0	-0.2	0.0	6.7	-0.3	-1.3
M1	454	-0.1	-0.8	-3.9	-0.6	-0.2	0.0	0.3	-1.2	-3.9
M2	452	0.2	1.0	-3.2	-0.3	-0.2	0.0	1.1	0.1	-3.2
M3	451	-0.2	2.4	-2.8	0.0	-0.2	-0.1	2.4	-0.2	-2.8
N1	810	-0.1	2.2	-1.9	-0.1	0.2	0.0	2.2	-0.1	-1.9
N2	807	-0.1	5.2	-0.5	-0.3	0.1	0.0	5.2	-0.1	-0.5
O1	524	0.0	-0.6	-1.3	0.0	-0.1	0.0	0.0	-0.6	-1.3
O2	521	0.0	2.0	0.0	-0.1	-0.1	0.0	2.0	0.0	0.0
P1	850	0.0	2.4	-4.1	-0.1	0.4	-0.1	2.4	0.0	-4.1
P2	847	-0.1	4.2	-1.9	-0.2	0.3	0.0	4.2	-0.1	-1.9
Q1	564	0.0	-0.1	-0.3	0.0	0.0	0.0	0.0	-0.1	-0.3
Q2	561	0.0	1.5	0.6	-0.1	0.0	0.0	1.5	0.6	0.0
R1	890	-0.8	-0.4	0.6	0.0	0.2	-0.2	0.6	-0.4	-0.8
R2	887	-1.0	-1.6	-5.0	0.1	0.1	-0.4	-0.9	-1.6	-5.1
S1	604	-0.3	0.4	0.3	0.0	0.0	-0.3	0.5	0.4	-0.5
S2	601	0.1	0.7	0.5	-0.1	0.0	-0.1	0.7	0.5	0.0
T1	897	0.3	-0.3	-1.7	0.0	0.1	-0.2	0.4	-0.3	-1.7

Table 2.10.4-17 Stress Components - Impact; 30-Foot Bottom Corner Drop; Drop Orientation = 24 Degrees; 3-D Bottom Model; 0-Degree Circumferential Location; Condition 1 (continued)

Stress Points Section <sup>1</sup> Node	Stress Components (ksi)						Principal Stresses (ksi)		
	S <sub>x</sub>	S <sub>y</sub>	S <sub>z</sub>	S <sub>xy</sub>	S <sub>yz</sub>	S <sub>xz</sub>	S1	S2	S3
T2 614	0.2	0.3	0.0	0.0	0.0	-0.4	0.4	0.3	-0.3
T3 611	-0.1	0.1	0.1	0.0	-0.1	-0.2	0.3	0.1	-0.3
U1 900	0.4	-0.1	-0.8	0.0	0.1	0.2	0.5	-0.1	-0.8
U2 910	0.7	-0.2	-0.5	0.1	0.0	0.2	0.7	-0.2	-0.5
V1 920	-0.4	-0.4	-0.4	0.1	0.0	0.2	-0.2	-0.5	-0.6
V2 930	-0.3	-1.1	-0.2	0.2	0.0	0.1	-0.1	-0.4	-1.1
W1 1216	1.5	2.6	-1.2	0.0	0.0	-0.3	2.6	1.5	-1.2
W2 1226	-0.3	-0.1	0.6	0.0	-0.1	-0.1	0.6	-0.1	-0.3
X1 1236	0.1	0.1	-0.7	0.0	-0.1	-0.1	0.2	0.1	-0.7
X2 1246	-1.8	-2.8	1.4	-0.1	0.0	-0.3	1.4	-1.9	-2.8

<sup>1</sup> Refer to Figure 2.10.2-34 for the identification of the representative sections.

Table 2.10.4-18 Stress Components - Impact; 30-Foot Bottom Oblique Drop; Drop Orientation = 15 Degrees; 3-D Bottom Model; 0-Degree Circumferential Location; Condition 1

Condition 1: 100°F Ambient with Contents

Stress Points		Stress Components (ksi)						Principal Stresses (ksi)		
Section <sup>1</sup>	Node	S <sub>x</sub>	S <sub>y</sub>	S <sub>z</sub>	S <sub>xy</sub>	S <sub>xz</sub>	S <sub>yz</sub>	S1	S2	S3
A1	1130	19.2	15.7	-7.0	-0.5	2.2	2.3	19.5	15.9	-7.4
A2	1129	2.6	1.1	-1.2	0.0	1.6	2.3	3.8	1.5	-2.8
A3	1128	-14.1	-13.4	4.6	0.5	2.1	2.3	5.1	-13.6	-14.4
B1	1185	11.3	5.2	-6.9	-0.6	2.6	2.5	11.6	5.8	-7.8
B2	1184	-3.7	-6.7	-2.0	-0.1	1.9	2.5	0.1	-4.9	-7.7
B3	1183	-19.0	-18.7	3.0	0.4	2.0	2.5	3.5	-18.8	-19.3
C1	90	-22.2	-5.3	-31.5	-1.4	-0.7	-6.0	-5.2	-19.4	-34.5
C2	80	-8.2	0.4	-17.5	-1.0	-0.5	-4.6	0.6	-6.4	-19.5
C3	70	-4.6	1.3	-10.5	-0.6	-0.4	-4.0	1.3	-2.6	-12.6
C4	60	-1.5	1.4	-6.1	-0.1	-0.4	-3.9	1.4	0.7	-8.4
C5	50	9.6	-1.6	-4.1	1.0	-0.2	-2.7	10.2	-1.7	-4.6
C6	40	17.6	-3.1	-4.3	1.8	-0.1	-1.6	17.9	-3.3	-4.4
D1	25	-28.5	-21.0	-33.9	-0.3	-0.7	-8.4	-21.0	-22.4	-40.1
D2	15	-3.9	-16.6	-15.6	0.7	-0.3	-3.8	-2.8	-16.6	-16.8
D3	5	3.1	-21.1	-7.8	1.6	-0.1	-1.2	3.3	-8.0	-21.2
E1	35	13.7	-5.8	-23.9	1.4	-0.4	-4.1	14.3	-5.9	-24.4
E2	34	4.0	-6.4	-18.5	0.7	-0.8	-7.8	6.4	-6.4	-21.0
E3	33	-2.9	-6.3	-11.3	0.2	-0.8	-8.1	2.1	-6.3	-16.3
E4	32	-4.2	-5.3	-6.1	0.1	-0.4	-5.0	0.0	-5.3	-10.3
E5	31	-4.6	-4.1	-1.1	0.0	-0.3	-3.0	0.7	-4.1	-6.4
F1	100	0.2	-1.7	-42.5	-0.1	-0.8	-4.1	0.6	-1.7	-42.9
F2	99	-2.6	3.4	-21.1	-0.6	-0.7	-2.4	3.4	-2.3	-21.5
F3	98	-2.8	5.8	-11.4	-0.7	-0.4	0.1	5.9	-2.9	-11.4
F4	97	-0.1	10.1	2.1	-0.8	-0.3	1.0	10.2	2.5	-0.5
G1	94	0.1	-1.9	-31.3	0.0	-0.4	-2.2	0.2	-1.9	-31.4
G2	93	-1.1	1.6	-17.1	-0.3	-0.4	-1.3	1.7	-1.0	-17.2
G3	92	-1.5	3.6	-9.0	-0.4	-0.2	-0.2	3.7	-1.6	-9.0
G4	91	-0.7	6.4	0.8	-0.5	-0.1	0.0	6.5	0.8	-0.8
H1	330	-0.2	2.3	-12.5	-0.2	-0.7	-0.1	2.3	-0.2	-12.5
H2	329	-0.4	1.6	-16.6	-0.1	-0.7	0.0	1.7	-0.5	-16.6

Table 2.10.4-18 Stress Components - Impact; 30-Foot Bottom Oblique Drop; Drop Orientation = 15 Degrees; 3-D Bottom Model; 0-Degree Circumferential Location; Condition 1 (continued)

Stress Points		Stress Components (ksi)						Principal Stresses (ksi)		
Section <sup>1</sup>	Node	S <sub>x</sub>	S <sub>y</sub>	S <sub>z</sub>	S <sub>xy</sub>	S <sub>xz</sub>	S <sub>yz</sub>	S1	S2	S3
H3	328	-0.6	1.1	-20.5	-0.1	-0.6	0.6	1.1	-0.6	-20.5
H4	327	-0.6	-0.2	-27.5	0.0	-0.5	1.5	-0.2	-0.5	-27.5
I1	244	0.0	2.1	-11.3	-0.1	-0.3	-0.1	2.1	0.0	-11.3
I2	243	0.0	2.3	-11.9	-0.2	-0.3	-0.1	2.3	0.0	-11.9
I3	242	0.0	2.5	-12.4	-0.2	-0.2	-0.1	2.6	0.0	-12.4
I4	241	0.0	2.7	-12.9	-0.2	-0.2	-0.1	2.8	0.0	-12.9
J1	550	-0.1	0.6	-13.6	-0.1	-0.5	0.0	0.7	-0.1	-13.6
J2	548	0.0	2.3	-13.1	-0.2	-0.5	0.0	2.4	-0.1	-13.1
J3	547	0.0	4.0	-12.6	-0.3	-0.5	0.0	4.0	0.0	-12.6
K1	344	0.0	-0.4	-9.9	0.0	-0.2	0.0	0.0	-0.4	-9.9
K2	342	0.0	0.7	-9.6	-0.1	-0.2	0.0	0.7	0.0	-9.6
K3	341	0.0	1.8	-9.3	-0.1	-0.2	0.0	1.8	0.0	-9.3
L1	740	0.1	0.8	-6.7	0.3	-0.2	0.0	0.9	0.0	-6.7
L2	738	-0.2	2.2	-6.2	-0.5	-0.2	0.0	2.3	-0.3	-6.2
L3	737	0.2	3.8	-5.6	-1.2	-0.2	0.0	4.2	-0.2	-5.6
M1	454	-0.1	-0.7	-6.4	-0.4	-0.2	0.0	0.1	-0.9	-6.4
M2	452	0.1	0.5	-6.0	-0.2	-0.2	0.0	0.6	0.0	-6.0
M3	451	-0.2	1.5	-5.8	0.0	-0.2	0.0	1.5	-0.2	-5.8
N1	810	0.0	1.6	-3.8	-0.1	0.0	0.0	1.6	-0.1	-3.8
N2	807	-0.1	3.1	-3.1	-0.2	0.0	0.0	3.2	-0.1	-3.1
O1	524	0.0	-0.7	-3.5	0.0	-0.1	0.0	0.0	-0.7	-3.5
O2	521	0.0	1.3	-2.6	-0.1	-0.1	0.0	1.3	0.0	-2.6
P1	850	0.0	1.6	-3.9	-0.1	0.2	-0.1	1.6	0.0	-3.9
P2	847	0.0	2.4	-3.0	-0.1	0.1	0.0	2.4	0.0	-3.0
Q1	564	0.0	0.1	-1.6	0.0	-0.1	0.0	0.1	0.0	-1.6
Q2	561	0.0	0.7	-2.0	0.0	-0.1	0.0	0.7	0.0	-2.0
R1	890	-0.2	0.4	-1.2	0.0	0.1	0.0	0.4	-0.2	-1.2
R2	887	-0.4	0.0	-3.1	0.0	0.0	-0.1	0.0	-0.4	-3.1
S1	604	-0.4	0.7	-1.5	0.0	-0.1	-0.1	0.7	-0.4	-1.5
S2	601	-0.1	1.4	0.4	-0.1	-0.1	0.0	1.4	0.4	-0.1
T1	897	-0.2	0.4	-1.3	0.0	0.0	0.0	0.4	-0.2	-1.3
T2	614	0.0	0.7	-0.6	0.0	-0.1	-0.1	0.7	0.0	-0.6

Table 2.10.4-18 Stress Components - Impact; 30-Foot Bottom Oblique Drop; Drop Orientation = 15 Degrees; 3-D Bottom Model; 0-Degree Circumferential Location; Condition 1 (continued)

Stress Points Section <sup>1</sup> Node	Stress Components (ksi)						Principal Stresses (ksi)		
	S <sub>x</sub>	S <sub>y</sub>	S <sub>z</sub>	S <sub>xy</sub>	S <sub>xz</sub>	S <sub>yz</sub>	S1	S2	S3
T3 611	0.0	0.6	-0.2	0.0	-0.1	-0.1	0.6	0.0	-0.3
U1 900	-0.5	0.4	-1.2	0.0	0.0	0.2	0.4	-0.4	-1.2
U2 910	1.2	0.3	-0.5	0.0	0.0	0.4	1.2	0.3	-0.6
V1 920	-1.0	-0.3	-0.5	0.0	0.0	0.4	-0.3	-0.3	-1.2
V2 930	0.4	-0.5	-0.4	0.1	0.0	0.2	0.4	-0.4	-0.5
W1 1216	1.8	2.4	-1.2	0.0	0.1	-0.3	2.4	1.9	-1.2
W2 1226	-0.3	-0.2	0.6	0.0	0.0	-0.2	0.7	-0.2	-0.3
X1 1236	0.2	0.2	-0.7	0.0	0.0	-0.2	0.2	0.2	-0.7
X2 1246	-2.1	-2.4	1.4	0.0	0.1	-0.3	1.4	-2.1	-2.5

<sup>1</sup> Refer to Figure 2.10.2-34 for the identification of the representative sections.

Table 2.10.4-19 Stress Components - Impact; 30-Foot Top Oblique Drop; Drop Orientation = 75 Degrees; 3-D Top Model; 0-Degree Circumferential Location; Condition 1

Condition 1: 100°F Ambient with Contents

Stress Points		Stress Components (ksi)						Principal Stresses (ksi)		
Section <sup>1</sup>	Node	S <sub>x</sub>	S <sub>y</sub>	S <sub>z</sub>	S <sub>xy</sub>	S <sub>xz</sub>	S <sub>yz</sub>	S1	S2	S3
A1	1949	-0.5	2.2	-0.1	-0.2	0.0	-0.1	2.2	-0.1	-0.6
A2	1950	-0.6	1.5	-0.1	-0.2	0.2	-0.1	1.6	-0.1	-0.6
A3	1951	-0.3	-0.1	0.2	-0.1	0.5	0.0	0.6	-0.3	-0.5
B1	1952	0.0	-0.7	-0.2	-0.2	0.5	-0.1	0.2	-0.1	-1.0
B2	93	0.2	-3.4	0.5	-0.4	0.2	-0.1	0.5	0.2	-3.5
C1	1925	2.2	-2.4	6.8	0.1	-0.5	0.4	6.9	2.2	-2.4
C2	1926	2.3	-3.6	1.3	0.2	-0.2	-0.2	2.3	1.3	-3.6
C3	1927	-1.1	-2.2	0.2	0.1	-0.1	0.2	0.2	-1.2	-2.3
D1	683	2.3	-2.0	0.3	0.5	-0.1	0.8	2.6	0.0	-2.0
D2	85	-3.2	-4.1	0.8	0.8	-0.1	0.2	0.8	-2.7	-4.5
E1	682	-1.8	-3.2	0.0	0.2	-0.1	1.1	0.6	-2.3	-3.3
E2	82	-1.5	-3.6	2.6	0.3	0.2	1.3	3.0	-1.9	-3.6
F1	1925	2.2	-2.4	6.8	0.1	-0.5	0.4	6.9	2.2	-2.4
F2	1325	0.5	-8.3	-13.6	0.5	-0.4	1.0	0.7	-8.3	-13.7
G1	680	2.2	-1.3	9.9	0.1	-0.1	2.0	10.4	1.7	-1.3
G2	80	2.0	-4.4	-2.3	0.4	-0.3	-0.2	2.1	-2.2	-4.4
H1	1921	-0.1	6.2	-3.0	-0.3	-1.3	0.1	6.4	-0.1	-3.1
H2	1321	-0.2	10.9	5.9	-0.7	-1.1	-0.3	11.1	5.7	-0.3
I1	676	-0.1	-0.2	5.4	0.1	-0.6	0.0	5.5	-0.1	-0.3
I2	76	-0.1	3.8	11.0	-0.2	-0.4	0.0	11.0	3.8	-0.1
J1	1916	-0.2	6.4	9.2	-0.5	-0.6	0.0	9.4	6.3	-0.3
J2	1316	-0.2	11.4	13.1	-0.8	-0.6	0.0	13.2	11.3	-0.2
K1	671	-0.1	-1.2	9.8	0.1	-0.4	0.0	9.9	-0.1	-1.2
K2	71	-0.1	5.9	13.2	-0.4	-0.2	0.0	13.2	5.9	-0.1
L1	1908	-0.9	3.5	12.6	-0.3	0.2	0.0	12.6	3.5	-0.9
L2	1308	0.0	10.4	15.5	1.8	0.2	0.0	15.5	10.7	-0.3
M1	663	-1.2	-2.2	10.7	0.1	0.1	0.0	10.7	-1.2	-2.2
M2	63	0.4	8.8	15.7	2.0	0.1	0.0	15.7	9.3	0.0

Table 2.10.4-19 Stress Components -- Impact; 30-Foot Top Oblique Drop; Drop Orientation = 75 Degrees; 3-D Top Model; 0-Degree Circumferential Location; Condition 1 (continued)

Stress Points Section <sup>1</sup> Node		Stress Components (ksi)						Principal Stresses (ksi)		
		S <sub>x</sub>	S <sub>y</sub>	S <sub>z</sub>	S <sub>xy</sub>	S <sub>yz</sub>	S <sub>xz</sub>	S1	S2	S3
N1	1877	-0.3	6.1	3.9	-0.5	1.1	0.0	6.6	3.5	-0.3
N2	1477	-0.2	8.9	5.7	-0.7	1.0	0.0	9.2	5.4	-0.2
N3	1277	-0.1	11.5	7.4	-0.8	1.0	0.0	11.8	7.2	-0.1
O1	647	-0.1	-1.1	8.2	0.0	0.5	0.0	8.3	-0.1	-1.1
O2	247	-0.1	2.5	9.9	-0.2	0.4	0.0	9.9	2.5	-0.1
O3	47	0.0	5.7	11.4	-0.4	0.2	0.0	11.4	5.8	-0.1
P1	1840	-0.3	6.2	-9.5	-0.4	1.7	0.0	6.4	-0.3	-9.7
P2	1640	-0.2	7.9	-6.8	-0.5	1.6	0.0	8.1	-0.3	-7.0
P3	1440	-0.1	9.5	-4.2	-0.6	1.5	0.0	9.8	-0.1	-4.4
P4	1240	0.0	11.1	-1.8	-0.7	1.5	0.1	11.4	0.0	-2.0
Q1	628	-0.4	0.3	2.1	-0.1	0.7	0.1	2.4	0.1	-0.4
Q2	428	-0.3	2.2	5.0	-0.2	0.6	0.1	5.1	2.0	-0.3
Q3	228	-0.1	3.9	7.8	-0.3	0.5	0.1	7.8	3.9	-0.1
Q4	28	0.0	5.6	10.6	-0.4	0.4	0.0	10.6	5.6	-0.1
R1	1816	-0.9	-10.4	2.3	0.8	1.1	0.2	2.4	-0.8	-10.6
R2	1616	-1.7	-12.4	-5.2	0.9	1.0	-0.1	-1.6	-5.0	-12.6
R3	1416	-4.1	-14.5	-12.0	1.0	0.7	-2.1	-3.5	-12.2	-15.0
R4	1216	-4.5	-16.5	-20.5	1.2	0.4	-4.9	-3.0	-16.5	-22.0
S1	616	4.3	-7.6	-2.1	0.6	0.6	-0.8	4.5	-2.1	-7.7
S2	416	0.1	-7.8	1.3	0.5	0.4	-1.0	1.9	-0.4	-7.9
S3	216	0.4	-6.7	4.5	0.5	0.3	-0.2	4.5	0.4	-6.8
S4	16	0.2	-5.7	7.6	0.4	0.2	-0.1	7.6	0.2	-5.8
T1	811	-18.9	-24.8	-16.4	1.1	0.3	-6.7	-10.8	-23.6	-25.7
T2	611	-10.2	-18.9	-4.8	0.9	0.1	-6.4	-0.6	-14.3	-19.1
T3	411	-4.8	-16.6	-2.5	1.0	0.1	-5.6	2.1	-9.3	-16.7
T4	211	-0.5	-14.7	-0.7	1.0	0.1	-3.3	2.7	-3.8	-14.8
T5	11	1.0	-12.3	5.7	0.9	0.1	-1.7	6.2	0.5	-12.4
U1	43058	5.2	1.5	-0.2	0.1	0.1	0.0	5.2	1.5	-0.2
U2	43057	2.6	0.0	-0.3	0.0	-0.1	0.0	2.6	0.0	-0.3
U3	43056	0.4	-1.5	-0.5	0.0	0.0	-0.1	0.4	-0.5	-1.5

Table 2.10.4-19 Stress Components - Impact; 30-Foot Top Oblique Drop; Drop Orientation = 75 Degrees; 3-D Top Model; 0-Degree Circumferential Location; Condition 1 (continued)

Stress Points		Stress Components (ksi)						Principal Stresses (ksi)		
Section <sup>1</sup>	Node	S <sub>x</sub>	S <sub>y</sub>	S <sub>z</sub>	S <sub>xy</sub>	S <sub>yz</sub>	S <sub>xz</sub>	S1	S2	S3
U4	43055	-1.8	-3.0	-0.8	0.1	0.0	-0.4	-0.6	-2.0	-3.0
U5	43054	-4.1	-4.6	-1.3	0.1	-0.1	-1.0	-1.0	-4.4	-4.6
U6	43053	-6.1	-6.2	-1.8	0.1	-0.2	-2.1	-0.9	-6.2	-7.0
U7	43052	-8.7	-7.7	-1.5	0.0	-0.2	-2.5	-0.7	-7.7	-9.5
U8	43051	-16.8	-11.1	-0.2	-0.1	0.1	1.8	0.0	-11.1	-17.0
V1	50024	-19.9	-13.2	0.1	-1.1	0.0	0.6	0.2	-13.0	-20.1
V2	50023	-20.2	-15.6	-0.8	-0.8	0.1	1.5	-0.7	-15.5	-20.5
V3	50022	-13.2	-15.8	-1.4	-0.3	0.1	2.0	-1.1	-13.5	-15.8
V4	50021	-16.0	-18.6	-1.0	-0.2	0.1	1.6	-0.8	-16.2	-18.7
W1	43278	-0.9	-4.5	-0.2	-0.2	-0.3	0.2	-0.1	-0.9	-4.5
W2	43274	-0.6	-5.1	-0.1	-0.1	-0.3	0.2	0.0	-0.6	-5.1
W3	43271	-0.1	-2.9	0.0	0.0	-0.5	0.1	0.1	-0.1	-3.0
X1	50084	9.7	0.0	-2.7	-0.2	0.2	-2.4	10.2	0.0	-3.2
X2	50083	2.5	-7.5	-1.7	0.0	0.2	-2.4	3.6	-2.8	-7.5
X3	50081	-10.5	-20.7	5.4	0.4	-0.3	-2.4	5.7	-10.8	-20.7

<sup>1</sup> Refer to Figures 2.10.2-34 for the identification of the representative sections.



Table 2.10.4-20 Stress Components -- Impact; 30-Foot Bottom Oblique Drop; Drop Orientation = 75 Degrees; 3-D Bottom Model; 0-Degree Circumferential Location; Condition 1

Condition 1: 100°F Ambient with Contents

Stress Points		Stress Components (ksi)						Principal Stresses (ksi)		
Section <sup>1</sup>	Node	S <sub>x</sub>	S <sub>y</sub>	S <sub>z</sub>	S <sub>xy</sub>	S <sub>yz</sub>	S <sub>xz</sub>	S1	S2	S3
A1	1130	4.3	-0.8	-2.2	-0.3	0.5	0.6	4.3	-0.6	-2.4
A2	1129	-0.3	-5.8	-0.4	-0.1	0.4	0.6	0.2	-0.9	-5.8
A3	1128	-4.9	-10.8	1.4	0.0	0.6	0.6	1.4	-4.9	-10.8
B1	1185	2.1	-5.4	-2.3	0.2	0.7	0.6	2.2	-2.3	-5.6
B2	1184	-2.1	-10.3	-0.5	0.3	0.4	0.6	-0.3	-2.3	-10.3
B3	1183	-6.3	-14.4	1.0	0.4	0.4	0.6	1.0	-6.3	-14.4
C1	90	-1.5	-7.1	10.9	-0.2	-0.8	0.3	10.9	-1.5	-7.1
C2	80	-7.9	-11.0	3.9	-0.2	-0.5	-0.6	3.9	-7.9	-11.0
C3	70	-8.3	-12.3	0.5	0.0	-0.4	-1.0	0.7	-8.4	-12.3
C4	60	-8.5	-13.0	-0.5	0.2	-0.2	-0.7	-0.5	-8.6	-13.1
C5	50	-10.8	-15.1	-0.4	0.3	-0.1	-0.2	-0.4	-10.8	-15.1
C6	40	-11.1	-15.9	-0.2	0.5	0.0	-0.1	-0.2	-11.0	-16.0
D1	25	-29.4	-23.7	-8.4	-0.6	-0.2	-5.0	-7.3	-23.6	-30.6
D2	15	-17.6	-20.4	-4.9	-0.3	0.0	-2.2	-4.6	-18.0	-20.5
D3	5	-10.8	-19.6	-2.4	-0.1	0.0	-0.7	-2.4	-10.9	-19.6
E1	35	-7.6	-16.4	-1.5	0.5	-0.1	-1.5	-1.1	-7.9	-16.5
E2	34	-8.4	-17.6	-5.0	0.5	-0.2	-3.3	-3.0	-10.4	-17.6
E3	33	-14.0	-19.4	-5.4	0.3	-0.3	-3.7	-4.0	-15.4	-19.4
E4	32	-16.2	-20.6	-7.0	0.3	-0.2	-2.4	-6.4	-16.8	-20.7
E5	31	-17.0	-21.6	-8.9	0.3	-0.2	-1.4	-8.7	-17.2	-21.6
F1	100	-1.1	-5.1	18.0	0.2	-1.2	1.6	18.2	-1.3	-5.1
F2	99	-2.4	-10.9	-1.9	0.5	-0.9	2.2	0.0	-4.2	-11.0
F3	98	-1.4	-14.2	-15.2	0.9	-0.6	3.9	-0.4	-14.0	-16.5
F4	97	0.6	-20.9	-42.5	1.5	-0.6	5.0	1.3	-20.9	-43.1
G1	94	1.3	-5.2	18.1	0.4	-0.4	4.1	19.0	0.4	-5.2
G2	93	1.8	-9.6	1.3	0.8	-0.3	3.2	4.8	-1.6	-9.7
G3	92	1.6	-10.8	-3.1	0.9	-0.2	1.5	2.0	-3.5	-10.9
G4	91	0.7	-12.3	-7.9	0.9	-0.2	0.6	0.8	-8.0	-12.4

Table 2.10.4-20 Stress Components - Impact; 30-Foot Bottom Oblique Drop; Drop Orientation = 75 Degrees; 3-D Bottom Model; 0-Degree Circumferential Location; Condition 1 (continued)

Stress Points		Stress Components (ksi)						Principal Stresses (ksi)		
Section <sup>1</sup>	Node	S <sub>x</sub>	S <sub>y</sub>	S <sub>z</sub>	S <sub>xy</sub>	S <sub>yz</sub>	S <sub>xz</sub>	S1	S2	S3
H1	330	-0.3	5.9	-9.2	-0.4	-1.7	0.0	6.1	-0.3	-9.4
H2	329	-0.2	7.5	-6.2	-0.5	-1.6	0.0	7.7	-0.2	-6.4
H3	328	0.0	9.1	-3.2	-0.6	-1.5	0.0	9.3	-0.1	-3.4
H4	327	0.1	10.6	-0.2	-0.7	-1.4	-0.1	10.9	0.1	-0.5
I1	244	-0.2	-0.8	-0.9	0.1	-0.8	0.0	0.0	-0.2	-1.7
I2	243	-0.1	1.0	2.2	-0.1	-0.7	-0.1	2.5	0.6	-0.1
I3	242	-0.1	2.6	5.3	-0.2	-0.5	-0.1	5.4	2.5	-0.1
I4	241	0.0	4.2	8.4	-0.3	-0.4	-0.1	8.5	4.1	0.0
J1	550	-0.3	6.3	5.9	-0.5	-0.9	0.0	7.0	5.2	-0.3
J2	548	-0.2	8.9	7.7	-0.7	-0.9	0.0	9.4	7.3	-0.2
J3	547	-0.1	11.3	9.5	-0.8	-0.8	0.0	11.7	9.2	-0.1
K1	344	-0.1	-0.9	6.9	0.0	-0.6	0.0	7.0	-0.1	-1.0
K2	342	-0.1	2.6	8.5	-0.2	-0.4	0.0	8.5	2.6	-0.1
K3	341	0.0	5.8	10.0	-0.5	-0.3	0.0	10.0	5.9	-0.1
L1	740	-0.1	3.8	13.3	0.3	-0.1	-0.1	13.3	3.9	-0.1
L2	738	-0.5	6.5	14.8	-1.1	-0.1	0.0	14.8	6.7	-0.7
L3	737	0.2	9.4	16.3	-2.4	-0.1	0.0	16.3	10.0	-0.4
M1	454	-0.3	-2.0	9.7	-1.9	-0.1	0.0	9.7	0.9	-3.2
M2	452	0.4	3.5	12.4	-0.9	-0.1	0.2	12.4	3.7	0.2
M3	451	-0.7	8.0	14.8	0.0	-0.1	-0.3	14.8	8.0	-0.7
N1	810	-0.2	6.6	9.0	-0.5	0.7	-0.1	9.2	6.4	-0.3
N2	807	-0.2	11.2	12.5	-0.8	0.7	0.0	12.8	11.0	-0.3
O1	524	-0.1	-0.8	9.6	0.1	0.4	0.0	9.6	-0.1	-0.9
O2	521	-0.1	5.7	12.9	-0.4	0.2	0.0	12.9	5.8	-0.1
P1	850	-0.1	6.3	-2.0	-0.3	1.3	-0.1	6.5	-0.2	-2.2
P2	847	-0.2	11.0	6.4	-0.7	1.1	0.3	11.3	6.2	-0.3
Q1	564	-0.1	0.0	6.3	0.0	0.5	0.0	6.3	0.0	-0.1
Q2	561	-0.1	4.0	11.1	-0.3	0.3	0.0	11.1	4.0	-0.1
R1	890	-3.0	-3.3	9.3	0.1	0.8	-0.6	9.4	-3.0	-3.4
R2	887	-2.9	-7.7	-10.2	0.4	0.5	-1.6	-2.6	-7.6	-10.7

Table 2.10.4-20 Stress Components - Impact; 30-Foot Bottom Oblique Drop; Drop Orientation = 75 Degrees; 3-D Bottom Model; 0-Degree Circumferential Location; Condition 1 (continued)

Stress Points Section <sup>1</sup> Node	Stress Components (ksi)						Principal Stresses (ksi)		
	S <sub>x</sub>	S <sub>y</sub>	S <sub>z</sub>	S <sub>w</sub>	S <sub>yz</sub>	S <sub>xy</sub>	S1	S2	S3
S1 604	-0.1	-1.2	8.1	0.0	0.2	-1.4	8.3	-0.4	-1.2
S2 601	0.7	-2.6	0.6	0.2	0.1	-0.6	1.3	0.1	-2.6
T1 897	3.0	-3.3	-2.3	0.3	0.3	-1.0	3.2	-2.3	-3.4
T2 614	0.8	-2.1	2.5	0.1	0.0	-1.2	3.2	0.2	-2.1
T3 611	-0.2	-2.5	1.3	0.1	-0.1	-0.7	1.5	-0.5	-2.5
U1 900	4.8	-1.7	1.9	0.2	0.4	-0.1	4.8	1.9	-1.7
U2 910	-2.0	-2.8	0.1	0.1	0.2	-0.9	0.4	-2.3	-2.8
V1 920	2.6	-1.1	0.8	0.4	0.1	-0.7	2.9	0.6	-1.2
V2 930	-4.0	-3.8	0.6	0.6	0.1	-0.2	0.6	-3.3	-4.5
W1 1216	-0.8	2.1	-0.4	-0.1	-0.3	0.1	2.2	-0.5	-0.8
W2 1226	-0.4	0.1	0.2	-0.1	-0.5	0.0	0.6	-0.3	-0.4
X1 1236	0.0	-0.7	-0.2	-0.2	-0.5	0.0	0.2	-0.1	-1.0
X2 1246	0.2	-3.3	0.5	-0.4	-0.3	0.0	0.6	0.2	-3.3

<sup>1</sup> Refer to Figure 2.10.2-34 for the identification of the representative sections.

Table 2.10.4-21 Primary Stresses; Heat Condition; 3-D Top Model; 0-Degree  
Circumferential Location; Condition 1

Condition 1: 100°F Ambient with Contents

Stress Points		Stress Components (ksi)						Principal Stresses (ksi)		
Section <sup>1</sup>	Node	S <sub>x</sub>	S <sub>y</sub>	S <sub>z</sub>	S <sub>xy</sub>	S <sub>yz</sub>	S <sub>xz</sub>	S1	S2	S3
A1	1949	-0.4	-0.4	0.0	0.0	0.0	-0.1	0.0	-0.4	-0.5
A2	1950	-0.3	-0.2	0.0	0.0	0.0	-0.1	0.0	-0.2	-0.3
A3	1951	0.1	0.1	-0.1	0.0	0.0	0.0	0.1	0.1	-0.1
B1	1952	0.0	0.0	0.1	0.0	0.0	0.0	0.1	0.0	-0.1
B2	93	0.4	0.4	-0.2	0.0	0.0	-0.1	0.4	0.4	-0.2
C1	1925	0.2	0.1	0.8	0.0	0.0	0.1	0.8	0.2	0.1
C2	1926	0.1	0.0	0.2	0.0	0.0	0.0	0.2	0.1	0.0
C3	1927	-0.1	0.0	0.1	0.0	0.0	0.0	0.1	0.0	-0.1
D1	683	0.1	0.1	0.0	0.0	0.0	0.0	0.2	0.1	0.0
D2	85	-0.1	0.2	0.1	0.0	0.0	0.0	0.2	0.1	-0.1
E1	682	-0.1	0.0	0.0	0.0	0.0	0.0	0.0	0.0	-0.1
E2	82	-0.1	0.0	0.1	0.0	0.0	0.1	0.1	0.0	-0.1
F1	1925	0.2	0.1	0.8	0.0	0.0	0.1	0.8	0.2	0.1
F2	1325	0.0	-0.4	-0.8	0.0	0.0	0.1	0.1	-0.4	-0.8
G1	680	0.0	0.0	0.3	0.0	0.0	0.1	0.3	0.0	0.0
G2	80	0.1	-0.1	0.0	0.0	0.0	0.0	0.1	0.0	-0.1
H1	1921	0.0	1.1	0.0	-0.1	0.0	0.0	1.1	0.0	0.0
H2	1321	0.0	1.3	0.7	-0.1	0.0	0.0	1.3	0.7	0.0
I1	676	0.0	-0.1	0.2	0.0	0.0	0.0	0.2	0.0	-0.1
I2	76	0.0	0.0	0.3	0.0	0.0	0.0	0.3	0.0	0.0
J1	1916	0.0	1.2	0.6	-0.1	0.0	0.0	1.2	0.6	0.0
J2	1316	0.0	1.3	0.7	-0.1	0.0	0.0	1.3	0.7	0.0
K1	671	0.0	0.0	0.2	0.0	0.0	0.0	0.2	0.0	0.0
K2	71	0.0	0.1	0.2	0.0	0.0	0.0	0.2	0.1	0.0
L1	1908	0.0	1.2	0.8	-0.1	0.0	0.0	1.2	0.8	-0.1
L2	1308	0.0	1.3	0.9	0.0	0.0	0.0	1.3	0.9	0.0
M1	663	0.0	0.0	0.2	0.0	0.0	0.0	0.2	0.0	0.0
M2	63	0.0	0.0	0.2	0.0	0.0	0.0	0.2	0.0	0.0
N1	1877	0.0	1.2	0.6	-0.1	0.0	0.0	1.2	0.6	0.0

Table 2.10.4-21 Primary Stresses; Heat Condition; 3-D Top Model; 0-Degree  
Circumferential Location; Condition 1 (continued)

Stress Points Section <sup>1</sup> Node		Stress Components (ksi)						Principal Stresses (ksi)		
		S <sub>x</sub>	S <sub>y</sub>	S <sub>z</sub>	S <sub>xy</sub>	S <sub>yz</sub>	S <sub>xz</sub>	S1	S2	S3
N2	1477	0.0	1.3	0.6	-0.1	0.0	0.0	1.3	0.6	0.0
N3	1277	0.0	1.3	0.7	-0.1	0.0	0.0	1.3	0.7	0.0
O1	647	0.0	0.1	0.1	0.0	0.0	0.0	0.1	0.1	0.0
O2	247	0.0	0.0	0.1	0.0	0.0	0.0	0.1	0.0	0.0
O3	47	0.0	0.0	0.1	0.0	0.0	0.0	0.1	0.0	0.0
P1	1840	0.0	1.1	-0.1	-0.1	0.0	0.0	1.1	0.0	-0.1
P2	1640	0.0	1.2	0.2	-0.1	0.0	0.0	1.2	0.2	0.0
P3	1440	0.0	1.3	0.5	-0.1	0.0	0.0	1.3	0.5	0.0
P4	1240	0.0	1.4	0.9	-0.1	0.0	0.1	1.4	0.9	0.0
Q1	628	0.0	-0.3	-0.2	0.0	0.0	0.0	0.0	-0.2	-0.3
Q2	428	0.0	-0.3	0.0	0.0	0.0	0.0	0.0	0.0	-0.3
Q3	228	0.0	-0.2	0.1	0.0	0.0	0.0	0.1	0.0	-0.2
Q4	28	0.0	-0.1	0.3	0.0	0.0	0.0	0.3	0.0	-0.2
R1	1816	-0.2	0.1	2.1	0.0	0.0	0.1	2.1	0.1	-0.2
R2	1616	-0.5	-0.3	0.7	0.0	0.0	0.2	0.7	-0.3	-0.5
R3	1416	-1.2	-0.8	-0.3	0.0	0.0	0.1	-0.3	-0.8	-1.2
R4	1216	-2.3	-1.4	-1.2	0.0	0.0	-0.2	-1.2	-1.4	-2.3
S1	616	-1.1	-0.7	0.6	0.0	0.0	0.2	0.6	-0.7	-1.1
S2	416	-0.5	-0.5	0.4	0.0	0.0	0.4	0.6	-0.5	-0.7
S3	216	0.0	-0.6	-0.3	0.0	0.0	0.5	0.3	-0.6	-0.7
S4	16	0.3	-0.6	-0.8	0.0	0.0	0.4	0.4	-0.6	-0.9
T1	811	0.3	0.1	0.2	0.0	0.0	0.4	0.6	0.1	-0.1
T2	611	0.5	-0.1	-0.6	0.0	0.0	0.1	0.5	-0.1	-0.6
T3	411	0.2	0.0	-0.2	0.0	0.0	0.1	0.2	0.0	-0.2
T4	211	0.1	0.0	0.1	0.0	0.0	0.1	0.1	0.0	0.0
T5	11	0.0	0.1	0.4	0.0	0.0	0.0	0.4	0.1	0.0
U1	43058	0.7	-0.6	-1.6	0.1	0.0	0.3	0.7	-0.6	-1.6
U2	43057	-0.4	-0.9	-1.7	0.0	0.0	0.4	-0.3	-0.9	-1.8
U3	43056	-0.6	-1.0	-2.0	0.0	0.0	0.6	-0.4	-1.0	-2.2
U4	43055	-0.3	-0.9	-2.3	0.0	0.0	0.4	-0.3	-0.9	-2.4
U5	43054	-0.2	-0.8	-2.4	0.0	0.0	-0.1	-0.2	-0.8	-2.4

Table 2.10.4-21 Primary Stresses; Heat Condition; 3-D Top Model; 0-Degree Circumferential Location; Condition 1 (continued)

Stress Points Section <sup>1</sup>	Node	Stress Components (ksi)						Principal Stresses (ksi)		
		S <sub>x</sub>	S <sub>y</sub>	S <sub>z</sub>	S <sub>xy</sub>	S <sub>yz</sub>	S <sub>xz</sub>	S1	S2	S3
U6	43053	-0.4	-0.7	-2.0	0.0	0.0	-0.4	-0.3	-0.7	-2.1
U7	43052	-0.7	-0.5	-1.3	0.0	0.0	-0.5	-0.5	-0.5	-1.6
U8	43051	0.8	0.5	-0.4	0.0	0.0	-0.4	0.9	0.5	-0.5
V1	50024	0.4	-0.2	-0.6	0.1	0.0	-0.1	0.5	-0.2	-0.6
V2	50023	0.2	-0.2	-0.8	0.0	0.0	0.0	0.2	-0.2	-0.8
V3	50022	-0.1	0.0	-0.2	0.0	0.0	0.0	0.0	-0.1	-0.2
V4	50021	-0.7	0.1	0.6	-0.1	0.0	0.0	0.6	0.1	-0.7
W1	43278	-0.8	-0.9	0.3	0.0	0.0	0.2	0.3	-0.9	-0.9
W2	43274	-0.1	-0.2	0.0	0.0	0.0	0.2	0.1	-0.2	-0.2
W3	43271	0.4	0.3	-0.2	0.0	0.0	0.1	0.4	0.3	-0.2
X1	50084	-0.4	-0.3	0.1	0.0	0.0	0.1	0.1	-0.3	-0.4
X2	50083	-0.1	-0.1	0.0	0.0	0.0	0.1	0.1	-0.1	-0.1
X3	50081	0.3	0.3	-0.2	0.0	0.0	0.1	0.4	0.3	-0.2

<sup>1</sup> Refer to Figure 2.10.2-34 for the identification of the representative sections.

Table 2.10.4-22 Primary + Secondary Stresses; Heat Condition; 3-D Top Model; 0-Degree Circumferential Location; Condition 1

Condition 1: 100°F Ambient with Contents

Stress Points		Stress Components (ksi)						Principal Stresses (ksi)		
Section <sup>1</sup>	Node	S <sub>x</sub>	S <sub>y</sub>	S <sub>z</sub>	S <sub>xy</sub>	S <sub>xz</sub>	S <sub>yz</sub>	S1	S2	S3
A1	1949	-0.8	-0.7	0.6	0.0	-0.1	0.6	0.9	-0.7	-1.0
A2	1950	-0.7	-0.6	0.5	0.0	-0.1	0.6	0.8	-0.7	-1.0
A3	1951	-1.5	-1.5	-0.8	0.0	-0.1	0.3	-0.7	-1.5	-1.7
B1	1952	0.7	0.7	0.7	0.0	-0.1	0.3	1.0	0.7	0.3
B2	93	0.6	0.5	-1.8	0.0	-0.2	0.7	0.8	0.5	-2.0
C1	1925	-1.0	-0.6	-0.6	0.0	-0.1	-0.8	0.0	-0.6	-1.7
C2	1926	0.8	-0.4	-0.8	0.1	-0.1	-0.7	1.1	-0.4	-1.1
C3	1927	-2.0	-2.1	-1.2	0.0	0.0	0.0	-1.2	-2.0	-2.1
D1	683	1.8	1.3	3.4	0.0	0.1	0.8	3.7	1.5	1.3
D2	85	-1.5	1.7	3.4	-0.1	0.1	0.6	3.5	1.7	-1.6
E1	682	-1.5	-0.4	2.4	-0.1	0.1	0.6	2.5	-0.4	-1.6
E2	82	-1.0	-0.5	-0.4	0.0	0.0	1.2	0.6	-0.5	-1.9
F1	1925	-1.0	-0.6	-0.6	0.0	-0.1	-0.8	0.0	-0.6	-1.7
F2	1325	0.6	-0.8	-1.5	0.1	0.0	-0.7	0.8	-0.8	-1.7
G1	680	0.0	0.2	1.0	0.0	0.0	0.2	1.1	0.2	-0.1
G2	80	-2.6	1.2	7.1	-0.2	0.1	1.3	7.2	1.2	-2.7
H1	1921	0.0	0.9	0.6	-0.1	0.1	0.0	1.0	0.6	0.0
H2	1321	-0.1	1.0	-0.4	-0.1	0.0	0.1	1.0	-0.1	-0.4
I1	676	-0.1	2.5	5.7	-0.2	0.1	0.1	5.7	2.5	-0.1
I2	76	-0.1	3.2	6.5	-0.2	-0.1	0.1	6.5	3.2	-0.2
J1	1916	-0.1	0.1	-1.5	0.0	0.0	0.0	0.1	-0.1	-1.5
J2	1316	-0.1	2.5	2.2	-0.2	0.0	0.0	2.5	2.2	-0.1
K1	671	-0.1	3.7	4.0	-0.3	0.0	0.0	4.0	3.7	-0.2
K2	71	-0.1	6.1	8.2	-0.5	0.0	0.0	8.2	6.2	-0.2
L1	1908	-0.9	-0.2	-1.1	0.0	0.0	0.0	-0.2	-0.9	-1.1
L2	1308	0.6	2.8	1.8	0.0	0.0	0.0	2.8	1.8	0.6
M1	663	-1.3	4.1	3.9	-0.4	0.0	0.0	4.1	3.9	-1.3
M2	63	0.7	7.7	8.0	-0.5	0.0	0.0	8.0	7.7	0.7
N1	1877	0.0	-0.6	-1.6	0.0	0.0	0.0	0.0	-0.6	-1.6

Table 2.10.4-22 Primary + Secondary Stresses; Heat Condition; 3-D Top Model; 0-Degree Circumferential Location; Condition 1 (continued)

Stress Points Section <sup>1</sup> Node		Stress Components (ksi)						Principal Stresses (ksi)		
		S <sub>x</sub>	S <sub>y</sub>	S <sub>z</sub>	S <sub>xy</sub>	S <sub>xz</sub>	S <sub>yz</sub>	S1	S2	S3
N2	1477	0.0	1.0	0.1	-0.1	0.0	0.0	1.0	0.1	0.0
N3	1277	0.0	2.5	1.7	-0.2	0.1	0.0	2.5	1.7	0.0
O1	647	-0.2	2.9	4.5	-0.2	-0.1	0.0	4.5	2.9	-0.3
O2	247	-0.1	4.7	6.2	-0.4	0.0	0.0	6.2	4.8	-0.2
O3	47	-0.1	6.4	7.9	-0.5	0.0	0.0	7.9	6.5	-0.1
P1	1840	0.0	-0.9	-1.7	0.1	0.0	0.0	0.0	-0.9	-1.7
P2	1640	0.0	0.3	-0.7	0.0	0.0	0.0	0.3	0.0	-0.7
P3	1440	0.1	1.6	0.3	-0.1	0.0	0.0	1.6	0.3	0.1
P4	1240	-0.2	2.7	1.5	-0.2	0.1	0.2	2.8	1.5	-0.2
Q1	628	-0.2	1.5	5.4	-0.1	0.0	0.1	5.4	1.5	-0.2
Q2	428	-0.2	2.6	6.1	-0.2	0.0	0.1	6.1	2.7	-0.2
Q3	228	-0.1	3.8	6.9	-0.3	0.0	0.1	6.9	3.8	-0.1
Q4	28	0.0	4.8	7.7	-0.4	0.0	0.0	7.7	4.9	0.0
R1	1816	0.0	-7.9	-1.0	0.6	0.0	1.0	0.7	-1.7	-7.9
R2	1616	-0.2	-6.7	-1.6	0.5	0.0	1.7	0.9	-2.7	-6.7
R3	1416	-2.0	-5.8	-1.7	0.2	0.0	2.8	1.0	-4.6	-5.8
R4	1216	-0.1	-3.5	0.4	0.1	0.0	2.2	2.4	-2.0	-3.5
S1	616	-3.2	-0.7	-2.4	-0.3	0.1	-1.7	-0.6	-1.1	-4.5
S2	416	-5.9	1.4	4.4	-0.5	-0.1	-2.3	4.9	1.4	-6.4
S3	216	-1.6	3.8	5.1	-0.4	0.1	-0.1	5.1	3.9	-1.7
S4	16	-0.7	5.6	7.4	-0.6	0.2	0.1	7.4	5.7	-0.8
T1	811	-1.8	-1.3	-4.8	-0.1	-0.1	-1.3	-1.3	-1.3	-5.2
T2	611	-1.0	0.8	-2.0	-0.1	-0.1	-0.7	0.8	-0.6	-2.3
T3	411	-0.4	2.5	0.1	-0.3	0.0	-0.4	2.5	0.3	-0.6
T4	211	-0.1	4.1	2.0	-0.3	0.0	-0.2	4.1	2.1	-0.2
T5	11	-0.1	5.6	3.9	-0.4	0.0	-0.1	5.6	3.9	-0.1
U1	43058	-2.6	-2.7	-7.4	0.1	0.2	1.0	-2.4	-2.7	-7.6
U2	43057	-0.1	-2.3	-6.4	0.2	0.1	1.2	0.1	-2.3	-6.6
U3	43056	-0.1	-2.3	-4.8	0.2	0.2	1.3	0.3	-2.3	-5.2
U4	43055	-0.1	-2.5	-4.2	0.2	0.2	0.9	0.1	-2.5	-4.4
U5	43054	-0.4	-2.8	-3.6	0.1	0.2	0.3	-0.4	-2.8	-3.6



Table 2.10.4-22 Primary + Secondary Stresses; Heat Conditions; 3-D Top Model;  
0-Degree Circumferential Location; Condition 1 (continued)

Stress Points Section <sup>1</sup> Node	Stress Components (ksi)						Principal Stresses (ksi)		
	S <sub>x</sub>	S <sub>y</sub>	S <sub>z</sub>	S <sub>xy</sub>	S <sub>yz</sub>	S <sub>xz</sub>	S1	S2	S3
U6 43053	-1.2	-3.2	-2.7	0.1	0.3	-0.1	-1.2	-2.6	-3.3
U7 43052	-2.6	-3.5	-1.6	0.1	0.5	-0.2	-1.5	-2.6	-3.7
U8 43051	3.1	3.7	5.3	-0.3	0.7	-1.1	6.0	3.5	2.6
V1 50024	1.3	0.2	0.0	0.1	-0.1	0.3	1.4	0.2	-0.1
V2 50023	0.6	-0.3	-0.5	0.1	-0.2	0.2	0.6	-0.2	-0.6
V3 50022	-0.3	-0.8	-0.3	0.0	-0.2	0.1	-0.2	-0.4	-0.9
V4 50021	-1.4	-1.2	0.5	-0.1	-0.1	0.1	0.5	-1.2	-1.4
W1 43278	1.9	2.0	-1.1	0.0	0.2	-0.6	2.0	1.9	-1.2
W2 43274	-0.9	-0.8	-0.6	0.0	0.2	-0.7	0.0	-0.8	-1.5
W3 43271	-2.8	-2.7	0.3	0.0	0.1	-0.3	0.3	-2.7	-2.8
X1 50084	1.6	1.7	-0.2	0.0	0.1	-0.3	1.7	1.7	-0.2
X2 50083	0.9	0.9	-0.1	0.0	0.1	-0.3	1.0	0.9	-0.2
X3 50081	-0.6	-0.7	0.4	0.0	0.1	-0.3	0.5	-0.7	-0.7

<sup>1</sup> Refer to Figure 2.10.2-34 for the identification of the representative sections.

Table 2.10.4-23  $P_m$  Stresses; Heat Condition; 3-D Top Model; 0-Degree  
Circumferential Location; Condition 1

Condition 1: 100°F Ambient with Contents

Section <sup>1</sup>	Node - Node	Stress Components (ksi)						Principal Stresses (ksi)			
		$S_x$	$S_y$	$S_z$	$S_{xy}$	$S_{yz}$	$S_{zx}$	S1	S2	S3	S.I.
A	1949 - 1951	-0.2	-0.1	0.0	0.0	0.0	-0.1	0.0	-0.1	-0.2	0.2
B	1952 - 93	0.2	0.2	-0.1	0.0	0.0	-0.1	0.2	0.2	-0.1	0.3
C	1925 - 1927	0.0	0.0	0.2	0.0	0.0	0.0	0.2	0.0	0.0	0.2
D	683 - 85	0.0	0.1	0.1	0.0	0.0	0.0	0.1	0.1	0.0	0.1
E	682 - 82	-0.1	0.0	0.1	0.0	0.0	0.1	0.1	0.0	-0.1	0.2
F	1925 - 1325	0.1	-0.1	0.0	0.0	0.0	0.1	0.1	0.0	-0.1	0.3
G	680 - 80	0.1	0.0	0.2	0.0	0.0	0.0	0.2	0.0	0.0	0.2
H	1921 - 1321	0.0	1.2	0.3	-0.1	0.0	0.0	1.2	0.3	0.0	1.3
I	676 - 76	0.0	0.0	0.2	0.0	0.0	0.0	0.2	0.0	0.0	0.2
J	1916 - 1316	0.0	1.3	0.7	-0.1	0.0	0.0	1.3	0.7	0.0	1.3
K	671 - 71	0.0	0.0	0.2	0.0	0.0	0.0	0.2	0.0	0.0	0.2
L	1908 - 1308	0.0	1.2	0.8	-0.1	0.0	0.0	1.2	0.8	0.0	1.3
M	663 - 63	0.0	0.0	0.2	0.0	0.0	0.0	0.2	0.0	0.0	0.2
N	1877 - 1277	0.0	1.3	0.6	-0.1	0.0	0.0	1.3	0.6	0.0	1.3
O	647 - 47	0.0	0.0	0.1	0.0	0.0	0.0	0.1	0.0	0.0	0.1
P	1840 - 1240	0.0	1.2	0.4	-0.1	0.0	0.0	1.2	0.4	0.0	1.2
Q	628 - 28	0.0	-0.2	0.1	0.0	0.0	0.0	0.1	0.0	-0.2	0.3
R	1816 - 1216	-1.0	-0.6	0.3	0.0	0.0	0.1	0.3	-0.6	-1.0	1.3
S	616 - 16	-0.3	-0.6	0.0	0.0	0.0	0.4	0.3	-0.6	-0.6	0.9
T	811 - 11	0.2	0.0	-0.1	0.0	0.0	0.1	0.3	0.0	-0.1	0.4
U	43058 - 43051	-0.2	-0.6	-1.7	0.0	0.0	0.0	-0.2	-0.6	-1.7	1.5
V	50024 - 50021	0.0	-0.1	-0.3	0.0	0.0	0.0	0.0	-0.1	-0.3	0.3
W	43278 - 43271	-0.1	-0.2	0.0	0.0	0.0	0.1	0.1	-0.2	-0.3	0.4
X	50084 - 50081	0.0	0.0	0.0	0.0	0.0	0.1	0.1	0.0	-0.1	0.2

<sup>1</sup> Refer to Figure 2.10.2-34 for the identification of the representative sections.

Table 2.10.4-24  $P_m + P_b$  Stresses; Heat Condition; 3-D Top Model; 0-Degree  
Circumferential Location; Condition 1

Condition 1: 100°F Ambient with Contents

Section <sup>1</sup>	Node - Node	Stress Components (ksi)							Principal Stresses (ksi)			
		$S_x$	$S_y$	$S_z$	$S_{xy}$	$S_{yz}$	$S_{zx}$		S1	S2	S3	S.I.
A I	1949 - 1951	-0.4	-0.4	0.0	0.0	0.0	-0.1	0.1	-0.4	-0.4	0.5	
B O	1952 - 93	0.4	0.4	-0.2	0.0	0.0	-0.1	0.4	0.4	-0.2	0.7	
C I	1925 - 1927	0.2	0.0	0.5	0.0	0.0	0.0	0.5	0.2	0.0	0.5	
D O	683 - 85	-0.1	0.2	0.1	0.0	0.0	0.0	0.2	0.1	-0.1	0.3	
E O	682 - 82	-0.1	0.0	0.1	0.0	0.0	0.1	0.1	0.0	-0.1	0.2	
F O	1925 - 1325	0.0	-0.4	-0.8	0.0	0.0	0.1	0.1	-0.4	-0.8	0.8	
G I	680 - 80	0.0	0.0	0.3	0.0	0.0	0.1	0.3	0.0	0.0	0.3	
H O	1921 - 1321	0.0	1.3	0.7	-0.1	0.0	0.0	1.3	0.7	0.0	1.4	
I O	676 - 76	0.0	0.0	0.3	0.0	0.0	0.0	0.3	0.0	0.0	0.3	
J O	1916 - 1316	0.0	1.3	0.7	-0.1	0.0	0.0	1.3	0.7	0.0	1.3	
K O	671 - 71	0.0	0.1	0.2	0.0	0.0	0.0	0.2	0.1	0.0	0.2	
L O	1908 - 1308	0.0	1.3	0.9	0.0	0.0	0.0	1.3	0.9	0.0	1.3	
M O	663 - 63	0.0	0.0	0.2	0.0	0.0	0.0	0.2	0.0	0.0	0.2	
N O	1877 - 1277	0.0	1.3	0.7	-0.1	0.0	0.0	1.3	0.7	0.0	1.3	
O I	647 - 47	0.0	0.1	0.1	0.0	0.0	0.0	0.1	0.1	0.0	0.1	
P O	1840 - 1240	0.0	1.4	0.8	-0.1	0.0	0.0	1.4	0.8	0.0	1.3	
Q O	628 - 28	0.0	-0.1	0.3	0.0	0.0	0.0	0.3	0.0	-0.1	0.5	
R I	1816 - 1216	0.1	0.2	1.9	0.0	0.0	0.2	1.9	0.2	0.1	1.9	
S I	616 - 16	-1.0	-0.6	0.8	0.0	0.0	0.3	0.8	-0.6	-1.1	1.9	
T I	811 - 11	0.5	0.0	-0.4	0.0	0.0	0.2	0.6	0.0	-0.5	1.0	
U I	43058 - 43051	-0.4	-1.1	-2.3	0.1	0.0	0.6	-0.2	-1.1	-2.4	2.2	
V I	50024 - 50021	0.5	-0.3	-1.0	0.1	0.0	-0.1	0.5	-0.3	-1.0	1.5	
W I	43278 - 43271	-0.8	-0.8	0.2	0.0	0.0	0.2	0.3	-0.8	-0.8	1.1	
X O	50084 - 50081	0.3	0.3	-0.2	0.0	0.0	0.1	0.4	0.3	-0.2	0.5	

<sup>1</sup> Refer to Figure 2.10.2-34 for the identification of the representative section.

Table 2.10.4-25  $S_n$  Stresses; Heat Condition; 3-D Top Model; 0-Degree Circumferential Location; Condition 1

Condition 1: 100°F Ambient with Contents

Section <sup>1</sup>	Node - Node	Stress Components (ksi)							Principal Stresses (ksi)			
		$S_x$	$S_y$	$S_z$	$S_{xy}$	$S_{yz}$	$S_{xz}$		S1	S2	S3	S.I.
A I	1949 - 1951	-0.6	-0.5	0.8	0.0	-0.2	0.7		1.1	-0.5	-0.9	2.0
B O	1952 - 93	0.6	0.5	-1.8	0.0	-0.2	0.7		0.8	0.5	-2.0	2.8
C I	1925 - 1927	0.5	-0.1	-0.7	0.0	-0.1	-0.9		1.0	-0.1	-1.2	2.1
D O	683 - 85	-1.5	1.7	3.4	-0.1	0.1	0.6		3.5	1.7	-1.6	5.1
E I	682 - 82	-1.5	-0.4	2.4	-0.1	0.1	0.6		2.5	-0.4	-1.6	4.1
F O	1925 - 1325	0.6	-0.8	-1.5	0.1	0.0	-0.7		0.8	-0.8	-1.7	2.5
G O	680 - 80	-2.6	1.2	7.1	-0.2	0.1	1.3		7.2	1.2	-2.7	10.0
H O	1921 - 1321	-0.1	1.0	-0.4	-0.1	0.0	0.1		1.0	-0.1	-0.4	1.4
I O	676 - 76	-0.1	3.2	6.5	-0.2	-0.1	0.1		6.5	3.2	-0.2	6.6
J O	1916 - 1316	-0.1	2.5	2.2	-0.2	0.0	0.0		2.5	2.2	-0.1	2.6
K O	671 - 71	-0.1	6.1	8.2	-0.5	0.0	0.0		8.2	6.2	-0.2	8.4
L O	1908 - 1308	0.6	2.8	1.8	0.0	0.0	0.0		2.8	1.8	0.6	2.2
M O	663 - 63	0.7	7.7	8.0	-0.5	0.0	0.0		8.0	7.7	0.7	7.4
N O	1877 - 1277	0.0	2.5	1.8	-0.2	0.1	0.0		2.5	1.8	0.0	2.5
O O	647 - 47	-0.1	6.5	7.9	-0.5	0.0	0.0		7.9	6.5	-0.1	8.0
P O	1840 - 1240	0.0	2.8	1.5	-0.2	0.1	0.1		2.8	1.5	0.0	2.8
Q O	628 - 28	0.0	4.9	7.7	-0.4	0.0	0.1		7.7	4.9	0.0	7.7
R I	1816 - 1216	-0.1	-8.1	-1.8	0.6	0.1	1.2		0.5	-2.4	-8.1	8.6
S O	616 - 16	-0.8	5.8	8.0	-0.6	0.2	0.3		8.0	5.9	-0.9	8.9
T O	811 - 11	0.3	5.7	4.1	-0.4	0.0	0.0		5.8	4.1	0.2	5.6
U I	43058 - 43051	-1.0	-3.5	-8.0	0.2	0.0	1.6		-0.6	-3.5	-8.4	7.7
V I	50024 - 50021	1.4	0.2	-0.5	0.2	-0.1	0.3		1.5	0.2	-0.5	2.0
W O	43278 - 43271	-3.0	-2.9	0.2	0.0	0.1	-0.4		0.3	-2.9	-3.0	3.3
X I	50084 - 50081	1.6	1.7	-0.3	0.0	0.1	-0.3		1.7	1.6	-0.3	2.0

<sup>1</sup> Refer to Figure 2.10.2-34 for the identification of the representative sections.

Table 2.10.4-26 Critical P<sub>m</sub> Stress Summary; Heat Condition; 3-D Top Model; Condition 1

**Condition 1: 100°F Ambient with Contents**

Comp. No. <sup>1</sup>	Section Cut Node-Node	P <sub>m</sub> Stresses (ksi)						Principal Stresses (ksi)				Allow. Stress	Margin of Safety
		S <sub>x</sub>	S <sub>y</sub>	S <sub>z</sub>	S <sub>w</sub>	S <sub>xx</sub>	S <sub>yy</sub>	S1	S2	S3			
1	1952- 93	0.2	0.2	-0.1	0.0	0.0	-0.1	0.2	0.2	-0.1	0.3	19.2	63.0
2	18679-18079	0.0	0.0	0.0	1.9	0.2	0.0	2.0	0.0	-1.9	3.9	18.5	3.7
3	1920- 1320	0.0	1.4	0.4	-0.1	0.0	0.0	1.4	0.4	0.0	1.4	31.4	21.4
4	1918- 1318	0.0	1.3	0.6	-0.1	0.0	0.0	1.3	0.6	0.0	1.3	19.6	14.1
5	625- 25	0.0	-0.4	0.1	0.0	0.0	0.0	0.1	0.0	-0.4	0.5	20.0	39.0
6	29216-29211	0.1	1.3	3.7	0.0	0.0	0.1	3.7	1.3	0.1	3.6	20.0	4.5
7	43021-43028	0.2	-2.5	-9.0	0.2	0.0	-0.1	-0.2	-2.5	-9.0	8.9	20.0	1.2
8	50916-50919	0.0	0.0	-0.1	0.0	0.0	0.2	0.2	0.0	-0.2	0.4	45.0	105.2

Locations of the most critical sections for each component are provided in the following:

Comp. No. <sup>1</sup>	Section Location					
	Inside Node			Outside Node		
	x (in)	y (deg)	z (in)	x (in)	y (deg)	z (in)
1	0.00	0.0	6.20	0.00	0.0	0.75
2	40.70	91.7	17.40	43.35	91.7	17.40
3	35.50	0.0	35.40	37.00	0.0	35.40
4	35.50	0.0	47.40	37.00	0.0	47.40
5	40.70	0.0	163.40	43.35	0.0	163.40
6	37.50	163.4	175.40	37.66	163.4	179.40
7	37.66	0.0	185.40	37.66	0.0	179.40
8	36.46	91.7	193.71	36.46	91.7	188.40

<sup>1</sup> Refer to Figure 2.10.2-33 for cask component identification.

Table 2.10.4-27 Critical  $P_m + P_b$  Stress Summary; Heat Condition; 3-D Top Model; Condition 1

Condition 1: 100°F Ambient with Contents

Comp. No. <sup>1</sup>	Section Cut Node-Node	$P_m + P_b$ Stresses (ksi)							Principal Stresses (ksi)			Allow. S.I. Stress	Margin of Safety
		$S_x$	$S_y$	$S_z$	$S_{xy}$	$S_{yz}$	$S_{zx}$	$S_{\theta}$	S1	S2	S3		
1	1952- 93	0.4	0.4	-0.2	0.0	0.0	-0.1	0.4	0.4	-0.2	0.7	28.7	40.0
2	18679-18079	0.1	0.1	0.0	2.1	0.4	0.0	2.2	0.0	-2.0	4.2	27.7	5.6
3	1920- 1320	0.0	1.4	0.6	-0.1	0.0	0.0	1.4	0.6	0.0	1.5	47.1	30.4
4	1911- 1311	0.0	1.3	0.9	-0.1	0.0	0.0	1.3	0.9	0.0	1.4	29.4	20.0
5	625- 25	0.0	-0.3	0.2	0.0	0.0	0.0	0.2	0.0	-0.3	0.5	30.0	59.0
6	29216-29211	1.8	3.7	10.3	0.0	0.0	0.1	10.6	3.7	1.8	8.8	30.0	2.4
7	43021-43028	-0.9	-3.4	-10.6	0.2	0.0	0.7	-0.9	-3.4	-10.6	9.8	30.0	2.1
8	50921-50924	1.0	0.1	-0.6	0.0	0.0	0.0	1.0	0.1	-0.6	1.6	67.3	41.2

Locations of the most critical sections for each component are provided in the following:

Comp. No. <sup>1</sup>	Section Location					
	Inside Node			Outside Node		
	x (in)	y (deg)	z (in)	x (in)	y (deg)	z (in)
1	0.00	0.0	6.20	0.00	0.0	0.75
2	40.70	91.7	17.40	43.35	91.7	17.40
3	35.50	0.0	35.40	37.00	0.0	35.40
4	35.50	0.0	83.69	37.00	0.0	83.69
5	40.70	0.0	163.40	43.35	0.0	163.40
6	37.50	163.4	175.40	37.66	163.4	179.40
7	37.66	0.0	185.40	37.66	0.0	179.40
8	35.21	91.7	193.71	35.21	91.7	188.40

<sup>1</sup> Refer to Figure 2.10.2-33 for cask component identification.

Table 2.10.4-28 Critical  $S_n$  Stress Summary; Heat Condition; 3-D Top Model; Condition 1  
Condition I: 100°F Ambient with Contents

Comp. No. <sup>1</sup>	Section Cut Node-Node	$S_n$ Stresses (ksi)						Principal Stresses (ksi)				Allow. Stress 3.0 $S_m$
		$S_x$	$S_y$	$S_z$	$S_{xy}$	$S_{xz}$	$S_{yz}$	S1	S2	S3	S.I.	
1	16683-16085	-1.5	1.4	3.5	0.0	0.0	0.6	3.5	1.4	-1.6	5.1	57.6
2	18680-18080	-2.6	1.3	7.3	-0.3	1.4	1.3	7.7	1.1	-2.8	10.6	55.5
3	1821- 1221	-0.1	-4.6	1.0	0.3	0.0	-0.4	1.2	-0.2	-4.6	5.7	94.2
4	1881- 1281	0.0	2.8	1.7	-0.2	0.1	0.0	2.8	1.7	0.0	2.8	58.8
5	669- 69	-0.1	6.9	8.3	-0.5	0.0	0.0	8.3	6.9	-0.2	8.4	60.0
6	10618-10018	-2.2	5.6	16.6	0.0	0.2	-1.4	16.7	5.6	-2.3	19.0	60.0
7	64571-64531	6.2	24.7	1.0	-0.1	0.0	-1.8	24.7	6.7	0.4	24.3	60.0
8	50036-50039	0.0	-0.7	-2.5	0.1	-0.5	-0.3	0.0	-0.6	-2.6	2.6	135.0

Locations of the most critical sections for each component are provided in the following:

Comp. No. <sup>1</sup>	Section Location					
	Inside Node			Outside Node		
	x (in)	y (deg)	z (in)	x (in)	y (deg)	z (in)
1	39.44	0.0	6.20	39.44	0.0	0.75
2	40.70	91.7	14.40	43.35	91.7	14.40
3	35.50	0.0	171.65	37.50	0.0	171.65
4	35.50	0.0	133.30	37.00	0.0	133.30
5	40.70	0.0	67.80	43.35	0.0	67.80
6	40.70	45.9	172.40	43.35	45.9	172.40
7	33.71	45.9	187.40	36.46	45.9	187.40
8	29.54	0.0	193.71	29.54	0.0	193.71

<sup>1</sup> Refer to Figure 2.10.2-33 for cask component identification.

Table 2.10.4-29 Primary Stresses; Cold Condition; 3-D Top Model; 0-Degree  
Circumferential Location; Condition 4

Condition 4: -40°F Ambient, No Decay Heat

Stress Points Section <sup>1</sup> Node	Stress Components (ksi)						Principal Stresses (ksi)		
	S <sub>x</sub>	S <sub>y</sub>	S <sub>z</sub>	S <sub>xy</sub>	S <sub>yz</sub>	S <sub>xz</sub>	S1	S2	S3
A1	1949	-0.1	-0.1	0.0	0.0	0.0	0.0	-0.1	-0.1
A2	1950	-0.1	0.0	0.0	0.0	0.0	0.0	0.0	-0.1
A3	1951	0.0	0.0	0.0	0.0	0.0	0.0	0.0	0.0
B1	1952	0.0	0.0	0.0	0.0	0.0	0.0	0.0	0.0
B2	93	0.1	0.1	-0.1	0.0	0.0	0.1	0.1	-0.1
C1	1925	0.0	0.0	0.3	0.0	0.0	0.3	0.0	0.0
C2	1926	0.0	0.0	0.1	0.0	0.0	0.1	0.0	0.0
C3	1927	0.0	0.0	0.0	0.0	0.0	0.0	0.0	0.0
D1	683	0.0	0.0	0.0	0.0	0.0	0.0	0.0	0.0
D2	85	0.0	0.1	0.0	0.0	0.0	0.1	0.0	0.0
E1	682	0.0	0.0	0.0	0.0	0.0	0.0	0.0	0.0
E2	82	0.0	0.0	0.1	0.0	0.0	0.1	0.0	0.0
F1	1925	0.0	0.0	0.3	0.0	0.0	0.3	0.0	0.0
F2	1325	0.0	-0.2	-0.4	0.0	0.0	0.0	-0.2	-0.4
G1	680	0.0	0.0	0.2	0.0	0.0	0.2	0.0	0.0
G2	80	0.0	0.0	0.1	0.0	0.0	0.1	0.0	0.0
H1	1921	0.0	0.4	-0.1	0.0	0.0	0.4	0.0	-0.1
H2	1321	0.0	0.5	0.2	0.0	0.0	0.5	0.2	0.0
I1	676	0.0	0.0	0.1	0.0	0.0	0.1	0.0	0.0
I2	76	0.0	0.0	0.2	0.0	0.0	0.2	0.0	0.0
J1	1916	0.0	0.4	0.3	0.0	0.0	0.4	0.3	0.0
J2	1316	0.0	0.5	0.4	0.0	0.0	0.5	0.4	0.0
K1	671	0.0	0.0	0.1	0.0	0.0	0.1	0.0	0.0
K2	71	0.0	0.1	0.2	0.0	0.0	0.2	0.1	0.0
L1	1908	0.0	0.3	0.5	0.0	0.0	0.5	0.3	0.0
L2	1308	0.0	0.6	0.6	0.0	0.0	0.6	0.6	0.0
M1	663	0.0	0.0	0.1	0.0	0.0	0.1	0.0	0.0
M2	63	0.0	0.0	0.1	0.0	0.0	0.1	0.0	0.0
N1	1877	0.0	0.4	0.3	0.0	0.0	0.4	0.3	0.0



Table 2.10.4-29 Primary Stresses; Cold Condition; 3-D Top Model; 0-Degree  
Circumferential Location; Condition 4 (continued)

Stress Points		Stress Components (ksi)						Principal Stresses (ksi)		
Section <sup>1</sup>	Node	S <sub>x</sub>	S <sub>y</sub>	S <sub>z</sub>	S <sub>xy</sub>	S <sub>yz</sub>	S <sub>xz</sub>	S1	S2	S3
N2	1477	0.0	0.5	0.3	0.0	0.0	0.0	0.5	0.3	0.0
N3	1277	0.0	0.5	0.4	0.0	0.0	0.0	0.5	0.4	0.0
O1	647	0.0	0.0	0.0	0.0	0.0	0.0	0.0	0.0	0.0
O2	247	0.0	0.0	0.0	0.0	0.0	0.0	0.0	0.0	0.0
O3	47	0.0	0.0	0.0	0.0	0.0	0.0	0.0	0.0	0.0
P1	1840	0.0	0.4	-0.1	0.0	0.0	0.0	0.4	0.0	-0.2
P2	1640	0.0	0.4	0.0	0.0	0.0	0.0	0.4	0.0	0.0
P3	1440	0.0	0.4	0.1	0.0	0.0	0.0	0.5	0.1	0.0
P4	1240	0.0	0.5	0.3	0.0	0.0	0.0	0.5	0.3	0.0
Q1	628	0.0	-0.3	-0.2	0.0	0.0	0.0	0.0	-0.2	-0.3
Q2	428	0.0	-0.2	-0.1	0.0	0.0	0.0	0.0	-0.1	-0.2
Q3	228	0.0	-0.2	0.1	0.0	0.0	0.0	0.1	0.0	-0.2
Q4	28	0.0	-0.1	0.2	0.0	0.0	0.0	0.2	0.0	-0.1
R1	1816	-0.2	-0.1	1.1	0.0	0.0	0.1	1.1	-0.1	-0.2
R2	1616	-0.3	-0.4	0.2	0.0	0.0	0.2	0.2	-0.4	-0.4
R3	1416	-0.9	-0.7	-0.3	0.0	0.0	0.1	-0.3	-0.7	-1.0
R4	1216	-1.9	-1.1	-0.7	0.0	0.0	-0.1	-0.7	-1.1	-1.9
S1	616	-1.2	-0.7	0.4	0.0	0.0	0.2	0.4	-0.7	-1.2
S2	416	-0.6	-0.6	0.4	0.0	0.0	0.4	0.5	-0.6	-0.8
S3	216	0.0	-0.6	-0.3	0.0	0.0	0.5	0.3	-0.6	-0.7
S4	16	0.3	-0.6	-0.7	0.0	0.0	0.3	0.4	-0.6	-0.8
T1	811	0.5	0.1	0.2	0.0	0.0	0.4	0.8	0.1	-0.1
T2	611	0.6	-0.1	-0.6	0.0	0.0	0.2	0.6	-0.1	-0.6
T3	411	0.2	-0.1	-0.2	0.0	0.0	0.2	0.3	-0.1	-0.3
T4	211	0.1	0.0	0.1	0.0	0.0	0.1	0.2	0.0	0.0
T5	11	0.0	0.0	0.4	0.0	0.0	0.1	0.4	0.0	0.0
U1	43058	0.2	-0.7	-2.1	0.0	0.0	0.3	0.2	-0.7	-2.1
U2	43057	-0.6	-0.9	-2.1	0.0	0.0	0.5	-0.5	-0.9	-2.2
U3	43056	-0.7	-1.0	-2.3	0.0	0.0	0.7	-0.5	-1.0	-2.5
U4	43055	-0.4	-0.9	-2.6	0.0	0.0	0.4	-0.3	-0.9	-2.6
U5	43054	-0.2	-0.8	-2.6	0.1	0.0	0.0	-0.2	-0.8	-2.6

Table 2.10.4-29 Primary Stresses; Cold Condition; 3-D Top Model; 0-Degree Circumferential Location; Condition 4 (continued)

Stress Points		Stress Components (ksi)						Principal Stresses (ksi)		
Section <sup>1</sup>	Node	S <sub>x</sub>	S <sub>y</sub>	S <sub>z</sub>	S <sub>xy</sub>	S <sub>yz</sub>	S <sub>xz</sub>	S1	S2	S3
U6	43053	-0.3	-0.7	-2.2	0.0	0.0	-0.4	-0.2	-0.7	-2.3
U7	43052	-0.6	-0.5	-1.5	0.0	0.0	-0.4	-0.4	-0.5	-1.7
U8	43051	1.0	0.3	-0.6	0.0	0.0	-0.3	1.0	0.3	-0.6
V1	50024	0.4	-0.1	-0.7	0.0	0.0	-0.1	0.4	-0.1	-0.7
V2	50023	0.2	-0.2	-0.9	0.0	0.0	0.0	0.2	-0.2	-0.9
V3	50022	-0.1	-0.1	-0.2	0.0	0.0	0.0	-0.1	-0.1	-0.2
V4	50021	-0.7	0.0	0.6	0.0	0.0	0.0	0.6	0.0	-0.7
W1	43278	-0.2	-0.3	0.1	0.0	0.0	0.1	0.1	-0.2	-0.3
W2	43274	0.0	-0.1	0.0	0.0	0.0	0.1	0.1	0.0	-0.1
W3	43271	0.2	0.1	0.0	0.0	0.0	0.0	0.2	0.1	-0.1
X1	50084	-0.1	-0.1	0.0	0.0	0.0	0.0	0.0	-0.1	-0.1
X2	50083	0.0	0.0	0.0	0.0	0.0	0.0	0.0	0.0	-0.1
X3	50081	0.1	0.1	-0.1	0.0	0.0	0.0	0.1	0.1	-0.1

<sup>1</sup> Refer to Figure 2.10.2-34 for the identification of the representative sections.

Table 2.10.4-30 Primary + Secondary Stresses; Cold Condition; 3-D Top Model; 0-Degree Circumferential Location; Condition 4

Condition 4: -40°F Ambient, No Decay Heat

Stress Points		Stress Components (ksi)						Principal Stresses (ksi)		
Section <sup>1</sup>	Node	S <sub>x</sub>	S <sub>y</sub>	S <sub>z</sub>	S <sub>xy</sub>	S <sub>yz</sub>	S <sub>xz</sub>	S1	S2	S3
A1	1949	0.1	0.1	0.0	0.0	0.0	0.1	0.1	0.1	-0.1
A2	1950	-0.1	-0.1	0.0	0.0	0.0	0.1	0.0	-0.1	-0.1
A3	1951	0.9	0.9	0.1	0.0	0.0	0.0	0.9	0.9	0.1
B1	1952	0.8	0.8	0.2	0.0	0.0	0.0	0.8	0.8	0.2
B2	93	-0.2	-0.2	-0.2	0.0	0.0	-0.1	-0.1	-0.2	-0.3
C1	1925	-1.1	-1.1	1.0	0.0	0.0	0.3	1.1	-1.1	-1.2
C2	1926	-1.3	-0.7	0.9	0.0	0.1	0.5	1.0	-0.7	-1.4
C3	1927	2.3	2.2	1.4	0.0	0.0	0.3	2.4	2.2	1.3
D1	683	-0.1	-0.6	-5.3	0.1	0.0	-0.4	0.0	-0.7	-5.3
D2	85	0.8	-2.3	-4.5	0.2	0.0	-0.7	0.9	-2.3	-4.6
E1	682	0.0	-0.5	-5.0	0.1	0.0	0.2	0.1	-0.5	-5.0
E2	82	-0.5	1.8	5.2	-0.2	0.0	-0.3	5.2	1.8	-0.5
F1	1925	-1.1	-1.1	1.0	0.0	0.0	0.3	1.1	-1.1	-1.2
F2	1325	0.2	-1.4	-1.7	0.1	0.0	0.4	0.2	-1.4	-1.7
G1	680	0.6	0.0	2.2	0.0	0.0	0.3	2.3	0.5	0.0
G2	80	0.4	-1.2	-2.4	0.1	0.0	-0.1	0.5	-1.2	-2.4
H1	1921	0.0	-3.0	-0.1	0.2	0.0	0.0	0.0	-0.1	-3.0
H2	1321	0.0	-2.8	-0.1	0.2	0.0	0.0	0.0	-0.1	-2.8
I1	676	0.0	-0.4	-0.1	0.0	0.0	0.0	0.0	-0.1	-0.4
I2	76	0.0	-0.2	0.6	0.0	0.0	0.0	0.6	0.0	-0.2
J1	1916	-0.1	-3.5	0.1	0.2	0.0	0.0	0.1	-0.1	-3.5
J2	1316	-0.1	-3.1	0.3	0.2	0.0	0.0	0.3	-0.1	-3.2
K1	671	0.0	0.1	0.2	0.0	0.0	0.0	0.2	0.1	0.0
K2	71	0.0	-0.1	0.2	0.0	0.0	0.0	0.2	0.0	-0.1
L1	1908	-0.1	-3.5	0.4	0.2	0.0	0.0	0.4	-0.1	-3.5
L2	1308	-0.1	-3.2	0.5	0.3	0.0	0.0	0.5	-0.1	-3.2
M1	663	0.1	0.5	0.2	0.0	0.0	0.0	0.5	0.2	0.1
M2	63	0.0	-0.4	-0.1	-0.2	0.0	0.0	0.0	-0.1	-0.5
N1	1877	-0.1	-3.2	0.3	0.2	0.0	0.0	0.3	-0.1	-3.2

Table 2.10.4-30 Primary + Secondary Stresses; Cold Condition; 3-D Top Model; 0-Degree Circumferential Location; Condition 4 (continued)

Stress Points		Stress Components (ksi)						Principal Stresses (ksi)		
Section <sup>1</sup>	Node	S <sub>x</sub>	S <sub>y</sub>	S <sub>z</sub>	S <sub>xy</sub>	S <sub>xz</sub>	S <sub>yz</sub>	S1	S2	S3
N2	1477	-0.3	-3.4	0.4	0.2	0.0	0.0	0.4	-0.3	-3.4
N3	1277	-0.4	-3.6	0.4	0.2	0.0	0.0	0.4	-0.4	-3.6
O1	647	0.0	1.1	-0.1	-0.1	0.1	0.0	1.1	0.0	-0.1
O2	247	0.0	0.1	-0.4	0.0	0.1	0.0	0.2	0.0	-0.4
O3	47	0.0	-0.8	-0.6	0.1	0.0	0.0	0.0	-0.6	-0.8
P1	1840	0.0	-2.2	0.0	0.2	0.1	0.0	0.0	-0.1	-2.2
P2	1640	0.0	-2.6	0.1	0.2	0.1	0.0	0.1	0.0	-2.6
P3	1440	0.0	-3.0	0.1	0.2	0.1	0.0	0.2	0.0	-3.0
P4	1240	0.0	-3.3	0.3	0.2	0.0	0.0	0.3	0.0	-3.3
Q1	628	0.0	0.2	-1.2	0.0	0.1	0.0	0.2	0.0	-1.2
Q2	428	0.0	-0.4	-1.0	0.0	0.1	0.0	0.0	-0.4	-1.0
Q3	228	0.0	-1.0	-0.8	0.1	0.1	0.0	0.0	-0.8	-1.0
Q4	28	0.0	-1.6	-0.7	0.1	0.1	0.0	0.0	-0.7	-1.6
R1	1816	-0.2	2.2	1.8	-0.2	0.0	0.5	2.2	1.9	-0.3
R2	1616	-0.4	1.2	0.2	-0.1	0.1	0.7	1.2	0.6	-0.9
R3	1416	-1.2	0.2	-0.7	-0.1	0.1	0.7	0.3	-0.3	-1.7
R4	1216	-2.9	-0.9	-1.5	0.0	0.1	0.3	-0.8	-1.4	-2.9
S1	616	-2.3	-1.0	3.4	0.1	-0.2	0.1	3.4	-1.0	-2.3
S2	416	-0.9	-1.8	1.0	0.1	0.0	1.0	1.4	-1.3	-1.8
S3	216	0.2	-3.0	-2.9	0.2	0.1	1.3	0.7	-3.0	-3.3
S4	16	1.1	-3.9	-5.9	0.4	0.1	0.9	1.3	-4.0	-6.1
T1	811	3.5	3.2	3.3	-0.2	-0.1	1.1	4.6	3.1	2.2
T2	611	0.6	1.2	0.8	-0.1	-0.1	0.5	1.3	1.0	0.2
T3	411	0.5	0.2	-0.8	0.0	0.0	0.1	0.5	0.2	-0.8
T4	211	0.2	-0.7	-2.2	0.1	0.0	0.0	0.2	-0.7	-2.2
T5	11	0.1	-1.5	-3.9	0.1	0.1	0.0	0.1	-1.5	-3.9
U1	43058	-4.1	-3.5	-5.2	0.2	0.0	0.8	-3.4	-3.8	-5.6
U2	43057	-2.5	-2.8	-4.6	0.2	0.0	1.0	-2.0	-2.8	-5.1
U3	43056	-1.7	-2.2	-4.0	0.2	0.0	1.2	-1.2	-2.2	-4.5
U4	43055	-0.8	-1.7	-3.8	0.2	0.0	0.8	-0.6	-1.8	-4.0
U5	43054	-0.2	-1.3	-3.5	0.2	-0.1	0.3	-0.1	-1.3	-3.6

Table 2.10.4-30 Primary + Secondary Stresses; Cold Condition; 3-D Top Model; 0-Degree Circumferential Location; Condition 4 (continued)

Stress Points Section <sup>1</sup> Node	Stress Components (ksi)						Principal Stresses (ksi)		
	S <sub>t</sub>	S <sub>r</sub>	S <sub>z</sub>	S <sub>xy</sub>	S <sub>xz</sub>	S <sub>yz</sub>	S1	S2	S3
U6 43053	-0.1	-0.9	-2.6	0.1	-0.1	-0.2	-0.1	-0.9	-2.7
U7 43052	0.4	-0.7	-3.1	0.1	-0.1	-0.4	0.5	-0.7	-3.1
U8 43051	1.3	0.4	-1.1	0.0	-0.1	-0.8	1.5	0.4	-1.4
V1 50024	-3.1	-2.5	-0.1	0.0	0.0	0.3	-0.1	-2.5	-3.2
V2 50023	-2.2	-1.8	-0.6	0.0	0.0	0.4	-0.6	-1.8	-2.3
V3 50022	-0.4	-0.6	-0.3	0.0	0.0	0.3	0.0	-0.6	-0.7
V4 50021	0.9	0.6	0.5	0.0	0.0	0.2	1.0	0.6	0.4
W1 43278	-1.0	-1.0	0.2	0.0	0.0	0.1	0.2	-1.0	-1.0
W2 43274	-0.5	-0.6	0.0	0.0	0.0	0.1	0.0	-0.5	-0.6
W3 43271	1.2	1.0	-0.1	0.0	0.0	0.1	1.2	1.0	-0.1
X1 50084	-1.6	-1.7	0.2	0.0	0.0	0.2	0.2	-1.6	-1.7
X2 50083	-1.1	-1.3	0.1	0.0	0.0	0.2	0.1	-1.1	-1.3
X3 50081	-0.1	-0.6	-0.4	0.0	0.0	0.2	0.0	-0.5	-0.6

<sup>1</sup> Refer to Figure 2.10.2-34 for the identification of the representative sections.

Table 2.10.4-31  $P_m$  Stresses; Cold Condition; 3-D Top Model; 0-Degree Circumferential Location; Condition 4

Condition 4: -40°F Ambient, No Decay Heat

Section <sup>1</sup>	Node - Node	Stress Components (ksi)						Principal Stresses (ksi)			
		$S_x$	$S_y$	$S_z$	$S_{xy}$	$S_{yz}$	$S_{xz}$	S1	S2	S3	S.L.
A	1949 - 1951	0.0	0.0	0.0	0.0	0.0	0.0	0.0	0.0	0.0	0.0
B	1952 - 93	0.0	0.0	0.0	0.0	0.0	0.0	0.0	0.0	0.0	0.1
C	1925 - 1927	0.0	0.0	0.1	0.0	0.0	0.0	0.1	0.0	0.0	0.1
D	683 - 85	0.0	0.1	0.0	0.0	0.0	0.0	0.1	0.0	0.0	0.1
E	682 - 82	0.0	0.0	0.0	0.0	0.0	0.0	0.0	0.0	0.0	0.1
F	1925 - 1325	0.0	-0.1	-0.1	0.0	0.0	0.0	0.0	-0.1	-0.1	0.1
G	680 - 80	0.0	0.0	0.1	0.0	0.0	0.0	0.1	0.0	0.0	0.1
H	1921 - 1321	0.0	0.4	0.1	0.0	0.0	0.0	0.4	0.1	0.0	0.4
I	676 - 76	0.0	0.0	0.2	0.0	0.0	0.0	0.2	0.0	0.0	0.2
J	1916 - 1316	0.0	0.4	0.4	0.0	0.0	0.0	0.5	0.4	0.0	0.5
K	671 - 71	0.0	0.0	0.1	0.0	0.0	0.0	0.1	0.0	0.0	0.1
L	1908 - 1308	0.0	0.4	0.5	0.0	0.0	0.0	0.5	0.4	0.0	0.6
M	663 - 63	0.0	0.0	0.1	0.0	0.0	0.0	0.1	0.0	0.0	0.1
N	1877 - 1277	0.0	0.5	0.3	0.0	0.0	0.0	0.5	0.3	0.0	0.5
O	647 - 47	0.0	0.0	0.0	0.0	0.0	0.0	0.0	0.0	0.0	0.0
P	1840 - 1240	0.0	0.4	0.1	0.0	0.0	0.0	0.4	0.1	0.0	0.4
Q	628 - 28	0.0	-0.2	0.0	0.0	0.0	0.0	0.0	0.0	-0.2	0.2
R	1816 - 1216	-0.8	-0.6	0.0	0.0	0.0	0.1	0.0	-0.6	-0.8	0.8
S	616 - 16	-0.4	-0.6	0.0	0.0	0.0	0.4	0.2	-0.6	-0.6	0.9
T	811 - 11	0.3	0.0	-0.1	0.0	0.0	0.2	0.4	0.0	-0.2	0.5
U	43058 - 43051	-0.3	-0.6	-1.9	0.0	0.0	0.0	-0.3	-0.6	-1.9	1.7
V	50024 - 50021	0.0	-0.1	-0.4	0.0	0.0	0.0	0.0	-0.1	-0.4	0.4
W	43278 - 43271	0.0	-0.1	0.0	0.0	0.0	0.1	0.1	-0.1	-0.1	0.2
X	50084 - 50081	0.0	0.0	0.0	0.0	0.0	0.0	0.0	0.0	0.0	0.1

<sup>1</sup> Refer to Figure 2.10.2-34 for the identification of the representative sections.

Table 2.10.4-32  $P_m + P_b$  Stresses; Cold Condition; 3-D Top Model; 0-Degree Circumferential Location; Condition 4

Condition 4: -40°F Ambient, No Decay Heat

Section <sup>1</sup>	Node - Node	Stress Components (ksi)						Principal Stresses (ksi)			
		$S_x$	$S_y$	$S_z$	$S_{xy}$	$S_{yz}$	$S_{xz}$	S1	S2	S3	S.L.
A I	1949 - 1951	-0.1	0.1	0.0	0.0	0.0	0.0	0.0	-0.1	-0.1	0.1
B O	1952 - 93	0.1	0.1	-0.1	0.0	0.0	0.0	0.1	0.1	-0.1	0.2
C I	1925 - 1927	0.0	0.0	0.2	0.0	0.0	0.0	0.2	0.0	0.0	0.2
D O	683 - 85	0.0	0.1	0.0	0.0	0.0	0.0	0.1	0.0	0.0	0.1
E O	682 - 82	0.0	0.0	0.1	0.0	0.0	0.0	0.1	0.0	0.0	0.1
F O	1925 - 1325	0.0	-0.2	-0.4	0.0	0.0	0.0	0.0	-0.2	-0.4	0.4
G I	680 - 80	0.0	0.0	0.2	0.0	0.0	0.0	0.2	0.0	0.0	0.2
H O	1921 - 1321	0.0	0.5	0.2	0.0	0.0	0.0	0.5	0.2	0.0	0.5
I O	676 - 76	0.0	0.0	0.2	0.0	0.0	0.0	0.2	0.0	0.0	0.2
J O	1916 - 1316	0.0	0.5	0.4	0.0	0.0	0.0	0.5	0.4	0.0	0.5
K O	671 - 71	0.0	0.1	0.2	0.0	0.0	0.0	0.2	0.1	0.0	0.2
L O	1908 - 1308	0.0	0.6	0.6	0.0	0.0	0.0	0.6	0.6	0.0	0.6
M O	663 - 63	0.0	0.0	0.1	0.0	0.0	0.0	0.1	0.0	0.0	0.1
N O	1877 - 1277	0.0	0.5	0.4	0.0	0.0	0.0	0.5	0.4	0.0	0.5
O I	647 - 47	0.0	0.0	0.0	0.0	0.0	0.0	0.0	0.0	0.0	0.0
P I	1840 - 1240	0.0	0.4	-0.2	0.0	0.0	0.0	0.4	0.0	-0.2	0.5
Q O	628 - 28	0.0	-0.1	0.2	0.0	0.0	0.0	0.2	0.0	-0.1	0.4
R I	1816 - 1216	0.1	-0.1	0.9	0.0	0.0	0.2	0.9	0.1	-0.1	1.0
S I	616 - 16	-1.1	-0.6	0.6	0.0	0.0	0.3	0.7	-0.6	-1.2	1.9
T I	811 - 11	0.7	0.0	-0.4	0.0	0.0	0.3	0.8	0.0	-0.5	1.3
U I	43058 - 43051	-0.6	-1.1	-2.7	0.0	0.0	0.7	-0.4	-1.2	-2.9	2.4
V I	50024 - 50021	0.5	-0.2	-1.1	0.1	0.0	-0.1	0.5	-0.2	-1.1	1.5
W I	43278 - 43271	-0.2	-0.3	0.1	0.0	0.0	0.1	0.1	-0.2	-0.3	0.4
X O	50084 - 50081	0.1	0.1	-0.1	0.0	0.0	0.0	0.1	0.1	-0.1	0.2

<sup>1</sup> Refer to Figure 2.10.2-34 for the identification of the representative sections.

Table 2.10.4-33  $S_n$  Stresses; Cold Condition; 3-D Top Model; 0-Degree Circumferential Location; Condition 4

Condition 4: -40°F Ambient, No Decay Heat

Section <sup>1</sup>	Node - Node	Stress Components (ksi)						Principal Stresses (ksi)			
		$S_x$	$S_y$	$S_z$	$S_{xy}$	$S_{yz}$	$S_{zx}$	S1	S2	S3	S.L
A O	1949 - 1951	0.8	0.8	0.1	0.0	0.0	0.0	0.8	0.8	0.1	0.8
B I	1952 - 93	0.8	0.8	0.2	0.0	0.0	0.0	0.8	0.8	0.2	0.6
C I	1925 - 1927	-1.9	-1.4	0.9	0.0	0.1	0.5	0.9	-1.4	-2.0	2.9
D O	683 - 85	0.8	-2.3	-4.5	0.2	0.0	-0.7	0.9	-2.3	-4.6	5.5
E O	682 - 82	-0.5	1.8	5.2	-0.2	0.0	-0.3	5.2	1.8	-0.5	5.8
F I	1925 - 1323	-1.1	-1.1	1.0	0.0	0.0	0.3	1.1	-1.1	-1.2	2.2
G O	680 - 80	0.4	-1.2	-2.4	0.1	0.0	-0.1	0.5	-1.2	-2.4	2.8
H I	1921 - 1321	0.0	-3.0	-0.1	0.2	0.0	0.0	0.0	-0.1	-3.0	3.0
I O	676 - 76	0.0	-0.2	0.6	0.0	0.0	0.0	0.6	0.0	-0.2	0.8
J I	1916 - 1316	-0.1	-3.5	0.1	0.2	0.0	0.0	0.1	-0.1	-3.5	3.6
K O	671 - 71	0.0	-0.1	0.2	0.0	0.0	0.0	0.2	0.0	-0.1	0.2
L I	1908 - 1308	-0.1	-3.5	0.4	0.2	0.0	0.0	0.4	-0.1	-3.5	3.9
M O	663 - 63	0.0	-0.4	-0.1	-0.2	0.0	0.0	0.0	-0.1	-0.5	0.5
N O	1877 - 1277	-0.4	-3.6	0.4	0.2	0.0	0.0	0.4	-0.4	-3.6	4.0
O I	647 - 47	0.0	1.1	-0.1	-0.1	0.1	0.0	1.1	0.0	-0.1	1.2
P O	1840 - 1240	0.0	-3.3	0.3	0.2	0.0	0.0	0.3	0.0	-3.3	3.6
Q O	628 - 28	0.0	-1.6	-0.7	0.1	0.1	0.0	0.0	-0.7	-1.6	1.6
R I	1816 - 216	0.2	2.2	1.4	-0.2	0.0	0.6	2.2	1.7	0.0	2.3
S O	616 - 16	1.3	-4.0	-6.0	0.4	0.1	1.4	1.5	-4.0	-6.2	7.8
T O	811 - 11	-0.5	-1.8	-4.0	0.1	0.1	-0.2	-0.4	-1.8	-4.0	3.6
U O	43058 - 43051	1.6	0.4	-1.7	0.1	-0.1	-0.9	1.8	0.4	-1.9	3.7
V I	50024 - 50021	-3.4	-2.7	-0.6	0.0	0.0	0.3	-0.6	-2.7	-3.4	2.9
W I	43278 - 43271	-1.3	-1.3	0.1	0.0	0.0	0.1	0.2	-1.3	-1.3	1.4
X I	50084 - 50081	-1.5	-1.7	0.2	0.0	0.0	0.2	0.3	-1.6	-1.7	1.9

<sup>1</sup> Refer to Figure 2.10.2-34 for the identification of the representative sections.



Table 2.10.4-34 Critical P<sub>m</sub> Stress Summary; Cold Condition; 3-D Top Model; Condition 4

Condition 4: -40°F Ambient, No Decay Heat

Comp. No. <sup>1</sup>	Section Cut Node-Node	P <sub>m</sub> Stresses (ksi)						Principal Stresses (ksi)			S.I. Stress	Allow. Stress	Margin of Safety
		S <sub>x</sub>	S <sub>y</sub>	S <sub>z</sub>	S <sub>x</sub>	S <sub>y</sub>	S <sub>z</sub>	S1	S2	S3			
1	683- 85	0.0	0.1	0.0	0.0	0.0	0.0	0.1	0.0	0.0	0.1	19.2	191.0
2	18679-18079	0.1	0.1	0.0	1.9	0.2	0.0	2.0	0.0	-1.9	3.9	18.5	3.7
3	15841-15241	0.0	0.3	0.2	0.0	0.3	0.0	0.6	0.0	-0.1	0.7	31.4	43.9
4	1907- 1307	0.0	0.4	0.5	-0.1	0.0	0.0	0.5	0.5	0.0	0.6	19.6	31.7
5	625- 25	0.0	-0.4	0.0	0.0	0.0	0.0	0.0	0.0	-0.4	0.4	20.0	49.0
6	29216-29211	0.1	1.3	3.9	0.0	0.0	0.2	3.9	1.3	0.1	3.8	20.0	4.3
7	43021-43028	-0.2	-2.5	-9.4	0.2	0.0	-0.1	-0.2	-2.6	-9.4	9.2	20.0	1.2
8	50916-50919	0.0	0.0	-0.1	0.0	0.0	0.2	0.2	0.0	-0.2	0.4	45.0	111.5

Locations of the most critical sections for each component are provided in the following:

Comp. No. <sup>1</sup>	Section Location					
	Inside Node			Outside Node		
	x (in)	y (deg)	z (in)	x (in)	y (deg)	z (in)
1	39.44	0.0	6.20	39.44	0.0	0.75
2	40.70	91.7	17.40	43.35	91.7	17.40
3	35.50	67.7	159.90	37.00	67.7	159.90
4	35.50	0.0	99.50	37.00	0.0	99.50
5	40.70	0.0	163.40	43.35	0.0	163.40
6	37.50	163.4	175.40	37.66	163.4	179.40
7	37.66	0.0	185.40	37.66	0.0	179.40
8	36.46	91.7	193.71	36.46	91.7	188.40

<sup>1</sup> Refer to Figure 2.10.2-33 for cask component identification.

Table 2.10.4-35 Critical  $P_m + P_b$  Stress Summary; Cold Condition; 3-D Top Model; Condition 4

Condition 4: -40°F Ambient, No Decay Heat

Comp. No. <sup>1</sup>	Section Cul Node-Node	P <sub>m</sub> + P <sub>b</sub> Stresses (ksi)							Principal Stresses (ksi)			Allow. S.I. Stress	Margin of Safety
		S <sub>x</sub>	S <sub>y</sub>	S <sub>z</sub>	S <sub>xy</sub>	S <sub>yz</sub>	S <sub>xz</sub>	S1	S2	S3			
1	1952- 93	0.1	0.1	-0.1	0.0	0.0	0.0	0.1	0.1	-0.1	0.2	28.7	142.3
2	18679-18079	0.1	0.2	0.1	2.1	0.4	0.0	2.3	0.1	-2.0	4.2	27.7	5.6
3	13841-13241	0.0	0.3	0.0	0.0	0.4	0.0	0.6	0.0	-0.3	0.8	47.1	57.9
4	1909- 1309	0.0	0.5	0.6	0.0	0.0	0.0	0.6	0.5	0.0	0.6	29.4	48.0
5	625- 25	0.0	-0.3	0.1	0.0	0.0	0.0	0.1	0.0	-0.3	0.5	30.0	59.0
6	29216-29211	1.9	3.7	10.8	0.0	0.0	0.2	10.8	3.7	1.9	8.9	30.0	2.4
7	43021-43028	-1.2	-3.4	-10.9	0.2	0.0	0.7	-1.2	-3.4	-10.9	9.8	30.0	2.1
8	50921-50924	1.0	0.2	-0.7	0.0	0.0	0.0	1.0	0.2	-0.7	1.7	67.5	38.7

Locations of the most critical sections for each component are provided in the following:

Comp. No. <sup>1</sup>	Section Location					
	Inside Node			Outside Node		
	x (in)	y (deg)	z (in)	x (in)	y (deg)	z (in)
1	0.00	0.0	6.20	0.00	0.0	0.75
2	40.70	91.7	17.40	43.35	91.7	17.40
3	35.50	56.5	159.90	37.00	56.5	159.90
4	35.50	0.0	93.56	37.00	0.0	93.56
5	40.70	0.0	163.40	43.35	0.0	163.40
6	37.50	163.4	175.40	37.66	163.4	179.40
7	37.66	0.0	185.40	37.66	0.0	179.40
8	35.21	91.7	193.71	35.21	91.7	188.40

<sup>1</sup> Refer to Figure 2.10.2-33 for cask component identification.

Table 2.10.4-36 Critical  $S_n$  Stress Summary; Cold Condition; 3-D Top Model; Condition 4

Condition 4: -40°F Ambient, No Decay Heat

Comp. No. <sup>1</sup>	Section Cut Node-Node	$S_n$ Stresses (ksi)						Principal Stresses (ksi)				Allow. Stress 3.0 $S_n$
		$S_x$	$S_y$	$S_z$	$S_{xy}$	$S_{yz}$	$S_{zx}$	S1	S2	S3	S.I.	
1	20683-20085	0.8	-2.3	-4.5	0.0	0.0	-0.7	0.9	-2.3	-4.6	5.5	57.6
2	682- 82	-0.5	1.8	5.2	-0.2	0.0	-0.3	5.2	1.8	-0.5	5.8	55.5
3	15847-15247	-0.1	-3.7	0.5	0.0	0.3	0.0	0.5	-0.1	-3.7	4.2	94.2
4	1875- 1275	-0.5	-3.6	0.4	0.2	0.0	0.0	0.4	-0.4	-3.6	4.1	58.8
5	10625-10025	0.1	-1.9	0.8	0.0	0.3	0.0	0.9	0.1	-2.0	2.9	60.0
6	11216-11211	1.3	2.0	11.4	-0.3	-0.3	-0.4	11.5	2.1	1.2	10.2	60.0
7	50030-63071	11.7	2.0	-3.5	0.5	-0.1	1.2	11.8	2.0	-3.6	15.4	60.0
8	50001-50004	-4.6	-1.8	3.5	-0.1	0.0	0.5	3.5	-1.8	-4.6	8.1	135.0

Locations of the most critical sections for each component are provided in the following:

Comp. No. <sup>1</sup>	Section Location					
	Inside Node			Outside Node		
	x (in)	y (deg)	z (in)	x (in)	y (deg)	z (in)
1	39.44	104.7	6.20	39.44	104.7	0.75
2	39.44	0.0	8.20	43.35	0.0	8.20
3	35.50	67.7	156.90	37.00	67.7	156.90
4	35.50	0.0	141.10	37.00	0.0	141.10
5	40.70	45.9	163.40	43.35	45.9	163.40
6	37.50	45.9	175.40	37.66	45.9	179.40
7	33.71	0.0	188.40	33.71	0.0	187.40
8	40.88	0.0	193.71	40.88	0.0	188.40

<sup>1</sup> Refer to Figure 2.10.2-33 for cask component identification.

Table 2.10.4-37 Primary Stresses; 1-Foot Top End Drop; Drop Orientation = 0 Degrees; 2-D Model; Condition 1

Condition 1: 100°F Ambient with Contents

Stress Points		Stress Components (ksi)						Principal Stresses (ksi)		
Section <sup>1</sup>	Node	S <sub>x</sub>	S <sub>y</sub>	S <sub>z</sub>	S <sub>xy</sub>	S <sub>yz</sub>	S <sub>xz</sub>	S1	S2	S3
A1	1	-0.7	0.0	-0.7	0.0	0.0	0.0	0.0	-0.7	-0.7
A1	1	0.9	0.0	0.9	0.0	0.0	0.0	0.9	0.9	0.0
A2	2	0.5	0.0	0.5	0.0	0.0	0.0	0.5	0.5	0.0
A3	3	0.1	0.0	0.1	0.0	0.0	0.0	0.1	0.1	0.0
A4	4	-0.2	0.0	-0.2	0.0	0.0	0.0	0.0	-0.2	-0.2
A5	5	-0.6	0.0	-0.6	0.0	0.0	0.0	0.0	-0.6	-0.6
B1	6	0.5	0.0	0.5	0.0	0.0	0.0	0.5	0.5	0.0
B2	7	0.2	0.0	0.2	0.0	0.0	0.0	0.2	0.2	0.0
B3	8	-0.1	0.0	-0.1	0.0	0.0	0.0	0.0	-0.1	-0.1
B4	9	-0.5	0.0	-0.5	0.0	0.0	0.0	0.0	-0.5	-0.5
B5	10	-0.8	0.0	-0.8	0.0	0.0	0.0	0.0	-0.8	-0.8
C1	251	-0.3	-0.1	0.2	-0.1	0.0	0.0	0.2	-0.1	-0.3
C2	252	-0.1	-0.1	0.2	-0.1	0.0	0.0	0.2	0.0	-0.2
C3	253	0.1	-0.1	0.1	-0.1	0.0	0.0	0.2	0.1	-0.1
C4	254	0.4	-0.1	0.1	-0.1	0.0	0.0	0.4	0.1	-0.1
C5	255	0.6	0.0	0.1	-0.1	0.0	0.0	0.6	0.1	0.0
D1	306	-0.7	-0.5	-0.3	-0.2	0.0	0.0	-0.3	-0.3	-0.8
D2	307	-0.2	-0.3	-0.2	-0.1	0.0	0.0	-0.2	-0.2	-0.4
D3	308	-0.1	-0.1	-0.1	0.0	0.0	0.0	-0.1	-0.1	-0.1
D4	309	0.1	-0.1	-0.1	0.0	0.0	0.0	0.1	-0.1	-0.1
D5	310	0.2	0.0	-0.2	0.0	0.0	0.0	0.3	0.0	-0.2
E1	305	0.7	0.0	0.2	-0.1	0.0	0.0	0.7	0.2	-0.1
E2	315	0.3	-0.2	0.1	-0.2	0.0	0.0	0.4	0.1	-0.2
E3	325	0.1	-0.2	0.0	-0.2	0.0	0.0	0.2	0.0	-0.2
E4	335	0.1	-0.1	0.0	-0.1	0.0	0.0	0.1	0.0	-0.2
E5	345	0.0	-0.1	0.0	-0.1	0.0	0.0	0.1	0.0	-0.2
E6	355	0.0	-0.2	0.0	0.0	0.0	0.0	0.0	0.0	-0.2
F1	251	-0.3	-0.1	0.2	-0.1	0.0	0.0	0.2	-0.1	-0.3
F2	261	-0.3	-0.2	0.1	0.0	0.0	0.0	0.1	-0.2	-0.3
F3	271	-0.4	-0.4	0.1	0.1	0.0	0.0	0.1	-0.3	-0.4
F4	281	-0.5	-0.6	0.0	0.1	0.0	0.0	0.0	-0.4	-0.7

Table 2.10.4-37 Primary Stresses; 1-Foot Top End Drop; Drop Orientation = 0 Degrees; 2-D Model; Condition 1 (continued)

Stress Points		Stress Components (ksi)						Principal Stresses (ksi)		
Section <sup>1</sup>	Node	S <sub>x</sub>	S <sub>y</sub>	S <sub>z</sub>	S <sub>xy</sub>	S <sub>yz</sub>	S <sub>xz</sub>	S1	S2	S3
G1	311	-0.3	-0.6	0.0	-0.1	0.0	0.0	0.0	-0.3	-0.6
G2	321	-0.2	-0.4	0.1	0.0	0.0	0.0	0.1	-0.2	-0.4
G3	331	-0.1	-0.2	0.1	0.0	0.0	0.0	0.1	-0.1	-0.2
G4	341	0.0	-0.1	0.2	0.0	0.0	0.0	0.2	0.0	-0.1
G5	351	0.0	0.1	0.2	0.0	0.0	0.0	0.2	0.1	0.0
H1	581	-0.1	-0.8	1.0	0.0	0.0	0.0	1.0	-0.1	-0.8
H2	582	0.0	-0.8	1.0	0.0	0.0	0.0	1.0	0.0	-0.8
H3	583	0.0	-0.8	1.0	0.0	0.0	0.0	1.0	0.0	-0.8
H4	584	0.0	-0.8	0.9	0.0	0.0	0.0	0.9	0.0	-0.8
I1	589	0.0	-0.3	0.1	0.0	0.0	0.0	0.1	0.0	-0.3
I2	590	0.0	-0.4	0.0	0.0	0.0	0.0	0.0	0.0	-0.4
I3	591	0.0	-0.4	0.0	0.0	0.0	0.0	0.0	0.0	-0.4
I4	592	0.0	-0.4	0.0	0.0	0.0	0.0	0.0	0.0	-0.4
I5	593	0.0	-0.4	0.0	0.0	0.0	0.0	0.0	0.0	-0.4
J1	971	-0.1	-1.0	1.2	0.0	0.0	0.0	1.2	-0.1	-1.0
J2	972	0.0	-1.0	1.2	0.0	0.0	0.0	1.2	0.0	-1.0
J3	973	0.0	-1.0	1.2	0.0	0.0	0.0	1.2	0.0	-1.0
J4	974	0.0	-1.0	1.2	0.0	0.0	0.0	1.2	0.0	-1.0
K1	979	0.0	-0.6	0.0	0.0	0.0	0.0	0.0	0.0	-0.6
K2	980	0.0	-0.6	0.0	0.0	0.0	0.0	0.0	0.0	-0.6
K3	981	0.0	-0.6	0.0	0.0	0.0	0.0	0.0	0.0	-0.6
K4	982	0.0	-0.6	0.0	0.0	0.0	0.0	0.0	0.0	-0.6
K5	983	0.0	-0.6	0.0	0.0	0.0	0.0	0.0	0.0	-0.6
L1	1601	-0.1	-1.4	1.2	0.0	0.0	0.0	1.2	-0.1	-1.4
L2	1602	0.0	-1.4	1.2	0.0	0.0	0.0	1.2	0.0	-1.4
L3	1603	0.0	-1.4	1.2	0.0	0.0	0.0	1.2	0.0	-1.4
L4	1604	0.0	-1.4	1.2	0.0	0.0	0.0	1.2	0.0	-1.4
M1	1609	0.0	-1.0	0.0	0.0	0.0	0.0	0.0	0.0	-1.0
M2	1610	0.0	-1.0	0.0	0.0	0.0	0.0	0.0	0.0	-1.0
M3	1611	0.0	-1.0	0.0	0.0	0.0	0.0	0.0	0.0	-1.0
M4	1612	0.0	-1.0	0.0	0.0	0.0	0.0	0.0	0.0	-1.0
M5	1613	0.0	-1.0	0.0	0.0	0.0	0.0	0.0	0.0	-1.0
N1	2216	-0.1	-1.7	1.2	0.0	0.0	0.0	1.2	-0.1	-1.7

Table 2.10.4-37 Primary Stresses; 1-Foot Top End Drop; Drop Orientation = 0 Degrees; 2-D Model; Condition 1 (continued)

Stress Points Section <sup>1</sup> Node		Stress Components (ksi)						Principal Stresses (ksi)		
		S <sub>x</sub>	S <sub>y</sub>	S <sub>z</sub>	S <sub>xy</sub>	S <sub>xz</sub>	S <sub>yz</sub>	S1	S2	S3
N2	2217	0.0	-1.7	1.2	0.0	0.0	0.0	1.2	0.0	-1.7
N3	2218	0.0	-1.7	1.2	0.0	0.0	0.0	1.2	0.0	-1.7
N4	2219	0.0	-1.7	1.2	0.0	0.0	0.0	1.2	0.0	-1.7
O1	2224	0.0	-1.3	0.0	0.0	0.0	0.0	0.0	0.0	-1.3
O2	2225	0.0	-1.3	0.0	0.0	0.0	0.0	0.0	0.0	-1.3
O3	2226	0.0	-1.3	0.0	0.0	0.0	0.0	0.0	0.0	-1.3
O4	2227	0.0	-1.3	0.0	0.0	0.0	0.0	0.0	0.0	-1.3
O5	2228	0.0	-1.3	0.0	0.0	0.0	0.0	0.0	0.0	-1.3
P1	2546	-0.1	-1.0	1.4	0.0	0.0	0.0	1.4	-0.1	-1.0
P2	2547	-0.1	-1.6	1.2	0.0	0.0	0.0	1.2	-0.1	-1.6
P3	2548	-0.1	-2.1	1.0	-0.1	0.0	0.0	1.0	-0.1	-2.1
P4	2549	0.0	-2.8	0.8	-0.2	0.0	0.0	0.8	0.0	-2.8
Q1	2554	0.0	-1.1	0.5	0.0	0.0	0.0	0.5	0.0	-1.1
Q2	2555	0.0	-1.3	0.4	0.0	0.0	0.0	0.4	0.0	-1.3
Q3	2556	0.0	-1.5	0.4	0.0	0.0	0.0	0.4	0.0	-1.5
Q4	2557	0.0	-1.7	0.3	0.0	0.0	0.0	0.3	0.0	-1.7
Q5	2558	0.0	-1.9	0.3	0.0	0.0	0.0	0.3	0.0	-1.9
R1	2771	-0.2	-6.5	0.0	0.1	0.0	0.0	0.0	-0.2	-6.5
R2	2772	0.0	-3.7	0.8	0.2	0.0	0.0	0.8	0.0	-3.7
R3	2773	0.1	-1.1	1.5	0.6	0.0	0.0	1.5	0.4	-1.4
R4	2774	-0.5	2.4	2.2	1.2	0.0	0.0	2.9	2.2	-0.9
S1	2779	-3.7	-4.7	-1.0	0.2	0.0	0.0	-1.0	-3.7	-4.7
S2	2780	-2.3	-2.7	-0.1	-0.1	0.0	0.0	-0.1	-2.3	-2.7
S3	2781	-1.2	-1.3	0.6	-0.4	0.0	0.0	0.6	-0.8	-1.7
S4	2782	-0.5	0.1	1.1	-0.3	0.0	0.0	1.1	0.2	-0.6
S5	2783	-0.2	1.9	1.6	-0.2	0.0	0.0	1.9	1.6	-0.2
T1	7066	4.0	3.7	1.9	1.2	0.0	0.0	5.0	2.6	1.9
T2	7067	3.0	0.8	0.9	0.3	0.0	0.0	3.0	0.9	0.8
T3	7068	2.0	-0.4	0.3	-0.1	0.0	0.0	2.0	0.3	-0.4
T4	7069	1.2	-1.2	-0.1	-0.4	0.0	0.0	1.2	-0.1	-1.2
T5	7070	0.6	-1.8	-0.4	-0.4	0.0	0.0	0.7	-0.4	-1.9
T6	7071	0.3	-2.6	-0.7	-0.3	0.0	0.0	0.3	-0.7	-2.6
T7	7072	0.1	-3.7	-1.0	-0.2	0.0	0.0	0.2	-1.0	-3.7

Table 2.10.4-37 Primary Stresses; 1-Foot Top End Drop; Drop Orientation = 0 Degrees; 2-D Model; Condition 1 (continued)

Stress Points		Stress Components (ksi)						Principal Stresses (ksi)		
Section <sup>1</sup>	Node	S <sub>x</sub>	S <sub>y</sub>	S <sub>z</sub>	S <sub>xy</sub>	S <sub>xz</sub>	S <sub>yz</sub>	S1	S2	S3
U1	3051	0.4	-4.5	1.7	1.2	0.0	0.0	1.7	0.7	-4.8
U2	3052	0.7	-4.7	0.8	1.4	0.0	0.0	1.1	0.8	-5.0
U3	3053	0.9	-4.4	0.2	1.3	0.0	0.0	1.2	0.2	-4.8
U4	3054	0.6	-3.9	-0.5	0.7	0.0	0.0	0.7	-0.5	-4.0
U5	3055	-0.2	-3.6	-1.3	0.7	0.0	0.0	0.0	-1.3	-3.7
U6	3056	0.0	-2.0	-1.4	1.2	0.0	0.0	0.6	-1.4	-2.5
V1	3611	-2.7	-1.2	2.3	-0.6	0.0	0.0	2.3	-1.0	-2.9
V2	3612	-1.8	-1.3	1.5	-0.8	0.0	0.0	1.5	-0.7	-2.4
V3	3613	-0.9	-1.5	0.7	-1.1	0.0	0.0	0.7	-0.1	-2.3
V4	3614	-0.1	-1.7	-0.2	-1.0	0.0	0.0	0.4	-0.2	-2.2
V5	3615	0.6	-2.0	-1.1	-0.9	0.0	0.0	0.9	-1.1	-2.2
V6	3616	0.6	-1.1	-1.9	-0.5	0.0	0.0	0.8	-1.3	-1.9
V7	3617	2.0	-0.2	-2.4	-0.3	0.0	0.0	2.1	-0.2	-2.4
W1	3241	-0.2	-0.3	-0.2	0.0	0.0	0.0	-0.2	-0.2	-0.3
W2	3242	0.3	-0.3	0.3	0.0	0.0	0.0	0.3	0.3	-0.3
W3	3243	0.8	-0.2	0.8	0.0	0.0	0.0	0.8	0.8	-0.2
W4	3244	1.2	-0.1	1.2	0.0	0.0	0.0	1.2	1.2	-0.1
W5	3245	1.7	-0.1	1.7	0.0	0.0	0.0	1.7	1.7	-0.1
W6	3246	2.2	0.0	2.2	0.0	0.0	0.0	2.2	2.2	0.0
X1	3801	18.5	-0.6	18.5	0.0	0.0	0.0	18.5	18.5	-0.6
X2	3802	12.5	-0.5	12.5	0.0	0.0	0.0	12.5	12.5	-0.5
X3	3803	6.5	-0.3	6.5	0.0	0.0	0.0	6.5	6.5	-0.3
X4	3804	0.4	-0.4	0.4	0.0	0.0	0.0	0.4	0.4	-0.4
X5	3805	-5.6	-0.5	-5.6	0.0	0.0	0.0	-0.5	-5.6	-5.6
X6	3806	-11.7	-0.4	-11.7	0.0	0.0	0.0	-0.4	-11.7	-11.7
X7	3807	-18.3	-0.3	-18.3	0.0	0.0	0.0	-0.3	-18.3	-18.3

<sup>1</sup> Refer to Figure 2.10.2-34 for the identification of the representative sections.

Table 2.10.4-38 Primary + Secondary Stresses; 1-Foot Top End Drop; Drop Orientation = 0 Degrees; 2-D Model; Condition 1

Condition 1: 100°F Ambient with Contents

Stress Points Section <sup>1</sup> Node	Stress Components (ksi)						Principal Stresses (ksi)		
	S <sub>x</sub>	S <sub>y</sub>	S <sub>z</sub>	S <sub>xy</sub>	S <sub>xz</sub>	S <sub>yz</sub>	S1	S2	S3
A1	1	1.3	-0.1	1.3	0.0	0.0	1.3	1.3	-0.1
A2	2	0.4	0.0	0.4	0.0	0.0	0.4	0.4	0.0
A3	3	-0.4	0.0	-0.4	0.0	0.0	0.0	-0.4	-0.4
A4	4	-1.2	0.0	-1.2	0.0	0.0	0.0	-1.2	-1.2
A5	5	-2.0	0.0	-2.0	0.0	0.0	0.0	-2.0	-2.0
B1	6	1.9	0.0	1.9	0.0	0.0	1.9	1.9	0.0
B2	7	1.5	0.0	1.5	0.0	0.0	1.5	1.5	0.0
B3	8	1.2	0.0	1.2	0.0	0.0	1.2	1.2	0.0
B4	9	0.8	0.0	0.8	0.0	0.0	0.8	0.8	0.0
B5	10	0.5	0.0	0.5	0.0	0.0	0.5	0.5	0.0
C1	251	-0.8	-2.9	-0.3	-0.6	0.0	-0.3	-0.6	-3.0
C2	252	0.1	-1.4	-0.1	-0.6	0.0	0.3	-0.1	-1.6
C3	253	-0.2	-1.1	-0.6	-0.6	0.0	0.1	-0.6	-1.3
C4	254	-0.4	-1.1	-1.2	-0.4	0.0	-0.2	-1.2	-1.2
C5	255	-0.8	-1.1	-1.9	-0.2	0.0	-0.7	-1.1	-1.9
D1	306	4.9	6.1	3.1	1.8	0.0	7.4	3.6	3.1
D2	307	0.8	3.4	1.3	1.3	0.0	3.9	1.3	0.2
D3	308	0.3	1.3	0.8	0.5	0.0	1.4	0.8	0.1
D4	309	-0.4	0.5	0.5	0.1	0.0	0.5	0.5	-0.4
D5	310	-1.3	0.2	0.2	0.0	0.0	0.2	0.2	-1.3
E1	305	-0.4	3.6	0.4	0.4	0.0	3.6	0.4	-0.5
E2	315	-0.4	2.3	0.3	1.3	0.0	2.8	0.3	-0.9
E3	325	0.2	1.3	0.2	1.5	0.0	2.3	0.2	-0.9
E4	335	0.1	0.6	0.1	1.2	0.0	1.6	0.1	-0.8
E5	345	0.1	-0.2	-0.1	0.7	0.0	0.7	-0.1	-0.7
E6	355	0.1	-1.1	-0.3	0.4	0.0	0.2	-0.3	-1.2
F1	251	-0.8	-2.9	-0.3	-0.6	0.0	-0.3	-0.6	-3.0
F2	261	-0.4	-1.3	0.2	-0.5	0.0	0.2	-0.2	-1.5
F3	271	0.3	-0.2	0.5	-0.5	0.0	0.6	0.5	-0.5
F4	281	0.5	1.5	0.9	-0.9	0.0	2.0	0.9	0.0
G1	311	-3.7	-0.3	-0.8	1.3	0.0	0.2	-0.8	-4.1



Table 2.10.4-38 Primary + Secondary Stresses; 1-Foot Top End Drop; Drop Orientation = 0 Degrees; 2-D Model; Condition 1 (continued)

Stress Points Section <sup>1</sup> Node		Stress Components (ksi)						Principal Stresses (ksi)		
		S <sub>x</sub>	S <sub>y</sub>	S <sub>z</sub>	S <sub>xy</sub>	S <sub>yz</sub>	S <sub>xz</sub>	S1	S2	S3
G2	321	-3.3	2.7	0.1	0.9	0.0	0.0	2.9	0.1	-3.4
G3	331	-1.6	4.2	1.0	0.2	0.0	0.0	4.2	1.0	-1.6
G4	341	-0.6	5.6	1.6	0.0	0.0	0.0	5.6	1.6	-0.6
G5	351	-0.2	7.7	2.3	-0.1	0.0	0.0	7.7	2.3	-0.2
H1	581	-0.1	-0.1	0.9	0.1	0.0	0.0	0.9	0.0	-0.2
H2	582	-0.1	-0.8	0.8	0.1	0.0	0.0	0.8	-0.1	-0.9
H3	583	0.0	-1.5	0.7	0.1	0.0	0.0	0.7	0.0	-1.5
H4	584	-0.2	-2.3	0.5	0.2	0.0	0.0	0.5	-0.1	-2.4
I1	589	-0.3	5.1	2.0	0.1	0.0	0.0	5.1	2.0	-0.3
I2	590	-0.2	5.1	2.1	0.1	0.0	0.0	5.1	2.1	-0.2
I3	591	-0.1	5.0	2.2	0.2	0.0	0.0	5.0	2.2	-0.2
I4	592	-0.1	4.9	2.4	0.1	0.0	0.0	4.9	2.4	-0.1
I5	593	0.0	4.9	2.5	0.1	0.0	0.0	4.9	2.5	0.0
J1	971	-0.1	-3.3	0.1	0.0	0.0	0.0	0.1	-0.1	-3.3
J2	972	0.0	-2.1	0.8	0.0	0.0	0.0	0.8	0.0	-2.1
J3	973	0.0	-0.8	1.6	0.0	0.0	0.0	1.6	0.0	-0.8
J4	974	0.0	0.4	2.3	0.0	0.0	0.0	2.3	0.4	0.0
K1	979	-0.3	2.6	3.5	0.0	0.0	0.0	3.5	2.6	-0.3
K2	980	-0.2	3.7	4.1	0.0	0.0	0.0	4.1	3.7	-0.2
K3	981	-0.2	4.8	4.8	0.0	0.0	0.0	4.8	4.8	-0.2
K4	982	-0.1	5.9	5.4	0.0	0.0	0.0	5.9	5.4	-0.1
K5	983	0.0	6.9	5.9	0.0	0.0	0.0	6.9	5.9	0.0
L1	1601	-0.1	-3.1	0.1	0.0	0.0	0.0	0.1	-0.1	-3.1
L2	1602	0.0	-2.2	0.8	0.0	0.0	0.0	0.8	0.0	-2.2
L3	1603	0.0	-1.3	1.5	0.0	0.0	0.0	1.5	0.0	-1.3
L4	1604	0.0	-0.5	2.2	0.0	0.0	0.0	2.2	0.0	-0.5
M1	1609	-0.4	2.4	4.6	0.0	0.0	0.0	4.6	2.4	-0.4
M2	1610	-0.3	3.4	5.3	0.0	0.0	0.0	5.3	3.4	-0.3
M3	1611	-0.2	4.4	6.0	0.0	0.0	0.0	6.0	4.4	-0.2
M4	1612	-0.1	5.5	6.6	0.0	0.0	0.0	6.6	5.5	-0.1
M5	1613	0.0	6.5	7.2	0.0	0.0	0.0	7.2	6.5	0.0

Table 2.10.4-38 Primary + Secondary Stresses; 1-Foot Top End Drop; Drop Orientation = 0 Degrees; 2-D Model; Condition 1 (continued)

Stress Points		Stress Components (ksi)						Principal Stresses (ksi)		
Section <sup>1</sup>	Node	S <sub>x</sub>	S <sub>y</sub>	S <sub>z</sub>	S <sub>xy</sub>	S <sub>yz</sub>	S <sub>zx</sub>	S1	S2	S3
N1	2216	-0.1	-3.8	-0.2	0.0	0.0	0.0	-0.1	-0.2	-3.8
N2	2217	0.0	-2.7	0.5	0.0	0.0	0.0	0.5	0.0	-2.7
N3	2218	0.0	-1.6	1.1	0.0	0.0	0.0	1.1	0.0	-1.6
N4	2219	0.0	-0.5	1.8	0.0	0.0	0.0	1.8	0.0	-0.5
O1	2224	-0.3	2.5	3.9	0.0	0.0	0.0	3.9	2.5	-0.3
O2	2225	-0.3	3.3	4.4	0.0	0.0	0.0	4.4	3.3	-0.3
O3	2226	-0.2	4.1	4.9	0.0	0.0	0.0	4.9	4.1	-0.2
O4	2227	-0.1	4.9	5.4	0.0	0.0	0.0	5.4	4.9	-0.1
O5	2228	0.0	5.7	5.9	0.0	0.0	0.0	5.9	5.7	0.0
P1	2546	-0.1	-1.7	0.9	0.0	0.0	0.0	0.9	-0.1	-1.7
P2	2547	-0.1	-2.1	0.9	0.0	0.0	0.0	0.9	-0.1	-2.1
P3	2548	0.1	-2.3	1.0	-0.1	0.0	0.0	1.0	0.1	-2.3
P4	2549	-0.2	-2.9	0.9	-0.1	0.0	0.0	0.9	-0.2	-2.9
Q1	2554	-0.1	3.5	3.2	0.1	0.0	0.0	3.5	3.2	-0.1
Q2	2555	-0.1	3.7	3.4	0.1	0.0	0.0	3.7	3.4	-0.1
Q3	2556	-0.1	3.9	3.6	0.1	0.0	0.0	3.9	3.6	-0.1
Q4	2557	0.0	4.2	3.8	0.1	0.0	0.0	4.2	3.8	0.0
Q5	2558	0.0	4.3	4.0	0.1	0.0	0.0	4.3	4.0	0.0
R1	2771	-0.5	-3.6	-3.0	0.2	0.0	0.0	-0.5	-3.0	-3.6
R2	2772	-0.7	-3.2	-2.4	0.4	0.0	0.0	-0.7	-2.4	-3.3
R3	2773	-1.5	-2.4	-1.9	0.9	0.0	0.0	-0.9	-1.9	-2.9
R4	2774	-3.5	-1.0	-1.5	1.1	0.0	0.0	-0.5	-1.5	-4.0
S1	2779	-0.9	3.8	1.3	-1.9	0.0	0.0	4.5	1.3	-1.6
S2	2780	0.2	3.3	1.7	-0.9	0.0	0.0	3.6	1.7	-0.1
S3	2781	0.1	2.7	1.8	-0.1	0.0	0.0	2.7	1.8	0.1
S4	2782	0.0	2.2	1.9	0.1	0.0	0.0	2.2	1.9	0.0
S5	2783	0.1	1.7	2.0	0.1	0.0	0.0	2.0	1.7	0.1
T1	7066	2.1	-2.8	1.2	-0.8	0.0	0.0	2.3	1.2	-2.9
T2	7067	1.1	-2.6	1.0	-0.8	0.0	0.0	1.3	1.0	-2.7
T3	7068	0.7	-1.6	1.3	-0.6	0.0	0.0	1.3	0.8	-1.7
T4	7069	0.4	-0.7	1.6	-0.6	0.0	0.0	1.6	0.6	-0.9
T5	7070	0.2	0.2	1.8	-0.4	0.0	0.0	1.8	0.6	-0.3
T6	7071	0.1	1.0	2.1	-0.2	0.0	0.0	2.1	1.0	0.0

Table 2.10.4-38 Primary + Secondary Stresses; 1-Foot Top End Drop; Drop Orientation = 0 Degrees; 2-D Model; Condition 1 (continued)

Stress Points		Stress Components (ksi)						Principal Stresses (ksi)		
Section <sup>1</sup>	Node	S <sub>x</sub>	S <sub>y</sub>	S <sub>z</sub>	S <sub>xy</sub>	S <sub>yz</sub>	S <sub>xz</sub>	S1	S2	S3
T7	7072	0.0	1.6	2.4	-0.1	0.0	0.0	2.4	1.7	0.0
U1	3051	-1.5	-5.9	-0.7	1.2	0.0	0.0	-0.7	-1.2	-6.2
U2	3052	0.4	-5.6	-0.9	1.3	0.0	0.0	0.7	-0.9	-5.9
U3	3053	0.9	-4.8	-1.2	1.0	0.0	0.0	1.1	-1.2	-4.9
U4	3054	0.8	-3.7	-1.6	0.2	0.0	0.0	0.8	-1.6	-3.7
U5	3055	0.3	-2.9	-2.1	0.1	0.0	0.0	0.3	-2.1	-2.9
U6	3056	1.2	-1.5	-2.0	1.0	0.0	0.0	1.6	-1.8	-2.0
V1	3611	-0.6	-0.2	1.1	-0.3	0.0	0.0	1.1	0.0	-0.8
V2	3612	-0.7	-0.3	0.6	-0.5	0.0	0.0	0.6	0.1	-1.0
V3	3613	-0.5	-0.6	0.0	-0.8	0.0	0.0	0.3	0.0	-1.4
V4	3614	-0.1	-1.1	-0.5	-0.9	0.0	0.0	0.5	-0.5	-1.6
V5	3615	0.4	-1.7	-1.2	-0.8	0.0	0.0	0.6	-1.2	-1.9
V6	3616	0.2	-1.1	-1.7	-0.5	0.0	0.0	0.4	-1.2	-1.7
V7	3617	0.6	-0.2	-1.9	-0.3	0.0	0.0	0.7	-0.2	-1.9
W1	3241	1.9	-0.3	1.9	0.0	0.0	0.0	1.9	1.9	-0.3
W2	3242	2.1	-0.3	2.1	0.0	0.0	0.0	2.1	2.1	-0.3
W3	3243	2.2	-0.2	2.2	0.0	0.0	0.0	2.2	2.2	-0.2
W4	3244	2.3	-0.1	2.3	0.0	0.0	0.0	2.3	2.3	-0.1
W5	3245	2.5	-0.1	2.5	0.0	0.0	0.0	2.5	2.5	-0.1
W6	3246	2.6	0.0	2.6	0.0	0.0	0.0	2.6	2.6	0.0
X1	3801	16.4	-0.4	16.4	0.0	0.0	0.0	16.4	16.4	-0.4
X2	3802	11.3	-0.4	11.3	0.0	0.0	0.0	11.3	11.3	-0.4
X3	3803	6.1	-0.3	6.1	0.0	0.0	0.0	6.1	6.1	-0.3
X4	3804	0.9	-0.4	0.9	0.0	0.0	0.0	0.9	0.9	-0.4
X5	3805	-4.3	-0.5	-4.3	0.0	0.0	0.0	-0.5	-4.3	-4.3
X6	3806	-9.6	-0.5	-9.6	0.0	0.0	0.0	-0.5	-9.6	-9.6
X7	3807	-15.4	-0.3	-15.4	0.0	0.0	0.0	-0.3	-15.4	-15.4

<sup>1</sup> Refer to Figure 2.10.2-34 for the identification of the representative sections.

Table 2.10.4-39  $P_m$  Stresses; 1-Foot Top End Drop; Drop Orientation = 0 Degrees; 2-D Model; Condition 1

Condition 1: 100°F Ambient with Contents

Section <sup>1</sup>	Node - Node	Stress Components (ksi)						Principal Stresses (ksi)			
		$S_x$	$S_y$	$S_z$	$S_{xy}$	$S_{yz}$	$S_{xz}$	S1	S2	S3	S.I.
A	1 - 5	0.1	0.0	0.1	0.0	0.0	0.0	0.1	0.1	0.0	0.2
B	6 - 10	-0.1	0.0	-0.1	0.0	0.0	0.0	0.0	-0.1	-0.1	0.1
C	251 - 255	0.2	-0.1	0.1	-0.1	0.0	0.0	0.2	0.1	-0.1	0.3
D	306 - 310	-0.1	-0.2	-0.2	0.0	0.0	0.0	-0.1	-0.2	-0.2	0.1
E	305 - 355	0.2	-0.1	0.0	-0.1	0.0	0.0	0.3	0.0	-0.2	0.5
F	251 - 281	-0.4	-0.3	0.1	0.0	0.0	0.0	0.1	-0.3	-0.4	0.5
G	311 - 351	-0.1	-0.2	0.1	0.0	0.0	0.0	0.1	-0.1	-0.2	0.3
H	581 - 584	0.0	-0.8	1.0	0.0	0.0	0.0	1.0	0.0	-0.8	1.7
I	589 - 593	0.0	-0.4	0.0	0.0	0.0	0.0	0.0	0.0	-0.4	0.4
J	971 - 974	0.0	-1.0	1.2	0.0	0.0	0.0	1.2	0.0	-1.0	2.2
K	979 - 983	0.0	-0.6	0.0	0.0	0.0	0.0	0.0	0.0	-0.6	0.6
L	1601 - 1604	0.0	-1.4	1.2	0.0	0.0	0.0	1.2	0.0	-1.4	2.6
M	1609 - 1613	0.0	-1.0	0.0	0.0	0.0	0.0	0.0	0.0	-1.0	1.0
N	2216 - 2219	0.0	-1.7	1.2	0.0	0.0	0.0	1.2	0.0	-1.7	2.9
O	2224 - 2228	0.0	-1.3	0.0	0.0	0.0	0.0	0.0	0.0	-1.3	1.3
P	2546 - 2549	-0.1	-1.9	1.1	0.0	0.0	0.0	1.1	-0.1	-1.9	3.0
Q	2554 - 2558	0.0	-1.5	0.4	0.0	0.0	0.0	0.4	0.0	-1.5	1.9
R	2771 - 2774	-0.1	-2.2	1.1	0.5	0.0	0.0	1.1	0.0	-2.4	3.5
S	2779 - 2783	-1.5	-1.3	0.5	-0.2	0.0	0.0	0.5	-1.2	-1.6	2.1
T	7066 - 7072	1.6	-0.9	0.1	0.0	0.0	0.0	1.6	0.1	-0.9	2.4
U	3051 - 3056	0.4	-4.1	-0.2	1.0	0.0	0.0	0.7	-0.2	-4.3	5.0
V	3611 - 3617	-0.3	-1.4	-0.2	-0.8	0.0	0.0	0.2	-0.2	-1.8	1.9
W	3241 - 3246	1.0	-0.2	1.0	0.0	0.0	0.0	1.0	1.0	-0.2	1.2
X	3801 - 3807	0.0	-0.4	0.0	0.0	0.0	0.0	0.0	0.0	-0.4	0.5

<sup>1</sup> Refer to Figure 2.10.2-34 for the identification of the representative sections.

Table 2.10.4-40  $P_m + P_b$  Stresses; 1-Foot Top End Drop; Drop Orientation = 0 Degrees; 2-D Model; Condition 1

Condition 1: 100°F Ambient with Contents

Section <sup>1</sup>	Node - Node	Stress Components (ksi)						Principal Stresses (ksi)			
		$S_x$	$S_y$	$S_z$	$S_{xy}$	$S_{xz}$	$S_{yz}$	S1	S2	S3	S.I.
A I	1 - 5	0.9	0.0	0.9	0.0	0.0	0.0	0.9	0.9	0.0	0.9
B O	6 - 10	-0.8	0.0	-0.8	0.0	0.0	0.0	0.0	-0.8	-0.8	0.8
C O	251 - 255	0.6	0.0	0.1	-0.1	0.0	0.0	0.6	0.1	-0.1	0.7
D O	306 - 310	0.3	0.0	-0.1	0.0	0.0	0.0	0.3	0.0	-0.1	0.4
E I	305 - 355	0.7	-0.1	0.1	-0.1	0.0	0.0	0.7	0.1	-0.1	0.8
F O	251 - 281	-0.5	-0.6	0.0	0.0	0.0	0.0	0.0	-0.5	-0.6	0.6
G I	311 - 351	-0.3	-0.5	0.0	0.0	0.0	0.0	0.0	-0.3	-0.5	0.5
H I	581 - 584	-0.1	-0.8	1.0	0.0	0.0	0.0	1.0	-0.1	-0.8	1.7
I O	589 - 593	0.0	-0.4	0.0	0.0	0.0	0.0	0.0	0.0	-0.4	0.5
J I	971 - 974	-0.1	-1.0	1.2	0.0	0.0	0.0	1.2	-0.1	-1.0	2.2
K I	979 - 983	0.0	-0.6	0.0	0.0	0.0	0.0	0.0	0.0	-0.6	0.6
L I	1601 - 1604	-0.1	-1.4	1.2	0.0	0.0	0.0	1.2	-0.1	-1.4	2.6
M O	1609 - 1613	0.0	-1.0	0.0	0.0	0.0	0.0	0.0	0.0	-1.0	1.0
N I	2216 - 2219	-0.1	-1.7	1.2	0.0	0.0	0.0	1.2	-0.1	-1.7	2.9
O I	2224 - 2228	0.0	-1.3	0.0	0.0	0.0	0.0	0.0	0.0	-1.3	1.3
P O	2546 - 2549	0.0	-2.7	0.9	0.0	0.0	0.0	0.9	0.0	-2.7	3.6
Q O	2554 - 2558	0.0	-1.9	0.3	0.0	0.0	0.0	0.3	0.0	-1.9	2.1
R I	2771 - 2774	-0.2	-6.6	0.0	0.5	0.0	0.0	0.0	-0.2	-6.7	6.7
S I	2779 - 2783	-3.7	-4.4	-0.8	-0.2	0.0	0.0	-0.8	-3.7	-4.5	3.7
T O	7066 - 7072	0.1	-3.9	-1.2	0.0	0.0	0.0	0.1	-1.2	-3.9	4.0
U I	3051 - 3056	0.9	-13.1	1.3	1.0	0.0	0.0	1.3	1.0	-13.2	14.5
V O	3611 - 3617	1.7	-0.2	-2.6	-0.8	0.0	0.0	2.0	-0.5	-2.6	4.6
W O	3241 - 3246	2.2	0.0	2.2	0.0	0.0	0.0	2.2	2.2	0.0	2.2
X I	3801 - 3807	18.3	-0.6	18.3	0.0	0.0	0.0	18.3	18.3	-0.6	18.9

<sup>1</sup> Refer to Figure 2.10.2-34 for the identification of the representative sections.

Table 2.10.4-41  $S_n$  Stresses; 1-Foot Top End Drop; Drop Orientation = 0 Degrees; 2-D Model; Condition 1

Condition 1: 100°F Ambient with Contents

Section <sup>1</sup>	Node - Node	Stress Components (ksi)						Principal Stresses (ksi)			
		$S_x$	$S_y$	$S_z$	$S_{xy}$	$S_{yz}$	$S_{zx}$	S1	S2	S3	S1
A O	1 - 5	-2.0	0.0	-2.0	0.0	0.0	0.0	0.0	-2.0	-2.0	2.0
B I	6 - 10	1.9	0.0	1.9	0.0	0.0	0.0	1.9	1.9	0.0	1.9
C I	251 - 255	-0.1	-2.9	0.1	-0.5	0.0	0.0	0.1	0.0	-2.9	3.1
D I	306 - 310	3.0	6.1	2.3	0.7	0.0	0.0	6.3	2.8	2.3	4.0
E I	305 - 355	-0.4	3.7	0.5	1.0	0.0	0.0	3.9	0.5	-0.6	4.5
F I	251 - 281	-0.8	-2.8	-0.2	-0.6	0.0	0.0	-0.2	-0.6	-2.9	2.7
G O	311 - 351	-0.2	7.6	2.4	0.4	0.0	0.0	7.6	2.4	-0.3	7.9
H O	581 - 584	-0.2	-2.2	0.6	0.1	0.0	0.0	0.6	-0.1	-2.2	2.8
I I	589 - 593	-0.3	5.1	2.0	0.1	0.0	0.0	5.1	2.0	-0.3	5.4
J I	971 - 974	-0.1	-3.3	0.1	0.0	0.0	0.0	0.1	-0.1	-3.3	3.4
K O	979 - 983	0.0	6.9	5.9	0.0	0.0	0.0	6.9	5.9	0.0	6.9
L I	1601 - 1604	-0.1	-3.1	0.2	0.0	0.0	0.0	0.2	-0.1	-3.1	3.3
M O	1609 - 1613	0.0	6.5	7.3	0.0	0.0	0.0	7.3	6.5	0.0	7.3
N I	2216 - 2219	-0.1	-3.8	-0.2	0.0	0.0	0.0	-0.1	-0.2	-3.8	3.7
O O	2224 - 2228	0.0	5.7	5.9	0.0	0.0	0.0	5.9	5.7	0.0	5.9
P O	2546 - 2549	-0.2	-2.8	1.0	-0.1	0.0	0.0	1.0	-0.2	-2.8	3.8
Q O	2554 - 2558	0.0	4.4	4.0	0.1	0.0	0.0	4.4	4.0	0.0	4.4
R I	2771 - 2774	-0.5	-3.9	-2.9	0.7	0.0	0.0	-0.4	-2.9	-4.0	3.7
S I	2779 - 2783	-0.9	3.8	1.5	-0.5	0.0	0.0	3.9	1.5	-1.0	4.8
T I	7066 - 7072	2.1	-3.2	0.9	-0.5	0.0	0.0	2.2	0.9	-3.3	5.4
U I	3051 - 3056	0.0	-17.1	-0.7	0.7	0.0	0.0	0.0	-0.7	-17.1	17.1
V O	3611 - 3617	0.6	-0.2	-2.1	-0.6	0.0	0.0	1.0	-0.5	-2.1	3.1
W O	3241 - 3246	2.6	0.0	2.6	0.0	0.0	0.0	2.6	2.6	0.0	2.6
X I	3801 - 3807	16.3	-0.4	16.3	0.0	0.0	0.0	16.3	16.3	-0.4	16.7

<sup>1</sup> Refer to Figure 2.10.2-34 for the identification of the representative sections.

Table 2.10.4-42 Critical P<sub>m</sub> Stress Summary; 1-Foot Top End Drop; Drop Orientation = 0 Degrees; 2-D Model; Condition 1

Condition 1: 100°F Ambient with Contents

Comp. No. <sup>1</sup>	Section Cut Node-Node	P <sub>m</sub> Stresses (ksi)							Principal Stresses (ksi)			Allow. S.I. Stress	Margin of Safety
		S <sub>x</sub>	S <sub>y</sub>	S <sub>z</sub>	S <sub>xy</sub>	S <sub>xz</sub>	S <sub>yz</sub>	S1	S2	S3			
1	256- 260	-0.1	0.0	-0.1	-0.1	0.0	0.0	0.0	-0.1	-0.2	0.2	19.2	95.0
2	386- 389	0.0	-0.5	0.3	0.1	0.0	0.0	0.3	0.0	-0.5	0.8	18.5	22.1
3	2711- 2714	0.0	-1.5	2.2	0.2	0.0	0.0	2.2	0.0	-1.5	3.7	31.4	7.5
4	2276- 2279	0.0	-1.8	1.2	0.0	0.0	0.0	1.2	0.0	-1.8	2.9	19.6	5.8
5	2599- 2603	-1.5	0.0	0.6	-0.1	0.0	0.0	0.6	0.0	-1.5	2.1	20.0	8.5
6	7064- 2774	0.1	3.4	1.6	1.0	0.0	0.0	3.7	1.6	-0.2	3.9	20.0	4.1
7	3021- 3026	0.2	-8.8	-1.5	0.2	0.0	0.0	0.2	-1.5	-8.8	9.1	20.0	1.2
8	3661- 3667	-0.2	-3.4	-0.9	1.0	0.0	0.0	0.1	-0.9	-3.7	3.8	43.0	10.8

Locations of the most critical sections for each component are provided in the following:

Comp. No. <sup>1</sup>	Section Location			
	Inside Node		Outside Node	
	x (in)	y (in)	z (in)	x (in)
1	35.50	6.20	35.50	0.75
2	35.50	16.40	37.50	16.40
3	35.50	171.40	37.50	171.40
4	35.50	142.40	37.00	142.40
5	40.70	163.40	43.35	163.40
6	37.655	179.40	37.50	175.40
7	37.655	179.40	37.655	185.40
8	26.158	188.40	26.158	193.71

<sup>1</sup> Refer to Figure 2.10.2-33 for cask component identification.

Table 2.10.4-43 Critical  $P_m + P_b$  Stress Summary; 1-Foot Top End Drop; Drop Orientation = 0 Degrees; 2-D Model; Condition 1

Condition 1: 100°F Ambient with Contents

Comp. No. <sup>1</sup>	Section Cut Node-Node	$P_m + P_b$ Stresses (ksi)							Principal Stresses (ksi)			Allow. S.L. Stress	Margin of Safety
		$S_x$	$S_y$	$S_z$	$S_{xy}$	$S_{yz}$	$S_{zx}$	$S_1$	$S_2$	$S_3$			
1	16- 20	-0.8	0.0	-0.8	0.0	0.0	0.0	0.0	-0.8	-0.8	0.8	28.7	34.9
2	371- 374	0.0	-0.8	0.1	0.1	0.0	0.0	0.1	0.0	-0.8	0.9	27.7	29.8
3	2711- 2714	-0.1	-4.0	1.6	0.2	0.0	0.0	1.6	0.0	-4.0	5.6	47.1	7.4
4	2276- 2279	-0.1	-1.8	1.2	0.0	0.0	0.0	1.2	-0.1	-1.8	3.0	29.4	8.8
5	2599- 2603	-1.7	0.0	0.6	-0.1	0.0	0.0	0.6	0.0	-1.7	2.2	30.0	12.6
6	7065- 2784	4.0	-7.6	-0.8	0.5	0.0	0.0	4.1	-0.8	-7.6	11.6	30.0	1.6
7	3107- 3108	14.6	-6.1	-0.3	0.2	0.0	0.0	14.6	-0.3	-6.1	20.7	30.0	0.4
8	3801- 3807	18.3	-0.6	18.3	0.0	0.0	0.0	18.3	18.3	-0.6	18.9	67.5	2.6

Locations of the most critical sections for each component are provided in the following:

Comp. No. <sup>1</sup>	Section Location			
	Inside Node		Outside Node	
	x (in)	y (in)	z (in)	x (in)
1	1.42	6.20	1.42	0.75
2	35.50	15.40	37.50	15.40
3	35.50	171.40	37.50	171.40
4	35.50	142.40	37.00	142.40
5	40.70	163.40	43.35	163.40
6	38.608	179.40	38.567	175.40
7	26.158	187.40	26.158	188.40
8	0.0	188.46	0.0	193.71

<sup>1</sup> Refer to Figure 2.10.2-33 for cask component identification.



Table 2.10.4-44 Critical  $S_n$  Stress Summary; 1-Foot Top End Drop; Drop Orientation = 0 Degrees; 2-D Model; Condition 1

Condition 1: 100°F Ambient with Contents

Comp. No. <sup>1</sup>	Section Cut Node-Node	$S_n$ Stresses (ksi)						Principal Stresses (ksi)				Allow. Stress 3.0 $S_n$
		$S_x$	$S_y$	$S_z$	$S_w$	$S_u$	$S_v$	S1	S2	S3	S.I.	
1	296-300	4.1	-0.8	1.4	1.1	0.0	0.0	4.3	1.4	-1.1	5.4	57.6
2	311-351	-0.2	7.6	2.4	0.4	0.0	0.0	7.6	2.4	-0.3	7.9	55.5
3	2291-2294	-0.4	-2.8	1.4	-0.1	0.0	0.0	1.4	-0.4	-2.9	4.2	94.2
4	2156-2159	-0.1	-3.7	0.2	0.0	0.0	0.0	0.2	-0.1	-3.7	3.8	58.8
5	1534-1538	6.6	0.0	7.3	0.0	0.0	0.0	7.3	6.6	0.0	7.3	60.0
6	7065-2784	5.7	-6.1	1.4	-0.9	0.0	0.0	5.8	1.4	-6.2	12.0	60.0
7	3107-3108	15.2	-6.3	0.5	0.1	0.0	0.0	15.2	0.5	-6.3	21.6	60.0
8	3801-3807	16.3	-0.4	16.3	0.0	0.0	0.0	16.3	16.3	-0.4	16.7	135.0

Locations of the most critical sections for each component are provided in the following:

Comp. No. <sup>1</sup>	Section Location			
	Inside Node		Outside Node	
	x (in)	y (in)	z (in)	x (in)
1	38.567	6.20	38.567	0.75
2	40.700	14.40	43.35	14.40
3	35.50	143.40	37.00	143.40
4	35.50	134.40	37.00	134.40
5	40.70	92.40	43.35	92.40
6	38.608	179.40	38.567	175.40
7	26.158	187.40	26.158	188.40
8	0.0	188.46	0.0	193.71

<sup>1</sup> Refer to Figure 2.10.2-33 for cask component identification.

Table 2.10.4-45 Critical P<sub>m</sub> Stress Summary; 1-Foot Top End Drop; Drop Orientation = 0 Degrees; 2-D Model; Condition 2

Condition 2: -20°F Ambient with Contents

Comp. No. <sup>1</sup>	Section Cut Node-Node	P <sub>m</sub> Stresses (ksi)						Principal Stresses (ksi)			S.I.	Allow. Stress	Margin of Safety
		S <sub>x</sub>	S <sub>y</sub>	S <sub>z</sub>	S <sub>xy</sub>	S <sub>xz</sub>	S <sub>yz</sub>	S1	S2	S3			
1	216- 220	-0.2	0.0	-0.2	-0.1	0.0	0.0	0.0	-0.2	-0.2	0.3	19.2	63.0
2	386- 389	0.0	-0.7	0.3	0.0	0.0	0.0	0.3	0.0	-0.7	1.0	18.5	17.5
3	2711-2714	0.0	-1.7	1.9	0.3	0.0	0.0	1.9	0.0	-1.8	3.7	31.4	7.5
4	2276-2279	0.0	-2.1	0.3	0.0	0.0	0.0	0.3	0.0	-2.1	2.4	19.6	7.2
5	2599-2603	-1.6	0.0	0.6	-0.1	0.0	0.0	0.6	0.0	-1.6	2.2	20.0	8.1
6	7064-2774	0.1	3.5	1.5	1.1	0.0	0.0	3.9	1.5	-0.2	4.1	20.0	3.9
7	3021-3026	0.2	-9.1	-1.5	0.2	0.0	0.0	0.2	-1.5	-9.1	9.3	20.0	1.1
8	3671-3677	0.0	-0.5	0.0	1.8	0.0	0.0	1.7	0.0	-2.1	3.7	45.0	11.1

Locations of the most critical sections for each component are provided in the following:

Comp. No. <sup>1</sup>	Section Location			
	Inside Node		Outside Node	
	x (in)	y (in)	z (in)	x (in)
1	29.820	6.20	29.820	0.75
2	35.50	16.40	37.50	16.40
3	35.50	171.40	37.50	171.40
4	35.50	142.40	37.00	142.40
5	40.70	163.40	43.35	163.40
6	37.655	179.40	37.50	175.40
7	37.655	179.40	37.655	185.40
8	24.289	188.46	24.289	193.71

<sup>1</sup> Refer to Figure 2.10.2-33 for cask component identification.

Table 2.10.4-46 Critical  $P_m + P_b$  Stress Summary; 1-Foot Top End Drop; Drop Orientation = 0 Degrees; 2-D Model; Condition 2

Condition 2: -20°F Ambient with Contents

Comp. No. <sup>1</sup>	Section Cut Node-Node	P <sub>m</sub> + P <sub>b</sub> Stresses (ksi)						Principal Stresses (ksi)			Allow. Stress	Margin of Safety	
		S <sub>x</sub>	S <sub>y</sub>	S <sub>z</sub>	S <sub>xy</sub>	S <sub>yz</sub>	S <sub>xz</sub>	S1	S2	S3			
1	16- 20	-1.3	0.0	-1.3	0.0	0.0	0.0	0.0	-1.3	-1.3	1.3	28.7	21.1
2	371- 374	0.1	-1.3	0.1	-0.1	0.0	0.0	0.1	0.1	-1.3	1.4	27.7	18.8
3	2711-2714	0.0	-4.4	1.2	0.3	0.0	0.0	1.2	0.0	-4.4	5.6	47.1	7.4
4	2276-2279	0.0	-2.1	0.3	0.0	0.0	0.0	0.3	0.0	-2.1	2.4	29.4	11.3
5	2599-2603	-1.7	0.0	0.6	-0.1	0.0	0.0	0.6	0.0	-1.7	2.3	30.0	12.0
6	7065-2784	4.2	-7.5	-0.9	0.6	0.0	0.0	4.3	-0.9	-7.5	11.8	30.0	1.6
7	3107-3108	14.0	-6.0	-0.6	0.2	0.0	0.0	14.0	-0.6	-6.0	20.0	30.0	0.5
8	3801-3807	18.6	-0.6	18.6	0.0	0.0	0.0	18.6	18.6	-0.6	19.2	67.5	2.5

Locations of the most critical sections for each component are provided in the following:

Comp. No. <sup>1</sup>	Section Location			
	Inside Node		Outside Node	
	x (in)	y (in)	z (in)	x (in)
1	1.42	6.20	1.42	0.75
2	35.50	15.40	37.50	15.40
3	35.50	171.40	37.50	171.40
4	35.50	142.40	37.00	142.40
5	40.70	163.40	43.35	163.40
6	38.608	179.40	38.567	175.40
7	26.158	187.40	26.158	188.40
8	0.0	188.46	0.0	193.71

<sup>1</sup> Refer to Figure 2.10.2-33 for cask component identification.

Table 2.10.4-47 Critical  $S_n$  Stress Summary; 1-Foot Top End Drop; Drop Orientation = 0 Degrees; 2-D Model; Condition 2  
Condition 2: -20°F Ambient with Contents

Comp. No. <sup>1</sup>	Section Cut Node-Node	$S_n$ Stresses (ksi)						Principal Stresses (ksi)				Allow. Stress $3.0 S_n$
		$S_x$	$S_y$	$S_z$	$S_{xy}$	$S_{yz}$	$S_{zx}$	S1	S2	S3	S.L.	
1	306-310	1.1	-2.0	0.8	0.0	0.0	0.0	1.1	0.8	-2.0	3.1	57.6
2	371-374	0.1	-4.0	-1.3	0.1	0.0	0.0	0.1	-1.3	-4.0	4.1	55.5
3	2531-2534	0.0	-5.4	0.0	-0.1	0.0	0.0	0.0	0.0	-5.4	5.4	94.2
4	2201-2204	0.0	-5.8	-0.7	0.0	0.0	0.0	0.0	-0.7	-5.8	5.7	58.8
5	1039-1043	0.0	4.4	2.0	0.0	0.0	0.0	4.4	2.0	0.0	4.4	60.0
6	7065-2784	4.8	-7.4	-0.2	-0.4	0.0	0.0	4.8	-0.2	-7.4	12.1	60.0
7	3107-3108	14.4	-5.8	-0.4	0.2	0.0	0.0	14.4	-0.4	-5.8	20.1	60.0
8	3801-3807	19.2	-0.6	19.2	0.0	0.0	0.0	19.2	19.2	-0.6	19.7	135.0

Locations of the most critical sections for each component are provided in the following:

Comp. No. <sup>1</sup>	Section Location			
	Inside Node		Outside Node	
	x (in)	y (in)	z (in)	x (in)
1	39.44	6.20	39.44	0.75
2	35.50	15.40	37.50	15.40
3	35.50	159.40	37.00	159.40
4	35.50	137.40	37.00	137.40
5	40.70	59.40	43.35	59.40
6	38.608	179.40	38.567	175.40
7	26.158	187.40	26.158	188.40
8	0.0	188.46	0.0	193.71

<sup>1</sup> Refer to Figure 2.10.2-33 for cask component identification.

Table 2.10.4-48 Critical P<sub>m</sub> Stress Summary; 1-Foot Top End Drop; Drop Orientation = 0 Degrees; 2-D Model; Condition 3

Condition 3: -20°F ambient without Contents

Comp. No. <sup>1</sup>	Section Cut Node-Node	P <sub>m</sub> Stresses (ksi)						Principal Stresses (ksi)			Allow. Stress	Margin of Safety	
		S <sub>x</sub>	S <sub>y</sub>	S <sub>z</sub>	S <sub>xy</sub>	S <sub>yz</sub>	S <sub>xz</sub>	S1	S2	S3			
1	206- 210	-0.2	0.0	-0.2	-0.1	0.0	0.0	0.0	-0.2	-0.2	0.3	19.2	63.0
2	386- 389	0.0	-0.8	0.3	0.0	0.0	0.0	0.3	0.0	-0.8	1.0	18.5	17.5
3	2711-2714	0.0	-1.8	2.0	0.3	0.0	0.0	2.0	0.0	-1.8	3.9	31.4	7.1
4	2261-2264	0.0	-2.1	0.3	0.0	0.0	0.0	0.3	0.0	-2.1	2.4	19.6	7.2
5	2599-2603	-1.5	0.0	0.7	-0.1	0.0	0.0	0.7	0.0	-1.6	2.2	20.0	8.1
6	7064-2774	0.1	3.8	1.6	1.3	0.0	0.0	4.2	1.6	-0.3	4.5	20.0	3.4
7	3021-3026	0.2	-9.1	-1.5	0.1	0.0	0.0	0.2	-1.5	-9.1	9.3	20.0	1.1
8	3671-3677	0.0	-0.4	0.0	1.5	0.0	0.0	1.4	0.0	-1.7	3.1	45.0	13.4

Locations of the most critical sections for each component are provided in the following:

Comp. No. <sup>1</sup>	Section Location			
	Inside Node		Outside Node	
	x (in)	y (in)	z (in)	x (in)
1	28.40	6.20	28.40	0.75
2	35.50	16.40	37.50	16.40
3	35.50	171.40	37.50	171.40
4	35.50	141.40	37.00	141.40
5	40.70	163.40	43.35	163.40
6	37.655	179.40	37.50	175.40
7	37.655	179.40	37.655	185.40
8	24.289	188.46	24.289	193.71

<sup>1</sup> Refer to Figure 2.10.2-33 for cask component identification.

Table 2.10.4-49 Critical  $P_m + P_b$  Stress Summary; 1-Foot Top End Drop; Drop Orientation = 0 Degrees; 2-D Model; Condition 3

Condition 3: -20°F Ambient without Contents

Comp. No. <sup>1</sup>	Section Cut Node-Node	$P_m + P_b$ Stresses (ksi)							Principal Stresses (ksi)			Allow. S.I. Stress	Margin of Safety
		$S_1$	$S_2$	$S_3$	$S_4$	$S_5$	$S_6$	$S_1$	$S_2$	$S_3$			
1	6- 20	-1.3	0.0	-1.3	0.0	0.0	0.0	0.0	-1.3	-1.3	1.3	28.7	21.1
2	371- 374	0.1	-1.3	0.1	-0.1	0.0	0.0	0.1	0.1	-1.3	1.4	27.7	18.8
3	2711-2714	0.0	-4.7	1.3	0.3	0.0	0.0	1.3	0.0	-4.7	6.0	47.1	6.9
4	2276-2279	0.0	-2.2	0.3	0.0	0.0	0.0	0.3	0.0	-2.2	2.5	29.4	10.8
5	2599-2603	-1.7	0.0	0.6	-0.1	0.0	0.0	0.6	0.0	-1.7	2.3	30.0	12.0
6	7065-2784	4.8	-6.8	-0.6	0.6	0.0	0.0	4.8	-0.6	-6.9	11.7	30.0	1.6
7	3051-3056	0.2	-16.3	1.7	0.9	0.0	0.0	1.7	0.3	-16.3	18.0	30.0	0.7
8	3801-3807	16.8	-0.7	16.8	0.0	0.0	0.0	16.8	16.8	-0.7	17.6	67.5	2.8

Locations of the most critical sections for each component are provided in the following:

Comp. No. <sup>1</sup>	Section Location			
	Inside Node		Outside Node	
	x (in)	y (in)	z (in)	x (in)
1	1.42	6.20	1.42	0.75
2	35.50	15.40	37.50	15.40
3	35.50	171.40	37.50	171.40
4	35.50	142.40	37.00	142.40
5	40.70	163.40	43.35	163.40
6	38.608	179.40	38.567	175.40
7	35.50	179.40	35.50	185.40
8	0.0	188.46	0.0	193.71

<sup>1</sup> Refer to Figure 2.10.2-33 for cask component identification.

Table 2.10.4-50 Critical  $S_n$  Stress Summary; 1-Foot Top End Drop; Drop Orientation = 0 Degrees; 2-D Model; Condition 3

Condition 3: -20°F Ambient without Contents

Comp. No. <sup>1</sup>	Section Cut Node-Node	$S_n$ Stresses (ksi)						Principal Stresses (ksi)				Allow. Stress 3.0 $S_n$
		$S_x$	$S_y$	$S_z$	$S_{xy}$	$S_{yz}$	$S_{zx}$	S1	S2	S3	S.L.	
1	16- 20	-1.5	0.0	-1.5	0.0	0.0	0.0	0.0	-1.5	-1.5	1.5	57.6
2	371- 374	0.1	-2.7	-0.8	-0.3	0.0	0.0	0.2	-0.8	-2.8	2.9	55.5
3	2711-2714	0.0	-4.9	0.3	0.2	0.0	0.0	0.3	0.0	-4.9	5.2	94.2
4	851- 854	0.0	-1.7	-2.9	0.0	0.0	0.0	0.0	-1.7	-2.9	2.9	58.8
5	2599-2603	-1.4	0.0	0.6	-0.1	0.0	0.0	0.6	0.0	-1.4	2.0	60.0
6	7065-2784	4.1	-7.1	-1.1	0.7	0.0	0.0	4.1	-1.1	-7.1	11.3	60.0
7	3051-3056	0.7	-15.9	1.4	1.1	0.0	0.0	1.4	0.8	-16.0	17.4	60.0
8	3801-3807	17.9	-0.5	17.9	0.0	0.0	0.0	17.9	17.9	-0.5	18.4	135.0

Locations of the most critical sections for each component are provided in the following:

Comp. No. <sup>1</sup>	Section Location			
	Inside Node		Outside Node	
	x (in)	y (in)	z (in)	x (in)
1	1.42	6.20	1.42	0.75
2	35.50	15.40	37.50	15.40
3	35.50	171.40	37.50	171.40
4	35.50	47.40	37.00	47.40
5	40.70	163.40	43.35	163.40
6	38.608	179.40	38.567	175.40
7	35.50	179.40	35.50	185.40
8	0.0	188.46	0.0	193.71

<sup>1</sup> Refer to Figure 2.10.2-33 for cask component identification.

Table 2.10.4-51 Primary Stresses; 1-Foot Bottom End Drop; Drop Orientation = 0 Degrees;  
2-D Model; Condition 1

Condition 1: 100°F Ambient with Contents

Stress Points Section <sup>1</sup> Node	Stress Components (ksi)						Principal Stresses (ksi)		
	$S_x$	$S_y$	$S_z$	$S_{xy}$	$S_{yz}$	$S_{xz}$	S1	S2	S3
A1	1	7.0	-0.4	7.0	0.0	0.0	7.0	7.0	-0.4
A2	2	4.0	-0.4	4.0	0.0	0.0	4.0	4.0	-0.4
A3	3	1.0	-0.5	1.0	0.0	0.0	1.0	1.0	-0.5
A4	4	-2.0	-0.6	-2.0	0.0	0.0	-0.6	-2.0	-2.0
A5	5	-5.0	-0.6	-5.0	0.0	0.0	-0.6	-5.0	-5.0
B1	6	4.0	-0.7	4.0	0.0	0.0	4.0	4.0	-0.7
B2	7	1.4	-0.7	1.4	0.0	0.0	1.4	1.4	-0.7
B3	8	-1.2	-0.7	-1.2	0.0	0.0	-0.7	-1.2	-1.2
B4	9	-3.9	-0.8	-3.9	0.0	0.0	-0.8	-3.9	-3.9
B5	10	-6.4	-0.8	-6.4	0.0	0.0	-0.8	-6.4	-6.4
C1	251	-3.5	-4.1	0.1	-0.7	0.0	0.1	-3.0	-4.6
C2	252	-0.6	-1.7	0.9	-0.5	0.0	0.9	-0.4	-1.9
C3	253	1.0	-0.8	0.9	-0.6	0.0	1.2	0.9	-1.0
C4	254	3.1	-0.5	0.9	-0.5	0.0	3.2	0.9	-0.6
C5	255	5.4	-0.5	0.9	-0.3	0.0	5.4	0.9	-0.5
D1	306	-6.0	-5.3	-2.8	-1.8	0.0	-2.8	-3.8	-7.5
D2	307	-1.6	-3.8	-1.6	-0.8	0.0	-1.3	-1.6	-4.0
D3	308	-0.4	-2.0	-1.3	0.0	0.0	-0.4	-1.3	-2.0
D4	309	0.8	-1.3	-1.3	0.2	0.0	0.8	-1.3	-1.3
D5	310	2.2	-1.0	-1.3	0.2	0.0	2.2	-1.0	-1.3
E1	305	5.1	-1.7	1.1	-1.2	0.0	5.3	1.1	-1.9
E2	315	2.4	-2.4	0.4	-1.5	0.0	2.9	0.4	-2.9
E3	325	1.0	-1.9	0.1	-1.5	0.0	1.7	0.1	-2.5
E4	335	0.5	-1.5	0.1	-1.2	0.0	1.0	0.1	-2.1
E5	345	0.2	-1.3	0.1	-0.7	0.0	0.5	0.1	-1.5
E6	355	0.1	-1.2	0.1	-0.4	0.0	0.2	0.1	-1.3
F1	251	-3.5	-4.1	0.1	-0.7	0.0	0.1	-3.0	-4.6
F2	261	-2.6	-1.9	0.9	-0.3	0.0	0.9	-1.8	-2.7
F3	271	-1.8	-0.2	1.5	0.0	0.0	1.5	-0.2	-1.8
F4	281	-1.8	1.1	1.7	-0.1	0.0	1.7	1.1	-1.8
G1	311	-2.7	-4.3	-0.3	-0.1	0.0	-0.3	-2.6	-4.3



Table 2.10.4-51 Primary Stresses; 1-Foot Bottom End Drop; Drop Orientation = 0 Degrees;  
2-D Model; Condition 1 (continued)

Stress Points Section <sup>1</sup> Node		Stress Components (ksi)						Principal Stresses (ksi)		
		S <sub>x</sub>	S <sub>y</sub>	S <sub>z</sub>	S <sub>xy</sub>	S <sub>yz</sub>	S <sub>xz</sub>	S1	S2	S3
G2	321	-1.9	-2.7	0.3	0.1	0.0	0.0	0.3	-1.9	-2.7
G3	331	-1.0	-1.6	0.8	0.3	0.0	0.0	0.8	-0.8	-1.8
G4	341	-0.4	-0.6	1.2	0.2	0.0	0.0	1.2	-0.2	-0.7
G5	351	-0.2	0.9	1.6	0.1	0.0	0.0	1.6	0.9	-0.2
H1	581	-0.1	-1.0	1.3	0.0	0.0	0.0	1.3	-0.1	-1.0
H2	582	-0.1	-1.5	1.1	0.0	0.0	0.0	1.1	-0.1	-1.5
H3	583	-0.1	-2.0	1.0	0.1	0.0	0.0	1.0	-0.1	-2.0
H4	584	0.0	-2.7	0.8	0.2	0.0	0.0	0.8	0.0	-2.7
I1	589	0.0	-1.2	0.4	0.0	0.0	0.0	0.4	0.0	-1.2
I2	590	0.0	-1.4	0.3	0.0	0.0	0.0	0.3	0.0	-1.4
I3	591	0.0	-1.6	0.3	0.0	0.0	0.0	0.3	0.0	-1.6
I4	592	0.0	-1.8	0.2	0.0	0.0	0.0	0.2	0.0	-1.8
I5	593	0.0	-2.0	0.1	0.0	0.0	0.0	0.1	0.0	-2.0
J1	971	-0.1	-1.7	1.2	0.0	0.0	0.0	1.2	-0.1	-1.7
J2	972	0.0	-1.7	1.2	0.0	0.0	0.0	1.2	0.0	-1.7
J3	973	0.0	-1.7	1.2	0.0	0.0	0.0	1.2	0.0	-1.7
J4	974	0.0	-1.7	1.2	0.0	0.0	0.0	1.2	0.0	-1.7
K1	979	0.0	-1.4	0.0	0.0	0.0	0.0	0.0	0.0	-1.4
K2	980	0.0	-1.4	0.0	0.0	0.0	0.0	0.0	0.0	-1.4
K3	981	0.0	-1.4	0.0	0.0	0.0	0.0	0.0	0.0	-1.4
K4	982	0.0	-1.4	0.0	0.0	0.0	0.0	0.0	0.0	-1.4
K5	983	0.0	-1.4	0.0	0.0	0.0	0.0	0.0	0.0	-1.4
L1	1601	-0.1	-1.3	1.2	0.0	0.0	0.0	1.2	-0.1	-1.3
L2	1602	0.0	-1.3	1.2	0.0	0.0	0.0	1.2	0.0	-1.3
L3	1603	0.0	-1.3	1.2	0.0	0.0	0.0	1.2	0.0	-1.3
L4	1604	0.0	-1.3	1.2	0.0	0.0	0.0	1.2	0.0	-1.3
M1	1609	0.0	-1.1	0.0	0.0	0.0	0.0	0.0	0.0	-1.1
M2	1610	0.0	-1.1	0.0	0.0	0.0	0.0	0.0	0.0	-1.1
M3	1611	0.0	-1.1	0.0	0.0	0.0	0.0	0.0	0.0	-1.1
M4	1612	0.0	-1.1	0.0	0.0	0.0	0.0	0.0	0.0	-1.1
M5	1613	0.0	-1.1	0.0	0.0	0.0	0.0	0.0	0.0	-1.1
N1	2216	-0.1	-1.0	1.2	0.0	0.0	0.0	1.2	-0.1	-1.0
N2	2217	0.0	-1.0	1.2	0.0	0.0	0.0	1.2	0.0	-1.0

Table 2.10.4-51 Primary Stresses; 1-Foot Bottom End Drop; Drop Orientation = 0 Degrees;  
2-D Model; Condition 1 (continued)

Stress Points Section <sup>1</sup> Node		Stress Components (ksi)						Principal Stresses (ksi)		
		S <sub>x</sub>	S <sub>y</sub>	S <sub>z</sub>	S <sub>xy</sub>	S <sub>yz</sub>	S <sub>xz</sub>	S1	S2	S3
N3	2218	0.0	-0.9	1.2	0.0	0.0	0.0	1.2	0.0	-0.9
N4	2219	0.0	-0.9	1.2	0.0	0.0	0.0	1.2	0.0	-0.9
O1	2224	0.0	-0.7	0.0	0.0	0.0	0.0	0.0	0.0	-0.7
O2	2225	0.0	-0.7	0.0	0.0	0.0	0.0	0.0	0.0	-0.7
O3	2226	0.0	-0.7	0.0	0.0	0.0	0.0	0.0	0.0	-0.7
O4	2227	0.0	-0.7	0.0	0.0	0.0	0.0	0.0	0.0	-0.7
O5	2228	0.0	-0.7	0.0	0.0	0.0	0.0	0.0	0.0	-0.7
P1	2546	-0.1	-0.6	1.0	0.0	0.0	0.0	1.0	-0.1	-0.6
P2	2547	0.0	-0.7	1.0	0.0	0.0	0.0	1.0	0.0	-0.7
P3	2548	0.0	-0.8	1.0	0.0	0.0	0.0	1.0	0.0	-0.8
P4	2549	0.0	-0.9	0.9	0.0	0.0	0.0	0.9	0.0	-0.9
Q1	2554	0.0	-0.4	0.1	0.0	0.0	0.0	0.1	0.0	-0.4
Q2	2555	0.0	-0.5	0.1	0.0	0.0	0.0	0.1	0.0	-0.5
Q3	2556	0.0	-0.5	0.1	0.0	0.0	0.0	0.1	0.0	-0.5
Q4	2557	0.0	-0.6	0.1	0.0	0.0	0.0	0.1	0.0	-0.6
Q5	2558	0.0	-0.7	0.0	0.0	0.0	0.0	0.0	0.0	-0.7
R1	2771	-0.3	-1.5	0.2	0.2	0.0	0.0	0.2	-0.3	-1.5
R2	2772	-0.2	-0.9	0.4	0.2	0.0	0.0	0.4	-0.2	-1.0
R3	2773	-0.4	-0.4	0.4	0.3	0.0	0.0	0.4	-0.1	-0.7
R4	2774	-1.0	0.8	0.6	0.3	0.0	0.0	0.9	0.6	-1.0
S1	2779	-0.9	-1.0	-0.1	0.0	0.0	0.0	-0.1	-0.9	-1.0
S2	2780	-0.5	-0.6	0.1	0.0	0.0	0.0	0.1	-0.5	-0.6
S3	2781	-0.3	-0.3	0.3	-0.1	0.0	0.0	0.3	-0.2	-0.4
S4	2782	-0.1	0.0	0.4	-0.1	0.0	0.0	0.4	0.0	-0.1
S5	2783	0.0	0.4	0.5	0.0	0.0	0.0	0.5	0.4	0.0
T1	7066	0.5	0.4	0.5	0.2	0.0	0.0	0.7	0.5	0.2
T2	7067	0.6	-0.3	0.2	0.0	0.0	0.0	0.6	0.2	-0.3
T3	7068	0.4	-0.4	0.2	0.0	0.0	0.0	0.4	0.2	-0.4
T4	7069	0.2	-0.4	0.1	0.0	0.0	0.0	0.2	0.1	-0.4
T5	7070	0.1	-0.4	0.1	0.0	0.0	0.0	0.1	0.1	-0.4
T6	7071	0.1	-0.5	0.1	0.0	0.0	0.0	0.1	0.1	-0.5
T7	7072	0.0	-0.6	0.1	0.0	0.0	0.0	0.1	0.0	-0.6
U1	3051	-0.3	-2.2	-0.2	0.5	0.0	0.0	-0.1	-0.2	-2.3

Table 2.10.4-51 Primary Stresses; 1-Foot Bottom End Drop; Drop Orientation = 0 Degrees;  
2-D Model; Condition 1 (continued)

Stress Points Section <sup>1</sup>	Node	Stress Components (ksi)						Principal Stresses (ksi)		
		S <sub>x</sub>	S <sub>y</sub>	S <sub>z</sub>	S <sub>xy</sub>	S <sub>yz</sub>	S <sub>xz</sub>	S1	S2	S3
U2	3052	-0.4	-2.5	-0.5	0.5	0.0	0.0	-0.3	-0.5	-2.6
U3	3053	0.0	-2.5	-0.5	0.2	0.0	0.0	0.0	-0.5	-2.5
U4	3054	0.2	-2.0	-0.5	-0.4	0.0	0.0	0.2	-0.5	-2.1
U5	3055	-0.2	-1.3	-0.4	-0.5	0.0	0.0	0.0	-0.4	-1.4
U6	3056	1.0	-0.2	0.2	-0.1	0.0	0.0	1.0	0.2	-0.2
V1	3611	1.0	0.0	0.9	0.0	0.0	0.0	1.0	0.9	0.0
V2	3612	0.5	-0.1	0.5	0.0	0.0	0.0	0.5	0.5	-0.1
V3	3613	0.3	-0.3	0.2	0.0	0.0	0.0	0.3	0.2	-0.3
V4	3614	0.1	-0.6	-0.1	0.0	0.0	0.0	0.1	-0.1	-0.6
V5	3615	-0.2	-1.0	-0.5	0.0	0.0	0.0	-0.2	-0.5	-1.0
V6	3616	-0.4	-0.5	-0.6	0.0	0.0	0.0	-0.4	-0.5	-0.6
V7	3617	-1.2	0.4	-0.7	0.0	0.0	0.0	0.4	-0.7	-1.2
W1	3241	0.9	0.0	0.9	0.0	0.0	0.0	0.9	0.9	0.0
W2	3242	0.6	0.0	0.6	0.0	0.0	0.0	0.6	0.6	0.0
W3	3243	0.3	0.0	0.3	0.0	0.0	0.0	0.3	0.3	0.0
W4	3244	0.0	0.0	0.0	0.0	0.0	0.0	0.0	0.0	0.0
W5	3245	-0.2	0.0	-0.2	0.0	0.0	0.0	0.0	-0.2	-0.2
W6	3246	-0.5	0.0	-0.5	0.0	0.0	0.0	0.0	-0.5	-0.5
X1	3801	1.4	0.0	1.4	0.0	0.0	0.0	1.4	1.4	0.0
X2	3802	1.0	0.0	1.0	0.0	0.0	0.0	1.0	1.0	0.0
X3	3803	0.5	0.0	0.5	0.0	0.0	0.0	0.5	0.5	0.0
X4	3804	0.0	0.0	0.0	0.0	0.0	0.0	0.0	0.0	0.0
X5	3805	-0.4	0.0	-0.4	0.0	0.0	0.0	0.0	-0.4	-0.4
X6	3806	-0.9	0.0	-0.9	0.0	0.0	0.0	0.0	-0.9	-0.9
X7	3807	-1.4	0.0	-1.4	0.0	0.0	0.0	0.0	-1.4	-1.4

<sup>1</sup> Refer to Figure 2.10.2-34 for the identification of the representative sections.

Table 2.10.4-52 Primary + Secondary Stresses; 1-Foot Bottom End Drop; Drop Orientation = 0 Degrees; 2-D Model; Condition 1

Condition 1: 100°F Ambient with Contents

Stress Points		Stress Components (ksi)						Principal Stresses (ksi)		
Section <sup>1</sup>	Node	S <sub>x</sub>	S <sub>y</sub>	S <sub>z</sub>	S <sub>xy</sub>	S <sub>xz</sub>	S <sub>yz</sub>	S1	S2	S3
A1	1	6.9	-0.4	6.9	0.0	0.0	0.0	6.9	6.9	-0.4
A2	2	3.7	-0.4	3.7	0.0	0.0	0.0	3.7	3.7	-0.4
A3	3	0.5	-0.5	0.5	0.0	0.0	0.0	0.5	0.5	-0.5
A4	4	-2.7	-0.6	-2.7	0.0	0.0	0.0	-0.6	-2.7	-2.7
A5	5	-6.0	-0.6	-6.0	0.0	0.0	0.0	-0.6	-6.0	-6.0
B1	6	6.0	-0.7	6.0	0.0	0.0	0.0	6.0	6.0	-0.7
B2	7	3.1	-0.7	3.1	0.0	0.0	0.0	3.1	3.1	-0.7
B3	8	0.1	-0.7	0.1	0.0	0.0	0.0	0.1	0.1	-0.7
B4	9	-2.9	-0.8	-2.9	0.0	0.0	0.0	-0.8	-2.9	-2.9
B5	10	-5.8	-0.8	-5.8	0.0	0.0	0.0	-0.8	-5.8	-5.8
C1	251	-3.9	-6.8	-0.4	-1.3	0.0	0.0	-0.4	-3.4	-7.3
C2	252	-0.3	-3.0	0.6	-1.1	0.0	0.0	0.6	0.1	-3.4
C3	253	0.7	-1.8	0.2	-1.1	0.0	0.0	1.1	0.2	-2.2
C4	254	2.2	-1.6	-0.4	-0.8	0.0	0.0	2.4	-0.4	-1.7
C5	255	3.8	-1.6	-1.1	-0.5	0.0	0.0	3.8	-1.1	-1.6
D1	306	-0.5	1.3	0.6	0.2	0.0	0.0	1.3	0.6	-0.6
D2	307	-0.7	0.0	-0.1	0.6	0.0	0.0	0.3	-0.1	-1.0
D3	308	-0.1	-0.5	-0.4	0.5	0.0	0.0	0.2	-0.4	-0.8
D4	309	0.4	-0.7	-0.7	0.3	0.0	0.0	0.4	-0.7	-0.8
D5	310	0.7	-0.8	-0.9	0.2	0.0	0.0	0.7	-0.8	-0.9
E1	305	4.0	1.9	1.4	-0.6	0.0	0.0	4.1	1.7	1.4
E2	315	1.7	0.1	0.6	-0.1	0.0	0.0	1.7	0.6	0.1
E3	325	1.0	-0.4	0.3	0.1	0.0	0.0	1.0	0.3	-0.4
E4	335	0.5	-0.7	0.2	0.2	0.0	0.0	0.6	0.2	-0.7
E5	345	0.2	-1.2	0.0	0.1	0.0	0.0	0.3	0.0	-1.2
E6	355	0.2	-2.0	-0.2	0.0	0.0	0.0	0.2	-0.2	-2.0
F1	251	-3.9	-6.8	-0.4	-1.3	0.0	0.0	-0.4	-3.4	-7.3
F2	261	-2.6	-2.9	0.9	-0.7	0.0	0.0	0.9	-2.0	-3.5
F3	271	-1.0	-0.1	1.9	-0.6	0.0	0.0	1.9	0.2	-1.3
F4	281	-0.7	3.1	2.6	-1.1	0.0	0.0	3.4	2.6	-1.0
G1	311	-5.7	-3.6	-1.0	1.3	0.0	0.0	-1.0	-3.0	-6.3

Table 2.10.4-52 Primary + Secondary Stresses; 1-Foot Bottom End Drop; Drop Orientation = 0 Degrees; 2-D Model; Condition 1 (continued)

Stress Points		Stress Components (ksi)						Principal Stresses (ksi)		
Section <sup>1</sup>	Node	S <sub>x</sub>	S <sub>y</sub>	S <sub>z</sub>	S <sub>xy</sub>	S <sub>xz</sub>	S <sub>yz</sub>	S1	S2	S3
G2	321	-4.7	0.6	0.4	1.1	0.0	0.0	0.8	0.4	-4.9
G3	331	-2.3	2.8	1.7	0.4	0.0	0.0	2.8	1.7	-2.4
G4	341	-0.9	5.0	2.6	0.2	0.0	0.0	5.0	2.6	-0.9
G5	351	-0.4	8.0	3.6	0.0	0.0	0.0	8.0	3.6	-0.4
H1	581	-0.1	-0.4	1.1	0.0	0.0	0.0	1.1	-0.1	-0.4
H2	582	-0.1	-1.6	0.8	0.1	0.0	0.0	0.8	-0.1	-1.6
H3	583	0.0	-2.8	0.6	0.2	0.0	0.0	0.6	0.0	-2.8
H4	584	-0.2	-4.3	0.3	0.3	0.0	0.0	0.3	-0.2	-4.3
I1	589	-0.3	3.8	2.8	0.0	0.0	0.0	3.8	2.8	-0.3
I2	590	-0.2	3.8	2.9	0.0	0.0	0.0	3.8	2.9	-0.2
I3	591	-0.1	3.8	3.0	0.1	0.0	0.0	3.8	3.0	-0.1
I4	592	-0.1	3.8	3.1	0.1	0.0	0.0	3.8	3.1	-0.1
I5	593	0.0	3.8	3.2	0.0	0.0	0.0	3.8	3.2	0.0
J1	971	-0.1	-3.9	0.1	0.0	0.0	0.0	0.1	-0.1	-3.9
J2	972	0.0	-2.7	0.8	0.0	0.0	0.0	0.8	0.0	-2.7
J3	973	0.0	-1.5	1.6	0.0	0.0	0.0	1.6	0.0	-1.5
J4	974	0.0	-0.3	2.3	0.0	0.0	0.0	2.3	0.0	-0.3
K1	979	-0.3	1.8	3.8	0.0	0.0	0.0	3.8	1.8	-0.3
K2	980	-0.3	2.9	4.5	0.0	0.0	0.0	4.5	2.9	-0.3
K3	981	-0.2	4.0	5.1	0.0	0.0	0.0	5.1	4.0	-0.2
K4	982	-0.1	5.1	5.7	0.0	0.0	0.0	5.7	5.1	-0.1
K5	983	0.0	6.1	6.2	0.0	0.0	0.0	6.2	6.1	0.0
L1	1601	-0.1	-3.1	0.1	0.0	0.0	0.0	0.1	-0.1	-3.1
L2	1602	0.0	-2.2	0.8	0.0	0.0	0.0	0.8	0.0	-2.2
L3	1603	0.0	-1.3	1.5	0.0	0.0	0.0	1.5	0.0	-1.3
L4	1604	0.0	-0.4	2.2	0.0	0.0	0.0	2.2	0.0	-0.4
M1	1609	-0.4	2.3	4.6	0.0	0.0	0.0	4.6	2.3	-0.4
M2	1610	-0.3	3.3	5.3	0.0	0.0	0.0	5.3	3.3	-0.3
M3	1611	-0.2	4.3	6.0	0.0	0.0	0.0	6.0	4.3	-0.2
M4	1612	-0.1	5.4	6.6	0.0	0.0	0.0	6.6	5.4	-0.1
M5	1613	0.0	6.4	7.2	0.0	0.0	0.0	7.2	6.4	0.0
N1	2216	-0.1	-3.0	-0.2	0.0	0.0	0.0	-0.1	-0.2	-3.0
N2	2217	0.0	-1.9	0.5	0.0	0.0	0.0	0.5	0.0	-1.9

Table 2.10.4-52 Primary + Secondary Stresses; 1-Foot Bottom End Drop; Drop Orientation = 0 Degrees; 2-D Model; Condition 1 (continued)

Stress Points		Stress Components (ksi)						Principal Stresses (ksi)		
Section <sup>1</sup>	Node	S <sub>x</sub>	S <sub>y</sub>	S <sub>z</sub>	S <sub>xy</sub>	S <sub>xz</sub>	S <sub>yz</sub>	S1	S2	S3
N3	2218	0.0	-0.9	1.1	0.0	0.0	0.0	1.1	0.0	-0.9
N4	2219	0.0	0.2	1.7	0.0	0.0	0.0	1.7	0.2	0.0
O1	2224	-0.3	3.1	3.6	0.0	0.0	0.0	3.6	3.1	-0.3
O2	2225	-0.2	3.9	4.1	0.0	0.0	0.0	4.1	3.9	-0.2
O3	2226	-0.2	4.7	4.6	0.0	0.0	0.0	4.7	4.6	-0.2
O4	2227	-0.1	5.5	5.1	0.0	0.0	0.0	5.5	5.1	-0.1
O5	2228	0.0	6.3	5.6	0.0	0.0	0.0	6.3	5.6	0.0
P1	2546	0.0	-1.4	0.7	0.0	0.0	0.0	0.7	0.0	-1.4
P2	2547	0.0	-1.3	0.8	0.0	0.0	0.0	0.8	0.0	-1.3
P3	2548	0.1	-1.1	1.1	0.0	0.0	0.0	1.1	0.1	-1.1
P4	2549	-0.2	-1.1	1.1	0.0	0.0	0.0	1.1	-0.2	-1.1
Q1	2554	-0.1	4.3	2.3	0.0	0.0	0.0	4.3	2.3	-0.1
Q2	2555	-0.1	4.6	2.6	0.1	0.0	0.0	4.6	2.6	-0.1
Q3	2556	-0.1	4.9	2.8	0.1	0.0	0.0	4.9	2.8	-0.1
Q4	2557	0.0	5.2	3.1	0.1	0.0	0.0	5.2	3.1	0.0
Q5	2558	0.0	5.5	3.3	0.0	0.0	0.0	5.5	3.3	0.0
R1	2771	-0.6	1.3	-2.9	0.3	0.0	0.0	1.4	-0.6	-2.9
R2	2772	-0.9	-0.5	-2.9	0.4	0.0	0.0	-0.3	-1.2	-2.9
R3	2773	-2.0	-1.7	-3.1	0.5	0.0	0.0	-1.3	-2.4	-3.1
R4	2774	-4.0	-2.6	-3.3	0.3	0.0	0.0	-2.5	-3.3	-4.0
S1	2779	1.2	6.7	1.6	-2.0	0.0	0.0	7.4	1.6	0.6
S2	2780	1.5	5.1	1.6	-0.8	0.0	0.0	5.3	1.6	1.4
S3	2781	0.8	3.8	1.4	0.2	0.0	0.0	3.8	1.4	0.8
S4	2782	0.3	2.5	1.1	0.3	0.0	0.0	2.6	1.1	0.3
S5	2783	0.2	1.1	1.0	0.3	0.0	0.0	1.1	1.0	0.1
T1	7066	-0.9	-5.0	-0.1	-1.5	0.0	0.0	-0.1	-0.4	-5.5
T2	7067	-0.9	-3.1	0.4	-1.0	0.0	0.0	0.4	-0.5	-3.5
T3	7068	-0.6	-1.2	1.1	-0.6	0.0	0.0	1.1	-0.3	-1.6
T4	7069	-0.4	0.3	1.7	-0.4	0.0	0.0	1.7	0.4	-0.6
T5	7070	-0.2	1.6	2.2	-0.2	0.0	0.0	2.2	1.6	-0.3
T6	7071	-0.1	3.0	2.7	-0.1	0.0	0.0	3.0	2.7	-0.1
T7	7072	-0.1	4.5	3.2	0.0	0.0	0.0	4.5	3.2	-0.1
U1	3051	-1.4	-3.4	-2.5	0.6	0.0	0.0	-1.2	-2.5	-3.6

Table 2.10.4-52 Primary + Secondary Stresses; 1-Foot Bottom End Drop; Drop Orientation = 0 Degrees; 2-D Model; Condition 1 (continued)

Stress Points Section <sup>1</sup>	Node	Stress Components (ksi)						Principal Stresses (ksi)		
		S <sub>x</sub>	S <sub>y</sub>	S <sub>z</sub>	S <sub>xy</sub>	S <sub>xz</sub>	S <sub>yz</sub>	S1	S2	S3
U2	3052	-0.4	-3.4	-2.3	0.5	0.0	0.0	-0.3	-2.3	-3.5
U3	3053	0.2	-3.0	-1.9	0.0	0.0	0.0	0.2	-1.9	-3.0
U4	3054	0.4	-2.1	-1.6	-0.7	0.0	0.0	0.6	-1.6	-2.3
U5	3055	0.0	-1.0	-1.3	-0.8	0.0	0.0	0.4	-1.3	-1.4
U6	3056	1.7	-0.3	-0.5	-0.2	0.0	0.0	1.7	-0.3	-0.5
V1	3611	1.2	-0.1	-1.3	-0.1	0.0	0.0	1.2	-0.1	-1.3
V2	3612	0.8	-0.1	-1.0	-0.1	0.0	0.0	0.8	-0.1	-1.0
V3	3613	0.4	-0.4	-0.8	-0.1	0.0	0.0	0.5	-0.4	-0.8
V4	3614	0.2	-0.8	-0.7	-0.1	0.0	0.0	0.2	-0.7	-0.8
V5	3615	-0.1	-1.5	-0.7	-0.1	0.0	0.0	-0.1	-0.7	-1.6
V6	3616	-0.3	-0.7	-0.2	0.0	0.0	0.0	-0.2	-0.3	-0.7
V7	3617	-1.5	0.7	0.2	0.0	0.0	0.0	0.7	0.2	-1.5
W1	3241	2.7	0.0	2.7	0.0	0.0	0.0	2.7	2.7	0.0
W2	3242	2.2	0.0	2.2	0.0	0.0	0.0	2.2	2.2	0.0
W3	3243	1.7	0.0	1.7	0.0	0.0	0.0	1.7	1.7	0.0
W4	3244	1.2	0.0	1.2	0.0	0.0	0.0	1.2	1.2	0.0
W5	3245	0.7	0.0	0.7	0.0	0.0	0.0	0.7	0.7	0.0
W6	3246	0.2	0.0	0.2	0.0	0.0	0.0	0.2	0.2	0.0
X1	3801	-0.5	0.0	-0.5	0.0	0.0	0.0	0.0	-0.5	-0.5
X2	3802	-0.2	0.0	-0.2	0.0	0.0	0.0	0.0	-0.2	-0.2
X3	3803	0.2	0.0	0.2	0.0	0.0	0.0	0.2	0.2	0.0
X4	3804	0.5	0.0	0.5	0.0	0.0	0.0	0.5	0.5	0.0
X5	3805	0.8	0.0	0.8	0.0	0.0	0.0	0.8	0.8	0.0
X6	3806	1.1	0.0	1.1	0.0	0.0	0.0	1.1	1.1	0.0
X7	3807	1.5	0.0	1.5	0.0	0.0	0.0	1.5	1.5	0.0

<sup>1</sup> Refer to Figure 2.10.2-34 for the identification of the representative sections.

Table 2.10.4-53  $P_m$  Stresses; 1-Foot Bottom End Drop; Drop Orientation = 0 Degrees; 2-D Model; Condition 1

Condition 1: 100°F Ambient with Contents

Section <sup>1</sup>	Node - Node	Stress Components (ksi)						Principal Stresses (ksi)			
		$S_x$	$S_y$	$S_z$	$S_{xy}$	$S_{yz}$	$S_{xz}$	S1	S2	S3	S.L
A	1 - 5	1.0	-0.5	1.0	0.0	0.0	0.0	1.0	1.0	-0.5	1.5
B	6 - 10	-1.2	-0.7	-1.2	0.0	0.0	0.0	-0.7	-1.2	-1.2	0.5
C	251 - 255	1.1	-1.3	0.8	-0.5	0.0	0.0	1.2	0.8	-1.5	2.7
D	306 - 310	-0.8	-2.5	-1.6	-0.4	0.0	0.0	-0.7	-1.6	-2.6	1.9
E	305 - 355	1.7	-1.8	0.3	-1.2	0.0	0.0	2.1	0.3	-2.1	4.2
F	251 - 281	-2.4	-1.2	1.1	-0.2	0.0	0.0	1.1	-1.2	-2.4	3.5
G	311 - 351	-1.2	-1.6	0.7	0.2	0.0	0.0	0.7	-1.1	-1.7	2.4
H	581 - 584	-0.1	-1.8	1.0	0.1	0.0	0.0	1.0	-0.1	-1.8	2.9
I	589 - 593	0.0	-1.6	0.3	0.0	0.0	0.0	0.3	0.0	-1.6	1.9
J	971 - 974	0.0	-1.7	1.2	0.0	0.0	0.0	1.2	0.0	-1.7	2.8
K	979 - 983	0.0	-1.4	0.0	0.0	0.0	0.0	0.0	0.0	-1.4	1.4
L	1601 - 1604	0.0	-1.3	1.2	0.0	0.0	0.0	1.2	0.0	-1.3	2.5
M	1609 - 1613	0.0	-1.1	0.0	0.0	0.0	0.0	0.0	0.0	-1.1	1.1
N	2216 - 2219	0.0	-1.0	1.2	0.0	0.0	0.0	1.2	0.0	-1.0	2.1
O	2224 - 2228	0.0	-0.7	0.0	0.0	0.0	0.0	0.0	0.0	-0.7	0.7
P	2546 - 2549	0.0	-0.7	1.0	0.0	0.0	0.0	1.0	0.0	-0.7	1.7
Q	2554 - 558	0.0	-0.5	0.1	0.0	0.0	0.0	0.1	0.0	-0.5	0.6
R	2771 - 2774	-0.4	-0.5	0.4	0.2	0.0	0.0	0.4	-0.2	-0.7	1.1
S	2779 - 2783	-0.3	-0.3	0.2	0.0	0.0	0.0	0.2	-0.3	-0.4	0.6
T	7066 - 7072	0.3	-0.4	0.2	0.0	0.0	0.0	0.3	0.2	-0.4	0.6
U	3051 - 3056	0.0	-1.9	-0.4	0.0	0.0	0.0	0.0	-0.4	-1.9	1.9
V	3611 - 3617	0.0	-0.3	-0.1	0.0	0.0	0.0	0.0	-0.1	-0.3	0.4
W	3241 - 3246	0.2	0.0	0.2	0.0	0.0	0.0	0.2	0.2	0.0	0.2
X	3801 - 3807	0.0	0.0	0.0	0.0	0.0	0.0	0.0	0.0	0.0	0.0

<sup>1</sup> Refer to Figure 2.10.2-34 for the identification of the representative sections.



Table 2.10.4-54  $P_m + P_b$  Stresses; 1-Foot Bottom End Drop; Drop Orientation = 0 Degrees;  
2-D Model; Condition 1

Condition 1: 100°F Ambient with Contents

Section <sup>1</sup>	Node - Node	Stress Components (ksi)						Principal Stresses (ksi)			
		$S_x$	$S_y$	$S_z$	$S_{xy}$	$S_{yz}$	$S_{xz}$	S1	S2	S3	S.L
AI	1 - 5	7.0	-0.4	7.0	0.0	0.0	0.0	7.0	7.0	-0.4	7.4
BO	6 - 10	-6.5	-0.8	-6.5	0.0	0.0	0.0	-0.8	-6.5	-6.5	5.6
CO	251 - 255	5.3	-0.5	1.1	-0.5	0.0	0.0	5.3	1.1	-0.6	5.9
DO	306 - 310	2.7	-1.0	-1.0	-0.4	0.0	0.0	2.7	-1.0	-1.1	3.8
EI	305 - 355	5.1	-2.3	0.8	-1.2	0.0	0.0	5.3	0.8	-2.5	7.8
FI	251 - 281	-3.5	-3.7	0.2	-0.2	0.0	0.0	0.2	-3.4	-3.9	4.1
GI	311 - 351	-2.7	-4.1	-0.2	0.2	0.0	0.0	-0.2	-2.6	-4.1	8.9
HO	581 - 584	0.0	-2.6	0.8	0.1	0.0	0.0	0.8	0.0	-2.6	3.4
IO	589 - 593	0.0	-2.0	0.1	0.0	0.0	0.0	0.1	0.0	-2.0	2.2
JI	971 - 974	-0.1	-1.7	1.2	0.0	0.0	0.0	1.2	-0.1	-1.7	2.9
KI	979 - 983	0.0	-1.4	0.0	0.0	0.0	0.0	0.0	0.0	-1.4	1.4
LI	1601 - 1604	-0.1	-1.3	1.2	0.0	0.0	0.0	1.2	-0.1	-1.3	2.5
MO	1609 - 1613	0.0	-1.1	0.0	0.0	0.0	0.0	0.0	0.0	-1.1	1.1
NI	2216 - 2219	-0.1	-1.0	1.2	0.0	0.0	0.0	1.2	-0.1	-1.0	2.2
OI	2224 - 2228	0.0	-0.7	0.0	0.0	0.0	0.0	0.0	0.0	-0.7	0.7
PO	2546 - 2549	0.0	-0.9	0.9	0.0	0.0	0.0	0.9	0.0	-0.9	1.8
QO	2554 - 2558	0.0	-0.7	0.0	0.0	0.0	0.0	0.0	0.0	-0.7	0.7
RI	2771 - 2774	-0.3	-1.6	0.2	0.2	0.0	0.0	0.2	-0.2	-1.7	1.9
SI	2779 - 2783	-0.9	-1.0	0.0	0.0	0.0	0.0	0.0	-0.9	-1.0	1.0
TO	7066 - 7072	0.0	-0.6	0.0	0.0	0.0	0.0	0.0	0.0	-0.6	0.6
UI	3051 - 3056	-0.4	-6.5	-0.6	0.0	0.0	0.0	-0.4	-0.6	-6.5	6.1
VI	3611 - 3617	0.9	2.5	0.8	0.0	0.0	0.0	2.5	0.9	0.8	1.8
WI	3241 - 3246	0.9	0.0	0.9	0.0	0.0	0.0	0.9	0.9	0.0	0.9
XI	3801 - 3807	1.4	0.0	1.4	0.0	0.0	0.0	1.4	1.4	0.0	1.5

<sup>1</sup> Refer to Figure 2.10.2-34 for the identification of the representative sections.

Table 2.10.4-55  $S_n$  Stresses; 1-Foot Bottom End Drop; Drop Orientation = 0 Degrees; 2-D Model; Condition 1

Condition 1: 100°F Ambient with Contents

Section <sup>1</sup>	Node - Node	Stress Components (ksi)						Principal Stresses (ksi)			
		$S_x$	$S_y$	$S_z$	$S_{xy}$	$S_{yz}$	$S_{zx}$	S1	S2	S3	S.L
A I	1 - 5	6.9	-0.4	6.9	0.0	0.0	0.0	6.9	6.9	-0.4	7.3
B I	6 - 10	6.1	-0.7	6.1	0.0	0.0	0.0	6.1	6.1	-0.7	6.7
C I	251 - 255	-2.7	-6.8	0.5	-1.0	0.0	0.0	0.5	-2.4	-7.0	7.5
D I	306 - 310	-0.9	1.3	0.4	0.4	0.0	0.0	1.4	0.4	-0.9	2.3
E I	305 - 355	4.0	1.5	1.2	0.0	0.0	0.0	4.0	1.5	1.2	2.8
F I	251 - 281	-3.9	-6.4	-0.2	-0.8	0.0	0.0	-0.2	-3.6	-6.7	6.5
G O	311 - 351	-0.4	7.9	3.8	0.6	0.0	0.0	7.9	3.8	-0.4	8.4
H O	581 - 584	-0.2	-4.1	0.3	0.2	0.0	0.0	0.3	-0.2	-4.1	4.5
I I	589 - 593	-0.3	3.8	2.8	0.0	0.0	0.0	3.8	2.8	-0.3	4.1
J I	971 - 974	-0.1	-3.9	0.1	0.0	0.0	0.0	0.1	-0.1	-3.9	4.0
K O	979 - 983	0.0	6.2	6.3	0.0	0.0	0.0	6.3	6.2	0.0	6.3
L I	1601 - 1604	-0.1	-3.1	0.2	0.0	0.0	0.0	0.2	-0.1	-3.1	3.2
M O	1609 - 1613	0.0	6.4	7.2	0.0	0.0	0.0	7.2	6.4	0.0	7.2
N I	2216 - 2219	-0.1	-3.0	-0.2	0.0	0.0	0.0	-0.1	-0.2	-3.0	3.0
O O	2224 - 2228	0.0	6.3	5.6	0.0	0.0	0.0	6.3	5.6	0.0	6.3
P O	2546 - 2549	-0.2	-1.0	1.2	0.0	0.0	0.0	1.2	-0.2	-1.0	2.2
Q O	2554 - 2558	0.0	5.5	3.3	0.1	0.0	0.0	5.5	3.3	0.0	5.5
R I	2771 - 2774	-0.6	1.0	-2.8	0.4	0.0	0.0	1.1	-0.7	-2.8	3.9
S I	2779 - 2783	1.2	6.6	1.8	-0.3	0.0	0.0	6.6	1.8	1.2	5.4
T O	7066 - 7072	-0.1	4.6	3.2	-0.5	0.0	0.0	4.7	3.2	-0.1	4.8
U I	3051 - 3056	-0.8	-10.0	-2.5	-0.2	0.0	0.0	-0.8	-2.5	-10.0	9.2
V I	3611 - 3617	1.1	2.4	-1.2	-0.1	0.0	0.0	2.4	1.0	-1.2	3.6
W I	3241 - 3246	2.7	0.0	2.7	0.0	0.0	0.0	2.7	2.7	0.0	2.7
X O	3801 - 3807	1.5	0.0	1.5	0.0	0.0	0.0	1.5	1.5	0.0	1.5

Table 2.10.4-56 Critical  $P_m$  Stress Summary; 1-Foot Bottom End Drop; Drop Orientation = 0 Degrees; 2-D Model; Condition 1

Condition 1: 100°F Ambient with Contents

Comp. No. <sup>1</sup>	Section Cut Node-Node	$P_m$ Stresses (ksi)						Principal Stresses (ksi)			S.I. Stress	Allow. Stress	Margin of Safety
		$S_x$	$S_y$	$S_z$	$S_{xy}$	$S_{yz}$	$S_{zx}$	S1	S2	S3			
1	306- 310	-0.8	-2.5	-1.6	-0.4	0.0	0.0	-0.7	-1.6	-2.6	1.9	19.2	9.1
2	305- 353	1.7	-1.8	0.3	-1.2	0.0	0.0	2.1	0.3	-2.1	4.2	18.5	3.4
3	416- 419	0.0	-1.5	2.1	-0.2	0.0	0.0	2.1	0.0	-1.5	3.6	31.4	7.7
4	851- 854	0.0	-1.7	1.2	0.0	0.0	0.0	1.2	0.0	-1.7	2.9	19.6	5.8
5	344- 548	0.0	-1.7	0.5	0.0	0.0	0.0	0.5	0.0	-1.7	2.1	20.0	8.5
6	7064-2774	0.0	4.0	1.5	0.1	0.0	0.0	4.0	1.5	0.0	4.0	20.0	4.0
7	3021-3026	0.2	-7.6	-1.8	-0.2	0.0	0.0	0.2	-1.8	-7.6	7.8	20.0	1.6
8	3521-3527	0.0	-0.4	-0.1	0.2	0.0	0.0	0.1	-0.1	-0.4	0.5	45.0	89.0

Locations of the most critical sections for each component are provided in the following:

Comp. No. <sup>1</sup>	Section Location			
	Inside Node		Outside Node	
	x (in)	y (in)	z (in)	x (in)
1	39.44	6.20	39.44	0.75
2	39.44	8.20	43.35	8.20
3	35.50	18.40	37.50	18.40
4	35.50	47.40	37.00	47.40
5	40.70	26.40	43.35	26.40
6	37.655	179.40	37.50	175.40
7	37.655	179.40	37.655	185.40
8	39.56	188.40	39.56	193.71

<sup>1</sup> Refer to Figure 2.10.2-33 for cast component identification.

Table 2.10.4-57 Critical  $P_m + P_b$  Stress Summary; 1-Foot Bottom End Drop; Drop Orientation = 0 Degrees; 2-D Model; Condition 1

Condition 1: 100°F Ambient with Contents

Comp. No. <sup>1</sup>	Section Cut Node-Node	P <sub>m</sub> + P <sub>b</sub> Stresses (ksi)							Principal Stresses (ksi)			Allow. S.L. Stress	Margin of Safety
		S <sub>x</sub>	S <sub>y</sub>	S <sub>z</sub>	S <sub>xy</sub>	S <sub>yz</sub>	S <sub>xz</sub>	S <sub>1</sub>	S <sub>2</sub>	S <sub>3</sub>			
1	16- 20	-6.4	-0.8	-6.4	0.0	0.0	0.0	-0.8	-6.4	-6.4	5.7	28.7	4.0
2	305- 335	5.1	-2.3	0.8	-1.2	0.0	0.0	5.3	0.8	-2.3	7.8	27.7	2.6
3	416- 419	-0.1	-3.3	1.7	-0.2	0.0	0.0	1.7	-0.1	-3.3	5.0	47.1	8.4
4	851- 854	-0.1	-1.8	1.2	0.0	0.0	0.0	1.2	-0.1	-1.8	3.0	29.4	8.8
5	544- 548	0.0	-2.0	0.4	0.0	0.0	0.0	0.4	0.0	-2.0	2.3	30.0	12.0
6	7064-2774	2.2	12.7	3.5	0.1	0.0	0.0	12.7	3.5	2.2	10.5	30.0	1.9
7	3021-3026	0.1	12.7	-1.1	-0.2	0.0	0.0	12.7	0.1	-1.1	13.8	30.0	1.2
8	3521-3527	0.1	-2.2	0.3	0.2	0.0	0.0	0.3	0.1	-2.2	2.5	67.5	26.0

Locations of the most critical sections for each component are provided in the following:

Comp. No. <sup>1</sup>	Section Location			
	Inside Node		Outside Node	
	x (in)	y (in)	z (in)	x (in)
1	1.42	6.20	1.42	0.75
2	39.44	8.20	43.35	8.20
3	35.50	18.40	37.50	18.40
4	35.50	47.40	37.00	47.40
5	40.70	26.40	43.35	26.40
6	37.655	179.40	37.50	175.40
7	37.655	179.40	37.655	185.40
8	39.56	188.40	39.56	193.71

<sup>1</sup> Refer to Figure 2.10.2-33 for cask component identification.

Table 2.10.4-58 Critical  $S_n$  Stress Summary; 1-Foot Bottom End Drop; Drop Orientation = 0 Degrees; 2-D Model; Condition 1

Condition 1: 100°F Ambient with Contents

Comp. No. <sup>1</sup>	Section Cut Node-Node	$S_n$ Stresses (ksi)						Principal Stresses (ksi)				Allow. Stress 3.0 $S_u$
		$S_x$	$S_y$	$S_z$	$S_{xy}$	$S_{yz}$	$S_{zx}$	S1	S2	S3	S.L.	
1	16- 20	6.0	-0.7	6.1	0.0	0.0	0.0	6.1	6.0	-0.7	6.8	57.6
2	371- 374	0.5	-8.9	1.2	-1.0	0.0	0.0	1.2	0.6	-9.0	10.1	55.5
3	416- 419	-0.2	-3.8	3.3	-0.4	0.0	0.0	3.3	-0.1	-3.9	7.2	94.2
4	971- 974	-0.1	-3.9	0.1	0.0	0.0	0.0	0.1	-0.1	-3.9	4.0	58.8
5	1519- 1523	6.4	0.0	7.3	0.0	0.0	0.0	7.3	6.4	0.0	7.3	60.0
6	2764- 2768	10.5	-0.4	2.2	0.5	0.0	0.0	0.5	2.2	-0.5	11.0	60.0
7	3021- 3026	1.0	12.2	-2.9	-0.5	0.0	0.0	12.2	1.0	-2.9	15.2	60.0
8	3611- 3617	1.1	2.4	-1.2	-0.1	0.0	0.0	2.4	1.0	-1.2	3.6	135.0

Locations of the most critical sections for each component are provided in the following:

Comp. No. <sup>1</sup>	Section Location			
	Inside Node		Outside Node	
	x (in)	y (in)	z (in)	x (in)
1	1.42	6.20	1.42	0.75
2	35.50	15.40	37.50	15.40
3	35.50	18.40	37.50	18.40
4	35.50	55.65	37.00	55.65
5	40.70	91.40	43.35	91.40
6	40.70	174.40	43.35	174.40
7	37.655	179.40	37.655	185.40
8	35.206	188.40	35.206	193.71

<sup>1</sup> Refer to Figure 2.10.2-33 for cask component identification.

Table 2.10.4-59 Critical P<sub>m</sub> Stress Summary; 1-Foot Bottom End Drop; Drop Orientation = 0 Degrees; 2-D Model; Condition 2

Condition 2: -20°F Ambient with Contents

Comp. No. <sup>1</sup>	Section Cut Node-Node	P <sub>m</sub> Stresses (ksi)						Principal Stresses (ksi)			Margin of Allow. Stress Safety	
		S <sub>1</sub>	S <sub>2</sub>	S <sub>3</sub>	S <sub>4</sub>	S <sub>5</sub>	S <sub>6</sub>	S1	S2	S3	S.L.	Stress
1	306- 310	-0.8	-2.6	-1.7	-0.4	0.0	0.0	-0.8	-1.7	-2.7	1.9	19.2
2	305- 355	1.8	-1.8	0.3	-1.2	0.0	0.0	2.2	0.3	-2.2	4.4	18.5
3	416- 419	0.0	-1.7	2.0	-0.2	0.0	0.0	2.0	0.0	-1.8	3.7	31.4
4	851- 854	0.0	-2.0	0.3	0.0	0.0	0.0	0.3	0.0	-2.0	2.3	19.6
5	544- 548	0.0	-1.7	0.5	0.0	0.0	0.0	0.5	0.0	-1.7	2.2	20.0
6	7064-2774	0.1	4.2	1.4	0.2	0.0	0.0	4.2	1.4	0.1	4.1	20.0
7	3021-3026	0.2	-7.8	-1.8	-0.3	0.0	0.0	0.2	-1.8	-7.8	8.0	20.0
8	3521-3527	0.0	-0.4	-0.1	0.2	0.0	0.0	0.1	-0.1	-0.5	0.5	45.0

Locations of the most critical sections for each component are provided in the following:

Comp. No. <sup>1</sup>	Section Location			
	Inside Node		Outside Node	
	x (in)	y (in)	z (in)	x (in)
1	39.44	6.20	39.44	0.75
2	39.44	8.20	43.35	8.20
3	35.50	18.40	37.50	18.40
4	35.50	47.40	37.00	47.40
5	40.70	26.40	43.35	26.40
6	37.655	179.40	37.50	175.40
7	37.655	179.40	37.655	185.40
8	39.56	188.40	39.56	193.71

<sup>1</sup> Refer to Figure 2.10.2-33 for cask component identification.

Table 2.10.4-60 Critical  $P_m + P_b$  Stress Summary; 1-Foot Bottom End Drop; Drop Orientation = 0 Degrees; 2-D Model; Condition 2

Condition 2: -20°F Ambient with Contents

Comp. No. <sup>1</sup>	Section Cnt Node-Node	P <sub>m</sub> + P <sub>b</sub> Stresses (ksi)							Principal Stresses (ksi)			Allow. S.L. Stress	Margin of Safety
		S <sub>x</sub>	S <sub>y</sub>	S <sub>z</sub>	S <sub>xy</sub>	S <sub>yz</sub>	S <sub>xz</sub>	S1	S2	S3			
1	16- 20	-6.9	-0.8	-7.0	0.0	0.0	0.0	-0.8	-6.9	-7.0	6.2	28.7	3.6
2	305- 355	5.5	-2.3	0.9	-1.2	0.0	0.0	5.7	0.9	-2.5	6.2	27.7	2.4
3	416- 419	0.0	-3.8	1.5	-0.2	0.0	0.0	1.5	0.0	-3.8	5.3	47.1	7.9
4	851- 854	0.0	-2.1	0.3	0.0	0.0	0.0	0.3	0.0	-2.1	2.4	29.4	11.3
5	544- 548	0.0	-2.0	0.4	0.0	0.0	0.0	0.4	0.0	-2.0	2.4	30.0	11.5
6	7064-2774	2.3	13.0	3.4	0.2	0.0	0.0	13.0	3.4	2.3	10.7	30.0	1.8
7	3021-3026	0.1	13.0	-1.0	-0.3	0.0	0.0	13.0	0.1	-1.0	14.0	30.0	1.1
8	3521-3527	0.1	-2.5	0.4	0.2	0.0	0.0	0.4	0.1	-2.5	2.9	67.5	22.3

Locations of the most critical sections for each component are provided in the following:

Comp. No. <sup>1</sup>	Section Location			
	Inside Node		Outside Node	
	x (in)	y (in)	z (in)	x (in)
1	1.42	6.20	1.42	0.75
2	39.44	8.20	43.35	8.20
3	35.50	18.40	37.50	18.40
4	35.50	47.40	37.00	47.40
5	40.70	26.40	43.35	26.40
6	37.655	179.40	37.50	175.40
7	37.655	179.40	37.655	185.40
8	39.56	188.40	39.56	193.71

<sup>1</sup> Refer to Figure 2.10.2-33 for cask component identification.

Table 2.10.4-61 Critical  $S_n$  Stress Summary; 1-Foot Bottom End Drop; Drop Orientation = 0 Degrees; 2-D Model; Condition 2

Condition 2: -20°F Ambient with Contents

Comp. No. <sup>1</sup>	Section Cut Node-Node	$S_n$ Stresses (ksi)						Principal Stresses (ksi)				Allow. Stress 3.0 $S_n$
		$S_1$	$S_2$	$S_3$	$S_4$	$S_5$	$S_6$	$S_1$	$S_2$	$S_3$	$S_4$	
1	306- 310	-2.7	-8.1	-1.4	-0.3	0.0	0.0	-1.4	-2.7	-8.1	6.7	57.6
2	301- 303	3.4	-6.3	0.0	0.8	0.0	0.0	3.5	0.0	-6.4	9.9	55.5
3	596- 599	0.0	-6.2	-0.8	0.2	0.0	0.0	0.0	-0.8	-6.2	6.2	94.2
4	926- 929	0.0	-6.0	-0.9	0.0	0.0	0.0	0.0	-0.9	-6.0	6.0	58.8
5	1579-1583	3.8	0.0	3.2	0.0	0.0	0.0	3.8	3.2	0.0	3.8	60.0
6	7064-2774	3.4	12.6	4.4	-0.1	0.0	0.0	12.6	4.4	3.4	9.2	60.0
7	3021-3026	0.3	12.6	-3.3	-0.3	0.0	0.0	12.6	0.3	-3.3	15.9	60.0
8	3801-3807	2.3	0.0	2.3	0.0	0.0	0.0	2.3	2.3	0.0	2.3	135.0

Locations of the most critical sections for each component are provided in the following:

Comp. No. <sup>1</sup>	Section Location			
	Inside Node		Outside Node	
	x (in)	y (in)	z (in)	x (in)
1	39.44	6.20	39.44	0.75
2	39.633	14.40	39.44	8.20
3	35.50	30.40	37.00	30.40
4	35.50	52.40	37.00	52.40
5	40.70	95.40	43.35	95.40
6	37.655	179.40	37.50	175.40
7	37.655	179.40	37.655	185.40
8	0.0	188.46	0.0	193.71

<sup>1</sup> Refer to Figure 2.10.2-33 for cask component identification.



Table 2.10.4-62 Critical P<sub>m</sub> Stress Summary; 1-Foot Bottom End Drop; Drop Orientation = 0 Degrees; 2-D Model; Condition 3  
Condition 3: -20°F Ambient without Contents

Comp. No. <sup>1</sup>	Section Cut Node-Node	P <sub>m</sub> Stresses (ksi)						Principal Stresses (ksi)			S.L.	Allow. Stress	Margin of Safety
		S <sub>x</sub>	S <sub>y</sub>	S <sub>z</sub>	S <sub>xy</sub>	S <sub>xz</sub>	S <sub>yz</sub>	S1	S2	S3			
1	306- 310	-1.0	-2.5	-1.8	-0.4	0.0	0.0	-0.9	-1.8	-2.6	1.7	19.2	10.3
2	305- 355	2.2	-1.7	0.4	-1.4	0.0	0.0	2.6	0.4	-2.1	4.7	18.5	2.9
3	416- 419	0.0	-1.8	2.2	-0.3	0.0	0.0	2.2	0.0	-1.8	4.0	31.4	6.9
4	866- 869	0.0	-2.1	0.3	0.0	0.0	0.0	0.3	0.0	-2.1	2.4	19.6	7.2
5	544- 548	0.0	-1.7	0.6	0.0	0.0	0.0	0.6	0.0	-1.7	2.3	20.0	7.7
6	7064-2774	0.1	4.2	1.4	0.2	0.0	0.0	4.2	1.4	0.1	4.2	20.0	3.8
7	3021-3026	0.2	-7.8	-1.8	-0.3	0.0	0.0	0.2	-1.8	-7.8	8.0	20.0	1.5
8	3521-3527	0.0	-0.4	-0.1	0.2	0.0	0.0	0.1	-0.1	-0.5	0.5	45.0	89.0

Locations of the most critical sections for each component are provided in the following:

Comp. No. <sup>1</sup>	Section Location			
	Inside Node		Outside Node	
	x (in)	y (in)	z (in)	x (in)
1	39.44	6.20	39.44	0.75
2	39.44	8.20	43.35	8.20
3	35.50	18.40	37.50	18.40
4	35.50	48.40	37.00	48.40
5	40.70	26.40	43.35	26.40
6	37.655	179.40	37.50	175.40
7	37.655	179.40	37.655	185.40
8	39.56	188.40	39.56	193.71

<sup>1</sup> Refer to Figure 2.10.2-33 for cask component identification.

Table 2.10.4-63 Critical  $P_m + P_b$  Stress Summary; 1-Foot Bottom End Drop; Drop Orientation = 0 Degrees; 2-D Model; Condition 3  
Condition 3: -20°F Ambient without Contents

Comp. No. <sup>1</sup>	Section Cut Node-Node	P <sub>m</sub> + P <sub>b</sub> Stresses (ksi)							Principal Stresses (ksi)			Allow. S.I. Stress	Margin of Safety	
		S <sub>x</sub>	S <sub>y</sub>	S <sub>z</sub>	S <sub>xy</sub>	S <sub>yz</sub>	S <sub>xz</sub>	S <sub>1</sub>	S <sub>2</sub>	S <sub>3</sub>				
1	16- 20	-7.9	-0.6	-7.9	0.0	0.0	0.0	0.0	-0.6	-7.9	-7.9	7.3	28.7	2.9
2	1- 5	8.6	-0.1	8.6	0.0	0.0	0.0	0.0	8.6	8.6	-0.1	8.7	27.7	2.2
3	416- 419	0.0	-4.2	1.6	-0.3	0.0	0.0	0.0	1.6	0.0	-4.3	5.9	47.1	7.0
4	851- 854	0.0	-2.2	0.3	0.0	0.0	0.0	0.0	0.3	0.0	-2.2	2.4	29.4	11.3
5	544- 548	0.0	-2.0	0.5	0.0	0.0	0.0	0.0	0.5	0.0	-2.0	2.5	30.0	11.0
6	7064-2774	2.4	13.1	3.3	0.2	0.0	0.0	0.0	13.1	3.3	2.4	10.7	30.0	1.8
7	3021-3026	0.1	13.1	-1.0	-0.3	0.0	0.0	0.0	13.1	0.1	-1.0	14.1	30.0	1.1
8	3521-3527	0.1	-2.5	0.4	0.2	0.0	0.0	0.0	0.4	0.1	-2.5	2.9	67.5	22.3

Locations of the most critical sections for each component are provided in the following:

Comp. No. <sup>1</sup>	Section Location			
	Inside Node		Outside Node	
	x (in)	y (in)	z (in)	x (in)
1	1.42	6.20	1.42	0.75
2	0.0	14.40	0.0	8.20
3	35.50	18.40	37.50	18.40
4	35.50	47.40	37.00	47.40
5	40.70	26.40	43.35	26.40
6	37.655	179.40	37.50	175.40
7	37.655	179.40	37.655	185.40
8	39.56	188.40	39.56	193.71

<sup>1</sup> Refer to Figure 2.10.2-33 for cask component identification.

Table 2.10.4-64 Critical  $S_n$  Stress Summary; 1-Foot Bottom End Drop; Drop Orientation = 0 Degrees; 2-D Model; Condition 3

Condition 3: -20°F Ambient without Contents

Comp. No.	Section Cut Node-Node	$S_n$ Stresses (ksi)						Principal Stresses (ksi)				Allow. Stress $3.0 S_u$
		$S_x$	$S_y$	$S_z$	$S_{xy}$	$S_{yz}$	$S_{zx}$	S1	S2	S3	S.L.	
1	296-300	-7.3	-0.4	-1.7	-1.2	0.0	0.0	-0.2	-1.7	-7.5	7.4	57.6
2	305-355	5.1	-5.2	0.2	-1.3	0.0	0.0	5.3	0.2	-5.5	10.7	55.5
3	416-419	0.0	-4.1	0.6	-0.2	0.0	0.0	0.6	0.0	-4.1	4.7	94.2
4	2276-2279	0.0	-1.7	-2.9	0.0	0.0	0.0	0.0	-1.7	-2.9	2.9	58.8
5	544-548	0.0	-1.8	0.3	0.0	0.0	0.0	0.3	0.0	-1.8	2.1	60.0
6	7064-2774	1.8	13.2	3.2	0.1	0.0	0.0	13.2	3.2	1.8	11.4	60.0
7	3021-3026	-0.5	13.2	-1.3	-0.2	0.0	0.0	13.2	-0.5	-1.3	14.5	60.0
8	3621-3627	0.2	-2.3	0.4	-0.1	0.0	0.0	0.4	0.2	-2.3	2.7	135.0

Locations of the most critical sections for each component are provided in the following:

Comp. No. <sup>1</sup>	Section Location			
	Inside Node		Outside Node	
	x (in)	y (in)	z (in)	x (in)
1	38.567	6.20	38.567	0.75
2	39.44	8.20	43.35	8.20
3	35.50	18.40	37.50	18.40
4	35.50	142.40	37.00	142.40
5	40.70	26.40	43.35	26.40
6	37.655	179.40	37.50	175.40
7	37.655	179.40	37.655	185.40
8	33.705	188.40	33.705	193.71

<sup>1</sup> Refer to Figure 2.10.2-33 for cask component identification.

Table 2.10.4-65 Primary Stresses; 1-Foot Side Drop; Drop Orientation = 90 Degrees; 3-D Model; 0-Degree Circumferential Location; Condition 1

Condition 1: 100°F Ambient with Contents

Stress Points		Stress Components (ksi)						Principal Stresses (ksi)		
Section <sup>1</sup>	Node	S <sub>x</sub>	S <sub>y</sub>	S <sub>z</sub>	S <sub>xy</sub>	S <sub>yz</sub>	S <sub>xz</sub>	S1	S2	S3
A1	1130	-0.3	-0.6	-0.1	0.0	0.0	0.0	-0.1	-0.3	-0.6
A2	1129	-0.3	-1.2	0.0	0.0	0.0	0.0	0.0	-0.3	-1.2
A3	1128	-0.4	-1.7	0.1	0.0	0.0	0.0	0.1	-0.4	-1.7
B1	1185	-0.5	-1.9	0.0	0.0	0.0	-0.1	0.0	-0.5	-1.9
B2	1184	-0.2	-2.1	0.0	0.0	0.0	-0.1	0.0	-0.2	-2.1
B3	1183	0.1	-2.4	0.0	0.0	0.0	-0.1	0.1	0.0	-2.4
C1	90	1.9	-0.9	6.3	0.0	-0.3	0.5	6.3	1.9	-0.9
C2	80	-1.3	-2.7	2.6	-0.1	-0.2	-0.1	2.6	-1.3	-2.7
C3	70	-1.6	-3.3	0.8	0.0	-0.2	-0.4	0.8	-1.7	-3.3
C4	60	-1.8	-3.5	0.0	0.1	-0.1	-0.2	0.1	-1.9	-3.5
C5	50	-3.3	-4.0	-0.1	0.1	0.0	0.0	-0.1	-3.3	-4.1
C6	40	-3.7	-4.3	-0.1	0.1	0.0	0.0	-0.1	-3.7	-4.3
D1	25	-1.8	-3.5	1.6	0.1	0.0	0.1	1.6	-1.8	-3.5
D2	15	-3.5	-4.0	0.6	0.1	0.0	-0.2	0.6	-3.5	-4.0
D3	5	-3.9	-4.1	0.1	0.1	0.0	-0.1	0.1	-3.9	-4.1
E1	35	-3.9	-4.2	1.2	0.1	0.0	0.7	1.3	-4.0	-4.2
E2	34	-2.8	-4.1	0.6	0.1	0.0	0.8	0.8	-3.0	-4.1
E3	33	-3.0	-4.4	0.0	0.1	0.0	0.7	0.1	-3.1	-4.4
E4	32	-3.1	-4.6	-0.7	0.1	0.0	0.4	-0.6	-3.2	-4.6
E5	31	-3.2	-4.9	-1.4	0.1	0.0	0.2	-1.4	-3.2	-4.9
F1	100	-0.6	-0.7	9.6	0.0	-0.5	0.9	9.7	-0.6	-0.7
F2	99	-0.7	-3.2	0.6	0.2	-0.4	1.0	1.1	-1.2	-3.3
F3	98	-0.3	-4.7	-5.3	0.3	-0.3	1.5	0.1	-4.6	-5.8
F4	97	0.3	-7.6	-16.9	0.6	-0.3	1.8	0.5	-7.6	-17.1
G1	94	0.3	-0.8	7.9	0.1	-0.1	1.1	8.0	0.1	-0.8
G2	93	0.5	-2.1	3.0	0.2	-0.1	0.8	3.2	0.3	-2.1
G3	92	0.5	-2.4	1.5	0.2	-0.1	0.3	1.5	0.4	-2.4
G4	91	0.2	-2.9	-0.3	0.2	0.0	0.1	0.3	-0.3	-3.0
H1	330	-0.1	3.4	-2.4	-0.2	-0.7	0.0	3.5	-0.1	-2.5
H2	329	-0.1	4.0	-1.0	-0.3	-0.7	0.0	4.1	-0.1	-1.1

Table 2.10.4-65 Primary Stresses; 1-Foot Side Drop; Drop Orientation = 90 Degrees; 3-D Model; 0-Degree Circumferential Location; Condition 1 (continued)

Stress Points Section <sup>1</sup> Node		Stress Components (ksi)						Principal Stresses (ksi)		
		S <sub>x</sub>	S <sub>y</sub>	S <sub>z</sub>	S <sub>xy</sub>	S <sub>yz</sub>	S <sub>xz</sub>	S1	S2	S3
H3	328	0.0	4.6	0.3	-0.3	-0.6	0.0	4.7	0.2	0.0
H4	327	0.1	5.2	1.9	-0.3	-0.6	-0.1	5.4	1.8	0.0
I1	244	-0.1	-0.6	2.0	0.0	-0.3	0.0	2.1	0.0	-0.7
I2	243	0.0	0.1	3.0	0.0	-0.2	0.0	3.0	0.1	0.0
I3	242	0.0	0.7	3.9	0.0	-0.1	0.0	3.9	0.7	0.0
I4	241	0.0	1.4	4.8	-0.1	-0.1	0.0	4.8	1.4	0.0
J1	550	-0.1	3.6	4.3	-0.3	-0.4	0.0	4.5	3.4	-0.2
J2	548	-0.1	4.5	4.9	-0.3	-0.4	0.0	5.2	4.3	-0.1
J3	547	0.0	5.4	5.6	-0.4	-0.4	0.0	5.9	5.1	-0.1
K1	344	-0.1	-1.0	3.7	0.1	-0.1	0.0	3.7	-0.1	-1.0
K2	342	0.0	0.6	4.5	-0.1	-0.1	0.0	4.5	0.6	0.0
K3	341	0.0	2.1	5.3	-0.2	-0.1	0.0	5.3	2.1	0.0
L1	740	0.0	3.1	7.3	0.0	0.0	-0.1	7.3	3.1	0.0
L2	738	-0.2	4.4	8.2	-0.6	0.0	0.0	8.2	4.5	-0.3
L3	737	0.1	5.8	9.0	-1.2	0.0	0.0	9.0	6.1	-0.1
M1	663	-0.4	-1.5	4.5	0.1	0.0	0.0	4.5	-0.4	-1.5
M2	63	0.2	2.7	6.2	0.8	0.0	0.0	6.2	2.9	-0.1
N1	1877	-0.1	3.4	3.6	-0.3	0.5	0.0	4.0	3.0	-0.1
N2	1477	-0.1	4.5	4.3	-0.3	0.4	0.0	4.8	3.9	-0.1
N3	1277	0.0	5.6	4.9	-0.4	0.4	0.0	5.8	4.7	-0.1
O1	647	0.0	-1.1	4.3	0.1	0.1	0.0	4.3	0.0	-1.1
O2	247	0.0	0.5	5.1	0.0	0.1	0.0	5.1	0.5	0.0
O3	47	0.0	2.0	5.8	-0.2	0.0	0.0	5.8	2.0	0.0
P1	1840	-0.1	3.4	-2.1	-0.2	0.7	0.0	3.5	-0.1	-2.2
P2	1640	-0.1	4.1	-0.9	-0.3	0.7	0.0	4.2	-0.1	-1.0
P3	1440	0.0	4.8	0.2	-0.3	0.6	0.0	4.9	0.2	0.0
P4	1240	0.1	5.5	1.6	-0.4	0.6	0.1	5.6	1.5	0.0
Q1	628	0.0	-0.3	3.8	0.0	0.2	0.0	3.8	0.0	-0.3
Q2	428	0.0	0.3	4.2	0.0	0.2	0.0	4.2	0.3	0.0
Q3	228	0.0	0.9	4.6	-0.1	0.1	0.0	4.6	0.9	0.0
Q4	28	0.0	1.5	5.0	-0.1	0.0	0.0	5.0	1.5	0.0
R1	1816	-0.5	-2.1	3.9	0.1	0.4	0.1	3.9	-0.5	-2.1

Table 2.10.4-65 Primary Stresses; 1-Foot Side Drop; Drop Orientation = 90 Degrees; 3-D Model; 0-Degree Circumferential Location; Condition 1 (continued)

Stress Points		Stress Components (ksi)						Principal Stresses (ksi)		
Section <sup>1</sup>	Node	S <sub>x</sub>	S <sub>y</sub>	S <sub>z</sub>	S <sub>xy</sub>	S <sub>yz</sub>	S <sub>xz</sub>	S1	S2	S3
R2	1616	-1.0	-3.2	-0.2	0.2	0.4	-0.1	-0.1	-1.0	-3.3
R3	1416	-2.5	-4.4	-3.7	0.3	0.3	-0.9	-2.0	-3.9	-4.7
R4	1216	-3.5	-3.7	-8.2	0.4	0.2	-2.1	-2.7	-5.7	-9.0
S1	616	1.1	-1.3	0.4	0.1	0.2	-0.1	1.2	0.4	-1.3
S2	416	0.1	-0.9	2.6	0.1	0.1	-0.1	2.6	0.1	-0.9
S3	216	0.1	-0.3	4.5	0.0	0.1	0.1	4.5	0.1	-0.3
S4	16	0.1	0.3	6.3	0.0	0.0	0.1	6.4	0.3	0.1
T1	811	-8.3	-8.0	-8.5	0.3	0.2	-2.2	-6.2	-8.0	-10.7
T2	611	-4.0	-5.1	-2.7	0.2	0.1	-1.8	-1.4	-5.0	-5.4
T3	411	-1.9	-3.5	0.9	0.1	0.1	-1.3	1.4	-2.3	-3.5
T4	211	-0.5	-2.1	4.0	0.1	0.0	-0.7	4.1	-0.5	-2.1
T5	11	0.0	-0.7	8.6	0.0	0.0	-0.3	8.6	0.0	-0.7
U1	43058	4.1	0.8	-0.1	0.1	0.0	-0.1	4.1	0.8	-0.1
U2	43057	1.2	-0.3	-0.4	0.1	0.0	0.1	1.2	-0.3	-0.4
U3	43056	0.1	-0.9	-1.0	0.0	0.0	0.4	0.2	-0.9	-1.1
U4	43055	-0.3	-1.3	-1.8	0.1	0.0	0.2	-0.3	-1.3	-1.8
U5	43054	-0.9	-1.7	-2.3	0.1	0.0	-0.4	-0.8	-1.7	-2.4
U6	43053	-1.7	-2.1	-2.3	0.1	-0.1	-1.1	-0.8	-2.1	-3.2
U7	43052	-2.9	-2.3	-1.4	0.0	-0.1	-1.4	-0.6	-2.3	-3.8
U8	43051	-4.2	-2.5	-0.1	0.0	0.0	-0.1	-0.1	-2.5	-4.2
V1	50024	1.4	-0.3	0.0	0.1	0.0	0.0	1.4	0.0	-0.3
V2	50023	-1.2	-1.6	-0.6	0.0	0.0	0.0	-0.6	-1.2	-1.6
V3	50022	-2.6	-2.2	-0.3	0.0	0.0	0.0	-0.3	-2.2	-2.6
V4	50021	-6.8	-3.6	0.5	-0.1	0.0	0.0	0.5	-3.6	-6.8
W1	43278	-0.7	-0.9	0.0	0.0	-0.1	0.1	0.0	-0.7	-0.9
W2	43274	-0.4	-1.1	0.0	0.0	-0.1	0.1	0.0	-0.4	-1.1
W3	43271	-0.1	-0.6	0.0	0.0	-0.1	0.0	0.0	-0.1	-0.7
X1	50084	-0.2	-1.9	0.0	0.0	0.0	0.1	0.0	-0.2	-1.9
X2	50083	-0.1	-2.1	0.0	0.0	0.0	0.1	0.0	-0.2	-2.1
X3	50081	0.1	-2.5	0.0	0.0	0.0	0.1	0.1	0.0	-2.5

<sup>1</sup> Refer to Figure 2.10.2-34 for the identification of the representative sections.

Table 2.10.4-66 Primary Plus Secondary Stresses; 1-Foot Side Drop; Drop Orientation = 90 Degrees; 3-D Model; 0-Degree Circumferential Location; Condition 1

Condition 1: 100°F Ambient with Contents

Stress Points		Stress Components (ksi)						Principal Stresses (ksi)		
Section <sup>1</sup>	Node	S <sub>x</sub>	S <sub>y</sub>	S <sub>z</sub>	S <sub>xy</sub>	S <sub>yz</sub>	S <sub>xz</sub>	S1	S2	S3
A1	1130	-0.1	-0.4	1.0	0.0	-0.1	0.3	1.1	-0.2	-0.4
A2	1129	-0.9	-1.7	0.0	0.0	-0.1	0.3	0.1	-1.0	-1.7
A3	1128	-1.6	-3.0	-1.0	0.0	-0.1	0.3	-0.9	-1.8	-3.0
B1	1185	1.7	0.4	0.8	-0.1	-0.1	0.3	1.8	0.7	0.4
B2	1184	0.9	-1.0	0.0	0.0	-0.1	0.3	1.0	-0.1	-1.0
B3	1183	0.2	-2.3	-0.8	0.0	0.0	0.3	0.2	-0.9	-2.3
C1	90	1.8	-1.3	6.1	0.0	-0.3	0.5	6.1	1.7	-1.3
C2	80	-1.9	-3.3	2.4	0.0	-0.2	-0.2	2.4	-1.9	-3.3
C3	70	-2.1	-3.9	0.3	0.0	-0.2	-0.5	0.4	-2.2	-4.0
C4	60	-2.2	-4.2	-0.4	0.1	-0.1	-0.3	-0.3	-2.3	-4.2
C5	50	-4.0	-4.7	-0.3	0.1	0.0	0.0	-0.3	-3.9	-4.7
C6	40	-3.8	-4.7	-0.1	0.1	0.0	0.0	-0.1	-3.8	-4.7
D1	25	0.2	-2.8	-0.2	0.2	0.0	0.9	1.0	-0.9	-2.8
D2	15	-2.7	-3.7	0.4	0.1	0.0	0.0	0.4	-2.7	-3.7
D3	5	-4.2	-4.7	0.0	0.1	0.0	-0.1	0.0	-4.1	-4.7
E1	35	-7.3	-6.1	-3.0	0.0	0.0	2.0	-2.3	-6.1	-8.1
E2	34	-5.2	-4.5	0.3	0.0	0.1	1.8	0.8	-4.5	-5.7
E3	33	-4.1	-4.0	1.1	0.0	0.1	1.4	1.5	-4.0	-4.5
E4	32	-3.6	-3.7	1.9	0.0	0.0	0.8	2.0	-3.7	-3.7
E5	31	-3.4	-3.4	2.9	0.0	0.0	0.5	3.0	-3.4	-3.4
F1	100	-0.6	-0.7	9.3	0.0	-0.4	1.0	9.4	-0.6	-0.8
F2	99	-0.6	-3.4	0.2	0.2	-0.3	1.1	0.9	-1.3	-3.5
F3	98	0.1	-5.0	-5.9	0.4	-0.3	1.2	0.4	-4.9	-6.2
F4	97	0.8	-7.3	-14.2	0.6	-0.3	1.3	0.9	-7.3	-14.3
G1	94	1.3	2.5	21.4	-0.1	0.0	2.7	21.8	2.5	1.0
G2	93	1.4	-1.2	7.6	0.2	0.0	1.6	8.0	1.0	-1.2
G3	92	1.0	-1.6	6.1	0.2	-0.1	0.3	6.2	1.0	-1.6
G4	91	0.3	-2.5	3.3	0.2	-0.1	0.0	3.3	0.3	-2.5
H1	330	-0.1	2.9	-1.7	-0.2	-0.6	0.1	3.0	-0.2	-1.8
H2	329	-0.1	3.6	-0.8	-0.2	-0.6	0.1	3.7	-0.1	-0.9

Table 2.10.4-66 Primary Plus Secondary Stresses; 1-Foot Side Drop; Drop Orientation = 90 Degrees; 3-D Model; 0-Degree Circumferential Location; Condition 1 (continued)

Stress Points Section <sup>1</sup> Node		Stress Components (ksi)						Principal Stresses (ksi)		
		S <sub>x</sub>	S <sub>y</sub>	S <sub>z</sub>	S <sub>xy</sub>	S <sub>yz</sub>	S <sub>xz</sub>	S1	S2	S3
H3	328	0.0	4.3	0.1	-0.3	-0.6	0.1	4.4	0.0	0.0
H4	327	-0.1	4.9	1.1	-0.3	-0.6	0.0	5.0	1.0	-0.1
I1	244	-0.1	2.4	8.1	-0.2	-0.2	0.0	8.1	2.4	-0.1
I2	243	-0.1	3.0	8.9	-0.2	-0.2	0.0	8.9	3.0	-0.1
I3	242	0.0	3.6	9.9	-0.3	-0.2	0.0	9.9	3.6	0.0
I4	241	0.0	4.2	10.8	-0.3	-0.1	0.0	10.8	4.2	0.0
J1	550	-0.1	2.4	1.9	-0.2	-0.3	0.0	2.6	1.7	-0.2
J2	548	-0.1	4.6	4.5	-0.3	-0.3	0.0	4.9	4.2	-0.1
J3	547	0.0	6.6	7.1	-0.5	-0.3	0.0	7.3	6.5	0.0
K1	344	-0.3	3.9	8.0	-0.3	-0.1	0.0	8.1	3.9	-0.3
K2	342	-0.2	6.2	10.8	-0.5	-0.1	0.0	10.8	6.2	-0.2
K3	341	-0.1	8.3	13.4	-0.6	-0.1	0.0	13.4	8.3	-0.1
L1	740	0.4	2.0	5.2	0.0	0.0	-0.1	5.2	2.0	0.4
L2	738	-0.6	3.5	6.5	-0.5	0.0	0.0	6.5	3.5	-0.7
L3	737	0.1	5.4	8.3	-0.8	0.0	0.0	8.3	5.5	0.0
M1	454	-0.8	4.2	8.6	-0.9	0.0	0.0	8.6	4.4	-1.0
M2	452	0.4	7.6	11.7	-0.7	0.0	0.2	11.7	7.7	0.3
M3	451	-0.9	10.0	14.2	-0.6	0.0	-0.4	14.2	10.1	-0.9
N1	1877	-0.2	1.9	1.4	-0.2	0.4	0.0	2.2	1.2	-0.2
N2	1477	-0.1	4.1	3.8	-0.3	0.4	0.0	4.4	3.6	-0.1
N3	1277	0.0	6.3	6.1	-0.5	0.4	0.0	6.6	5.8	-0.1
O1	647	-0.3	3.9	9.2	-0.3	0.1	0.0	9.2	3.9	-0.3
O2	247	-0.2	5.9	11.3	-0.4	0.1	0.0	11.3	5.9	-0.2
O3	47	-0.1	7.7	13.4	-0.6	0.1	0.0	13.4	7.7	-0.1
P1	1840	-0.1	2.8	-2.5	-0.2	0.7	0.0	2.9	-0.1	-2.6
P2	1640	-0.1	3.7	-1.3	-0.3	0.6	0.0	3.8	-0.1	-1.3
P3	1440	0.1	4.7	0.0	-0.3	0.6	0.0	4.8	0.1	0.0
P4	1240	-0.2	5.6	1.4	-0.4	0.6	0.1	5.7	1.4	-0.2
Q1	628	-0.3	3.6	8.5	-0.3	0.2	0.1	8.5	3.6	-0.3
Q2	428	-0.2	4.4	9.7	-0.3	0.2	0.1	9.7	4.4	-0.2
Q3	228	0.0	5.2	11.0	-0.4	0.2	0.1	11.0	5.2	-0.1
Q4	28	0.0	5.9	12.2	-0.4	0.1	0.1	12.2	6.0	0.0
R1	1816	-0.1	-6.4	-1.2	0.5	0.4	0.9	0.5	-1.7	-6.4



Table 2.10.4-66 Primary Plus Secondary Stresses; 1-Foot Side Drop; Drop Orientation = 90 Degrees; 3-D Model; 0-Degree Circumferential Location; Condition 1 (continued)

Stress Points		Stress Components (ksi)						Principal Stresses (ksi)		
Section <sup>1</sup>	Node	S <sub>x</sub>	S <sub>y</sub>	S <sub>z</sub>	S <sub>xy</sub>	S <sub>xz</sub>	S <sub>yz</sub>	S1	S2	S3
R2	1616	-0.4	-6.3	-3.1	0.5	0.4	1.4	0.3	-3.7	-6.3
R3	1416	-2.1	-6.5	-4.8	0.5	0.4	2.0	-1.0	-5.8	-6.6
R4	1216	0.6	-5.0	-4.8	0.5	0.3	0.7	0.7	-4.8	-5.1
S1	616	-0.9	-2.2	-2.3	0.1	0.2	-1.5	0.0	-2.2	-3.2
S2	416	-5.0	-0.7	6.5	-0.3	0.0	-2.1	6.8	-0.7	-5.4
S3	216	-1.2	1.6	9.4	-0.2	0.1	0.1	9.4	1.6	-1.2
S4	16	-0.4	3.3	13.6	-0.3	0.1	0.2	13.6	3.4	-0.4
T1	811	-10.6	-10.4	-15.3	0.3	0.0	-3.9	-8.4	-10.4	-17.5
T2	611	-5.6	-5.9	-5.0	0.1	0.0	-2.1	-3.2	-5.9	-7.5
T3	411	-2.4	-3.1	1.3	0.1	0.1	-1.1	1.6	-2.7	-3.1
T4	211	-0.6	-0.7	7.2	0.0	0.1	-0.5	7.2	-0.7	-0.7
T5	11	-0.1	1.7	14.5	-0.1	0.1	-0.2	14.5	1.7	-0.1
U1	43058	1.1	-1.0	-4.3	0.1	0.2	0.8	1.2	-1.0	-4.4
U2	43057	0.8	-1.7	-4.0	0.1	0.1	1.1	1.1	-1.7	-4.3
U3	43056	0.2	-2.3	-3.6	0.2	0.1	1.3	0.7	-2.4	-4.1
U4	43055	-0.3	-3.1	-3.6	0.2	0.1	0.9	-0.1	-3.1	-3.9
U5	43054	-1.3	-3.9	-3.5	0.2	0.1	0.1	-1.3	-3.4	-3.9
U6	43053	-2.7	-4.7	-3.0	0.1	0.2	-0.7	-2.1	-3.5	-4.7
U7	43052	-4.9	-5.4	-1.3	0.1	0.3	-1.0	-1.0	-5.1	-5.5
U8	43051	-2.2	0.7	5.9	-0.4	0.5	-0.7	6.0	0.7	-2.3
V1	50024	4.2	1.3	0.0	0.2	-0.1	-0.1	4.2	1.3	0.0
V2	50023	0.4	-0.8	-0.5	0.1	-0.1	-0.1	0.4	-0.5	-0.8
V3	50022	-2.4	-2.5	-0.3	0.0	-0.1	0.0	-0.3	-2.4	-2.5
V4	50021	-7.0	-4.6	0.5	-0.1	-0.1	0.0	0.5	-4.6	-7.0
W1	43278	3.0	2.4	-1.4	0.0	0.2	-0.8	3.1	2.4	-1.6
W2	43274	-0.6	-1.7	-0.6	0.0	0.2	-0.9	0.3	-1.4	-1.7
W3	43271	-3.0	-3.9	0.5	0.0	0.0	-0.4	0.6	-3.1	-3.9
X1	50084	2.3	1.6	-0.4	0.0	0.1	-0.4	2.4	1.6	-0.4
X2	50083	1.2	0.1	-0.2	0.0	0.1	-0.4	1.3	0.1	-0.4
X3	50081	-1.0	-2.9	0.9	0.0	0.1	-0.4	0.9	-1.0	-2.9

<sup>1</sup> Refer to Figure 2.10.2-34 for the identification of the representative sections.

Table 2.10.4-67  $P_m$  Stresses; 1-Foot Side Drop; Drop Orientation = 90 Degrees; 3-D Model; 0-Degree Circumferential Location; Condition 1

Condition 1: 100°F Ambient with Contents

Section <sup>1</sup>	Node - Node	Stress Components (ksi)						Principal Stresses (ksi)			
		$S_x$	$S_y$	$S_z$	$S_{xy}$	$S_{yz}$	$S_{zx}$	S1	S2	S3	S.L.
A	1130 - 1128	-0.3	-1.2	0.0	0.0	0.0	0.0	0.0	-0.3	-1.2	1.2
B	1185 - 1183	-0.2	-2.1	0.0	0.0	0.0	-0.1	0.0	-0.2	-2.1	2.1
C	90 - 40	-2.1	-3.5	0.8	0.0	-0.1	-0.1	0.8	-2.1	-3.5	4.3
D	25 - 5	-3.2	-3.9	0.7	0.1	0.0	-0.1	0.7	-3.2	-3.9	4.6
E	35 - 31	-3.1	-4.4	0.0	0.1	0.0	0.6	0.2	-3.2	-4.4	4.5
F	100 - 97	-0.4	-4.0	-2.8	0.3	-0.3	1.3	0.1	-3.2	-4.2	4.4
G	94 - 91	0.4	-2.1	2.7	0.2	-0.1	0.6	2.9	0.3	-2.1	5.0
H	330 - 327	0.0	4.3	-0.3	-0.3	-0.6	0.0	4.4	0.0	-0.4	4.8
I	244 - 241	0.0	0.4	3.4	0.0	-0.2	0.0	3.4	0.4	0.0	3.5
J	550 - 547	-0.1	4.5	4.9	-0.3	-0.4	0.0	5.2	4.3	-0.1	5.3
K	344 - 341	0.0	0.6	4.5	-0.1	-0.1	0.0	4.5	0.6	0.0	4.5
L	740 - 737	-0.1	4.5	8.2	-0.6	0.0	0.0	8.2	4.5	-0.2	8.3
M	663 - 63	-0.1	0.6	5.4	0.5	0.0	0.0	5.4	0.8	-0.3	5.7
N	1877 - 1277	-0.1	4.5	4.2	-0.3	0.4	0.0	4.8	3.9	-0.1	4.9
O	647 - 47	0.0	0.5	5.1	0.0	0.1	0.0	5.1	0.5	0.0	5.1
P	1840 - 1240	0.0	4.4	-0.3	-0.3	0.6	0.0	4.5	0.0	-0.4	5.0
Q	628 - 28	0.0	0.6	4.4	-0.1	0.1	0.0	4.4	0.6	0.0	4.4
R	1816 - 1216	-1.8	-3.8	-2.0	0.3	0.3	-0.7	-1.3	-2.5	-3.9	2.7
S	616 - 16	0.3	-0.6	3.5	0.0	0.1	0.0	3.5	0.3	-0.6	4.1
T	811 - 11	-2.6	-3.8	0.5	0.2	0.1	-1.3	1.0	-3.0	-3.8	4.8
U	43058 - 43051	-1.0	-1.5	-1.3	0.0	0.0	-0.4	-0.7	-1.5	-1.6	0.8
V	50024 - 50021	-2.2	-1.9	-0.2	0.0	0.0	0.0	-0.2	-1.9	-2.2	2.0
W	43278 - 43271	-0.4	-0.9	0.0	0.0	-0.1	0.1	0.0	-0.4	-0.9	0.9
X	50084 - 50081	-0.1	-2.2	0.0	0.0	0.0	0.1	0.0	-0.1	-2.2	2.2

<sup>1</sup> Refer to Figure 2.10.2-34 for the identification of the representative sections.

Table 2.10.4-68  $P_m + P_b$  Stresses; 1-Foot Side Drop; Drop Orientation = 90 Degrees; 3-D Model; 0-Degree Circumferential Location; Condition 1

Condition 1: 100°F Ambient with Contents

Section <sup>1</sup>	Node - Node	Stress Components (ksi)						Principal Stresses (ksi)			
		$S_x$	$S_y$	$S_z$	$S_{xy}$	$S_{yz}$	$S_{xz}$	S1	S2	S3	S.I.
A O	1130 - 1128	-0.4	-1.7	0.1	0.0	0.0	0.0	0.1	-0.4	1.7	1.8
B O	1185 - 1183	0.1	-2.4	0.0	0.0	0.0	-0.1	0.1	0.0	-2.4	2.5
C I	90 - 40	-0.2	-2.3	2.9	0.0	-0.2	-0.1	2.9	-0.2	-2.3	5.2
D I	25 - 5	-2.1	-3.6	1.5	0.1	0.0	0.0	1.5	-2.1	-3.6	5.1
E I	35 - 31	-3.3	-4.0	1.4	0.1	0.0	0.9	1.5	-3.5	-4.0	5.5
F O	100 - 97	0.1	-7.2	-15.1	0.5	-0.3	1.8	0.3	-7.2	-15.3	15.6
G I	94 - 91	0.4	-1.2	6.4	0.1	-0.1	1.1	6.6	0.2	-1.2	7.8
H I	330 - 327	-0.1	3.4	-2.5	-0.2	-0.7	0.0	3.5	-0.1	-2.5	6.0
I O	244 - 241	0.0	1.4	4.8	-0.1	-0.1	0.0	4.8	1.4	0.0	4.8
J O	550 - 547	0.0	5.4	5.6	-0.4	-0.4	0.0	5.9	5.1	-0.1	5.9
K O	344 - 341	0.0	2.1	5.3	-0.2	-0.1	0.0	5.3	2.1	0.0	5.3
L O	740 - 737	0.0	5.8	9.0	-1.2	0.0	0.0	9.0	6.1	-0.2	9.3
M O	663 - 63	0.2	2.7	6.2	0.8	0.0	0.0	6.2	2.9	-0.1	6.3
N O	1877 - 1277	0.0	5.6	4.9	-0.4	0.4	0.0	5.8	4.7	-0.1	5.8
O O	647 - 47	0.0	2.0	5.8	-0.2	0.0	0.0	5.8	2.1	0.0	5.9
P I	1840 - 1240	-0.1	3.4	-2.2	-0.2	0.7	0.0	3.5	-0.1	-2.2	5.7
Q O	628 - 28	0.0	1.5	5.0	-0.1	0.0	0.0	5.0	1.5	0.0	5.1
R I	1816 - 1216	-0.2	-2.0	3.9	0.2	0.5	0.4	4.0	-0.2	-2.1	6.0
S O	616 - 16	-0.1	0.3	6.4	0.0	0.0	0.2	6.4	0.3	-0.1	6.6
T O	811 - 11	1.3	-0.4	8.4	0.1	0.0	-0.2	8.4	1.3	-0.4	8.8
U O	43058 - 43051	-4.5	-3.0	-1.5	0.0	-0.1	-1.1	-1.1	-3.0	-4.8	3.7
V O	50024 - 50021	-5.8	-3.4	0.1	0.0	0.0	0.0	0.1	-3.4	-5.8	6.0
W I	43278 - 43271	-0.7	-1.0	0.0	0.0	-0.1	0.1	0.0	-0.7	-1.0	1.0
X O	50084 - 50081	0.1	-2.5	0.0	0.0	0.0	0.1	0.1	0.0	-2.5	2.6

<sup>1</sup> Refer to Figure 2.10.2-34 for the identification of the representative sections.

Table 2.10.4-69  $S_n$  Stresses; 1-Foot Side Drop; Drop Orientation = 90 Degrees; 3-D Model; 0-Degree Circumferential Location; Condition 1

Condition 1: 100°F Ambient with Contents

Section <sup>1</sup>	Node - Node	Stress Components (ksi)						Principal Stresses (ksi)			
		$S_x$	$S_y$	$S_z$	$S_{xy}$	$S_{yz}$	$S_{zx}$	S1	S2	S3	S.I.
A O	1130 - 1128	-1.6	-3.0	-1.1	0.0	-0.1	0.3	-0.9	-1.8	-3.0	2.1
B O	1185 - 1183	0.2	-2.3	-0.8	0.0	0.0	0.3	0.2	-0.9	-2.3	2.6
C I	90 - 40	-0.6	-2.9	2.5	0.0	-0.2	-0.2	2.5	-0.6	-2.9	5.5
D O	25 - 5	-4.5	-4.7	0.3	0.1	0.0	-0.3	0.3	-4.5	-4.7	5.0
E O	35 - 31	-2.7	-3.1	3.2	0.0	0.0	0.6	3.3	-2.8	-3.1	6.4
F O	100 - 97	0.6	-7.2	-13.9	0.5	-0.3	1.3	0.8	-7.2	-14.0	14.8
G I	94 - 91	1.6	1.1	16.2	0.0	0.0	2.6	16.6	1.2	1.1	15.5
H O	330 - 327	0.0	4.9	1.0	-0.3	-0.6	0.0	5.0	1.0	0.0	5.1
I O	244 - 241	0.0	4.2	10.8	-0.3	-0.1	0.0	10.8	4.2	0.0	10.8
J O	550 - 547	0.0	6.7	7.1	-0.5	-0.3	0.0	7.3	6.5	0.0	7.3
K O	344 - 341	-0.1	8.3	13.4	-0.6	-0.1	0.0	13.4	8.3	-0.1	13.6
L O	740 - 737	-0.3	5.3	8.2	-0.8	0.0	0.0	8.2	5.4	-0.4	8.6
M O	454 - 451	-0.3	10.3	14.3	-0.6	0.0	-0.2	14.3	10.3	-0.3	14.6
N O	1877 - 1277	0.0	6.3	6.1	-0.5	0.4	0.0	6.6	5.8	-0.1	6.7
O O	647 - 47	-0.1	7.7	13.4	-0.6	0.1	0.0	13.4	7.8	-0.1	13.5
P O	1840 - 1240	0.0	5.6	1.4	-0.4	0.6	0.1	5.7	1.3	0.0	5.8
Q O	628 - 28	0.0	6.0	12.2	-0.4	0.1	0.1	12.2	6.0	0.0	12.2
R I	1816 - 1216	-0.4	-6.6	-1.7	0.5	0.5	1.3	0.4	-2.5	-6.7	7.1
S O	616 - 16	-0.8	3.4	14.3	-0.3	0.1	0.5	14.3	3.4	-0.8	15.2
T O	811 - 11	1.7	2.2	14.6	-0.1	0.1	0.3	14.6	2.2	1.6	13.0
U I	43058 - 43051	1.4	-2.3	-6.0	0.3	0.0	1.5	1.8	-2.3	-6.3	8.1
V O	50024 - 50021	-6.5	-4.6	0.1	-0.1	-0.1	0.0	0.1	-4.6	-6.5	6.6
W O	43278 - 43271	-3.3	-4.4	0.5	0.0	0.0	-0.5	0.6	-3.4	-4.4	4.9
X O	50084 - 50081	-1.0	-2.9	0.8	0.0	0.1	-0.4	0.9	-1.1	-2.9	3.8

<sup>1</sup> Refer to Figure 2.10.2-34 for the identification of the representative sections.

Table 2.10.4-70 Critical P<sub>m</sub> Stress Summary; 1-Foot Side Drop; Drop Orientation = 90 Degrees; 3-D Model; Condition 1

Condition 1: 100°F Ambient with Contents

Comp. No. <sup>1</sup>	Section Cut Node-Node	P <sub>m</sub> Stresses (ksi)							Principal Stresses (ksi)			Allow. S.I. Stress	Margin of Safety
		S <sub>x</sub>	S <sub>y</sub>	S <sub>z</sub>	S <sub>xy</sub>	S <sub>yz</sub>	S <sub>xz</sub>	S <sub>xy</sub>	S1	S2	S3		
1	25- 5	-3.2	-3.9	0.7	0.1	0.0	-0.1	0.7	-3.2	-3.9	4.6	19.2	3.2
2	14140-14137	0.0	0.3	0.5	0.0	-5.4	0.0	5.8	0.0	-5.0	10.9	18.5	0.7
3	14340-14337	0.0	1.8	0.7	0.1	-6.8	0.0	8.1	0.0	-5.6	13.7	31.4	1.3
4	14520-14517	0.0	1.9	0.6	0.0	-4.7	0.0	6.0	0.0	-3.5	9.5	19.6	1.1
5	662- 62	0.1	0.4	5.4	-0.9	0.0	0.0	5.4	1.1	-0.6	6.0	20.0	2.3
6	401- 1	-3.9	-12.7	0.1	0.6	0.1	0.6	0.1	-3.9	-12.7	12.9	20.0	0.6
7	43021-43028	-0.6	-3.5	-9.5	0.2	0.0	0.4	-0.6	-3.6	-9.5	8.9	20.0	1.2
8	51501-51504	-1.7	-1.2	1.2	0.1	0.0	0.0	1.2	-1.2	-1.7	2.8	45.0	15.0

Locations of the most critical sections for each component are provided in the following:

Comp. No. <sup>1</sup>	Section Location					
	Inside Node			Outside Node		
	x (in)	y (deg)	z (in)	x (in)	y (deg)	z (in)
1	39.44	0.0	6.20	39.44	0.0	0.75
2	35.50	67.7	17.40	37.50	67.7	17.40
3	35.50	67.7	29.90	37.00	67.7	29.90
4	35.50	67.7	47.40	37.00	67.7	47.40
5	40.70	0.0	99.50	43.35	0.0	99.50
6	40.88	0.0	193.71	43.35	0.0	193.71
7	37.66	0.0	185.40	37.66	0.0	179.40
8	40.88	180.0	193.71	40.88	180.0	188.40

<sup>1</sup> Refer to Figure 2.10.2-33 for cask component identification.

Table 2.10.4-71 Critical  $P_m + P_b$  Stress Summary; 1-Foot Side Drop; Drop Orientation = 90 Degrees; 3-D Model; Condition 1

Condition 1: 100°F Ambient with Contents

Comp. No. <sup>1</sup>	Section Cut Node-Node	P <sub>b</sub> + P <sub>b</sub> Stresses (ksi)							Principal Stresses (ksi)			Allow. Stress	Margin of Safety
		S <sub>x</sub>	S <sub>y</sub>	S <sub>z</sub>	S <sub>xy</sub>	S <sub>yz</sub>	S <sub>zx</sub>	S1	S2	S3			
1	25- 3	-2.1	-3.6	1.5	0.1	0.0	0.0	1.5	-2.1	-3.6	5.1	28.7	4.6
2	100- 97	0.1	-7.2	-15.1	0.5	-0.3	1.8	0.3	-7.2	-15.3	15.6	27.7	0.8
3	14350-14347	0.0	2.0	0.2	0.0	-7.4	0.0	8.6	0.0	-6.3	14.8	47.1	2.2
4	14320-14317	0.0	2.6	0.9	0.0	-5.0	0.0	6.8	0.0	-3.4	10.2	29.4	1.9
5	662- 62	0.2	2.4	6.3	-1.0	0.0	0.0	6.3	2.8	-0.2	6.5	30.0	3.6
6	403- 3	-2.8	-9.8	7.5	0.5	0.2	1.2	7.6	-2.9	-9.8	17.4	30.0	0.7
7	43021-43028	0.9	-3.0	-11.1	0.2	0.1	1.9	1.2	-3.0	-11.4	12.6	30.0	1.4
8	51501-51504	-5.0	-2.8	1.8	0.3	0.0	0.3	1.8	-2.7	-5.0	6.8	67.5	8.9

Locations of the most critical sections for each component are provided in the following:

Comp. No. <sup>1</sup>	Section Location					
	Inside Node			Outside Node		
	x (in)	y (deg)	z (in)	x (in)	y (deg)	z (in)
1	39.44	0.0	6.20	39.44	0.0	0.75
2	35.50	0.0	15.00	37.50	0.0	15.00
3	35.50	67.7	30.40	37.00	67.7	30.40
4	35.50	67.7	47.40	37.00	67.7	47.40
5	40.70	0.0	99.50	43.35	0.0	99.50
6	40.88	0.0	190.15	43.35	0.0	190.15
7	37.66	0.0	185.40	37.66	0.0	179.40
8	40.88	180.0	193.71	40.88	180.0	188.40

<sup>1</sup> Refer to Figure 2.10.2-33 for cask component identification.

Table 2.10.4-72 Critical  $S_n$  Stress Summary; 1-Foot Side Drop; Drop Orientation = 90 Degrees; 3-D Model; Condition 1

Condition 1: 100°F Ambient with Contents

Comp. No. <sup>1</sup>	Section Cut Node-Node	$S_x$ Stresses (ksi)						Principal Stresses (ksi)				Allow. Stress 3.0 $S_m$
		$S_x$	$S_y$	$S_z$	$S_w$	$S_x$	$S_y$	S1	S2	S3	S.L.	
1	20025-20005	1.6	0.9	-1.1	-1.4	-1.6	0.6	3.3	0.2	-2.0	5.2	57.6
2	104- 101	-1.3	0.1	14.2	-0.1	-0.1	1.1	14.3	0.1	-1.4	15.7	55.5
3	13842-13242	-0.1	2.7	-0.1	0.0	6.0	0.0	7.5	-0.1	-4.9	12.4	94.2
4	13874-13274	0.0	2.7	-0.1	-0.1	4.3	0.0	5.9	0.0	-3.2	9.1	58.8
5	664- 64	-0.2	10.4	15.2	-0.8	0.0	0.0	15.2	10.4	-0.2	15.4	60.0
6	401- 1	-8.5	-22.6	4.0	1.1	0.1	1.9	4.2	-8.7	-22.7	26.9	60.0
7	67571-67531	6.2	24.0	-0.1	1.8	0.1	-1.8	24.2	6.5	-0.6	24.8	60.0
8	50001-50004	-5.7	-3.9	2.4	-0.1	0.0	-0.3	2.4	-3.9	-5.7	8.1	135.0

Locations of the most critical sections for each component are provided in the following:

Comp. No. <sup>1</sup>	Section Location					
	Inside Node			Outside Node		
	x (in)	y (deg)	z (in)	x (in)	y (deg)	z (in)
1	39.44	104.7	6.20	39.44	104.7	0.75
2	40.70	0.0	16.20	43.35	0.0	16.20
3	35.50	56.5	159.40	37.00	56.5	159.40
4	35.50	56.5	142.40	37.00	56.5	142.40
5	40.70	0.0	93.56	43.35	0.0	93.56
6	40.88	0.0	193.71	43.35	0.0	193.71
7	33.71	180.0	187.40	36.46	180.0	187.40
8	40.88	0.0	193.71	40.88	0.0	188.40

<sup>1</sup> Refer to Figure 2.10.2-33 for cask component identification.

Table 2.10.4-73  $P_m$  Stresses; 1-Foot Side Drop; Drop Orientation = 90 Degrees; 3-D Model; 45.9-Degree Circumferential Location; Condition 1

Condition 1: 100°F Ambient with Contents

Section <sup>1</sup>	Node - Node	Stress Components (ksi)						Principal Stresses (ksi)			
		$S_x$	$S_y$	$S_z$	$S_{xy}$	$S_{yz}$	$S_{xz}$	S1	S2	S3	S.I.
A	1130 - 1128	-0.3	-1.2	0.0	0.0	0.0	0.0	0.0	-0.3	-1.2	1.2
B	1185 - 1183	-0.2	-2.1	0.0	0.0	0.0	-0.1	0.0	-0.2	-2.1	2.1
C	10090 - 10040	-1.5	-2.1	0.5	-0.4	-1.0	-0.1	0.8	-1.4	-2.6	3.4
D	10025 - 10005	-1.9	-2.9	0.6	-0.1	-0.3	0.0	0.6	-1.9	-3.0	3.5
E	10035 - 10031	-1.9	-2.8	0.1	0.3	-0.6	0.5	0.3	-1.9	-3.0	3.3
F	10100 - 10097	-0.2	-1.9	-1.3	0.0	-4.3	0.7	2.8	-0.3	-5.9	8.7
G	10094 - 10091	0.1	-0.9	1.6	0.0	-0.9	0.1	1.9	0.1	-1.2	3.1
H	10330 - 10327	0.0	3.1	0.2	0.2	-5.9	0.0	7.8	0.0	-4.5	12.2
I	10244 - 10241	0.0	0.3	1.8	0.0	-1.3	0.0	2.5	0.0	-0.4	2.9
J	10550 - 10547	0.0	3.2	2.7	0.0	-3.5	0.0	6.4	0.0	-0.6	7.0
K	10344 - 10341	0.0	0.4	2.2	0.0	-0.8	0.0	2.5	0.1	0.0	2.5
L	10740 - 10737	0.0	3.2	3.9	0.1	0.1	0.0	3.9	3.1	0.0	4.0
M	10663 - 10063	0.1	0.3	2.6	-0.1	-0.1	0.0	2.6	0.4	0.0	2.6
N	11877 - 11277	0.0	3.2	2.4	0.0	3.8	0.0	6.6	0.0	-1.1	7.6
O	10647 - 10047	0.0	0.3	2.5	0.0	0.5	0.0	2.6	0.2	0.0	2.6
P	11840 - 11240	0.0	3.2	0.3	0.2	5.8	0.0	7.7	0.0	-4.2	11.9
Q	10628 - 10028	0.0	0.5	2.2	0.0	0.9	0.0	2.6	0.1	0.0	2.6
R	11816 - 11216	-0.9	-1.3	-0.8	1.0	3.5	-0.3	2.6	-0.8	-4.8	7.4
S	10616 - 10016	-0.2	-0.2	2.0	-0.2	0.8	0.0	2.3	-0.1	-0.6	2.9
T	10811 - 10011	3	-2.2	0.4	0.6	1.6	-0.6	1.2	-1.0	-3.3	4.4
U	44558 - 44551	-0.8	-1.2	-1.3	0.0	0.0	-0.2	-0.7	-1.2	-1.4	0.7
V	50524 - 50521	-1.1	-1.3	-0.2	0.3	0.1	0.0	-0.2	-0.9	-1.5	1.4
W	43278 - 43271	-0.4	-0.9	0.0	0.0	-0.1	0.1	0.0	-0.4	-0.9	0.9
X	50084 - 50081	-0.1	-2.2	0.0	0.0	0.0	0.1	0.0	-0.1	-2.2	2.2

<sup>1</sup> Refer to Figure 2.10.2-34 for the identification of the representative sections.



Table 2.10.4-74  $P_m + P_b$  Stresses; 1-Foot Side Drop; Drop Orientation = 90 Degrees; 3-D Model; 45.9-Degree Circumferential Location; Condition 1

Condition 1: 100°F Ambient with Contents

Section <sup>1</sup>	Node - Node	Stress Components (ksi)						Principal Stresses (ksi)			
		$S_x$	$S_y$	$S_z$	$S_{xy}$	$S_{yz}$	$S_{xz}$	S1	S2	S3	S.I.
A O	1130 - 1128	-0.4	-1.7	0.1	0.0	0.0	0.0	0.1	-0.4	-1.7	1.8
B O	1185 - 1183	0.1	-2.4	0.0	0.0	0.0	-0.1	0.1	0.0	-2.4	2.5
C I	10090 - 10040	-0.4	-1.1	1.6	-1.5	-2.2	0.0	3.0	0.1	-3.0	6.0
D I	10025 - 10005	-1.0	-2.4	1.1	-0.4	-0.6	0.1	1.2	-0.9	-2.6	3.8
E I	10035 - 10031	-2.1	-2.6	1.0	0.6	-0.9	0.7	1.3	-1.7	-3.3	4.6
F I	10100 - 10097	-0.5	-0.3	5.0	0.0	-4.8	0.5	7.9	-0.5	-3.1	11.0
G I	10094 - 10091	0.1	-0.8	1.6	0.0	-1.4	0.2	2.3	0.1	-1.5	3.8
H I	10330 - 10327	-0.1	2.5	-1.2	0.1	-6.4	0.1	7.2	-0.1	-6.0	13.2
I I	10244 - 10241	0.0	0.6	1.5	0.0	-1.8	0.0	2.8	0.0	-0.8	3.6
J I	10550 - 10547	-0.1	2.8	2.4	0.0	-3.9	0.0	6.5	-0.1	-1.3	7.8
K I	10344 - 10341	0.0	1.1	2.3	0.0	-1.1	0.0	2.9	0.5	0.0	2.9
L O	10740 - 10737	0.0	3.4	4.1	0.2	0.1	0.0	4.1	3.4	0.0	4.1
M O	10663 - 10063	-0.1	-0.7	2.3	-0.2	-0.1	0.0	2.4	0.0	-0.7	3.1
N I	11877 - 11277	-0.1	2.9	2.1	0.0	4.2	0.0	6.8	-0.1	-1.7	8.4
O I	10647 - 10047	0.0	0.9	2.6	0.0	0.8	0.0	2.9	0.6	0.0	2.9
P I	11840 - 11240	-0.1	2.9	-0.7	0.0	6.2	0.0	7.5	-0.1	-5.4	12.9
Q I	10628 - 10028	0.0	0.8	2.2	0.0	1.3	0.0	2.9	0.0	0.0	3.0
R I	11816 - 11216	-0.1	-0.5	1.4	0.0	4.0	0.1	4.5	-0.1	-3.6	8.1
S O	10616 - 10016	0.0	0.5	4.8	0.1	0.4	0.0	4.8	0.5	-0.1	4.9
T I	10811 - 10011	-3.5	-4.1	-4.5	1.6	2.9	-1.1	-1.3	-2.8	-8.0	6.8
U I	44558 - 44551	1.4	0.0	-1.3	-0.5	0.1	0.5	1.7	-0.1	-1.4	3.0
V O	50524 - 50521	-3.8	-2.6	0.2	1.0	0.1	0.0	0.2	-2.1	-4.4	4.5
W I	43278 - 43271	-0.7	-1.0	0.0	0.0	-0.1	0.1	0.0	-0.7	-1.0	1.0
X O	50084 - 50081	0.1	-2.5	0.0	0.0	0.0	0.1	0.1	0.0	-2.5	2.6

<sup>1</sup> Refer to Figure 2.10.2-34 for the identification of the representative sections.

Table 2.10.4-75  $S_n$  Stresses; 1-Foot Side Drop; Drop Orientation = 90 Degrees; 3-D Model; 45.9-Degree Circumferential Location; Condition 1

Condition 1: 100°F Ambient with Contents

Section <sup>1</sup>	Node - Node	Stress Components (ksi)							Principal Stresses (ksi)			
		$S_x$	$S_y$	$S_z$	$S_{xy}$	$S_{yz}$	$S_{xz}$	$S_{\theta}$	S1	S2	S3	S.L
A O	1130 - 1128	-1.6	-3.0	-1.1	0.0	-0.1	0.3	-0.9	-1.8	-3.0	2.1	
B O	1185 - 1183	0.2	-2.3	-0.8	0.0	0.0	0.3	0.2	-0.9	-2.3	2.6	
C I	10090 - 10040	-0.4	-1.6	1.1	-1.4	-1.8	-0.1	2.2	0.0	-3.1	5.3	
D O	10025 - 10005	-3.0	-3.9	0.2	0.3	0.0	-0.3	0.3	-2.9	-4.0	4.2	
E I	10035 - 10031	-5.4	-4.2	-2.1	0.5	-1.0	1.8	-1.2	-4.0	-6.5	5.4	
F I	10100 - 10097	-0.4	-0.6	2.9	0.0	-4.1	0.7	5.7	-0.4	-3.3	9.0	
G I	10094 - 10091	1.3	1.5	11.9	-0.1	-2.2	1.9	12.7	1.3	0.8	11.9	
H I	10330 - 10327	0.0	2.4	-0.1	0.0	-3.7	0.1	7.0	0.0	-4.7	11.7	
I O	10244 - 10241	0.0	3.5	8.4	0.0	-1.4	0.0	8.8	3.2	0.0	8.8	
J I	10550 - 10547	0.0	1.5	-0.3	-0.1	-3.4	0.0	4.1	0.0	-2.9	7.0	
K O	10344 - 10341	0.0	6.7	10.8	0.0	-1.0	0.0	11.0	6.5	0.0	11.1	
L O	10740 - 10737	-0.1	5.1	4.8	0.6	0.0	0.1	5.2	4.8	-0.1	5.3	
M O	10454 - 10451	-0.1	7.3	10.5	0.0	0.0	-0.1	10.5	7.3	-0.1	10.6	
N I	11877 - 11277	0.0	1.4	-0.3	0.0	3.8	0.0	4.5	0.0	-3.3	7.8	
O O	10647 - 10047	0.0	6.3	10.3	0.0	0.6	0.0	10.4	6.2	0.0	10.5	
P I	11840 - 11240	0.0	2.7	-0.7	0.0	5.7	-0.1	7.0	0.0	-5.0	12.0	
Q O	10628 - 10028	0.0	5.0	9.7	0.0	1.1	0.1	10.0	4.8	0.0	9.9	
R I	11816 - 11216	-0.5	-4.2	-4.5	0.0	3.6	0.8	0.0	-1.2	-7.9	7.9	
S O	10616 - 10016	-0.7	2.9	12.4	0.1	1.1	0.3	12.6	2.8	-0.7	13.3	
T O	10811 - 10011	1.3	1.4	11.3	-0.4	0.8	0.3	11.4	1.8	0.8	10.6	
U I	44558 - 44551	1.7	-1.1	-5.2	-0.6	0.1	1.9	2.3	-1.2	-5.7	8.0	
V O	50524 - 50521	-5.0	-4.5	0.3	1.0	0.1	0.2	0.3	-3.7	-5.7	6.0	
W O	43278 - 43271	-3.3	-4.4	0.5	0.0	0.0	-0.5	0.6	-3.4	-4.4	4.9	
X O	50084 - 50081	-1.0	-2.9	0.8	0.0	0.1	-0.4	0.9	-1.1	-2.9	3.8	

<sup>1</sup> Refer to Figure 2.10.2-34 for the identification of the representative sections.

Table 2.10.4-76  $P_m$  Stresses; 1-Foot Side Drop; Drop Orientation = 90 Degrees; 3-D Model; 91.7-Degree Circumferential Location; Condition 1

Condition 1: 100°F Ambient with Contents

Section <sup>1</sup>	Node - Node	Stress Components (ksi)						Principal Stresses (ksi)			
		$S_x$	$S_y$	$S_z$	$S_{xy}$	$S_{yz}$	$S_{zx}$	S1	S2	S3	S.L.
A	1130 - 1128	-0.3	-1.2	0.0	0.0	0.0	0.0	0.0	-0.3	-1.2	1.2
B	1185 - 1183	-0.2	-2.1	0.0	0.0	0.0	-0.1	0.0	-0.2	-2.1	2.1
C	18090 - 18040	-0.2	-0.1	-0.2	-0.5	-1.1	0.1	1.0	-0.3	-1.4	2.4
D	18025 - 18005	0.0	-0.8	0.3	-0.8	-0.7	0.0	0.8	0.2	-1.5	2.3
E	18035 - 18031	0.2	-0.2	0.0	0.3	-1.4	-0.1	1.4	0.2	-1.5	2.9
F	18100 - 18097	0.1	1.3	1.8	0.0	-4.7	-0.5	6.3	0.2	-3.2	9.6
G	18094 - 18091	-0.2	0.5	-1.0	-0.1	-1.4	-0.2	1.3	-0.1	-1.9	3.2
H	18330 - 18327	-0.1	0.4	0.8	0.3	-5.9	-0.1	6.4	-0.1	-5.3	11.7
I	18244 - 18241	0.0	0.2	-1.0	0.0	-1.3	0.0	1.0	0.0	-1.8	2.8
J	18550 - 18547	-0.2	0.6	-1.4	0.0	-3.5	0.0	3.2	-0.2	-4.0	7.2
K	18344 - 18341	0.0	0.0	-1.2	0.0	-0.8	0.0	0.4	0.0	-1.6	2.0
L	18740 - 18737	-0.2	1.0	-2.4	0.0	0.1	0.0	1.0	-0.2	-2.4	3.4
M	18663 - 18063	0.1	0.0	-1.3	0.1	-0.1	0.0	0.1	-0.1	-1.4	1.5
N	19877 - 19277	-0.2	0.7	-1.1	0.0	3.7	0.0	3.6	-0.2	-4.0	7.5
O	18647 - 18047	0.0	0.0	-1.3	0.0	0.6	0.0	0.2	0.0	-1.6	1.8
P	19840 - 19240	-0.1	0.6	0.8	0.3	5.7	0.1	6.4	-0.1	-5.0	11.3
Q	18628 - 18028	0.0	0.1	-1.3	0.0	1.1	0.0	0.7	0.0	-1.8	2.6
R	19816 - 19216	0.9	2.4	1.1	1.3	4.0	0.4	6.1	0.7	-2.3	8.4
S	18616 - 18016	-0.5	0.5	-1.1	-0.1	1.1	0.1	1.1	-0.5	-1.7	2.8
T	18811 - 18011	0.5	0.7	-0.3	0.8	2.0	0.5	2.7	0.2	-1.9	4.6
U	45758 - 45751	-0.5	-0.9	-1.6	-0.2	0.1	0.0	-0.5	-0.9	-1.7	1.2
V	50924 - 50921	0.0	-0.6	-0.2	-0.1	0.1	0.0	0.0	-0.2	-0.7	0.7
W	43278 - 43271	-0.4	-0.9	0.0	0.0	-0.1	0.1	0.0	-0.4	-0.9	0.9
X	50084 - 50081	-0.1	-2.2	0.0	0.0	0.0	0.1	0.0	-0.1	-2.2	2.2

<sup>1</sup> Refer to Figure 2.10.2-34 for the identification of the representative sections.

Table 2.10.4-77  $P_m + P_b$  Stresses; 1-Foot Side Drop; Drop Orientation = 90 Degrees; 3-D Model; 91.7-Degree Circumferential Location; Condition 1

Condition 1: 100°F Ambient with Contents

Section <sup>1</sup>	Node - Node	Stress Components (ksi)						Principal Stresses (ksi)			
		$S_x$	$S_y$	$S_z$	$S_{xy}$	$S_{yz}$	$S_{xz}$	S1	S2	S3	S.L
A O	1130 - 1128	-0.4	-1.7	0.1	0.0	0.0	0.0	0.1	-0.4	-1.7	1.8
B O	1185 - 1183	0.1	-2.4	0.0	0.0	0.0	-0.1	0.1	0.0	-2.4	2.5
C I	18090 - 18040	0.0	0.4	-1.0	-1.5	-2.4	0.1	2.8	-0.4	-3.1	5.9
D I	18025 - 18005	0.0	-0.4	0.7	-1.2	-1.3	0.0	1.9	0.3	-1.9	3.8
E I	18035 - 18031	0.4	0.0	1.0	0.8	-1.7	-0.2	2.5	0.3	-1.5	3.9
F O	18100 - 18097	0.0	2.8	7.5	0.1	-4.6	-0.8	10.3	0.3	-0.4	10.7
G I	18094 - 18091	-0.2	-0.2	-3.3	-0.1	-1.6	-0.4	0.5	-0.1	-4.0	4.5
H O	18330 - 18327	0.0	-0.6	0.4	0.4	-6.0	-0.1	6.0	0.0	-6.1	12.1
I O	18244 - 18241	0.0	-0.1	-1.3	0.0	-1.4	0.0	0.8	0.0	-2.2	3.0
J I	18550 - 18547	-0.2	2.6	-0.7	0.0	-3.5	0.0	4.8	-0.2	-2.9	7.7
K I	18344 - 18341	0.0	0.5	-0.9	0.0	-0.8	0.0	0.9	0.0	-1.2	2.1
L I	19908 - 19308	0.4	3.3	-1.4	0.0	0.3	0.0	3.3	0.4	-1.4	4.7
M I	18663 - 18063	0.2	0.9	-1.0	0.0	-0.1	0.0	0.9	0.2	-1.0	1.9
N I	19877 - 19277	-0.2	2.5	-0.4	0.0	3.7	0.0	5.0	-0.2	-2.9	7.9
O O	18647 - 18047	0.0	-0.7	-1.6	0.0	0.7	0.0	0.0	-0.3	-2.0	2.0
P O	19840 - 19240	0.0	-0.4	0.4	0.4	5.8	0.1	5.8	0.0	-5.8	11.7
Q O	18628 - 18028	0.0	-0.3	-1.8	0.0	1.2	0.0	0.3	0.0	-2.4	2.7
R O	19816 - 19216	1.8	3.7	5.7	2.6	3.9	1.1	9.5	2.1	-0.5	10.0
S I	18616 - 18016	-1.0	0.3	-2.1	-0.2	1.2	0.3	0.8	-0.9	-2.7	3.5
T I	18811 - 18011	1.2	1.3	0.6	1.9	2.9	0.9	4.9	0.2	-2.1	7.0
U I	45758 - 45751	-1.1	-1.0	-2.3	-0.6	0.1	0.6	-0.4	-1.4	-2.6	2.2
V I	50924 - 50921	0.8	-0.1	-0.7	-0.6	0.1	-0.1	1.1	-0.4	-0.7	1.8
W I	43278 - 43271	-0.7	-1.0	0.0	0.0	-0.1	0.1	0.0	-0.7	-1.0	1.0
X O	50084 - 50081	0.1	-2.5	0.0	0.0	0.0	0.1	0.1	0.0	-2.5	2.6

<sup>1</sup> Refer to Figure 2.10.2-34 for the identification of the representative sections.

Table 2.10.4-78  $S_n$  Stresses; 1-Foot Side Drop; Drop Orientation = 90 Degrees; 3-D Model; 91.7-Degree Circumferential Location; Condition 1

**Condition 1: 100°F Ambient with Contents**

Section <sup>1</sup>	Node - Node	Stress Components (ksi)						Principal Stresses (ksi)			
		$S_x$	$S_y$	$S_z$	$S_{xy}$	$S_{yz}$	$S_{xz}$	S1	S2	S3	S.L
A O	1130 - 1128	-1.6	-3.0	-1.1	0.0	-0.1	0.3	-0.9	-1.8	-3.0	2.1
B O	1185 - 1183	0.2	-2.3	-0.8	0.0	0.0	0.3	0.2	-0.9	-2.3	2.6
C I	18090 - 18040	-0.5	-0.1	-0.7	-1.5	-1.6	0.0	1.9	-0.6	-2.6	4.4
D I	18025 - 18005	2.0	0.5	-0.9	-1.4	-1.5	0.7	3.2	0.2	-1.8	5.1
E I	18035 - 18031	-3.0	-1.6	-2.6	0.8	-1.9	1.1	-0.1	-2.1	-5.0	4.9
F O	18100 - 18097	0.8	2.6	7.8	-0.1	-2.4	-1.1	8.9	1.9	0.4	8.5
G I	18094 - 18091	0.9	2.1	6.6	-0.3	-3.4	0.9	8.5	0.8	0.2	8.3
H O	18330 - 18327	-0.1	0.3	0.3	0.3	-3.6	0.0	3.9	0.0	-3.3	7.2
I I	18244 - 18241	0.0	2.7	5.4	0.0	-2.6	0.0	7.0	1.2	0.0	7.0
J I	18550 - 18547	-0.1	2.5	-2.7	0.1	-2.0	0.0	3.2	-0.1	-3.4	6.6
K O	18344 - 18341	0.0	5.6	6.8	0.0	-1.5	0.0	7.9	4.5	0.0	7.9
M O	18454 - 18451	-0.1	6.4	6.3	0.0	0.0	-0.1	6.4	6.3	-0.1	6.5
L I	19908 - 19308	-0.2	3.5	-3.6	0.2	0.2	0.0	3.5	-0.2	-3.6	7.1
N I	19877 - 19277	-0.1	2.0	-2.4	0.1	2.2	0.0	2.9	-0.1	-3.3	6.2
O O	18647 - 18047	0.0	4.9	5.3	0.0	1.4	0.0	6.5	3.7	0.0	6.6
P O	19840 - 19240	0.0	0.9	1.1	0.3	3.7	0.1	4.7	0.0	-2.7	7.4
Q O	18628 - 18028	0.0	3.5	4.1	0.0	2.4	0.1	6.2	1.4	0.0	6.2
R O	19816 - 19216	0.9	0.7	6.1	0.9	2.0	4.1	9.0	0.1	-1.4	10.4
S I	18616 - 18016	-6.3	-1.5	-3.1	-1.5	2.8	-2.2	1.4	-4.9	-7.5	8.9
T I	18811 - 18011	1.3	-0.4	-1.6	1.4	3.0	0.1	2.9	0.5	-4.1	7.0
U I	45758 - 45751	-0.1	-1.8	-7.6	-0.2	0.0	1.9	0.4	-1.8	-8.1	8.5
V O	50924 - 50921	-2.1	-3.1	0.4	0.4	0.0	0.3	0.4	-2.0	-3.3	3.7
W O	43278 - 43271	-3.3	-4.4	0.5	0.0	0.0	-0.5	0.6	-3.4	-4.4	4.9
X O	50084 - 50081	-1.0	-2.9	0.8	0.0	0.1	-0.4	0.9	-1.1	-2.9	3.8

<sup>1</sup> Refer to Figure 2.10.2-34 for the identification of the representative sections.

Table 2.10.4-79  $P_m$  Stresses; 1-Foot Side Drop; Drop Orientation = 90 Degrees;  
3-D Model; 180-Degree Circumferential Location; Condition 1

Condition 1: 100°F Ambient with Contents

Section <sup>1</sup>	Node - Node	Stress Components (ksi)						Principal Stresses (ksi)			
		$S_x$	$S_y$	$S_z$	$S_{xy}$	$S_{yz}$	$S_{zx}$	S1	S2	S3	S.I.
A	1130 - 1128	-0.3	-1.2	0.0	0.0	0.0	0.0	0.0	-0.3	-1.2	1.2
B	1183 - 1183	-0.2	-2.1	0.0	0.0	0.0	-0.1	0.0	-0.2	-2.1	2.1
C	30090 - 30040	0.0	0.9	-0.3	0.1	-0.1	0.0	0.9	0.0	-0.4	1.3
D	30025 - 30005	-0.9	1.5	-0.2	0.1	-0.1	0.0	1.5	-0.2	-0.9	2.4
E	30035 - 30031	0.6	1.1	-0.3	0.1	-0.2	-0.4	1.2	0.7	-0.5	1.7
F	30100 - 30097	0.0	0.8	0.3	0.1	-0.4	-0.5	1.2	0.4	-0.3	1.5
G	30094 - 30091	-0.1	0.3	-1.3	0.0	-0.2	-0.1	0.3	-0.1	-1.4	1.7
H	30330 - 30327	-0.1	-1.8	-0.9	-0.2	-0.4	0.0	0.0	-0.7	-2.0	2.0
I	30244 - 30241	0.0	-0.3	-1.8	0.0	-0.2	0.0	0.0	-0.3	-1.8	1.8
J	30550 - 30547	-0.2	-1.3	-2.6	-0.2	-0.2	0.0	-0.2	-1.3	-2.6	2.4
K	30344 - 30341	0.0	-0.3	-2.4	0.0	-0.1	0.0	0.0	-0.3	-2.4	2.4
L	30740 - 30737	0.0	-1.2	-3.5	0.3	0.0	0.0	0.1	-1.2	-3.5	3.6
M	30663 - 30063	-0.1	-0.3	-2.8	-0.4	0.0	0.0	0.2	-0.6	-2.8	3.0
N	31877 - 31277	-0.2	-1.2	-2.0	-0.2	0.3	0.0	-0.2	-1.2	-2.1	1.9
O	30647 - 30047	0.0	-0.3	-2.6	0.0	0.1	0.0	0.0	-0.3	-2.6	2.6
P	31840 - 31240	-0.1	-1.8	-0.6	-0.2	0.4	0.0	-0.1	-0.5	-2.0	1.9
Q	30628 - 30028	0.0	-0.5	-2.2	-0.1	0.1	0.0	0.0	-0.5	-2.2	2.2
R	31816 - 31216	0.2	2.4	0.3	0.4	0.3	0.6	2.5	0.6	-0.4	2.9
S	30616 - 30016	-0.2	1.6	-1.8	0.3	0.2	0.0	1.7	-0.2	-1.8	3.5
T	30811 - 30011	0.3	3.6	-0.9	0.6	0.2	0.4	3.7	0.3	-1.0	4.7
U	47558 - 47551	-1.1	-1.6	-2.6	-0.1	0.0	0.1	-1.1	-1.7	-2.6	1.4
V	51524 - 51521	-1.6	-1.4	-0.4	0.0	0.0	0.2	-0.4	-1.4	-1.7	1.3
W	43278 - 43271	-0.4	-0.9	0.0	0.0	-0.1	0.1	0.0	-0.4	-0.9	0.9
X	50084 - 50081	-0.1	-2.2	0.0	0.0	0.0	0.1	0.0	-0.1	-2.2	2.2

<sup>1</sup> Refer to Figure 2.10.2-34 for the identification of the representative sections.

Table 2.10.4-80  $P_m + P_b$  Stresses; 1-Foot Side Drop; Drop Orientation = 90 Degrees; 3-D Model; 180-Degree Circumferential Location; Condition 1

**Condition 1: 100°F Ambient with Contents**

Section <sup>1</sup>	Node - Node	Stress Components (ksi)						Principal Stresses (ksi)			
		$S_x$	$S_y$	$S_z$	$S_{xy}$	$S_{yz}$	$S_{xz}$	S1	S2	S3	S.I.
A O	1130 - 1128	-0.4	-1.7	0.1	0.0	0.0	0.0	0.1	-0.4	-1.7	1.8
B O	1185 - 1183	0.1	-2.4	0.0	0.0	0.0	-0.1	0.1	0.0	-2.4	2.5
C I	30090 - 30040	-0.9	0.2	-1.1	0.0	-0.2	-0.1	0.2	-0.9	-1.1	1.4
D O	30025 - 30005	-0.7	2.0	-0.3	0.1	0.0	0.3	2.0	-0.1	-0.9	2.9
E O	30035 - 30031	-0.1	0.6	-1.2	0.1	-0.2	-0.2	0.7	-0.1	-1.2	1.9
F O	30100 - 30097	-0.1	1.7	3.6	0.3	-0.4	-0.5	3.8	1.6	-0.2	4.0
G I	30094 - 30091	-0.1	0.1	-1.8	0.0	-0.2	-0.2	0.1	0.0	-1.8	2.0
H O	30330 - 30327	-0.1	-1.7	-1.4	-0.2	-0.5	0.0	0.0	-1.0	-2.1	2.0
I O	30244 - 30241	0.0	-0.2	-2.0	0.0	-0.2	0.0	0.0	-0.1	-2.0	2.0
J I	30550 - 30547	-0.2	-2.0	-2.8	-0.3	-0.2	0.0	-0.1	-2.0	-2.8	2.7
K I	30344 - 30341	0.0	-0.8	-2.5	-0.1	-0.1	0.0	0.0	-0.8	-2.5	2.5
L O	31908 - 31308	-0.4	0.7	-2.7	-1.7	0.0	0.0	2.0	-1.7	-2.7	4.7
M O	30663 - 30063	-0.1	0.5	-2.6	-0.6	0.0	0.0	0.9	-0.5	-2.6	3.5
N I	31877 - 31277	-0.1	-1.9	-2.2	-0.3	0.2	0.0	-0.1	-1.8	-2.3	2.2
O I	30647 - 30047	0.0	-0.8	-2.7	-0.1	0.1	0.0	0.0	-0.8	-2.7	2.7
P I	31840 - 31240	-0.1	-1.9	0.1	-0.3	0.4	0.0	0.1	-0.1	-2.0	2.1
Q O	30628 - 30028	0.0	-0.4	-2.7	-0.1	0.2	0.0	0.0	-0.4	-2.7	2.7
R I	31816 - 31216	0.1	1.9	-1.7	0.3	0.3	0.2	1.9	0.1	-1.7	3.7
S O	30616 - 30016	0.1	1.3	-3.4	0.2	0.1	0.1	1.4	0.0	-3.4	4.8
T O	30811 - 30011	-0.3	2.6	-3.8	0.4	0.2	-0.2	2.7	-0.4	-3.8	6.5
U O	47558 - 47551	1.3	0.4	-1.1	-0.1	0.2	-0.8	1.6	0.4	-1.4	3.0
V I	51524 - 51521	-4.0	-3.1	-1.2	0.0	0.0	0.1	-1.2	-3.1	-4.0	2.8
W I	43278 - 43271	-0.7	-1.0	0.0	0.0	-0.1	0.1	0.0	-0.7	-1.0	1.0
X O	50084 - 50081	0.1	-2.5	0.0	0.0	0.0	0.1	0.1	0.0	-2.5	2.6

<sup>1</sup> Refer to Figure 2.10.2-34 for the identification of the representative sections.

Table 2.10.4-81  $S_n$  Stresses; 1-Foot Side Drop; Drop Orientation = 90 Degrees; 3-D Model; 180-Degree Circumferential Location; Condition 1

Condition 1: 100°F Ambient with Contents

Section <sup>1</sup>	Node - Node	Stress Components (ksi)						Principal Stresses (ksi)			
		$S_x$	$S_y$	$S_z$	$S_{xy}$	$S_{yz}$	$S_{xz}$	S1	S2	S3	S.L
A O	1130 - 1128	-1.6	-3.0	-1.1	0.0	-0.1	0.3	-0.9	-1.8	-3.0	2.1
B O	1185 - 1183	0.2	-2.3	-0.8	0.0	0.0	0.3	0.2	-0.9	-2.3	2.6
C I	30090 - 30040	-2.6	-0.9	-0.2	0.1	-0.1	-0.4	-0.2	-0.9	-2.6	2.4
D I	30025 - 30005	1.1	2.1	-2.1	0.0	-0.3	0.6	2.1	1.2	-2.2	4.3
E O	30035 - 30031	0.1	3.0	4.7	0.4	-0.3	0.1	4.8	3.0	0.0	4.7
F O	30100 - 30097	0.5	-0.9	-3.1	-0.1	-0.1	0.0	0.5	-0.9	-3.1	3.6
G I	30094 - 30091	0.9	2.2	8.1	0.2	-0.7	0.8	8.2	2.2	0.8	7.4
H O	30330 - 30327	-0.1	0.3	-3.0	0.1	-0.1	0.2	0.3	-0.1	-3.0	3.3
I I	30244 - 30241	0.0	1.0	5.2	0.1	-0.4	0.0	5.3	1.0	0.0	5.3
J I	30550 - 30547	-0.1	-0.6	-4.0	-0.1	0.0	0.0	-0.1	-0.6	-4.0	3.9
K O	30344 - 30341	0.0	5.5	5.6	0.8	-0.2	0.0	5.8	5.4	-0.1	5.8
L I	30740 - 30737	-0.2	-0.6	-3.4	-0.4	0.0	-0.1	0.0	-0.8	-3.4	3.4
M O	30454 - 30451	-0.1	6.6	4.3	0.9	0.0	-0.1	6.8	4.3	-0.2	6.9
N I	31877 - 31277	-0.1	-0.9	-3.3	-0.1	0.0	0.0	-0.1	-0.9	-3.3	3.3
O O	30647 - 30047	0.0	4.9	4.9	0.7	0.2	0.0	5.2	4.8	-0.1	5.2
P O	31840 - 31240	-0.1	0.7	-1.7	0.1	0.1	-0.1	0.7	-0.1	-1.7	2.4
Q I	30628 - 30028	-0.1	1.6	4.3	0.2	0.3	0.0	4.4	1.6	-0.1	4.5
R O	31816 - 31216	-0.9	-0.2	-1.4	0.1	-0.3	3.4	2.2	-0.2	-4.5	6.8
S O	30616 - 30016	-0.6	5.2	6.8	0.9	0.3	0.4	6.8	5.3	-0.7	7.5
T I	30811 - 30011	-2.9	2.4	-4.2	0.8	0.5	-0.6	2.5	-2.7	-4.6	7.1
U I	47558 - 47551	-3.2	-5.0	-9.8	-0.3	-0.4	2.6	-2.3	-5.1	-10.7	8.5
V O	51524 - 51521	-0.7	-1.5	0.1	-0.1	0.0	0.2	0.2	-0.7	-1.6	1.8
W O	43278 - 43271	-3.3	-4.4	0.5	0.0	0.0	-0.5	0.6	-3.4	-4.4	4.9
X O	50084 - 50081	-1.0	-2.9	0.8	0.0	0.1	-0.4	0.9	-1.1	-2.9	3.8

<sup>1</sup> Refer to Figure 2.10.2-34 for the identification of the representative sections.



Table 2.10.4-82  $P_m$  Stresses; 1-Foot Side Drop; Drop Orientation = 90 Degrees; 3-D Model; 67.7-Degree Circumferential Location; Condition 1

Condition 1: 100°F Ambient with Contents

Section <sup>1</sup>	Node - Node	Stress Components (ksi)						Principal Stresses (ksi)			
		$S_x$	$S_y$	$S_z$	$S_{xy}$	$S_{yz}$	$S_{zx}$	S1	S2	S3	S.L
A	1130 - 1128	0.3	-1.2	0.0	0.0	0.0	0.0	0.0	-0.3	-1.2	1.2
B	1185 - 1183	-0.2	-2.1	0.0	0.0	0.0	-0.1	0.0	-0.2	-2.1	2.1
C	14090 -14040	-0.7	-1.1	0.1	-0.4	-1.2	0.0	0.9	-0.6	-1.9	2.8
D	14025 -14005	-0.6	-1.9	0.4	-0.3	-0.5	0.0	0.5	-0.6	-2.1	2.6
E	14035 -14031	-0.7	-1.3	0.1	0.3	-1.0	0.2	0.6	-0.5	-1.9	2.6
F	14100 -14097	0.0	-0.1	0.4	0.1	-5.2	0.1	5.3	0.0	-5.0	10.3
G	14094 -14091	-0.1	0.0	0.3	-0.1	-1.2	-0.1	1.3	-0.1	-1.1	2.4
H	14330 -14327	0.0	1.8	0.7	0.2	-6.8	0.0	8.1	0.0	-5.6	13.6
I	14244 -14241	0.0	0.3	0.4	0.0	-1.4	0.0	1.7	0.0	-1.0	2.7
J	14550 -14547	0.0	2.0	0.6	0.0	-3.9	0.0	5.2	0.0	-2.7	7.9
K	14344 -14341	0.0	0.2	0.4	0.0	-0.9	0.0	1.2	0.0	-0.6	1.8
L	14740 -14737	-0.1	2.1	0.5	0.1	0.1	0.0	2.1	0.5	-0.1	2.2
M	14454 -14451	-0.1	0.3	0.4	0.0	-0.1	0.0	0.4	0.2	-0.1	0.5
N	15877 -15277	0.0	2.0	0.6	0.0	4.2	0.0	5.5	0.0	-3.0	8.5
O	14647 -14047	0.0	0.2	0.4	0.0	0.6	0.0	0.9	0.0	-0.3	1.3
P	15840 -15240	0.0	2.0	0.7	0.2	6.6	0.0	8.0	0.0	-5.2	13.2
Q	14628 -14028	0.0	0.4	0.4	0.0	1.0	0.0	1.4	0.0	-0.7	2.0
R	15816 -15216	-0.1	0.8	0.3	1.3	4.2	0.0	4.9	-0.1	-3.8	8.8
S	14616 -14016	0.3	0.0	0.3	-0.2	1.0	0.1	1.2	-0.3	-0.9	2.2
T	14811 -14011	-0.2	-0.9	0.1	0.7	2.0	0.0	1.7	-0.2	-2.6	4.3
U	45158 -45151	-0.5	-0.9	-1.5	0.0	0.0	-0.1	-0.5	-0.9	-1.5	1.0
V	50724 -50721	-0.2	-0.8	-0.2	0.2	0.1	0.0	-0.1	-0.2	-0.9	0.8
W	43278 -43271	-0.4	-0.9	0.0	0.0	-0.1	0.1	0.0	-0.4	-0.9	0.9
X	50084 -50081	-0.1	-2.2	0.0	0.0	0.0	0.1	0.0	-0.1	-2.2	2.2

<sup>1</sup> Refer to Figure 2.10.2-34 for the identification of the representative sections.

Table 2.10.4-83  $P_m + P_b$  Stresses; 1-Foot Side Drop; Drop Orientation = 90 Degrees; 3-D Model; 67.7-Degree Circumferential Location; Condition 1

Condition 1: 100°F Ambient with Contents

Section <sup>1</sup>	Node - Node	Stress Components (ksi)						Principal Stresses (ksi)			
		$S_x$	$S_y$	$S_z$	$S_{xy}$	$S_{yz}$	$S_{xz}$	S1	S2	S3	S.I.
A O	1130 - 1128	-0.4	-1.7	0.1	0.0	0.0	0.0	0.1	-0.4	-1.7	1.8
B O	1185 - 1183	0.1	-2.4	0.0	0.0	0.0	-0.1	0.1	0.0	-2.4	2.5
C I	14090 - 14040	0.0	-0.3	0.3	-1.6	-2.7	0.1	3.1	0.0	-3.1	6.3
D I	14025 - 14005	-0.1	-1.3	0.9	-0.8	-1.0	0.1	1.3	0.1	-2.0	3.3
E I	14035 - 14031	-0.7	-1.3	0.9	0.8	-1.4	0.2	1.6	-0.3	-2.4	3.9
F I	14100 - 14097	-0.1	-0.2	0.4	0.0	-5.7	0.2	5.8	-0.1	-5.6	11.5
G I	14094 - 14091	-0.1	-0.5	-1.3	-0.1	-1.5	-0.2	0.7	-0.1	-2.5	3.2
H I	14330 - 14327	0.0	1.9	0.2	0.0	-7.3	0.0	8.4	0.0	-6.3	14.6
I I	14244 - 14241	0.0	0.6	0.5	0.0	-1.6	0.0	2.1	0.0	-1.0	3.2
J I	14550 - 14547	0.0	2.9	0.9	0.0	-4.1	0.0	6.1	0.0	-2.4	8.5
K I	14344 - 14341	0.0	1.1	0.7	0.0	-1.0	0.0	1.9	0.0	-0.1	2.0
M I	14454 - 14451	-0.2	1.6	0.8	0.0	0.0	0.0	1.6	0.8	-0.2	1.8
L I	15908 - 15308	0.3	3.8	1.1	-0.1	0.4	0.0	3.8	1.0	0.3	3.5
N I	15877 - 15277	0.0	2.9	0.9	0.0	4.5	0.0	6.5	0.0	-2.7	9.2
O I	14647 - 14047	0.0	1.1	0.8	0.0	0.7	0.0	1.7	0.2	0.0	1.7
P I	15840 - 15240	0.0	2.3	0.5	0.0	6.9	0.0	8.4	0.0	-5.6	14.0
Q I	14628 - 14028	0.0	0.9	0.6	0.0	1.2	0.0	2.0	0.0	-0.4	2.3
R O	15816 - 15216	-0.2	1.0	1.6	2.5	3.8	0.2	5.7	0.2	-3.5	9.3
S I	14616 - 14016	-0.7	-0.4	-1.5	-0.4	1.4	0.2	0.6	-0.6	-2.5	3.1
T I	14811 - 14011	-0.7	-1.3	-1.5	1.9	3.3	0.0	2.5	-0.9	-5.1	7.6
U I	45158 - 45151	0.4	-0.2	-1.9	-0.5	0.1	0.5	0.8	-0.5	-2.0	2.8
V O	50724 - 50721	-1.8	-1.9	0.3	0.9	0.1	0.0	0.3	-1.0	-2.7	3.0
W I	43278 - 43271	-0.7	-1.0	0.0	0.0	-0.1	0.1	0.0	-0.7	-1.0	1.0
X O	50084 - 50081	0.1	-2.5	0.0	0.0	0.0	0.1	0.1	0.0	-2.5	2.6

<sup>1</sup> Refer to Figure 2.10.2-34 for the identification of the representative sections.

Table 2.10.4-84 Primary Stresses; 1-Foot Top Corner Drop; Drop Orientation = 24 Degrees; 3-D Top Model; 0-Degree Circumferential Location; Condition 1

Condition 1: 100°F Ambient with Contents

Stress Points		Stress Components (ksi)						Principal Stresses (ksi)		
Section <sup>1</sup>	Node	S <sub>x</sub>	S <sub>y</sub>	S <sub>z</sub>	S <sub>xy</sub>	S <sub>yz</sub>	S <sub>xz</sub>	S1	S2	S3
A1	1949	0.3	0.7	-0.1	0.0	0.0	0.1	0.7	0.3	-0.1
A2	1950	0.2	0.5	-0.1	0.0	0.0	0.1	0.5	0.2	-0.1
A3	1951	-0.1	-0.1	0.1	0.0	0.0	0.0	0.1	-0.1	-0.1
B1	1952	0.0	0.0	-0.1	0.0	0.0	0.0	0.0	0.0	-0.1
B2	93	-0.3	-0.6	0.2	0.0	0.0	0.0	0.2	-0.3	-0.6
C1	1925	-0.1	0.0	0.9	0.0	-0.1	0.0	0.9	0.0	-0.1
C2	1926	0.0	-0.1	0.1	0.0	0.0	-0.1	0.2	-0.1	-0.2
C3	1927	0.2	0.0	0.0	0.0	0.0	0.0	0.2	0.0	-0.1
D1	683	0.1	-0.1	-0.2	0.0	0.0	0.1	0.1	-0.1	-0.2
D2	85	-0.1	-0.3	-0.1	0.1	0.0	0.0	-0.1	-0.1	-0.3
E1	682	0.1	-0.1	-0.3	0.0	0.0	0.1	0.1	-0.1	-0.3
E2	82	0.1	0.1	0.5	0.0	0.0	0.2	0.6	0.1	0.0
F1	1925	-0.1	0.0	0.9	0.0	-0.1	0.0	0.9	0.0	-0.1
F2	1325	-0.6	-1.1	-2.7	0.1	-0.1	0.2	-0.6	-1.1	-2.7
G1	680	-0.3	-0.1	0.4	0.0	0.0	0.2	0.5	-0.1	-0.4
G2	80	0.0	0.1	0.5	0.0	0.0	0.0	0.5	0.1	0.0
H1	1921	0.0	2.1	-1.6	-0.1	-0.2	0.0	2.2	0.0	-1.6
H2	1321	0.0	2.6	-0.2	-0.2	-0.2	0.0	2.6	0.0	-0.2
I1	676	0.0	0.0	0.2	0.0	0.0	0.0	0.2	0.0	0.0
I2	76	0.0	0.3	0.4	0.0	0.0	0.0	0.4	0.2	0.0
J1	1916	0.0	2.3	-0.1	-0.2	-0.1	0.0	2.3	-0.1	-0.1
J2	1316	0.0	2.8	0.3	-0.2	-0.1	0.0	2.8	0.3	-0.1
K1	671	0.0	-0.1	-0.3	0.0	0.0	0.0	0.0	-0.1	-0.3
K2	71	0.0	0.4	0.0	0.0	0.0	0.0	0.4	0.0	0.0
L1	1908	-0.2	1.9	-0.8	-0.1	0.1	0.0	1.9	-0.2	-0.8
L2	1308	0.0	3.2	-0.2	0.3	0.1	0.0	3.3	0.0	-0.2
M1	663	-0.1	-0.5	-1.3	0.0	0.0	0.0	-0.1	-0.5	-1.3
M2	63	0.1	0.8	-0.9	0.2	0.1	0.0	0.9	0.0	-0.9

Table 2.10.4-84 Primary Stresses; 1-Foot Top Corner Drop; Drop Orientation = 24 Degrees; 3-D Top Model; 0-Degree Circumferential Location; Condition 1 (continued)

Stress Points		Stress Components (ksi)						Principal Stresses (ksi)		
Section <sup>1</sup>	Node	S <sub>x</sub>	S <sub>y</sub>	S <sub>z</sub>	S <sub>xy</sub>	S <sub>yz</sub>	S <sub>xz</sub>	S1	S2	S3
N1	1877	-0.1	1.9	-4.1	-0.1	0.3	0.0	1.9	-0.1	-4.1
N2	1477	0.0	2.5	-3.9	-0.2	0.3	0.0	2.6	-0.1	-3.9
N3	1277	0.0	3.2	-3.6	-0.2	0.3	0.0	3.2	0.0	-3.6
O1	647	0.0	-0.4	-2.4	0.0	0.1	0.0	0.0	-0.4	-2.4
O2	247	0.0	0.1	-2.2	0.0	0.1	0.0	0.1	0.0	-2.2
O3	47	0.0	0.5	-2.1	0.0	0.0	0.0	0.6	0.0	-2.1
P1	1840	-0.1	2.2	-5.0	-0.2	0.4	0.0	2.2	-0.1	-5.0
P2	1640	-0.2	2.1	-5.9	-0.2	0.4	0.0	2.2	-0.2	-6.0
P3	1440	-0.2	2.1	-6.8	-0.1	0.3	-0.2	2.1	-0.2	-6.8
P4	1240	-0.2	1.8	-8.6	-0.1	0.3	-0.5	1.8	-0.2	-8.7
Q1	628	0.0	0.8	-2.4	-0.1	0.1	0.0	0.8	0.0	-2.4
Q2	428	0.0	0.9	-2.8	-0.1	0.1	0.0	0.9	0.0	-2.8
Q3	228	0.0	0.9	-3.1	-0.1	0.1	0.0	0.9	0.0	-3.1
Q4	28	0.0	1.0	-3.4	-0.1	0.0	0.0	1.0	0.0	-3.4
R1	1816	-0.1	-1.0	-10.7	0.1	0.3	0.1	0.0	-1.0	-10.7
R2	1616	0.0	-0.2	-8.1	0.0	0.2	0.2	0.0	-0.2	-8.1
R3	1416	-0.2	0.5	-5.6	0.0	0.2	0.4	0.5	-0.2	-5.6
R4	1216	1.8	1.8	-2.8	0.1	0.2	0.4	1.9	1.8	-2.8
S1	616	-3.7	-2.0	-11.6	-0.1	0.2	1.4	-2.0	-3.4	-11.8
S2	416	-3.6	-0.4	-5.2	-0.2	0.0	-0.4	-0.4	-3.5	-5.3
S3	216	-1.3	1.4	-0.8	-0.2	0.0	-0.5	1.4	-0.5	-1.6
S4	16	-0.5	3.0	4.4	-0.3	0.0	-0.4	4.5	3.0	-0.5
T1	811	-0.6	-1.7	-1.3	0.2	0.2	0.5	-0.3	-1.4	-1.8
T2	611	0.4	-1.8	-2.9	0.2	0.1	-0.3	0.4	-1.8	-2.9
T3	411	0.3	-1.8	-2.8	0.2	0.1	-0.3	0.3	-1.8	-2.8
T4	211	0.3	-1.6	-2.4	0.1	0.1	-0.2	0.3	-1.6	-2.4
T5	11	0.3	-1.5	-1.8	0.1	0.0	-0.1	0.3	-1.5	-1.8
U1	43058	2.1	3.0	-6.1	-0.2	0.2	1.3	3.1	2.2	-6.3
U2	43057	1.6	2.0	-5.7	-0.1	0.1	1.9	2.1	1.9	-6.2
U3	43056	1.0	1.1	-5.4	-0.1	0.2	2.6	1.9	1.1	-6.4

Table 2.10.4-84 Primary Stresses; 1-Foot Top Corner Drop; Drop Orientation = 24 Degrees; 3-D Top Model; 0-Degree Circumferential Location; Condition 1 (continued)

Stress Points Section <sup>1</sup> Node	Stress Components (ksi)						Principal Stresses (ksi)		
	S <sub>x</sub>	S <sub>y</sub>	S <sub>z</sub>	S <sub>w</sub>	S <sub>xy</sub>	S <sub>yz</sub>	S1	S2	S3
U4 43055	0.7	0.2	-5.5	0.0	0.2	2.5	1.6	0.2	-6.4
U5 43054	0.3	-0.8	-5.6	0.1	0.1	2.0	0.9	-0.8	-6.2
U6 43053	-0.6	-1.5	-4.5	0.1	0.1	1.2	-0.3	-1.5	-4.9
U7 43052	-1.2	-2.8	-5.8	0.2	0.1	1.2	-0.9	-2.8	-6.1
U8 43051	-2.9	-4.3	-4.8	0.2	0.1	2.4	-1.2	-4.3	-6.4
V1 50024	-5.8	0.4	-2.1	-0.5	-0.1	-0.9	0.4	-1.9	-6.1
V2 50023	-4.0	-1.6	-2.5	-0.2	-0.1	-0.7	-1.6	-2.2	-4.3
V3 50022	-1.8	-3.3	-2.1	0.1	0.0	-0.2	-1.6	-2.2	-3.4
V4 50021	0.2	-5.1	-1.2	0.4	0.0	0.0	0.2	-1.2	-5.1
W1 43278	0.2	-0.7	-0.1	-0.1	-0.3	0.1	0.3	0.0	-0.9
W2 43274	0.4	-0.3	-0.1	0.0	-0.4	0.1	0.4	0.1	-0.6
W3 43271	0.3	0.1	-0.1	0.0	-0.4	0.0	0.4	0.3	-0.5
X1 50084	13.3	10.5	-3.2	-0.4	0.1	-3.2	13.9	10.5	-3.8
X2 50083	4.1	2.0	-2.1	-0.1	0.1	-3.2	5.5	2.0	-3.4
X3 50081	-12.5	-13.2	6.6	0.4	-0.3	-3.2	7.1	-12.8	-13.5

<sup>1</sup> Refer to Figure 2.10.2-34 for the identification of the representative sections.

Table 2.10.4-85 Primary + Secondary Stresses; 1-Foot Top Corner Drop; Drop Orientation = 24 Degrees; 3-D Top Model; 0-Degree Circumferential Location; Condition 1

Condition 1: 100°F Ambient with Contents

Stress Points		Stress Components (ksi)						Principal Stresses (ksi)		
Section <sup>1</sup>	Node	S <sub>x</sub>	S <sub>y</sub>	S <sub>z</sub>	S <sub>xy</sub>	S <sub>yz</sub>	S <sub>xz</sub>	S1	S2	S3
A1	1949	0.0	0.4	0.5	0.0	-0.2	0.7	1.1	0.4	-0.5
A2	1950	-0.3	0.0	0.4	0.0	-0.2	0.7	0.9	0.0	-0.8
A3	1951	-1.7	-1.7	-0.6	0.0	0.0	0.4	-0.5	-1.7	-1.8
B1	1952	0.7	0.7	0.4	0.0	-0.1	0.4	1.0	0.7	0.1
B2	93	-0.2	-0.5	-1.4	0.0	-0.2	0.8	0.3	-0.5	-1.8
C1	1925	-1.1	-0.6	-0.7	0.0	-0.1	-0.8	-0.1	-0.6	-1.7
C2	1926	0.7	-0.5	-1.0	0.1	-0.1	-0.8	1.0	-0.5	-1.3
C3	1927	-1.7	-2.2	-1.3	0.0	0.0	-0.1	-1.3	-1.7	-2.2
D1	683	1.7	1.1	3.1	0.0	0.1	0.8	3.5	1.3	1.1
D2	85	-1.5	1.1	3.2	-0.1	0.1	0.6	3.3	1.1	-1.6
E1	682	-1.3	-0.5	2.1	0.0	0.1	0.7	2.3	-0.5	-1.4
E2	82	-0.7	-0.5	-0.1	0.0	0.0	1.3	0.9	-0.5	-1.7
F1	1925	-1.1	-0.6	-0.7	0.0	-0.1	-0.8	-0.1	-0.6	-1.7
F2	1325	-0.1	-1.5	-3.5	0.1	-0.1	-0.5	0.0	-1.5	-3.5
G1	680	-0.4	0.1	1.2	0.0	0.0	0.4	1.3	0.1	-0.5
G2	80	-2.3	1.2	7.1	-0.2	0.1	1.2	7.3	1.2	-2.5
H1	1921	0.0	1.7	-1.4	-0.1	-0.1	0.1	1.7	0.0	-1.4
H2	1321	-0.1	2.3	-1.8	-0.2	-0.1	0.1	2.3	-0.1	-1.8
I1	676	-0.1	2.6	5.5	-0.2	0.1	0.1	5.5	2.6	-0.1
I2	76	-0.1	3.4	6.5	-0.3	-0.1	0.1	6.5	3.4	-0.2
J1	1916	-0.2	0.6	-2.9	0.0	-0.1	0.0	0.6	-0.2	-2.9
J2	1316	-0.1	4.3	1.3	-0.3	-0.1	0.0	4.3	1.3	-0.2
K1	671	-0.1	3.8	3.5	-0.3	0.1	0.0	3.8	3.5	-0.2
K2	71	-0.1	6.5	8.0	-0.5	0.0	0.0	8.0	6.5	-0.2
L1	1908	-1.1	-0.2	-3.5	-0.1	0.1	0.0	-0.1	-1.1	-3.5
L2	1308	0.6	5.1	0.3	0.7	0.1	0.0	5.2	0.5	0.3
M1	663	-1.3	4.4	2.7	-0.4	0.0	0.0	4.5	2.7	-1.3
M2	63	0.7	8.1	6.9	-0.5	0.0	0.0	8.1	6.9	0.6

Table 2.10.4-85 Primary + Secondary Stresses; 1-Foot Top Corner Drop; Drop Orientation = 24 Degrees; 3-D Top Model; 0-Degree Circumferential Location; Condition 1 (continued)

Stress Points		Stress Components (ksi)						Principal Stresses (ksi)		
Section <sup>1</sup>	Node	S <sub>x</sub>	S <sub>y</sub>	S <sub>z</sub>	S <sub>xy</sub>	S <sub>xz</sub>	S <sub>yz</sub>	S1	S2	S3
N1	1877	-0.1	0.2	-6.7	0.0	0.3	0.0	0.2	-0.1	-6.7
N2	1477	0.0	2.2	-4.7	-0.2	0.3	0.0	2.2	-0.1	-4.8
N3	1277	0.0	4.0	-2.8	-0.3	0.3	0.0	4.0	0.0	-2.8
O1	647	-0.3	4.1	2.0	-0.3	0.1	0.0	4.1	2.0	-0.3
O2	247	-0.2	5.4	3.7	-0.4	0.1	0.0	5.4	3.7	-0.2
O3	47	-0.1	6.5	5.3	-0.5	0.1	0.0	6.6	5.3	-0.1
P1	1840	-0.1	1.7	-5.9	-0.1	0.4	0.0	1.7	-0.1	-5.9
P2	1640	-0.2	1.8	-6.9	-0.1	0.3	0.0	1.8	-0.2	-6.9
P3	1440	-0.1	2.1	-7.7	-0.1	0.3	-0.2	2.1	-0.1	-7.7
P4	1240	-0.4	1.9	-9.6	-0.1	0.3	-0.5	1.9	-0.4	-9.7
Q1	628	-0.2	4.3	2.2	-0.3	0.1	0.1	4.4	2.2	-0.2
Q2	428	-0.1	4.7	2.5	-0.4	0.1	0.2	4.8	2.6	-0.2
Q3	228	0.0	5.2	3.0	-0.4	0.1	0.2	5.2	3.0	-0.1
Q4	28	0.0	5.5	3.5	-0.4	0.1	0.1	5.6	3.5	0.0
R1	1816	0.2	-5.5	-15.6	0.4	0.3	0.8	0.3	-5.6	-15.6
R2	1616	0.2	-3.7	-11.4	0.3	0.3	1.4	0.4	-3.7	-11.6
R3	1416	-0.8	-2.3	-7.2	0.2	0.4	2.9	0.4	-2.3	-8.4
R4	1216	4.4	1.4	-1.0	0.2	0.3	2.7	5.5	1.4	-2.1
S1	616	-5.7	-3.1	-13.9	-0.2	0.3	0.2	-3.1	-5.7	-13.9
S2	416	-8.3	-0.2	-1.4	-0.5	-0.1	-2.2	-0.2	-0.7	-9.0
S3	216	-2.5	3.2	4.1	-0.4	0.0	-0.5	4.1	3.2	-2.6
S4	16	-0.9	5.9	11.7	-0.5	0.0	-0.3	11.8	6.0	-1.0
T1	811	-2.5	-4.3	-8.0	0.3	0.1	-1.3	-2.2	-4.4	-8.3
T2	611	-1.1	-2.9	-5.1	0.2	0.0	-0.6	-1.0	-2.9	-5.2
T3	411	-0.3	-1.7	-2.2	0.1	0.1	-0.3	-0.3	-1.7	-2.3
T4	211	0.1	-0.5	0.8	0.0	0.1	-0.1	0.8	0.1	-0.5
T5	11	0.2	0.7	4.3	0.0	0.1	0.0	4.3	0.7	0.2
U1	43058	-2.1	1.0	-11.9	-0.3	0.5	2.2	1.0	-1.6	-12.4
U2	43057	0.9	0.6	-10.6	-0.1	0.2	2.9	1.6	0.6	-11.3
U3	43056	0.8	-0.3	-8.7	0.0	0.4	3.6	2.0	-0.3	-9.9

Table 2.10.4-85 Primary + Secondary Stresses; 1-Foot Top Corner Drop; Drop Orientation = 24 Degrees; 3-D Top Model; 0-Degree Circumferential Location; Condition 1 (continued)

Stress Points Section <sup>1</sup> Node	Stress Components (ksi)						Principal Stresses (ksi)		
	S <sub>x</sub>	S <sub>y</sub>	S <sub>z</sub>	S <sub>xy</sub>	S <sub>yz</sub>	S <sub>xz</sub>	S1	S2	S3
U4 43055	0.6	-1.5	-7.9	0.1	0.4	3.2	1.7	-1.5	-9.0
U5 43054	-0.2	-2.8	-7.3	0.2	0.5	2.5	0.6	-2.8	-8.1
U6 43053	-1.6	-4.0	-5.7	0.2	0.6	1.6	-1.0	-4.0	-6.3
U7 43052	-3.0	-5.9	-7.0	0.3	0.8	1.5	-2.5	-5.7	-7.7
U8 43051	-0.9	-1.2	-0.7	-0.3	1.3	2.1	1.5	-0.9	-3.5
V1 50024	-2.7	1.8	-5.0	-0.3	-0.7	-1.0	1.9	-2.4	-5.4
V2 50023	-1.7	-0.5	-4.1	-0.2	-0.6	-0.7	-0.3	-1.5	-4.4
V3 50022	-1.8	-3.6	-2.6	0.0	-0.5	-0.4	-1.6	-2.6	-3.8
V4 50021	-1.7	-6.5	-1.5	0.2	-0.3	-0.1	-1.4	-1.8	-6.5
W1 43278	4.0	2.9	-1.6	-0.1	-0.1	-0.8	4.1	2.9	-1.7
W2 43274	0.1	-0.9	-0.7	0.0	-0.1	-0.9	0.7	-0.8	-1.4
W3 43271	-2.8	-3.3	0.5	0.0	-0.3	-0.4	0.6	-2.9	-3.3
X1 50084	16.7	14.6	-3.7	-0.4	0.3	-3.7	17.4	14.6	-4.3
X2 50083	5.9	4.5	-2.4	-0.1	0.3	-3.7	7.4	4.5	-3.8
X3 50081	-13.5	-13.9	7.6	0.4	-0.1	-3.7	8.3	-13.6	-14.4

<sup>1</sup> Refer to Figure 2.10.2-34 for the identification of the representative sections.



Table 2.10.4-86  $P_m$  Stresses; 1-Foot Top Corner Drop; Drop Orientation = 24 Degrees; 3-D Top Model; 0-Degree Circumferential Location; Condition 1

Condition 1: 100°F Ambient with Contents

Section <sup>1</sup>	Node - Node	Stress Components (ksi)						Principal Stresses (ksi)			
		$S_x$	$S_y$	$S_z$	$S_{xy}$	$S_{yz}$	$S_{xz}$	S1	S2	S3	S.I.
A	1949 - 1951	0.1	0.3	0.0	0.0	0.0	0.0	0.3	0.1	-0.1	0.4
B	1952 - 93	-0.2	-0.3	0.0	0.0	0.0	0.0	0.1	-0.2	-0.3	0.4
C	1925 - 1927	0.1	-0.1	0.2	0.0	0.0	-0.1	0.2	0.0	-0.1	0.3
D	683 - 85	0.0	-0.2	-0.1	0.0	0.0	0.0	0.0	-0.1	-0.2	0.2
E	682 - 82	0.1	0.0	0.1	0.0	0.0	0.2	0.3	0.0	-0.1	0.3
F	1925 - 1325	-0.4	-0.5	-0.9	0.0	-0.1	0.1	-0.4	-0.5	-0.9	0.6
G	680 - 80	-0.2	0.0	0.5	0.0	0.0	0.1	0.5	0.0	-0.2	0.7
H	1921 - 1321	0.0	2.4	-0.9	-0.2	-0.2	0.0	2.4	0.0	-0.9	3.3
I	676 - 76	0.0	0.1	0.3	0.0	0.0	0.0	0.3	0.1	0.0	0.3
J	1916 - 1316	0.0	2.6	0.1	-0.2	-0.1	0.0	2.6	0.1	-0.1	2.6
K	671 - 71	0.0	0.1	-0.2	0.0	0.0	0.0	0.1	0.0	-0.2	0.3
L	1908 - 1308	-0.1	2.5	-0.5	0.1	0.1	0.0	2.6	-0.1	-0.5	3.1
M	663 - 63	0.0	0.2	-1.1	0.1	0.1	0.0	0.2	-0.1	-1.1	1.3
N	1877 - 1277	0.0	2.5	-3.9	-0.2	0.3	0.0	2.6	-0.1	-3.9	6.4
O	647 - 47	0.0	0.1	-2.2	0.0	0.1	0.0	0.1	0.0	-2.2	2.3
P	1840 - 1240	-0.2	2.1	-6.5	-0.1	0.3	-0.1	2.1	-0.2	-6.5	8.6
Q	628 - 28	0.0	0.9	-2.9	-0.1	0.1	0.0	0.9	0.0	-2.9	3.8
R	1816 - 1216	0.2	0.2	-6.8	0.0	0.2	0.3	0.3	0.2	-6.8	7.1
S	616 - 16	-2.3	0.5	-3.2	-0.2	0.1	-0.1	0.5	-2.3	-3.2	3.7
T	811 - 11	0.2	-1.7	-2.4	0.2	0.1	-0.1	0.2	-1.7	-2.4	2.7
U	43058 - 43051	-0.1	-0.7	-5.4	0.0	0.1	1.9	0.5	-0.8	-6.0	6.5
V	50024 - 50021	-2.8	-2.5	-2.1	-0.1	-0.1	-0.5	-1.9	-2.4	-3.1	1.2
W	43278 - 43271	0.3	-0.3	-0.1	0.0	-0.4	0.1	0.3	0.2	-0.6	0.9
X	50084 - 50081	-0.1	-1.8	0.7	0.0	0.0	-3.2	3.5	-1.8	-2.9	6.4

<sup>1</sup> Refer to Figure 2.10.2-34 for the identification of the representative sections.

Table 2.10.4-87  $P_m + P_b$  Stresses; 1-Foot Top Corner Drop; Drop Orientation = 24 Degrees; 3-D Top Model; 0-Degree Circumferential Location; Condition 1

Condition 1: 100°F Ambient with Contents

Section <sup>1</sup>	Node - Node	Stress Components (ksi)						Principal Stresses (ksi)			
		$S_x$	$S_y$	$S_z$	$S_{xy}$	$S_{yz}$	$S_{xz}$	S1	S2	S3	S.L
A I	1949 - 1951	0.3	0.7	-0.1	0.0	0.0	0.1	0.7	0.3	-0.1	0.8
B O	1952 - 93	-0.3	-0.6	0.2	0.0	0.0	0.0	0.2	-0.3	-0.6	0.9
C I	1925 - 1927	-0.1	-0.1	0.5	0.0	-0.1	-0.1	0.5	-0.1	-0.1	0.6
D I	683 - 85	0.1	-0.1	-0.2	0.0	0.0	0.1	0.1	-0.1	-0.2	0.3
E O	682 - 82	0.1	0.1	0.5	0.0	0.0	0.2	0.6	0.1	0.0	0.6
F O	1925 - 1325	-0.6	-1.1	-2.7	0.1	-0.1	0.2	-0.6	-1.1	-2.7	2.1
G I	680 - 80	-0.3	-0.1	0.4	0.0	0.0	0.2	0.5	-0.1	-0.4	0.9
H I	1921 - 1321	0.0	2.1	-1.6	-0.1	-0.2	0.0	2.2	0.0	-1.6	3.7
I O	676 - 76	0.0	0.3	0.4	0.0	0.0	0.0	0.4	0.2	0.0	0.4
J O	1916 - 1316	0.0	2.8	0.3	-0.2	-0.1	0.0	2.8	0.3	-0.1	2.9
K O	671 - 71	0.0	0.4	0.0	0.0	0.0	0.0	0.4	0.0	0.0	0.4
L O	1908 - 1308	0.0	3.2	-0.2	0.3	0.1	0.0	3.3	0.0	-0.2	3.5
M O	663 - 63	0.1	0.8	-0.9	0.2	0.1	0.0	0.9	0.0	-0.9	1.7
N O	1877 - 1277	0.0	3.2	-3.6	-0.2	0.3	0.0	3.2	0.0	-3.6	6.8
O O	647 - 47	0.0	0.6	-2.1	0.0	0.0	0.0	0.6	0.0	-2.1	2.7
P O	1840 - 1240	-0.2	1.9	-8.2	-0.1	0.3	-0.4	1.9	-0.2	-8.2	10.2
Q O	628 - 28	0.0	1.0	-3.4	-0.1	0.0	0.0	1.0	0.0	-3.4	4.4
R I	1816 - 1216	-0.4	-1.1	-10.7	0.1	0.3	0.1	-0.4	-1.1	-10.7	10.3
S I	616 - 16	-4.3	-2.0	-10.9	-0.1	0.2	0.6	-2.0	-4.3	-10.9	8.9
T O	811 - 11	0.5	-1.5	-2.4	0.1	0.0	-0.3	0.5	-1.6	-2.4	2.9
U I	43058 - 43051	2.3	2.9	-5.8	-0.2	0.2	2.1	3.0	2.7	-6.3	9.3
V I	50024 - 50021	-5.9	0.3	-2.6	-0.5	-0.1	-1.0	0.3	-2.3	-6.2	6.6
W I	43278 - 43271	0.3	-0.7	-0.1	-0.1	-0.3	0.1	0.3	0.0	-0.8	1.2
X O	50084 - 50081	-12.8	-13.5	5.9	0.4	-0.2	-3.2	6.5	13.0	13.8	20.2

<sup>1</sup> Refer to Figure 2.10.2-34 for the identification of the representative sections.

Table 2.10.4-88  $S_n$  Stresses; 1-Foot Top Corner Drop; Drop Orientation = 24 Degrees; 3-D Top Model; 0-Degree Circumferential Location; Condition 1

Condition 1: 100°F Ambient with Contents

Section <sup>1</sup>	Node - Node	Stress Components (ksi)						Principal Stresses (ksi)			
		$S_x$	$S_y$	$S_z$	$S_{xy}$	$S_{yz}$	$S_{zx}$	S1	S2	S3	S.L
A I	1949 - 1951	0.1	0.6	0.6	0.0	-0.2	0.8	1.3	0.5	-0.5	1.7
B O	1952 - 93	-0.2	-0.5	-1.4	0.0	-0.2	0.8	0.3	-0.5	-1.8	2.1
C I	1925 - 1927	0.4	-0.2	-0.8	0.0	-0.1	-0.9	0.9	-0.2	-1.3	2.2
D O	683 - 85	-1.5	1.1	3.2	-0.1	0.1	0.6	3.3	1.1	-1.6	4.9
E I	682 - 82	-1.3	-0.5	2.1	0.0	0.1	0.7	2.3	-0.5	-1.4	3.7
F O	1925 - 1325	-0.1	-1.5	-3.5	0.1	-0.1	-0.5	0.0	-1.5	-3.5	3.5
G O	680 - 80	-2.3	1.2	7.1	-0.2	0.1	1.2	7.3	1.2	-2.5	9.8
H O	1921 - 1321	-0.1	2.3	-1.8	-0.2	-0.1	0.1	2.3	-0.1	-1.8	4.2
I O	676 - 76	-0.1	3.4	6.5	-0.3	-0.1	0.1	6.5	3.4	-0.2	6.7
J O	1916 - 1316	-0.1	4.3	1.3	-0.3	-0.1	0.0	4.3	1.3	-0.2	4.5
K O	671 - 71	-0.1	6.5	8.0	-0.5	0.0	0.0	8.0	6.5	-0.2	8.1
L O	1908 - 1308	0.6	5.1	0.3	0.7	0.1	0.0	5.2	0.5	0.3	4.8
M O	663 - 63	0.7	8.1	6.9	-0.5	0.0	0.0	8.1	6.9	0.6	7.5
N I	1877 - 1277	-0.1	0.3	-6.7	0.0	0.3	0.0	0.3	-0.1	-6.7	7.0
O O	647 - 47	-0.1	6.6	5.3	-0.5	0.1	0.0	6.6	5.3	-0.1	6.7
P O	1840 - 1240	-0.3	2.1	-9.1	-0.1	0.3	-0.4	2.1	-0.3	-9.2	11.3
Q O	628 - 28	0.0	5.5	3.5	-0.4	0.1	0.2	5.6	3.5	0.0	5.6
R I	1816 - 1216	-0.7	-5.9	-16.0	0.4	0.3	0.8	-0.6	-5.9	16.1	15.4
S O	616 - 16	-0.9	6.1	12.3	-0.5	0.0	-0.6	12.4	6.1	-1.0	13.3
T I	811 - 11	-1.9	-4.2	-8.2	0.3	0.0	-1.0	-1.7	-4.2	-8.3	6.6
U I	43058 - 43051	0.8	0.6	-11.5	0.0	0.1	3.3	1.6	0.6	-12.3	13.9
V I	50024 - 50021	-2.2	2.1	-5.2	-0.3	-0.7	-1.0	2.2	-1.9	-5.6	7.8
W I	43278 - 43271	3.7	2.5	-1.7	-0.1	-0.1	-1.0	3.9	2.5	-1.9	5.8
X I	50084 - 50081	16.0	14.0	-5.2	-0.4	0.4	-3.7	16.7	13.9	-5.9	22.6

<sup>1</sup> Refer to Figure 2.10.2-34 for the identification of the representative sections.

Table 2.10.4-89 Critical P<sub>m</sub> Stress Summary; 1-Foot Top Corner Drop; Drop Orientation = 24 Degrees; 3-D Top Model; Condition 1

Condition 1: 100°F Ambient with Contents

Comp. No. <sup>1</sup>	Section Cut Node-Node	P <sub>m</sub> Stresses (ksi)						Principal Stresses (ksi)			Allow. Stress	Margin of Safety	
		S <sub>1</sub>	S <sub>2</sub>	S <sub>3</sub>	S <sub>4</sub>	S <sub>5</sub>	S <sub>6</sub>	S1	S2	S3			
1	1952- 93	-0.2	-0.3	0.0	0.0	0.0	0.0	0.1	-0.2	-0.3	0.4	19.2	47.0
2	13924-13324	0.0	0.5	-0.3	0.0	-1.5	0.1	1.6	0.0	-1.4	3.0	18.5	5.2
3	11841-11241	-0.1	1.7	-5.2	0.0	3.3	-0.1	3.0	-0.1	-6.5	9.5	31.4	2.3
4	13874-13274	0.0	1.8	-3.3	0.0	3.1	0.0	3.2	0.0	-4.8	8.0	19.6	1.5
5	10625-10025	0.0	1.2	-3.2	0.0	0.9	0.1	1.4	0.0	-3.4	4.8	20.0	3.2
6	401- 1	-2.0	-13.7	-1.7	0.8	0.0	-0.2	-1.6	-2.0	13.7	12.1	20.0	0.7
7	43021-43028	-0.9	-2.8	-12.3	0.1	0.0	1.2	-0.7	-2.8	-12.4	11.7	20.0	0.7
8	50081-50084	-0.1	-1.8	0.7	0.0	0.0	-3.2	3.5	-1.8	-2.9	6.4	45.0	6.0

Locations of the most critical sections for each component are provided in the following:

Comp. No. <sup>1</sup>	Section Location					
	Inside Node			Outside Node		
	x (in)	y (deg)	z (in)	x (in)	y (deg)	z (in)
1	0.00	0.0	6.20	0.00	0.0	0.75
2	35.50	56.5	17.40	37.50	56.5	17.40
3	35.50	45.9	159.90	37.00	45.9	159.90
4	35.50	56.5	142.40	37.00	56.5	142.40
5	40.70	45.9	163.40	43.35	45.9	163.40
6	40.88	0.0	193.71	43.35	0.0	193.71
7	37.66	0.0	185.40	37.66	0.0	179.40
8	0.00	0.0	193.71	0.00	0.0	188.46

<sup>1</sup> Refer to Figure 2.10.2-33 for cask component identification.

Table 2.10.4-90 Critical  $P_m + P_b$  Stress Summary; 1-Foot Top Corner Drop; Drop Orientation = 24 Degrees; 3-D Top Model; Condition 1  
Condition 1: 100°F Ambient with Contents

Comp. No. <sup>1</sup>	Section Cut Node-Node	P <sub>m</sub> + P <sub>b</sub> Stresses (ksi)							Principal Stresses (ksi)			Allow. S.L. Stress	Margin of Safety
		S <sub>1</sub>	S <sub>y</sub>	S <sub>z</sub>	S <sub>xy</sub>	S <sub>xz</sub>	S <sub>yz</sub>	S1	S2	S3			
1	1952- 93	-0.3	-0.6	0.2	0.0	0.0	0.0	0.2	-0.3	-0.6	0.9	28.7	30.9
2	13924-13324	0.0	0.6	-0.1	0.0	-1.9	0.1	2.2	0.0	-1.7	3.9	27.7	6.1
3	11821-11221	-0.1	1.8	-7.7	0.0	3.1	0.2	2.7	-0.1	-8.6	11.3	47.1	3.2
4	13874-13274	0.0	2.1	-3.3	0.0	3.3	0.0	3.7	0.0	-4.8	8.5	29.4	2.5
5	12625-12025	0.0	0.9	-3.4	0.0	1.1	0.1	1.1	0.0	-3.7	4.9	30.0	5.1
6	401- 1	-1.7	-13.9	-2.1	0.8	0.0	-0.1	-1.6	-2.2	-13.9	12.3	30.0	1.4
7	50150-63451	-29.1	-14.5	-8.2	0.3	0.0	-0.4	-8.2	-14.4	-29.1	20.9	30.0	0.4
8	50071-50074	-25.5	-20.0	-1.5	0.0	0.0	0.0	-1.5	-20.0	-25.5	23.9	67.5	1.8

Locations of the most critical sections for each component are provided in the following:

Comp. No. <sup>1</sup>	Section Location					
	Inside Node			Outside Node		
	x (in)	y (deg)	z (in)	x (in)	y (deg)	z (in)
1	0.00	0.0	6.20	0.00	0.0	0.75
2	35.50	56.5	17.40	37.50	56.5	17.40
3	35.50	45.9	171.65	37.00	45.9	171.65
4	35.50	56.5	142.40	37.00	56.5	142.40
5	40.70	56.5	163.40	43.35	56.5	163.40
6	40.88	0.0	193.71	43.35	0.0	193.71
7	25.00	8.3	188.40	25.00	8.3	187.40
8	9.00	0.0	193.71	9.00	0.0	188.46

<sup>1</sup> Refer to Figure 2.10.2-33 for cask component identification.

Table 2.10.4-91 Critical  $S_n$  Stress Summary; 1-Foot Top Corner Drop; Drop Orientation = 24 Degrees; 3-D Top Model; Condition 1

Condition 1: 100°F Ambient with Contents

Comp. No. <sup>1</sup>	Section Cut Node-Node	$S_n$ Stresses (ksi)							Principal Stresses (ksi)				Allow. Stress 3.0 $S_n$
		$S_1$	$S_2$	$S_3$	$S_4$	$S_5$	$S_6$	$S_7$	$S_1$	$S_2$	$S_3$	$S_4$	
1	683- 85	-1.5	1.1	3.2	-0.1	0.1	0.6	3.3	1.1	-1.6	4.9		57.6
2	16680-16080	-2.6	1.7	7.1	-0.1	-0.2	1.2	7.3	1.6	-2.7	10.0		55.3
3	1841- 1241	-0.1	2.1	-9.2	-0.2	0.3	-0.2	2.1	-0.1	-9.2	11.3		94.2
4	13874-13274	0.0	1.8	-5.0	0.0	3.0	0.0	3.0	0.0	-6.1	9.1		58.8
5	664- 64	-0.2	7.9	7.3	-0.6	0.0	0.0	8.0	7.2	-0.2	8.2		60.0
6	401- 1	-2.1	-22.4	-1.4	1.4	0.0	0.2	-1.4	-2.0	-22.4	21.0		60.0
7	50050-63151	-26.9	-0.9	3.9	-0.9	-0.2	-0.5	3.9	-0.9	-27.0	30.8		60.0
8	50071-50074	-26.8	-21.4	-1.6	0.0	0.0	0.0	-1.6	-21.4	-26.8	25.2		135.0

Locations of the most critical sections for each component are provided in the following:

Comp. No. <sup>1</sup>	Section Location					
	Inside Node			Outside Node		
	x (in)	y (deg)	z (in)	x (in)	y (deg)	z (in)
1	39.44	0.0	6.20	39.44	0.0	0.75
2	40.70	79.4	14.40	43.35	79.4	14.40
3	35.50	0.0	159.90	37.00	0.0	159.90
4	35.50	56.5	142.40	37.00	56.5	142.40
5	40.70	0.0	93.56	43.35	0.0	93.56
6	40.88	0.0	193.71	43.35	0.0	193.71
7	25.00	0.0	188.40	25.00	0.0	187.40
8	9.00	0.0	193.71	9.00	0.0	188.46

<sup>1</sup> Refer to Figure 2.10.2-33 for cask component identification.

Table 2.10.4-92  $P_m$  Stresses; 1-Foot Top Corner Drop; Drop Orientation = 24 Degrees; 3-D Top Model; 45.9-Degree Circumferential Location; Condition 1

**Condition 1: 100°F Ambient with Contents**

Section <sup>1</sup>	Node - Node	Stress Components (ksi)						Principal Stresses (ksi)			
		$S_x$	$S_y$	$S_z$	$S_{xy}$	$S_{yz}$	$S_{zx}$	S1	S2	S3	S.I.
A	1949 - 1951	0.1	0.3	0.0	0.0	0.0	0.0	0.3	0.1	-0.1	0.4
B	1952 - 93	-0.2	-0.3	0.0	0.0	0.0	0.0	0.1	-0.2	-0.3	0.4
C	11925 - 11927	0.0	0.1	0.1	-0.1	-0.2	0.0	0.3	0.1	-0.2	0.5
D	10683 - 10085	0.0	-0.3	-0.1	0.0	0.0	0.0	0.0	-0.1	-0.3	0.3
E	10682 - 10082	0.1	0.0	0.0	0.0	0.0	0.0	0.1	0.0	0.0	0.1
F	11925 - 11325	-0.2	0.0	-0.4	0.0	-0.7	0.1	0.5	-0.2	-0.9	1.4
G	10680 - 10080	-0.2	0.1	0.1	0.2	0.2	0.0	0.4	0.0	-0.2	0.6
H	11921 - 11321	0.0	1.7	-0.5	0.0	-1.5	0.0	2.5	0.0	-1.3	3.8
I	10676 - 10076	0.0	0.1	-0.1	0.0	0.3	0.0	0.3	0.0	-0.3	0.6
J	11916 - 11316	0.0	1.9	-0.5	0.0	-0.5	0.0	2.0	0.0	-0.5	2.6
K	10671 - 10071	0.0	0.1	-0.5	0.0	0.4	0.0	0.3	0.0	-0.7	1.0
L	11908 - 11308	0.0	2.0	-1.4	-0.1	1.1	0.0	2.3	0.0	-1.7	4.0
M	10663 - 10063	0.0	0.1	-1.3	0.0	0.6	0.0	0.3	0.0	-1.5	1.8
N	11877 - 11277	0.0	2.0	-3.5	0.0	2.6	0.0	3.0	0.0	-4.5	7.5
O	10647 - 10047	0.0	0.1	-2.3	0.0	0.8	0.0	0.3	0.0	-2.6	2.9
P	11840 - 11240	-0.1	1.8	-5.2	0.1	3.2	-0.1	3.0	-0.1	-6.4	9.5
Q	10628 - 10028	0.0	0.8	-3.1	0.0	0.9	0.0	1.0	0.0	-3.3	4.3
R	11816 - 11216	0.4	1.1	-5.6	0.5	2.2	0.4	2.0	0.2	-6.2	8.2
S	10616 - 10016	-2.2	0.8	-3.4	-0.3	0.9	0.0	1.0	-2.2	-3.6	4.6
T	10811 - 10011	0.6	-0.8	-2.3	0.6	1.3	0.1	0.9	-0.3	-3.0	4.0
U	44558 - 44551	0.2	-0.4	-5.2	-0.1	-0.1	1.8	0.8	-0.4	-5.7	6.5
V	50524 - 50521	-2.1	-1.9	-2.3	0.2	0.0	-0.4	-1.6	-2.0	-2.6	1.0
W	43278 - 43271	0.3	-0.3	-0.1	0.0	-0.4	0.1	0.3	0.2	-0.6	0.9
X	50084 - 50081	-0.1	-1.8	0.7	0.0	0.0	-3.2	3.5	-1.8	-2.9	6.4

<sup>1</sup> Refer to Figure 2.10.2-34 for the identification of the representative sections.

Table 2.10.4-93  $P_m + P_b$  Stresses; 1-Foot Top Corner Drop; Drop Orientation = 24 Degrees; 3-D Top Model; 45.9-Degree Circumferential Location; Condition 1

Condition 1: 100°F Ambient with Contents

Section <sup>1</sup>	Node - Node	Stress Components (ksi)						Principal Stresses (ksi)			
		$S_x$	$S_y$	$S_z$	$S_{xy}$	$S_{yz}$	$S_{xz}$	S1	S2	S3	S.L
A I	1949 - 1951	0.3	0.7	-0.1	0.0	0.0	0.1	0.7	0.3	-0.1	0.8
B O	1952 - 93	-0.3	-0.6	0.2	0.0	0.0	0.0	0.2	-0.3	-0.6	0.9
C I	11925 - 11927	0.0	0.2	0.2	-0.1	-0.5	0.0	0.7	0.0	-0.3	1.1
D O	10683 - 10085	0.0	-0.4	-0.1	0.1	0.0	0.0	0.0	-0.1	-0.4	0.4
E I	10682 - 10082	0.1	-0.1	-0.2	0.0	0.0	0.0	0.1	-0.1	-0.2	0.3
F O	11925 - 11325	-0.4	-0.3	-1.3	0.1	-0.6	0.1	0.0	-0.4	-1.6	1.6
G O	10680 - 10080	-0.1	0.3	0.4	0.1	0.2	0.0	0.6	0.1	-0.1	0.7
H I	11921 - 11321	0.0	1.4	-1.0	0.0	-1.9	0.0	2.4	0.0	-2.0	4.4
I O	10676 - 10076	0.0	0.1	-0.1	0.0	0.3	0.0	0.3	0.0	-0.4	0.7
J O	11916 - 11316	0.0	2.3	-0.3	0.0	-0.4	0.0	2.3	0.0	-0.3	2.7
K I	10671 - 10071	0.0	0.2	-0.5	0.0	0.3	0.0	0.3	0.0	-0.6	1.0
L I	11908 - 11308	0.0	1.9	-1.4	-0.1	1.1	0.0	2.3	0.0	-1.7	4.0
M I	10663 - 10063	0.1	0.4	-1.2	0.0	0.6	0.0	0.5	0.1	-1.4	1.9
N I	11877 - 11277	0.0	2.2	-3.4	0.0	2.7	0.0	3.3	0.0	-4.5	7.9
O I	10647 - 10047	0.0	0.3	-2.2	0.0	0.8	0.0	0.6	0.0	-2.5	3.1
P O	11840 - 11240	-0.2	1.1	-7.0	0.2	3.1	-0.3	2.2	-0.2	-8.1	10.3
Q O	10628 - 10028	0.0	0.5	-3.8	0.0	0.8	0.0	0.6	0.0	-4.0	4.6
R I	11816 - 11216	-0.4	-0.4	-10.5	0.0	2.6	-0.1	0.2	-0.4	-11.1	11.3
S I	10616 - 10016	-4.2	-1.5	-10.3	-0.7	1.3	0.7	-1.2	-4.2	-10.6	9.4
T I	10811 - 10011	1.1	-0.4	-1.4	1.4	2.3	0.5	2.7	-0.1	-3.3	6.0
U I	44558 - 44551	1.4	2.9	-5.6	-1.1	0.0	2.1	3.6	1.3	-6.2	9.8
V I	50524 - 50521	-5.2	0.7	-3.1	-1.1	0.0	-0.8	0.9	-2.9	-5.6	6.6
W I	43278 - 43271	0.3	-0.7	-0.1	-0.1	-0.3	0.1	0.3	0.0	-0.8	1.2
X O	50084 - 50081	-12.8	-13.5	5.9	0.4	-0.2	-3.2	6.5	-13.0	-13.8	20.2

<sup>1</sup> Refer to Figure 2.10.2-34 for the identification of the representative sections.



Table 2.10.4-94  $P_m$  Stresses; 1-Foot Top Corner Drop; Drop Orientation = 24 Degrees; 3-D Top Model; 91.7-Degree Circumferential Location; Condition 1

Condition 1: 100°F Ambient with Contents

Section <sup>1</sup>	Node - Node	Stress Components (ksi)						Principal Stresses (ksi)			
		$S_x$	$S_y$	$S_z$	$S_{xy}$	$S_{yz}$	$S_{xz}$	S1	S2	S3	S.I.
A	1949 - 1951	0.1	0.3	0.0	0.0	0.0	0.0	0.3	0.1	-0.1	0.4
B	1952 - 93	-0.2	-0.3	0.0	0.0	0.0	0.0	0.1	-0.2	-0.3	0.4
C	19925 - 19927	0.0	0.2	-0.1	0.0	-0.2	0.0	0.3	0.0	-0.2	0.6
D	18683 - 18085	0.0	-0.3	-0.1	-0.1	-0.1	-0.1	0.0	0.0	-0.4	0.4
E	18682 - 18082	0.1	0.0	-0.2	0.1	-0.1	-0.1	0.2	0.0	-0.3	0.5
F	19925 - 19325	0.1	0.7	0.3	0.1	-0.6	-0.1	1.1	0.1	-0.1	1.2
G	18680 - 18080	-0.1	0.2	-0.5	0.1	0.1	-0.1	0.3	-0.1	-0.6	0.8
H	19921 - 19321	0.0	0.6	-0.2	0.1	-0.9	0.0	1.2	0.0	-0.8	2.1
I	18676 - 18076	0.0	0.1	-0.8	0.0	0.3	0.0	0.2	0.0	-0.9	1.0
J	19916 - 19316	0.0	0.8	-1.4	0.0	-0.1	0.0	0.8	0.0	-1.4	2.2
K	18671 - 18071	0.0	0.0	-0.9	0.0	0.5	0.0	0.2	0.0	-1.1	1.3
L	19908 - 19308	0.1	0.9	-1.9	0.2	1.4	0.0	1.4	0.1	-2.5	3.9
M	18663 - 18063	0.0	0.0	-1.1	0.0	0.8	0.0	0.4	0.0	-1.6	1.9
N	19877 - 19277	-0.1	0.9	-1.3	0.0	2.9	0.0	2.9	-0.1	-3.3	6.2
O	18647 - 18047	0.0	0.0	-1.3	0.0	1.1	0.0	0.6	0.0	-2.0	2.6
P	19840 - 19240	-0.3	0.6	-0.4	0.2	3.6	0.0	3.8	-0.3	-3.6	7.3
Q	18628 - 18028	0.0	0.2	-1.3	0.0	1.4	0.0	1.0	0.0	-2.2	3.2
R	19816 - 19216	0.1	1.9	-0.4	0.6	2.9	0.7	4.1	-0.1	-2.4	6.5
S	18616 - 18016	-1.4	0.8	-1.2	-0.6	1.6	-0.2	1.8	-1.5	-2.1	3.9
T	18811 - 18011	0.7	1.0	-0.5	0.8	2.1	0.2	2.8	0.4	-2.0	4.8
U	45758 - 45751	-0.1	-0.8	-2.9	-0.2	0.2	0.5	0.0	-0.8	-3.0	3.0
V	50924 - 50921	-0.4	-0.9	0.0	-0.2	0.1	-0.4	0.3	-0.6	-1.0	1.3
W	43278 - 43271	0.3	-0.3	-0.1	0.0	-0.4	0.1	0.3	0.2	-0.6	0.9
X	50084 - 50081	-0.1	-1.8	0.7	0.0	0.0	-3.2	3.5	-1.8	-2.9	6.4

<sup>1</sup> Refer to Figure 2.10.2-34 for the identification of the representative sections.

Table 2.10.4-95  $P_m + P_b$  Stresses; 1-Foot Top Corner Drop; Drop Orientation = 24 Degrees; 3-D Top Model; 91.7-Degree Circumferential Location; Condition 1

Condition 1: 100°F Ambient with Contents

Section <sup>1</sup>	Node - Node	Stress Components (ksi)						Principal Stresses (ksi)			
		$S_x$	$S_y$	$S_z$	$S_{xy}$	$S_{yz}$	$S_{xz}$	S1	S2	S3	S.L
A I	1949 - 1951	0.3	0.7	-0.1	0.0	0.0	0.1	0.7	0.3	-0.1	0.8
B O	1952 - 93	-0.3	-0.6	0.2	0.0	0.0	0.0	0.2	-0.3	-0.6	0.9
C I	19925 - 19927	0.0	0.5	-0.3	0.0	-0.4	0.0	0.7	0.0	-0.5	1.1
D O	18683 - 18085	0.1	-0.4	-0.1	0.0	-0.1	0.0	0.1	-0.1	-0.4	0.6
E O	18682 - 18082	0.1	0.0	-0.3	0.1	-0.1	-0.1	0.2	-0.1	-0.4	0.6
F O	19925 - 19325	0.2	0.9	1.2	0.2	-0.6	-0.1	1.7	0.4	0.1	1.6
G I	18680 - 18080	-0.1	0.1	-0.9	0.2	0.1	-0.2	0.3	-0.1	-1.0	1.3
H O	19921 - 19321	0.0	0.3	-0.4	0.1	-1.0	0.0	1.0	0.0	-1.1	2.2
I I	18676 - 18076	0.0	0.2	-0.6	0.0	0.3	0.0	0.3	0.0	-0.8	1.1
J I	19916 - 19316	0.0	1.6	-1.1	0.0	-0.1	0.0	1.6	0.0	-1.1	2.6
K I	18671 - 18071	0.0	0.1	-0.9	0.0	0.5	0.0	0.4	0.0	-1.1	1.4
L I	19908 - 19308	0.1	2.0	-1.6	0.1	1.4	0.0	2.4	0.1	-2.0	4.5
M I	18663 - 18063	0.0	0.1	-1.1	0.0	0.8	0.0	0.5	0.0	-1.5	2.0
N I	19877 - 19277	-0.1	1.5	-1.1	0.0	2.9	0.0	3.3	-0.1	-3.0	6.3
O I	18647 - 18047	0.0	0.0	-1.3	0.0	1.1	0.0	0.6	0.0	-2.0	2.6
P O	19840 - 19240	-0.6	0.1	-1.5	0.3	3.9	-0.1	3.3	-0.6	-4.7	8.0
Q O	18628 - 18028	0.0	0.1	-1.8	0.0	1.5	0.0	0.9	0.0	-2.6	3.6
R I	19816 - 19216	-0.1	0.9	-4.1	-0.1	3.3	-0.1	2.6	-0.1	-5.7	8.3
S I	18616 - 18016	-2.7	-0.2	-3.7	-1.2	2.1	-0.1	1.1	-2.9	-4.8	5.9
T I	18811 - 18011	1.6	1.9	2.0	2.0	3.3	0.8	6.1	1.0	-1.6	7.7
U I	45758 - 45751	-1.3	-0.7	-4.6	-1.5	0.1	1.1	0.6	-2.2	-5.0	5.6
V I	50924 - 50921	-2.2	-0.6	-0.3	-1.8	0.1	-0.4	0.7	-0.4	-3.4	4.1
W I	43278 - 43271	0.3	-0.7	-0.1	-0.1	-0.3	0.1	0.3	0.0	-0.8	1.2
X O	50084 - 50081	-12.8	-13.5	5.9	0.4	-0.2	-3.2	6.5	-13.0	-13.8	20.2

<sup>1</sup> Refer to Figure 2.10.2-34 for the identification of the representative sections.

Table 2.10.4-96  $P_m$  Stresses; 1-Foot Top Corner Drop; Drop Orientation = 24 Degrees; 3-D Top Model; 180-Degree Circumferential Location; Condition 1

Condition 1: 100°F Ambient with Contents

Section <sup>1</sup>	Node - Node	Stress Components (ksi)						Principal Stresses (ksi)			
		$S_x$	$S_y$	$S_z$	$S_{xy}$	$S_{yz}$	$S_{xz}$	S1	S2	S3	S.I.
A	1949 - 95	0.1	0.3	0.0	0.0	0.0	0.0	0.3	0.1	-0.1	0.4
B	1952 - 93	-0.2	-0.3	0.0	0.0	0.0	0.0	0.1	-0.2	-0.3	0.4
C	31925 - 31927	0.0	0.1	-0.1	0.0	0.0	-0.1	0.1	0.1	-0.2	0.2
D	30683 - 30085	0.0	0.0	-0.3	0.0	0.0	0.0	0.1	0.0	-0.3	0.3
E	30682 - 30082	0.3	0.1	-0.3	0.0	0.0	0.0	0.3	0.1	-0.3	0.6
F	31925 - 31325	-0.3	0.0	-0.3	0.0	0.0	0.0	0.0	-0.3	-0.3	0.3
G	30680 - 30080	0.0	-0.1	-0.6	0.0	0.1	0.0	0.0	-0.1	-0.7	0.6
H	31921 - 31321	0.0	0.0	-0.8	0.0	0.0	0.0	0.0	0.0	-0.8	0.8
I	30676 - 30076	0.0	-0.1	-0.7	0.0	0.1	0.0	0.0	-0.1	-0.7	0.7
J	31916 - 31316	-0.1	0.1	-0.7	0.0	0.1	0.0	0.1	-0.1	-0.8	0.9
K	30671 - 30071	0.0	-0.1	-0.6	0.0	0.1	0.0	0.0	-0.1	-0.6	0.6
L	31908 - 31308	-0.1	0.3	-0.1	-0.1	0.2	0.0	0.3	-0.1	-0.2	0.5
M	30663 - 30063	0.0	-0.1	-0.4	0.0	0.1	0.0	0.0	-0.1	-0.4	0.4
N	31877 - 31277	-0.1	0.2	1.1	0.0	0.2	0.0	1.1	0.1	-0.1	1.2
O	30647 - 30047	0.0	-0.1	0.0	0.0	0.1	0.0	0.1	0.0	-0.2	0.3
P	31840 - 31240	-0.4	-0.4	2.0	0.0	0.3	0.0	2.0	-0.4	-0.5	2.5
Q	30628 - 30028	0.0	-0.3	0.3	0.0	0.1	0.0	0.3	0.0	-0.3	0.7
R	31816 - 31216	-0.4	2.5	1.3	0.5	0.1	0.9	2.6	1.6	-0.9	3.5
S	30616 - 30016	-0.8	1.7	0.1	0.3	0.1	-0.2	1.8	0.2	-0.9	2.7
T	30811 - 30011	0.1	3.4	-0.2	0.5	0.1	0.2	3.5	0.1	-0.3	3.7
U	47558 - 47551	-1.2	-1.4	-2.6	-0.1	0.0	-0.1	-1.1	-1.4	-2.6	1.5
V	51524 - 51521	-1.5	-1.2	-0.2	0.0	0.0	-0.2	-0.1	-1.2	-1.6	1.4
W	43278 - 43271	0.3	-0.3	-0.1	0.0	-0.4	0.1	0.3	0.2	-0.6	0.9
X	50084 - 50081	-0.1	-1.8	0.7	0.0	0.0	-3.2	3.5	-1.8	-2.9	6.4

<sup>1</sup> Refer to Figure 2.10.2-34 for the identification of the representative sections.

Table 2.10.4-97  $P_m + P_b$  Stresses; 1-Foot Top Corner Drop; Drop Orientation = 24 Degrees; 3-D Top Model; 180-Degree Circumferential Location; Condition 1

Condition 1: 100°F Ambient with Contents

Section <sup>1</sup>	Node - Node	Stress Components (ksi)						Principal Stresses (ksi)			
		$S_x$	$S_y$	$S_z$	$S_{xy}$	$S_{yz}$	$S_{zx}$	S1	S2	S3	S.I
A I	1949 - 1951	0.3	0.7	-0.1	0.0	0.0	0.1	0.7	0.3	-0.1	0.8
B O	1952 - 93	-0.3	-0.6	0.2	0.0	0.0	0.0	0.2	-0.3	-0.6	0.9
C O	31925 - 31927	0.3	0.1	0.0	0.0	0.0	-0.1	0.3	0.1	-0.1	0.4
D O	30683 - 30085	0.4	0.1	-0.3	0.0	0.0	0.0	0.4	0.1	-0.3	0.7
E O	30682 - 30082	0.3	0.1	-0.4	0.0	0.1	0.0	0.3	0.1	-0.4	0.7
F O	31925 - 31325	-0.3	0.0	-0.3	0.0	0.0	0.0	0.0	-0.3	-0.4	0.3
G O	30680 - 30080	0.0	-0.2	-1.0	0.0	0.1	0.0	0.0	-0.2	-1.0	1.0
H O	31921 - 31321	0.0	0.0	-0.9	0.0	0.0	0.0	0.0	0.0	-0.9	0.9
I O	30676 - 30076	0.0	-0.1	-0.7	0.0	0.0	0.0	0.0	-0.1	-0.7	0.7
J O	31916 - 31316	-0.1	0.2	-0.7	0.0	0.1	0.0	0.3	-0.1	-0.7	1.0
K I	30671 - 30071	0.0	-0.2	-0.6	0.0	0.1	0.0	0.0	-0.2	-0.6	0.6
L O	31908 - 31308	-0.1	0.5	0.0	-0.2	0.2	0.0	0.6	0.0	-0.2	0.8
M I	30663 - 30063	0.0	-0.1	-0.4	0.0	0.1	0.0	0.0	-0.1	-0.4	0.4
N O	31877 - 31277	-0.1	0.1	1.1	0.0	0.2	0.0	1.1	0.1	-0.1	1.2
O O	30647 - 30047	0.0	-0.2	0.0	0.0	0.1	0.0	0.1	0.0	-0.2	0.3
P I	31840 - 31240	0.0	0.1	3.3	0.0	0.3	0.0	3.3	0.1	0.0	3.3
Q I	30628 - 30028	0.0	-0.1	0.9	0.0	0.2	0.0	0.9	0.0	-0.1	1.0
R O	31816 - 31216	-0.9	2.5	2.2	0.6	-0.1	1.5	2.9	2.5	-1.6	4.5
S I	30616 - 30016	-1.6	1.7	0.5	0.4	0.2	-0.6	1.7	0.7	-1.8	3.5
T O	30811 - 30011	-0.2	2.7	-1.9	0.4	0.1	-0.3	2.7	-0.2	-2.0	4.7
U O	47558 - 47551	2.0	0.5	-0.5	-0.1	0.2	-1.1	2.4	0.5	-0.9	3.3
V I	51524 - 51521	-5.2	-2.4	-0.6	0.1	0.0	-0.2	-0.6	-2.4	-5.2	4.6
W I	43278 - 43271	0.3	-0.7	-0.1	-0.1	-0.3	0.1	0.3	0.0	-0.8	1.2
X O	50084 - 50081	-12.8	-13.5	5.9	0.4	-0.2	-3.2	6.3	-13.0	-13.8	20.2

<sup>1</sup> Refer to Figure 2.10.2-34 for the identification of the representative sections.

Table 2.10.4-98 Primary Stresses; 1-Foot Bottom Corner Drop; Drop Orientation = 24 Degrees; 3-D Bottom Model; 0-Degree Circumferential Location; Condition 1

Condition 1: 100°F Ambient with Contents

Stress Points		Stress Components (ksi)						Principal Stresses (ksi)		
Section <sup>1</sup>	Node	S <sub>x</sub>	S <sub>y</sub>	S <sub>z</sub>	S <sub>xy</sub>	S <sub>yz</sub>	S <sub>xz</sub>	S1	S2	S3
A1	1130	6.1	4.5	-2.3	-0.2	0.8	0.7	6.1	4.6	-2.4
A2	1129	0.9	0.0	-0.5	0.0	0.6	0.7	1.2	0.2	-1.1
A3	1128	-4.3	-4.5	1.3	0.2	0.8	0.7	1.5	-4.4	-4.6
B1	1185	3.4	1.1	-2.3	-0.2	0.9	0.8	3.5	1.3	-2.6
B2	1184	-1.3	-2.8	-0.7	0.0	0.6	0.8	-0.1	-1.8	-3.0
B3	1183	-6.1	-6.6	0.9	0.1	0.7	0.8	1.0	-6.2	-6.7
C1	90	-6.2	-1.6	-7.1	-0.4	-0.3	-1.5	-1.6	-5.1	-8.2
C2	80	-3.1	-0.5	-4.3	-0.3	-0.2	-1.1	-0.5	-2.4	-5.0
C3	70	-2.0	-0.4	-2.8	-0.2	-0.1	-0.9	-0.3	-1.4	-3.4
C4	60	-1.1	-0.3	-1.6	0.0	-0.1	-0.8	-0.3	-0.5	-2.2
C5	50	2.2	-1.0	-0.5	0.3	-0.1	-0.6	2.3	-0.7	-1.0
C6	40	5.3	-1.0	-0.1	0.5	0.0	-0.4	5.4	-0.1	-1.0
D1	25	-12.0	-9.1	-15.0	-0.1	-0.2	-3.2	-9.1	-9.9	-17.1
D2	15	-2.0	-6.9	-6.4	0.2	-0.1	-1.6	-1.5	-6.9	-6.9
D3	5	0.7	-8.5	-3.0	0.6	0.0	-0.5	0.8	-3.1	-8.6
E1	35	2.5	-4.0	-11.8	0.5	-0.1	-1.1	2.6	-4.0	-11.8
E2	34	-0.3	-3.4	-7.7	0.2	-0.3	-2.9	0.7	-3.4	-8.7
E3	33	-2.5	-3.0	-4.0	0.0	-0.3	-3.2	0.0	-3.0	-6.5
E4	32	-2.7	-2.3	-1.1	0.0	-0.2	-2.0	0.2	-2.3	-4.0
E5	31	-2.8	-1.6	2.0	-0.1	-0.1	-1.2	2.3	-1.6	-3.1
F1	100	-0.1	-0.4	-9.1	-0.1	-0.3	-0.9	0.0	-0.4	-9.2
F2	99	-1.0	0.2	-6.1	-0.1	-0.3	-0.4	0.2	-1.0	-6.1
F3	98	-1.0	0.3	-5.3	-0.1	-0.2	0.6	0.4	-0.9	-5.4
F4	97	0.0	0.5	-5.8	-0.1	-0.1	0.9	0.5	0.1	-6.0
G1	94	0.1	-0.8	-7.7	0.0	-0.1	-0.3	0.1	-0.8	-7.7
G2	93	-0.2	-0.2	-5.2	0.0	-0.1	-0.2	-0.2	-0.2	-5.2
G3	92	-0.3	0.3	-3.1	0.0	-0.1	0.0	0.3	-0.3	-3.1
G4	91	-0.2	1.0	-0.7	-0.1	0.0	0.0	1.0	-0.2	-0.7

Table 2.10.4-98 Primary Stresses; 1-Foot Bottom Corner Drop; Drop Orientation = 24 Degrees; 3-D Bottom Model; 0-Degree Circumferential Location; Condition 1 (continued)

Stress Points		Stress Components (ksi)						Principal Stresses (ksi)		
Section <sup>1</sup>	Node	S <sub>x</sub>	S <sub>y</sub>	S <sub>z</sub>	S <sub>xy</sub>	S <sub>yz</sub>	S <sub>xz</sub>	S1	S2	S3
H1	330	-0.1	2.2	-5.0	-0.2	-0.4	0.0	2.2	-0.1	-5.0
H2	329	-0.2	2.1	-5.8	-0.2	-0.3	0.0	2.1	-0.2	-5.8
H3	328	-0.2	2.1	-6.6	-0.1	-0.3	0.2	2.1	-0.2	-6.6
H4	327	-0.2	1.8	-8.3	-0.1	-0.3	0.4	1.8	-0.1	-8.3
I1	244	0.0	0.1	-3.6	0.0	-0.1	0.0	0.1	0.0	-3.6
I2	243	0.0	0.4	-3.6	0.0	-0.1	0.0	0.4	0.0	-3.6
I3	242	0.0	0.6	-3.6	0.0	-0.1	0.0	0.6	0.0	-3.6
I4	241	0.0	0.8	-3.6	-0.1	0.0	0.0	0.8	0.0	-3.6
J1	550	-0.1	2.1	-3.4	-0.2	-0.3	0.0	2.1	-0.1	-3.5
J2	548	0.0	2.5	-3.3	-0.2	-0.3	0.0	2.6	-0.1	-3.3
J3	547	0.0	3.0	-3.1	-0.2	-0.2	0.0	3.0	0.0	-3.1
K1	344	0.0	-0.7	-3.0	0.0	-0.1	0.0	0.0	-0.7	-3.0
K2	342	0.0	0.2	-2.6	0.0	-0.1	0.0	0.2	0.0	-2.6
K3	341	0.0	1.0	-2.3	-0.1	-0.1	0.0	1.0	0.0	-2.3
L1	740	0.0	2.1	-0.4	-0.1	-0.1	0.0	2.1	0.0	-0.4
L2	738	-0.1	2.5	-0.1	-0.3	-0.1	0.0	2.6	-0.1	-0.1
L3	737	0.0	3.0	0.1	-0.5	-0.1	0.0	3.1	0.1	0.0
M1	454	0.0	-0.6	-1.7	-0.3	0.0	0.0	0.1	-0.7	-1.7
M2	452	0.1	0.2	-1.4	-0.1	-0.1	0.0	0.3	0.0	-1.4
M3	451	-0.1	0.8	-1.2	0.0	-0.1	0.0	0.8	-0.1	-1.2
N1	810	0.0	2.4	0.0	-0.2	0.1	0.0	2.4	0.0	-0.1
N2	807	-0.1	2.7	0.3	-0.2	0.1	0.0	2.7	0.3	-0.1
O1	524	0.0	-0.2	-0.5	0.0	0.0	0.0	0.0	-0.2	-0.5
O2	521	0.0	0.4	-0.2	0.0	-0.1	0.0	0.4	0.0	-0.2
P1	850	0.0	2.1	-1.5	-0.1	0.2	0.0	2.2	0.0	-1.5
P2	847	0.0	2.6	-0.2	-0.2	0.2	0.0	2.6	0.0	-0.2
Q1	564	0.0	0.1	0.1	0.0	0.0	0.0	0.2	0.0	0.0
Q2	561	0.0	0.3	0.2	0.0	0.0	0.0	0.3	0.2	0.0
R1	890	-0.5	0.0	1.1	0.0	0.1	-0.1	1.1	0.0	-0.5
R2	887	-0.6	-0.8	-2.3	0.0	0.1	-0.2	-0.6	-0.8	-2.3

Table 2.10.4-98 Primary Stresses; 1-Foot Bottom Corner Drop; Drop Orientation = 24 Degrees; 3-D Bottom Model; 0-Degree Circumferential Location; Condition 1 (continued)

Stress Points		Stress Components (ksi)						Principal Stresses (ksi)		
Section <sup>1</sup>	Node	S <sub>x</sub>	S <sub>y</sub>	S <sub>z</sub>	S <sub>xy</sub>	S <sub>yz</sub>	S <sub>xz</sub>	S1	S2	S3
S1	604	-0.3	0.1	0.1	0.0	0.0	-0.2	0.2	0.1	-0.4
S2	601	0.0	0.4	0.7	0.0	0.0	-0.1	0.7	0.4	0.0
T1	897	0.3	-0.1	-0.7	0.0	0.0	-0.1	0.3	-0.1	-0.7
T2	614	0.2	0.1	0.1	0.0	0.0	-0.2	0.3	0.1	-0.1
T3	611	0.0	0.1	0.3	0.0	0.0	-0.1	0.3	0.1	0.0
U1	900	0.3	0.1	-0.1	0.0	0.0	0.1	0.3	0.1	-0.1
U2	910	0.1	-0.1	-0.2	0.0	0.0	0.0	0.1	-0.1	-0.2
V1	920	0.0	-0.1	-0.1	0.0	0.0	0.0	0.0	-0.1	-0.1
V2	930	-0.2	-0.3	0.0	0.1	0.0	0.0	0.0	-0.2	-0.3
W1	1216	0.3	0.7	-0.3	0.0	0.0	0.0	0.7	0.3	-0.3
W2	1226	-0.1	0.0	0.1	0.0	0.0	0.0	0.1	0.0	-0.1
X1	1236	0.0	0.0	-0.2	0.0	0.0	0.0	0.0	0.0	-0.2
X2	1246	-0.4	-0.7	0.3	0.0	0.0	0.0	0.3	-0.4	-0.7

<sup>1</sup> Refer to Figure 2.10.2-34 for the identification of the representative sections.

Table 2.10.4-99 Primary + Secondary Stresses; 1-Foot Bottom Corner Drop; Drop Orientation = 24 Degrees; 3-D Bottom Model; 0-Degree Circumferential Location; Condition 1

Condition 1: 100°F Ambient with Contents

Stress Points		Stress Components (ksi)						Principal Stresses (ksi)		
Section <sup>1</sup>	Node	S <sub>x</sub>	S <sub>y</sub>	S <sub>z</sub>	S <sub>xy</sub>	S <sub>yz</sub>	S <sub>xz</sub>	S1	S2	S3
A1	1130	6.2	4.8	-1.2	-0.2	0.7	1.0	6.4	4.9	-1.4
A2	1129	0.2	-0.7	-0.5	0.0	0.3	1.1	1.0	-0.5	-1.4
A3	1128	-5.9	-6.2	0.3	0.2	0.6	1.0	0.5	-6.0	-6.2
B1	1185	5.3	3.0	-1.3	-0.2	0.8	1.1	5.5	3.1	-1.6
B2	1184	-0.1	-1.5	-0.7	0.0	0.6	1.1	0.8	-1.1	-2.0
B3	1183	-5.5	-5.9	-0.1	0.1	0.6	1.1	0.2	-5.7	-6.0
C1	90	-7.7	-2.7	-9.0	-0.4	-0.3	-2.0	-2.6	-6.3	-10.5
C2	80	-4.2	-1.4	-5.5	-0.4	-0.2	-1.8	-1.3	-2.9	-6.8
C3	70	-2.9	-1.3	-3.9	-0.2	-0.2	-1.7	-1.3	-1.6	-5.2
C4	60	-1.7	-1.3	-2.6	0.0	-0.1	-1.5	-0.5	-1.3	-3.7
C5	50	1.8	-2.4	-1.9	0.4	-0.1	-1.0	2.1	-2.1	-2.4
C6	40	5.1	-2.7	-1.9	0.6	0.0	-0.6	5.2	-2.0	-2.8
D1	25	-7.8	-6.8	-11.4	0.0	-0.2	-1.9	-6.8	-7.0	-12.2
D2	15	-1.8	-6.0	-5.0	0.2	-0.1	-1.1	-1.4	-5.3	-6.0
D3	5	-0.7	-8.2	-2.7	0.5	0.0	-0.5	-0.5	-2.8	-8.2
E1	35	0.4	-4.6	-10.7	0.4	-0.1	0.0	0.4	-4.7	-10.7
E2	34	-1.7	-3.6	-5.9	0.1	-0.2	-1.3	-1.3	-3.6	-6.3
E3	33	-2.9	-3.0	-2.8	0.0	-0.2	-1.6	-1.2	-3.0	-4.5
E4	32	-2.8	-2.3	-0.3	0.0	-0.1	-1.0	0.0	-2.3	-3.2
E5	31	-2.8	-1.6	2.3	-0.1	-0.1	-0.6	2.4	-1.6	-2.9
F1	100	-0.1	-0.8	-11.7	0.0	-0.3	-1.1	0.0	-0.8	-11.8
F2	99	-1.1	-0.1	-7.6	-0.1	-0.3	-0.5	0.0	-1.0	-7.6
F3	98	-0.7	0.2	-6.4	-0.1	-0.2	0.3	0.2	-0.7	-6.4
F4	97	0.6	1.3	-2.5	-0.1	-0.2	0.5	1.3	0.6	-2.6
G1	94	1.0	2.1	4.2	-0.1	0.0	1.0	4.5	2.1	0.7
G2	93	0.6	0.8	-0.5	-0.1	-0.1	0.5	0.9	0.7	-0.7
G3	92	0.0	1.3	1.7	-0.1	-0.1	0.0	1.7	1.3	0.0
G4	91	-0.1	1.7	3.4	-0.1	-0.1	-0.1	3.4	1.7	-0.1



Table 2.10.4-99 Primary + Secondary Stresses; 1-Foot Bottom Corner Drop; Drop  
Orientation = 24 Degrees; 3-D Bottom Model; 0-Degree  
Circumferential Location; Condition 1 (continued)

Stress Points Section <sup>1</sup> Node		Stress Components (ksi)						Principal Stresses (ksi)		
		S <sub>x</sub>	S <sub>y</sub>	S <sub>z</sub>	S <sub>xy</sub>	S <sub>yz</sub>	S <sub>xz</sub>	S1	S2	S3
H1	330	-0.1	1.8	-4.8	-0.1	-0.4	0.0	1.8	-0.1	-4.8
H2	329	-0.2	1.7	-6.4	-0.1	-0.3	0.1	1.7	-0.2	-6.4
H3	328	-0.2	1.7	-7.8	-0.1	-0.3	0.3	1.7	-0.2	-7.8
H4	327	-0.4	1.3	-10.4	-0.1	-0.3	0.6	1.3	-0.3	-10.5
I1	244	0.0	3.3	2.2	-0.2	-0.1	0.0	3.3	2.2	-0.1
I2	243	0.0	3.5	2.2	-0.3	-0.1	-0.1	3.5	2.2	0.0
I3	242	0.0	3.8	2.3	-0.3	-0.1	-0.1	3.9	2.3	0.0
I4	241	0.0	4.1	2.4	-0.3	-0.1	0.0	4.1	2.4	0.0
J1	550	-0.1	0.5	-6.4	0.0	-0.3	0.0	0.5	-0.1	-6.4
J2	548	0.0	2.6	-4.2	-0.2	-0.2	0.0	2.6	0.0	-4.2
J3	547	0.0	4.5	-2.0	-0.3	-0.2	0.0	4.6	0.0	-2.0
K1	344	-0.3	4.1	1.0	-0.3	-0.1	0.0	4.1	1.0	-0.3
K2	342	-0.2	5.7	3.3	-0.4	-0.1	0.0	5.7	3.3	-0.2
K3	341	-0.1	7.2	5.6	-0.5	-0.1	0.0	7.2	5.6	-0.1
L1	740	0.4	0.5	-2.6	0.2	-0.1	-0.1	0.7	0.3	-2.6
L2	738	-0.6	2.3	-1.2	-0.4	-0.1	0.1	2.4	-0.7	-1.2
L3	737	0.3	4.7	0.7	-1.0	-0.1	0.0	4.9	0.7	0.1
M1	454	-0.7	4.7	2.4	-0.4	0.0	0.0	4.7	2.4	-0.8
M2	452	0.3	6.6	4.7	-0.5	0.0	0.1	6.7	4.7	0.2
M3	451	-0.7	7.8	6.3	-0.6	-0.1	-0.3	7.8	6.3	-0.7
N1	810	0.3	0.6	-2.6	0.0	0.1	0.0	0.6	0.3	-2.6
N2	807	0.3	3.8	0.9	-0.3	0.1	0.0	3.8	0.9	0.3
O1	524	-0.1	3.9	4.0	-0.3	-0.1	0.0	4.0	3.9	-0.2
O2	521	-0.1	6.3	7.4	-0.5	0.0	0.0	7.4	6.3	-0.2
P1	850	0.2	1.9	-1.7	-0.1	0.1	0.0	1.9	0.2	-1.7
P2	847	-0.3	2.7	-1.7	-0.2	0.1	0.0	2.7	-0.4	-1.7
Q1	564	0.0	3.4	5.7	-0.2	0.0	0.1	5.7	3.4	0.0
Q2	561	-0.1	4.3	6.4	-0.3	0.0	0.0	6.4	4.4	-0.1
R1	890	-0.4	-4.2	-4.3	0.2	0.1	0.3	-0.4	-4.2	-4.4
R2	887	0.1	-1.7	-2.2	0.1	0.1	0.2	0.1	-1.7	-2.2

Table 2.10.4-99 Primary + Secondary Stresses; 1-Foot Bottom Corner Drop; Drop Orientation = 24 Degrees; 3-D Bottom Model; 0-Degree Circumferential Location; Condition 1 (continued)

Stress Points Section <sup>1</sup> Node	Stress Components (ksi)						Principal Stresses (ksi)		
	S <sub>x</sub>	S <sub>y</sub>	S <sub>z</sub>	S <sub>xy</sub>	S <sub>yz</sub>	S <sub>xz</sub>	S1	S2	S3
S1 604	0.1	0.5	1.5	0.0	-0.1	-0.5	1.7	0.5	-0.1
S2 601	0.2	3.3	7.3	-0.3	0.1	-0.7	7.3	3.3	0.1
T1 897	-1.0	-1.7	-1.1	0.1	0.0	-0.3	-0.8	-1.3	-1.7
T2 614	-0.4	-0.8	0.3	0.1	-0.1	-1.2	1.2	-0.8	-1.3
T3 611	0.9	-0.3	2.5	0.1	-0.1	-1.1	3.1	0.3	-0.3
U1 900	-1.0	-1.0	-1.3	0.0	0.1	1.2	0.1	-1.0	-2.4
U2 910	0.8	-0.3	3.7	0.1	0.0	0.6	3.8	0.7	-0.3
V1 920	6.3	5.3	4.6	0.0	0.0	-0.9	6.7	5.3	4.2
V2 930	-5.8	-2.6	0.5	-0.1	0.0	-1.7	0.9	-2.6	-6.2
W1 1216	1.9	2.4	-1.7	0.0	0.1	-0.6	2.4	2.0	-1.8
W2 1226	-2.5	-2.4	1.0	0.0	0.0	-0.3	1.0	-2.4	-2.5
X1 1236	1.8	1.8	-1.1	0.0	0.1	-0.4	1.9	1.8	-1.1
X2 1246	-0.1	-0.5	2.4	0.0	0.2	-0.8	2.7	-0.4	-0.5

<sup>1</sup> Refer to Figure 2.10.2-34 for the identification of the representative sections.

Table 2.10.4-100  $P_m$  Stresses; 1-Foot Bottom Corner Drop; Drop Orientation = 24 Degrees;  
3-D Bottom Model; 0-Degree Circumferential Location; Condition 1

Condition 1: 100°F Ambient with Contents

Section <sup>1</sup>	Node - Node	Stress Components (ksi)						Principal Stresses (ksi)			
		$S_x$	$S_y$	$S_z$	$S_{xy}$	$S_{yz}$	$S_{xz}$	S1	S2	S3	S.I.
A	1130 - 1128	0.9	0.0	-0.5	0.0	0.7	0.7	1.2	0.3	-1.2	2.4
B	1185 - 1183	-1.4	-2.8	-0.7	0.0	0.7	0.8	-0.1	-1.8	-3.0	3.0
C	90 - 40	-0.1	-0.7	-2.0	0.0	-0.1	-0.8	0.2	-0.7	-2.3	2.5
D	25 - 5	-3.8	-7.8	-7.7	0.2	-0.1	-1.7	-3.2	-7.9	-8.4	5.2
E	35 - 31	-1.2	-3.0	-4.9	0.1	-0.2	-2.3	-0.1	-3.0	-6.0	5.9
F	100 - 97	-0.7	0.2	-6.3	-0.1	-0.2	0.1	0.2	-0.7	-6.3	6.5
G	94 - 91	-0.2	0.1	-4.2	0.0	-0.1	-0.1	0.1	-0.2	-4.2	4.3
H	330 - 327	-0.2	2.0	-6.3	-0.1	-0.3	0.1	2.1	-0.2	-6.3	8.4
I	244 - 241	0.0	0.5	-3.6	0.0	-0.1	0.0	0.5	0.0	-3.6	4.1
J	550 - 547	0.0	2.5	-3.3	-0.2	-0.3	0.0	2.6	-0.1	-3.3	5.8
K	344 - 341	0.0	0.2	-2.6	0.0	-0.1	0.0	0.2	0.0	-2.6	2.8
L	740 - 737	0.0	2.5	-0.1	-0.3	-0.1	0.0	2.6	-0.1	-0.1	2.7
M	454 - 451	0.0	0.1	-1.4	-0.1	-0.1	0.0	0.2	-0.1	-1.4	1.6
N	810 - 807	-0.1	2.6	0.1	-0.2	0.1	0.0	2.6	0.1	-0.1	2.6
O	524 - 521	0.0	0.1	-0.3	0.0	0.0	0.0	0.1	0.0	-0.3	0.5
P	850 - 847	0.0	2.4	-0.8	-0.2	0.2	0.0	2.4	0.0	-0.8	3.2
Q	564 - 561	0.0	0.2	0.2	0.0	0.0	0.0	0.2	0.1	0.0	0.2
R	890 - 887	-0.6	-0.4	-0.6	0.0	0.1	-0.1	-0.4	-0.5	-0.7	0.4
S	604 - 601	-0.2	0.2	0.4	0.0	0.0	-0.1	0.4	0.2	-0.2	0.6
T	614 - 611	0.1	0.1	0.2	0.0	0.0	-0.1	0.3	0.1	0.0	0.3
U	900 - 910	0.2	0.0	-0.1	0.0	0.0	0.0	0.2	0.0	-0.1	0.4
V	920 - 930	-0.1	-0.2	-0.1	0.0	0.0	0.0	-0.1	-0.1	-0.2	0.1
W	1216 - 1226	0.1	0.3	-0.1	0.0	0.0	0.0	0.3	0.1	-0.1	0.4
X	1236 - 1246	-0.2	-0.3	0.1	0.0	0.0	0.0	0.1	-0.2	-0.3	0.4

<sup>1</sup> Refer to Figure 2.10.2-34 for the identification of the representative sections.

Table 2.10.4-101  $P_m + P_b$  Stresses; 1-Foot Bottom Corner Drop; Drop Orientation = 24 Degrees; 3-D Bottom Model; 0-Degree Circumferential Location; Condition 1

Condition 1: 100°F Ambient with Contents

Section <sup>1</sup>	Node - Node	Stress Components (ksi)						Principal Stresses (ksi)			
		$S_x$	$S_y$	$S_z$	$S_{xy}$	$S_{yz}$	$S_{zx}$	S1	S2	S3	S.L
AI	1130 - 1128	6.1	4.5	-2.3	-0.2	0.7	0.7	6.1	4.6	-2.4	8.5
BO	1185 - 1183	-6.1	-6.7	0.9	0.1	0.6	0.8	1.0	-6.2	-6.7	7.7
CO	90 - 40	4.6	-0.9	0.8	0.5	0.0	-0.4	4.7	0.8	-0.9	5.6
DO	25 - 5	2.5	-7.6	-1.7	0.6	0.0	-0.3	2.5	-1.7	-7.6	10.1
EI	35 - 31	1.7	-4.1	-11.9	0.4	-0.3	-2.4	2.1	-4.1	-12.4	14.5
FI	100 - 97	-0.7	-0.2	-7.8	-0.1	-0.4	-1.0	-0.2	-0.6	-8.0	7.8
GI	94 - 91	0.0	-0.8	-7.6	0.0	-0.1	-0.3	0.0	-0.8	-7.6	7.6
HO	330 - 327	-0.2	1.9	-7.8	-0.1	-0.3	0.4	1.9	-0.2	-7.9	9.8
IO	244 - 241	0.0	0.8	-3.6	-0.1	0.0	0.0	0.8	0.0	-3.6	4.4
JO	550 - 547	0.0	3.0	-3.1	-0.2	-0.2	0.0	3.0	0.0	-3.1	6.1
KO	344 - 341	0.0	1.0	-2.3	-0.1	-0.1	0.0	1.1	0.0	-2.3	3.4
LO	740 - 737	0.0	3.0	0.1	-0.5	-0.1	0.0	3.0	0.1	-0.1	3.1
MO	454 - 451	0.0	0.8	-1.2	0.0	-0.1	0.0	0.9	0.0	-1.2	2.0
NO	810 - 807	-0.1	2.7	0.3	-0.2	0.1	0.0	2.7	0.3	-0.1	2.8
OO	524 - 521	0.0	0.4	-0.2	0.0	-0.1	0.0	0.4	0.0	-0.2	0.6
PI	850 - 847	0.0	2.1	-1.5	-0.1	0.2	0.0	2.2	0.0	-1.5	3.7
QO	564 - 561	0.0	0.3	0.2	0.0	0.0	0.0	0.3	0.2	0.0	0.3
RO	890 - 887	-0.6	-0.8	-2.3	0.0	0.1	-0.2	-0.6	-0.8	-2.3	1.7
SO	604 - 601	0.0	0.4	0.7	0.0	0.0	-0.1	0.7	0.4	0.0	0.7
TO	614 - 611	0.0	0.1	0.3	0.0	0.0	-0.1	0.3	0.1	0.0	0.4
UI	900 - 910	0.3	0.1	-0.1	0.0	0.0	0.1	0.3	0.1	-0.1	0.4
VO	920 - 930	-0.2	-0.3	0.0	0.1	0.0	0.0	0.0	-0.2	-0.3	0.3
WI	1216 - 1226	0.3	0.7	-0.3	0.0	0.0	0.0	0.7	0.3	-0.3	0.9
XO	1236 - 1246	-0.4	-0.7	0.3	0.0	0.0	0.0	0.3	-0.4	-0.7	0.9

<sup>1</sup> Refer to Figure 2.10.2-34 for the identification of the representative sections.

Table 2.10.4-102  $S_n$  Stresses; 1-Foot Bottom Corner Drop; Drop Orientation = 24 Degrees;  
3-D Bottom Model; 0-Degree Circumferential Location; Condition 1

Condition 1: 100°F Ambient with Contents

Section <sup>1</sup>	Node - Node	Stress Components (ksi)						Principal Stresses (ksi)			
		$S_x$	$S_y$	$S_z$	$S_{xy}$	$S_{yz}$	$S_{zx}$	S1	S2	S3	S.I.
A I	1130 - 1128	6.2	4.8	-1.2	-0.2	0.6	1.0	6.4	4.9	-1.4	7.8
B I	1185 - 1183	5.3	3.0	-1.3	-0.2	0.8	1.1	5.5	3.1	-1.6	7.1
C O	90 - 40	4.6	-2.4	-0.5	0.6	0.0	-0.6	4.7	-0.6	-2.5	7.2
D O	25 - 5	0.6	-7.4	-1.6	0.5	0.0	-0.4	0.7	-1.7	-7.4	8.1
E I	35 - 31	-0.4	-4.6	-10.3	0.3	-0.1	-0.8	-0.3	-4.6	-10.4	10.0
F I	100 - 97	-0.9	-0.8	-11.0	-0.1	-0.3	-1.0	-0.7	-0.8	-11.1	10.4
G O	94 - 91	-0.3	1.3	2.1	-0.1	-0.1	-0.3	2.1	1.3	-0.3	2.4
H O	330 - 327	-0.3	1.5	-9.9	-0.1	-0.3	0.5	1.5	-0.3	-9.9	11.4
I O	244 - 241	0.0	4.1	2.4	-0.3	-0.1	-0.1	4.1	2.4	0.0	4.1
J I	550 - 547	-0.1	0.5	-6.4	0.0	-0.3	0.0	0.5	-0.1	-6.4	6.9
K O	344 - 341	-0.1	7.2	5.6	-0.5	-0.1	0.0	7.3	5.6	-0.1	7.4
L O	740 - 737	-0.2	4.5	0.5	-1.0	0.0	0.1	4.7	0.5	-0.4	5.1
M O	454 - 451	-0.2	8.0	6.5	-0.6	-0.1	-0.1	8.0	6.5	-0.2	8.2
N O	810 - 807	0.3	3.8	0.9	-0.3	0.1	0.0	3.8	0.9	0.3	3.6
O O	524 - 521	-0.1	6.3	7.4	-0.5	0.0	0.0	7.4	6.3	-0.2	7.6
P O	850 - 847	-0.3	2.7	-1.7	-0.2	0.1	0.0	2.7	-0.4	-1.7	4.4
Q O	564 - 561	-0.1	4.3	6.4	-0.3	0.0	0.0	6.4	4.4	-0.1	6.4
R I	890 - 887	-0.4	-4.2	-4.3	0.2	0.1	0.3	-0.4	-4.2	-4.4	4.0
S O	604 - 601	0.2	3.3	7.3	-0.3	0.1	-0.7	7.3	3.3	0.1	7.2
T O	614 - 611	0.9	-0.3	2.5	0.1	-0.1	-1.1	3.1	0.3	-0.3	3.4
U O	900 - 910	0.8	-0.3	3.7	0.1	0.0	0.6	3.8	0.7	-0.3	4.1
V O	920 - 930	-5.8	-2.6	0.5	-0.1	0.0	-1.7	0.9	-2.6	-6.2	7.1
W I	1216 - 1226	1.9	2.4	-1.7	0.0	0.1	-0.6	2.4	2.0	-1.8	4.2
X O	1236 - 1246	-0.1	-0.5	2.4	0.0	0.2	-0.8	2.7	-0.4	-0.5	3.1

<sup>1</sup> Refer to Figure 2.10.2-34 for the identification of the representative sections.

Table 2.10.4-103 Critical  $P_m$  Stress Summary; 1-Foot Bottom Corner Drop; Drop Orientation = 24 Degrees; 3-D Bottom Model; Condition 1

Condition 1: 100°F Ambient with Contents

Comp. No. <sup>1</sup>	Section Cut Node-Node	P <sub>m</sub> Stresses (ksi)						Principal Stresses (ksi)			Allow. S.I. Stress	Margin of Safety	
		S <sub>x</sub>	S <sub>y</sub>	S <sub>z</sub>	S <sub>xy</sub>	S <sub>yz</sub>	S <sub>xz</sub>	S1	S2	S3			
1	14025-14003	-1.5	-4.9	-6.9	-0.7	-1.1	-1.4	-1.1	-4.4	-7.8	6.7	19.2	1.9
2	12140-12137	0.0	1.8	-3.8	0.0	-3.3	-0.1	3.3	0.0	-5.3	8.6	18.3	1.2
3	12340-12337	-0.1	1.3	-4.0	0.1	-3.8	0.1	3.4	-0.1	-6.0	9.4	31.4	2.3
4	12520-12517	0.0	1.8	-3.0	0.0	-3.1	0.0	3.3	0.0	-4.5	7.8	19.6	1.5
5	12204-12201	0.0	0.6	-3.5	0.0	-1.3	0.0	1.0	0.0	-3.9	4.9	20.0	3.1
6	12880-12877	0.0	0.6	-0.3	0.0	1.5	-0.1	1.8	0.0	-1.4	3.2	20.0	5.3
7	897- 907	0.2	-0.1	-0.4	0.0	0.0	-0.1	0.2	-0.1	-0.4	0.6	20.0	32.3
8	31234-31244	-0.4	-0.2	0.0	0.0	0.0	0.0	0.0	-0.2	-0.4	0.4	45.0	111.3

Locations of the most critical sections for each component are provided in the following:

Comp. No. <sup>1</sup>	Section Location					
	Inside Node			Outside Node		
	x (in)	y (deg)	z (in)	x (in)	y (deg)	z (in)
1	39.44	67.7	6.20	39.44	67.7	0.75
2	35.50	56.5	17.40	37.45	56.5	17.40
3	35.50	56.5	29.90	37.00	56.5	29.90
4	35.50	56.5	47.40	37.00	56.5	47.40
5	40.70	56.5	26.40	43.35	56.5	26.40
6	35.50	56.5	172.40	37.50	56.5	175.40
7	37.50	0.0	179.40	37.00	0.0	185.40
8	10.00	180.0	187.40	10.00	180.0	193.71

<sup>1</sup> Refer to Figure 2.10.2-33 for cask component identification.

Table 2.10.4-104 Critical  $P_m + P_b$  Stress Summary; 1-Foot Bottom Corner Drop; Drop Orientation = 24 Degrees; 3-D Bottom Model; Condition 1

Condition 1: 100°F Ambient with Contents

Comp. No. <sup>1</sup>	Section Cnt Node-Node	$P_m + P_b$ Stresses (ksi)							Principal Stresses (ksi)			Allow. S.L. Stress	Margin of Safety
		$S_x$	$S_y$	$S_z$	$S_{xy}$	$S_{xz}$	$S_{yz}$	$S_1$	$S_2$	$S_3$			
1	1167- 1165	-16.2	-12.3	-1.7	0.0	0.0	-0.1	-1.7	-12.3	-16.2	14.5	28.7	1.0
2	12035-12031	1.9	-2.8	-11.9	1.6	-2.4	-2.1	2.9	-3.0	-12.7	15.6	27.7	0.8
3	12150-12147	-0.1	1.5	-5.5	0.0	-3.6	-0.1	3.0	-0.1	-7.1	10.1	47.1	3.7
4	12520-12517	0.0	1.9	-3.0	0.0	-3.3	0.0	3.5	0.0	-4.7	8.2	29.4	2.6
5	10204-10201	0.0	0.9	-3.6	0.0	-1.2	-0.1	1.2	0.0	-3.9	5.0	30.0	5.0
6	12880-12877	0.0	0.7	-0.1	0.0	1.9	-0.1	2.3	0.0	-1.6	3.9	30.0	6.7
7	897- 907	0.3	-0.1	-0.7	0.0	0.0	-0.1	0.3	-0.1	-0.7	1.0	30.0	29.0
8	1236- 1246	-0.4	-0.7	0.3	0.0	0.0	0.0	0.3	-0.4	-0.7	0.9	67.5	74.0

Locations of the most critical sections for each component are provided in the following:

Comp. No. <sup>1</sup>	Section Location					
	Inside Node			Outside Node		
	x (in)	y (deg)	z (in)	x (in)	y (deg)	z (in)
1	17.67	0.0	6.20	17.67	0.0	0.75
2	39.44	56.5	8.20	43.35	56.5	8.20
3	35.50	56.5	18.15	37.50	56.5	18.15
4	35.50	56.5	47.40	37.00	56.5	47.40
5	40.70	45.9	26.40	43.35	45.9	26.40
6	35.50	56.5	172.40	37.50	56.5	172.40
7	37.50	0.0	179.40	37.00	0.0	185.40
8	0.0	0.0	187.40	0.0	0.0	193.71

<sup>1</sup> Refer to Figure 2.10.2-33 for cask component identification.

Table 2.10.4-105 Critical  $S_n$  Stress Summary; 1-Foot Bottom Corner Drop; Drop Orientation = 24 Degrees; 3-D Bottom Model; Condition 1

Condition 1: 100°F Ambient with Contents

Comp. No. <sup>1</sup>	Section Cut Node-Node	$S_n$ Stresses (ksi)							Principal Stresses (ksi)				Allow. Stress $3.0 S_u$
		$S_x$	$S_y$	$S_z$	$S_{xy}$	$S_{yz}$	$S_{zx}$	$S_1$	$S_2$	$S_3$	$S_1$		
1	1170- 1168	-14.9	-10.8	-1.7	0.0	0.0	0.0	-1.7	-10.8	-14.9	13.2	57.6	
2	12100-12097	-0.5	-0.2	-11.4	-0.2	-3.6	-0.8	0.9	-0.4	-12.3	13.4	55.5	
3	10150-10147	-0.1	3.0	-7.7	0.0	-3.0	-0.4	3.7	-0.1	-8.3	12.2	94.2	
4	10520-10517	0.2	1.5	-5.8	0.0	-2.8	0.0	2.4	0.2	-6.7	9.1	58.8	
5	424- 421	-0.1	8.2	6.6	-0.6	-0.1	0.0	8.2	6.6	-0.1	8.3	60.0	
6	14644-14641	-1.9	-9.9	-1.2	0.1	0.0	1.3	-0.2	-2.9	-9.9	9.7	60.0	
7	1211- 1221	6.4	4.1	0.0	0.1	0.0	0.1	6.4	4.1	0.0	6.3	60.0	
8	920- 930	-5.8	-2.6	0.5	-0.1	0.0	-1.7	0.9	-2.6	-6.2	7.1	135.0	

Locations of the most critical sections for each component are provided in the following:

Comp. No. <sup>1</sup>	Section Location					
	Inside Node			Outside Node		
	x (in)	y (deg)	z (in)	x (in)	y (deg)	z (in)
1	14.72	0.0	6.20	14.72	0.0	0.75
2	35.50	56.5	15.00	37.50	56.5	15.00
3	35.50	45.9	18.15	37.50	45.9	18.15
4	35.50	45.9	47.40	37.00	45.9	47.40
5	40.70	0.0	85.50	43.35	0.0	85.50
6	40.70	67.7	193.71	43.35	67.7	193.71
7	25.00	0.0	179.40	25.00	0.0	185.40
8	35.50	0.0	187.40	35.50	0.0	193.71

<sup>1</sup> Refer to Figure 2.10.2-33 for cask component identification.



Table 2.10.4-106  $P_m$  Stresses; 1-Foot Bottom Corner Drop; Drop Orientation = 24 Degrees;  
3-D Bottom Model; 45.9-Degree Circumferential Location; Condition 1

Condition 1: 100°F Ambient with Contents

Section <sup>1</sup>	Node - Node	Stress Components (ksi)						Principal Stresses (ksi)			
		$S_x$	$S_y$	$S_z$	$S_{xy}$	$S_{yz}$	$S_{xz}$	S1	S2	S3	S.I.
A	1130 - 1128	0.9	0.0	-0.5	0.0	0.7	0.7	1.2	0.3	-1.2	2.4
B	1185 - 1183	-1.4	-2.8	-0.7	0.0	0.7	0.8	-0.1	-1.8	-3.0	3.0
C	10090 - 10040	0.4	-0.1	-1.8	0.1	-0.7	-0.6	0.7	0.0	-2.2	2.9
D	10025 - 10005	-2.7	-6.7	-7.6	-0.4	-0.6	-1.6	-2.2	-6.5	-8.3	6.1
E	10035 - 10031	-0.5	-1.8	-4.7	0.5	-0.9	-2.1	0.6	-2.0	-5.7	6.3
F	10100 - 10097	-0.5	0.9	-5.0	-0.1	-2.7	-0.1	2.0	-0.5	-6.0	8.0
G	10094 - 10091	-0.3	0.5	-4.3	-0.1	-1.0	-0.3	0.7	-0.2	-4.5	5.3
H	10330 - 10327	-0.1	1.7	-4.9	0.1	-3.3	0.1	3.1	-0.1	-6.2	9.3
I	10244 - 10241	0.0	0.5	-3.6	0.0	-1.0	0.0	0.7	0.0	-3.9	4.6
J	10550 - 10547	0.0	2.0	-2.9	0.0	-2.4	0.0	3.0	0.0	-3.9	6.9
K	10344 - 10341	0.0	0.1	-2.7	0.0	-0.9	0.0	0.4	0.0	-3.0	3.4
L	10740 - 10737	0.0	2.0	-1.0	0.0	-0.9	0.0	2.2	0.0	-1.3	3.4
M	10454 - 10451	0.0	0.1	-1.5	0.0	-0.7	0.0	0.4	0.0	-1.7	2.1
N	10810 - 10807	0.0	1.9	-0.4	0.0	0.7	0.0	2.1	0.0	-0.6	2.7
O	10524 - 10521	0.0	0.1	-0.6	0.0	-0.5	0.0	0.3	0.0	-0.9	1.2
P	10850 - 10847	0.0	1.7	-0.5	0.0	1.6	0.0	2.5	0.0	-1.3	3.9
Q	10564 - 10561	0.0	0.2	-0.2	0.0	-0.4	0.0	0.4	0.0	-0.5	0.9
R	10890 - 10887	-0.3	0.2	-0.3	0.4	0.9	-0.1	0.9	-0.3	-1.1	1.9
S	10604 - 10601	-0.1	0.3	0.1	0.2	-0.2	0.0	0.5	-0.1	-0.2	0.7
T	10614 - 10611	0.1	0.2	0.0	0.0	-0.1	-0.1	0.2	0.1	-0.1	0.3
U	10900 - 10910	0.1	0.1	-0.1	-0.1	0.2	0.0	0.2	0.1	-0.2	0.5
V	10920 - 10930	0.0	-0.3	-0.1	0.0	0.0	0.0	0.0	-0.1	-0.3	0.3
W	1216 - 1226	0.1	0.3	-0.1	0.0	0.0	0.0	0.3	0.1	-0.1	0.4
X	1236 - 1246	-0.2	-0.3	0.1	0.0	0.0	0.0	0.1	-0.2	-0.3	0.4

<sup>1</sup> Refer to Figure 2.10.2-34 for the identification of the representative sections.

Table 2.10.4-107  $P_m$  Stresses; 1-Foot Bottom Corner Drop; Drop Orientation = 24 Degrees;  
3-D Bottom Model; 45.9-Degree Circumferential Location; Condition 1

Condition 1: 100°F Ambient with Contents

Section <sup>1</sup>	Node - Node	Stress Components (ksi)						Principal Stresses (ksi)			
		$S_x$	$S_y$	$S_z$	$S_{xy}$	$S_{yz}$	$S_{xz}$	S1	S2	S3	S.L
A I	1130 - 1128	6.1	4.5	-2.3	-0.2	0.7	0.7	6.1	4.6	-2.4	8.5
B O	1185 - 1183	-6.1	-6.7	0.9	0.1	0.6	0.8	1.0	-6.2	-6.7	7.7
C I	10090 - 10040	-4.5	-0.1	-4.5	-1.7	-1.6	-1.0	0.8	-3.5	-6.3	7.1
D O	10025 - 10005	3.1	-6.6	-1.6	0.8	0.1	-0.4	3.2	-1.6	-6.7	9.8
E I	10035 - 10031	1.8	-3.3	-12.1	1.3	-1.8	-2.2	2.6	-3.5	-12.7	15.3
F I	10100 - 10097	-0.5	0.2	-7.8	-0.2	-3.4	-0.9	1.4	-0.5	-9.2	10.6
G I	10094 - 10091	-0.2	-0.4	-8.1	-0.2	-1.6	-0.6	0.0	-0.2	-8.4	8.4
H O	10330 - 10327	-0.2	1.2	-6.4	0.2	-3.2	0.3	2.4	-0.1	-7.6	10.0
I I	10244 - 10241	0.0	0.8	-3.2	0.0	-1.1	0.0	1.1	0.0	-3.5	4.6
J I	10550 - 10547	0.0	2.0	-2.9	0.0	-2.6	0.0	3.1	0.0	-4.0	7.1
K I	10344 - 10341	0.0	0.6	-2.5	0.0	-1.0	0.0	0.8	0.0	-2.8	3.6
L O	10740 - 10737	0.0	2.1	-1.0	0.1	-0.8	0.0	2.3	0.0	-1.2	3.5
M I	10454 - 10451	0.0	0.4	-1.4	0.0	-0.7	0.0	0.6	0.0	-1.7	2.3
N O	10810 - 10807	0.0	2.3	-0.2	0.0	0.6	0.0	2.4	0.0	-0.3	2.8
O O	10524 - 10521	0.0	0.0	-0.6	0.0	-0.5	0.0	0.3	0.0	-0.9	1.2
P I	10850 - 10847	0.0	1.4	-1.0	0.0	1.9	0.0	2.4	0.0	-2.0	4.5
Q O	10564 - 10561	0.0	0.1	-0.3	0.0	-0.5	0.0	0.4	0.0	-0.6	1.0
R I	10890 - 10887	-0.3	0.4	0.5	0.3	1.0	-0.1	1.5	-0.1	-0.8	2.3
S O	10604 - 10601	-0.1	0.5	0.5	0.1	-0.3	0.0	0.7	0.2	-0.1	0.8
T I	10614 - 10611	0.1	0.2	-0.1	0.0	-0.1	-0.1	0.2	0.1	-0.1	0.4
U I	10900 - 10910	0.1	0.2	-0.1	-0.2	0.3	0.0	0.5	0.1	-0.3	0.8
V O	10920 - 10930	0.0	-0.4	-0.1	0.1	0.0	0.0	0.0	-0.1	-0.5	0.5
W I	1216 - 1226	0.3	0.7	-0.3	0.0	0.0	0.0	0.7	0.3	-0.3	0.9
X O	1236 - 1246	-0.4	-0.7	0.3	0.0	0.0	0.0	0.3	-0.4	-0.7	0.9

<sup>1</sup> Refer to Figure 2.10.2-34 for the identification of the representative sections.

Table 2.10.4-108  $P_m$  Stresses; 1-Foot Bottom Corner Drop; Drop Orientation = 24 Degrees;  
3-D Bottom Model; 91.7-Degree Circumferential Location; Condition 1

**Condition 1: 100°F Ambient with Contents**

Section <sup>1</sup>	Node - Node	Stress Components (ksi)						Principal Stresses (ksi)			
		$S_x$	$S_y$	$S_z$	$S_{xy}$	$S_{yz}$	$S_{zx}$	S1	S2	S3	S.L.
A	1130 - 1128	0.9	0.0	-0.5	0.0	0.7	0.7	1.2	0.3	-1.2	2.4
B	1185 - 1183	-1.4	-2.8	-0.7	0.0	0.7	0.8	-0.1	-1.8	-3.0	3.0
C	18090 - 18040	1.0	0.7	-0.3	0.0	-0.9	0.1	1.2	1.0	-0.8	2.0
D	18025 - 18005	-0.7	-1.7	-2.7	-1.1	-1.2	-0.2	0.1	-1.4	-3.7	3.8
E	18035 - 18031	1.0	0.3	-0.8	0.5	-2.1	-1.4	2.9	0.3	-2.6	5.5
F	18100 - 18097	0.0	1.1	0.5	-0.2	-3.5	-0.3	4.2	0.1	-2.7	7.0
G	18094 - 18091	-0.1	0.4	-1.0	-0.2	-2.0	-0.1	1.8	-0.1	-2.4	4.2
H	18330 - 18327	-0.5	0.3	-0.4	0.2	-3.7	0.0	3.7	-0.5	-3.7	7.4
I	18244 - 18241	0.0	0.0	-1.3	0.0	-1.5	0.0	1.1	0.0	-2.3	3.3
J	18550 - 18547	-0.1	0.9	-1.4	0.0	-2.7	0.0	2.6	-0.1	-3.2	5.8
K	18344 - 18341	0.0	0.0	-1.4	0.0	-1.3	0.0	0.7	0.0	-2.1	2.9
L	18740 - 18737	-0.1	1.0	-1.9	0.0	-1.1	0.0	1.4	-0.1	-2.3	3.7
M	18454 - 18451	0.0	0.0	-1.2	0.0	-0.9	0.0	0.5	0.0	-1.7	2.2
N	18810 - 18807	0.0	0.8	-1.2	0.0	0.3	0.0	0.9	0.0	-1.3	2.1
O	18524 - 18521	0.0	0.0	-1.1	0.0	-0.6	0.0	0.3	0.0	-1.3	1.6
P	18850 - 18847	0.0	0.6	-0.2	0.1	1.0	0.0	1.3	0.0	-0.9	2.3
Q	18564 - 18561	0.0	0.1	-0.9	0.0	-0.5	0.0	0.2	0.0	-1.1	1.4
R	18890 - 18887	0.2	0.9	0.2	0.3	0.7	0.1	1.4	0.1	-0.3	1.7
S	18604 - 18601	-0.1	0.3	-0.6	0.2	-0.1	0.1	0.4	-0.1	-0.7	1.1
T	18614 - 18611	0.0	0.1	-0.4	0.0	0.0	0.1	0.2	0.0	-0.4	0.6
U	18900 - 18910	0.0	0.2	0.0	0.0	0.2	0.0	0.3	0.0	-0.2	0.5
V	18920 - 18930	-0.1	-0.3	-0.1	-0.1	0.1	0.1	0.0	-0.1	-0.3	0.3
W	1216 - 1226	0.1	0.3	-0.1	0.0	0.0	0.0	0.3	0.1	-0.1	0.4
X	1236 - 1246	-0.2	-0.3	0.1	0.0	0.0	0.0	0.1	-0.2	-0.3	0.4

<sup>1</sup> Refer to Figure 2.10.2-34 for the identification of the representative sections.

Table 2.10.4-109  $P_m + P_b$  Stresses; 1-Foot Bottom Corner Drop; Drop Orientation = 24 Degrees; 3-D Bottom Model; 91.7-Degree Circumferential Location; Condition 1

Condition 1: 100°F Ambient with Contents

Section <sup>1</sup>	Node - Node	Stress Components (ksi)						Principal Stresses (ksi)			
		$S_x$	$S_y$	$S_z$	$S_{xy}$	$S_{yz}$	$S_{xz}$	S1	S2	S3	S.L.
A I	1130 - 1128	6.1	4.5	-2.3	-0.2	0.7	0.7	6.1	4.6	-2.4	8.5
B O	1185 - 1183	-6.1	-6.7	0.9	0.1	0.6	0.8	1.0	-6.2	-6.7	7.7
C I	18090 - 18040	-2.3	-0.1	-1.0	-2.0	-2.0	0.1	2.1	-1.6	-3.8	5.9
D I	18025 - 18005	-5.2	-2.9	-5.3	-3.3	-2.6	-1.0	0.0	-4.3	-9.1	9.1
E I	18035 - 18031	2.6	-0.2	-4.3	1.6	-3.2	-1.7	4.4	-0.2	-6.2	10.6
F I	18100 - 18097	0.0	0.3	-2.6	-0.2	-4.0	-0.2	3.1	0.0	-5.5	8.6
G I	18094 - 18091	0.0	0.1	-2.1	-0.3	-2.4	-0.2	1.7	0.0	-3.7	5.4
H O	18330 - 18327	-1.0	-0.5	-1.8	0.3	-3.9	0.0	2.8	-1.0	-5.1	7.9
I O	18244 - 18241	0.0	0.1	-1.4	0.0	-1.6	0.0	1.2	0.0	-2.4	3.6
J I	18550 - 18547	-0.1	1.6	-1.2	0.0	-2.7	0.0	3.2	-0.1	-2.8	6.0
K I	18344 - 18341	0.0	-0.1	-1.4	0.0	-1.3	0.0	0.7	0.0	-2.2	2.9
L I	18740 - 18737	0.0	1.8	-1.6	0.1	-1.1	0.0	2.2	0.0	-1.9	4.1
M I	18454 - 18451	0.0	0.1	-1.2	0.0	-1.0	0.0	0.6	0.0	-1.7	2.4
N I	18810 - 18807	0.0	1.5	-0.9	0.0	0.3	0.0	1.5	0.0	-1.0	2.5
O I	18524 - 18521	0.0	0.1	-1.0	0.0	-0.7	0.0	0.4	0.0	-1.3	1.7
P O	18850 - 18847	0.0	0.3	-0.4	0.1	1.1	0.0	1.1	0.0	-1.2	2.3
Q I	18564 - 18561	0.0	0.2	-0.8	0.0	-0.5	0.0	0.4	0.0	-1.0	1.4
R I	18890 - 18887	0.1	0.7	-0.8	0.3	0.8	0.0	1.1	0.1	-1.1	2.2
S I	18604 - 18601	0.0	0.3	-1.0	0.2	-0.2	0.1	0.4	-0.1	-1.0	1.4
T I	18614 - 18611	0.0	0.2	-0.4	0.0	0.0	0.1	0.2	0.0	-0.4	0.6
U I	18900 - 18910	-0.2	0.4	0.0	-0.1	0.3	0.0	0.5	-0.2	-0.2	0.7
V O	18920 - 18930	0.1	-0.4	-0.1	0.0	0.1	0.0	0.1	-0.1	-0.5	0.6
W I	1216 - 1226	0.3	0.7	-0.3	0.0	0.0	0.0	0.7	0.3	-0.3	0.9
X O	1236 - 1246	-0.4	-0.7	0.3	0.0	0.0	0.0	0.3	-0.4	-0.7	0.9

<sup>1</sup> Refer to Figure 2.10.2-34 for the identification of the representative sections.

Table 2.10.4-110  $P_m$  Stresses; 1-Foot Bottom Corner Drop; Drop Orientation = 24 Degrees;  
3-D Bottom Model; 180-Degree Circumferential Location; Condition 1

Condition 1: 100°F Ambient with Contents

Section <sup>1</sup>	Node - Node	Stress Components (ksi)						Principal Stresses (ksi)			
		$S_x$	$S_y$	$S_z$	$S_w$	$S_{xz}$	$S_{yz}$	S1	S2	S3	S.I.
A	1130 - 1128	0.9	0.0	-0.5	0.0	0.7	0.7	1.2	0.3	-1.2	2.4
B	1185 - 1183	-1.4	-2.8	-0.7	0.0	0.7	0.8	-0.1	-1.8	-3.0	3.0
C	30090 - 30040	0.4	1.0	0.4	0.1	-0.1	0.4	1.0	0.8	0.0	1.0
D	30025 - 30005	-0.6	1.0	-1.0	0.1	-0.1	0.1	1.0	-0.5	-1.1	2.1
E	30035 - 30031	0.6	1.2	0.0	0.1	-0.1	-0.6	1.3	0.9	-0.4	1.7
F	30100 - 30097	0.2	0.6	1.8	0.0	-0.3	-0.1	1.8	0.5	0.1	1.7
G	30094 - 30091	0.1	0.2	0.9	0.0	-0.2	0.0	0.9	0.1	0.1	0.8
H	30330 - 30327	-0.5	-0.6	1.7	0.0	-0.3	0.0	1.7	-0.5	-0.6	2.3
I	30244 - 30241	0.0	-0.3	0.6	0.0	-0.2	0.0	0.6	0.0	-0.3	0.9
J	30550 - 30547	-0.1	0.0	0.7	0.0	-0.2	0.0	0.7	0.0	-0.1	0.9
K	30344 - 30341	0.0	-0.1	0.2	0.0	-0.1	0.0	0.2	0.0	-0.2	0.4
L	30740 - 30737	-0.1	0.2	-0.4	0.1	-0.1	0.0	0.2	-0.1	-0.4	0.6
M	30454 - 30451	0.0	-0.1	-0.3	0.0	-0.1	0.0	0.0	-0.1	-0.3	0.3
N	30810 - 30807	-0.1	0.1	-0.8	0.0	-0.1	0.0	0.1	-0.1	-0.8	0.9
O	30524 - 30521	0.0	-0.1	-0.6	0.0	-0.1	0.0	0.0	-0.1	-0.6	0.6
P	30850 - 30847	0.0	0.0	-0.7	0.0	0.0	0.0	0.0	0.0	-0.7	0.7
Q	30564 - 30561	0.0	-0.1	-0.6	0.0	-0.1	0.0	0.0	-0.1	-0.7	0.7
R	30890 - 30887	0.0	0.0	-0.3	0.0	0.0	0.0	0.1	0.0	-0.3	0.3
S	30604 - 30601	0.0	0.0	-0.5	0.0	0.0	0.0	0.0	0.0	-0.5	0.5
T	30614 - 30611	0.0	0.0	-0.4	0.0	0.0	0.1	0.0	0.0	-0.4	0.4
U	30900 - 30910	0.1	0.1	-0.1	0.0	0.0	0.1	0.2	0.1	-0.1	0.3
V	30920 - 30930	-0.1	0.1	-0.1	0.0	0.0	0.1	0.1	0.0	-0.2	0.3
W	1216 - 1226	0.1	0.3	-0.1	0.0	0.0	0.0	0.3	0.1	-0.1	0.4
X	1236 - 1246	-0.2	-0.3	0.1	0.0	0.0	0.0	0.1	-0.2	-0.3	0.4

<sup>1</sup> Refer to Figure 2.10.2-34 for the identification of the representative sections.

Table 2.10.4-111  $P_m + P_b$  Stresses; 1-Foot Bottom Corner Drop; Drop Orientation = 24 Degrees; 3-D Bottom Model; 180-Degree Circumferential Location; Condition 1

Condition 1: 100°F Ambient with Contents

Section <sup>1</sup>	Node - Node	Stress Components (ksi)						Principal Stresses (ksi)			
		$S_x$	$S_y$	$S_z$	$S_{xy}$	$S_{yz}$	$S_{xz}$	S1	S2	S3	S.L
A I	1130 - 1128	6.1	4.5	-2.3	-0.2	0.7	0.7	6.1	4.6	-2.4	8.5
B O	1185 - 1183	-6.1	-6.7	0.9	0.1	0.6	0.8	1.0	-6.2	-6.7	7.7
C I	30090 - 30040	-1.8	-0.1	1.0	0.0	-0.2	0.5	1.2	-0.2	-1.9	3.1
D I	30025 - 30005	-3.3	-0.1	-2.0	0.2	-0.1	-0.3	-0.1	-2.0	-3.4	3.3
E I	30035 - 30031	1.5	1.1	-1.4	0.1	-0.1	-0.8	1.7	1.1	-1.6	3.3
F I	30100 - 30097	0.1	0.6	1.9	0.0	-0.4	0.1	2.0	0.5	0.1	2.0
G I	30094 - 30091	0.2	0.6	2.2	0.0	-0.3	0.2	2.3	0.6	0.2	2.1
H I	30330 - 30327	0.0	-0.1	2.8	0.0	-0.3	0.0	2.8	0.0	-0.1	2.9
I O	30244 - 30241	0.0	-0.4	0.5	-0.1	-0.1	0.0	0.5	0.0	-0.4	0.9
J O	30550 - 30547	-0.1	0.0	0.7	0.0	-0.2	0.0	0.8	0.0	-0.1	0.9
K O	30344 - 30341	0.0	-0.2	0.1	0.0	-0.1	0.0	0.2	0.0	-0.3	0.5
L O	30740 - 30737	0.0	0.3	-0.3	0.3	-0.1	0.0	0.5	-0.1	-0.3	0.8
M I	30454 - 30451	0.0	-0.1	-0.3	0.0	-0.1	0.0	0.0	-0.1	-0.3	0.3
N O	30810 - 30807	0.0	0.2	-0.8	0.0	0.0	0.0	0.2	-0.1	-0.8	1.0
O I	30524 - 30521	0.0	-0.2	-0.6	0.0	-0.1	0.0	0.0	-0.2	-0.6	0.6
P O	30850 - 30847	0.0	0.0	-0.8	0.0	0.0	0.0	0.0	0.0	-0.8	0.8
Q O	30564 - 30561	0.0	-0.1	-0.6	0.0	0.0	0.0	0.0	-0.1	-0.7	0.7
R I	30890 - 30887	0.0	0.0	-0.3	0.0	0.0	0.0	0.0	0.0	-0.3	0.4
S O	30604 - 30601	0.0	-0.1	-0.6	0.0	0.0	0.0	0.0	-0.1	-0.6	0.5
T O	30614 - 30611	0.0	0.0	-0.4	0.0	0.0	0.1	0.0	0.0	-0.4	0.5
U O	30900 - 30910	0.4	0.2	0.0	0.0	0.0	0.1	0.4	0.2	-0.1	0.5
V I	30920 - 30930	-0.4	-0.1	-0.1	0.0	0.0	0.2	0.0	-0.1	-0.5	0.5
W I	1216 - 1226	0.3	0.7	-0.3	0.0	0.0	0.0	0.7	0.3	-0.3	0.9
X O	1236 - 1246	-0.4	-0.7	0.3	0.0	0.0	0.0	0.3	-0.4	-0.7	0.9

<sup>1</sup> Refer to Figure 2.10.2-34 for the identification of the representative sections.

Table 2.10.4-112 Primary Stresses; 30-Foot Top End Drop; Drop Orientation = 0 Degrees;  
2-D Model; Condition 1

Condition 1: 100°F Ambient with Contents

Stress Points		Stress Components (ksi)						Principal Stresses (ksi)		
Section <sup>1</sup>	Node	S <sub>x</sub>	S <sub>y</sub>	S <sub>z</sub>	S <sub>xy</sub>	S <sub>xz</sub>	S <sub>yz</sub>	S1	S2	S3
A1	1	3.7	-0.1	3.7	0.0	0.0	0.0	3.7	3.7	-0.1
A2	2	2.1	0.0	2.1	0.0	0.0	0.0	2.1	2.1	0.0
A3	3	0.5	0.0	0.5	0.0	0.0	0.0	0.5	0.5	0.0
A4	4	-1.1	0.0	-1.1	0.0	0.0	0.0	0.0	-1.1	-1.1
A5	5	-2.7	0.0	-2.7	0.0	0.0	0.0	0.0	-2.7	-2.7
B1	6	2.3	0.0	2.3	0.0	0.0	0.0	2.3	2.3	0.0
B2	7	0.8	0.0	0.8	0.0	0.0	0.0	0.8	0.8	0.0
B3	8	-0.6	0.0	-0.6	0.0	0.0	0.0	0.0	-0.6	-0.6
B4	9	-2.0	0.0	-2.0	0.0	0.0	0.0	0.0	-2.0	-2.0
B5	10	-3.5	0.0	-3.5	0.0	0.0	0.0	0.0	-3.5	-3.5
C1	251	-2.1	-2.4	-0.1	-0.5	0.0	0.0	-0.1	-1.7	-2.7
C2	252	-0.4	-1.0	0.4	-0.4	0.0	0.0	0.4	-0.2	-1.2
C3	253	0.6	-0.5	0.4	-0.4	0.0	0.0	0.7	0.4	-0.6
C4	254	1.6	-0.2	0.4	-0.3	0.0	0.0	1.7	0.4	-0.3
C5	255	2.8	-0.1	0.3	-0.2	0.0	0.0	2.8	0.3	-0.2
D1	306	-2.9	-1.7	-1.2	-0.8	0.0	0.0	-1.2	-1.3	-3.3
D2	307	-0.9	-1.3	-0.8	-0.3	0.0	0.0	-0.7	-0.8	-1.4
D3	308	-0.2	-0.5	-0.6	0.1	0.0	0.0	-0.2	-0.5	-0.6
D4	309	0.4	-0.2	-0.6	0.1	0.0	0.0	0.4	-0.2	-0.6
D5	310	1.1	-0.1	-0.6	0.1	0.0	0.0	1.1	-0.1	-0.6
E1	305	2.7	0.1	0.7	-0.6	0.0	0.0	2.9	0.7	-0.1
E2	315	1.4	-0.7	0.2	-0.7	0.0	0.0	1.6	0.2	-0.9
E3	325	0.6	-0.6	0.1	-0.7	0.0	0.0	0.9	0.1	-0.9
E4	335	0.3	-0.5	0.0	-0.5	0.0	0.0	0.6	0.0	-0.8
E5	345	0.1	-0.5	-0.1	-0.3	0.0	0.0	0.2	-0.1	-0.7
E6	355	0.1	-0.7	-0.1	-0.2	0.0	0.0	0.1	-0.1	-0.7
F1	251	-2.1	-2.4	-0.1	-0.5	0.0	0.0	-0.1	-1.7	-2.7
F2	261	-1.7	-1.5	0.2	-0.2	0.0	0.0	0.2	-1.4	-1.8
F3	271	-1.4	-0.9	0.4	0.2	0.0	0.0	0.4	-0.9	-1.5
F4	281	-1.6	-0.7	0.4	0.3	0.0	0.0	0.4	-0.6	-1.7
G1	311	-1.2	-2.1	-0.1	-0.2	0.0	0.0	-0.1	-1.2	-2.1

Table 2.10.4-112 Primary Stresses; 30-Foot Top End Drop; Drop Orientation = 0 Degrees;  
2-D Model; Condition 1 (continued)

Stress Points Section <sup>1</sup> Node	Stress Components (ksi)						Principal Stresses (ksi)		
	S <sub>x</sub>	S <sub>y</sub>	S <sub>z</sub>	S <sub>xy</sub>	S <sub>yz</sub>	S <sub>xz</sub>	S1	S2	S3
G2	321	-0.8	-1.3	0.2	0.0	0.0	0.2	-0.8	-1.3
G3	331	-0.4	-0.8	0.4	0.1	0.0	0.4	-0.4	-0.8
G4	341	-0.2	-0.2	0.6	0.1	0.0	0.6	-0.1	-0.3
G5	351	-0.1	0.5	0.8	0.1	0.0	0.8	0.5	-0.1
H1	581	-0.1	-2.2	1.1	0.0	0.0	1.1	-0.1	-2.2
H2	582	-0.1	-2.6	1.0	0.0	0.0	1.0	-0.1	-2.6
H3	583	-0.1	-2.9	0.9	0.1	0.0	0.9	-0.1	-2.9
H4	584	0.0	-3.5	0.7	0.2	0.0	0.7	0.0	-3.6
I1	589	0.0	-1.1	0.2	0.0	0.0	0.2	0.0	-1.1
I2	590	0.0	-1.2	0.2	0.0	0.0	0.2	0.0	-1.2
I3	591	0.0	-1.3	0.1	0.0	0.0	0.1	0.0	-1.3
I4	592	0.0	-1.4	0.1	0.0	0.0	0.1	0.0	-1.4
I5	593	0.0	-1.5	0.1	0.0	0.0	0.1	0.0	-1.5
J1	971	-0.1	-3.5	1.2	0.0	0.0	1.2	-0.1	-3.5
J2	972	0.0	-3.5	1.2	0.0	0.0	1.2	0.0	-3.5
J3	973	0.0	-3.5	1.2	0.0	0.0	1.2	0.0	-3.5
J4	974	0.0	-3.5	1.2	0.0	0.0	1.2	0.0	-3.5
K1	979	0.0	-1.9	0.0	0.0	0.0	0.0	0.0	-1.9
K2	980	0.0	-1.9	0.0	0.0	0.0	0.0	0.0	-1.9
K3	981	0.0	-1.9	0.0	0.0	0.0	0.0	0.0	-1.9
K4	982	0.0	-1.9	0.0	0.0	0.0	0.0	0.0	-1.9
K5	983	0.0	-1.9	0.0	0.0	0.0	0.0	0.0	-1.9
L1	1601	-0.1	-4.5	1.2	0.0	0.0	1.2	-0.1	-4.5
L2	1602	0.0	-4.5	1.2	0.0	0.0	1.2	0.0	-4.5
L3	1603	0.0	-4.5	1.2	0.0	0.0	1.2	0.0	-4.5
L4	1604	0.0	-4.5	1.2	0.0	0.0	1.2	0.0	-4.5
M1	1609	0.0	-2.9	0.0	0.0	0.0	0.0	0.0	-2.9
M2	1610	0.0	-2.9	0.0	0.0	0.0	0.0	0.0	-2.9
M3	1611	0.0	-2.9	0.0	0.0	0.0	0.0	0.0	-2.9
M4	1612	0.0	-2.9	0.0	0.0	0.0	0.0	0.0	-2.9
M5	1613	0.0	-2.9	0.0	0.0	0.0	0.0	0.0	-2.9
N1	2216	-0.1	-5.6	1.2	0.0	0.0	1.2	-0.1	-5.6
N2	2217	0.0	-5.5	1.2	0.0	0.0	1.2	0.0	-5.5



Table 2.10.4-112 Primary Stresses; 30-Foot Top End Drop; Drop Orientation = 0 Degrees;  
2-D Model; Condition 1 (continued)

Stress Points		Stress Components (ksi)						Principal Stresses (ksi)		
Section <sup>1</sup>	Node	S <sub>x</sub>	S <sub>y</sub>	S <sub>z</sub>	S <sub>xy</sub>	S <sub>yz</sub>	S <sub>xz</sub>	S1	S2	S3
N3	2218	0.0	-5.5	1.2	0.0	0.0	0.0	1.2	0.0	-5.5
N4	2219	0.0	-5.5	1.2	0.0	0.0	0.0	1.2	0.0	-5.5
O1	2224	0.0	-3.8	-0.1	0.0	0.0	0.0	0.0	-0.1	-3.8
O2	2225	0.0	-3.8	-0.1	0.0	0.0	0.0	0.0	-0.1	-3.8
O3	2226	0.0	-3.8	-0.1	0.0	0.0	0.0	0.0	-0.1	-3.8
O4	2227	0.0	-3.8	-0.1	0.0	0.0	0.0	0.0	-0.1	-3.8
O5	2228	0.0	-3.8	-0.1	0.0	0.0	0.0	0.0	-0.1	-3.8
P1	2546	-0.1	-3.3	1.8	0.0	0.0	0.0	1.8	-0.1	-3.3
P2	2547	-0.2	-4.9	1.3	0.0	0.0	0.0	1.3	-0.2	-4.9
P3	2548	-0.1	-6.6	0.9	-0.2	0.0	0.0	0.9	-0.1	-6.6
P4	2549	-0.1	-8.8	0.2	-0.5	0.0	0.0	0.2	-0.1	-8.9
Q1	2554	0.0	-3.4	1.3	0.0	0.0	0.0	1.3	0.0	-3.4
Q2	2555	0.0	-3.9	1.1	0.0	0.0	0.0	1.1	0.0	-3.9
Q3	2556	0.0	-4.4	1.0	0.1	0.0	0.0	1.0	0.0	-4.4
Q4	2557	0.0	-4.8	0.8	0.0	0.0	0.0	0.8	0.0	-4.8
Q5	2558	0.0	-5.3	0.7	0.0	0.0	0.0	0.7	0.0	-5.3
R1	2771	-0.1	-18.1	-0.6	0.0	0.0	0.0	-0.1	-0.6	-18.1
R2	2772	0.3	-10.6	1.6	0.3	0.0	0.0	1.6	0.4	-10.6
R3	2773	1.1	-3.5	3.7	1.4	0.0	0.0	3.7	1.5	-3.9
R4	2774	0.3	5.4	5.8	3.1	0.0	0.0	6.8	5.8	-1.1
S1	2779	-9.6	-12.6	-2.7	0.7	0.0	0.0	-2.7	-9.4	-12.7
S2	2780	-6.0	-7.5	-0.4	-0.3	0.0	0.0	-0.4	-5.9	-7.6
S3	2781	-3.1	-3.9	1.2	-1.1	0.0	0.0	1.2	-2.3	-4.7
S4	2782	-1.2	-0.3	2.7	-0.9	0.0	0.0	2.7	0.3	-1.8
S5	2783	-0.5	4.4	4.1	-0.6	0.0	0.0	4.4	4.1	-0.6
T1	7066	11.2	8.9	4.8	2.8	0.0	0.0	13.1	7.0	4.8
T2	7067	7.8	2.2	2.1	0.9	0.0	0.0	7.9	2.1	2.1
T3	7068	5.2	-1.1	0.6	-0.2	0.0	0.0	5.2	0.6	-1.1
T4	7069	3.1	-3.2	-0.5	-0.9	0.0	0.0	3.2	-0.5	-3.3
T5	7070	1.6	-5.1	-1.3	-1.0	0.0	0.0	1.8	-1.3	-5.3
T6	7071	0.7	-7.3	-2.1	-0.7	0.0	0.0	0.8	-2.1	-7.3
T7	7072	0.4	-10.3	-3.0	-0.4	0.0	0.0	0.4	-3.0	-10.3
U1	3051	-1.7	-10.7	5.7	2.2	0.0	0.0	5.7	-1.2	-11.2

Table 2.10.4-112 Primary Stresses; 30-Foot Top End Drop; Drop Orientation = 0 Degrees;  
2-D Model; Condition 1 (continued)

Stress Points Section <sup>1</sup>	Node	Stress Components (ksi)						Principal Stresses (ksi)		
		S <sub>x</sub>	S <sub>y</sub>	S <sub>z</sub>	S <sub>xy</sub>	S <sub>yz</sub>	S <sub>xz</sub>	S1	S2	S3
U2	3052	1.7	-10.3	3.8	2.6	0.0	0.0	3.8	2.2	-10.9
U3	3053	2.4	-9.2	1.7	2.6	0.0	0.0	2.9	1.7	-9.8
U4	3054	2.2	-8.7	-0.8	1.9	0.0	0.0	2.5	-0.8	-9.0
U5	3055	1.6	-9.4	-3.6	2.1	0.0	0.0	2.0	-3.6	-9.8
U6	3056	-0.6	-6.6	-5.7	3.9	0.0	0.0	1.3	-5.7	-8.6
V1	3611	-7.3	-4.7	5.5	-1.4	0.0	0.0	5.5	-4.1	-8.0
V2	3612	-4.3	-4.6	3.8	-1.8	0.0	0.0	3.8	-2.7	-6.3
V3	3613	-2.1	-4.3	1.8	-2.2	0.0	0.0	1.8	-0.7	-5.7
V4	3614	-0.2	-4.1	-0.4	-2.1	0.0	0.0	0.7	-0.4	-5.0
V5	3615	1.4	-3.7	-2.6	-1.7	0.0	0.0	2.0	-2.6	-4.3
V6	3616	1.4	-2.5	-5.1	-1.1	0.0	0.0	1.6	-2.7	-5.1
V7	3617	5.6	-1.5	-6.4	-0.6	0.0	0.0	5.6	-1.5	-6.4
W1	3241	20.7	-1.1	20.7	0.0	0.0	0.0	20.7	20.7	-1.1
W2	3242	13.4	-1.3	13.4	0.0	0.0	0.0	13.4	13.4	-1.3
W3	3243	6.2	-1.8	6.2	0.0	0.0	0.0	6.2	6.2	-1.8
W4	3244	-0.7	-2.3	-0.7	0.0	0.0	0.0	-0.7	-0.7	-2.3
W5	3245	-7.9	-2.8	-7.9	0.0	0.0	0.0	-2.8	-7.9	-7.9
W6	3246	-15.5	-3.0	-15.5	0.0	0.0	0.0	-3.0	-15.5	-15.5
X1	3801	26.5	-3.5	26.5	0.0	0.0	0.0	26.5	26.5	-3.5
X2	3802	18.4	-3.3	18.4	0.0	0.0	0.0	18.4	18.4	-3.3
X3	3803	9.5	-3.1	9.5	0.0	0.0	0.0	9.5	9.5	-3.1
X4	3804	0.5	-2.9	0.5	0.0	0.0	0.0	0.5	0.5	-2.9
X5	3805	-8.6	-2.6	-8.6	0.0	0.0	0.0	-2.6	-8.6	-8.6
X6	3806	-17.5	-2.2	-17.5	0.0	0.0	0.0	-2.2	-17.5	-17.5
X7	3807	-27.0	-1.8	-27.0	0.0	0.0	0.0	-1.8	-27.0	-27.0

<sup>1</sup> Refer to Figure 2.10.2-34 for the identification of the representative sections.

Table 2.10.4-113  $P_m$  Stresses; 30-Foot Top End Drop; Drop Orientation = 0 Degrees; 2-D Model; Condition 1

Condition 1: 100°F Ambient with Contents

Section <sup>1</sup>	Node - Node	Stress Components (ksi)						Principal Stresses (ksi)			
		$S_x$	$S_y$	$S_z$	$S_w$	$S_{yz}$	$S_{xz}$	S1	S2	S3	S.I.
A	1 - 5	0.5	0.0	0.5	0.0	0.0	0.0	0.5	0.5	0.0	0.5
B	6 - 10	-0.6	0.0	-0.6	0.0	0.0	0.0	0.0	-0.6	-0.6	0.6
C	251 - 255	0.5	-0.7	0.3	-0.3	0.0	0.0	0.6	0.3	-0.8	1.5
D	306 - 310	-0.4	-0.7	-0.7	-0.1	0.0	0.0	-0.4	-0.7	-0.8	0.4
E	305 - 355	1.0	-0.5	0.2	-0.5	0.0	0.0	1.1	0.2	-0.7	1.8
F	251 - 281	-1.6	-1.3	0.2	0.0	0.0	0.0	0.2	-1.3	-1.6	1.9
G	311 - 351	-0.5	-0.8	0.4	0.0	0.0	0.0	0.4	-0.5	-0.8	1.2
H	581 - 584	-0.1	-2.8	0.9	0.1	0.0	0.0	0.9	-0.1	-2.8	3.7
I	589 - 593	0.0	-1.3	0.2	0.0	0.0	0.0	0.2	0.0	-1.3	1.4
J	971 - 974	0.0	-3.5	1.2	0.0	0.0	0.0	1.2	0.0	-3.5	4.7
K	979 - 983	0.0	-1.9	0.0	0.0	0.0	0.0	0.0	0.0	-1.9	1.9
L	1601 - 1604	0.0	-4.5	1.2	0.0	0.0	0.0	1.2	0.0	-4.5	5.7
M	1609 - 1613	0.0	-2.9	0.0	0.0	0.0	0.0	0.0	0.0	-2.9	2.9
N	2216 - 2219	0.0	-5.5	1.2	0.0	0.0	0.0	1.2	0.0	-5.5	6.7
O	2224 - 2228	0.0	-3.8	-0.1	0.0	0.0	0.0	0.0	-0.1	-3.8	3.8
P	2546 - 2549	-0.1	-5.9	1.1	-0.2	0.0	0.0	1.1	-0.1	-5.9	6.9
Q	2554 - 2558	0.0	-4.4	1.0	0.0	0.0	0.0	1.0	0.0	-4.4	5.4
R	2771 - 2774	0.5	-6.7	2.7	1.1	0.0	0.0	2.7	0.7	-6.9	9.5
S	2779 - 2783	-3.8	-3.9	1.0	-0.6	0.0	0.0	1.0	-3.3	-4.4	5.5
T	7066 - 7072	4.1	-2.5	0.0	-0.1	0.0	0.0	4.1	0.0	-2.5	6.7
U	3051 - 3056	1.4	-9.5	0.1	2.4	0.0	0.0	1.9	0.1	-10.0	11.9
V	3611 - 3617	-0.6	-3.7	-0.7	-1.6	0.0	0.0	0.1	-0.7	-4.4	4.5
W	3241 - 3246	2.7	-2.1	2.7	0.0	0.0	0.0	2.7	2.7	-2.1	4.8
X	3801 - 3807	-0.2	-2.8	-0.2	0.0	0.0	0.0	-0.2	-0.2	-2.8	2.6

<sup>1</sup> Refer to Figure 2.10.2-34 for the identification of the representative sections.

Table 2.10.4-114  $P_m + P_b$  Stresses; 30-Foot Top End Drop; Drop Orientation = 0 Degrees;  
2-D Model; Condition 1

Condition 1: 100°F Ambient with Contents

Section <sup>1</sup>	Node - Node	Stress Components (ksi)						Principal Stresses (ksi)			
		$S_x$	$S_y$	$S_z$	$S_{xy}$	$S_{yz}$	$S_{xz}$	S1	S2	S3	S.I.
A I	1 - 5	3.7	-0.1	3.7	0.0	0.0	0.0	3.7	3.7	-0.1	3.7
B D	6 - 10	-3.5	0.0	-3.5	0.0	0.0	0.0	0.0	-3.5	-3.5	3.5
C D	251 - 255	2.8	-0.1	0.5	-0.3	0.0	0.0	2.9	0.5	-0.2	3.0
D O	306 - 310	1.3	-0.1	-0.5	-0.1	0.0	0.0	1.3	-0.1	-0.5	1.8
E I	305 - 355	2.7	-0.3	0.6	-0.5	0.0	0.0	2.8	0.6	-0.4	3.2
F I	251 - 281	-2.1	-2.2	0.0	0.0	0.0	0.0	0.0	-2.1	-2.2	2.2
G I	311 - 331	-1.2	-2.0	-0.1	0.0	0.0	0.0	-0.1	-1.2	-2.0	1.9
H O	581 - 584	0.0	-3.4	0.7	0.1	0.0	0.0	0.7	0.0	-3.4	4.2
I O	589 - 593	0.0	-1.5	0.1	0.0	0.0	0.0	0.1	0.0	-1.5	1.6
J I	971 - 974	-0.1	-3.5	1.2	0.0	0.0	0.0	1.2	-0.1	-3.5	4.7
K I	979 - 983	0.0	-1.9	0.0	0.0	0.0	0.0	0.0	0.0	-1.9	1.9
L I	1601 - 1604	-0.1	-4.5	1.2	0.0	0.0	0.0	1.2	-0.1	-4.5	5.7
M O	1609 - 1613	0.0	-2.9	0.0	0.0	0.0	0.0	0.0	0.0	-2.9	2.9
N I	2216 - 2219	-0.1	-5.6	1.2	0.0	0.0	0.0	1.2	-0.1	-5.6	6.8
O I	2224 - 2228	0.0	-3.8	-0.1	0.0	0.0	0.0	0.0	-0.1	-3.8	3.8
P O	2546 - 2549	-0.1	-8.6	0.3	-0.2	0.0	0.0	0.3	-0.1	-8.6	8.8
Q O	2554 - 2558	0.0	-5.3	0.7	0.0	0.0	0.0	0.7	0.0	-5.3	6.0
R I	2771 - 2774	-0.1	-18.3	-0.5	1.1	0.0	0.0	0.0	-0.5	-18.4	18.4
S I	2779 - 2783	-9.6	-12.0	-2.3	-0.6	0.0	0.0	-2.3	-9.4	-12.1	9.8
T O	7066 - 7072	0.4	-10.5	-3.5	-0.1	0.0	0.0	0.4	-3.5	-10.6	10.9
U I	3051 - 3056	1.3	-31.4	5.5	2.4	0.0	0.0	5.5	1.5	-31.6	37.1
V I	3611 - 3617	-5.7	-3.5	5.2	-1.6	0.0	0.0	5.2	-2.7	-6.6	11.8
W I	3241 - 3246	20.6	-1.1	20.6	0.0	0.0	0.0	20.6	20.6	-1.1	21.7
X I	3801 - 3807	26.7	-3.5	26.7	0.0	0.0	0.0	26.7	26.7	-3.5	30.2

<sup>1</sup> Refer to Figure 2.10.2-34 for the identification of the representative sections.

Table 2.10.4-115 Critical  $P_m$  Stress Summary; 30-Foot Top End Drop; Drop Orientation = 0 Degrees; 2-D Model; Condition 1

Condition 1: 100°F Ambient with Contents

Comp. No. <sup>1</sup>	Section Cut Node-Node	P <sub>m</sub> Stresses (ksi)							Principal Stresses (ksi)			Allow. S.L. Stress	Margin of Safety	
		S <sub>x</sub>	S <sub>y</sub>	S <sub>z</sub>	S <sub>xy</sub>	S <sub>xz</sub>	S <sub>yz</sub>	S <sub>m</sub>	S1	S2	S3			
1	246- 250	-0.6	0.0	-0.6	-0.2	0.0	0.0	0.0	0.0	-0.6	-0.7	0.7	45.6	64.1
2	386- 389	0.0	-1.9	0.9	-0.1	0.0	0.0	0.0	0.9	0.0	-1.9	2.7	44.9	15.6
3	2711- 2714	0.0	-4.7	4.9	0.6	0.0	0.0	0.0	4.9	0.1	-4.8	9.7	66.0	5.8
4	2276- 2279	0.0	-5.6	1.2	0.0	0.0	0.0	0.0	1.2	0.0	-5.6	6.8	45.8	5.7
5	2599- 2603	-4.4	0.0	1.6	-0.1	0.0	0.0	0.0	1.6	0.0	-4.4	6.1	46.4	6.6
6	2726- 2729	-0.1	-4.8	4.8	0.7	0.0	0.0	0.0	4.8	0.0	-4.9	9.7	49.3	4.1
7	3117- 3118	-13.1	1.1	-12.6	-3.7	0.0	0.0	0.0	2.0	-12.6	-14.0	16.0	48.0	2.0
8	3661- 3667	-0.4	-6.7	-1.6	2.5	0.0	0.0	0.0	0.5	-1.6	-7.6	8.1	94.5	10.7

Locations of the most critical sections for each component are provided in the following:

Comp. No. <sup>1</sup>	Section Location			
	Inside Node		Outside Node	
	x (in)	y (in)	z (in)	x (in)
1	34.08	6.20	34.08	0.75
2	35.50	16.40	37.50	16.40
3	35.50	171.40	37.50	171.40
4	35.50	142.20	37.00	142.40
5	40.70	163.40	43.35	163.40
6	35.50	172.40	37.50	172.40
7	24.289	187.40	24.289	188.40
8	26.158	188.40	26.158	193.71

<sup>1</sup> Refer to Figure 2.10.2-33 for cask component identification.

Table 2.10.4-116 Critical  $P_m + P_b$  Stress Summary; 30-Foot Top End Drop; Drop Orientation = 0 Degrees; 2-D Model; Condition 1

Condition 1: 100°F Ambient with Contents

Comp. No. <sup>1</sup>	Section Cut Node-Node	P <sub>m</sub> + P <sub>b</sub> Stresses (ksi)							Principal Stresses (ksi)			Allow. Stress	Margin of Safety
		S <sub>x</sub>	S <sub>y</sub>	S <sub>z</sub>	S <sub>xy</sub>	S <sub>yz</sub>	S <sub>xz</sub>	S1	S2	S3			
1	16- 20	-3.5	0.0	-3.5	0.0	0.0	0.0	0.0	-3.5	-3.5	3.5	65.2	17.6
2	1- 5	3.7	-0.1	3.7	0.0	0.0	0.0	3.7	3.7	-0.1	3.7	64.2	16.4
3	2711- 2714	-0.1	-11.3	3.3	0.6	0.0	0.0	3.3	0.0	-11.4	14.6	94.3	5.5
4	2276- 2279	-0.1	-5.7	1.2	0.0	0.0	0.0	1.2	-0.1	-5.7	6.9	65.5	8.5
5	2599- 2603	-4.8	0.0	1.5	-0.1	0.0	0.0	1.5	0.0	-4.8	6.2	66.4	9.7
6	2756- 2759	-18.5	0.3	0.5	-0.9	0.0	0.0	0.5	0.4	-18.5	19.0	70.9	2.7
7	3051- 3056	1.3	-31.4	5.5	2.4	0.0	0.0	5.5	1.5	-31.6	37.1	69.8	0.9
8	3761- 3767	28.5	-2.4	27.9	-0.4	0.0	0.0	28.5	27.9	-2.4	30.9	135.0	3.4

Locations of the most critical sections for each component are provided in the following:

Comp. No. <sup>1</sup>	Section Location			
	Inside Node		Outside Node	
	x (in)	y (in)	z (in)	x (in)
1	1.42	6.20	1.42	0.75
2	0.00	14.40	0.00	8.20
3	35.50	171.40	37.50	171.40
4	35.50	142.40	37.00	142.40
5	40.70	163.40	43.35	163.40
6	35.50	174.40	37.50	174.40
7	35.50	179.40	35.50	185.40
8	7.4737	188.46	7.4737	193.71

<sup>1</sup> Refer to Figure 2.10.2-33 for cask component identification.

Table 2.10.4-117 Critical P<sub>m</sub> Stress Summary; 30-Foot Top End Drop; Drop Orientation = 0 Degrees; 2-D Model; Condition 2

Condition 2: -20°F Ambient with Contents

Comp. No. <sup>1</sup>	Section Cut Node-Node	P <sub>m</sub> Stresses (ksi)							Principal Stresses (ksi)			Allow. S.I. Stress	Margin of Safety
		S <sub>x</sub>	S <sub>y</sub>	S <sub>z</sub>	S <sub>xy</sub>	S <sub>xz</sub>	S <sub>yz</sub>	S1	S2	S3			
1	206- 210	-0.7	0.0	-0.7	-0.2	0.0	0.0	0.1	-0.7	-0.8	0.8	45.6	56.0
2	386- 389	0.0	-2.1	0.8	-0.2	0.0	0.0	0.8	0.0	-2.1	2.9	44.9	14.5
3	2711- 2714	0.0	-5.0	4.6	0.7	0.0	0.0	4.6	0.1	-5.1	9.6	66.0	5.9
4	2276- 2279	0.0	-5.9	0.3	0.0	0.0	0.0	0.3	0.0	-5.9	6.2	45.8	6.4
5	2599- 2603	-4.5	0.0	1.6	-0.1	0.0	0.0	1.6	0.0	-4.5	6.1	46.4	6.6
6	2771- 2774	-7.0	0.7	2.5	-1.2	0.0	0.0	2.5	0.8	-7.2	9.7	49.3	4.1
7	3117- 3118	-13.5	1.1	-13.0	-3.7	0.0	0.0	2.0	-13.0	-14.4	16.4	48.0	1.9
8	3661- 3667	-0.4	-6.7	-1.7	2.6	0.0	0.0	0.5	-1.7	-7.6	8.1	94.5	10.7

Locations of the most critical sections for each component are provided in the following:

Comp. No. <sup>1</sup>	Section Location			
	Inside Node		Outside Node	
	x (in)	y (in)	z (in)	x (in)
1	28.40	6.20	28.40	0.75
2	35.50	16.40	37.50	16.40
3	35.50	171.40	37.50	171.40
4	35.50	142.40	37.00	142.40
5	40.70	163.40	43.35	163.40
6	35.50	175.40	37.50	175.40
7	24.289	187.40	24.289	188.40
8	26.158	188.40	26.158	193.71

<sup>1</sup> Refer to Figure 2.10.2-33 for cask component identification.

Table 2.10.4-118 Critical  $P_m + P_b$  Stress Summary; 30-Foot Top End Drop; Drop Orientation = 0 Degrees; 2-D Model; Condition 2

Condition 2: -20°F Ambient with Contents

Comp. No. <sup>1</sup>	Section Cut Node-Node	P <sub>m</sub> + P <sub>b</sub> Stresses (ksi)							Principal Stresses (ksi)			Allow. S.I. Stress	Margin of Safety	
		S <sub>1</sub>	S <sub>2</sub>	S <sub>3</sub>	S <sub>4</sub>	S <sub>5</sub>	S <sub>6</sub>	S <sub>7</sub>	S1	S2	S3			
1	16- 20	-4.0	0.0	-4.0	0.0	0.0	0.0	0.0	0.0	-4.0	-4.0	4.0	65.2	15.3
2	371- 374	0.3	-4.4	0.2	-0.2	0.0	0.0	0.0	0.3	0.2	-4.4	4.7	64.2	12.7
3	2711- 2714	0.0	-11.7	2.9	0.7	0.0	0.0	0.0	2.9	0.0	-11.8	14.7	94.3	5.4
4	2276- 2279	0.0	-6.1	0.3	0.0	0.0	0.0	0.0	0.3	0.0	-6.1	6.3	63.5	9.4
5	2599- 2603	-4.8	0.0	1.5	-0.1	0.0	0.0	0.0	1.5	0.0	-4.8	6.2	66.4	9.7
6	2756- 2759	-19.3	0.4	0.1	-1.0	0.0	0.0	0.0	0.4	0.1	-19.3	19.8	70.9	2.6
7	3051- 3056	1.2	-32.7	5.6	2.5	0.0	0.0	0.0	5.6	1.4	-32.9	38.5	69.8	0.8
8	3761- 3767	29.4	-2.4	28.8	-0.4	0.0	0.0	0.0	29.4	28.8	-2.4	31.7	135.0	3.3

Locations of the most critical sections for each component are provided in the following:

Comp. No. <sup>1</sup>	Section Location			
	Inside Node		Outside Node	
	x (in)	y (in)	z (in)	x (in)
1	1.42	6.20	1.42	0.75
2	35.50	15.40	37.50	15.40
3	35.50	171.40	37.50	171.40
4	35.50	142.40	37.00	142.40
5	40.70	163.40	43.35	163.40
6	35.50	174.40	37.50	174.40
7	35.50	179.40	35.50	185.40
8	7.4737	188.46	7.4737	193.71

<sup>1</sup> Refer to Figure 2.10.2-33 for cask component identification.



Table 2.10.4-119 Critical P<sub>m</sub> Stress Summary; 30-Foot Top End Drop; Drop Orientation = 0 Degrees; 2-D Model; Condition 3

Condition 3: -20°F Ambient without Contents.

Comp. No. <sup>1</sup>	Section Cut Node-Node	P <sub>m</sub> Stresses (ksi)							Principal Stresses (ksi)			Allow. S.I. Stress	Margin of Safety	
		S <sub>x</sub>	S <sub>y</sub>	S <sub>z</sub>	S <sub>xy</sub>	S <sub>yz</sub>	S <sub>xz</sub>	S <sub>m</sub>	S1	S2	S3			
1	206- 210	-0.5	0.0	-0.5	-0.2	0.0	0.0	0.0	0.0	-0.5	-0.6	0.6	45.6	75.0
2	386- 389	0.0	-1.8	0.6	-0.1	0.0	0.0	0.0	0.6	0.0	-1.8	2.5	44.7	17.0
3	2711- 2714	0.0	-4.2	4.2	0.6	0.0	0.0	0.0	4.2	0.1	-4.2	8.5	66.0	6.8
4	2276- 2279	0.0	-5.0	0.3	0.0	0.0	0.0	0.0	0.3	0.0	-5.0	5.2	45.8	7.8
5	2599- 2603	-3.6	0.0	1.5	-0.1	0.0	0.0	0.0	1.5	0.0	-3.6	5.1	46.4	8.1
6	2771- 2774	-6.1	0.5	2.3	-1.1	0.0	0.0	0.0	2.3	0.7	-6.2	8.5	49.3	4.8
7	3117- 3118	-12.7	0.9	-12.4	-2.8	0.0	0.0	0.0	1.4	-12.4	-13.2	14.6	48.0	2.3
8	3671- 3677	0.0	-0.9	0.0	3.2	0.0	0.0	0.0	2.8	0.0	-3.7	6.5	94.5	13.5

Locations of the most critical sections for each component are provided in the following:

Comp. No. <sup>1</sup>	Section Location			
	Inside Node		Outside Node	
	x (in)	y (in)	z (in)	x (in)
1	28.40	6.20	28.40	0.75
2	35.50	16.40	37.50	16.40
3	35.50	171.40	37.50	171.40
4	35.50	142.40	37.00	142.40
5	40.70	163.40	43.35	163.40
6	35.50	175.40	37.50	175.40
7	24.289	187.40	24.289	188.40
8	24.289	188.46	24.289	193.71

<sup>1</sup> Refer to Figure 2.10.2-33 for cask component identification.

Table 2.10.4-120 Critical  $P_m + P_b$  Stress Summary; 30-Foot Top End Drop; Drop Orientation = 0 Degrees; 2-D Model; Condition 3

Condition 3: -20°F Ambient without Contents

Comp. No. <sup>1</sup>	Section Cut Node-Node	P <sub>m</sub> + P <sub>b</sub> Stresses (ksi)							Principal Stresses (ksi)			Allow. Stress	Margin of Safety
		S <sub>x</sub>	S <sub>y</sub>	S <sub>z</sub>	S <sub>xy</sub>	S <sub>yz</sub>	S <sub>xz</sub>	S1	S2	S3			
1	16- 20	-3.2	0.0	-3.2	0.0	0.0	0.0	0.0	-3.2	-3.2	3.2	65.2	19.4
2	371- 374	0.2	-3.5	0.1	-0.2	0.0	0.0	0.2	0.1	-3.5	3.7	64.2	16.4
3	2711- 2714	0.0	-10.5	2.6	0.6	0.0	0.0	2.6	0.0	-10.5	13.2	94.3	6.1
4	2276- 2279	0.0	-5.1	0.3	0.0	0.0	0.0	0.3	0.0	-5.1	5.3	65.5	11.4
5	2599- 2603	-3.9	0.0	1.4	-0.1	0.0	0.0	1.4	0.0	-3.9	5.2	66.4	11.8
6	2756- 2759	-17.5	0.4	0.1	-0.9	0.0	0.0	0.4	0.1	-17.6	18.0	70.9	2.9
7	3051- 3056	0.5	-31.0	5.1	2.1	0.0	0.0	5.1	0	-31.1	36.2	69.8	0.9
8	3801- 3807	29.7	-2.3	29.7	0.0	0.0	0.0	29.7	29.7	-2.3	32.0	135.0	3.2

Locations of the most critical sections for each component are provided in the following:

Comp. No. <sup>1</sup>	Section Location			
	Inside Node		Outside Node	
	x (in)	y (in)	z (in)	x (in)
1	1.42	6.20	1.42	0.75
2	35.50	15.40	37.50	15.40
3	35.50	171.40	37.50	171.40
4	35.50	142.40	37.00	142.40
5	40.70	163.40	43.35	163.40
6	35.50	174.40	37.50	174.40
7	35.50	179.40	35.50	185.40
8	0.0	188.46	0.0	193.71

<sup>1</sup> Refer to Figure 2.10.2-33 for cask component identification.

Table 2.10.4-121 Primary Stresses; 30-Foot Bottom End Drop; Drop Orientation = 0 Degrees; 2-D Model; Condition 1

Condition 1: 100°F Ambient with Contents

Stress Points Section <sup>1</sup> Node		Stress Components (ksi)						Principal Stresses (ksi)		
		S <sub>x</sub>	S <sub>y</sub>	S <sub>z</sub>	S <sub>xy</sub>	S <sub>yz</sub>	S <sub>xz</sub>	S1	S2	S3
A1	1	21.0	-1.0	21.0	0.0	0.0	0.0	21.0	21.0	-1.0
A2	2	11.9	-1.1	11.9	0.0	0.0	0.0	11.9	11.9	-1.1
A3	3	2.9	-1.3	2.9	0.0	0.0	0.0	2.9	2.9	-1.3
A4	4	-6.1	-1.5	-6.1	0.0	0.0	0.0	-1.5	-6.1	-6.1
A5	5	-15.2	-1.6	-15.2	0.0	0.0	0.0	-1.6	-15.2	-15.2
B1	6	12.2	-1.8	12.2	0.0	0.0	0.0	12.2	12.2	-1.8
B2	7	4.3	-1.9	4.3	0.0	0.0	0.0	4.3	4.3	-1.9
B3	8	-3.6	-2.1	-3.6	0.0	0.0	0.0	-2.1	-3.6	-3.6
B4	9	-11.5	-2.2	-11.5	0.0	0.0	0.0	-2.2	-11.5	-11.5
B5	10	-19.3	-2.4	-19.3	0.0	0.0	0.0	-2.4	-19.3	-19.3
C1	251	-11.2	-13.5	-0.4	-2.3	0.0	0.0	-0.4	-9.7	-14.9
C2	252	-1.8	-5.6	2.4	-1.7	0.0	0.0	2.4	-1.2	-6.2
C3	253	3.1	-2.5	2.7	-1.8	0.0	0.0	3.6	2.7	-3.0
C4	254	9.3	-1.6	2.7	-1.4	0.0	0.0	9.4	2.7	-1.8
C5	255	16.1	-1.4	2.5	-1.0	0.0	0.0	16.2	2.5	-1.5
D1	306	-17.9	-15.3	-8.4	-5.3	0.0	0.0	-8.4	-11.1	-22.1
D2	307	-4.7	-11.0	-4.7	-2.3	0.0	0.0	-4.0	-4.7	-11.7
D3	308	-1.2	-5.6	-3.7	0.0	0.0	0.0	-1.2	-3.7	-5.6
D4	309	2.3	-3.6	-3.8	0.5	0.0	0.0	2.3	-3.7	-3.8
D5	310	6.6	-2.9	-3.9	0.5	0.0	0.0	6.6	-2.9	-3.9
E1	305	15.2	-4.7	3.5	-3.5	0.0	0.0	15.8	3.5	-5.3
E2	315	7.3	-6.9	1.0	-4.5	0.0	0.0	8.6	1.0	-8.2
E3	325	3.1	-5.4	0.3	-4.4	0.0	0.0	5.0	0.3	-7.3
E4	335	1.5	-4.4	0.2	-3.4	0.0	0.0	3.1	0.2	-6.0
E5	345	0.6	-3.7	0.2	-2.0	0.0	0.0	1.4	0.2	-4.5
E6	355	0.2	-3.6	0.1	-1.2	0.0	0.0	0.6	0.1	-3.9
F1	251	-11.2	-13.5	-0.4	-2.3	0.0	0.0	-0.4	-9.7	-14.9
F2	261	-8.1	-6.1	2.2	-0.8	0.0	0.0	2.2	-5.8	-8.4
F3	271	-5.4	-0.6	4.2	0.1	0.0	0.0	4.2	-0.6	-5.4
F4	281	-5.4	4.0	5.3	-0.2	0.0	0.0	5.3	4.0	-5.4
G1	311	-7.8	-12.6	-1.0	-0.4	0.0	0.0	-1.0	-7.8	-12.6

Table 2.10.4-121 Primary Stresses; 30-Foot Bottom End Drop; Drop Orientation = 0 Degrees; 2-D Model; Condition 1 (continued)

Stress Points Section <sup>1</sup> Node		Stress Components (ksi)						Principal Stresses (ksi)		
		S <sub>x</sub>	S <sub>y</sub>	S <sub>z</sub>	S <sub>xy</sub>	S <sub>yz</sub>	S <sub>xz</sub>	S1	S2	S3
G2	321	-5.5	-7.9	0.8	0.3	0.0	0.0	0.8	-5.4	-7.9
G3	331	-2.8	-4.7	2.3	0.9	0.0	0.0	2.3	-2.5	-5.1
G4	341	-1.1	-1.5	3.5	0.7	0.0	0.0	3.5	-0.6	-2.0
G5	351	-0.5	2.6	4.7	0.4	0.0	0.0	4.7	2.7	-0.6
H1	581	-0.1	-3.0	1.7	0.0	0.0	0.0	1.7	-0.1	-3.0
H2	582	-0.2	-4.8	1.2	0.0	0.0	0.0	1.2	-0.2	-4.8
H3	583	-0.1	-6.6	0.7	0.2	0.0	0.0	0.7	-0.1	-6.6
H4	584	-0.1	-9.1	0.0	0.5	0.0	0.0	0.0	-0.1	-9.2
I1	589	0.0	-3.6	1.1	0.0	0.0	0.0	1.1	0.0	-3.6
I2	590	0.0	-4.2	0.9	0.0	0.0	0.0	0.9	0.0	-4.2
I3	591	0.0	-4.7	0.8	0.0	0.0	0.0	0.8	0.0	-4.7
I4	592	0.0	-5.3	0.6	0.0	0.0	0.0	0.6	0.0	-5.3
I5	593	0.0	-5.9	0.4	0.0	0.0	0.0	0.4	0.0	-5.9
J1	971	-0.1	-5.4	1.2	0.0	0.0	0.0	1.2	-0.1	-5.4
J2	972	0.0	-5.4	1.2	0.0	0.0	0.0	1.2	0.0	-5.4
J3	973	0.0	-5.4	1.2	0.0	0.0	0.0	1.2	0.0	-5.4
J4	974	0.0	-5.4	1.2	0.0	0.0	0.0	1.2	0.0	-5.4
K1	979	0.0	-4.2	0.0	0.0	0.0	0.0	0.0	0.0	-4.2
K2	980	0.0	-4.2	0.0	0.0	0.0	0.0	0.0	0.0	-4.2
K3	981	0.0	-4.1	0.0	0.0	0.0	0.0	0.0	0.0	-4.1
K4	982	0.0	-4.1	0.0	0.0	0.0	0.0	0.0	0.0	-4.1
K5	983	0.0	-4.1	0.0	0.0	0.0	0.0	0.0	0.0	-4.1
L1	1601	-0.1	-4.4	1.2	0.0	0.0	0.0	1.2	-0.1	-4.4
L2	1602	0.0	-4.4	1.2	0.0	0.0	0.0	1.2	0.0	-4.4
L3	1603	0.0	-4.4	1.2	0.0	0.0	0.0	1.2	0.0	-4.4
L4	1604	0.0	-4.4	1.2	0.0	0.0	0.0	1.2	0.0	-4.4
M1	1609	0.0	-3.2	0.0	0.0	0.0	0.0	0.0	0.0	-3.2
M2	1610	0.0	-3.2	0.0	0.0	0.0	0.0	0.0	0.0	-3.2
M3	1611	0.0	-3.2	0.0	0.0	0.0	0.0	0.0	0.0	-3.2
M4	1612	0.0	-3.2	0.0	0.0	0.0	0.0	0.0	0.0	-3.2
M5	1613	0.0	-3.2	0.0	0.0	0.0	0.0	0.0	0.0	-3.2
N1	2216	-0.1	-3.4	1.2	0.0	0.0	0.0	1.2	-0.1	-3.4
N2	2217	0.0	-3.4	1.2	0.0	0.0	0.0	1.2	0.0	-3.4

Table 2.10.4-121 Primary Stresses; 30-Foot Bottom End Drop; Drop Orientation = 0 Degrees; 2-D Model; Condition 1 (continued)

Stress Points		Stress Components (ksi)						Principal Stresses (ksi)		
Section <sup>1</sup>	Node	S <sub>x</sub>	S <sub>y</sub>	S <sub>z</sub>	S <sub>xy</sub>	S <sub>yz</sub>	S <sub>xz</sub>	S1	S2	S3
N3	2218	0.0	-3.4	1.2	0.0	0.0	0.0	1.2	0.0	-3.4
N4	2219	0.0	-3.4	1.2	0.0	0.0	0.0	1.2	0.0	-3.4
O1	2224	0.0	-2.2	0.0	0.0	0.0	0.0	0.0	0.0	-2.2
O2	2225	0.0	-2.2	0.0	0.0	0.0	0.0	0.0	0.0	-2.2
O3	2226	0.0	-2.2	0.0	0.0	0.0	0.0	0.0	0.0	-2.2
O4	2227	0.0	-2.2	0.0	0.0	0.0	0.0	0.0	0.0	-2.2
O5	2228	0.0	-2.2	0.0	0.0	0.0	0.0	0.0	0.0	-2.2
P1	2546	-0.1	-2.1	1.1	0.0	0.0	0.0	1.1	-0.1	-2.1
P2	2547	-0.1	-2.6	1.0	0.0	0.0	0.0	1.0	-0.1	-2.6
P3	2548	-0.1	-3.0	0.9	-0.1	0.0	0.0	0.9	-0.1	-3.0
P4	2549	0.0	-3.6	0.7	-0.2	0.0	0.0	0.7	0.0	-3.7
Q1	2554	0.0	-1.4	0.3	0.0	0.0	0.0	0.3	0.0	-1.4
Q2	2555	0.0	-1.5	0.3	0.0	0.0	0.0	0.3	0.0	-1.5
Q3	2556	0.0	-1.7	0.2	0.0	0.0	0.0	0.2	0.0	-1.7
Q4	2557	0.0	-1.8	0.2	0.0	0.0	0.0	0.2	0.0	-1.8
Q5	2558	0.0	-1.9	0.1	0.0	0.0	0.0	0.1	0.0	-1.9
R1	2771	-0.3	-4.4	0.0	0.2	0.0	0.0	0.0	-0.3	-4.4
R2	2772	-0.1	-2.9	0.4	0.3	0.0	0.0	0.4	-0.1	-2.9
R3	2773	-0.2	-1.4	0.8	0.4	0.0	0.0	0.8	-0.1	-1.5
R4	2774	-0.7	1.0	1.3	0.5	0.0	0.0	1.3	1.2	-0.9
S1	2779	-2.1	-2.9	-0.4	0.2	0.0	0.0	-0.4	-2.0	-2.9
S2	2780	-1.3	-1.8	0.1	0.0	0.0	0.0	0.1	-1.3	-1.8
S3	2781	-0.7	-1.1	0.4	-0.2	0.0	0.0	0.4	-0.5	-1.2
S4	2782	-0.3	-0.3	0.7	-0.2	0.0	0.0	0.7	-0.1	-0.5
S5	2783	-0.1	0.7	1.0	-0.1	0.0	0.0	1.0	0.8	-0.1
T1	7066	1.9	1.6	1.1	0.5	0.0	0.0	2.3	1.2	1.1
T2	7067	1.5	0.1	0.5	0.1	0.0	0.0	1.5	0.5	0.1
T3	7068	1.0	-0.5	0.3	0.0	0.0	0.0	1.0	0.3	-0.5
T4	7069	0.6	-0.8	0.1	-0.1	0.0	0.0	0.6	0.1	-0.8
T5	7070	0.3	-1.1	-0.1	-0.1	0.0	0.0	0.3	-0.1	-1.1
T6	7071	0.1	-1.4	-0.2	-0.1	0.0	0.0	0.1	-0.2	-1.4
T7	7072	0.1	-1.9	-0.3	-0.1	0.0	0.0	0.1	-0.3	-1.9
U1	3051	-1.2	-3.6	0.6	0.7	0.0	0.0	0.6	-1.0	-3.8

Table 2.10.4-121 Primary Stresses; 30-Foot Bottom End Drop; Drop Orientation = 0 Degrees; 2-D Model; Condition 1 (continued)

Stress Points Section <sup>1</sup> Node	Stress Components (ksi)						Principal Stresses (ksi)		
	S <sub>x</sub>	S <sub>y</sub>	S <sub>z</sub>	S <sub>xy</sub>	S <sub>xz</sub>	S <sub>yz</sub>	S1	S2	S3
U2 3052	-0.4	-3.7	0.1	0.7	0.0	0.0	0.1	-0.2	-3.9
U3 3053	0.3	-3.5	-0.2	0.3	0.0	0.0	0.3	-0.2	-3.5
U4 3054	0.6	-2.9	-0.5	-0.3	0.0	0.0	0.6	-0.5	-2.9
U5 3055	0.4	-2.3	-0.9	-0.3	0.0	0.0	0.4	-0.9	-2.3
U6 3056	1.2	-1.0	-0.7	0.4	0.0	0.0	1.2	-0.7	-1.0
V1 3611	0.6	-0.1	1.8	-0.1	0.0	0.0	1.8	0.6	-0.1
V2 3612	0.3	-0.2	1.1	-0.1	0.0	0.0	1.1	0.3	-0.2
V3 3613	0.1	-0.4	0.5	-0.1	0.0	0.0	0.5	0.2	-0.5
V4 3614	0.0	-0.7	-0.1	-0.1	0.0	0.0	0.0	-0.1	-0.7
V5 3615	-0.1	-1.1	-0.8	0.0	0.0	0.0	-0.1	-0.8	-1.1
V6 3616	-0.3	-0.5	-1.2	0.0	0.0	0.0	-0.3	-0.5	-1.2
V7 3617	-0.8	0.4	-1.7	0.0	0.0	0.0	0.4	-0.8	-1.7
W1 3241	4.7	0.0	4.7	0.0	0.0	0.0	4.7	4.7	0.0
W2 3242	3.0	0.0	3.0	0.0	0.0	0.0	3.0	3.0	0.0
W3 3243	1.4	0.0	1.4	0.0	0.0	0.0	1.4	1.4	0.0
W4 3244	-0.2	0.0	-0.2	0.0	0.0	0.0	0.0	-0.2	-0.2
W5 3245	-1.9	0.0	-1.9	0.0	0.0	0.0	0.0	-1.9	-1.9
W6 3246	-3.5	0.0	-3.5	0.0	0.0	0.0	0.0	-3.5	-3.5
X1 3801	4.6	-0.1	4.6	0.0	0.0	0.0	4.6	4.6	-0.1
X2 3802	3.1	-0.1	3.1	0.0	0.0	0.0	3.1	3.1	-0.1
X3 3803	1.6	0.0	1.6	0.0	0.0	0.0	1.6	1.6	0.0
X4 3804	0.1	0.0	0.1	0.0	0.0	0.0	0.1	0.1	0.0
X5 3805	-1.4	0.0	-1.4	0.0	0.0	0.0	0.0	-1.4	-1.4
X6 3806	-2.9	0.1	-2.9	0.0	0.0	0.0	0.1	-2.9	-2.9
X7 3807	-4.6	0.1	-4.6	0.0	0.0	0.0	0.1	-4.6	-4.6

<sup>1</sup> Refer to Figure 2.10.2-34 for the identification of the representative sections.

Table 2.10.4-122  $P_m$  Stresses; 30-Foot Bottom End Drop; Drop Orientation = 0 Degrees; 2-D Model; Condition 1

Condition 1: 100°F Ambient with Contents

Section <sup>1</sup>	Node - Node	Stress Components (ksi)						Principal Stresses (ksi)			
		$S_x$	$S_y$	$S_z$	$S_{xy}$	$S_{yz}$	$S_{xz}$	S1	S2	S3	S.I.
A	1 - 5	2.9	-1.3	2.9	0.0	0.0	0.0	2.9	2.9	-1.3	4.2
B	6 - 10	-3.6	-2.1	-3.6	0.0	0.0	0.0	-2.1	-3.6	-3.6	1.5
C	251 - 255	3.2	-4.3	2.2	-1.6	0.0	0.0	3.6	2.2	-4.6	8.2
D	306 - 310	-2.3	-7.3	-4.6	-1.1	0.0	0.0	-2.1	-4.6	-7.5	5.4
E	305 - 355	5.1	-5.0	1.0	-3.4	0.0	0.0	6.2	1.0	-6.1	12.3
F	251 - 281	-7.3	-3.7	3.0	-0.6	0.0	0.0	3.0	-3.6	-7.4	10.3
G	311 - 351	-3.4	-4.7	2.1	0.5	0.0	0.0	2.1	-3.2	-4.9	7.0
H	581 - 584	-0.1	-5.9	0.9	0.2	0.0	0.0	0.9	-0.1	-5.9	6.8
I	589 - 593	0.0	-4.8	0.8	0.0	0.0	0.0	0.8	0.0	-4.8	5.5
J	971 - 974	0.0	-5.4	1.2	0.0	0.0	0.0	1.2	0.0	-5.4	6.6
K	979 - 983	0.0	-4.1	0.0	0.0	0.0	0.0	0.0	0.0	-4.1	4.1
L	1601 - 1604	0.0	-4.4	1.2	0.0	0.0	0.0	1.2	0.0	-4.4	5.6
M	1609 - 1613	0.0	-3.2	0.0	0.0	0.0	0.0	0.0	0.0	-3.2	3.2
N	2216 - 2219	0.0	-3.4	1.2	0.0	0.0	0.0	1.2	0.0	-3.4	4.6
O	2224 - 2228	0.0	-2.2	0.0	0.0	0.0	0.0	0.0	0.0	-2.2	2.2
P	2546 - 2549	-0.1	-2.8	0.9	-0.1	0.0	0.0	0.9	-0.1	-2.8	3.7
Q	2554 - 2558	0.0	-1.7	0.2	0.0	0.0	0.0	0.2	0.0	-1.7	1.9
R	2771 - 2774	-0.3	-2.0	0.6	0.3	0.0	0.0	0.6	-0.2	-2.0	2.7
S	2779 - 2783	-0.8	-1.0	0.4	-0.1	0.0	0.0	0.4	-0.8	-1.1	1.5
T	7066 - 7072	0.8	-0.6	0.2	0.0	0.0	0.0	0.8	0.2	-0.6	1.4
U	3051 - 3056	0.2	-3.0	-0.4	0.2	0.0	0.0	0.2	-0.4	-3.0	3.2
V	3611 - 3617	0.0	-0.4	-0.1	-0.1	0.0	0.0	0.0	-0.1	-0.4	0.4
W	3241 - 3246	0.6	0.0	0.6	0.0	0.0	0.0	0.6	0.6	0.0	0.6
X	3801 - 3807	0.0	0.0	0.0	0.0	0.0	0.0	0.0	0.0	0.0	0.0

<sup>1</sup> Refer to Figure 2.10.2-34 for the identification of the representative sections.

Table 2.10.4-123  $P_m + P_b$  Stresses; 30-Foot Bottom End Drop; Drop Orientation = 0 Degrees; 2-D Model; Condition 1

**Condition 1: 100°F Ambient with Contents**

Section <sup>1</sup>	Node - Node	Stress Components (ksi)						Principal Stresses (ksi)			
		$S_x$	$S_y$	$S_z$	$S_{xy}$	$S_{yz}$	$S_{zx}$	S1	S2	S3	S.L
A I	1 - 5	21.0	-1.0	21.0	0.0	0.0	0.0	21.0	21.0	-1.0	22.0
B O	6 - 10	-19.4	-2.4	-19.4	0.0	0.0	0.0	-2.4	-19.4	-19.4	17.0
C O	251 - 255	13.9	-1.4	3.2	-1.6	0.0	0.0	16.1	3.2	-1.6	17.7
D O	306 - 310	7.9	-2.9	-2.8	-1.1	0.0	0.0	8.0	-2.8	-3.0	11.0
E I	305 - 355	15.2	-6.4	2.5	-3.4	0.0	0.0	15.7	2.5	-7.0	22.7
F I	251 - 281	-11.2	-12.4	0.1	-0.6	0.0	0.0	0.1	-10.9	-12.7	12.7
G I	311 - 351	-7.8	-11.9	-0.7	0.5	0.0	0.0	-0.7	-7.8	-12.0	11.3
H O	581 - 584	-0.1	-8.8	0.1	0.2	0.0	0.0	0.1	-0.1	-8.8	8.9
I O	589 - 593	0.0	-5.9	0.4	0.0	0.0	0.0	0.4	0.0	-5.9	6.3
J I	971 - 974	-0.1	-5.4	1.2	0.0	0.0	0.0	1.2	-0.1	-5.4	6.6
K I	979 - 983	0.0	-4.2	0.0	0.0	0.0	0.0	0.0	0.0	-4.2	4.2
L I	1601 - 1604	-0.1	-4.4	1.2	0.0	0.0	0.0	1.2	-0.1	-4.4	5.6
M O	1609 - 1613	0.0	-3.2	0.0	0.0	0.0	0.0	0.0	0.0	-3.2	3.2
N I	2216 - 2219	-0.1	-3.4	1.2	0.0	0.0	0.0	1.2	-0.1	-3.4	4.6
O I	2224 - 2228	0.0	-2.2	0.0	0.0	0.0	0.0	0.0	0.0	-2.2	2.2
P O	2546 - 2549	0.0	-3.5	0.7	-0.1	0.0	0.0	0.7	0.0	-3.5	4.2
Q O	2554 - 2558	0.0	-1.9	0.1	0.0	0.0	0.0	0.1	0.0	-1.9	2.1
R I	2771 - 2774	-0.3	-4.6	0.0	0.3	0.0	0.0	0.0	-0.2	-4.6	4.6
S I	2779 - 2783	-2.1	-2.8	-0.3	-0.1	0.0	0.0	-0.3	-2.0	-2.8	2.5
T O	7066 - 7072	0.1	-2.0	-0.4	0.0	0.0	0.0	0.1	-0.4	-2.0	2.1
U I	3051 - 3056	-0.7	-11.2	0.3	0.2	0.0	0.0	0.3	-0.7	-11.2	11.4
V O	3611 - 3617	-0.6	0.4	-1.8	-0.1	0.0	0.0	0.4	-0.6	-1.8	2.2
W I	3241 - 3246	4.7	0.0	4.7	0.0	0.0	0.0	4.7	4.7	0.0	4.7
X O	3801 - 3807	-4.5	0.1	-4.5	0.0	0.0	0.0	0.1	-4.5	-4.5	4.7

<sup>1</sup> Refer to Figure 2.10.2-34 for the identification of the representative sections.



Table 2.10.4-124 Critical P<sub>m</sub> Stress Summary; 30-Foot Bottom End Drop; Drop Orientation = 0 Degrees; 2-D Model; Condition 1

Condition 1: 100°F Ambient with Contents

Comp. No. <sup>1</sup>	Section Cut Node-Node	P <sub>m</sub> Stresses (ksi)							Principal Stresses (ksi)			Allow. Stress	Margin of Safety
		S <sub>x</sub>	S <sub>y</sub>	S <sub>z</sub>	S <sub>xy</sub>	S <sub>yz</sub>	S <sub>xz</sub>	S1	S2	S3			
1	306- 310	-2.3	-7.3	-4.6	-1.1	0.0	0.0	-2.1	-4.6	-7.5	5.4	45.6	7.4
2	305- 355	5.1	-5.0	1.0	-3.4	0.0	0.0	6.2	1.0	-6.1	12.3	44.9	2.7
3	416- 419	-0.1	-4.7	5.6	-0.6	0.0	0.0	5.6	0.0	-4.8	10.4	66.0	5.3
4	851- 854	0.0	-5.6	1.2	0.0	0.0	0.0	1.2	0.0	-5.6	6.8	45.8	5.7
5	544- 548	0.0	-4.8	1.4	-0.1	0.0	0.0	1.4	0.0	-4.8	6.2	46.4	6.5
6	7064- 2774	0.0	3.8	1.7	0.4	0.0	0.0	3.8	1.7	0.0	3.9	49.3	11.6
7	3021- 3026	0.2	-8.0	-1.7	-0.2	0.0	0.0	0.2	-1.7	-8.0	8.3	48.0	4.8
8	3621- 3627	0.0	-0.6	-0.2	-0.1	0.0	0.0	0.0	-0.2	-0.6	0.6	94.5	156.5

Locations of the most critical sections for each component are provided in the following:

Comp. No. <sup>1</sup>	Section Location			
	Inside Node		Outside Node	
	x (in)	y (in)	z (in)	x (in)
1	39.44	6.20	39.44	0.75
2	39.44	8.20	43.35	8.20
3	35.50	18.40	37.50	18.40
4	35.50	47.40	37.00	47.40
5	40.70	26.40	43.35	26.40
6	37.655	179.40	37.50	175.40
7	37.655	179.40	37.655	185.40
8	33.705	188.40	33.705	193.71

<sup>1</sup> Refer to Figure 2.10.2-33 for cask component identification.

Table 2.10.4-125 Critical  $P_m + P_b$  Stress Summary; 30-Foot Bottom End Drop; Drop Orientation = 0 Degrees; 2-D Model; Condition 1

Condition 1: 100°F Ambient with Contents

Comp. No. <sup>1</sup>	Section Cut Node-Node	$P_m + P_b$ Stresses (ksi)							Principal Stresses (ksi)				Allow. Stress	Margin of Safety
		$S_x$	$S_y$	$S_z$	$S_{xy}$	$S_{yz}$	$S_{zx}$	$S_1$	$S_2$	$S_3$	S.I.			
1	16- 20	-19.3	-2.2	-19.3	-0.1	0.0	0.0	-2.2	-19.3	-19.3	17.1	65.2	2.8	
2	305- 355	15.2	-6.4	2.5	-3.4	0.0	0.0	15.7	2.5	-7.0	22.7	64.2	1.8	
3	416- 419	-0.1	-10.5	4.2	-0.6	0.0	0.0	4.2	-0.1	-10.5	14.7	94.3	5.4	
4	851- 854	-0.1	-3.7	1.2	0.0	0.0	0.0	1.2	-0.1	-5.7	6.9	65.3	8.5	
5	544- 548	0.0	-3.6	1.1	-0.1	0.0	0.0	1.1	0.0	-5.6	6.7	66.4	8.9	
6	7064- 2774	2.6	12.2	3.3	0.4	0.0	0.0	12.2	3.3	2.6	9.6	70.9	5.4	
7	3021- 3026	0.1	12.2	-0.1	-0.2	0.0	0.0	12.2	0.1	-0.1	12.3	69.8	4.7	
8	3801- 3807	-4.5	0.1	-4.5	0.0	0.0	0.0	0.1	-4.5	-4.5	4.7	135.0	27.7	

Locations of the most critical sections for each component are provided in the following:

Comp. No. <sup>1</sup>	Section Location			
	Inside Node		Outside Node	
	x (in)	y (in)	z (in)	x (in)
1	1.42	6.20	1.42	0.75
2	39.44	8.20	43.35	8.20
3	35.50	18.40	37.50	18.40
4	35.50	47.40	37.00	47.40
5	40.70	26.40	43.35	26.40
6	37.655	179.40	37.50	175.40
7	37.655	179.40	37.655	185.40
8	0.0	188.46	0.0	193.71

<sup>1</sup> Refer to Figure 2.10.2-33 for cask component identification.

Table 2.10.4-126 Critical P<sub>m</sub> Stress Summary; 30-Foot Bottom End Drop; Drop Orientation = 0 Degrees; 2-D Model; Condition 2

Condition 2: -20°F Ambient with Contents

Comp. No. <sup>1</sup>	Section Cut Node-Node	P <sub>m</sub> Stresses (ksi)						Principal Stresses (ksi)			S.I.	Allow. Stress	Margin of Safety
		S <sub>x</sub>	S <sub>y</sub>	S <sub>z</sub>	S <sub>xy</sub>	S <sub>yz</sub>	S <sub>xz</sub>	S1	S2	S3			
1	306- 310	-2.4	-7.4	-4.7	-1.1	0.0	0.0	-2.2	-4.7	-7.6	5.5	45.6	7.3
2	305- 355	5.3	-5.1	1.0	-3.5	0.0	0.0	6.3	1.0	-6.1	12.5	44.9	2.6
3	416- 419	0.0	-5.0	5.4	-0.7	0.0	0.0	5.4	0.1	-5.1	10.5	66.0	5.3
4	851- 854	0.0	-5.9	0.3	0.0	0.0	0.0	0.3	0.0	-5.9	6.2	45.8	6.4
5	544- 548	0.0	-4.9	1.4	-0.1	0.0	0.0	1.4	0.0	-4.9	6.3	46.4	6.4
6	7064- 2774	0.1	4.0	1.6	0.5	0.0	0.0	4.0	1.6	0.0	4.0	49.3	11.3
7	3021- 3026	0.2	-8.3	-1.7	-0.3	0.0	0.0	0.2	-1.7	-8.3	8.5	48.0	4.6
8	3621- 3627	0.0	-0.6	-0.2	-0.1	0.0	0.0	0.0	-0.2	-0.7	0.7	94.5	134.0

Locations of the most critical sections for each component are provided in the following:

Comp. No. <sup>1</sup>	Section Location			
	Inside Node		Outside Node	
	x (in)	y (in)	z (in)	x (in)
1	39.44	6.20	39.44	0.75
2	39.44	8.20	43.35	8.20
3	35.50	18.40	37.50	18.40
4	35.50	47.40	37.00	47.40
5	40.70	26.40	43.35	26.40
6	37.655	179.40	37.50	175.40
7	37.655	179.40	37.655	185.40
8	33.705	188.40	33.705	193.716

<sup>1</sup> Refer to Figure 2.10.2-33 for cask component identification.

Table 2.10.4-127 Critical  $P_m + P_b$  Stress Summary; 30-Foot Bottom End Drop; Drop Orientation = 0 Degrees; 2-D Model; Condition 2

Condition 2: -20°F Ambient with Contents

Comp. No. <sup>1</sup>	Section Cut Node-Node	$P_m + P_b$ Stresses (ksi)							Principal Stresses (ksi)				Allow. Stress	Margin of Safety
		$S_x$	$S_y$	$S_z$	$S_{xy}$	$S_{yz}$	$S_{zx}$	S1	S2	S3	S.I.			
1	16- 20	-19.8	-2.2	-19.8	-0.1	0.0	0.0	-2.2	-19.8	-19.8	17.6	65.2	2.7	
2	305- 333	15.5	-6.5	2.5	-3.5	0.0	0.0	16.1	2.5	-7.0	23.1	64.2	1.8	
3	416- 419	-0.1	-11.0	4.0	-0.7	0.0	0.0	4.0	0.0	-11.0	15.0	94.3	3.3	
4	831- 854	0.0	-6.1	0.3	0.0	0.0	0.0	0.3	0.0	-6.1	6.3	65.5	9.4	
5	544- 548	0.0	-5.7	1.1	-0.1	0.0	0.0	1.1	0.0	-5.7	6.8	66.4	8.8	
6	7064- 2774	2.8	12.5	3.3	0.5	0.0	0.0	12.6	3.3	2.8	9.8	70.9	6.2	
7	3051- 3056	-0.8	-12.6	0.4	0.2	0.0	0.0	0.4	-0.8	-12.6	12.9	69.8	4.4	
8	3801- 3807	-4.8	0.1	-4.8	0.0	0.0	0.0	0.1	-4.8	-4.8	5.0	135.0	26.0	

Locations of the most critical sections for each component are provided in the following:

Comp. No. <sup>1</sup>	Section Location			
	Inside Node		Outside Node	
	x (in)	y (in)	z (in)	x (in)
1	1.42	6.20	1.42	0.75
2	39.44	8.20	43.35	8.20
3	35.50	18.40	37.50	18.40
4	35.50	47.40	37.00	47.40
5	40.70	26.40	43.35	26.40
6	37.655	179.40	37.50	175.40
7	35.50	179.40	35.50	185.40
8	0.0	188.46	0.0	193.71

<sup>1</sup> Refer to Figure 2.10.2-33 for cask component identification.

Table 2.10.4-128 Critical P<sub>m</sub> Stress Summary; 30-Foot Bottom End Drop; Drop Orientation = 0 Degrees; 2-D Model; Condition 3

Condition 3: -20°F Ambient without Contents

Comp. No. <sup>1</sup>	Section Cut Node-Node	P <sub>m</sub> Stresses (ksi)							Principal Stresses (ksi)			S.I.	Allow. Stress	Margin of Safety
		S <sub>x</sub>	S <sub>y</sub>	S <sub>z</sub>	S <sub>xy</sub>	S <sub>yz</sub>	S <sub>xz</sub>	S <sub>max</sub>	S1	S2	S3			
1	306- 310	-2.4	-6.3	-4.5	-0.9	0.0	0.0	0.0	-2.2	-4.5	-6.5	4.3	45.6	9.6
2	305- 355	5.5	-4.2	0.9	-3.4	0.0	0.0	0.0	6.5	0.9	-5.3	11.8	44.9	2.8
3	416- 419	0.0	-4.5	5.5	-0.7	0.0	0.0	0.0	5.5	0.1	-4.6	10.1	66.0	5.5
4	866- 869	0.0	-5.3	0.3	0.0	0.0	0.0	0.0	0.3	0.0	-5.3	5.6	45.8	7.2
5	544- 548	0.0	-4.2	1.4	-0.1	0.0	0.0	0.0	1.4	0.0	-4.2	5.7	46.4	7.1
6	7064- 2774	0.1	4.0	1.5	0.4	0.0	0.0	0.0	4.0	1.5	0.0	4.0	49.7	11.3
7	3021- 3026	0.2	-8.2	-1.7	-0.3	0.0	0.0	0.0	0.2	-1.7	-8.2	8.4	48.0	4.7
8	3621- 3627	0.0	-0.6	-0.2	-0.1	0.0	0.0	0.0	0.0	-0.2	-0.6	0.6	94.5	156.5

Locations of the most critical sections for each component are provided in the following:

Comp. No. <sup>1</sup>	Section Location			
	Inside Node		Outside Node	
	x (in)	y (in)	z (in)	x (in)
1	39.44	6.20	39.44	0.75
2	39.44	8.20	43.35	8.20
3	35.50	18.40	37.50	18.40
4	35.50	48.40	37.00	48.40
5	40.70	26.40	43.35	26.40
6	35.50	79.40	37.50	175.40
7	37.65	179.40	37.66	185.40
8	33.05	188.40	33.71	193.71

<sup>1</sup> Refer to Figure 2.10.2-33 for cask component identification.

Table 2.10.4-129 Critical  $P_m + P_b$  Stress Summary; 30-Foot Bottom End Drop; Drop Orientation = 0 Degrees; 2-D Model; Condition 3

Condition 3: -20°F Ambient without Contents

Comp. No. <sup>1</sup>	Section Cut Node-Node	$P_m + P_b$ Stresses (ksi)							Principal Stresses (ksi)			S.L.	Allow. Stress	Margin of Safety
		$S_x$	$S_y$	$S_z$	$S_{xy}$	$S_{yz}$	$S_{zx}$	$S_{xy}$	S1	S2	S3			
1	16- 20	-19.8	-1.5	-19.8	-0.1	0.0	0.0	0.0	-1.5	-19.8	-19.8	18.3	65.2	2.6
2	1- 5	21.4	-0.4	21.4	0.0	0.0	0.0	0.0	21.4	21.4	-0.4	21.7	64.2	2.0
3	416- 419	-0.1	10.7	4.0	-0.7	0.0	0.0	0.0	4.0	0.0	-10.7	14.7	94.3	5.4
4	851- 854	0.0	-5.5	0.3	0.0	0.0	0.0	0.0	0.3	0.0	-5.5	5.7	65.5	10.5
5	544- 548	0.0	-3.1	1.2	-0.1	0.0	0.0	0.0	1.2	0.0	-3.1	6.2	66.4	9.7
6	7064- 2774	2.7	12.7	3.4	0.4	0.0	0.0	0.0	12.7	3.4	2.7	10.0	70.9	6.1
7	3021- 3026	0.1	12.7	-0.1	-0.3	0.0	0.0	0.0	12.7	0.1	-0.1	12.8	69.8	4.5
8	3521- 3527	0.0	-3.6	0.9	0.1	0.0	0.0	0.0	0.9	0.0	-3.6	4.5	135.0	29.0

Locations of the most critical sections for each component are provided in the following:

Comp. No. <sup>1</sup>	Section Location			
	Inside Node		Outside Node	
	x (in)	y (in)	z (in)	x (in)
1	1.42	6.20	1.42	0.75
2	0.0	14.40	0.0	8.20
3	35.50	18.40	37.50	18.40
4	35.50	47.40	37.00	47.40
5	40.70	26.40	43.35	26.40
6	37.66	179.40	37.50	175.40
7	37.66	179.40	37.66	185.40
8	39.56	188.40	39.56	193.71

<sup>1</sup> Refer to Figure 2.10.2-33 for cask component identification.

Table 2.10.4-130 Primary Stresses; 30-Foot Side Drop; Drop Orientation = 90 Degrees; 3-D Model; 0-Degree Circumferential Location; Condition 1

Condition 1: 100°F Ambient with Contents

Stress Points		Stress Components (ksi)						Principal Stresses (ksi)		
Section <sup>1</sup>	Node	S <sub>x</sub>	S <sub>y</sub>	S <sub>z</sub>	S <sub>xy</sub>	S <sub>yz</sub>	S <sub>xz</sub>	S1	S2	S3
A1	1130	-0.8	-1.9	-0.3	-0.1	0.1	0.0	-0.3	-0.7	-1.9
A2	1129	-1.0	-3.2	0.0	-0.1	0.1	0.0	0.0	-1.0	-3.2
A3	1128	-1.3	-4.4	0.3	0.0	0.1	0.0	0.3	-1.3	-4.4
B1	1185	-1.1	-5.3	0.0	-0.1	0.0	-0.2	0.0	-1.1	-5.3
B2	1184	-0.3	-6.0	0.0	-0.1	0.0	-0.2	0.1	-0.4	-6.0
B3	1183	0.4	-6.7	0.0	-0.1	0.1	-0.2	0.5	-0.1	-6.7
C1	90	5.9	-2.4	15.3	0.0	-0.8	1.5	15.6	5.7	-2.5
C2	80	-2.4	-7.0	6.6	-0.1	-0.5	0.0	6.6	-2.4	-7.0
C3	70	-3.5	-8.6	2.2	0.1	-0.4	-0.8	2.3	-3.6	-8.6
C4	60	-4.6	-9.5	0.3	0.2	-0.2	-0.5	0.4	-4.7	-9.5
C5	50	-9.8	-11.5	-0.1	0.2	-0.1	-0.1	-0.1	-9.8	-11.6
C6	40	-12.0	-12.5	-0.1	0.2	0.0	0.0	-0.1	-12.0	-12.6
D1	25	-4.9	-9.6	5.6	0.3	-0.1	0.1	5.6	-4.9	-9.6
D2	15	-9.8	-11.4	1.8	0.1	-0.1	-0.5	1.9	-9.8	-11.4
D3	5	-10.8	-11.6	0.4	0.2	0.0	-0.4	0.4	-10.8	-11.7
E1	35	-10.5	-11.4	4.9	0.2	-0.2	1.6	5.0	-10.6	-11.5
E2	34	-7.5	-11.5	2.1	0.3	0.0	1.8	2.5	-7.8	-11.5
E3	33	-8.0	-12.4	-0.3	0.3	0.0	1.5	0.0	-8.2	-12.4
E4	32	-8.6	-13.4	-2.8	0.4	0.0	0.9	-2.7	-8.7	-13.4
E5	31	-8.8	-14.3	-5.4	0.4	0.0	0.5	-5.3	-8.8	-14.3
F1	100	-1.3	-2.3	23.1	0.0	-1.2	2.3	23.4	-1.5	-2.4
F2	99	-1.5	-8.1	2.3	0.4	-0.9	2.5	3.5	-2.6	-8.2
F3	98	-0.5	-11.3	-11.0	0.8	-0.7	3.3	0.5	-10.7	-12.6
F4	97	0.6	-17.8	-36.7	1.3	-0.7	3.9	1.1	-17.8	-37.1
G1	94	0.8	-2.3	21.3	0.2	-0.5	3.3	21.8	0.3	-2.3
G2	93	1.5	-5.9	7.1	0.5	-0.3	2.4	8.0	0.6	-6.0
G3	92	1.5	-7.1	2.4	0.6	-0.3	1.0	3.1	0.9	-7.1
G4	91	0.7	-8.6	-3.1	0.7	-0.2	0.4	0.8	-3.1	-8.7
H1	330	-0.3	7.3	-4.6	-0.5	-1.6	0.1	7.6	-0.3	-4.8
H2	329	-0.1	9.1	-0.8	-0.6	-1.5	0.0	9.4	-0.2	-1.0

Table 2.10.4-130 Primary Stresses; 30-Foot Side Drop; Drop Orientation = 90 Degrees; 3-D Model; 0-Degree Circumferential Location; Condition 1 (continued)

Stress Points Section <sup>1</sup> Node		Stress Components (ksi)						Principal Stresses (ksi)		
		S <sub>x</sub>	S <sub>y</sub>	S <sub>z</sub>	S <sub>xy</sub>	S <sub>yz</sub>	S <sub>xz</sub>	S1	S2	S3
H3	328	0.1	10.8	2.9	-0.7	-1.5	-0.2	11.1	2.7	0.0
H4	327	0.2	12.8	7.4	-0.8	-1.4	-0.5	13.1	7.1	0.1
I1	244	-0.2	-0.4	4.8	0.0	-0.8	0.0	5.0	-0.2	-0.5
I2	243	-0.1	1.2	7.4	-0.1	-0.7	0.0	7.5	1.2	-0.1
I3	242	-0.1	2.8	10.0	-0.2	-0.5	0.0	10.0	2.7	-0.1
I4	241	0.0	4.2	12.5	-0.3	-0.4	0.0	12.6	4.3	0.0
J1	550	-0.3	7.9	10.8	-0.6	-0.8	0.0	11.0	7.7	-0.4
J2	548	-0.2	10.3	12.7	-0.8	-0.8	0.0	12.9	10.2	-0.2
J3	547	-0.1	12.7	14.5	-0.9	-0.7	0.0	14.8	12.5	-0.1
K1	344	-0.1	-1.3	11.2	0.0	-0.5	0.0	11.2	-0.1	-1.3
K2	342	-0.1	2.5	13.0	-0.2	-0.4	0.0	13.0	2.5	-0.1
K3	341	0.0	6.0	14.7	-0.5	-0.3	0.0	14.7	6.0	-0.1
L1	740	-0.1	4.8	16.7	0.3	0.0	-0.2	16.7	4.8	-0.1
L2	738	-0.6	7.7	18.3	-1.2	0.0	0.0	18.3	7.8	-0.7
L3	737	0.2	10.7	20.0	-2.6	0.0	0.0	20.0	11.3	-0.4
M1	663	-1.3	-2.5	13.9	0.1	0.0	0.0	13.9	-1.3	-2.5
M2	63	0.5	9.3	19.3	2.2	0.0	0.0	19.3	9.8	0.0
N1	1877	-0.3	7.6	9.2	-0.6	1.0	0.0	9.6	7.2	-0.4
N2	1477	-0.2	10.4	10.9	-0.8	0.9	0.0	11.6	9.7	-0.2
N3	1277	-0.1	13.0	12.7	-1.0	0.9	0.0	13.8	12.0	-0.1
O1	647	-0.1	-1.7	12.7	0.1	0.4	0.0	12.7	-0.1	-1.7
O2	247	-0.1	2.4	14.6	-0.2	0.3	0.0	14.6	2.4	-0.1
O3	47	0.0	6.1	16.5	-0.5	0.2	0.0	16.5	6.2	-0.1
P1	1840	-0.3	7.6	-4.4	-0.5	1.6	0.0	7.8	-0.3	-4.6
P2	1640	-0.2	9.5	-1.2	-0.7	1.6	0.0	9.8	-0.2	-1.4
P3	1440	0.0	11.4	1.9	-0.7	1.5	0.1	11.7	1.7	0.0
P4	1240	0.2	13.5	5.6	-0.9	1.5	0.4	13.8	5.4	0.1
Q1	628	-0.3	0.4	8.4	-0.1	0.7	0.1	8.5	0.3	-0.3
Q2	428	-0.2	2.3	10.7	-0.2	0.6	0.1	10.7	2.3	-0.2
Q3	228	-0.1	4.1	12.9	-0.3	0.4	0.1	12.9	4.2	-0.1
Q4	28	0.0	5.9	15.2	-0.4	0.3	0.1	15.2	5.9	-0.1
R1	1816	-1.0	-7.5	5.9	0.5	1.1	-0.2	6.0	-1.0	-7.6
R2	1616	-2.0	-9.2	-1.2	0.6	1.0	-0.5	-0.9	-2.1	-9.4



Table 2.10.4-130 Primary Stresses; 30-Foot Side Drop; Drop Orientation = 90 Degrees; 3-D Model; 0-Degree Circumferential Location; Condition 1 (continued)

Stress Points Section <sup>1</sup> Node	Stress Components (ksi)						Principal Stresses (ksi)		
	S <sub>x</sub>	S <sub>y</sub>	S <sub>z</sub>	S <sub>xy</sub>	S <sub>yz</sub>	S <sub>xz</sub>	S1	S2	S3
R3	1416	-4.8	-11.1	-7.4	0.7	0.7	-2.1	-3.6	-8.2
R4	1216	-6.4	-13.1	-15.7	0.8	0.4	-4.3	-4.6	-13.1
S1	616	2.8	-4.3	1.3	0.2	0.6	-0.2	2.8	1.3
S2	416	0.4	-3.3	6.4	0.2	0.5	-0.1	6.4	0.4
S3	216	0.4	-1.7	11.1	0.1	0.3	0.3	11.1	0.4
S4	16	0.2	-0.2	15.6	0.0	0.2	0.2	15.6	0.2
T1	811	-19.4	-21.7	-19.3	0.9	0.5	-5.4	-13.9	-21.4
T2	611	-9.6	-14.7	-5.4	0.7	0.4	-4.5	-2.5	-12.2
T3	411	-4.5	-10.8	2.5	0.5	0.3	-3.3	3.8	-5.7
T4	211	-1.0	-7.6	9.5	0.5	0.2	-1.8	9.8	-1.3
T5	11	0.2	-4.2	20.0	0.3	0.1	-0.9	20.0	0.2
U1	43058	6.9	0.4	-0.1	0.2	0.0	-0.1	6.9	0.4
U2	43057	3.3	-0.9	-0.4	0.2	0.0	-0.1	3.3	-0.4
U3	43056	1.0	-2.0	-1.0	0.1	0.0	-0.1	1.0	-1.1
U4	43055	-0.6	-2.9	-1.9	0.1	0.0	-0.4	-0.4	-2.0
U5	43054	-2.3	-3.9	-2.7	0.1	-0.1	-1.3	-1.1	-3.8
U6	43053	-4.1	-4.9	-3.2	0.1	-0.2	-2.7	-0.9	-4.9
U7	43052	-7.0	-5.6	-1.6	0.0	-0.3	-3.4	0.0	-5.6
U8	43051	-13.1	-7.3	0.2	-0.1	0.0	-0.1	0.2	-7.3
V1	50024	2.4	-1.4	0.1	0.1	0.0	0.0	2.4	0.1
V2	50023	-3.7	-4.3	-0.8	0.1	0.0	0.1	-0.8	-3.7
V3	50022	-6.9	-6.0	-0.6	0.1	0.0	0.1	-0.6	-6.0
V4	50021	-17.1	-9.5	0.6	-0.1	0.0	0.0	0.6	-9.5
W1	43278	-2.1	-2.8	0.1	-0.1	-0.2	0.2	0.1	-2.1
W2	43274	-1.4	-3.2	0.0	0.0	-0.2	0.2	0.0	-1.4
W3	43271	-0.3	-1.8	0.0	0.0	-0.3	0.1	0.0	-0.4
X1	50084	-0.7	-5.6	0.0	-0.1	0.0	0.2	0.1	-0.7
X2	50083	-0.3	-5.9	0.0	-0.1	0.0	0.2	0.1	-0.4
X3	50081	0.4	-6.6	0.0	0.0	-0.1	0.2	0.5	-0.1

<sup>1</sup> Refer to Figure 2.10.2-34 for the identification of the representative sections.

Table 2.10.4-131  $P_m$  Stresses; 30-Foot Side Drop; Drop Orientation = 90 Degrees; 3-D Model; 0-Degree Circumferential Location; Condition 1

Condition 1: 100°F Ambient with Contents

Section <sup>1</sup>	Node - Node	Stress Components (ksi)						Principal Stresses (ksi)			
		$S_x$	$S_y$	$S_z$	$S_{xy}$	$S_{yz}$	$S_{zx}$	S1	S2	S3	S.I.
A	1130 - 1128	-1.0	-3.2	0.0	-0.1	0.1	0.0	0.0	-1.0	-3.2	3.1
B	1185 - 1183	-0.3	-6.0	0.0	-0.1	0.0	-0.2	0.1	-0.4	-6.0	6.0
C	90 - 40	-5.9	-9.5	2.2	0.1	-0.3	-0.2	2.2	-5.9	-9.5	11.7
D	25 - 5	-8.8	-11.0	2.4	0.2	-0.1	-0.3	2.4	-8.8	-11.0	13.4
E	35 - 31	-8.5	-12.4	0.1	0.3	0.0	1.4	0.3	-8.6	-12.5	12.7
F	100 - 97	-0.8	-9.8	-5.2	0.6	-0.8	3.0	0.7	-6.4	-10.1	10.8
G	94 - 91	1.2	-6.2	6.2	0.5	-0.3	1.8	6.8	0.7	-6.2	13.0
H	330 - 327	0.0	10.0	1.2	-0.7	-1.5	-0.1	10.3	1.0	-0.1	10.4
I	244 - 241	-0.1	2.0	8.7	-0.1	-0.6	0.0	8.8	1.9	-0.1	8.9
J	550 - 547	-0.2	10.3	12.7	-0.8	-0.8	0.0	12.9	10.1	-0.2	13.2
K	344 - 341	-0.1	2.4	13.0	-0.2	-0.4	0.0	13.0	2.4	-0.1	13.1
L	740 - 737	-0.3	7.7	18.3	-1.2	0.0	0.0	18.3	7.9	-0.4	18.8
M	663 - 63	-0.4	3.4	16.6	1.1	0.0	0.0	16.6	3.7	-0.7	17.3
N	1877 - 1277	-0.2	10.3	10.9	-0.8	0.9	0.0	11.6	9.7	-0.2	11.9
O	647 - 47	-0.1	2.3	14.6	-0.2	0.3	0.0	14.6	2.3	-0.1	14.7
P	1840 - 1240	-0.1	10.5	0.4	-0.7	1.5	0.1	10.8	0.3	-0.2	11.0
Q	628 - 28	-0.2	3.2	11.8	-0.3	0.5	0.1	11.8	3.2	-0.2	12.0
R	1816 - 1216	-3.5	-10.2	-4.5	0.7	0.8	-1.6	-2.3	-5.5	-10.4	8.1
S	616 - 16	0.8	-2.4	8.6	0.1	0.4	0.1	8.7	0.8	-2.5	11.1
T	811 - 11	-6.2	-11.5	1.7	0.6	0.3	-3.2	2.9	-7.2	-11.6	14.5
U	43058 - 43051	-2.9	-3.8	-1.4	0.1	-0.1	-1.2	-0.7	-3.6	-3.8	3.0
V	50024 - 50021	-6.1	-5.2	-0.3	0.1	0.0	0.0	-0.3	-5.2	-6.1	5.7
W	43278 - 43271	-1.3	-2.7	0.0	0.0	-0.2	0.2	0.1	-1.3	-2.8	2.8
X	50084 - 50081	-0.1	-6.1	0.0	0.0	0.0	0.2	0.1	-0.3	-6.1	6.2

<sup>1</sup> Refer to Figure 2.10.2-34 for the identification of the representative sections.

Table 2.10.4-132  $P_m + P_b$  Stresses; 30-Foot Side Drop; Drop Orientation = 90 Degrees; 3-D Model; 0-Degree Circumferential Location; Condition 1

Condition 1: 100°F Ambient with Contents

Section <sup>1</sup>	Node - Node	Stress Components (ksi)						Principal Stresses (ksi)			
		$S_x$	$S_y$	$S_z$	$S_{xy}$	$S_{yz}$	$S_{zx}$	S1	S2	S3	S.I.
A O	1130 - 1128	-1.3	-4.4	0.3	0.0	0.1	0.0	0.3	-1.3	-4.4	4.7
B O	1185 - 1183	0.4	-6.7	0.0	-0.1	0.1	-0.2	0.5	-0.1	-6.7	7.2
C I	90 - 40	1.0	-5.7	7.3	0.0	-0.6	0.0	7.3	1.0	-5.7	13.1
D I	25 - 5	-5.9	-10.0	5.0	0.2	-0.1	-0.1	5.0	-5.9	-10.0	15.0
E I	35 - 31	-8.8	-10.8	5.3	0.3	-0.1	2.0	5.5	-9.1	-10.9	16.4
F O	100 - 97	0.3	-16.9	-32.8	1.2	-0.6	3.8	0.8	-16.9	-33.3	34.1
G I	94 - 91	1.3	-3.3	17.2	0.3	-0.5	3.4	17.9	0.6	-3.3	21.2
H O	330 - 327	0.2	12.7	7.1	-0.8	-1.4	-0.4	13.0	6.8	0.1	12.9
I O	244 - 241	0.0	4.3	12.6	-0.3	-0.4	0.0	12.6	4.3	0.0	12.6
J O	550 - 547	-0.1	12.7	14.6	-0.9	-0.7	0.0	14.8	12.5	-0.1	14.9
K O	344 - 341	0.0	6.1	14.7	-0.5	-0.3	0.0	14.7	6.1	-0.1	14.8
L O	740 - 737	-0.1	10.6	20.0	-2.6	0.0	0.0	20.0	11.2	-0.7	20.7
M O	663 - 63	0.5	9.3	19.3	2.2	0.0	0.0	19.3	9.8	0.0	19.3
N O	1877 - 1277	-0.1	13.0	12.7	-1.0	0.9	0.0	13.8	12.0	-0.1	13.9
O O	647 - 47	0.0	6.2	16.5	-0.5	0.2	0.0	16.5	6.2	-0.1	16.6
P O	1840 - 1240	0.2	13.4	5.4	-0.8	1.5	0.3	13.7	5.2	0.1	13.6
Q O	628 - 28	0.0	6.0	15.2	-0.4	0.3	0.1	15.2	6.0	0.0	15.2
R I	1816 - 1216	-0.5	-7.4	5.9	0.5	1.2	0.5	6.1	-0.5	-7.5	13.6
S O	616 - 16	-0.3	-0.3	15.8	0.0	0.2	0.4	15.8	-0.2	-0.3	16.1
T O	811 - 11	3.2	-3.4	19.6	0.3	0.1	-0.8	19.6	3.1	-3.4	23.0
U O	43058 - 43051	-11.9	-7.5	-1.7	-0.1	-0.2	-2.5	-1.1	-7.5	-12.5	11.4
V O	50024 - 50021	-14.8	-9.0	0.0	0.0	0.0	0.1	0.0	-9.0	-14.8	14.7
W I	43278 - 43271	-2.2	-3.2	0.1	-0.1	-0.1	0.2	0.1	-2.2	-3.3	3.4
X O	50084 - 50081	0.4	-6.6	0.0	0.0	-0.1	0.2	0.5	-0.1	-6.6	7.1

<sup>1</sup> Refer to Figure 2.10.2-34 for the identification of the representative sections.

Table 2.10.4-133 Critical  $P_m$  Stress Summary; 30-Foot Side Drop; Drop Orientation = 90 Degrees; 3-D Model; Condition 1

Condition 1: 100°F Ambient with Contents

Comp. No. <sup>1</sup>	Section Cut Node-Node	$P_m$ Stresses (ksi)							Principal Stresses (ksi)				Allow. Stress	Margin of Safety
		$S_x$	$S_y$	$S_z$	$S_{xy}$	$S_{yz}$	$S_{zx}$	$S_{\theta}$	S1	S2	S3	S.L.		
1	25- 5	-8.8	-11.0	2.4	0.2	-0.1	-0.3	2.4	-8.8	-11.0	13.4	45.6	2.4	
2	16140-16137	0.0	1.3	1.1	0.0	-12.4	-0.2	13.7	0.0	-11.1	24.8	44.9	0.8	
3	14340-14337	-0.1	3.9	0.7	0.2	-15.4	-0.1	17.8	-0.1	-13.2	31.0	66.0	1.1	
4	14520-14517	-0.1	3.7	0.9	0.0	-10.7	0.0	13.1	-0.1	-8.5	21.6	45.8	1.1	
5	662- 62	0.2	2.9	16.7	-2.6	0.0	0.1	16.7	4.5	-1.4	18.0	46.4	1.6	
6	401- 1	-10.7	-35.3	0.1	1.8	0.2	1.6	0.4	-10.8	-35.6	36.0	49.3	0.4	
7	43071-43031	-12.0	-6.9	-0.3	-0.1	-0.2	-2.0	-0.1	-6.9	-12.3	12.2	48.0	2.9	
8	51501-51504	-4.5	-3.3	3.2	0.2	0.1	0.1	3.2	-3.3	-4.6	7.8	94.5	11.1	

Locations of the most critical sections for each component are provided in the following:

Comp. No. <sup>1</sup>	Section Location					
	Inside Node			Outside Node		
	x (in)	y (deg)	z (in)	x (in)	y (deg)	z (in)
1	39.44	0.0	6.20	39.44	0.0	0.75
2	35.50	79.4	17.40	37.50	79.4	17.40
3	35.50	67.7	29.90	37.00	67.7	29.90
4	35.50	67.7	47.40	37.00	67.7	47.40
5	40.70	0.0	99.50	43.35	0.0	99.50
6	40.88	0.0	193.71	43.35	0.0	193.71
7	33.71	0.0	185.40	36.46	0.0	185.40
8	40.88	180.0	193.71	40.88	180.0	188.40

<sup>1</sup> Refer to Figure 2.10.2-33 for cask component identification.

Table 2.10.4-134 Critical  $P_m + P_b$  Stress Summary; 30-Foot Side Drop; Drop Orientation = 90 Degrees; 3-D Model; Condition 1

Condition 1: 100°F Ambient with Contents

Comp. No. <sup>1</sup>	Section Cnt Node-Node	$P_m + P_b$ Stresses (ksi)							Principal Stresses (ksi)				ABow. Stress	Margin of Safety
		$S_x$	$S_y$	$S_z$	$S_{xy}$	$S_{yz}$	$S_{xz}$	$S_1$	$S_2$	$S_3$	S.I.			
1	25- 5	-5.9	-10.0	5.0	0.2	-0.1	-0.1	5.0	-5.9	-10.0	15.0	65.2	3.3	
2	100- 97	0.3	-16.9	-32.8	1.2	-0.6	3.8	0.8	-16.9	-33.3	34.1	64.2	0.9	
3	12350-12347	-0.2	6.0	-0.7	0.0	-16.0	-0.1	18.9	-0.2	-13.7	32.6	94.3	1.9	
4	14520-14517	-0.2	6.4	1.9	0.0	-11.4	0.0	15.7	-0.2	-7.5	23.2	65.5	1.8	
5	662- 62	0.5	8.5	19.6	-2.9	0.0	0.0	19.6	9.5	-0.4	20.0	66.4	2.3	
6	403- 3	-7.4	-27.7	21.2	1.5	0.5	3.4	21.6	-7.7	-27.8	49.4	70.9	0.4	
7	43001-43008	-20.3	-7.0	10.0	-0.7	0.3	1.0	10.1	-7.0	-20.3	30.4	69.8	1.3	
8	51501-51504	-13.3	-7.9	4.9	0.7	0.0	0.8	4.9	-7.8	-13.3	18.4	135.0	6.3	

Locations of the most critical sections for each component are provided in the following:

Comp. No. <sup>1</sup>	Section Location Inside Node			Outside Node		
	x (in)	y (deg)	z (in)	x (in)	y (deg)	z (in)
1	39.44	0.0	6.20	39.44	0.0	0.75
2	35.50	0.0	15.00	37.50	0.0	15.00
3	35.50	56.5	30.40	37.00	56.5	30.40
4	35.50	67.7	142.40	37.00	67.7	142.40
5	40.70	0.0	99.50	43.35	0.0	99.50
6	40.88	0.0	190.15	43.35	0.0	190.15
7	39.53	0.0	185.40	39.53	0.0	179.40
8	40.88	180.0	193.71	40.88	180.0	188.40

<sup>1</sup> Refer to Figure 2.10.2-33 for cask component identification.

Table 2.10.4-135  $P_m$  Stresses; 30-Foot Side Drop; Drop Orientation = 90 Degrees; 3-D Model; 45.9-Degree Circumferential Location; Condition 1

Condition 1: 100°F Ambient with Contents

Section <sup>1</sup>	Node - Node	Stress Components (ksi)						Principal Stresses (ksi)			
		$S_x$	$S_y$	$S_z$	$S_{xy}$	$S_{yz}$	$S_{xz}$	S1	S2	S3	S.L
A	1130 - 1128	-1.0	-3.2	0.0	-0.1	0.1	0.0	0.0	-1.0	-3.2	3.1
B	1185 - 1183	-0.3	-6.0	0.0	-0.1	0.0	-0.2	0.1	-0.4	-6.0	6.0
C	10090 - 10040	-4.1	-5.9	0.9	-1.1	-2.4	0.0	1.7	-3.7	-7.1	8.8
D	10025 - 10005	-5.2	-8.2	1.7	-0.2	-0.9	-0.2	1.8	-5.2	-8.2	10.0
E	10035 - 10031	-5.3	-7.8	0.3	0.8	-1.7	1.1	0.8	-5.1	-8.5	9.3
F	10100 - 10097	-0.4	-4.6	-2.5	-0.1	-9.7	1.5	6.5	-0.6	-13.4	19.9
G	10094 - 10091	0.4	-2.5	3.8	-0.3	-4.2	0.7	6.0	0.3	-4.6	10.7
H	10330 - 10327	0.0	6.8	0.7	0.4	-13.4	-0.1	17.5	0.0	-10.0	27.5
I	10244 - 10241	0.0	1.5	4.9	-0.1	-5.1	0.0	8.5	0.0	-2.1	10.6
J	10550 - 10547	0.0	6.7	6.3	0.0	-7.4	0.0	13.9	0.0	-0.9	14.9
K	10344 - 10341	0.0	1.6	6.4	-0.1	-3.3	0.0	8.0	0.1	-0.1	8.1
L	10740 - 10737	0.1	5.7	9.9	0.1	0.1	0.0	10.0	5.7	0.1	9.8
M	10663 - 10063	0.1	2.0	7.6	-0.6	-0.2	0.0	7.7	2.2	-0.1	7.8
N	11877 - 11277	0.0	6.7	5.4	0.0	8.4	0.0	14.5	0.0	-2.4	16.9
O	10647 - 10047	0.0	1.6	7.1	-0.1	2.5	0.0	8.1	0.6	0.0	8.1
P	11840 - 11240	0.0	7.0	0.7	0.4	13.5	0.0	17.7	0.0	-10.0	27.7
Q	10628 - 10028	0.0	2.0	6.0	-0.1	4.1	0.0	8.6	0.0	-0.5	9.1
R	11816 - 11216	-1.4	-3.3	-1.7	1.9	8.8	-0.8	6.4	-1.0	-11.7	18.1
S	10616 - 10016	-0.3	-1.2	5.0	-1.3	3.7	0.1	6.7	0.2	-3.4	10.1
T	10811 - 10011	-3.4	-6.6	1.2	1.8	4.7	-1.5	3.5	-2.6	-9.7	13.1
U	44558 - 44551	-2.3	-2.7	-1.2	-0.1	-0.1	-0.9	-0.7	-2.6	-2.9	2.2
V	50524 - 50521	-3.1	-3.4	-0.2	0.9	0.2	-0.1	-0.2	-2.3	-4.2	3.9
W	43278 - 43271	-1.3	-2.7	0.0	0.0	-0.2	0.2	0.1	-1.3	-2.8	2.8
X	50084 - 50081	-0.1	-6.1	0.0	0.0	0.0	0.2	0.1	-0.3	-6.1	6.2

<sup>1</sup> Refer to Figure 2.10.2-34 for the identification of the representative sections.

Table 2.10.4-136  $P_m + P_b$  Stresses; 30-Foot Side Drop; Drop Orientation = 90 Degrees; 3-D Model; 45.9-Degree Circumferential Location; Condition 1

Condition 1: 100°F Ambient with Contents

Section <sup>1</sup>	Node - Node	Stress Components (ksi)						Principal Stresses (ksi)			
		$S_x$	$S_y$	$S_z$	$S_{xy}$	$S_{yz}$	$S_{zx}$	S1	S2	S3	S.I.
A O	1130 - 1128	-1.3	-4.4	0.3	0.0	0.1	0.0	0.3	-1.3	-4.4	4.7
B O	1185 - 1183	0.4	-6.7	0.0	-0.1	0.1	-0.2	0.5	-0.1	-6.7	7.2
C I	10090 - 10040	-0.3	-3.1	3.2	-4.3	-5.5	0.0	7.1	0.8	-8.1	15.3
D I	10025 - 10005	-2.9	-6.6	3.4	-1.3	-1.8	0.1	3.8	-2.6	-7.3	11.1
E I	10035 - 10031	-5.8	-7.1	3.3	1.9	-2.9	1.6	4.1	-4.4	-9.3	13.4
F I	10100 - 10097	-1.0	-1.4	9.9	-0.2	-11.7	1.0	17.3	-1.0	-8.8	26.1
G I	10094 - 10091	0.5	-2.0	5.5	-0.4	-6.6	1.3	9.5	0.4	-5.9	15.4
H I	10330 - 10327	-0.1	6.1	-2.2	0.0	-14.5	0.1	17.0	-0.1	-13.2	30.2
I I	10244 - 10241	-0.1	1.2	3.3	-0.2	-6.8	0.0	9.2	-0.1	-4.7	13.9
J I	10550 - 10547	-0.1	6.4	6.0	-0.1	-8.2	0.0	14.4	-0.1	-2.0	16.3
K I	10344 - 10341	0.0	2.0	6.2	-0.2	-4.2	0.0	8.8	0.0	-0.6	9.4
L O	10740 - 10737	0.2	6.9	10.6	0.2	0.2	0.0	10.6	6.9	0.2	10.4
M O	10663 - 10063	-0.1	0.6	7.4	-0.9	-0.2	0.0	7.4	1.2	-0.8	8.1
N I	11877 - 11277	-0.1	6.6	5.2	-0.1	9.2	0.0	15.2	-0.1	-3.4	18.5
O I	10647 - 10047	0.0	2.0	7.0	-0.2	3.4	0.0	8.7	0.3	-0.1	8.8
P I	11840 - 11240	-0.1	6.6	-1.4	0.0	14.5	-0.1	17.6	-0.1	-12.4	30.0
Q I	10628 - 10028	-0.1	2.2	5.4	-0.2	5.7	0.0	9.7	-0.1	-2.1	11.9
R I	11816 - 11216	-0.3	-2.0	1.9	0.0	10.6	0.1	10.7	-0.3	-10.8	21.5
S I	10616 - 10016	-0.4	-2.9	-2.0	-3.0	5.6	0.3	4.1	-0.5	-8.7	12.8
T I	10811 - 10011	-8.6	-11.2	-10.7	4.9	8.7	-2.9	-1.9	-6.7	-21.9	20.0
U O	44558 - 44551	-8.6	-6.1	-1.4	1.3	-0.3	-1.8	-0.9	-5.8	-9.4	8.5
V O	50524 - 50521	-9.0	-6.7	0.1	2.9	0.2	-0.1	0.1	-4.7	-11.0	11.1
W I	43278 - 43271	-2.2	-3.2	0.1	-0.1	-0.1	0.2	0.1	-2.2	-3.3	3.4
X O	50084 - 50081	0.4	-6.6	0.0	0.0	-0.1	0.2	0.5	-0.1	-6.6	7.1

<sup>1</sup> Refer to Figure 2.10.2-34 for the identification of the representative sections.

Table 2.10.4-137  $P_m$  Stresses; 30-Foot Side Drop; Drop Orientation = 90 Degrees; 3-D Model; 91.7-Degree Circumferential Location; Condition 1

Condition 1: 100°F Ambient with Contents

Section <sup>1</sup>	Node - Node	Stress Components (ksi)						Principal Stresses (ksi)			
		$S_x$	$S_y$	$S_z$	$S_{xy}$	$S_{yz}$	$S_{xz}$	S1	S2	S3	S.L.
A	1130 - 1128	-1.0	-3.2	0.0	-0.1	0.1	0.0	0.0	-1.0	-3.2	3.1
B	1185 - 1183	-0.3	-6.0	0.0	-0.1	0.0	-0.2	0.1	-0.4	-6.0	6.0
C	18090 - 18040	-0.6	-0.4	-0.7	-1.5	-2.7	0.1	2.6	-0.7	-3.6	6.2
D	18025 - 18005	0.1	-2.0	0.4	-2.3	-2.0	0.0	2.4	0.3	-4.1	6.5
E	18035 - 18031	0.3	-0.1	0.2	0.8	-4.0	0.1	4.1	0.3	-4.1	8.2
F	18100 - 18097	0.1	2.3	1.9	-0.1	-11.6	-0.8	13.7	0.2	-9.5	23.2
G	18094 - 18091	-0.5	1.7	-1.1	-0.4	-4.9	-0.6	5.4	-0.4	-4.9	10.3
H	18330 - 18327	0.0	0.4	0.2	0.6	-14.1	0.0	14.4	0.0	-13.8	28.1
I	18244 - 18241	0.0	0.5	-1.9	0.0	-4.5	-0.1	4.0	0.0	-5.3	9.3
J	18550 - 18547	0.1	0.7	-3.2	0.1	-8.2	0.0	7.2	0.1	-9.7	16.9
K	18344 - 18341	0.0	0.1	-3.6	0.1	-2.9	0.0	1.7	0.0	-5.2	6.9
L	19908 - 19308	0.6	0.8	-4.9	0.8	0.8	0.0	1.6	-0.1	-5.0	6.6
M	18663 - 18063	0.4	-0.1	-4.7	0.5	-0.3	0.0	0.7	-0.4	-4.7	5.4
N	19877 - 19277	0.1	0.7	-2.7	0.1	8.9	0.0	8.1	0.1	-10.1	18.2
O	18647 - 18047	0.0	0.1	-4.0	0.1	2.4	0.0	1.2	0.0	-5.1	6.3
P	19840 - 19240	0.1	0.4	0.5	0.6	13.8	0.0	14.3	0.1	-13.4	27.7
Q	18628 - 18028	0.0	0.4	-3.0	0.0	3.9	0.0	2.9	0.0	-5.5	8.4
R	19816 - 19216	1.7	5.3	1.2	3.1	9.8	0.7	13.9	1.2	-7.1	21.0
S	18616 - 18016	-1.2	1.7	-1.9	-0.5	3.9	0.2	4.2	-1.2	-4.5	8.7
T	18811 - 18011	0.5	2.0	-0.3	2.0	5.8	1.0	7.5	-0.1	-5.1	12.6
U	45758 - 45751	-1.4	-1.9	-2.4	-0.5	0.2	0.2	-1.1	-1.9	-2.6	1.5
V	50924 - 50921	-0.1	-1.7	-0.5	-0.3	0.2	-0.1	0.0	-0.5	-1.8	1.8
W	43278 - 43271	-1.3	-2.7	0.0	0.0	-0.2	0.2	0.1	-1.3	-2.8	2.8
X	50084 - 50081	-0.1	-6.1	0.0	0.0	0.0	0.2	0.1	-0.3	-6.1	6.2

<sup>1</sup> Refer to Figure 2.10.2-34 for the identification of the representative sections.



Table 2.10.4-138  $P_m + P_b$  Stresses; 30-Foot Side Drop; Drop Orientation = 90 Degrees; 3-D Model; 91.7-Degree Circumferential Location; Condition 1

Condition 1: 100°F Ambient with Contents

Section <sup>1</sup>	Node - Node	Stress Components (ksi)						Principal Stresses (ksi)			
		$S_x$	$S_y$	$S_z$	$S_{xy}$	$S_{yz}$	$S_{xz}$	S1	S2	S3	S.I.
A O	1130 - 1128	-1.3	-4.4	0.3	0.0	0.1	0.0	0.3	-1.3	-4.4	4.7
B O	1185 - 1183	0.4	-6.7	0.0	-0.1	0.1	-0.2	0.5	-0.1	-6.7	7.2
C I	18090 - 18040	-1.4	0.4	-2.4	-4.1	-6.1	0.0	6.6	-1.7	-8.3	14.9
D I	18025 - 18005	0.3	-0.9	0.9	-3.5	-3.8	0.0	5.1	0.6	-5.4	10.5
E I	18035 - 18031	0.5	-0.2	1.2	2.2	-4.9	0.0	5.8	0.6	-5.0	10.8
F I	18100 - 18097	0.3	-0.2	-7.7	-0.2	-12.4	-0.6	9.0	0.4	-16.9	25.9
G I	18094 - 18091	-0.4	-0.1	-8.2	-0.5	-5.6	-1.2	2.7	-0.3	-11.2	13.9
H O	18330 - 18327	0.1	-0.9	-0.8	1.1	-14.4	0.0	13.6	0.1	-15.2	28.8
I O	18244 - 18241	0.0	-0.8	-3.1	0.0	-4.8	-0.1	3.0	0.0	-6.9	9.9
J I	18550 - 18547	0.1	3.1	-2.2	0.1	-8.1	0.0	9.0	0.1	-8.1	17.1
K I	18344 - 18341	0.0	2.8	-2.3	0.1	-2.7	0.0	4.0	0.0	-3.4	7.4
L I	19908 - 19308	0.9	5.4	-3.3	0.3	0.8	0.0	5.5	0.9	-3.4	8.9
M I	18663 - 18063	0.9	4.3	-3.0	0.2	-0.3	0.0	4.3	0.9	-3.0	7.3
N I	19877 - 19277	0.1	3.2	-1.7	0.1	8.8	0.0	9.9	0.1	-8.4	18.2
O I	18647 - 18047	0.0	3.1	-2.6	0.1	2.2	0.0	3.8	0.0	-3.3	7.1
P O	19840 - 19240	0.1	-1.2	-1.1	1.1	14.2	-0.1	13.1	0.1	-15.4	28.5
Q O	18628 - 18028	0.0	-1.5	-4.5	0.0	4.2	0.0	1.5	0.0	-7.5	9.0
R O	19816 - 19216	3.3	7.1	8.5	6.4	9.5	1.9	19.4	3.3	-3.8	23.2
S I	18616 - 18016	-2.6	0.9	-5.2	-1.2	4.1	0.8	3.0	-2.3	-7.6	10.6
T I	18811 - 18011	1.5	2.7	-0.1	5.0	7.8	1.8	11.7	-0.5	-7.1	18.8
U I	45758 - 45751	-3.8	-2.3	-3.5	-1.7	0.2	1.0	-1.2	-3.1	-5.4	4.2
V I	50924 - 50921	0.0	-1.3	-1.4	-1.5	0.2	-0.2	1.0	-1.4	-2.3	3.3
W I	43278 - 43271	-2.2	-3.2	0.1	-0.1	-0.1	0.2	0.1	-2.2	-3.3	3.4
X O	50084 - 50081	0.4	-6.6	0.0	0.0	-0.1	0.2	0.5	-0.1	-6.6	7.1

<sup>1</sup> Refer to Figure 2.10.2-34 for the identification of the representative sections.

Table 2.10.4-139 P<sub>m</sub> Stresses; 30-Foot Side Drop; Drop Orientation = 90 Degrees; 3-D Model; 180-Degree Circumferential Location; Condition 1

Condition 1: 100°F Ambient with Contents

Section <sup>1</sup>	Node - Node	Stress Components (ksi)						Principal Stresses (ksi)			
		S <sub>x</sub>	S <sub>y</sub>	S <sub>z</sub>	S <sub>xy</sub>	S <sub>yz</sub>	S <sub>xz</sub>	S1	S2	S3	S.L.
A	1130 - 1128	-1.0	-3.2	0.0	-0.1	0.1	0.0	0.0	-1.0	-3.2	3.1
B	1185 - 1183	-0.3	-6.0	0.0	-0.1	0.0	-0.2	0.1	-0.4	-6.0	6.0
C	30090 - 30040	0.0	2.4	-0.9	0.3	-0.3	0.0	2.5	-0.1	-0.9	3.4
D	30025 - 30005	-2.4	4.2	-0.4	0.3	-0.2	0.0	4.2	-0.5	-2.4	6.6
E	30035 - 30031	1.6	3.0	-0.8	0.3	-0.6	-1.3	3.3	1.9	-1.4	4.7
F	30100 - 30097	0.2	2.5	1.7	0.4	-1.1	-1.4	3.6	1.3	-0.7	4.3
G	30094 - 30091	-0.2	0.6	-4.0	0.1	-0.6	-0.2	0.6	-0.2	-4.1	4.7
H	30330 - 30327	-0.2	-5.4	-1.9	-0.7	-1.3	0.0	0.0	-1.5	-6.0	5.9
I	30244 - 30241	0.0	-0.9	-5.1	-0.1	-0.4	0.0	0.0	-0.9	-5.2	5.2
J	30550 - 30547	-0.4	-4.4	-7.2	-0.6	-0.8	-0.1	-0.4	-4.2	-7.4	7.1
K	30344 - 30341	0.0	-0.9	-6.3	-0.1	-0.2	0.0	0.0	-0.9	-6.3	6.3
L	30740 - 30737	0.0	-4.0	-10.4	0.4	0.0	0.0	0.1	-4.1	-10.4	10.5
M	30663 - 30063	-0.4	-0.6	-7.2	-1.3	0.0	0.0	0.7	-1.8	-7.2	8.0
N	31877 - 31277	-0.4	-4.4	-5.6	-0.6	0.9	0.0	-0.3	-4.0	-6.0	5.7
O	30647 - 30047	0.0	-0.9	-6.9	-0.1	0.1	0.0	0.0	-0.9	-6.9	6.9
P	31840 - 31240	-0.4	-5.7	-1.0	-0.8	1.3	-0.1	-0.1	-0.8	-6.2	6.1
Q	30628 - 30028	0.0	-1.5	-6.1	-0.2	0.3	-0.1	0.0	-1.5	-6.1	6.2
R	31816 - 31216	1.3	6.6	1.3	1.1	0.8	1.3	7.0	2.2	-0.1	7.0
S	30616 - 30016	-0.3	4.3	-5.1	0.7	0.4	0.1	4.4	-0.4	-5.1	9.6
T	30811 - 30011	0.4	9.6	-2.1	1.6	0.6	1.1	9.9	0.5	-2.5	12.4
U	47558 - 47551	-3.1	-3.8	-3.7	-0.1	0.0	0.2	-3.0	-3.7	-3.9	0.9
V	51524 - 51521	-4.5	-3.5	-0.2	-0.1	0.0	0.4	-0.2	-3.5	-4.6	4.4
W	43278 - 43271	-1.3	-2.7	0.0	0.0	-0.2	0.2	0.1	-1.3	-2.8	2.8
X	50084 - 50081	-0.1	-6.1	0.0	0.0	0.0	0.2	0.1	-0.3	-6.1	6.2

<sup>1</sup> Refer to Figure 2.10.2-34 for the identification of the representative sections.

Table 2.10.4-140  $P_m + P_b$  Stresses; 30-Foot Side Drop; Drop Orientation = 90 Degrees; 3-D Model; 180-Degree Circumferential Location; Condition 1

Condition 1: 100°F Ambient with Contents

Section <sup>1</sup>	Node - Node	Stress Components (ksi)						Principal Stresses (ksi)			
		$S_x$	$S_y$	$S_z$	$S_{xy}$	$S_{yz}$	$S_{zx}$	S1	S2	S3	S.I.
A O	1130 - 1128	-1.3	-4.4	0.3	0.0	0.1	0.0	0.3	-1.3	-4.4	4.7
B O	1185 - 1183	0.4	-6.7	0.0	-0.1	0.1	-0.2	0.5	-0.1	-6.7	7.2
C I	30090 - 30040	-2.1	0.5	-3.0	0.1	-0.6	-0.2	0.6	-2.1	-3.1	3.7
D O	30025 - 30005	-1.9	5.7	-0.7	0.2	-0.1	0.8	5.7	-0.3	-2.3	8.0
E O	30035 - 30031	-0.4	1.6	-3.4	0.3	-0.7	-0.7	1.7	-0.3	-3.6	5.3
F O	30100 - 30097	-0.1	5.2	12.1	0.9	-1.2	-1.5	12.5	5.1	-0.4	12.9
G I	30094 - 30091	-0.1	0.3	-4.6	0.0	-0.5	-0.4	0.3	-0.1	-4.7	5.0
H O	30330 - 30327	-0.2	-5.2	-3.3	-0.7	-1.5	0.1	0.0	-2.6	-6.1	6.0
I O	30244 - 30241	0.0	-0.4	-5.6	-0.1	-0.5	0.0	0.0	-0.3	-5.6	5.7
J I	30550 - 30547	-0.3	-5.9	-7.6	-0.8	-0.7	-0.1	-0.2	-5.8	-7.8	7.7
K I	30344 - 30341	-0.1	-2.3	-6.7	-0.3	-0.2	0.0	0.0	-2.4	-6.7	6.7
L O	31908 - 31308	-0.9	0.0	-8.5	-4.1	0.1	0.0	3.7	-4.6	-8.5	12.2
M O	30663 - 30063	-0.3	1.9	-6.5	-2.1	0.0	0.0	3.2	-1.5	-6.5	9.7
N I	31877 - 31277	-0.2	-6.0	-5.9	-0.8	0.8	0.1	-0.1	-5.2	-6.8	6.7
O I	30647 - 30047	-0.1	-2.5	-7.4	-0.4	0.1	0.0	0.0	-2.5	-7.4	7.3
P I	31840 - 31240	-0.1	-5.9	0.9	-0.9	1.2	0.0	1.1	0.0	-6.3	7.4
Q O	30628 - 30028	0.0	-0.9	-7.4	-0.1	0.4	-0.1	0.0	-0.9	-7.4	7.4
R I	31816 - 31216	0.3	4.8	-4.2	0.7	1.0	0.3	5.0	0.2	-4.3	9.3
S O	30616 - 30016	0.1	3.4	-10.0	0.5	0.4	0.2	3.5	0.1	-10.0	13.5
T O	30811 - 30011	-1.0	7.0	-10.5	1.1	0.6	-0.5	7.2	-1.1	-10.5	17.7
U O	47558 - 47551	3.6	1.5	-1.0	-0.3	0.3	-1.2	4.0	1.5	-1.3	5.3
V I	51524 - 51521	-11.7	-8.5	-0.5	0.1	0.0	0.4	-0.5	-8.5	-11.7	11.2
W I	43278 - 43271	-2.2	-3.2	0.1	-0.1	-0.1	0.2	0.1	-2.2	-3.3	3.4
X O	50084 - 50081	0.4	-6.6	0.0	0.0	-0.1	0.2	0.5	-0.1	-6.6	7.1

<sup>1</sup> Refer to Figure 2.10.2-34 for the identification of the representative sections.

Table 2.10.4-141 Primary Stresses; 30-Foot Top Corner Drop; Drop Orientation = 24 Degrees; 3-D Top Model; 0-Degree Circumferential Location; Condition 1

Condition 1: 100°F Ambient with Contents

Stress Points		Stress Components (ksi)						Principal Stresses (ksi)		
Section <sup>1</sup>	Node	S <sub>x</sub>	S <sub>y</sub>	S <sub>z</sub>	S <sub>xy</sub>	S <sub>yz</sub>	S <sub>xz</sub>	S1	S2	S3
A1	1949	1.7	2.7	-0.3	0.0	-0.1	0.3	2.7	1.8	-0.4
A2	1950	1.0	1.7	-0.3	0.0	-0.1	0.3	1.8	1.0	-0.4
A3	1951	-0.4	-0.3	0.4	0.0	0.1	0.2	0.4	-0.3	-0.4
B1	1952	0.0	0.0	-0.5	0.0	0.1	0.1	0.1	0.0	-0.6
B2	93	-1.6	-2.5	1.0	-0.1	0.0	0.3	1.0	-1.6	-2.5
C1	1925	-0.2	0.0	1.3	-0.1	-0.1	0.0	1.3	0.0	-0.2
C2	1926	0.3	-0.3	0.0	0.0	-0.1	-0.3	0.5	-0.2	-0.3
C3	1927	0.5	-0.2	-0.1	0.0	0.0	-0.2	0.6	-0.2	-0.2
D1	683	-0.1	-0.5	-0.5	0.1	0.0	0.0	-0.1	-0.5	-0.5
D2	85	-0.2	-0.9	-0.4	0.2	0.0	0.0	-0.1	-0.4	-1.0
E1	682	0.4	-0.3	-0.6	0.1	0.0	0.2	0.5	-0.3	-0.6
E2	82	0.4	-0.1	0.6	0.1	0.1	0.2	0.7	0.3	-0.1
F1	1925	-0.2	0.0	1.3	-0.1	-0.1	0.0	1.3	0.0	-0.2
F2	1325	-1.2	-2.2	-5.6	0.1	-0.1	0.4	-1.2	-2.2	-5.7
G1	680	-0.4	0.0	1.2	0.0	0.0	0.6	1.4	0.0	-0.6
G2	80	0.3	-0.1	-0.2	0.0	0.0	0.0	0.3	-0.1	-0.2
H1	1921	0.0	3.6	-3.9	-0.2	-0.4	0.1	3.6	0.0	-3.9
H2	1321	-0.1	5.3	-1.2	-0.3	-0.3	0.0	5.3	-0.1	-1.2
I1	676	0.0	-0.3	-0.1	0.0	-0.1	0.0	0.0	-0.1	-0.3
I2	76	0.0	1.4	1.1	-0.1	0.0	0.0	1.4	1.1	0.0
J1	1916	-0.1	3.3	-1.4	-0.2	-0.2	0.0	3.4	-0.1	-1.4
J2	1316	-0.1	6.4	0.1	-0.5	-0.1	0.0	6.4	0.1	-0.1
K1	671	0.0	-0.7	-0.9	0.0	0.0	0.0	0.0	-0.7	-0.9
K2	71	0.0	2.1	0.5	-0.2	0.1	0.0	2.1	0.5	0.0
L1	1908	-0.7	1.8	-3.9	-0.2	0.3	0.0	1.9	-0.7	-3.9
L2	1308	0.1	7.9	-1.6	1.7	0.3	0.0	8.3	-0.2	-1.6
M1	663	-0.4	-0.9	-3.2	0.0	0.2	0.0	-0.4	-0.8	-3.2
M2	63	0.2	2.7	-1.8	0.7	0.2	0.0	2.9	0.0	-1.8

Table 2.10.4-141 Primary Stresses; 30-Foot Top Corner Drop; Drop Orientation = 24 Degrees; 3-D Top Model; 0-Degree Circumferential Location; Condition 1 (continued)

Stress Points Section <sup>1</sup> Node	Stress Components (ksi)							Principal Stresses (ksi)		
	S <sub>x</sub>	S <sub>y</sub>	S <sub>z</sub>	S <sub>xy</sub>	S <sub>yz</sub>	S <sub>xz</sub>	S <sub>xx</sub>	S1	S2	S3
N1	1877	-0.1	2.5	-12.2	-0.2	0.7	0.0	2.6	-0.2	-12.3
N2	1477	-0.1	4.9	-11.3	-0.4	0.7	0.0	4.9	-0.1	-11.3
N3	1277	0.0	7.1	-10.4	-0.5	0.6	0.0	7.2	-0.1	-10.4
O1	647	-0.1	-0.3	-6.5	0.0	0.3	0.0	-0.1	-0.3	-6.5
O2	247	0.0	1.0	-6.0	-0.1	0.2	0.0	1.0	0.0	-6.0
O3	47	0.0	2.3	-5.6	-0.2	0.2	0.0	2.3	0.0	-5.6
P1	1840	-0.3	3.9	-13.7	-0.3	1.0	0.1	4.0	-0.3	-13.8
P2	1640	-0.5	3.8	-16.5	-0.3	0.9	0.0	3.9	-0.5	-16.6
P3	1440	-0.5	3.8	-19.1	-0.3	0.8	-0.6	3.9	-0.5	-19.1
P4	1240	-0.5	3.1	-24.5	-0.2	0.7	-1.3	3.1	-0.4	-24.6
Q1	628	-0.2	2.7	-7.9	-0.2	0.4	0.1	2.8	-0.2	-7.9
Q2	428	-0.1	3.1	-8.2	-0.2	0.3	0.1	3.1	-0.1	-8.3
Q3	228	0.0	3.4	-8.6	-0.3	0.3	0.1	3.4	-0.1	-8.6
Q4	28	0.0	3.7	-8.9	-0.3	0.2	0.0	3.7	0.0	-8.9
R1	1816	0.0	-3.3	-29.9	0.3	0.6	0.1	0.0	-3.3	-29.9
R2	1616	0.1	-1.1	-22.3	0.2	0.6	0.2	0.1	-1.1	-22.3
R3	1416	-0.2	0.9	-15.0	0.1	0.6	0.9	0.9	-0.2	-15.1
R4	1216	6.1	4.7	-8.1	0.2	0.4	0.9	6.2	4.6	-8.1
S1	616	-8.8	-5.4	-30.4	-0.3	0.7	4.0	-5.4	-8.1	-31.1
S2	416	-8.8	-1.4	-14.6	-0.5	0.2	-0.7	-1.4	-8.7	-14.7
S3	216	-3.1	3.1	-3.4	-0.4	0.1	-1.2	3.1	-2.1	-4.4
S4	16	-1.2	7.0	9.8	-0.6	0.0	-0.9	9.9	7.1	-1.3
T1	811	-0.5	-5.2	-4.3	0.7	0.5	0.8	-0.3	-4.3	-5.5
T2	611	0.9	-5.6	-7.8	0.6	0.3	-0.4	0.9	-5.6	-7.9
T3	411	0.6	-5.5	-7.6	0.5	0.3	-0.4	0.7	-5.5	-7.7
T4	211	0.8	-5.2	-6.8	0.4	0.2	-0.4	0.8	-5.2	-6.9
TS	11	0.8	-4.6	-5.1	0.4	0.1	-0.2	0.9	-4.6	-5.2
U1	43058	2.1	8.2	-14.5	-0.7	0.6	3.2	8.3	2.6	-15.1
U2	43057	3.4	6.2	-13.2	-0.5	0.1	4.4	6.4	4.4	-14.3
U3	43056	2.5	4.0	-11.8	-0.3	0.4	5.9	4.6	4.0	-13.9
U4	43055	1.8	1.6	-11.5	-0.1	0.4	5.9	4.0	1.6	-13.7
U5	43054	0.7	-1.0	-11.5	0.1	0.3	5.3	2.7	-1.0	-13.4
U6	43053	-1.0	-3.1	-9.2	0.2	0.2	3.7	0.5	-3.1	-10.6

Table 2.10.4-141 Primary Stresses; 30-Foot Top Corner Drop; Drop Orientation = 24 Degrees; 3-D Top Model; 0-Degree Circumferential Location; Condition 1 (continued)

Stress Points		Stress Components (ksi)						Principal Stresses (ksi)		
Section <sup>1</sup>	Node	S <sub>x</sub>	S <sub>y</sub>	S <sub>z</sub>	S <sub>xy</sub>	S <sub>xz</sub>	S <sub>yz</sub>	S1	S2	S3
U7	43052	-1.7	-6.9	-14.0	0.5	0.2	3.8	-0.6	-6.9	-15.1
U8	43051	-8.3	-12.7	-13.2	0.5	0.4	7.1	-3.2	-12.7	-18.2
V1	50024	-15.6	0.8	-6.2	-1.3	-0.2	-2.2	0.9	-5.7	-16.2
V2	50023	-10.7	-4.3	-6.3	-0.6	-0.2	-1.2	-4.3	-6.0	-11.1
V3	50022	-5.1	-9.3	-5.5	0.3	0.0	0.0	-5.1	-5.5	-9.3
V4	50021	0.0	-14.4	-4.4	1.0	0.0	0.3	0.1	-4.4	-14.5
W1	43278	9.6	6.1	-3.6	-0.7	-1.4	-2.0	10.0	6.3	-4.1
W2	43274	1.7	-0.2	-1.2	-0.1	-1.4	-2.0	2.8	0.4	-2.8
W3	43271	-3.6	-3.7	-0.3	0.2	-1.7	-1.0	0.6	-3.8	-4.5
X1	50084	22.8	16.8	-8.2	-0.5	0.1	-5.1	23.7	16.8	-9.1
X2	50083	6.7	1.3	-5.9	-0.2	0.3	-5.2	8.6	1.3	-7.8
X3	50081	-23.0	-26.8	10.5	0.5	-0.1	-5.1	11.3	-23.7	-26.9

<sup>1</sup> Refer to Figure 2.10.2-34 for the identification of the representative sections.

Table 2.10.4-142  $P_m$  Stresses; 30-Foot Top Corner Drop; Drop Orientation = 24 Degrees;  
3-D Top Model; 0-Degree Circumferential Location; Condition 1

**Condition 1: 100°F Ambient with Contents**

Section <sup>1</sup>	Node - Node	Stress Components (ksi)						Principal Stresses (ksi)			
		$S_x$	$S_y$	$S_z$	$S_{xy}$	$S_{yz}$	$S_{xz}$	S1	S2	S3	S.I.
A	1949 - 1951	0.6	1.1	0.0	0.0	0.0	0.2	1.1	0.7	-0.1	1.2
B	1952 - 93	-0.8	-1.3	0.2	-0.1	0.0	0.2	0.3	-0.8	-1.3	1.6
C	1925 - 1927	0.3	-0.2	0.1	0.0	-0.1	-0.2	0.5	0.0	-0.2	0.7
D	683 - 85	-0.1	-0.7	-0.4	0.2	0.0	0.0	-0.1	-0.4	-0.8	0.7
E	682 - 82	0.4	-0.2	0.0	0.1	0.0	0.2	0.5	-0.1	-0.2	0.7
F	1925 - 1325	-0.7	-1.1	-2.2	0.0	-0.1	0.2	-0.7	-1.1	-2.2	1.5
G	680 - 80	-0.1	0.0	0.5	0.0	0.0	0.3	0.6	0.0	-0.2	0.8
H	1921 - 1321	0.0	4.4	-2.5	-0.2	-0.4	0.0	4.5	-0.1	-2.6	7.0
I	676 - 76	0.0	0.6	0.5	0.0	0.0	0.0	0.6	0.5	0.0	0.6
J	1916 - 1316	-0.1	4.9	-0.6	-0.3	-0.1	0.0	4.9	-0.1	-0.6	5.5
K	671 - 71	0.0	0.7	-0.2	-0.1	0.1	0.0	0.7	0.0	-0.2	0.9
L	1908 - 1308	-0.3	4.9	-2.8	0.7	0.3	0.0	5.0	-0.4	-2.8	7.8
M	663 - 63	-0.1	0.9	-2.5	0.4	0.2	0.0	1.0	-0.2	-2.5	3.6
N	1877 - 1277	-0.1	4.9	-11.3	-0.4	0.7	0.0	4.9	-0.1	-11.3	16.2
O	647 - 47	0.0	1.0	-6.0	-0.1	0.2	0.0	1.0	0.0	-6.0	7.0
P	1840 - 1240	-0.5	3.7	-18.2	-0.3	0.9	-0.4	3.8	-0.5	-18.3	22.0
Q	628 - 28	-0.1	3.2	-8.4	-0.2	0.3	0.1	3.3	-0.1	-8.4	11.7
R	1816 - 1216	1.0	0.2	-18.8	0.2	0.5	0.5	1.0	0.2	-18.8	19.8
S	616 - 16	-5.7	0.8	-9.4	-0.5	0.2	-0.1	0.9	-5.7	-9.4	10.3
T	811 - 11	0.6	-5.3	-6.8	0.5	0.3	-0.2	0.7	-5.3	-6.8	7.5
U	43058 - 43051	-0.3	-1.4	-12.3	0.1	0.3	4.9	1.5	-1.4	-14.1	15.6
V	50024 - 50021	-7.8	-6.9	-5.7	-0.1	-0.1	-0.7	-5.5	-6.8	-8.1	2.6
W	43278 - 43271	2.4	0.5	-1.6	-0.2	-1.5	-1.7	3.1	1.1	-2.9	5.9
X	50084 - 50081	-0.8	-5.7	-0.7	0.0	0.1	-5.2	4.4	-5.7	-6.0	10.4

<sup>1</sup> Refer to Figure 2.10.2-34 for the identification of the representative sections.

Table 2.10.4-143  $P_m + P_b$  Stresses; 30-Foot Top Corner Drop; Drop Orientation = 24 Degrees; 3-D Top Model; 0-Degree Circumferential Location; Condition 1

Condition 1: 100°F Ambient with Contents

Section <sup>1</sup>	Node - Node	Stress Components (ksi)						Principal Stresses (ksi)			
		$S_x$	$S_y$	$S_z$	$S_{xy}$	$S_{yz}$	$S_{zx}$	S1	S2	S3	S.L.
A I	1949 - 1951	1.6	2.6	-0.4	0.0	-0.1	0.3	2.6	1.6	-0.5	3.1
B O	1952 - 93	-1.6	-2.5	1.0	-0.1	0.0	0.3	1.0	-1.6	-2.5	3.6
C O	1925 - 1927	0.6	-0.3	-0.4	0.1	0.0	-0.2	0.7	-0.3	-0.4	1.1
D O	683 - 85	-0.2	-0.9	-0.4	0.2	0.0	0.0	-0.1	-0.4	-1.0	0.9
E I	682 - 82	0.4	-0.3	-0.6	0.1	0.0	0.2	0.5	-0.3	-0.6	1.1
F O	1925 - 1325	-1.2	-2.2	-5.6	0.1	-0.1	0.4	-1.2	-2.2	-5.7	4.5
G I	680 - 80	-0.4	0.0	1.2	0.0	0.0	0.6	1.4	0.0	-0.6	2.0
H I	1921 - 1321	0.0	3.6	-3.9	-0.2	-0.4	0.1	3.6	0.0	-3.9	7.5
I O	676 - 76	0.0	1.4	1.1	-0.1	0.0	0.0	1.4	1.1	0.0	1.4
J O	1916 - 1316	-0.1	6.4	0.1	-0.5	-0.1	0.0	6.4	0.1	-0.1	6.5
K O	671 - 71	0.0	2.1	0.5	-0.2	0.1	0.0	2.1	0.5	0.0	2.1
L O	1908 - 1308	0.1	7.9	-1.6	1.7	0.3	0.0	8.3	-0.2	-1.6	9.9
M O	663 - 63	0.2	2.7	-1.8	0.7	0.2	0.0	2.9	0.0	-1.8	4.7
N O	1877 - 1277	0.0	7.2	-10.4	-0.5	0.6	0.0	7.2	-0.1	-10.4	17.6
O O	647 - 47	0.0	2.3	-5.6	-0.2	0.2	0.0	2.3	0.0	-5.6	7.9
P O	1840 - 1240	-0.6	3.4	-23.3	-0.2	0.7	-1.1	3.4	-0.5	-23.4	26.8
Q O	628 - 28	0.0	3.7	-8.9	-0.3	0.2	0.1	3.7	0.0	-8.9	12.7
R I	1816 - 1216	-1.3	-3.6	-29.7	0.2	0.7	0.0	-1.3	-3.6	-29.7	28.4
S I	616 - 16	-10.5	-5.5	-28.8	-0.3	0.5	1.9	-5.5	-10.3	-29.0	23.5
T O	811 - 11	1.0	-4.9	-6.6	0.4	0.1	-0.5	1.0	-5.0	-6.7	7.7
U I	43058 - 43051	4.9	9.1	-12.2	-0.6	0.3	4.6	9.2	5.9	-13.4	22.6
V I	50024 - 50021	-15.8	0.7	-6.7	-1.4	-0.2	-2.1	0.8	-6.2	-16.4	17.2
W I	43278 - 43271	9.0	5.4	-3.2	-0.6	-1.3	-2.2	9.4	5.6	-3.8	13.2
X O	50084 - 50081	-23.5	-27.3	9.3	0.5	-0.1	-5.2	10.1	-24.2	-27.4	37.5

<sup>1</sup> Refer to Figure 2.10.2-34 for the identification of the representative sections.



Table 2.10.4-144 Critical P<sub>m</sub> Stress Summary; 30-Foot Top Corner Drop; Drop Orientation = 24 Degrees; 3-D Top Model; Condition 1

Condition 1: 100°F Ambient with Contents

Comp. No. <sup>1</sup>	Section Cut Node-Node	P <sub>m</sub> Stresses (ksi)						Principal Stresses (ksi)				Allow. S.L. Stress	Margin of Safety
		S <sub>x</sub>	S <sub>y</sub>	S <sub>z</sub>	S <sub>xy</sub>	S <sub>xz</sub>	S <sub>yz</sub>	S1	S2	S3	S.L.		
1	1932- 93	-0.8	-1.3	0.2	-0.1	0.0	0.2	0.3	-0.8	-1.3	1.6	45.6	27.5
2	1592-15324	0.1	1.7	-0.7	0.1	-3.2	-0.1	3.9	0.1	-2.9	6.8	44.9	5.6
3	11841-11241	-0.2	2.7	-14.7	0.1	8.2	-0.3	6.0	-0.2	-18.0	24.0	66.0	1.8
4	13874-13274	-0.1	3.0	-10.2	0.0	7.8	0.0	6.6	-0.1	-13.8	20.4	45.8	1.2
5	10625-10025	0.0	3.7	-9.0	0.0	3.4	0.2	4.6	0.0	-9.9	14.5	46.4	2.2
6	401- 1	-5.4	-37.8	-4.7	2.2	0.0	-0.5	-4.5	-5.5	-37.9	33.4	49.3	0.5
7	50055-63171	-24.1	-15.3	-0.1	-0.2	-1.8	-4.2	0.8	-15.5	-24.9	25.7	48.0	0.9
8	50051-50054	-7.3	-3.8	-2.1	-0.2	0.5	6.2	2.0	-3.8	-11.5	13.5	94.5	6.0

Locations of the most critical sections for each component are provided in the following:

Comp. No. <sup>1</sup>	Section Location					
	Inside Node			Outside Node		
	x (in)	y (deg)	z (in)	x (in)	y (deg)	z (in)
1	0.00	0.0	6.20	0.00	0.0	0.75
2	35.50	67.7	17.40	37.50	67.7	17.40
3	35.50	45.9	159.90	37.50	45.9	159.90
4	35.50	56.5	142.40	37.00	56.5	142.40
5	40.70	45.9	163.40	43.35	45.9	163.40
6	40.88	0.0	193.71	43.35	0.0	193.71
7	23.00	8.3	188.40	23.00	8.3	187.40
8	23.00	0.0	193.71	23.00	0.0	188.46

<sup>1</sup> Refer to Figure 2.10.2-33 for cask component identification.

Table 2.10.4-145 Critical  $P_m + P_b$  Stresses; 30-Foot Top Corner Drop; Drop Orientation = 24 Degrees; 3-D Top Model; Condition 1

Condition 1: 100°F Ambient with Contents

Comp. No. <sup>1</sup>	Section Cut Node-Node	$P_m + P_b$ Stresses (ksi)							Principal Stresses (ksi)			Allow. Stress	Margin of Safety
		$S_x$	$S_y$	$S_z$	$S_{xy}$	$S_{yz}$	$S_{xz}$	$S_1$	$S_2$	$S_3$	$S_1$		
1	1952- 93	-1.6	-2.5	1.0	-0.1	0.0	0.3	1.0	-1.6	-2.5	3.6	65.2	17.1
2	15924-15324	0.0	1.4	-2.5	0.1	-4.0	-0.1	3.9	0.0	-5.0	8.9	64.2	6.2
3	11821-11221	-0.1	4.3	-21.8	0.0	8.1	0.7	6.6	-0.1	-24.1	30.7	94.3	2.1
4	13874-13274	-0.1	5.1	-9.6	0.0	8.2	0.0	8.7	-0.1	-13.2	21.9	65.5	2.0
5	10625-10025	0.0	4.1	-8.1	-0.1	4.1	0.2	5.4	0.1	-9.4	14.7	66.4	3.5
6	401- 1	-4.7	-38.3	-5.8	2.3	0.0	-0.4	-4.4	-6.0	-38.4	34.0	70.9	1.1
7	50150-63451	-69.2	-37.5	-17.4	1.0	0.0	-0.8	-17.4	-37.5	-69.2	51.8	69.8	0.3
8	50071-50074	-55.0	-38.4	-4.8	-0.2	-0.3	-1.4	-4.8	-38.4	-55.1	50.3	135.0	1.7

Locations of the most critical sections for each component are provided in the following:

Comp. No. <sup>1</sup>	Section Location					
	Inside Node			Outside Node		
	x (in)	y (deg)	z (in)	x (in)	y (deg)	z (in)
1	0.00	0.0	6.20	0.00	0.0	0.75
2	35.50	67.7	17.40	37.50	67.7	17.40
3	35.50	45.9	171.65	37.50	45.9	171.65
4	35.50	56.5	142.40	37.00	56.5	142.40
5	40.70	45.9	163.40	43.35	45.9	163.40
6	40.88	0.0	193.71	43.35	0.0	193.71
7	25.00	8.3	188.40	25.00	8.3	187.40
8	9.00	0.0	193.71	9.00	0.0	188.46

<sup>1</sup> Refer to Figure 2.10.2-33 for cask component identification.

Table 2.10.4-146  $P_m$  Stresses; 30-Foot Top Corner Drop; Drop Orientation = 24 Degrees;  
3-D Top Model; 45.9-Degree Circumferential Location; Condition 1

Condition 1: 100°F Ambient with Contents

Section <sup>1</sup>	Node - Node	Stress Components (ksi)						Principal Stresses (ksi)			
		$S_x$	$S_y$	$S_z$	$S_{xy}$	$S_{yz}$	$S_{xz}$	S1	S2	S3	S.I.
A	1949 - 1951	0.6	1.1	0.0	0.0	0.0	0.2	1.1	0.7	-0.1	1.2
B	1952 - 93	-0.8	-1.3	0.2	-0.1	0.0	0.2	0.3	-0.8	-1.3	1.6
C	11925 - 11927	0.1	0.2	-0.2	-0.2	-0.6	-0.2	0.6	0.2	-0.6	1.3
D	10683 - 10085	0.0	-1.0	-0.4	0.1	-0.1	0.0	0.0	-0.4	-1.0	1.0
E	10682 - 10082	0.5	0.0	0.0	0.1	0.0	0.0	0.5	0.0	0.0	0.5
F	11925 - 11325	-0.8	0.3	-1.1	-0.2	-1.4	0.1	1.2	-0.8	-2.0	3.2
G	10680 - 10080	-0.6	0.5	0.2	0.1	0.2	0.0	0.6	0.1	-0.7	1.3
H	11921 - 11321	0.0	3.2	-1.7	0.1	-3.1	0.0	4.7	0.0	-3.2	7.9
I	10676 - 10076	0.0	0.5	-0.6	0.0	0.1	0.0	0.5	0.0	-0.6	1.1
J	11916 - 11316	0.0	3.4	-2.0	0.0	-0.8	0.0	3.6	0.0	-2.1	5.7
K	10671 - 10071	0.0	0.4	-1.6	0.0	0.6	0.0	0.6	0.0	-1.8	2.4
L	11908 - 11308	0.1	3.4	-4.8	-0.4	3.0	0.0	4.4	0.1	-5.8	10.2
M	10663 - 10063	0.0	0.6	-3.6	-0.3	1.5	0.0	1.2	0.0	-4.1	5.2
N	11877 - 11277	0.0	3.6	-10.6	0.0	6.5	0.0	6.1	0.0	-13.1	19.2
O	10647 - 10047	0.0	0.7	-6.5	0.0	2.5	0.0	1.5	0.0	-7.3	8.8
P	11840 - 11240	-0.4	3.0	-14.6	0.3	8.1	-0.3	6.2	-0.4	-17.8	23.9
Q	10628 - 10028	0.0	2.7	-8.6	0.0	3.3	0.0	3.6	0.0	-9.5	13.1
R	11816 - 11216	1.8	3.1	-15.5	1.1	5.6	0.9	5.1	1.3	-17.0	22.2
S	10616 - 10016	-5.9	2.0	-9.8	-1.1	3.1	0.0	2.9	-6.0	-10.6	13.5
T	10811 - 10011	1.4	-2.4	-6.2	1.5	3.7	0.4	2.3	-1.0	-8.5	10.9
U	44558 - 44551	0.5	-0.4	-11.8	-0.2	-0.3	4.9	2.3	-0.5	-13.5	15.8
V	50524 - 50521	-5.7	-5.2	-6.3	0.7	0.0	-0.6	-4.6	-5.8	-6.7	2.1
W	43278 - 43271	2.4	0.5	-1.6	-0.2	-1.5	-1.7	3.1	1.1	-2.9	5.9
X	50084 - 50081	-0.8	-5.7	-0.7	0.0	0.1	-5.2	4.4	-5.7	-6.0	10.4

<sup>1</sup> Refer to Figure 2.10.2-34 for the identification of the representative sections.

Table 2.10.4-147  $P_m + P_b$  Stresses; 30-Foot Top Corner Drop; Drop Orientation = 24 Degrees; 3-D Top Model; 45.9-Degree Circumferential Location; Condition 1

Condition 1: 100°F Ambient with Contents

Section <sup>1</sup>	Node - Node	Stress Components (ksi)						Principal Stresses (ksi)			
		$S_x$	$S_y$	$S_z$	$S_{xy}$	$S_{yz}$	$S_{zx}$	S1	S2	S3	S.L.
A I	1949 - 1951	1.6	2.6	-0.4	0.0	-0.1	0.3	2.6	1.6	-0.5	3.1
B O	1952 - 93	-1.6	-2.5	1.0	-0.1	0.0	0.3	1.0	-1.6	-2.5	3.6
C I	11925 - 11927	-0.4	0.6	-0.2	-0.5	-1.1	-0.1	1.5	-0.2	-1.2	2.6
D O	10683 - 10085	0.2	-1.5	-0.4	0.2	-0.1	0.0	0.2	-0.4	-1.5	1.8
E I	10682 - 10082	0.5	-0.2	-0.6	0.1	-0.2	0.0	0.5	-0.1	-0.6	1.1
F I	11925 - 11325	-0.4	0.7	-0.1	-0.5	-1.6	0.0	2.0	-0.4	-1.5	3.4
G O	10680 - 10080	-0.3	1.0	1.6	0.0	0.3	0.1	1.7	0.8	-0.3	2.0
H I	11921 - 11321	0.0	3.0	-2.4	0.1	-3.7	0.1	4.9	0.0	-4.4	9.2
I O	10676 - 10076	0.0	0.1	-0.9	0.0	0.5	0.0	0.3	0.0	-1.1	1.4
J I	11916 - 11316	0.0	3.8	-2.0	0.0	-1.2	0.0	4.0	0.0	-2.3	6.3
K I	10671 - 10071	0.0	1.2	-1.4	-0.1	0.3	0.0	1.2	0.0	-1.4	2.7
L I	11908 - 11308	0.2	4.7	-4.4	-0.1	3.0	0.0	5.6	0.2	-5.3	11.0
M I	10663 - 10063	0.1	1.2	-3.4	-0.1	1.6	0.0	1.7	0.1	-3.9	5.6
N I	11877 - 11277	-0.1	4.8	-10.1	-0.1	7.0	0.0	7.5	-0.1	-12.9	20.4
O I	10647 - 10047	0.0	1.0	-6.3	-0.1	2.8	0.0	2.0	0.0	-7.2	9.3
P O	11840 - 11240	-0.5	0.8	-20.2	0.5	7.7	-0.9	3.4	-0.4	-22.8	26.1
Q O	10628 - 10028	0.0	2.0	-10.4	0.0	2.8	0.0	2.6	0.0	-11.0	13.6
R I	11816 - 11216	-1.2	-1.7	-30.1	0.0	6.8	-0.5	-0.1	-1.2	-31.6	31.5
S I	10616 - 10016	-11.1	-4.1	-28.2	-2.5	4.4	2.1	-2.8	-11.3	-29.3	26.6
T I	10811 - 10011	2.6	-1.5	-4.0	3.9	6.5	1.4	7.2	-0.6	-9.6	16.8
U I	44558 - 44551	2.6	9.2	-11.9	-3.2	0.1	4.6	10.6	2.6	-13.3	23.8
V O	50524 - 50521	2.8	-12.4	-4.3	4.5	0.0	0.6	4.0	-4.4	-13.6	17.7
W I	43278 - 43271	9.0	5.4	-3.2	-0.6	-1.3	-2.2	9.4	5.6	-3.8	13.2
X O	50084 - 50081	-23.5	-27.3	9.3	0.5	-0.1	-5.2	10.1	-24.2	-27.4	37.5

<sup>1</sup> Refer to Figure 2.10.2-34 for the identification of the representative sections.

Table 2.10.4-148  $P_m$  Stresses; 30-Foot Top Corner Drop; Drop Orientation = 24 Degrees;  
3-D Top Model; 91.7-Degree Circumferential Location; Condition 1

**Condition 1: 100°F Ambient with Contents**

Section <sup>1</sup>	Node - Node	Stress Components (ksi)						Principal Stresses (ksi)			
		$S_x$	$S_y$	$S_z$	$S_{xy}$	$S_{yz}$	$S_{zx}$	S1	S2	S3	S.I.
A	1949 - 1951	0.6	1.1	0.0	0.0	0.0	0.2	1.1	0.7	-0.1	1.2
B	1952 - 93	-0.8	-1.3	0.2	-0.1	0.0	0.2	0.3	-0.8	-1.3	1.6
C	19925 - 19927	-0.1	0.6	-0.7	0.1	-0.5	-0.1	0.8	-0.1	-0.9	1.7
D	18683 - 18085	-0.1	-0.9	-0.4	-0.2	-0.4	-0.2	0.0	-0.2	-1.1	1.1
E	18682 - 18082	0.6	0.1	-0.5	0.2	-0.5	-0.3	0.8	0.1	-0.7	1.6
F	19925 - 19325	-0.4	1.6	0.2	0.2	-1.4	-0.2	2.5	-0.4	-0.7	3.2
G	18680 - 18080	-0.5	0.8	-1.1	0.3	0.1	-0.2	0.8	-0.5	-1.2	2.0
H	19921 - 19321	0.0	0.3	-1.8	0.1	-2.2	0.0	1.7	0.0	-3.2	4.9
I	18676 - 18076	0.0	0.2	-2.1	0.0	0.6	0.0	0.4	0.0	-2.2	2.6
J	19916 - 19316	0.0	0.8	-4.1	0.0	0.2	0.0	0.9	0.0	-4.1	5.0
K	18671 - 18071	0.0	0.0	-2.8	0.0	1.1	0.0	0.4	0.0	-3.2	3.6
L	19908 - 19308	0.2	1.0	-5.3	0.5	3.9	0.0	2.9	0.1	-7.1	10.0
M	18663 - 18063	0.1	0.0	-3.8	0.2	2.1	0.0	0.9	0.0	-4.7	5.6
N	19877 - 19277	0.1	1.1	-4.0	0.0	7.5	0.0	6.5	0.1	-9.4	15.9
O	18647 - 18047	0.0	-0.1	-4.1	0.0	3.3	0.0	1.8	0.0	-5.9	7.7
P	19840 - 19240	0.0	0.6	-2.2	0.5	9.1	-0.1	8.4	0.0	-10.1	18.5
Q	18628 - 18028	0.0	0.6	-3.6	0.1	4.2	0.0	3.1	0.0	-6.2	9.3
R	19816 - 19216	0.4	4.6	-2.2	1.3	7.7	1.8	10.0	0.0	-7.3	17.4
S	18616 - 18016	-3.8	2.4	-3.0	-1.8	4.8	-0.6	5.6	-4.1	-5.9	11.5
T	18811 - 18011	1.5	2.9	-1.5	2.3	5.8	0.4	7.7	0.9	-5.7	13.4
U	45758 - 45751	-0.5	-1.6	-5.8	-0.7	0.5	1.1	0.0	-1.7	-6.1	6.0
V	50924 - 50921	-0.9	-2.5	0.5	-0.6	0.3	-0.7	0.9	-1.1	-2.7	3.5
W	43278 - 43271	2.4	0.5	-1.6	-0.2	-1.5	-1.7	3.1	1.1	-2.9	5.9
X	50084 - 50081	-0.8	-5.7	-0.7	0.0	0.1	-5.2	4.4	-5.7	-6.0	10.4

<sup>1</sup> Refer to Figure 2.10.2-34 for the identification of the representative sections.

Table 2.10.4-149  $P_m + P_b$  Stresses; 30-Foot Top Corner Drop; Drop Orientation = 24 Degrees; 3-D Top Model; 91.7-Degree Circumferential Location; Condition 1

Condition 1: 100°F Ambient with Contents

Section <sup>1</sup>	Node - Node	Stress Components (ksi)						Principal Stresses (ksi)			
		$S_x$	$S_y$	$S_z$	$S_{xy}$	$S_{yz}$	$S_{xz}$	S1	S2	S3	S.L
A I	1949 - 1951	1.6	2.6	-0.4	0.0	-0.1	0.3	2.6	1.6	-0.5	3.1
B O	1952 - 93	-1.6	-2.5	1.0	-0.1	0.0	0.3	1.0	-1.6	-2.5	3.6
C I	19925 - 19927	-0.6	1.1	-1.6	0.0	-1.0	-0.1	1.5	-0.6	-1.9	3.4
D O	18683 - 18085	0.6	-1.3	-0.5	-0.1	-0.3	-0.1	0.6	-0.4	-1.4	2.0
E I	18682 - 18082	0.6	0.1	-0.3	0.2	-0.5	-0.3	0.9	0.2	-0.7	1.6
F O	19925 - 19325	-0.2	2.3	2.9	0.4	-1.5	-0.3	4.2	1.1	-0.3	4.5
G I	18680 - 18080	-0.6	0.4	-2.8	0.4	0.2	-0.4	0.5	-0.7	-2.9	3.5
H O	19921 - 19321	0.0	-0.7	-2.9	0.1	-2.2	0.1	0.7	0.0	-4.3	5.0
I I	18676 - 18076	0.0	0.6	-1.6	0.0	0.8	0.0	0.9	0.0	-1.9	2.7
J I	19916 - 19316	0.0	1.9	-3.7	0.0	0.3	0.0	2.0	0.0	-3.7	5.7
K I	18671 - 18071	0.0	0.5	-2.6	0.0	1.3	0.0	1.0	0.0	-3.1	4.0
L I	19908 - 19308	0.2	1.7	-5.0	0.1	4.0	0.0	3.6	0.2	-6.8	10.4
M I	18663 - 18063	0.2	0.8	-3.4	0.1	2.2	0.0	1.7	0.2	-4.4	6.1
N O	19877 - 19277	0.1	1.4	-3.9	0.0	7.5	0.0	6.7	0.1	-9.3	16.0
O I	18647 - 18047	0.0	0.5	-3.8	0.1	3.3	0.0	2.2	0.0	-5.6	7.8
P O	19840 - 19240	-0.1	0.5	-3.8	0.7	10.1	-0.2	8.7	-0.1	-12.0	20.7
Q O	18628 - 18028	0.0	0.0	-5.0	0.0	4.6	0.0	2.8	0.0	-7.8	10.5
R I	19816 - 19216	-0.3	2.3	-10.7	-0.3	8.9	0.0	6.8	-0.3	-15.3	22.0
S I	18616 - 18016	-7.4	-0.4	-10.3	-3.8	6.1	-0.3	3.7	-8.2	-13.6	17.3
T I	18811 - 18011	3.7	5.0	3.8	5.7	9.2	1.5	15.9	2.4	-5.8	21.6
U I	45758 - 45751	-4.7	-1.0	-10.0	-4.0	0.2	2.0	1.6	-6.4	-11.0	12.6
V O	50924 - 50921	3.8	-4.0	0.6	3.4	0.3	-0.8	5.1	0.5	-5.4	10.5
W I	43278 - 43271	9.0	5.4	-3.2	-0.6	-1.3	-2.2	9.4	5.6	-3.8	13.2
X O	50084 - 50081	-23.5	-27.3	9.3	0.5	-0.1	-5.2	10.1	-24.2	-27.4	37.5

<sup>1</sup> Refer to Figure 2.10.2-34 for the identification of the representative sections.

Table 2.10.4-150  $P_m$  Stresses; 30-Foot Top Corner Drop; Drop Orientation = 24 Degrees;  
3-D Top Model; 180-Degree Circumferential Location; Condition 1

**Condition 1: 100°F Ambient with Contents**

Section <sup>1</sup>	Node - Node	Stress Components (ksi)						Principal Stresses (ksi)			
		$S_x$	$S_y$	$S_z$	$S_{xy}$	$S_{yz}$	$S_{xz}$	S1	S2	S3	S.L.
A	1949 - 1951	0.6	1.1	0.0	0.0	0.0	0.2	1.1	0.7	-0.1	1.2
B	1952 - 93	-0.8	-1.3	0.2	-0.1	0.0	0.2	0.3	-0.8	-1.3	1.6
C	31925 - 31927	0.1	0.2	-0.6	0.0	0.0	-0.2	0.2	0.2	-0.7	0.9
D	30683 - 30085	0.0	-0.1	-0.8	0.1	0.0	-0.1	0.1	-0.1	-0.8	0.9
E	30682 - 30082	1.1	0.4	-0.9	0.0	0.1	-0.2	1.1	0.4	-0.9	2.0
F	31925 - 31325	-1.0	0.1	-0.9	0.1	0.0	-0.1	0.2	-0.8	-1.0	1.1
G	30680 - 30080	-0.2	-0.1	-2.0	0.0	0.2	0.1	-0.1	-0.2	-2.0	1.9
H	31921 - 31321	-0.1	-1.4	-2.4	-0.2	0.0	0.1	0.0	-1.5	-2.4	2.4
I	30676 - 30076	0.0	-0.3	-2.1	-0.1	0.2	0.0	0.0	-0.3	-2.1	2.1
J	31916 - 31316	-0.1	-1.2	-2.6	-0.2	0.2	0.0	-0.1	-1.2	-2.6	2.5
K	30671 - 30071	0.0	-0.4	-1.8	-0.1	0.2	0.0	0.0	-0.3	-1.9	1.9
L	31908 - 31308	-0.2	-0.8	-1.0	-0.4	0.4	0.0	0.0	-0.6	-1.4	1.4
M	30663 - 30063	0.0	-0.3	-1.2	-0.1	0.3	0.0	0.0	-0.3	-1.2	1.2
N	31877 - 31277	-0.2	-0.9	2.4	-0.1	0.7	0.0	2.6	-0.2	-1.1	3.6
O	30647 - 30047	0.0	-0.3	-0.2	-0.1	0.3	0.0	0.0	0.0	-0.6	0.6
P	31840 - 31240	-1.0	-2.3	5.2	-0.2	0.9	0.0	5.3	-1.0	-2.5	7.7
Q	30628 - 30028	0.0	-0.9	0.4	-0.1	0.4	-0.1	0.6	0.0	-1.0	1.6
R	31816 - 31216	-0.6	6.6	3.7	1.2	0.3	2.3	7.0	4.5	-1.7	8.7
S	30616 - 30016	-1.6	4.7	-0.1	0.8	0.4	-0.5	4.8	0.0	-1.9	6.6
T	30811 - 30011	-0.9	9.0	-0.6	1.6	0.4	0.3	9.3	-0.5	-1.2	10.5
U	47558 - 47551	-3.1	-3.2	-4.3	-0.1	0.1	-0.6	-2.8	-3.2	-4.6	1.7
V	51524 - 51521	-4.2	-3.5	-0.3	-0.1	0.1	-0.2	-0.3	-3.4	-4.3	4.0
W	43278 - 43271	2.4	0.5	-1.6	-0.2	-1.5	-1.7	3.1	1.1	-2.9	5.9
X	50084 - 50081	-0.8	-5.7	-0.7	0.0	0.1	-5.2	4.4	-5.7	-6.0	10.4

<sup>1</sup> Refer to Figure 2.10.2-34 for the identification of the representative sections.

Table 2.10.4-151  $P_m + P_b$  Stresses; 30-Foot Top Corner Drop; Drop Orientation = 24 Degrees; 3-D Top Model; 180-Degree Circumferential Location; Condition 1

Condition 1: 100°F Ambient with Contents

Section <sup>1</sup>	Node - Node	Stress Components (ksi)						Principal Stresses (ksi)			
		$S_x$	$S_y$	$S_z$	$S_{xy}$	$S_{yz}$	$S_{zx}$	S1	S2	S3	S.I.
A I	1949 - 1951	1.6	2.6	-0.4	0.0	-0.1	0.3	2.6	1.6	-0.5	3.1
B O	1952 - 93	-1.6	-2.5	1.0	-0.1	0.0	0.3	1.0	-1.6	-2.5	3.6
C I	31925 - 31927	-0.8	0.1	-1.2	0.1	0.0	-0.2	0.1	-0.7	-1.3	1.5
D O	30683 - 30085	1.3	0.1	-0.9	0.1	0.1	-0.1	1.3	0.1	-0.9	2.2
E O	30682 - 30082	1.1	0.3	-1.3	0.0	0.3	-0.2	1.1	0.4	-1.4	2.5
F I	31925 - 31325	-1.0	-0.1	-1.7	0.1	0.0	-0.2	-0.1	-0.9	-1.8	1.7
G O	30680 - 30080	-0.2	-0.3	-2.8	0.0	0.2	0.0	-0.1	-0.3	-2.8	2.7
H O	31921 - 31321	-0.1	-1.4	-3.0	-0.2	0.0	0.1	-0.1	-1.5	-3.0	3.0
I O	30676 - 30076	0.0	-0.3	-2.2	0.0	0.1	0.0	0.0	-0.3	-2.2	2.2
J I	31916 - 31316	-0.1	-1.5	-2.7	-0.2	0.2	0.0	-0.1	-1.5	-2.7	2.6
K I	30671 - 30071	0.0	-0.5	-1.9	-0.1	0.2	0.0	0.0	-0.5	-2.0	1.9
L O	31908 - 31308	-0.2	-0.4	-0.9	-0.6	0.4	0.0	0.3	-0.6	-1.3	1.6
M I	30663 - 30063	0.0	-0.4	-1.2	-0.1	0.2	0.0	0.0	-0.3	-1.3	1.2
N O	31877 - 31277	-0.2	-1.0	2.4	-0.1	0.7	0.0	2.5	-0.2	-1.2	3.7
O O	30647 - 30047	0.0	-0.5	-0.2	-0.1	0.3	0.0	0.0	0.0	-0.7	0.7
P I	31840 - 31240	0.1	-1.0	8.5	-0.1	0.9	-0.1	8.6	0.1	-1.1	9.6
Q I	30628 - 30028	0.0	-0.4	1.9	-0.1	0.4	-0.1	2.0	0.0	-0.5	2.5
R O	31816 - 31216	-1.3	6.7	5.6	1.4	0.0	3.8	7.6	6.5	-3.2	10.8
S I	30616 - 30016	-3.1	4.9	1.9	1.0	0.6	-1.4	5.1	2.2	-3.6	8.7
T I	30811 - 30011	-1.5	10.3	3.5	2.0	0.4	1.4	10.7	3.8	-2.1	12.9
U O	47558 - 47551	5.6	1.3	0.8	-0.4	0.2	-2.0	6.4	1.3	0.0	6.4
V I	51524 - 51521	-14.6	-6.0	-0.9	0.4	0.1	-0.3	-0.9	-6.0	-14.7	13.7
W I	43278 - 43271	9.0	5.4	-3.2	-0.6	-1.3	-2.2	9.4	5.6	-3.8	13.2
X O	50084 - 50081	-23.5	-27.3	9.3	0.5	-0.1	-5.2	10.1	-24.2	-27.4	37.5

<sup>1</sup> Refer to Figure 2.10.2-34 for the identification of the representative sections.



Table 2.10.4-152 Primary Stresses; 30-Foot Bottom Corner Drop; Drop Orientation = 24 Degrees; 3-D Bottom Model; 0-Degree Circumferential Location; Condition 1

Condition 1: 100°F Ambient with Contents

Stress Points Section <sup>1</sup> Node		Stress Components (ksi)						Principal Stresses (ksi)		
		S <sub>x</sub>	S <sub>y</sub>	S <sub>z</sub>	S <sub>xy</sub>	S <sub>yz</sub>	S <sub>xz</sub>	S1	S2	S3
A1	1130	17.5	13.4	-6.5	-0.5	2.1	2.1	17.7	13.6	-6.9
A2	1129	2.2	-0.1	-1.2	0.0	1.5	2.1	3.3	0.5	-2.9
A3	1128	-13.0	-13.6	4.1	0.5	2.0	2.1	4.6	-13.2	-13.9
B1	1185	10.1	3.3	-6.5	-0.5	2.5	2.3	10.4	3.9	-7.3
B2	1184	-3.6	-7.8	-1.9	0.0	1.8	2.3	0.0	-4.9	-8.4
B3	1183	-17.5	-18.8	2.7	0.4	1.9	2.3	3.1	-17.8	-19.0
C1	90	-19.6	-5.7	-24.9	-1.2	-0.7	-5.1	-5.6	-16.6	-28.1
C2	80	-8.8	-1.6	-14.4	-1.0	-0.5	-4.2	-1.4	-6.7	-16.7
C3	70	-5.7	-1.1	-9.1	-0.5	-0.4	-3.8	-1.1	-3.3	-11.6
C4	60	-3.0	-1.2	-5.4	-0.1	-0.4	-3.6	-0.3	-1.2	-8.1
C5	50	6.5	-4.1	-3.5	1.0	-0.2	-2.5	7.2	-4.1	-4.2
C6	40	13.7	-5.5	-3.5	1.6	-0.1	-1.5	14.0	-3.7	-5.6
D1	25	-30.3	-22.9	-31.9	-0.4	-0.6	-8.4	-22.6	-23.0	-39.5
D2	15	-6.7	-18.5	-14.8	0.6	-0.3	-3.8	-5.1	-16.3	-18.5
D3	5	0.5	-22.3	-7.5	1.4	-0.1	-1.2	0.7	-7.6	-22.4
E1	35	10.5	-8.3	-21.9	1.3	-0.4	-3.8	11.0	-8.4	-22.4
E2	34	1.8	-8.9	-17.5	0.7	-0.8	-7.4	4.3	-9.0	-20.0
E3	33	-5.2	-9.1	-11.1	0.3	-0.7	-7.8	0.2	-9.1	-16.5
E4	32	-6.7	-8.4	-6.7	0.1	-0.4	-4.8	-1.9	-8.4	-11.5
E5	31	-7.3	-7.6	-2.5	0.0	-0.3	-2.9	-1.1	-7.6	-8.6
F1	100	-0.1	-2.1	-32.9	-0.1	-0.9	-3.2	0.2	-2.1	-33.2
F2	99	-2.8	1.0	-18.9	-0.4	-0.8	-1.6	1.1	-2.7	-19.1
F3	98	-2.8	2.3	-13.4	-0.5	-0.4	1.0	2.4	-2.7	-13.6
F4	97	0.1	4.6	-8.0	-0.4	-0.4	2.0	4.6	0.5	-8.5
G1	94	0.3	-2.6	-24.2	0.1	-0.4	-1.1	0.4	-2.6	-24.3
G2	93	-0.6	-0.3	-14.8	-0.1	-0.4	-0.5	-0.2	-0.6	-14.9
G3	92	-1.1	1.3	-8.4	-0.2	-0.2	0.1	1.3	-1.1	-8.4
G4	91	-0.5	3.5	-0.7	-0.3	-0.1	0.1	3.5	-0.5	-0.8
H1	330	-0.3	4.0	-13.1	-0.3	-1.0	-0.1	4.1	-0.3	-13.2
H2	329	-0.5	3.8	-16.1	-0.3	-0.9	0.0	3.9	-0.5	-16.1

Table 2.10.4-152 Primary Stresses; 30-Foot Bottom Corner Drop; Drop Orientation = 24 Degrees; 3-D Bottom Model; 0-Degree Circumferential Location; Condition 1 (continued)

Stress Points Section <sup>1</sup> Node		S <sub>x</sub>	Stress Components (ksi)					Principal Stresses (ksi)		
			S <sub>y</sub>	S <sub>z</sub>	S <sub>xy</sub>	S <sub>yz</sub>	S <sub>xz</sub>	S1	S2	S3
H3	328	-0.5	3.7	-18.8	-0.3	-0.8	0.6	3.8	-0.5	-18.9
H4	327	-0.5	2.9	-24.3	-0.2	-0.7	1.3	3.0	-0.4	-24.4
I1	244	0.0	1.8	-10.1	-0.1	-0.4	-0.1	1.8	0.0	-10.1
I2	243	0.0	2.3	-10.1	-0.2	-0.4	-0.1	2.3	0.0	-10.1
I3	242	0.0	2.7	-9.9	-0.2	-0.3	-0.1	2.8	0.0	-9.9
I4	241	0.0	3.2	-9.9	-0.2	-0.2	-0.1	3.2	0.0	-9.9
J1	550	-0.1	2.5	-10.8	-0.2	-0.7	0.0	2.5	-0.2	-10.8
J2	548	-0.1	4.9	-9.9	-0.4	-0.6	0.0	4.9	-0.1	-9.9
J3	547	0.0	7.1	-9.0	-0.5	-0.6	0.0	7.2	-0.1	-9.0
K1	344	-0.1	-0.3	-7.6	0.0	-0.3	0.0	-0.1	-0.3	-7.6
K2	342	0.0	1.2	-7.0	-0.1	-0.3	0.0	1.2	0.0	-7.0
K3	341	0.0	2.5	-6.4	-0.2	-0.2	0.0	2.6	0.0	-6.5
L1	740	0.1	2.4	-2.9	0.4	-0.2	-0.1	2.4	0.0	-2.9
L2	738	-0.3	4.7	-2.0	-0.9	-0.2	0.0	4.8	-0.5	-2.0
L3	737	0.3	7.2	-0.9	-2.1	-0.2	0.0	7.8	-0.3	-0.9
M1	454	-0.1	-0.9	-3.9	-0.6	-0.2	0.0	0.2	-1.2	-3.9
M2	452	0.2	0.9	-3.2	-0.3	-0.2	0.0	1.0	0.1	-3.2
M3	451	-0.2	2.4	-2.7	0.0	-0.2	-0.1	2.4	-0.2	-2.7
N1	810	-0.1	3.5	-1.4	-0.2	0.2	0.0	3.5	-0.1	-1.4
N2	807	-0.1	6.3	-0.1	-0.4	0.1	0.0	6.3	-0.1	-0.1
O1	524	0.0	-0.7	-1.2	0.0	-0.1	0.0	0.0	-0.6	-1.2
O2	521	0.0	2.0	0.1	-0.1	-0.1	0.0	2.0	0.1	0.0
P1	850	0.0	3.5	-4.0	-0.2	0.4	-0.1	3.6	0.0	-4.0
P2	847	-0.1	5.3	-1.3	-0.3	0.3	0.0	5.4	-0.1	-1.3
Q1	564	0.0	-0.2	-0.2	0.0	0.0	0.0	0.0	-0.2	-0.3
Q2	561	0.0	1.5	0.7	-0.1	0.0	0.0	1.5	0.7	0.0
R1	890	-1.0	-0.2	1.5	0.0	0.2	-0.2	1.5	-0.2	-1.0
R2	887	-1.2	-1.7	-5.2	0.1	0.1	-0.5	-1.1	-1.7	-5.2
S1	604	-0.4	0.3	0.4	0.0	0.0	-0.4	0.6	0.3	-0.6
S2	601	0.0	0.7	0.5	-0.1	-0.1	-0.1	0.7	0.5	0.0
T1	897	0.5	-0.3	-1.6	0.0	0.1	-0.2	0.6	-0.3	-1.6

Table 2.10.4-152 Primary Stresses; 30-Foot Bottom Corner Drop; Drop Orientation = 24 Degrees; 3-D Bottom Model; 0-Degree Circumferential Location; Condition 1 (continued)

Stress Points Section <sup>1</sup> Node	Stress Components (ksi)						Principal Stresses (ksi)		
	$S_x$	$S_y$	$S_z$	$S_{xy}$	$S_{yz}$	$S_{xz}$	S1	S2	S3
T2 614	0.3	0.2	0.0	0.0	0.0	-0.4	0.5	0.3	-0.3
T3 611	-0.1	0.1	0.0	0.0	-0.1	-0.2	0.2	0.1	-0.3
U1 900	0.7	0.1	-0.4	0.0	0.1	0.1	0.7	0.1	-0.5
U2 910	0.5	-0.2	-0.4	0.0	0.0	0.1	0.5	-0.2	-0.4
V1 920	-0.2	-0.4	-0.3	0.1	0.0	0.1	-0.1	-0.4	-0.4
V2 930	-0.5	-1.0	-0.2	0.2	0.0	0.1	-0.1	-0.5	-1.0
W1 1216	1.2	2.3	-1.0	0.0	0.0	-0.2	2.3	1.2	-1.0
W2 1226	-0.3	-0.1	0.5	0.0	-0.1	-0.1	0.5	-0.1	-0.3
X1 1236	0.1	0.0	-0.6	0.0	-0.1	-0.1	0.1	0.0	-0.6
X2 1246	-1.5	-2.4	1.1	-0.1	0.0	-0.2	1.1	-1.5	-2.5

<sup>1</sup> Refer to Figure 2.10.2-34 for the identification of the representative sections.

Table 2.10.4-153  $P_m$  Stresses; 30-Foot Bottom Corner Drop; Drop Orientation = 24 Degrees; 3-D Bottom Model; 0-Degree Circumferential Location; Condition 1

Condition 1: 100°F Ambient with Contents

Section <sup>1</sup>	Node - Node	Stress Components (ksi)						Principal Stresses (ksi)			
		$S_x$	$S_y$	$S_z$	$S_{xy}$	$S_{yz}$	$S_{zx}$	S1	S2	S3	S.L
A	1130 - 1128	2.2	-0.1	-1.2	0.0	1.8	2.1	3.4	0.6	-3.1	6.4
B	1185 - 1183	-3.7	-7.8	-1.9	0.0	2.0	2.3	0.0	-4.9	-8.5	8.5
C	90 - 40	-0.5	-2.9	-7.6	0.2	-0.4	-3.2	0.8	-2.9	-8.8	9.6
D	25 - 5	-10.8	-20.5	-17.2	0.5	-0.3	-4.3	-8.6	-19.4	-20.6	12.0
E	33 - 31	-1.3	-8.6	-12.6	0.5	-0.6	-5.8	1.2	-8.6	-15.1	16.3
F	100 - 97	-1.9	1.5	-17.6	-0.4	-0.6	-0.4	1.6	-1.9	-17.6	19.2
G	94 - 91	-0.6	0.5	-11.9	-0.1	-0.3	-0.3	0.5	-0.6	-11.9	12.4
H	330 - 327	-0.5	3.7	-17.9	-0.3	-0.9	0.4	3.7	-0.5	-17.9	21.6
I	244 - 241	0.0	2.5	-10.0	-0.2	-0.3	-0.1	2.5	0.0	-10.0	12.5
J	550 - 547	-0.1	4.8	-9.9	-0.4	-0.6	0.0	4.9	-0.1	-9.9	14.8
K	344 - 341	0.0	1.1	-7.0	-0.1	-0.3	0.0	1.2	0.0	-7.0	8.2
L	740 - 737	-0.1	4.7	-1.9	-0.9	-0.2	0.0	4.9	-0.2	-1.9	6.8
M	454 - 451	0.0	0.9	-3.2	-0.3	-0.2	0.0	0.9	-0.1	-3.2	4.2
N	810 - 807	-0.1	4.9	-0.8	-0.3	0.2	0.0	4.9	-0.1	-0.8	5.7
O	524 - 521	0.0	0.7	-0.6	0.0	-0.1	0.0	0.7	0.0	-0.6	1.3
P	850 - 847	0.0	4.4	-2.6	-0.2	0.4	0.0	4.5	-0.1	-2.6	7.1
Q	564 - 561	0.0	0.6	0.2	0.0	0.0	0.0	0.6	0.2	0.0	0.7
R	890 - 887	-1.1	-1.0	-1.8	0.0	0.2	-0.3	-0.9	-1.0	-2.0	1.1
S	604 - 601	-0.2	0.5	0.4	0.0	0.0	-0.2	0.5	0.5	-0.3	0.8
T	614 - 611	0.1	0.2	0.0	0.0	-0.1	-0.3	0.4	0.2	-0.3	0.6
U	900 - 910	0.6	-0.1	-0.4	0.0	0.1	0.1	0.6	-0.1	-0.5	1.1
V	920 - 930	-0.4	-0.7	-0.2	0.1	0.0	0.1	-0.1	-0.4	-0.7	0.6
W	1216 - 1226	0.5	1.1	-0.3	0.0	0.0	-0.2	1.1	0.5	-0.3	1.4
X	1236 - 1246	-0.7	-1.2	0.3	-0.1	0.0	-0.2	0.3	-0.7	-1.2	1.5

<sup>1</sup> Refer to Figure 2.10.2-34 for the identification of the representative sections.

Table 2.10.4-154  $P_m + P_b$  Stresses; 30-Foot Bottom Corner Drop; Drop Orientation = 24 Degrees; 3-D Bottom Model; 0-Degree Circumferential Location; Condition 1

Condition 1: 100°F Ambient with Contents

Section <sup>1</sup>	Node - Node	Stress Components (ksi)						Principal Stresses (ksi)			
		$S_x$	$S_y$	$S_z$	$S_{xy}$	$S_{yz}$	$S_{zx}$	S1	S2	S3	S.I.
A I	1130 - 1128	17.5	13.4	-6.5	-0.5	1.8	2.1	17.7	13.5	-6.8	24.5
B O	1185 - 1183	-17.5	-18.8	2.7	0.4	1.7	2.3	3.1	-17.7	-19.0	22.1
C I	90 - 40	-14.1	-1.4	-15.6	-1.3	-0.6	-4.7	-1.3	-10.1	-19.7	18.5
D O	25 - 5	-4.6	-20.3	-5.0	1.4	0.0	-0.7	4.7	-5.1	-20.3	25.1
E I	35 - 31	8.2	-8.9	-23.1	1.2	-0.7	-6.6	9.6	-9.0	-24.4	34.1
F I	100 - 97	-2.0	-1.5	-29.1	-0.2	-1.0	-3.3	-1.4	-1.7	-29.5	28.1
G I	94 - 91	-0.1	-2.4	-23.2	0.0	-0.5	-1.0	-0.1	-2.4	-23.2	23.2
H O	330 - 327	-0.6	3.2	-23.1	-0.2	-0.7	1.1	3.3	-0.5	-23.2	26.5
I O	244 - 241	0.0	3.2	-9.8	-0.2	-0.2	-0.1	3.2	0.0	-9.9	13.1
J O	550 - 547	0.0	7.1	-9.0	-0.5	-0.6	0.0	7.2	-0.1	-9.0	16.2
K O	344 - 341	0.0	2.6	-6.4	-0.2	-0.2	0.0	2.6	0.0	-6.4	9.0
L O	740 - 737	0.0	7.1	-0.9	-2.1	-0.2	0.0	7.7	-0.5	-0.9	8.6
M O	454 - 451	-0.1	2.5	-2.6	0.0	-0.2	0.0	2.5	-0.1	-2.6	5.1
N O	810 - 807	-0.1	6.3	-0.1	-0.4	0.1	0.0	6.3	-0.1	-0.1	6.4
O O	524 - 521	0.0	2.0	0.1	-0.1	-0.1	0.0	2.0	0.1	0.0	2.1
P I	850 - 847	0.0	3.5	-4.0	-0.2	0.4	-0.1	3.6	0.0	-4.0	7.6
Q O	564 - 561	0.0	1.5	0.7	-0.1	0.0	0.0	1.5	0.7	0.0	1.5
R O	890 - 887	-1.2	-1.7	-5.2	0.1	0.1	-0.5	-1.1	-1.7	-5.2	4.1
S I	604 - 601	-0.4	0.3	0.4	0.0	0.0	-0.4	0.6	0.3	-0.6	1.1
T I	614 - 611	0.3	0.2	0.0	0.0	0.0	-0.4	0.5	0.3	-0.3	0.8
U I	900 - 910	0.7	0.1	-0.4	0.0	0.1	0.1	0.7	0.1	-0.5	1.2
V O	920 - 930	-0.5	-1.0	-0.2	0.2	0.0	0.1	-0.1	-0.5	-1.0	0.9
W I	1216 - 1226	1.2	2.3	-1.0	0.0	0.0	-0.2	2.3	1.2	-1.0	3.3
X O	1236 - 1246	-1.5	-2.4	1.1	-0.1	0.0	-0.2	1.1	-1.5	-2.5	3.6

<sup>1</sup> Refer to Figure 2.10.2-34 for the identification of the representative sections.

Table 2.10.4-155 Critical P<sub>m</sub> Stress Summary; 30-Foot Bottom Corner Drop; Drop Orientation = 24 Degrees; 3-D Bottom Model; Condition 1

Condition 1: 100°F Ambient with Contents

Comp. No. <sup>1</sup>	Section Cut Node-Node	P <sub>m</sub> Stresses (ksi)						Principal Stresses (ksi)			S.I.	Allow. Stress	Margin of Safety
		S <sub>x</sub>	S <sub>y</sub>	S <sub>z</sub>	S <sub>xy</sub>	S <sub>xz</sub>	S <sub>yz</sub>	S1	S2	S3			
1	27- 7	-13.0	-17.0	-3.7	0.1	-0.5	-6.2	-0.6	-16.1	-17.0	16.4	43.6	1.8
2	10140-10137	0.0	6.4	-12.9	0.0	-6.6	-0.8	8.5	0.0	-14.9	23.4	44.9	0.9
3	10160-10157	0.0	6.9	-12.5	0.0	-6.6	-0.6	8.9	0.0	-14.6	23.5	66.0	1.8
4	12520-12517	-0.1	3.0	-9.7	0.0	-7.6	0.0	6.5	-0.1	-13.3	19.8	45.8	1.3
5	12204-12201	-0.2	2.6	-9.7	0.0	-4.4	-0.2	4.0	-0.2	-11.1	15.1	46.4	2.1
6	14880-14877	-0.1	1.7	-0.8	-0.1	3.3	0.1	4.0	-0.1	-3.1	7.1	49.3	5.9
7	16900-16910	-0.2	0.5	-0.8	-0.1	0.6	0.2	0.7	-0.1	-1.1	1.8	48.0	25.2
8	1236- 1246	-0.7	-1.2	0.3	-0.1	0.0	-0.2	0.3	-0.7	-1.2	1.5	94.5	62.0

Locations of the most critical sections for each component are provided in the following:

Comp. No. <sup>1</sup>	Section Location Inside Node			Section Location Outside Node		
	x (in)	y (deg)	z (in)	x (in)	y (deg)	z (in)
1	37.50	0.0	6.20	37.50	0.0	0.75
2	35.50	45.9	17.40	37.50	45.9	17.40
3	35.50	45.9	18.90	37.50	45.9	18.90
4	35.50	56.5	47.40	37.00	56.5	47.40
5	40.70	56.5	26.40	43.35	56.5	26.40
6	35.50	67.7	172.40	37.50	67.7	172.40
7	35.50	79.4	179.40	35.50	79.4	185.40
8	0.0	0.0	187.40	0.0	0.0	193.71

<sup>1</sup> Refer to Figure 2.10.2-33 for cask component identification.

Table 2.10.4-156 Critical  $P_m + P_b$  Stress Summary; 30-Foot Bottom Corner Drop; Drop Orientation = 24 Degrees; 3-D Bottom Model; Condition 1

Condition 1: 100°F Ambient with Contents

Comp. No. <sup>1</sup>	Section Cnt Node-Node	$P_m + P_b$ Stresses (ksi)						Principal Stresses (ksi)				Allow. Stress	Margin of Safety
		$S_x$	$S_y$	$S_z$	$S_{xy}$	$S_{yz}$	$S_{zx}$	S1	S2	S3	S.L.		
1	1170- 1168	-44.2	-33.1	-4.6	-0.1	-0.1	-0.1	-4.6	-33.1	-44.2	39.6	65.2	0.6
2	14035-14031	9.1	-3.6	-21.0	5.2	-8.6	-5.2	12.9	-3.6	-24.8	37.7	64.2	0.7
3	10150-10147	-0.1	4.6	-21.5	0.0	-7.9	-0.7	6.8	-0.1	-23.7	30.5	94.3	2.1
4	12520-12517	-0.1	5.0	-9.1	0.0	-8.0	0.0	8.6	-0.1	-12.8	21.4	65.5	2.1
5	10204-10201	-0.3	2.9	-10.6	0.0	-4.3	-0.2	4.2	-0.3	-11.9	16.0	66.4	3.2
6	14880-14877	-0.1	1.7	-1.8	-0.1	4.0	0.1	4.3	-0.1	-4.4	8.7	70.9	7.1
7	1216- 1226	1.2	2.3	-1.0	0.0	0.0	-0.2	2.3	1.2	-1.0	3.3	69.8	20.2
8	1236- 1246	-1.5	-2.4	1.1	-0.1	0.0	-0.2	1.1	-1.5	-2.5	3.6	135.0	36.5

Locations of the most critical sections for each component are provided in the following:

Comp. No. <sup>1</sup>	Section Location Inside Node			Outside Node		
	x (in)	y (deg)	z (in)	x (in)	y (deg)	z (in)
1	14.73	0.0	6.20	14.73	0.0	0.75
2	39.44	67.7	8.20	43.35	67.7	8.20
3	35.50	45.9	18.15	37.50	45.9	18.15
4	35.50	56.5	47.40	37.00	56.5	47.40
5	40.70	45.9	26.40	43.35	45.9	26.40
6	35.50	67.7	172.40	37.50	67.7	172.40
7	0.0	0.0	179.40	0.0	0.0	185.40
8	0.0	0.0	187.40	0.0	0.0	193.71

<sup>1</sup> Refer to Figure 2.10.2-33 for cask component identification.

Table 2.10.4-157  $P_m$  Stresses; 30-Foot Bottom Corner Drop; Drop Orientation = 24 Degrees; 3-D Bottom Model; 45.9-Degree Circumferential Location; Condition 1

Condition 1: 100°F Ambient with Contents

Section <sup>1</sup>	Node - Node	Stress Components (ksi)						Principal Stresses (ksi)			
		$S_x$	$S_y$	$S_z$	$S_{xy}$	$S_{yz}$	$S_{zx}$	S1	S2	S3	S.I.
A	1130 - 1128	2.2	-0.1	-1.2	0.0	1.8	2.1	3.4	0.6	-3.1	6.4
B	1185 - 1183	-3.7	-7.8	-1.9	0.0	2.0	2.3	0.0	-4.9	-8.5	8.5
C	10090 - 10040	0.9	-1.1	-7.2	0.3	-1.8	-2.7	1.9	-0.9	-8.4	10.3
D	10025 - 10005	-7.7	-17.4	-16.8	-0.9	-1.5	-4.0	-6.2	-16.0	-19.6	13.4
E	10035 - 10031	0.4	-5.5	-11.9	1.4	-2.5	-5.4	3.0	-5.7	-14.3	17.3
F	10100 - 10097	-1.4	4.0	-13.5	-0.5	-6.5	-1.0	6.1	-1.3	-15.7	21.8
G	10094 - 10091	-0.8	2.0	-12.1	-0.4	-3.5	-0.7	2.9	-0.8	-13.0	15.9
H	10330 - 10327	-0.4	3.0	-14.0	0.3	-8.0	0.3	6.2	-0.4	-17.2	23.4
I	10244 - 10241	0.0	2.2	-9.9	0.0	-3.5	-0.1	3.2	0.0	-10.9	14.1
J	10550 - 10547	0.0	3.5	-9.5	0.0	-6.1	0.0	5.9	0.0	-11.9	17.8
K	10344 - 10341	0.0	0.9	-7.2	0.0	-2.8	0.0	1.7	0.0	-8.0	9.8
L	10740 - 10737	-0.1	3.5	-4.3	0.1	-2.4	0.0	4.2	-0.1	-5.0	9.2
M	10454 - 10451	0.0	0.7	-4.0	0.0	-1.8	0.0	1.2	0.0	-4.6	5.9
N	10810 - 10807	0.0	3.4	-1.9	0.0	1.2	0.0	3.7	0.0	-2.2	5.9
O	10524 - 10521	0.0	0.4	-1.9	0.0	-0.8	0.0	0.6	0.0	-2.2	2.8
P	10850 - 10847	0.0	3.1	-1.8	0.1	3.2	0.0	4.7	0.0	-3.4	8.1
Q	10564 - 10561	0.0	0.5	-0.9	0.0	-0.4	0.0	0.6	0.0	-1.0	1.6
R	10890 - 10887	-0.5	0.7	-1.2	0.7	1.9	-0.1	2.0	-0.5	-2.5	4.5
S	10604 - 10601	-0.3	1.0	0.0	0.2	-0.3	0.0	1.1	0.0	-0.3	1.5
T	10614 - 10611	0.1	0.5	0.0	0.0	-0.2	-0.1	0.6	0.1	-0.1	0.7
U	10900 - 10910	0.2	0.2	-0.6	-0.3	0.6	0.2	0.6	0.2	-0.9	1.5
V	10920 - 10930	-0.1	-1.0	-0.3	0.1	0.2	0.2	0.0	-0.4	-1.0	1.0
W	1216 - 1226	0.5	1.1	-0.3	0.0	0.0	-0.2	1.1	0.5	-0.3	1.4
X	1236 - 1246	-0.7	-1.2	0.3	-0.1	0.0	-0.2	0.3	-0.7	-1.2	1.5

<sup>1</sup> Refer to Figure 2.10.2-34 for the identification of the representative sections.



Table 2.10.4-158  $P_m + P_b$  Stresses; 30-Foot Bottom Corner Drop; Drop Orientation = 24 Degrees; 3-D Bottom Model; 45.9-Degree Circumferential Location; Condition 1

Condition 1: 100°F Ambient with Contents

Section <sup>1</sup>	Node - Node	Stress Components (ksi)						Principal Stresses (ksi)			
		$S_x$	$S_y$	$S_z$	$S_{xy}$	$S_{yz}$	$S_{zx}$	S1	S2	S3	S.I.
A I	1130 - 1128	17.5	13.4	-6.5	-0.5	1.8	2.1	17.7	13.5	-6.8	24.5
B O	1185 - 1183	-17.5	-18.8	2.7	0.4	1.7	2.3	3.1	-17.7	-19.0	22.1
C I	10090 - 10040	-12.7	0.2	-15.1	-4.7	-4.1	-4.0	2.2	-9.9	-19.9	22.1
D O	10025 - 10005	6.2	-17.7	-4.8	2.0	0.4	-0.8	6.4	-4.9	-17.9	24.3
E I	10035 - 10031	8.5	-6.7	-23.4	3.5	-4.8	-6.2	10.8	-6.9	-25.5	36.3
F I	10100 - 10097	-1.3	-0.5	-30.6	-0.6	-8.8	-3.2	1.9	-1.0	-33.4	35.3
G I	10094 - 10091	-0.4	-1.2	-24.7	-0.6	-5.5	-1.7	0.2	-0.4	-26.0	26.2
H O	10330 - 10327	-0.5	0.8	-19.6	0.5	-7.7	0.9	3.4	-0.4	-22.2	25.6
I I	10244 - 10241	0.0	2.7	-8.9	0.0	-4.1	-0.1	4.0	0.0	-10.2	14.2
J I	10550 - 10547	-0.1	4.8	-9.0	-0.1	-6.5	0.0	7.4	-0.1	-11.6	19.0
K I	10344 - 10341	0.0	1.2	-7.0	-0.1	-3.1	0.0	2.2	0.0	-8.0	10.3
L I	10740 - 10737	0.0	4.5	-4.0	-0.2	-2.4	0.0	5.1	0.0	-4.7	9.8
M I	10454 - 10451	-0.1	1.2	-4.0	0.1	-1.8	0.0	1.7	-0.1	-4.5	6.2
N I	10810 - 10807	0.0	3.8	-2.0	0.0	1.6	0.0	4.2	0.0	-2.4	6.6
O I	10524 - 10521	0.0	1.1	-1.7	-0.1	-0.5	0.0	1.2	0.0	-1.8	3.0
P I	10850 - 10847	0.0	2.9	-2.5	0.1	3.8	-0.1	4.9	0.0	-4.5	9.4
Q O	10564 - 10561	0.0	0.1	-1.3	0.0	-0.8	0.0	0.5	0.0	-1.6	2.1
R I	10890 - 10887	-0.3	0.9	-0.4	0.6	2.4	0.0	2.8	-0.3	-2.3	5.1
S I	10604 - 10601	-0.5	0.7	-1.3	0.3	-0.1	-0.1	0.8	-0.6	-1.4	2.1
T I	10614 - 10611	0.2	0.6	-0.3	-0.1	-0.1	-0.1	0.6	0.2	-0.4	1.0
U I	10900 - 10910	-0.2	0.5	-0.7	-0.6	0.8	0.2	1.1	-0.2	-1.3	2.4
V O	10920 - 10930	0.2	-1.5	-0.2	0.4	0.1	0.1	0.3	-0.3	-1.6	1.9
W I	1216 - 1226	1.2	2.3	-1.0	0.0	0.0	-0.2	2.3	1.2	-1.0	3.3
X O	1236 - 1246	-1.5	-2.4	1.1	-0.1	0.0	-0.2	1.1	-1.5	-2.5	3.6

<sup>1</sup> Refer to Figure 2.10.2-34 for the identification of the representative sections.

Table 2.10.4-159  $P_m$  Stresses; 30-Foot Bottom Corner Drop; Drop Orientation = 24 Degrees; 3-D Bottom Model; 91.7-Degree Circumferential Location; Condition 1

Condition 1: 100°F Ambient with Contents

Section <sup>1</sup>	Node - Node	Stress Components (ksi)						Principal Stresses (ksi)			
		$S_x$	$S_y$	$S_z$	$S_{xy}$	$S_{yz}$	$S_{xz}$	S1	S2	S3	S.L
A	1130 - 1128	2.2	-0.1	-1.2	0.0	1.8	2.1	3.4	0.6	-3.1	6.4
B	1185 - 1183	-3.7	-7.8	-1.9	0.0	2.0	2.3	0.0	-4.9	-8.5	8.5
C	18090 - 18040	2.6	1.5	-1.6	-0.1	-2.4	-0.3	2.8	2.6	-2.9	5.7
D	18025 - 18005	-2.0	-4.2	-5.2	-3.0	-3.4	-0.6	0.6	-3.0	-9.0	9.6
E	18035 - 18031	3.9	0.8	-2.0	1.7	-5.9	-3.3	8.2	1.4	-6.9	15.1
F	18100 - 18097	-0.1	3.2	-0.5	-0.6	-8.8	-0.7	10.3	0.0	-7.8	18.1
G	18094 - 18091	-0.4	1.8	-2.3	-0.7	-6.0	-0.5	6.2	-0.3	-6.7	12.9
H	18330 - 18327	0.0	0.7	-2.3	0.5	-8.9	0.1	8.2	0.0	-9.8	18.1
I	18244 - 18241	0.0	0.4	-3.4	0.1	-4.7	0.0	3.5	0.0	-6.5	10.1
J	18550 - 18547	0.1	1.1	-4.3	0.0	-6.9	0.0	5.8	0.1	-9.0	14.8
K	18344 - 18341	0.0	0.0	-4.2	0.0	-3.6	0.0	2.1	0.0	-6.3	8.4
L	18740 - 18737	0.1	1.1	-5.4	-0.1	-3.3	0.0	2.5	0.0	-6.8	9.2
M	18454 - 18451	0.0	0.0	-3.9	0.0	-2.4	0.0	1.2	0.0	-5.0	6.2
N	18810 - 18807	0.0	0.8	-4.1	0.1	0.4	0.0	0.8	0.0	-4.1	5.0
O	18524 - 18521	0.0	0.0	-3.0	0.0	-1.4	0.0	0.5	0.0	-3.6	4.1
P	18850 - 18847	0.0	0.3	-2.1	0.1	2.4	-0.1	1.7	0.0	-3.5	5.3
Q	18564 - 18561	0.0	0.2	-2.4	0.0	-1.0	0.0	0.5	0.0	-2.7	3.3
R	18890 - 18887	0.7	2.1	-0.9	0.8	1.7	0.3	3.2	0.4	-1.7	4.8
S	18604 - 18601	-0.1	1.1	-1.3	0.3	-0.2	0.3	1.2	-0.1	-1.4	2.6
T	18614 - 18611	-0.1	0.5	-0.7	0.1	0.2	0.2	0.6	-0.1	-0.8	1.4
U	18900 - 18910	-0.2	0.5	-0.8	0.0	0.6	0.2	0.7	-0.1	-1.0	1.7
V	18920 - 18930	-0.1	-0.9	-0.4	-0.2	0.3	0.2	0.0	-0.3	-1.1	1.1
W	1216 - 1226	0.5	1.1	-0.3	0.0	0.0	-0.2	1.1	0.5	-0.3	1.4
X	1236 - 1246	-0.7	-1.2	0.3	-0.1	0.0	-0.2	0.3	-0.7	-1.2	1.5

<sup>1</sup> Refer to Figure 2.10.2-34 for the identification of the representative sections.

Table 2.10.4-160  $P_m + P_b$  Stresses; 30-Foot Bottom Corner Drop; Drop Orientation = 24 Degrees; 3-D Bottom Model; 91.7-Degree Circumferential Location; Condition 1

Condition 1: 100°F Ambient with Contents

Section <sup>1</sup>	Node - Node	Stress Components (ksi)						Principal Stresses (ksi)			
		$S_x$	$S_y$	$S_z$	$S_{xy}$	$S_{yz}$	$S_{xz}$	S1	S2	S3	S.I.
A I	1130 - 1128	17.5	13.4	-6.5	-0.5	1.8	2.1	17.7	13.5	-6.8	24.5
B O	1185 - 1183	-17.5	-18.8	2.7	0.4	1.7	2.3	3.1	-17.7	-19.0	22.1
C I	18090 - 18040	-8.7	-0.6	-4.4	-5.9	-5.3	-0.5	4.8	-5.5	-13.1	17.8
D I	18025 - 18005	-12.6	-6.9	-10.2	-8.6	-7.1	-2.5	1.3	-8.7	-22.2	23.4
E I	18035 - 18031	9.7	0.9	-6.9	4.8	-8.9	-4.3	14.8	1.7	-12.8	27.5
F I	18100 - 18097	-0.1	0.4	-10.7	-0.8	-10.7	-1.0	6.9	0.0	-17.3	24.1
G I	18094 - 18091	-0.1	0.2	-8.4	-0.9	-7.6	-0.9	4.7	0.0	-12.9	17.6
H O	18330 - 18327	0.0	0.9	-3.4	0.7	-9.8	0.2	8.8	0.0	-11.3	20.1
I O	18244 - 18241	0.0	0.1	-4.2	0.0	-5.0	0.0	3.4	0.0	-7.5	10.9
J O	18550 - 18547	0.1	1.4	-4.3	0.0	-6.9	0.0	6.0	0.1	-8.9	14.9
K I	18344 - 18341	0.0	0.6	-3.9	0.1	-3.7	0.0	2.7	0.0	-5.9	8.6
L I	18740 - 18737	0.2	1.5	-5.1	0.3	-3.5	0.0	3.1	0.1	-6.6	9.6
M I	18454 - 18451	-0.1	0.9	-3.6	-0.1	-2.5	0.0	2.0	-0.1	-4.7	6.8
N I	18810 - 18807	0.0	1.9	-3.7	0.1	0.2	0.0	1.9	0.0	-3.7	5.6
O I	18524 - 18521	0.0	0.5	-2.8	0.0	-1.6	0.0	1.1	0.0	-3.5	4.6
P I	18850 - 18847	0.0	1.3	-1.0	0.1	2.4	0.0	2.8	0.0	-2.5	5.3
Q I	18564 - 18561	0.0	0.6	-1.9	0.0	-1.2	0.0	1.1	0.0	-2.4	3.5
R I	18890 - 18887	0.6	1.5	-3.6	0.7	1.8	0.2	2.4	0.3	-4.2	6.6
S I	18604 - 18601	0.0	0.9	-2.6	0.5	-0.3	0.4	1.1	-0.2	-2.7	3.8
T I	18614 - 18611	-0.2	0.7	-0.9	0.1	0.2	0.3	0.7	-0.1	-1.0	1.7
U I	18900 - 18910	-1.2	0.7	-1.1	-0.2	0.7	0.1	1.0	-1.1	-1.5	2.4
V O	18920 - 18930	0.7	-1.3	-0.3	-0.1	0.2	0.1	0.7	-0.3	-1.4	2.0
W I	1216 - 1226	1.2	2.3	-1.0	0.0	0.0	-0.2	2.3	1.2	-1.0	3.3
X O	1236 - 1246	-1.5	-2.4	1.1	-0.1	0.0	-0.2	1.1	-1.5	-2.5	3.6

<sup>1</sup> Refer to Figure 2.10.2-34 for the identification of the representative sections.

Table 2.10.4-161  $P_m$  Stresses; 30-Foot Bottom Corner Drop; Drop Orientation = 24 Degrees; 3-D Bottom Model; 180-Degree Circumferential Location; Condition 1

Condition 1: 100°F Ambient with Contents

Section <sup>1</sup>	Node - Node	Stress Components (ksi)						Principal Stresses (ksi)			
		$S_x$	$S_y$	$S_z$	$S_{xy}$	$S_{yz}$	$S_{xz}$	S1	S2	S3	S.L
A	1130 - 1128	2.2	-0.1	-1.2	0.0	1.8	2.1	3.4	0.6	-3.1	6.4
B	1185 - 1183	-3.7	-7.8	-1.9	0.0	2.0	2.3	0.0	-4.9	-8.5	8.5
C	30090 - 30040	1.2	2.5	0.6	0.1	-0.3	1.0	2.6	1.9	-0.2	2.8
D	30025 - 30005	-1.7	2.9	-1.9	0.3	-0.3	0.3	3.0	-1.5	-2.1	5.1
E	30035 - 30031	2.4	3.1	-0.1	0.3	-0.2	-1.7	3.5	2.8	-1.0	4.4
F	30100 - 30097	0.4	2.3	4.8	0.2	-0.7	-0.6	5.1	2.1	0.3	4.8
G	30094 - 30091	0.2	0.8	1.9	0.0	-0.4	0.0	2.1	0.7	0.2	1.9
H	30330 - 30327	-1.1	-2.2	4.3	-0.2	-0.9	0.0	4.4	-1.1	-2.4	6.8
I	30244 - 30241	0.0	-0.5	1.2	-0.1	-0.4	0.0	1.3	0.0	-0.6	1.9
J	30550 - 30547	-0.2	-1.0	1.1	-0.1	-0.7	0.0	1.3	-0.2	-1.2	2.5
K	30344 - 30341	0.0	-0.3	0.3	-0.1	-0.3	0.0	0.5	0.0	-0.4	0.9
L	30740 - 30737	-0.1	-0.9	-1.9	0.0	-0.4	0.0	-0.1	-0.8	-2.0	1.9
M	30454 - 30451	0.0	-0.3	-0.8	0.0	-0.3	0.0	0.0	-0.2	-1.0	0.9
N	30810 - 30807	-0.1	-1.2	-2.9	-0.2	-0.1	0.0	-0.1	-1.2	-2.9	2.8
O	30524 - 30521	0.0	-0.4	-1.7	0.0	-0.2	0.0	0.0	-0.3	-1.7	1.7
P	30850 - 30847	-0.1	-1.5	-2.4	-0.2	0.0	-0.1	0.0	-1.5	-2.4	2.4
Q	30564 - 30561	0.0	-0.4	-2.0	-0.1	-0.2	0.0	0.0	-0.4	-2.0	2.0
R	30890 - 30887	0.4	0.1	-1.3	0.0	0.1	0.1	0.4	0.1	-1.3	1.7
S	30604 - 30601	0.0	0.0	-1.5	0.0	0.0	0.1	0.0	0.0	-1.5	1.6
T	30614 - 30611	-0.1	0.1	-1.0	0.1	0.0	0.2	0.1	-0.1	-1.1	1.2
U	30900 - 30910	0.3	0.2	-0.5	0.0	0.0	0.3	0.4	0.2	-0.6	1.0
V	30920 - 30930	-0.3	0.0	-0.4	0.1	0.0	0.4	0.1	0.0	-0.8	0.9
W	1216 - 1226	0.5	1.1	-0.3	0.0	0.0	-0.2	1.1	0.5	-0.3	1.4
X	1236 - 1246	-0.7	-1.2	0.3	-0.1	0.0	-0.2	0.3	-0.7	-1.2	1.5

<sup>1</sup> Refer to Figure 2.10.2-34 for the identification of the representative sections.

Table 2.10.4-162  $P_m + P_b$  Stresses; 30-Foot Bottom Corner Drop; Drop Orientation = 24 Degrees; 3-D Bottom Model; 180-Degree Circumferential Location; Condition 1

Condition 1: 100°F Ambient with Contents

Section <sup>1</sup>	Node - Node	Stress Components (ksi)							Principal Stresses (ksi)			
		$S_x$	$S_y$	$S_z$	$S_{xy}$	$S_{yz}$	$S_{xz}$	$S_{xx}$	S1	S2	S3	S.I.
A I	1130 - 1128	17.5	13.4	-6.5	-0.5	1.8	2.1	17.7	13.5	-6.8	24.5	
B O	1185 - 1183	-17.5	-18.8	2.7	0.4	1.7	2.3	3.1	-17.7	-19.0	22.1	
C O	30090 - 30040	8.9	5.5	-0.1	0.0	-0.1	0.8	9.0	5.5	-0.1	9.1	
D I	30025 - 30005	-8.4	0.1	-3.5	0.6	-0.4	-0.9	0.2	-3.4	-8.6	8.8	
E I	30035 - 30031	5.7	3.9	-1.2	0.1	-0.3	-2.2	6.4	3.9	-1.8	8.2	
F O	30100 - 30097	0.5	3.1	8.4	0.4	-0.4	-1.0	8.6	3.1	0.3	8.3	
G I	30094 - 30091	0.4	1.6	4.1	0.1	-0.6	0.3	4.3	1.4	0.4	3.9	
H I	30330 - 30327	0.1	-0.9	7.2	-0.1	-0.9	0.0	7.3	0.1	-1.0	8.3	
I I	30244 - 30241	0.0	-0.2	1.6	0.0	-0.4	0.0	1.7	0.0	-0.3	2.0	
J O	30550 - 30547	-0.3	-1.1	1.1	-0.1	-0.7	0.0	1.3	-0.2	-1.3	2.6	
K O	30344 - 30341	0.0	-0.6	0.3	-0.1	-0.3	0.0	0.4	0.0	-0.7	1.1	
L I	30740 - 30737	-0.2	-1.2	-2.1	-0.3	-0.3	0.0	-0.1	-1.1	-2.2	2.1	
M I	30454 - 30451	0.0	-0.3	-0.9	-0.1	-0.3	0.0	0.0	-0.2	-1.0	1.0	
N I	30810 - 30807	-0.1	-1.5	-3.0	-0.2	-0.1	0.0	-0.1	-1.6	-3.1	3.0	
O I	30524 - 30521	0.0	-0.6	-1.8	-0.1	-0.2	0.0	0.0	-0.6	-1.9	1.8	
P O	30850 - 30847	-0.1	-1.4	-2.9	-0.2	0.0	-0.1	0.0	-1.4	-2.9	2.8	
Q O	30564 - 30561	0.0	-0.2	-2.0	0.0	-0.1	0.0	0.0	-0.2	-2.0	2.0	
R I	30890 - 30887	0.4	-0.2	-2.3	0.0	0.1	0.0	0.4	-0.2	-2.3	2.7	
S O	30604 - 30601	-0.1	-0.1	-1.7	0.0	0.0	0.1	-0.1	-0.1	-1.7	1.7	
T O	30614 - 30611	0.0	0.1	-1.2	0.0	0.1	0.2	0.1	0.0	-1.2	1.3	
U O	30900 - 30910	1.3	0.5	-0.2	0.0	0.0	0.5	1.5	0.5	-0.3	1.8	
V I	30920 - 30930	-1.5	-0.3	-0.5	0.1	0.0	0.5	-0.2	-0.3	-1.7	1.5	
W I	1216 - 1226	1.2	2.3	-1.0	0.0	0.0	-0.2	2.3	1.2	-1.0	3.3	
X O	1236 - 1246	-1.5	-2.4	1.1	-0.1	0.0	-0.2	1.1	-1.5	-2.5	3.6	

<sup>1</sup> Refer to Figure 2.10.2-34 for the identification of the representative sections.

Table 2.10.4-163 Primary Stresses; 30-Foot Bottom Oblique Drop; Drop Orientation = 15 Degrees; 3-D Bottom Model; 0-Degree Circumferential Location; Condition 1

Condition 1: 100°F Ambient with Contents

Stress Points		Stress Components (ksi)						Principal Stresses (ksi)		
Section <sup>1</sup>	Node	S <sub>x</sub>	S <sub>y</sub>	S <sub>z</sub>	S <sub>xy</sub>	S <sub>xz</sub>	S <sub>yz</sub>	S1	S2	S3
A1	1130	18.7	15.1	-6.8	-0.5	2.2	2.2	18.9	15.3	-7.2
A2	1129	2.6	1.1	-1.3	0.0	1.6	2.2	3.7	1.5	-2.8
A3	1128	-13.6	-12.9	4.3	0.5	2.1	2.2	4.8	-13.1	-13.9
B1	1185	10.9	4.9	-6.8	-0.6	2.6	2.4	11.3	5.4	-7.7
B2	1184	-3.6	-6.6	-2.0	-0.1	1.9	2.4	0.1	-4.8	-7.6
B3	1183	-18.4	-18.1	2.8	0.4	2.1	2.4	3.3	-18.3	-18.7
C1	90	-21.3	-4.9	-30.1	-1.3	-0.7	-5.7	-4.7	-18.6	-33.0
C2	80	-8.0	0.6	-16.9	-1.0	-0.5	-4.5	0.7	-6.2	-18.8
C3	70	-4.5	1.3	-10.2	-0.6	-0.4	-4.0	1.3	-2.5	-12.3
C4	60	-1.5	1.3	-5.9	-0.1	-0.4	-3.9	1.4	0.7	-8.2
C5	50	9.3	-1.7	-4.1	1.0	-0.2	-2.7	9.9	-1.7	-4.6
C6	40	17.1	-3.2	-4.3	1.7	-0.1	-1.6	17.3	-3.3	-4.4
D1	25	-28.1	-20.8	-33.8	-0.3	-0.7	-8.3	-20.8	-22.1	-39.8
D2	15	-3.9	-16.5	-15.5	0.7	-0.3	-3.8	-2.7	-16.5	-16.7
D3	5	2.9	-21.0	-7.8	1.6	-0.1	-1.2	3.1	-8.0	-21.1
E1	35	13.3	-6.0	-24.0	1.4	-0.4	-4.0	13.8	-6.1	-24.4
E2	34	3.7	-6.4	-18.5	0.7	-0.8	-7.6	6.1	-6.4	-20.9
E3	33	-3.0	-6.2	-11.3	0.2	-0.8	-8.0	1.9	-6.3	-16.2
E4	32	-4.2	-5.2	-6.1	0.1	-0.4	-4.9	-0.1	-5.2	-10.2
E5	31	-4.7	-4.1	-1.0	0.0	-0.3	-3.0	0.7	-4.1	-6.3
F1	100	0.2	-1.4	-40.6	-0.1	-0.8	-3.9	0.5	-1.3	-41.0
F2	99	-2.6	3.4	-20.5	-0.6	-0.7	-2.2	3.5	-2.4	-20.8
F3	98	-2.7	5.7	-11.4	-0.7	-0.4	0.2	5.8	-2.8	-11.4
F4	97	0.0	9.7	1.0	-0.8	-0.3	1.1	9.8	1.6	-0.7
G1	94	0.1	-1.9	-30.9	0.0	-0.4	-2.1	0.2	-1.9	-31.0
G2	93	-1.1	1.6	-17.0	-0.3	-0.4	-1.2	1.6	-1.0	-17.1
G3	92	-1.5	3.6	-9.0	-0.4	-0.2	-0.2	3.6	-1.5	-9.0
G4	91	-0.7	6.3	0.6	-0.5	-0.1	0.0	6.3	0.6	-0.8
H1	330	-0.3	3.3	-12.5	-0.2	-0.7	-0.1	3.4	-0.3	-12.5
H2	329	-0.5	2.7	-16.4	-0.2	-0.7	0.0	2.8	-0.5	-16.4

Table 2.10.4-163 Primary Stresses; 30-Foot Bottom Oblique Drop; Drop Orientation = 15 Degrees; 3-D Bottom Model; 0-Degree Circumferential Location; Condition 1 (continued)

Stress Points Section <sup>1</sup> Node		Stress Components (ksi)						Principal Stresses (ksi)		
		S <sub>x</sub>	S <sub>y</sub>	S <sub>z</sub>	S <sub>xy</sub>	S <sub>yz</sub>	S <sub>xz</sub>	S1	S2	S3
H3	328	-0.6	2.2	-20.0	-0.2	-0.6	0.6	2.3	-0.6	-20.0
H4	327	-0.6	1.0	-26.6	-0.1	-0.5	1.4	1.0	-0.5	-26.7
I1	244	0.0	2.0	-11.2	-0.1	-0.3	-0.1	2.0	0.0	-11.3
I2	243	0.0	2.3	-11.8	-0.2	-0.3	-0.1	2.3	0.0	-11.8
I3	242	0.0	2.5	-12.3	-0.2	-0.2	-0.1	2.5	0.0	-12.3
I4	241	0.0	2.7	-12.8	-0.2	-0.2	-0.1	2.7	0.0	-12.8
J1	550	-0.1	1.9	-13.2	-0.2	-0.5	0.0	1.9	-0.1	-13.2
J2	548	-0.1	3.5	-12.7	-0.3	-0.5	0.0	3.6	-0.1	-12.7
J3	547	0.0	5.1	-12.2	-0.4	-0.5	0.0	5.1	-0.1	-12.2
K1	344	0.0	-0.4	-9.9	0.0	-0.2	0.0	0.0	-0.4	-9.9
K2	342	0.0	0.7	-9.5	-0.1	-0.2	0.0	0.7	0.0	-9.5
K3	341	0.0	1.8	-9.2	-0.1	-0.2	0.0	1.8	0.0	-9.2
L1	740	0.0	2.1	-6.2	0.2	-0.2	0.0	2.1	0.0	-6.2
L2	738	-0.2	3.4	-5.8	-0.6	-0.2	0.0	3.5	-0.3	-5.8
L3	737	0.2	4.9	-5.2	-1.3	-0.2	0.0	5.2	-0.1	-5.2
M1	454	-0.1	-0.8	-6.3	-0.4	-0.2	0.0	0.1	-1.0	-6.3
M2	452	0.1	0.5	-5.9	-0.2	-0.2	0.0	0.6	0.0	-5.9
M3	451	-0.2	1.5	-5.7	0.0	-0.2	0.0	1.5	-0.2	-5.7
N1	810	-0.1	2.9	-3.4	-0.2	0.0	0.0	2.9	-0.1	-3.4
N2	807	-0.1	4.2	-2.7	-0.3	0.0	0.0	4.2	-0.1	-2.7
O1	524	0.0	-0.7	-3.4	0.0	-0.1	0.0	0.0	-0.7	-3.4
O2	521	0.0	1.2	-2.6	-0.1	-0.1	0.0	1.3	0.0	-2.6
P1	850	0.0	2.7	-3.7	-0.2	0.2	-0.1	2.7	0.0	-3.7
P2	847	0.0	3.5	-2.4	-0.2	0.1	0.0	3.5	0.0	-2.4
Q1	564	0.0	0.1	-1.5	0.0	-0.1	0.0	0.1	0.0	-1.5
Q2	561	0.0	0.7	-1.9	0.0	-0.1	0.0	0.7	0.0	-1.9
R1	890	-0.4	0.6	-0.3	-0.1	0.1	-0.1	0.6	-0.3	-0.5
R2	887	-0.7	-0.1	-3.2	0.0	0.0	-0.2	-0.1	-0.6	-3.2
S1	604	-0.5	0.6	-1.4	0.0	-0.1	-0.1	0.6	-0.5	-1.4
S2	601	-0.1	1.3	0.4	-0.1	-0.1	0.0	1.3	0.4	-0.1
T1	897	0.0	0.4	-1.2	0.0	0.0	0.0	0.4	0.0	-1.2
T2	614	0.1	0.7	-0.6	0.0	-0.1	-0.1	0.7	0.1	-0.6

Table 2.10.4-163 Primary Stresses; 30-Foot Bottom Oblique Drop; Drop Orientation = 15 Degrees; 3-D Bottom Model; 0-Degree Circumferential Location; Condition 1 (continued)

Stress Points		Stress Components (ksi)						Principal Stresses (ksi)		
Section <sup>1</sup>	Node	S <sub>x</sub>	S <sub>y</sub>	S <sub>z</sub>	S <sub>xy</sub>	S <sub>yz</sub>	S <sub>xz</sub>	S1	S2	S3
T3	611	0.0	0.6	-0.3	0.0	-0.1	-0.1	0.6	0.0	-0.3
U1	900	-0.2	0.5	-0.8	0.0	0.0	0.2	0.5	-0.1	-0.8
U2	910	0.9	0.3	-0.5	0.0	0.0	0.3	1.0	0.3	-0.5
V1	920	-0.8	-0.2	-0.5	0.0	0.0	0.3	-0.2	-0.3	-1.0
V2	930	0.3	-0.4	-0.3	0.1	0.0	0.2	0.3	-0.3	-0.4
W1	1216	1.6	2.2	-1.1	0.0	0.1	-0.3	2.2	1.6	-1.1
W2	1226	-0.2	-0.1	0.5	0.0	0.0	-0.1	0.5	-0.1	-0.3
X1	1236	0.1	0.1	-0.6	0.0	0.0	-0.1	0.2	0.1	-0.6
X2	1246	-1.8	-2.1	1.2	0.0	0.1	-0.3	1.2	-1.8	-2.1

<sup>1</sup> Refer to Figure 2.10.2-34 for the identification of the representative sections.



Table 2.10.4-164  $P_m$  Stresses; 30-Foot Bottom Oblique Drop; Drop Orientation = 15 Degrees; 3-D Bottom Model; 0-Degree Circumferential Location; Condition 1

Condition 1: 100°F Ambient with Contents

Section <sup>1</sup>	Node - Node	Stress Components (ksi)						Principal Stresses (ksi)			
		$S_x$	$S_y$	$S_z$	$S_{xy}$	$S_{yz}$	$S_{xz}$	S1	S2	S3	S.L.
A	1130 - 1128	2.5	1.1	-1.2	0.0	1.9	2.2	3.8	1.5	-3.0	6.8
B	1185 - 1183	-3.7	-6.6	-2.0	-0.1	2.1	2.4	0.2	-4.7	-7.7	7.9
C	90 - 40	1.2	-0.6	-8.7	0.2	-0.3	-3.5	2.4	-0.6	-9.8	12.2
D	25 - 5	-8.3	-18.7	-18.2	0.7	-0.3	-4.3	-6.6	-18.7	-19.8	13.1
E	35 - 31	1.0	-5.8	-13.0	0.5	-0.6	-6.0	3.3	-5.8	-15.2	18.5
F	100 - 97	-1.7	4.4	-17.2	-0.6	-0.5	-1.1	4.5	-1.7	-17.3	21.8
G	94 - 91	-1.0	2.4	-13.7	-0.3	-0.3	-0.8	2.5	-1.0	-13.8	16.2
H	330 - 327	-0.5	2.4	-18.6	-0.2	-0.6	0.4	2.4	-0.5	-18.7	21.1
I	244 - 241	0.0	2.4	-12.0	-0.2	-0.3	-0.1	2.4	0.0	-12.0	14.4
J	550 - 547	-0.1	3.5	-12.7	-0.3	-0.5	0.0	3.5	-0.1	-12.7	16.2
K	344 - 341	0.0	0.7	-9.5	-0.1	-0.2	0.0	0.7	0.0	-9.5	10.2
L	740 - 737	0.0	3.4	-5.8	-0.6	-0.2	0.0	3.5	-0.1	-5.8	9.3
M	454 - 451	0.0	0.5	-5.9	-0.2	-0.2	0.0	0.5	-0.1	-5.9	6.5
N	810 - 807	-0.1	3.5	-3.1	-0.2	0.0	0.0	3.6	-0.1	-3.1	6.6
O	524 - 521	0.0	0.3	-3.0	0.0	-0.1	0.0	0.3	0.0	-3.0	3.3
P	850 - 847	0.0	3.1	-3.1	-0.2	0.1	0.0	3.1	0.0	-3.1	6.2
Q	564 - 561	0.0	0.4	-1.7	0.0	-0.1	0.0	0.4	0.0	-1.7	2.1
R	890 - 887	-0.5	0.2	-1.8	0.0	0.1	-0.1	0.2	-0.5	-1.8	2.0
S	604 - 601	-0.3	1.0	-0.5	-0.1	-0.1	0.0	1.0	-0.3	-0.5	1.5
T	614 - 611	0.0	0.7	-0.4	0.0	-0.1	-0.1	0.7	0.1	-0.5	1.1
U	900 - 910	0.4	0.4	-0.6	0.0	0.0	0.2	0.4	0.4	-0.7	1.1
V	920 - 930	-0.3	-0.3	-0.4	0.0	0.0	0.2	-0.1	-0.3	-0.6	0.5
W	1216 - 1226	0.7	1.0	-0.3	0.0	0.0	-0.2	1.0	0.7	-0.3	1.4
X	1236 - 1246	-0.8	-1.0	0.3	0.0	0.0	-0.2	0.3	-0.9	-1.0	1.3

<sup>1</sup> Refer to Figure 2.10.2-34 for the identification of the representative sections.

Table 2.10.4-165  $P_m + P_b$  Stresses; 30-Foot Bottom Oblique Drop; Drop Orientation = 15 Degrees; 3-D Bottom Model; 0-Degree Circumferential Location; Condition 1

Condition 1: 100°F Ambient with Contents

Section <sup>1</sup>	Node - Node	Stress Components (ksi)						Principal Stresses (ksi)			
		$S_x$	$S_y$	$S_z$	$S_{xy}$	$S_{yz}$	$S_{xz}$	S1	S2	S3	S.L.
A I	1130 - 1128	18.7	15.1	-6.8	-0.5	1.9	2.2	18.9	15.2	-7.2	26.1
B O	1185 - 1183	-18.3	-18.1	2.8	0.4	1.8	2.4	3.3	-18.2	-18.7	21.9
C I	90 - 40	-14.2	0.6	-18.2	-1.4	-0.6	-5.1	0.7	-10.8	-21.8	22.5
D O	25 - 5	7.2	-18.8	-5.2	1.6	0.0	-0.7	7.4	-5.2	-18.9	26.2
E I	35 - 31	10.4	-6.7	-25.1	1.2	-0.8	-6.9	11.8	-6.8	-26.5	38.3
F I	100 - 97	-1.6	-0.6	-36.4	-0.3	-0.9	-3.9	-0.5	-1.3	-36.9	36.3
G I	94 - 91	-0.5	-1.4	-28.6	-0.1	-0.5	-2.0	-0.4	-1.4	-28.8	28.4
H O	330 - 327	-0.6	1.3	-25.3	-0.1	-0.5	1.2	1.3	-0.6	-25.4	26.7
I O	244 - 241	0.0	2.7	-12.8	-0.2	-0.2	-0.1	2.7	0.0	-12.8	15.5
J O	550 - 547	0.0	5.1	-12.2	-0.4	-0.5	0.0	5.1	-0.1	-12.2	17.3
K O	344 - 341	0.0	1.8	-9.2	-0.1	-0.2	0.0	1.8	0.0	-9.2	11.0
L O	740 - 737	0.0	4.8	-5.2	-1.3	-0.2	0.0	5.2	-0.3	-5.2	10.4
M O	454 - 451	-0.1	1.6	-5.6	0.0	-0.2	0.0	1.6	-0.1	-5.6	7.2
N O	810 - 807	-0.1	4.2	-2.7	-0.3	0.0	0.0	4.2	-0.1	-2.7	7.0
O O	524 - 521	0.0	1.2	-2.6	-0.1	-0.1	0.0	1.3	0.0	-2.6	3.8
P I	850 - 847	0.0	2.7	-3.7	-0.2	0.2	-0.1	2.7	0.0	-3.7	6.4
Q O	564 - 561	0.0	0.7	-1.9	0.0	-0.1	0.0	0.7	0.0	-1.9	2.6
R O	890 - 887	-0.7	-0.1	-3.2	0.0	0.0	-0.2	-0.1	-0.6	-3.2	3.1
S I	604 - 601	-0.5	0.6	-1.4	0.0	-0.1	-0.1	0.6	-0.5	-1.4	2.1
T I	614 - 611	0.1	0.7	-0.6	0.0	-0.1	-0.1	0.7	0.1	-0.6	1.3
U O	900 - 910	0.9	0.3	-0.5	0.0	0.0	0.3	1.0	0.3	-0.5	1.5
V I	920 - 930	-0.8	-0.2	-0.5	0.0	0.0	0.3	-0.2	-0.3	-1.0	0.8
W I	1216 - 1226	1.6	2.2	-1.1	0.0	0.1	-0.3	2.2	1.6	-1.1	3.3
X O	1236 - 1246	-1.8	-2.1	1.2	0.0	0.1	-0.3	1.2	-1.8	-2.1	3.3

<sup>1</sup> Refer to Figure 2.10.2-34 for the identification of the representative sections.

Table 2.10.4-166 Critical P<sub>m</sub> Stress Summary; 30-Foot Bottom Oblique Drop; Drop Orientation = 15 Degrees; 3-D Bottom Model; Condition 1  
Condition 1: 100°F Ambient with Contents

Comp. No. <sup>1</sup>	Section Cut Node-Node	P <sub>m</sub> Stresses (ksi)						Principal Stresses (ksi)			S.I.	Allow. Stress	Margin of Safety
		S <sub>1</sub>	S <sub>2</sub>	S <sub>3</sub>	S <sub>4</sub>	S <sub>5</sub>	S <sub>6</sub>	S1	S2	S3			
1	14025-14005	-3.9	-11.9	-16.3	-2.3	-3.3	-3.5	-2.8	-10.2	-19.1	16.4	45.6	1.8
2	140- 137	0.0	7.3	-16.7	-0.5	-0.5	-0.9	7.4	0.0	-16.8	24.1	44.9	0.9
3	160- 157	0.0	7.9	-16.4	-0.6	-0.5	-0.7	7.9	-0.1	-16.4	24.3	66.0	1.7
4	8520- 8517	0.0	3.0	-13.3	0.0	-4.3	0.0	4.1	0.0	-14.3	18.5	45.8	1.5
5	8204- 8201	-0.1	3.1	-12.1	0.0	-2.3	-0.2	3.4	-0.1	-12.5	15.9	46.4	1.9
6	12880-12877	-0.1	1.3	-1.6	0.0	1.4	0.0	1.9	-0.1	-2.1	4.0	49.3	11.3
7	1216- 1226	0.7	1.0	-0.3	0.0	0.0	-0.2	1.0	0.7	-0.3	1.4	48.0	34.3
8	1236- 1246	-0.8	-1.0	0.3	0.0	0.0	-0.2	0.3	-0.9	-1.0	1.3	94.5	71.7

Locations of the most critical sections for each component are provided in the following:

Comp. No. <sup>1</sup>	Section Location			Section Location		
	Inside Node			Outside Node		
	x (in)	y (deg)	z (in)	x (in)	y (deg)	z (in)
1	39.44	67.7	6.20	39.44	67.7	0.75
2	35.50	0.0	17.40	37.50	0.0	17.40
3	35.50	0.0	18.90	37.50	0.0	18.90
4	35.50	35.8	47.40	37.00	35.8	47.40
5	40.70	35.8	26.40	43.35	35.8	26.40
6	35.50	56.5	172.40	37.50	56.5	172.40
7	0.00	0.0	179.40	0.00	0.0	185.40
8	0.00	0.0	187.40	0.00	0.0	193.71

<sup>1</sup> Refer to Figure 2.10.2-33 for cask component identification.

Table 2.10.4-167 Critical  $P_m + P_b$  Stress Summary; 30-Foot Bottom Oblique Drop; Drop Orientation = 15 Degrees; 3-D Bottom Model; Condition 1

Condition 1: 100°F Ambient with Contents

Comp. No. <sup>1</sup>	Section Cut Node-Node	$P_m + P_b$ Stresses (ksi)							Principal Stresses (ksi)				Allow. Stress	Margin of Safety
		$S_x$	$S_y$	$S_z$	$S_{xy}$	$S_{yz}$	$S_{zx}$	$S_{yz}$	S1	S2	S3	S.I.		
1	1170- 1168	-43.5	-34.0	-4.8	0.0	-0.1	-0.1	-0.1	-4.8	-34.0	-43.5	38.7	65.2	0.7
2	12035-12031	10.1	-4.2	-24.7	4.5	-6.8	-6.1	13.0	4.5	-27.3	40.3	64.2	64.2	0.6
3	6150- 6147	-0.1	5.2	-25.6	0.0	-3.9	-0.9	5.7	-0.1	-26.1	31.8	94.3	94.3	2.0
4	10520-10517	-0.1	3.7	-12.0	0.0	-5.6	0.0	5.5	-0.1	-13.8	19.3	65.5	65.5	2.4
5	8204- 8201	-0.3	3.0	-12.1	0.0	-2.7	-0.2	3.5	-0.3	-12.6	16.1	66.4	66.4	3.1
6	880- 877	0.1	0.0	-3.0	0.0	0.1	-0.3	0.1	0.0	-5.0	5.1	70.9	70.9	12.9
7	1216- 1226	1.6	2.2	-1.1	0.0	0.1	-0.3	2.2	1.6	-1.1	3.3	69.8	69.8	20.2
8	1236- 1246	-1.8	-2.1	1.2	0.0	0.1	-0.3	1.2	-1.8	-2.1	3.3	135.0	135.0	39.9

Locations of the most critical sections for each component are provided in the following:

Comp. No. <sup>1</sup>	Section Location					
	Inside Node			Outside Node		
	x (in)	y (deg)	z (in)	x (in)	y (deg)	z (in)
1	14.73	0.0	6.20	14.73	0.0	0.75
2	39.44	56.5	8.20	43.35	56.5	8.20
3	35.50	26.2	18.15	37.50	26.2	18.15
4	35.50	45.9	47.40	37.00	45.9	47.40
5	40.70	35.8	26.40	43.35	35.8	26.40
6	35.50	0.0	172.40	37.50	0.0	172.40
7	0.00	0.0	179.40	0.00	0.0	185.40
8	0.00	0.0	187.40	0.00	0.0	193.71

<sup>1</sup> Refer to Figure 2.10.2-33 for cask component identification.

Table 2.10.4-168 Primary Stresses; 30-Foot Top Oblique Drop; Drop Orientation = 75 Degrees; 3-D Top Model; 0-Degree Circumferential Location; Condition 1

Condition 1: 100°F Ambient with Contents

Stress Points		Stress Components (ksi)						Principal Stresses (ksi)		
Section <sup>1</sup>	Node	S <sub>x</sub>	S <sub>y</sub>	S <sub>z</sub>	S <sub>xy</sub>	S <sub>xz</sub>	S <sub>yz</sub>	S1	S2	S3
A1	1949	-1.0	1.8	-0.1	-0.2	0.0	-0.2	1.8	-0.1	-1.0
A2	1950	-0.9	1.3	-0.1	-0.2	0.2	-0.2	1.3	-0.1	-0.9
A3	1951	-0.2	-0.1	0.1	-0.1	0.5	-0.1	0.5	-0.2	-0.5
B1	1952	0.0	-0.8	-0.1	-0.2	0.5	-0.1	0.3	-0.1	-1.0
B2	93	0.6	-3.0	0.3	-0.4	0.3	-0.2	0.7	0.2	-3.1
C1	1925	2.5	-2.3	7.5	0.1	-0.5	0.4	7.6	2.5	-2.3
C2	1926	2.4	-3.5	1.5	0.2	-0.2	-0.1	2.4	1.5	-3.6
C3	1927	-1.3	-2.2	0.2	0.1	-0.1	0.2	0.3	-1.3	-2.3
D1	683	2.4	-1.9	0.3	0.5	-0.1	0.8	2.8	0.1	-2.0
D2	85	-3.3	-4.0	0.9	0.8	-0.1	0.2	0.9	-2.8	-4.5
E1	682	-2.0	-3.2	0.1	0.2	-0.1	1.1	0.6	-2.4	-3.3
E2	82	-1.7	-3.6	2.6	0.3	0.2	1.4	3.0	-2.0	-3.6
F1	1925	2.5	-2.3	7.5	0.1	-0.5	0.4	7.6	2.5	-2.3
F2	1325	0.7	-8.4	-13.8	0.6	-0.4	1.1	0.8	-8.4	-13.9
G1	680	2.3	-1.3	10.1	0.2	-0.1	2.0	10.6	1.8	-1.3
G2	80	2.1	-4.5	-2.4	0.4	-0.3	-0.2	2.2	-2.4	-4.5
H1	1921	-0.1	7.3	-2.8	-0.4	-1.3	0.1	7.4	-0.2	-3.0
H2	1321	-0.2	12.0	6.6	-0.7	-1.1	-0.3	12.2	6.5	-0.3
I1	676	-0.1	-0.3	5.4	0.1	-0.6	0.0	5.5	-0.1	-0.4
I2	76	-0.1	3.8	11.1	-0.2	-0.4	0.0	11.1	3.8	-0.1
J1	1916	-0.2	7.6	9.6	-0.6	-0.6	0.0	9.8	7.5	-0.3
J2	1316	-0.2	12.5	13.4	-0.9	-0.6	0.0	13.7	12.3	-0.3
K1	671	-0.1	-1.2	9.9	0.1	-0.4	0.0	9.9	-0.1	-1.3
K2	71	-0.1	5.9	13.3	-0.4	-0.2	0.0	13.3	6.0	-0.1
L1	1908	-0.9	4.5	12.9	-0.4	0.2	0.0	12.9	4.6	-0.9
L2	1308	0.0	11.5	15.9	1.7	0.2	0.0	15.9	11.7	-0.3
M1	663	-1.2	-2.2	10.8	0.1	0.1	0.0	10.8	-1.2	-2.2
M2	63	0.4	8.9	15.8	2.0	0.1	0.0	15.8	9.3	0.0
N1	1877	-0.3	7.4	4.5	-0.6	1.0	0.0	7.8	4.2	-0.4
N2	1477	-0.2	10.0	6.2	-0.8	1.0	0.0	10.3	6.0	-0.2

Table 2.10.4-168 Primary Stresses; 30-Foot Top Oblique Drop; Drop Orientation = 75 Degrees; 3-D Top Model; 0-Degree Circumferential Location; Condition 1  
(continued)

Stress Points		Stress Components (ksi)						Principal Stresses (ksi)		
Section <sup>1</sup>	Node	S <sub>x</sub>	S <sub>y</sub>	S <sub>z</sub>	S <sub>xy</sub>	S <sub>xz</sub>	S <sub>yz</sub>	S1	S2	S3
N3	1277	-0.1	12.6	7.9	-0.9	0.9	0.0	12.8	7.7	-0.1
O1	647	-0.1	-1.1	8.3	0.0	0.5	0.0	8.3	-0.1	-1.2
O2	247	-0.1	2.4	9.9	-0.2	0.4	0.0	9.9	2.4	-0.1
O3	47	0.0	5.8	11.5	-0.4	0.3	0.0	11.5	5.8	-0.1
P1	1840	-0.3	7.2	-9.1	-0.5	1.7	0.0	7.4	-0.3	-9.3
P2	1640	-0.2	8.9	-6.3	-0.6	1.6	0.0	9.2	-0.3	-6.4
P3	1440	-0.1	10.6	-3.4	-0.7	1.5	0.0	10.9	-0.1	-3.6
P4	1240	0.1	12.3	-0.6	-0.8	1.5	0.1	12.5	0.1	-0.8
Q1	628	-0.4	0.3	2.2	-0.1	0.7	0.1	2.4	0.0	-0.4
Q2	428	-0.3	2.1	5.0	-0.2	0.6	0.1	5.1	2.0	-0.3
Q3	228	-0.1	3.8	7.7	-0.3	0.5	0.1	7.8	3.8	-0.1
Q4	28	0.0	5.5	10.5	-0.4	0.4	0.0	10.5	5.5	-0.1
R1	1816	-1.0	-9.7	4.1	0.7	1.1	0.2	4.2	-0.9	-9.8
R2	1616	-1.8	-11.9	-4.1	0.9	1.0	-0.1	-1.7	-4.0	-12.1
R3	1416	-4.4	-14.3	-11.7	1.0	0.7	-2.1	-3.8	-11.9	-14.7
R4	1216	-5.1	-16.5	-20.7	1.2	0.3	-5.0	-3.5	-16.5	-22.3
S1	616	5.0	-7.2	-1.8	0.6	0.6	-0.8	5.1	-1.8	-7.3
S2	416	0.3	-7.6	1.3	0.5	0.4	-1.0	1.9	-0.2	-7.7
S3	216	0.5	-6.6	4.3	0.5	0.3	-0.2	4.3	0.5	-6.6
S4	16	0.3	-5.7	7.2	0.4	0.2	0.0	7.2	0.3	-5.8
T1	811	-20.6	-25.0	-17.0	1.0	0.3	-6.4	-12.2	-24.2	-26.3
T2	611	-10.6	-18.8	-5.6	0.9	0.1	-6.4	-1.2	-14.8	-19.0
T3	411	-5.0	-16.3	-2.7	0.9	0.1	-5.5	1.8	-9.4	-16.4
T4	211	-0.6	-14.3	-0.4	1.0	0.1	-3.2	2.7	-3.6	-14.4
T5	11	1.0	-11.8	6.5	0.9	0.1	-1.6	7.0	0.6	-11.8
U1	43058	7.9	2.2	-0.3	0.2	0.1	-0.2	7.9	2.2	-0.3
U2	43057	3.1	-0.1	-0.6	0.1	-0.1	0.0	3.1	0.0	-0.6
U3	43056	0.1	-1.9	-1.3	0.1	0.0	0.1	0.1	-1.3	-1.9
U4	43055	-2.1	-3.6	-2.2	0.1	0.0	-0.2	-2.0	-2.3	-3.6
U5	43054	-4.4	-5.2	-3.0	0.1	-0.1	-1.0	-2.4	-4.9	-5.2
U6	43053	-6.7	-6.8	-3.4	0.1	-0.2	-2.5	-2.0	-6.8	-8.0
U7	43052	-9.6	-8.2	-2.5	0.0	-0.3	-2.9	-1.4	-8.2	-10.7

Table 2.10.4-168 Primary Stresses; 30-Foot Top Oblique Drop; Drop Orientation = 75 Degrees; 3-D Top Model; 0-Degree Circumferential Location; Condition 1  
(continued)

Stress Points		Stress Components (ksi)						Principal Stresses (ksi)		
Section <sup>1</sup>	Node	S <sub>x</sub>	S <sub>y</sub>	S <sub>z</sub>	S <sub>xy</sub>	S <sub>yz</sub>	S <sub>xz</sub>	S1	S2	S3
U8	49051	-16.4	-10.9	-0.2	-0.1	0.1	1.5	0.0	-10.9	-16.6
V1	50024	-18.4	-12.7	0.0	-1.1	0.0	0.6	0.0	-12.5	-18.6
V2	50023	-19.7	-15.5	-1.2	-0.8	0.1	1.5	-1.1	-15.4	-20.0
V3	50022	-13.3	-15.8	-1.5	-0.3	0.1	2.0	-1.2	-13.6	-15.8
V4	50021	-17.4	-18.9	-0.4	-0.2	0.1	1.6	-0.3	-17.5	-18.9
W1	43278	-1.6	-5.3	0.1	-0.2	-0.4	0.3	0.1	-1.6	-5.4
W2	43274	-0.6	-5.2	-0.1	-0.1	-0.4	0.3	0.0	-0.7	-5.2
W3	43271	0.2	-2.6	-0.2	0.0	-0.5	0.1	0.2	-0.1	-2.7
X1	50084	9.4	-0.3	-2.6	-0.2	0.2	-2.3	9.8	-0.3	-3.1
X2	50083	2.4	-7.5	-1.7	0.0	0.1	-2.3	3.5	-2.7	-7.5
X3	50081	-10.1	-20.2	5.1	0.4	-0.4	-2.3	5.5	-10.4	-20.2

<sup>1</sup> Refer to Figure 2.10.2-34 for the identification of the representative sections.

Table 2.10.4-169  $P_m$  Stresses; 30-Foot Top Oblique Drop; Drop Orientation = 75 Degrees;  
3-D Top Model; 0-Degree Circumferential Location; Condition 1

Condition 1: 100°F Ambient with Contents

Section <sup>1</sup>	Node - Node	Stress Components (ksi)							Principal Stresses (ksi)			
		$S_x$	$S_y$	$S_z$	$S_{xy}$	$S_{yz}$	$S_{zx}$		S1	S2	S3	S.I.
A	1949 - 1951	-0.6	0.9	-0.1	-0.1	0.3	-0.1		1.0	-0.1	-0.7	1.6
B	1952 - 93	0.3	-1.9	0.1	-0.3	0.4	-0.1		0.4	0.0	-2.0	2.4
C	1925 - 1927	1.0	-2.9	1.8	0.2	-0.2	0.1		1.9	1.0	-2.9	4.8
D	683 - 85	-0.4	-2.9	0.6	0.6	-0.1	0.5		0.8	-0.5	-3.1	3.9
E	682 - 82	-1.8	-3.4	1.3	0.2	0.0	1.3		1.8	-2.2	-3.5	5.2
F	1925 - 1325	1.6	-5.3	-3.2	0.4	-0.5	0.7		1.7	-3.2	-5.5	7.2
G	680 - 80	2.2	-2.9	3.8	0.3	-0.2	0.9		4.2	1.8	-2.9	7.1
H	1921 - 1321	-0.2	9.6	1.9	-0.6	-1.2	-0.1		9.8	1.7	-0.2	10.1
I	676 - 76	-0.1	1.8	8.3	-0.1	-0.5	0.0		8.3	1.7	-0.1	8.4
J	1916 - 1316	-0.2	10.1	11.5	-0.7	-0.6	0.0		11.7	9.9	-0.3	12.0
K	671 - 71	-0.1	2.3	11.6	-0.2	-0.3	0.0		11.6	2.3	-0.1	11.7
L	1908 - 1308	-0.5	8.0	14.4	0.6	0.2	0.0		14.4	8.1	-0.5	14.9
M	663 - 63	-0.4	3.3	13.3	1.0	0.1	0.0		13.3	3.6	-0.6	14.0
N	1877 - 1277	-0.2	10.0	6.2	-0.7	1.0	0.0		10.3	6.0	-0.2	10.5
O	647 - 47	-0.1	2.4	9.9	-0.2	0.4	0.0		9.9	2.4	-0.1	10.0
P	1840 - 1240	-0.1	9.8	-4.8	-0.7	1.6	0.0		10.0	-0.2	-5.0	15.0
Q	628 - 28	-0.2	2.9	6.3	-0.2	0.6	0.1		6.4	2.9	-0.2	6.7
R	1816 - 1216	-3.1	-13.1	-8.0	1.0	0.8	-1.5		-2.6	-8.2	-13.4	10.8
S	616 - 16	1.2	-6.9	2.8	0.5	0.4	-0.5		2.9	1.0	-7.0	9.9
T	811 - 11	-6.5	-17.0	-3.5	0.9	0.1	-4.8		0.0	-9.9	-17.1	17.1
U	43058 - 43051	-4.6	-5.0	-1.8	0.0	-0.1	-0.8		-1.6	-4.8	-5.0	3.4
V	50024 - 50021	-17.0	-15.7	-1.0	-0.6	0.1	1.5		-0.8	-15.5	-17.3	16.5
W	43278 - 43271	-0.6	-4.6	-0.1	-0.1	-0.4	0.3		0.1	-0.7	-4.6	4.7
X	50084 - 50081	-0.7	-10.6	0.5	0.1	0.0	-2.3		2.3	-2.5	-10.6	12.9

<sup>1</sup> Refer to Figure 2.10.2-34 for the identification of the representative sections.



Table 2.10.4-170  $P_m + P_b$  Stresses; 30-Foot Top Oblique Drop; Drop Orientation = 75 Degrees; 3-D Top Model; 0-Degree Circumferential Location; Condition 1

Condition 1: 100°F Ambient with Contents

Section <sup>1</sup>	Node - Node	Stress Components (ksi)						Principal Stresses (ksi)			
		$S_x$	$S_y$	$S_z$	$S_{xy}$	$S_{yz}$	$S_{xz}$	S1	S2	S3	S.I.
A I	1949 - 1951	-1.0	1.8	-0.1	-0.2	0.0	-0.2	1.8	-0.1	-1.1	2.9
B O	1952 - 93	0.6	-3.0	0.3	-0.4	0.3	-0.2	0.7	0.2	-3.1	3.8
C I	1925 - 1927	3.1	-3.2	4.5	0.2	-0.4	0.0	4.5	3.1	-3.2	7.8
D O	683 - 85	-3.3	-4.0	0.9	0.8	-0.1	0.2	0.9	-2.8	-4.5	5.3
E O	682 - 82	-1.7	-3.6	2.6	0.3	0.2	1.4	3.0	-2.0	-3.6	6.6
F O	1925 - 1325	0.7	-8.4	-13.8	0.6	-0.4	1.1	0.8	-8.4	-13.9	14.8
G I	680 - 80	2.3	-1.3	10.1	0.2	-0.1	2.0	10.6	1.8	-1.3	11.8
H O	1921 - 1321	-0.2	12.0	6.6	-0.7	-1.1	-0.3	12.2	6.5	-0.3	12.5
I O	676 - 76	-0.1	3.8	11.1	-0.2	-0.4	0.0	11.1	3.8	-0.1	11.2
J O	1916 - 1316	-0.2	12.5	13.4	-0.9	-0.6	0.0	13.7	12.2	-0.3	13.9
K O	671 - 71	-0.1	5.9	13.3	-0.4	-0.2	0.0	13.3	6.0	-0.1	13.4
L O	1908 - 1308	0.0	11.5	15.9	1.7	0.2	0.0	15.9	11.7	-0.3	16.2
M O	663 - 63	0.4	8.9	15.8	2.0	0.1	0.0	15.8	9.3	0.0	15.8
N O	1877 - 1277	-0.1	12.6	7.9	-0.9	0.9	0.0	12.8	7.7	-0.1	13.0
O O	647 - 47	0.0	5.8	11.5	-0.4	0.3	0.0	11.5	5.8	-0.1	11.6
P I	1840 - 1240	-0.3	7.2	-9.1	-0.5	1.7	0.0	7.5	-0.4	-9.3	16.7
Q O	628 - 28	0.0	5.5	10.5	-0.4	0.4	0.0	10.5	5.5	0.0	10.6
R O	1816 - 1216	-5.6	-16.6	-20.2	1.2	0.4	-4.3	-4.3	-16.5	-21.4	17.1
S O	616 - 16	-0.6	-6.0	7.2	0.4	0.2	0.1	7.2	-0.6	-6.0	13.2
T O	811 - 11	4.0	-11.1	5.8	1.0	0.0	-2.1	7.2	2.7	-11.2	18.4
U O	43058 - 43051	-15.6	-11.3	-2.3	0.0	-0.2	-1.5	-2.2	-11.3	-15.7	13.6
V I	50024 - 50021	-19.5	-13.2	-0.7	-1.0	0.0	1.0	-0.7	-13.0	-19.7	19.0
W I	43278 - 43271	-1.5	-5.9	0.0	-0.2	-0.3	0.3	0.1	-1.6	-6.0	6.1
X O	50084 - 50081	-10.3	-20.4	4.6	0.4	-0.3	-2.3	5.0	-10.6	-20.5	25.5

<sup>1</sup> Refer to Figure 2.10.2-34 for the identification of the representative sections.

Table 2.10.4-171 Critical P<sub>m</sub> Stress Summary; 30-Foot Top Oblique Drop; Drop Orientation = 75 Degrees; 3-D Top Model; Condition 1

Condition 1: 100°F Ambient with Contents

Comp. No. <sup>1</sup>	Section Cut Node-Node	P <sub>m</sub> Stresses (ksi)						Principal Stresses (ksi)			S.L.	Allow. Stress	Margin of Safety
		S <sub>x</sub>	S <sub>y</sub>	S <sub>z</sub>	S <sub>xy</sub>	S <sub>yz</sub>	S <sub>xz</sub>	S1	S2	S3			
1	30683-30083	0.1	3.7	-1.0	0.6	-0.2	-0.6	3.8	0.2	-1.2	5.1	43.6	7.9
2	17924-17324	0.0	2.5	1.0	0.2	-10.7	-0.3	12.5	0.0	-9.0	21.5	44.9	1.1
3	15841-15241	-0.2	3.9	-2.1	0.2	15.9	0.0	17.1	-0.2	-15.3	32.4	66.0	1.0
4	15874-15274	-0.2	3.7	-1.7	0.0	11.6	0.0	12.9	-0.2	-10.9	23.9	43.8	0.9
5	662- 62	0.2	2.9	13.3	-2.4	0.1	0.0	13.3	4.3	-1.3	14.5	46.4	2.2
6	403- 3	-21.4	-35.5	-1.2	0.6	0.3	3.1	-0.7	-21.9	-35.5	34.8	49.3	0.4
7	43071-43031	-14.7	-10.2	-0.6	-0.1	-0.1	-1.1	-0.5	-10.2	-14.8	14.3	48.0	2.4
8	50101-50104	-19.8	-19.2	-0.5	0.0	-0.1	0.0	-0.5	-19.2	-19.8	19.3	94.5	3.9

Locations of the most critical sections for each component are provided in the following:

Comp. No. <sup>1</sup>	Section Location					
	Inside Node			Outside Node		
	x (in)	y (deg)	z (in)	x (in)	y (deg)	z (in)
1	39.44	180.0	6.20	39.44	180.0	0.75
2	35.50	79.4	17.40	37.50	79.4	17.40
3	35.50	67.7	159.90	37.00	67.7	159.90
4	35.50	67.7	142.40	37.00	67.7	142.40
5	40.70	0.0	99.50	43.35	0.0	99.50
6	40.88	0.0	190.15	43.35	0.0	190.15
7	33.71	0.0	185.40	36.46	0.0	185.40
8	40.88	8.3	193.71	40.88	8.3	188.40

<sup>1</sup> Refer to Figure 2.10.2-33 for cask component identification.

Table 2.10.4-172 Critical  $P_m + P_b$  Stress Summary; 30-Foot Top Oblique Drop; Drop Orientation = 75 Degrees; 3-D Top Model; Condition 1

Condition 1: 100°F Ambient with Contents

Comp. No. <sup>1</sup>	Section Cui Node-Node	$P_m + P_b$ Stresses (ksi)							Principal Stresses (ksi)			Allow. Stress	Margin of Safety
		$S_x$	$S_y$	$S_z$	$S_{xy}$	$S_{yz}$	$S_{xz}$	$S_1$	$S_2$	$S_3$	$S_{I1}$		
1	30683-30085	3.0	5.9	-1.2	0.7	-0.2	-0.3	6.1	2.8	-1.2	7.3	65.2	7.9
2	15924-15324	-0.2	1.6	-0.6	0.3	-12.3	0.0	12.9	-0.2	-11.8	24.8	64.2	1.6
3	13842-13242	-0.1	6.6	-3.0	0.0	16.4	0.0	18.9	-0.1	-15.3	34.2	94.3	1.8
4	15874-15274	-0.2	7.1	-0.5	0.0	12.3	0.0	16.2	-0.2	-9.6	25.8	65.5	1.5
5	664-64	-0.1	8.5	16.3	-0.7	0.0	0.0	16.3	8.5	-0.1	16.5	66.4	3.0
6	404-4	-2.0	-26.0	13.2	1.1	0.6	10.4	18.5	-7.3	-26.1	44.5	70.9	0.6
7	43001-43008	-26.3	-14.6	-0.9	-0.6	0.3	1.2	-0.9	-14.6	-26.4	25.5	69.8	1.7
8	50001-50004	-32.0	-20.4	1.2	-0.8	-0.2	-0.2	1.2	-20.3	-32.1	33.2	135.0	3.1

Locations of the most critical sections for each component are provided in the following:

Comp. No. <sup>1</sup>	Section Location					
	Inside Node			Outside Node		
	x (in)	y (deg)	z (in)	x (in)	y (deg)	z (in)
1	39.44	180.0	6.20	39.44	180.0	0.75
2	35.50	67.7	17.40	37.50	67.7	17.40
3	35.50	56.5	159.40	37.00	56.5	159.40
4	35.50	67.7	142.40	37.00	67.7	142.40
5	40.70	0.0	93.60	43.35	0.0	93.60
6	40.88	0.0	188.40	43.35	0.0	188.40
7	39.53	0.0	185.40	39.53	0.0	179.40
8	40.88	0.0	193.71	40.88	0.0	188.40

<sup>1</sup> Refer to Figure 2.10.2-33 for cask component identification.

Table 2.10.4-173 Primary Stresses; 30-Foot Bottom Oblique Drop; Drop Orientation = 75 Degrees; 3-D Bottom Model; 0-Degree Circumferential Location; Condition 1

Condition 1: 100°F Ambient with Contents

Stress Points Section <sup>1</sup> Node		Stress Components (ksi)						Principal Stresses (ksi)		
		S <sub>x</sub>	S <sub>y</sub>	S <sub>z</sub>	S <sub>xy</sub>	S <sub>xz</sub>	S <sub>yz</sub>	S1	S2	S3
A1	1130	3.7	-1.4	-2.0	-0.3	0.6	0.5	3.8	-1.0	-2.4
A2	1129	-0.4	-5.8	-0.4	-0.1	0.4	0.5	0.1	-0.9	-5.9
A3	1128	-4.4	-10.3	1.1	0.0	0.6	0.5	1.2	-4.5	-10.4
B1	1185	1.7	-5.9	-2.1	0.2	0.7	0.6	1.8	-2.1	-6.0
B2	1184	-2.0	-10.2	-0.5	0.3	0.5	0.6	-0.3	-2.2	-10.2
B3	1183	-5.7	-13.8	0.7	0.4	0.5	0.6	0.8	-5.7	-13.8
C1	90	-0.6	-6.6	12.2	-0.1	-0.8	0.5	12.3	-0.6	-6.6
C2	80	-7.6	-10.8	4.6	-0.2	-0.5	-0.5	4.6	-7.6	-10.8
C3	70	-8.1	-12.2	0.9	0.0	-0.3	-0.9	1.0	-8.2	-12.3
C4	60	-8.5	-13.1	-0.4	0.2	-0.2	-0.6	-0.3	-8.6	-13.1
C5	50	-11.2	-15.1	-0.3	0.3	-0.1	-0.2	-0.3	-11.2	-15.2
C6	40	-11.7	-16.0	-0.2	0.4	-0.0	-0.1	-0.2	-11.6	-16.1
D1	25	-29.0	-23.5	-8.2	-0.6	-0.2	-4.9	-7.2	-23.5	-30.1
D2	15	-17.6	-20.3	-4.8	-0.3	0.0	-2.2	-4.5	-18.0	-20.4
D3	5	-11.0	-19.5	-2.4	-0.1	0.0	-0.7	-2.3	-11.1	-19.5
E1	35	-8.0	-16.5	-1.5	0.5	-0.1	-1.4	-1.2	-8.3	-16.6
E2	34	-8.6	-17.6	-4.9	0.5	-0.2	-3.2	-3.1	-10.4	-17.7
E3	33	-14.1	-19.4	-5.4	0.3	-0.3	-3.6	-4.1	-15.4	-19.5
E4	32	-16.2	-20.6	-6.9	0.3	-0.2	-2.4	-6.4	-16.8	-20.7
E5	31	-17.0	-21.6	-8.9	0.3	-0.2	-1.4	-8.6	-17.2	-21.6
F1	100	-1.2	-4.7	19.8	0.1	-1.1	1.8	20.0	-1.4	-4.7
F2	99	-2.4	-10.8	-1.2	0.5	-0.9	2.4	0.6	-4.1	-10.9
F3	98	-1.3	-14.3	-15.1	0.9	-0.6	4.0	-0.2	-14.0	-16.5
F4	97	0.7	-21.2	-43.4	1.5	-0.6	5.0	1.3	-21.2	-44.0
G1	94	1.3	-5.2	18.4	0.4	-0.4	4.2	19.4	0.4	-5.2
G2	93	1.8	-9.7	1.4	0.8	-0.3	3.2	4.9	-1.5	-9.8
G3	92	1.6	-10.9	-3.1	0.9	-0.2	1.5	2.1	-3.5	-11.0
G4	91	0.7	-12.4	-8.1	1.0	-0.2	0.6	0.8	-8.2	-12.5
H1	330	-0.3	6.9	-9.1	-0.5	-1.7	0.0	7.1	-0.3	-9.3
H2	329	-0.2	8.6	-5.8	-0.6	-1.6	0.0	8.8	-0.2	-6.0

Table 2.10.4-173 Primary Stresses; 30-Foot Bottom Oblique Drop; Drop Orientation = 75 Degrees; 3-D Bottom Model; 0-Degree Circumferential Location; Condition 1 (continued)

Stress Points Section <sup>1</sup> Node		Stress Components (ksi)						Principal Stresses (ksi)		
		S <sub>x</sub>	S <sub>y</sub>	S <sub>z</sub>	S <sub>xy</sub>	S <sub>yz</sub>	S <sub>xz</sub>	S1	S2	S3
H3	328	0.0	10.2	-2.6	-0.7	-1.5	0.0	10.4	-0.1	-2.8
H4	327	0.1	11.9	0.7	-0.8	-1.4	-0.2	12.1	0.7	-0.1
I1	244	-0.2	-0.8	-0.9	0.1	-0.8	0.0	0.0	-0.2	-1.7
I2	243	-0.1	0.9	2.2	-0.1	-0.7	-0.1	2.6	0.6	-0.1
I3	242	-0.1	2.6	5.4	-0.2	-0.5	-0.1	5.5	2.5	-0.1
I4	241	0.0	4.1	8.5	-0.3	-0.4	-0.1	8.5	4.1	0.0
J1	550	-0.3	7.6	6.3	-0.6	-0.9	0.0	8.1	5.8	-0.4
J2	548	-0.2	10.1	8.1	-0.8	-0.8	0.0	10.4	7.8	-0.2
J3	547	-0.1	12.4	9.8	-0.9	-0.8	0.0	12.7	9.6	-0.1
K1	344	-0.1	-1.0	7.0	0.0	-0.6	0.0	7.1	-0.1	-1.0
K2	42	-0.1	2.6	8.6	-0.2	-0.4	0.0	8.6	2.5	-0.1
K3	341	0.0	5.9	10.1	-0.5	-0.3	0.0	10.1	5.9	-0.1
L1	740	-0.1	4.9	13.6	0.2	-0.1	-0.1	13.6	4.9	-0.1
L2	738	-0.5	7.6	15.1	-1.2	-0.1	0.0	15.1	7.8	-0.7
L3	737	0.2	10.5	16.7	-2.5	-0.1	0.0	16.7	11.0	-0.4
M1	454	-0.3	-2.0	9.8	-1.9	-0.1	0.0	9.8	0.9	-3.2
M2	452	0.4	3.5	12.5	-0.9	-0.1	0.2	12.5	3.8	0.2
M3	451	-0.7	8.1	14.9	0.0	-0.1	-0.3	14.9	8.1	-0.7
N1	810	-0.3	7.8	9.4	-0.6	0.7	-0.1	9.7	7.6	-0.3
N2	807	-0.2	12.4	12.8	-0.9	0.6	0.0	13.3	11.9	-0.3
O1	524	-0.1	-0.9	9.7	0.1	0.4	0.0	9.7	-0.1	-0.9
O2	521	-0.1	5.7	13.0	-0.4	0.2	0.0	13.0	5.8	-0.1
P1	850	-0.2	7.5	-1.8	-0.4	1.2	-0.1	7.6	-0.2	-1.9
P2	847	-0.2	12.2	7.1	-0.8	1.1	0.3	12.4	6.9	-0.3
Q1	564	-0.1	-0.1	6.3	0.0	0.5	0.0	6.4	-0.1	-0.2
Q2	561	-0.1	4.0	11.1	-0.3	0.3	0.0	11.1	4.0	-0.1
R1	890	-3.2	-3.1	10.2	0.1	0.8	-0.7	10.3	-3.1	-3.3
R2	887	-3.1	-7.7	-10.3	0.4	0.5	-1.6	-2.7	-7.7	-10.7
S1	604	-0.2	-1.3	8.1	0.0	0.2	-1.5	8.4	-0.5	-1.3
S2	601	0.7	-2.7	0.6	0.2	0.1	-0.6	1.2	0.0	-2.7
T1	897	3.2	-3.3	-2.2	0.3	0.3	-1.0	3.4	-2.3	-3.4
T2	614	0.9	-2.1	2.5	0.1	0.0	-1.3	3.2	0.2	-2.2

Table 2.10.4-173 Primary Stresses; 30-Foot Bottom Oblique Drop; Drop Orientation = 75 Degrees; 3-D Bottom Model; 0-Degree Circumferential Location; Condition 1 (continued)

Stress Points		Stress Components (ksi)						Principal Stresses (ksi)		
Section <sup>1</sup>	Node	S <sub>x</sub>	S <sub>y</sub>	S <sub>z</sub>	S <sub>xy</sub>	S <sub>xz</sub>	S <sub>yz</sub>	S1	S2	S3
T3	611	-0.2	-2.5	1.2	0.1	-0.1	-0.7	1.5	-0.5	-2.5
U1	900	5.1	-1.5	2.3	0.2	0.4	-0.1	5.1	2.3	-1.6
U2	910	-2.2	-2.8	0.2	0.1	0.2	-1.0	0.5	-2.5	-2.9
V1	920	2.8	-1.0	0.9	0.4	0.1	-0.8	3.1	0.6	-1.1
V2	930	-4.1	-3.8	0.6	0.6	0.1	-0.2	0.7	-3.3	-4.6
W1	1216	-1.1	1.9	-0.3	-0.1	-0.3	0.1	1.9	-0.3	-1.1
W2	1226	-0.3	0.2	0.1	-0.1	-0.5	0.1	0.6	-0.3	-0.4
X1	1236	0.0	-0.7	-0.1	-0.2	-0.5	0.1	0.3	-0.1	-1.0
X2	1246	0.5	-2.9	0.3	-0.4	-0.3	0.1	0.6	0.3	-3.0

<sup>1</sup> Refer to Figure 2.10.2-34 for the identification of the representative sections.

Table 2.10.4-174 P<sub>m</sub> Stresses; 30-Foot Bottom Oblique Drop; Drop Orientation = 75 Degrees; 3-D Bottom Model; 0-Degree Circumferential Location; Condition 1

Condition 1: 100°F Ambient with Contents

Section <sup>1</sup>	Node - Node	Stress Components (ksi)						Principal Stresses (ksi)			
		S <sub>x</sub>	S <sub>y</sub>	S <sub>z</sub>	S <sub>xy</sub>	S <sub>yz</sub>	S <sub>xz</sub>	S1	S2	S3	S.I.
A	1130 - 1128	-0.4	-5.9	-0.4	-0.1	0.5	0.5	0.1	-0.9	-5.9	6.0
B	1185 - 1183	-2.0	-10.0	-0.6	0.3	0.5	0.6	-0.4	-2.2	-10.0	9.6
C	90 - 40	-9.0	-13.2	1.3	0.2	-0.2	-0.4	1.3	-9.0	-13.2	14.5
D	25 - 5	-18.8	-20.9	-5.1	-0.3	-0.1	-2.5	-4.6	-19.2	-21.0	16.3
E	35 - 31	-12.4	-19.0	-5.4	0.4	-0.2	-2.6	-4.5	-13.3	-19.0	14.5
F	100 - 97	-1.3	-12.7	-9.4	0.7	-0.8	3.3	-0.2	-10.2	-13.1	12.9
G	94 - 91	1.5	-9.8	1.1	0.8	-0.3	2.4	3.7	-1.0	-9.9	13.6
H	330 - 327	-0.1	9.4	-4.2	-0.6	-1.5	0.0	9.6	-0.2	-4.4	14.0
I	244 - 241	-0.1	1.7	3.8	-0.1	-0.6	-0.1	4.0	1.5	-0.1	4.1
J	550 - 547	-0.2	10.0	8.0	-0.7	-0.8	0.0	10.4	7.7	-0.2	10.6
K	344 - 341	-0.1	2.5	8.6	-0.2	-0.4	0.0	8.6	2.5	-0.1	8.7
L	740 - 737	-0.3	7.6	15.1	-1.1	-0.1	0.0	15.1	7.8	-0.4	15.6
M	454 - 451	0.0	3.3	12.4	-0.9	-0.1	0.0	12.4	3.5	-0.3	12.7
N	810 - 807	-0.2	10.1	11.1	-0.7	0.7	0.0	11.5	9.8	-0.3	11.8
O	524 - 521	-0.1	2.4	11.3	-0.2	0.3	0.0	11.3	2.4	-0.1	11.4
P	850 - 847	-0.2	9.8	2.7	-0.6	1.2	0.1	10.0	2.5	-0.2	10.3
Q	564 - 561	-0.1	2.0	8.7	-0.1	0.4	0.0	8.8	1.9	-0.1	8.9
R	890 - 887	-3.2	-5.4	0.0	0.2	0.6	-1.1	0.4	-3.5	-5.6	5.9
S	604 - 601	0.2	-2.0	4.4	0.1	0.1	-1.0	4.6	0.0	-2.0	6.6
T	614 - 611	0.3	-2.3	1.9	0.1	0.0	-1.0	2.3	-0.1	-2.3	4.7
U	900 - 910	1.4	-2.2	1.2	0.2	0.3	-0.5	1.9	0.8	-2.2	4.1
V	920 - 930	-0.7	-2.4	0.8	0.5	0.1	-0.5	0.9	-0.7	-2.6	3.5
W	1216 - 1226	-0.7	1.0	-0.1	-0.1	-0.4	0.1	1.1	-0.2	-0.7	1.8
X	1236 - 1246	0.2	-1.8	0.1	-0.3	-0.4	0.1	0.4	0.1	-1.9	2.3

<sup>1</sup> Refer to Figure 2.10.2-34 for the identification of the representative sections.

Table 2.10.4-175  $P_m + P_b$  Stresses; 30-Foot Bottom Oblique Drop; Drop Orientation = 75 Degrees; 3-D Bottom Model; 0-Degree Circumferential Location; Condition 1

Condition 1: 100°F Ambient with Contents

Section <sup>1</sup>	Node - Node	Stress Components (ksi)						Principal Stresses (ksi)			
		$S_x$	$S_y$	$S_z$	$S_{xy}$	$S_{yz}$	$S_{zx}$	S1	S2	S3	S.L.
A O	1130 - 1128	-4.4	-10.3	1.1	0.0	0.5	0.5	1.2	-4.5	-10.4	11.6
B O	1185 - 183	-5.7	-13.9	0.8	0.4	0.4	0.6	0.9	-5.7	-14.0	14.9
C I	90 - 40	-5.3	-9.6	5.1	-0.2	-0.5	-0.5	5.2	-5.3	-9.6	14.8
D I	25 - 5	-27.8	-22.9	-8.0	-0.5	-0.2	-4.6	-7.0	-22.9	-28.9	21.9
E I	35 - 31	-6.6	-16.2	-2.2	0.5	-0.2	-2.7	-0.8	-7.9	-16.2	15.4
F O	100 - 97	-0.3	-20.2	-38.6	1.4	-0.4	5.1	0.5	-20.3	-39.3	39.8
G I	94 - 91	1.8	-6.6	13.0	0.6	-0.4	4.3	14.5	0.4	-6.7	21.1
H I	330 - 327	-0.3	6.9	-9.1	-0.5	-1.7	0.0	7.1	-0.4	-9.3	16.4
I O	244 - 241	0.0	4.2	8.5	-0.3	-0.4	-0.1	8.6	4.2	0.0	8.6
J O	550 - 547	-0.1	12.4	9.8	-0.9	-0.8	0.0	12.7	9.6	-0.1	12.9
K O	344 - 341	0.0	5.9	10.1	-0.5	-0.3	0.0	10.2	5.9	-0.1	10.2
L O	740 - 737	-0.1	10.4	16.7	-2.5	-0.1	0.0	16.7	11.0	-0.7	17.3
M O	454 - 451	-0.3	8.3	14.9	0.0	-0.1	-0.2	15.0	8.3	-0.3	15.2
N O	810 - 807	-0.2	12.4	12.8	-0.9	0.6	0.0	13.3	11.9	-0.3	13.6
O O	524 - 521	-0.1	5.7	13.0	-0.4	0.2	0.0	13.0	5.8	-0.1	13.1
P O	850 - 847	-0.2	12.2	7.1	-0.8	1.1	0.3	12.4	6.9	-0.3	12.8
Q O	564 - 561	-0.1	4.0	11.1	-0.3	0.3	0.0	11.1	4.0	-0.1	11.3
R I	890 - 887	-3.2	-3.1	10.2	0.1	0.8	-0.7	10.3	-3.1	-3.3	13.6
S I	604 - 601	-0.2	-1.3	8.1	0.0	0.2	-1.5	8.4	-0.5	-1.3	9.7
T I	614 - 611	0.9	-2.1	2.5	0.1	0.0	-1.3	3.2	0.2	-2.2	5.4
U I	900 - 910	5.1	-1.5	2.3	0.2	0.4	-0.1	5.1	2.3	-1.6	6.6
V O	920 - 930	-4.1	-3.8	0.6	0.6	0.1	-0.2	0.7	-3.3	-4.6	5.2
W I	1216 - 1226	-1.1	1.9	-0.3	-0.1	-0.3	0.1	1.9	-0.3	-1.1	3.0
X O	1236 - 1246	0.5	-2.9	0.3	-0.4	-0.3	0.1	0.6	0.3	-3.0	3.6

<sup>1</sup> Refer to Figure 2.10.2-34 for the identification of the representative sections.



Table 2.10.4-176 Critical  $P_m$  Stress Summary; 30-Foot Bottom Oblique Drop; Drop Orientation = 75 Degrees; 3-D Bottom Model; Condition 1

Condition 1: 100°F Ambient with Contents

Comp. No. <sup>1</sup>	Section Cut Node-Node	P <sub>m</sub> Stresses (ksi)							Principal Stresses (ksi)				Allow. Stress	Margin of Safety
		S <sub>x</sub>	S <sub>y</sub>	S <sub>z</sub>	S <sub>xy</sub>	S <sub>yz</sub>	S <sub>zx</sub>	S1	S2	S3	S.L.			
1	28- 8	-20.6	-19.0	-1.1	-0.5	-0.1	-2.9	-0.7	-18.9	-21.1	20.5	45.6	1.2	
2	16140-16137	0.0	1.0	0.1	0.0	-12.6	-0.1	13.2	0.0	-12.0	25.2	44.9	0.8	
3	14340-14337	-0.2	3.8	-1.7	0.2	-15.9	0.0	17.2	-0.2	-15.1	32.3	66.0	1.0	
4	14520-14517	-0.2	3.7	-1.3	0.0	-11.5	0.0	13.0	-0.2	-10.6	23.5	45.8	0.9	
5	14204-14201	0.0	1.1	-1.3	0.0	-6.5	-0.1	6.5	0.0	-6.8	13.3	46.4	2.5	
6	16880-16877	-0.1	2.9	1.0	-0.3	10.8	0.3	12.8	-0.1	-8.9	21.6	49.3	1.3	
7	14900-14910	-0.4	-0.1	-0.5	-1.2	3.3	-0.1	3.3	-0.5	-3.8	7.0	48.0	5.9	
8	30907-30927	-0.4	3.6	0.0	0.6	0.2	0.9	3.8	0.7	-1.2	4.9	94.5	18.3	

Locations of the most critical sections for each component are provided in the following:

Comp. No. <sup>1</sup>	Section Location					
	Inside Node			Outside Node		
	x (in)	y (deg)	z (in)	x (in)	y (deg)	z (in)
1	36.83	0.0	6.20	36.83	0.0	0.75
2	35.50	79.4	17.40	37.50	79.4	17.40
3	35.50	67.7	29.90	37.00	67.7	29.90
4	35.50	67.7	47.40	37.00	67.7	47.40
5	40.70	67.7	26.40	43.35	67.7	26.40
6	35.50	79.4	172.40	37.50	79.4	172.40
7	35.50	67.7	179.40	35.50	67.7	185.40
8	37.00	180.0	185.40	37.00	180.0	193.71

<sup>1</sup> Refer to Figure 2.10.2-33 for cask component identification.

Table 2.10.4-177 Critical  $P_m + P_b$  Stress Summary; 30-Foot Bottom Oblique Drop; Drop Orientation = 75 Degrees; 3-D Bottom Model; Condition 1

Condition 1: 100°F Ambient with Contents

Comp. No. <sup>1</sup>	Section Cut Node-Node	$P_m + P_b$ Stresses (ksi)							Principal Stresses (ksi)			S.I. Stress	Margin of Safety
		$S_1$	$S_2$	$S_3$	$S_4$	$S_5$	$S_6$	$S_7$	S1	S2	S3		
1	27- 7	-33.5	-20.5	0.2	-1.2	-0.3	-3.8	0.5	-20.4	-34.1	34.7	65.2	0.9
2	100- 97	-0.3	-20.2	-38.6	1.4	-0.4	5.1	0.5	-20.3	-39.3	39.8	64.2	0.6
3	12350-12347	-0.1	6.2	-3.2	0.0	-16.4	0.0	18.6	-0.1	-15.6	34.2	94.3	1.8
4	14520-14517	-0.2	6.8	-0.2	0.0	-12.2	0.0	16.0	-0.2	-9.4	25.4	65.3	1.6
5	12204-12201	0.1	1.5	-1.6	-0.2	-8.3	-0.1	8.3	0.1	-8.3	16.8	66.4	3.0
6	14880-14877	-0.2	2.5	-0.2	-0.2	11.8	0.0	13.1	-0.2	-10.7	23.8	70.7	2.0
7	14900-14910	-0.3	0.7	-0.3	-3.0	4.0	0.1	5.1	-0.3	-5.0	10.1	69.8	5.9
8	30920-30930	2.1	5.6	-0.5	0.6	0.2	0.4	5.7	2.0	-0.6	6.3	135.0	20.4

Locations of the most critical sections for each component are provided in the following:

Comp. No. <sup>1</sup>	Section Location Inside Node			Section Location Outside Node		
	x (in)	y (deg)	z (in)	x (in)	y (deg)	z (in)
1	37.50	0.0	6.20	37.50	0.0	0.75
2	35.50	0.0	15.00	37.50	0.0	15.00
3	35.50	56.5	30.40	37.00	56.5	30.40
4	35.50	67.7	47.40	37.00	67.7	47.40
5	40.70	56.5	26.40	43.35	56.5	26.40
6	35.50	67.7	172.40	37.50	67.7	172.40
7	35.50	67.7	179.40	35.50	67.7	185.40
8	35.50	180.0	187.40	35.50	180.0	193.71

<sup>1</sup> Refer to Figure 2.10.2-33 for cask component identification.

Table 2.10.4-178 Primary + Secondary Stresses; Thermal (Fire) Transient; Time = 30 Minutes; With Contents; 2-D Model

Stress Points Section <sup>1</sup> Node	Stress Components (ksi)						Principal Stresses (ksi)		
	S <sub>x</sub>	S <sub>y</sub>	S <sub>z</sub>	S <sub>xy</sub>	S <sub>xz</sub>	S <sub>yz</sub>	S1	S2	S3
A1	1	7.8	-0.1	7.8	0.0	0.0	7.8	7.8	-0.1
A2	2	6.8	-0.1	6.8	0.0	0.0	6.8	6.8	-0.1
A3	3	5.7	-0.1	5.7	0.0	0.0	5.7	5.7	-0.1
A4	4	4.5	0.0	4.5	0.0	0.0	4.5	4.5	0.0
A5	5	3.3	0.0	3.3	0.0	0.0	3.3	3.3	0.0
B1	6	-0.3	0.0	-0.3	0.0	0.0	0.0	-0.3	-0.3
B2	7	-0.3	0.0	-0.3	0.0	0.0	0.0	-0.3	-0.3
B3	8	-0.3	0.0	-0.3	0.0	0.0	0.0	-0.3	-0.3
B4	9	-0.2	0.0	-0.2	0.0	0.0	0.0	-0.2	-0.2
B5	10	-0.2	0.0	-0.2	0.0	0.0	0.0	-0.2	-0.2
C1	251	7.4	0.4	6.6	0.2	0.0	7.4	6.6	0.4
C2	252	9.1	0.9	6.4	-0.3	0.0	9.1	6.4	0.8
C3	253	6.8	0.5	4.7	-0.5	0.0	6.9	4.7	0.5
C4	254	3.1	-0.6	2.1	-0.1	0.0	3.1	2.1	-0.6
C5	255	-3.8	-1.2	-1.3	0.1	0.0	-1.2	-1.3	-3.8
D1	306	5.7	19.9	6.3	1.4	0.0	20.0	6.3	5.6
D2	307	-1.2	8.5	1.5	1.6	0.0	8.8	1.5	-1.5
D3	308	-1.4	3.2	0.2	0.0	0.0	3.2	0.2	-1.4
D4	309	-2.3	1.2	-0.6	-0.3	0.0	1.2	-0.6	-2.3
D5	310	-3.9	0.5	-1.4	-0.2	0.0	0.5	-1.4	-4.0
E1	305	7.0	22.0	5.5	-3.8	0.0	23.0	6.1	5.5
E2	315	4.3	7.5	0.4	-1.0	0.0	7.8	4.0	0.4
E3	325	3.8	1.4	-1.1	-0.3	0.0	3.9	1.3	-1.1
E4	335	3.3	-4.2	-2.5	-0.1	0.0	3.3	-2.5	-4.2
E5	345	1.4	-11.6	-5.9	0.2	0.0	1.4	-5.9	-11.6
E6	355	-0.2	-20.0	-9.5	0.2	0.0	-0.2	-9.5	-20.0
F1	251	7.4	0.4	6.6	0.2	0.0	7.4	6.6	0.4
F2	261	6.3	3.7	6.1	-0.3	0.0	6.3	6.1	3.6
F3	271	7.3	6.6	6.0	-1.7	0.0	8.7	6.0	5.2
F4	281	9.9	10.0	5.5	-3.0	0.0	12.9	7.0	5.5
G1	311	5.6	10.5	-19.6	5.0	0.0	13.6	2.4	-19.6
G2	321	1.1	4.3	-32.0	4.1	0.0	7.1	-1.7	-32.0

Table 2.10.4-178 Primary + Secondary Stresses; Thermal (Fire) Transient; Time = 30 Minutes; With Contents; 2-D Model (continued)

Stress Points Section <sup>1</sup> Node		Stress Components (ksi)						Principal Stresses (ksi)		
		S <sub>x</sub>	S <sub>y</sub>	S <sub>z</sub>	S <sub>xy</sub>	S <sub>yz</sub>	S <sub>xz</sub>	S1	S2	S3
G3	331	2.6	5.0	-40.7	2.3	0.0	0.0	6.4	1.2	-40.7
G4	341	-0.4	-8.9	-69.9	1.0	0.0	0.0	-0.2	-9.0	-69.9
G5	351	-7.9	-15.1	-97.3	0.3	0.0	0.0	-7.8	-15.1	-97.3
H1	581	0.0	8.3	2.8	0.1	0.0	0.0	8.3	2.8	0.0
H2	582	0.0	8.7	3.1	0.1	0.0	0.0	8.7	3.1	0.0
H3	583	0.1	9.0	3.3	-0.1	0.0	0.0	9.0	3.3	0.1
H4	584	0.0	10.0	3.8	-0.4	0.0	0.0	10.0	3.8	0.0
I1	589	-0.4	4.4	6.2	0.0	0.0	0.0	6.2	4.4	-0.4
I2	590	-0.2	3.8	5.7	0.0	0.0	0.0	5.7	3.8	-0.2
I3	591	-0.1	3.1	5.2	0.0	0.0	0.0	5.2	3.1	-0.1
I4	592	0.0	0.9	3.3	0.0	0.0	0.0	3.3	0.9	0.0
I5	593	0.0	-1.2	1.4	0.0	0.0	0.0	1.4	0.0	-1.2
J1	971	-0.1	7.5	1.9	0.0	0.0	0.0	7.5	1.9	-0.1
J2	972	-0.1	8.6	2.5	0.0	0.0	0.0	8.6	2.5	-0.1
J3	973	-0.1	9.7	3.2	0.0	0.0	0.0	9.7	3.2	-0.1
J4	974	0.0	10.9	3.9	0.0	0.0	0.0	10.9	3.9	0.0
K1	979	-0.4	3.0	6.8	0.0	0.0	0.0	6.8	3.0	-0.4
K2	980	-0.3	3.0	6.4	0.0	0.0	0.0	6.4	3.0	-0.3
K3	981	-0.1	3.0	6.0	0.0	0.0	0.0	6.0	3.0	-0.1
K4	982	-0.1	1.6	4.3	0.0	0.0	0.0	4.3	1.6	-0.1
K5	983	0.0	0.3	2.7	0.0	0.0	0.0	2.7	0.3	0.0
L1	1601	-0.1	8.1	2.2	0.0	0.0	0.0	8.1	2.2	-0.1
L2	1602	-0.1	8.8	2.7	0.0	0.0	0.0	8.8	2.7	-0.1
L3	1603	0.0	9.5	3.3	0.0	0.0	0.0	9.5	3.3	0.0
L4	1604	0.0	10.2	3.8	0.0	0.0	0.0	10.2	3.8	0.0
M1	1609	-0.4	3.2	7.1	0.0	0.0	0.0	7.1	3.2	-0.4
M2	1610	-0.2	3.1	6.7	0.0	0.0	0.0	6.7	3.1	-0.2
M3	1611	-0.1	3.0	6.2	0.0	0.0	0.0	6.2	3.0	-0.1
M4	1612	-0.1	1.5	4.5	0.0	0.0	0.0	4.5	1.5	-0.1
M5	1613	0.0	0.1	2.9	0.0	0.0	0.0	2.9	0.1	0.0
N1	2216	-0.1	7.6	2.0	0.0	0.0	0.0	7.6	2.0	-0.1
N2	2217	-0.1	8.6	2.5	0.0	0.0	0.0	8.6	2.5	-0.1

Table 2.10.4-178 Primary + Secondary Stresses; Thermal (Fire) Transient; Time = 30 Minutes; With Contents; 2-D Model (continued)

Stress Points Section <sup>1</sup> Node	Stress Components (ksi)							Principal Stresses (ksi)		
	S <sub>x</sub>	S <sub>y</sub>	S <sub>z</sub>	S <sub>xy</sub>	S <sub>yz</sub>	S <sub>xz</sub>	S <sub>xx</sub>	S1	S2	S3
N3	2218	0.0	9.7	3.0	0.0	0.0	0.0	9.7	3.0	0.0
N4	2219	0.0	10.7	3.5	0.0	0.0	0.0	10.7	3.5	0.0
O1	2224	-0.3	4.0	4.5	-0.1	0.0	0.0	4.5	4.0	-0.3
O2	2225	-0.2	3.6	3.9	-0.2	0.0	0.0	3.9	3.6	-0.2
O3	2226	-0.1	3.0	3.3	-0.3	0.0	0.0	3.3	3.0	-0.1
O4	2227	0.0	1.1	1.3	-0.2	0.0	0.0	1.3	1.2	-0.1
O5	2228	0.0	-0.7	-0.6	-0.1	0.0	0.0	0.0	-0.6	-0.7
P1	2546	-0.4	27.1	7.7	-0.2	0.0	0.0	27.1	7.7	-0.4
P2	2547	-0.3	15.3	4.0	-0.5	0.0	0.0	15.4	4.0	-0.4
P3	2548	-1.1	3.0	0.1	-0.9	0.0	0.0	3.2	0.1	-1.3
P4	2549	0.9	-9.5	-3.1	-1.8	0.0	0.0	1.2	-3.1	-9.8
Q1	2554	-0.4	25.0	24.9	0.2	0.0	0.0	25.0	24.9	-0.4
Q2	2555	-0.2	14.3	20.9	0.4	0.0	0.0	20.9	14.3	-0.2
Q3	2556	-0.2	3.6	16.8	0.9	0.0	0.0	16.8	3.8	-0.4
Q4	2557	-0.1	-9.0	11.4	0.9	0.0	0.0	11.4	0.0	-9.1
Q5	2558	0.0	-22.3	5.8	0.7	0.0	0.0	5.8	0.0	-22.4
R1	2771	3.7	-51.1	42.6	-1.2	0.0	0.0	42.6	3.7	-51.2
R2	2772	9.0	-14.2	51.2	-0.9	0.0	0.0	51.2	9.0	-14.2
R3	2773	20.0	15.2	59.2	2.9	0.0	0.0	59.2	21.3	13.9
R4	2774	34.6	49.1	64.9	7.7	0.0	0.0	64.9	52.4	31.3
S1	2779	21.4	12.6	-16.9	-6.6	0.0	0.0	25.0	9.1	-16.9
S2	2780	16.5	5.9	-34.7	-6.1	0.0	0.0	19.3	3.1	-34.7
S3	2781	8.7	0.7	-52.4	-4.2	0.0	0.0	10.5	-1.1	-52.4
S4	2782	3.9	-8.5	-72.3	-2.3	0.0	0.0	4.3	-8.9	-72.3
S5	2783	0.8	-19.2	-91.3	-1.2	0.0	0.0	0.9	-19.3	-91.3
T1	7066	-21.0	-6.2	10.3	-0.6	0.0	0.0	10.3	-6.1	-21.1
T2	7067	-11.1	1.4	5.4	0.2	0.0	0.0	5.4	1.4	-11.1
T3	7068	-6.4	5.3	-4.0	1.5	0.0	0.0	5.5	-4.0	-6.6
T4	7069	-3.5	3.4	-17.6	2.1	0.0	0.0	3.9	-4.1	-17.6
T5	7070	-0.8	1.9	-32.1	2.0	0.0	0.0	3.0	-1.8	-32.1
T6	7071	-0.9	-6.6	-56.3	1.3	0.0	0.0	-0.6	-6.9	-56.3
T7	7072	-4.4	-10.3	-79.1	0.7	0.0	0.0	-4.3	-10.4	-79.1

Table 2.10.4-178 Primary + Secondary Stresses; Thermal (Fire) Transient; Time = 30 Minutes; With Contents; 2-D Model (continued)

Stress Points Section <sup>1</sup> Node		Stress Components (ksi)						Principal Stresses (ksi)		
		S <sub>x</sub>	S <sub>y</sub>	S <sub>z</sub>	S <sub>xy</sub>	S <sub>yz</sub>	S <sub>xz</sub>	S1	S2	S3
U1	3051	-0.8	-1.1	-7.5	-0.2	0.0	0.0	-0.7	-1.2	-7.3
U2	3052	2.0	0.1	-4.4	-0.4	0.0	0.0	2.1	0.0	-4.4
U3	3053	2.4	0.0	-2.5	-0.7	0.0	0.0	2.6	-0.2	-2.5
U4	3054	1.8	0.6	-1.2	-1.1	0.0	0.0	2.3	-0.1	-1.2
U5	3055	-0.4	1.7	-0.8	-1.2	0.0	0.0	2.2	-0.8	-0.9
U6	3056	-0.3	2.2	0.1	-0.5	0.0	0.0	2.3	0.1	-0.4
V1	3611	5.0	-0.1	2.0	0.1	0.0	0.0	5.0	2.0	-0.1
V2	3612	3.1	-0.3	1.3	0.2	0.0	0.0	3.1	1.3	-0.3
V3	3613	1.6	-0.8	0.5	0.3	0.0	0.0	1.6	0.5	-0.8
V4	3614	0.2	-1.7	-0.4	0.3	0.0	0.0	0.3	-0.4	-1.8
V5	3615	-1.1	-3.4	-1.5	0.3	0.0	0.0	-1.1	-1.5	-3.4
V6	3616	-2.7	-1.5	-1.7	0.2	0.0	0.0	-1.4	-1.7	-2.8
V7	3617	-5.9	1.5	-2.1	0.1	0.0	0.0	1.5	-2.1	-5.9
W1	3241	0.1	-0.1	0.1	0.0	0.0	0.0	0.1	0.1	-0.1
W2	3242	0.7	-0.1	0.7	0.0	0.0	0.0	0.7	0.7	-0.1
W3	3243	1.4	-0.1	1.4	0.0	0.0	0.0	1.4	1.4	-0.1
W4	3244	2.0	-0.1	2.0	0.0	0.0	0.0	2.0	2.0	-0.1
W5	3245	2.7	0.0	2.7	0.0	0.0	0.0	2.7	2.7	0.0
W6	3246	3.3	0.0	3.3	0.0	0.0	0.0	3.3	3.3	0.0
X1	3801	0.3	0.0	0.3	0.0	0.0	0.0	0.3	0.3	0.0
X2	3802	0.3	0.0	0.3	0.0	0.0	0.0	0.3	0.3	0.0
X3	3803	0.2	0.0	0.2	0.0	0.0	0.0	0.2	0.2	0.0
X4	3804	0.1	0.0	0.1	0.0	0.0	0.0	0.1	0.1	0.0
X5	3805	0.0	0.0	0.0	0.0	0.0	0.0	0.0	0.0	0.0
X6	3806	-0.1	0.0	-0.1	0.0	0.0	0.0	0.0	-0.1	-0.1
X7	3807	-0.2	0.0	-0.2	0.0	0.0	0.0	0.0	-0.2	-0.2

<sup>1</sup> Refer to Figure 2.10.2-34 for the identification of the representative sections.

Table 2.10.4-179  $S_n$  Stresses; Thermal (Fire) Transient; Time = 30 Minutes; With Contents;  
2-D Model

Section <sup>1</sup>	Node - Node	Stress Components (ksi)						Principal Stresses (ksi)			
		$S_x$	$S_y$	$S_z$	$S_{xy}$	$S_{yz}$	$S_{xz}$	S1	S2	S3	S.I.
A I	1 - 5	7.9	-0.1	7.9	0.0	0.0	0.0	7.9	7.9	-0.1	8.0
B I	6 - 10	-0.3	0.0	-0.3	0.0	0.0	0.0	0.0	-0.3	-0.3	0.3
C I	251 - 255	10.9	0.4	8.0	-0.2	0.0	0.0	10.9	8.0	0.4	10.6
D I	306 - 310	2.4	19.9	4.1	0.5	0.0	0.0	19.9	4.1	2.4	17.5
E O	305 - 355	-0.2	-18.8	-8.2	-0.8	0.0	0.0	-0.2	-8.2	-18.8	18.6
F I	251 - 281	7.4	0.4	6.5	-1.1	0.0	0.0	7.5	6.5	0.2	7.3
G O	311 - 351	-7.9	-13.4	-88.7	2.5	0.0	0.0	-6.9	-14.4	-88.7	81.8
H O	581 - 584	0.0	9.7	3.7	-0.1	0.0	0.0	9.7	3.7	0.0	9.7
I I	589 - 593	-0.4	5.2	6.9	0.0	0.0	0.0	6.9	5.2	-0.4	7.3
J O	971 - 974	0.0	10.9	3.9	0.0	0.0	0.0	10.9	3.9	0.0	10.9
K I	979 - 983	-0.4	3.7	7.4	0.0	0.0	0.0	7.4	3.7	-0.4	7.8
L O	1601 - 1604	0.0	10.2	3.8	0.0	0.0	0.0	10.2	3.8	0.0	10.2
M I	1609 - 1613	-0.4	3.9	7.7	0.0	0.0	0.0	7.7	3.9	-0.4	8.1
N O	2216 - 2219	0.0	10.7	3.5	0.0	0.0	0.0	10.7	3.5	0.0	10.7
O I	2224 - 2228	-0.3	4.7	5.2	-0.2	0.0	0.0	5.2	4.7	-0.3	5.4
P I	2546 - 2549	-0.4	27.4	7.6	-0.8	0.0	0.0	27.4	7.6	-0.4	27.8
Q O	2554 - 2558	0.0	-21.0	6.6	0.7	0.0	0.0	6.6	0.0	-21.0	27.6
R I	2771 - 2774	3.7	-48.8	43.3	1.8	0.0	0.0	43.3	3.8	-48.8	92.2
S O	2779 - 2783	0.8	-16.7	-90.7	-4.1	0.0	0.0	1.7	-17.6	-90.7	92.4
T O	7066 - 7072	-4.4	-4.5	-67.5	1.2	0.0	0.0	-3.3	-5.6	-67.5	64.2
U I	3051 - 3056	1.8	-3.6	-3.4	-0.8	0.0	0.0	1.9	-3.4	-3.7	5.6
V O	3611 - 3617	-4.7	1.5	-2.6	0.2	0.0	0.0	1.5	-2.6	-4.7	6.2
W O	3241 - 3246	3.3	0.0	3.3	0.0	0.0	0.0	3.3	3.3	0.0	3.3
X I	3801 - 3807	0.3	0.0	0.3	0.0	0.0	0.0	0.3	0.3	0.0	0.4

<sup>1</sup> Refer to Figure 2.10.2-34 for the identification of the representative sections.

Table 2.10.4-180 Critical  $S_n$  Stress Summary; Thermal (Fire) Transient; Time = 30 Minutes; With Contents; 2-D Model

Comp. No. <sup>1</sup>	Section Cnt Node-Node	P <sub>n</sub> Stresses (ksi)							Principal Stresses (ksi)			Allow. Stress	Margin of Safety	
		S <sub>x</sub>	S <sub>y</sub>	S <sub>z</sub>	S <sub>xy</sub>	S <sub>yz</sub>	S <sub>xz</sub>	S1	S2	S3				
1	306- 310	2.4	19.9	4.1	0.5	0.0	0.0	0.0	19.9	4.1	2.4	17.5	730.0	40.7
2	311- 351	-7.9	-13.4	-88.7	2.5	0.0	0.0	0.0	-6.9	-14.4	-88.7	81.8	730.0	7.9
3	2711- 2714	-0.6	2.3	46.2	3.8	0.0	0.0	0.0	46.2	4.9	-3.3	49.3	730.0	13.7
4	926- 929	0.0	11.0	3.7	0.0	0.0	0.0	0.0	11.0	3.7	0.0	11.0	730.0	63.1
5	2539- 2543	-22.0	0.4	8.7	-0.3	0.0	0.0	0.0	8.7	0.4	-22.0	30.7	730.0	22.8
6	2719- 2723	17.1	-0.2	-77.7	1.5	0.0	0.0	0.0	17.3	-0.3	-77.7	95.0	730.0	6.7
7	3021- 3026	1.8	21.6	-13.5	0.6	0.0	0.0	0.0	21.6	1.8	-13.5	35.1	730.0	19.8
8	3601- 3607	4.1	-2.7	1.8	0.9	0.0	0.0	0.0	4.2	1.8	-2.8	7.1	730.0	102.2

Locations of the most critical sections for each component are provided in the following:

Comp. No. <sup>1</sup>	Section Location			
	Inside Node		Outside Node	
	x (in)	y (in)	z (in)	x (in)
1	39.44	6.20	39.44	0.75
2	40.70	14.40	43.35	14.40
3	35.50	171.40	37.50	171.40
4	35.50	52.40	37.00	52.40
5	40.70	159.40	43.35	159.40
6	40.70	171.40	43.35	171.40
7	37.66	179.40	37.66	185.40
8	36.46	188.40	36.46	193.71

<sup>1</sup> Refer to Figure 2.10.2-33 for cask component identification.



## 2.10.5 Inner Shell Buckling Analysis

Code Case N-284 (Metal Containment Shell Buckling Design Methods) of the "ASME Boiler and Pressure Vessel Code" is used to analyze the NAC-STC inner shell and transition sections for structural stability. Structural stability ensures that the inner shell and transition sections do not buckle during cask fabrication, normal conditions of transport, or hypothetical accident conditions. The buckling evaluation requirements of Regulatory Guide 7.6, Paragraph C.5, are shown to be satisfied by the results of the interaction equation calculations of Code Case N-284.

The inner shell buckling design criteria, specifically the criteria of Code Case N-284, are described in detail in Section 2.1.3.4.

### 2.10.5.1 Buckling Analysis

The structural stability analysis of the NAC-STC inner shell and transition sections is performed by an NAC proprietary computer program in accordance with the ASME Code Case N-284. The data considered for an ASME Code Case N-284 buckling evaluation includes shell geometry parameters, shell fabrication tolerances, shell material properties, theoretical elastic buckling stress values for the shell, and primary plus secondary ( $P + Q$ ) stresses at the sections of the shell to be evaluated. The axial, hoop, and in-plane shear components of the  $P + Q$  stresses in the inner shell and in the transition sections are obtained from the ANSYS finite element analyses for each of the normal conditions of transport and hypothetical accident conditions. Since the inner shell and the transition sections of the primary containment vessel are different materials and have different operating temperatures, a separate buckling evaluation is performed for the inner shell and for the transition sections. The fixity provided by the thick end forgings precludes buckling in the regions of the inner shell immediately adjacent to the forgings.

Nodal  $P + Q$  stress components are conservatively used for the buckling evaluation of the inner shell and the transition sections of the directly loaded fuel configuration of the NAC-STC for the heat condition, the cold condition, all of the 1-foot drop conditions, the 30-foot top and bottom end drops, the 30-foot side drop, and the 30-foot top and bottom corner drops (nodal stresses include any peaking effects that are present at the node location). Sectional  $P + Q$  stress components, as required by ASME Code Case N-284, are used for the buckling evaluation of the inner shell and the transition sections of the directly loaded fuel configuration of the NAC-STC for the 30-foot top and bottom 75-degree oblique drops and for the 30-foot bottom 15-degree oblique drop. Buckling is evaluated for the canistered fuel configuration of the NAC-STC only

for the 30-foot side drop condition. The 1-foot side drop condition is less critical than the 30-foot side drop condition (refer to Table 2.10.5-1). For the other drop orientations, the directly loaded fuel configuration has been shown to bound the canistered fuel configuration (Sections 2.7.1.1 - 2.7.1.4). For each load condition evaluated, the maximum compressive axial stress component calculated anywhere in the inner shell is combined with the maximum compressive hoop stress component calculated anywhere in the inner shell and the maximum in-plane shear stress component calculated anywhere in the inner shell; this produces a grossly conservative, bounding case buckling evaluation of the inner shell. The same analysis is used in the buckling evaluation of the transition sections. The stress component values used in the buckling evaluations are documented in Table 2.10.5-1.

The maximum temperatures for normal conditions of transport in the inner shell and the transition section are 331°F and 300°F, respectively, for the directly loaded fuel configuration; 311°F and 300°F, respectively, for the Yankee-MPC canistered fuel configuration; and 331°F and 331°F, respectively, for the CY-MPC canistered fuel configuration (Table 3.4-5). Therefore, previously analyzed and conservative higher temperatures are not revised throughout these analyses and a temperature of 353°F is used to determine the values of the modulus of elasticity and yield stress to be used in the buckling evaluation of the Type 304 stainless steel inner shell. Similarly, a temperature of 338°F is used for the transition sections.

#### 2.10.5.2 Analysis Results

The results of the buckling evaluation of the NAC-STC inner shell and transition sections are summarized in Table 2.10.5-1 for the directly loaded fuel configuration and in Sections 2.10.5.4 and 2.10.5.5 for the canistered fuel configurations. All interaction equations yield values less than 1.0. Also, there are no concentrated loads on the inner shell or transition sections that would lead to localized buckling. Therefore, the buckling criteria of Code Case N-284 are satisfied and it is concluded that buckling of the NAC-STC inner shell and transition sections will not occur.

2.10.5.3      Verification of the Code Case N-284 Buckling Evaluation of the NAC-STC Inner Shell and Transition Sections

The results of the proprietary NAC computer program that performs the Code Case N-284 buckling evaluation are verified by a hand calculation of load case "J<sub>T</sub>" (Table 2.10.5-1). This step-by-step analysis procedure reflects the procedure diagrammed in paragraph-1800 of Code Case N-284. The geometry parameters for the NAC-STC inner shell and transition sections are defined in Table 2.10.5-2.

Step 1

For load case "J<sub>T</sub>", the compressive stresses from Table 2.10.5-1 are:

$$S_f = 16,445 \text{ psi}$$

$$S_q = 10,356 \text{ psi}$$

$$S_{fq} = 14,515 \text{ psi}$$

Step 2

For accident conditions, the factor of safety (FS) is 1.34. Multiplying the stress components by this factor of safety yields:

$$FS(S_f) = 22,036 \text{ psi}$$

$$FS(S_q) = 13,877 \text{ psi}$$

$$FS(S_{fq}) = 19,450 \text{ psi}$$

Step 3

Capacity reduction factors, calculated per Section 2.1.3.4.3, are as follows for the load case "J<sub>T</sub>" transition section temperature of 338°F:

$$\alpha_{\phi L} = 0.393$$

$$\alpha_{\theta L} = 0.8$$

$$\alpha_{\theta\phi L} = 0.8$$

In order to directly use the capacity reduction factors from Table 2.10.5-3, the tolerance requirements of Article NE-4220 of the "ASME Boiler and Pressure Vessel Code," Subsection NE must be satisfied. Article NE-4221.1 and Article NE-4221.2 set forth the "maximum difference in cross-sectional diameters" and "maximum deviation from true theoretical form for external pressure". Table 2.10.5-4 shows that the requirements of Articles NE-4221.1 and NE-4221.2 are satisfied, as long as the maximum tolerances and configuration constraints are met during manufacturing.

#### Step 4

Plasticity reduction factors are determined using the equations presented in Section 2.1.3.4.4 as follows ( $S_y$  available from Table 2.10.5-5):

##### 1. Axial Compression

$$S_{\phi} (FS)/S_y = (22,036)/(42,600) = 0.5173$$

$$\eta_{\phi} = 1.0$$

##### 2. Hoop Compression

$$S_{\theta} (FS)/S_y = (13,877)/(42,600) = 0.3258$$

$$\eta_{\theta} = 1.0$$

### 3. Shear

$$S_{\phi\theta} (FS)/S_y = (19,450)/(42,600) = 0.4566$$

$$\eta_{\phi\theta} = 1.0$$

From Section-1600 of Code Case N-284, as an upper limit, the compressive stresses,  $S_i$  ( $\phi = f$  or  $\theta$ ), must be less than the yield strength,  $S_y$ , divided by the appropriate factor of safety ( $S_i < S_y/FS$ ). Similarly, for shear,  $S_{\phi\theta}$  must be less than or equal to  $0.6 S_y$  divided by the appropriate factor of safety ( $S_{\phi\theta} < 0.6 S_y/FS$ ). As stated in Section 2.1.3.4.1, there is a factor of safety of 2.0 for normal transport conditions and a factor of safety of 1.34 for hypothetical accident conditions. Table 2.10.5-6 presents the elastic upper bound compressive and shear stresses, evaluated using normal and accident condition factors of safety. Under no circumstances can the elastic values presented in the table be exceeded. However, satisfying these limits alone is not sufficient to demonstrate that buckling will not occur. As stated in Section 2.1.3.4.1, the interaction equations must also be satisfied.

#### Step 5

Compute elastic stress components per the following equation:

$$S_{is} = S_i(FS)/\alpha_{iL}$$

$$S_{\phi s} = S_{\phi} (FS)/\alpha_{\phi L} = (22,036)/(0.393) = 56,071 \text{ psi}$$

$$S_{0s} = S_0 (FS)/\alpha_{0L} = (13,877)/(0.8) = 17,346 \text{ psi}$$

$$S_{\phi 0s} = S_{\phi 0} (FS)/\alpha_{\phi 0L} = (19,450)/(0.8) = 24,313 \text{ psi}$$

Step 6

Compute inelastic stress components per the following equation:

$$S_{ip} = S_{is}/\eta_i$$

$$S_{\phi p} = S_{\phi s}/\eta_{\phi} = (56,071)/(1.0) = 56,071 \text{ psi}$$

$$S_{\theta p} = S_{\theta s}/\eta_{\theta} = (17,346)/(1.0) = 17,346 \text{ psi}$$

$$S_{\phi\theta p} = S_{\phi\theta s}/\eta_{\phi\theta} = (24,313)/(1.0) = 24,313 \text{ psi}$$

Step 7

For the NAC-STC, the buckling evaluation approach, consistent with the vessel design and method of analysis, is that of paragraph-1710 of Code Case N-284.

Step 8

Theoretical uniaxial buckling values are available from Section 2.1.3.4.2. For the transition section at 338°F, these theoretical values are as follows (Table 2.10.5-7 and Table 2.10.5-8):

$$S_{\phi cL} = 668,435 \text{ psi}$$

$$S_{\theta cL} = S_{rcL} = 49,155 \text{ psi}$$

$$S_{\eta cL} = 47,927 \text{ psi}$$

$$S_{\phi\theta cL} = 176,487 \text{ psi}$$

Applicable elastic and inelastic interaction equations in paragraph-1713.1.1 and paragraph-1713.2.1 of Code Case N-284 are checked as follows:

1. Elastic Buckling (Paragraph-1713.1.1, Code Case N-284)

a. Axial Compression Plus Hoop Compression

$$(S_{\phi s} < 0.5 S_{\theta s})$$

$$56,071 > (0.5)(17,346); \text{ therefore, not applicable.}$$

b. Axial Compression Plus Hoop Compression

$$(S_{\phi s} \geq 0.5 S_{\theta s})$$

$$[(S_{\phi s} - 0.5 S_{\theta s}) / (S_{\phi eL} - 0.5 S_{\theta eL})] + (S_{\theta s} / S_{\theta eL})^2 \leq 1.0$$

$$\frac{56,071 - (0.5)(47,927)}{668,435 - (0.5)(47,927)} + (17,346/47,927)^2 \leq 1.0$$

$$0.1779 \leq 1.0$$

therefore,

$$Q1 = 0.1779 < 1.0$$

c. Axial Compression Plus Shear

$$(S_{\phi s} / S_{\phi eL}) + (S_{\theta s} / S_{\theta eL})^2 \leq 1.0$$

$$(56,071/668,435) + (24,313/176,487)^2 \leq 1.0$$

$$0.1029 \leq 1.0$$

therefore,

$$Q2 = 0.1029 < 1.0$$

d. Hoop Compression Plus Shear

$$(S_{\theta s}/S_{reL}) + (S_{\phi \theta s}/S_{\phi \theta eL})^2 \leq 1.0$$

$$(17,346/49,165) + (24,313/176,487)^2 \leq 1.0$$

$$0.372 \leq 1.0$$

therefore,

$$Q3 = 0.372 < 1.0$$

e. Axial Compression Plus Hoop Compression Plus Shear

$$K = 1 - (S_{\phi \theta s}/S_{\phi \theta eL})^2 = 1 - (24,313/176,487)^2 = 0.981$$

and, therefore, Equation B (above) becomes:

$$+ [(17,346/(0.981)(48,465))]^2 = 0.1832$$

therefore,

$$Q4 = 0.1846 < 1.0$$

2. Inelastic Buckling (Paragraph-1713.2.1, Code Case N-284)

a. Axial Compression Plus Shear

$$(S_{\phi p}/S_{\phi eL})^2 + (S_{\phi \theta p}/S_{\phi \theta eL})^2 \leq 1.0$$

$$(56,071/668,435)^2 + (24,313/176,487)^2 \leq 1.0$$

$$0.026 \leq 1.0$$



therefore,

$$Q5 = 0.026 < 1.0$$

b. Hoop Compression Plus Shear

$$(S_{\theta p}/S_{reL})^2 + (S_{\phi \theta p}/S_{\phi \theta eL})^2 \leq 1.0$$

$$(17,346/49,155)^2 + (24,313/176,487)^2 \leq 1.0$$

$$0.144 \leq 1.0$$

therefore,

$$Q6 = 0.144 < 1.0$$

The results of the hand calculation of load case "J<sub>T</sub>" are identical to the results in Table 2.10.5-1 that were calculated by the NAC proprietary computer program, which performs the Code Case N-284 buckling evaluation. Thus, the computer program results in Table 2.10.5-1 and the buckling stability of the NAC-STC inner shell are verified.

2.10.5.4 Buckling Evaluation of the Inner Shell for the Yankee-MPC Fuel Configuration

In the Yankee-MPC canistered fuel configuration for a side drop load condition, the fuel load is applied to the support disks which transmit the load to the canister and then to the inner shell of the NAC-STC. Thus, the loading on the cask inner shell for a side drop load condition is different than that for the directly loaded fuel configuration where the support disks directly load the cask inner shell. To demonstrate that the NAC-STC will resist buckling of the inner shell in the side drop, the methodology described in 2.10.5.3 will be applied with stresses determined for the side drop using the canistered fuel configuration. The canistered fuel configuration loading on the cask cavity for an end drop condition is essentially the same as for the directly loaded fuel configuration, so no additional evaluation is required.

The section with the maximum compressive stress (hoop and axial) for the inner shell and transition shell occurs at the weld connecting the inner shell to the bottom forging). As a result of computing the linearized stress at this section, the maximum axial stress is -12,800 psi and the maximum hoop stress is -16,200 psi. The corresponding shear stress is 1,100 psi. These values are obtained from Table 2.7.1.2-1. These stresses are for the 30-ft side drop condition and they envelop the 1-ft side drop condition. Thermal compressive forces are included by using the largest thermal membrane stresses from Tables 2.10.4-5, 2.10.4-6, and 2.10.4-7.

Step 1

$$S_{\phi} = -12,800 + (-2,700) = -15,500 \text{ psi}$$

$$S_{\theta} = -16,200 + (-1,800) = -16,700 \text{ psi}$$

$$S_{\phi\theta} = 1,100 + 1,200 = 2,300 \text{ psi}$$

Step 2

$$FS(S_{\phi}) = 20,770 \text{ psi}$$

$$FS(S_{\theta}) = 22,378 \text{ psi}$$

$$FS(S_{\phi\theta}) = 3,082 \text{ psi}$$

Step 3

$$\alpha_{\phi L} = 0.393$$

$$\alpha_{\theta L} = 0.800$$

$$\alpha_{\phi\theta L} = 0.800$$

Step 4

1. Axial Compression

$$S_{\phi}(FS)/S_y = (20,700)/(42,600) = 0.486$$

$$\eta_{\phi} = 1.0$$

2. Hoop Compression

$$S_{\theta}(FS)/S_y = (22,378)/(42,600) = 0.525$$

$$\eta_{\theta} = 1.0$$

3. Shear

$$S_{\phi\theta}(FS)/S_y = (3,082)/(42,600) = 0.072$$

$$\eta_{\phi\theta} = 1.0$$

Step 5

$$S_{is} = S_i(FS)/\alpha_{iL}$$

$$S_{\phi s} = S_{\phi}(FS)/\alpha_{\phi L} = (20,770)/(0.393) = 52,850 \text{ psi}$$

$$S_{\theta s} = S_{\theta}(FS)/\alpha_{\theta L} = (22,378)/(0.800) = 27,973 \text{ psi}$$

$$S_{\phi\theta s} = S_{\phi\theta}(FS)/\alpha_{\phi\theta L} = (3,082)/(0.800) = 3,853 \text{ psi}$$

Step 6

$$S_{ip} = S_{ip}/\eta_i$$

$$S_{\phi p} = S_{\phi p} / \eta_{\phi} = (52,850) / (1.0) = 52,850 \text{ psi}$$

$$S_{\theta p} = S_{\theta p} / \eta_{\theta} = (27,973) / (1.0) = 27,973 \text{ psi}$$

$$S_{\phi \theta p} = S_{\phi \theta p} / \eta_{\phi \theta} = (3,853) / (1.0) = 3,853 \text{ psi}$$

Step 7

For the NAC-STC, the buckling evaluation approach, consistent with the vessel design and method of analysis, is that of Paragraph-1710 of Code Case N-284.

Step 8

From Table 2.10.5-8 the theoretical elastic buckling stresses at 353 °F are:

$$S_{\phi cL} = 668,435 \text{ psi}$$

$$S_{\theta cL} = S_{rel} = 49,115 \text{ psi}$$

$$S_{hcL} = 47,927 \text{ psi}$$

$$S_{\phi \theta cL} = 176,487 \text{ psi}$$

1. Elastic Buckling (Paragraph-1713.1.1, Code Case N-284)

a.  $52,850 > (0.5)(27,973)$ ; therefore, not applicable.

b.  $0.381 < 1.0$

therefore,

$$Q1 = 0.381 < 1.0$$

c.  $0.0795 \leq 1.0$

therefore,

$$Q2 = 0.0795 < 1.0$$

d.  $0.584 \leq 1.0$

therefore,

$$Q3 = 0.584 < 1.0$$

e.  $K = 0.9995$

therefore,

$$Q4 = 0.381 < 1.0$$

**2. Inelastic Buckling (Paragraph-1713.2.1, Code Case N-284)**

a.  $0.0067 \leq 1.0$

therefore,

$$Q5 = 0.0067 < 1.0$$

b.  $0.3368 \leq 1.0$

therefore,

$$Q6 = 0.3368 < 1.0$$

Using the methodology presented in Section 2.10.5.3, the buckling stability of the inner shell and the transition shell of the NAC-STC for the canistered fuel configuration is verified.

2.10.5.5 Buckling Evaluation of the Inner Shell for the CY-MPC Fuel Configuration

The section with the maximum compressive stress (hoop and axial) for the inner shell and transition shell occurs in the transition shell where the thickness is 2.0 inches. This evaluation conservatively uses a thickness of 1.5 inches for all sections on the inner shell. As a result of computing the linearized stress at this section, the maximum axial stress is -8,490 psi and the maximum hoop stress is -14,740 psi. The corresponding shear stress is 965 psi. These values are obtained from Table 2.7.1.1-2. These stresses are for the 30-foot side drop condition and they envelop the 1-foot side drop event. Thermal compressive forces are included by using the largest thermal membrane stresses from Tables 2.10.4-5, 2.10.4-6 and 2.10.4-7. Use of these thermal stresses is conservative because the heat load in the CY-MPC is less than the heat load in the NAC-STC directly loaded fuel configuration.

$$\text{Maximum axial stress, } S_{\phi} = -8,490 + (-2,700) = -11,190 \text{ psi}$$

$$\text{Maximum hoop stress, } S_{\theta} = -14,740 + (-1,800) = -16,540 \text{ psi}$$

$$\text{Maximum shear stress, } S_{\phi\theta} = 965 + 1,200 = +2,165 \text{ psi}$$

Because the stress values for the CY-MPC are less than the corresponding stress values calculated for the Yankee-MPC canistered fuel configuration determined in Section 2.10.5.4.1, the Yankee-MPC configuration evaluated in Section 2.10.5.4 is bounding for the CY-MPC configuration.

Table 2.10.5-1 Buckling Evaluation Results NAC-STC Inner Shell

Load Case	Load Condition	Analysis Section Location	Axial Stress (psi)	Hoop Stress (psi)	Inplane Shear Stress (psi)	Elastic Buckling Interaction Equations				Plastic Buckling Interaction Equations	
						Q1	Q2	Q3	Q4	Q5	Q6
A <sub>IS</sub>	Heat	Inner Shell	-1634	-830	322	.00	.02	.04	.00	.00	.00
B <sub>IS</sub>	Cold	Inner Shell	-321	-3838	315	.00	.00	.19	.00	.00	.04
C <sub>IS</sub>	1-Ft Top End	Inner Shell	-5755	-2867	0	.09	.04	.29	.09	.00	.08
D <sub>IS</sub>	1-Ft Bottom End	Inner Shell	-5988	-2864	0	.10	.04	.30	.10	.00	.09
E <sub>IS</sub>	1-Ft Side	Inner Shell	-4911	-1829	4338	.04	.07	.10	.04	.01	.01
F <sub>IS</sub>	1-Ft Top Corner	Inner Shell	-6729	-937	3029	.06	.10	.05	.07	.02	.00
G <sub>IS</sub>	1-Ft Bottom Corner	Inner Shell	-6819	-847	-2945	.07	.10	.04	.07	.02	.00
H <sub>IS</sub>	30-Ft Top End	Inner Shell	-10409	-2705	0	.07	.10	.09	.07	.03	.01
I <sub>IS</sub>	30-Ft Bottom End	Inner Shell	-10649	-2679	0	.08	.10	.09	.08	.03	.01
J <sub>IS</sub>	30-Ft Side	Inner Shell	-9836	-7346	9724	.12	.10	.26	.13	.08	.13
K <sub>IS</sub>	30-Ft Top Corner	Inner Shell	-16021	-2484	8083	.13	.16	.09	.13	.72	.02
L <sub>IS</sub>	30-Ft Bottom Corner	Inner Shell	-15916	-2154	-7853	.13	.16	.08	.13	.65	.01
M <sub>IS</sub>	30-Ft Top Obliq. (75°)	Inner Shell	-9659	-6848	9460	.11	.10	.24	.12	.07	.11
N <sub>IS</sub>	30-Ft Bott. Obliq. (15°)	Inner Shell	-16170	-1595	-6427	.13	.16	.06	.13	.81	.01
O <sub>IS</sub>	30-Ft Bott. Obliq. (75°)	Inner Shell	-10161	-5650	-9286	.10	.10	.20	.10	.07	.08

Table 2.10.5-1 Buckling Evaluation Results NAC-STC Inner Shell (continued)

Load		Analysis	Axial	Hoop	Inplane	Elastic Buckling				Plastic Buckling	
		Section	Stress	Stress	Shear	Interaction Equations				Interaction	
Case	Load Condition	Location	(psi)	(psi)	(psi)	Q1	Q2	Q3	Q4	Q5	Q6
A <sub>T</sub>	Heat	Transition	-2956	-5218	-694	.00	.02	.26	.00	.00	.07
B <sub>T</sub>	Cold	Transition	-2988	-4135	503	.00	.02	.21	.00	.00	.04
C <sub>T</sub>	1-Ft Top End	Transition	-2960	-5727	0	.00	.02	.29	.00	.00	.08
D <sub>T</sub>	1-Ft Bottom End	Transition	-2955	-6581	0	.00	.02	.33	.00	.00	.11
E <sub>T</sub>	1-Ft Side	Transition	-7482	-3994	6037	.06	.06	.21	.06	.01	.05
F <sub>T</sub>	1-Ft Top Corner	Transition	-9626	-1473	3679	.04	.08	.07	.04	.01	.01
G <sub>T</sub>	1-Ft Bottom Corner	Transition	-10422	-1704	-3467	.05	.08	.09	.05	.01	.01
H <sub>T</sub>	30-Ft Top End	Transition	-2984	-14144	0	.00	.01	.48	.00	.00	.23
I <sub>T</sub>	30-Ft Bottom End	Transition	-2973	-14362	0	.00	.01	.48	.00	.00	.23
J <sub>T</sub>	30-Ft Side	Transition	-16445	-10356	14515	.17	.10	.37	.18	.03	.14
K <sub>T</sub>	30-Ft Top Corner	Transition	-26632	-898	9400	.10	.14	.04	.10	.13	.01
L <sub>T</sub>	30-Ft Bottom Corner	Transition	-27565	-2122	-9183	.11	.14	.08	.11	.17	.01
M <sub>T</sub>	30-Ft Top Obliq. (75°)	Transition	-13488	-9023	15240	.13	.09	.32	.13	.02	.11
N <sub>T</sub>	30-Ft Bott. Obliq. (15°)	Transition	-30799	-1935	-7402	.12	.16	.07	.13	.47	.01
O <sub>T</sub>	30-Ft Bott. Obliq. (75°)	Transition	-17164	-10107	-15101	.17	.10	.36	.18	.03	.14



Table 2.10.5-2 Geometry Parameters for the NAC-STC Inner Shell and Transition Sections

Parameter	Inner Shell	Transition Section <sup>1</sup>
R = radius (in) [to centerline of shell]	36.25	36.25
t = thickness (in)	1.5	1.5
$(Rt)^{0.5}$	7.37	7.37
$L_{\phi}$ = length (in)	161.00	161.00
$L_{\theta}$ = $2\pi R$ = circumference (in)	227.8	227.8
$M_{\phi} = L_{\phi}/(Rt)^{0.5}$	21.83	21.83
$M_{\theta} = L_{\theta}/(Rt)^{0.5}$	30.89	30.89
M = lesser of $M_{\phi}$ or $M_{\theta}$	21.83	21.83
$\nu$ = Poisson's Ratio	0.275	0.275

1 Conservatively consider the thinner portion of the Transition Section.

Table 2.10.5-3 Capacity Reduction Factors for the NAC-STC Inner Shell and Transition Sections

Capacity Reduction Factor	Temperature (°F)		
	70	338	353
SA-240, Type 304 Stainless Steel			
$a_{\phi L}$ (axial)	0.67	0.207	0.207
$a_{\theta L}$ (hoop)	0.8	0.8	0.8
$a_{\phi\theta L}$ (shear)	0.8	0.8	0.8
SA-240, Type XM-19 Stainless Steel			
$a_{\phi L}$ (axial)	0.517	0.393	0.389
$a_{\theta L}$ (hoop)	0.8	0.8	0.8
$a_{\phi\theta L}$ (shear)	0.8	0.8	0.8

Table 2.10.5-4 Fabrication Tolerances for the NAC-STC Inner Shell

Requirement	Parameter	Inner Shell Data (inch)
	Maximum Inside Diameter (I.D.)	71.06
	Minimum I.D.	70.96
	Nominal I.D.	71.00
NE-4221.1	a) (Max I.D. - Min I.D.)	0.10
	b) $(0.01) \times (\text{Nominal I.D.})$	0.710
	Tolerance Check	Yes
	$(a < b)$	$(0.10 \text{ in} < 0.710 \text{ in})$
	Nominal Shell Thickness	1.50
	Minimum Shell Thickness	1.48
	Shell Length	161.00
	Nominal Shell Outside Diameter (O.D.)	74.00
	Minimum Shell O.D.	73.92
NE-4221.2	c) Permissible Deviation, e	0.54
	(Figure -4221.2-1)	
	d) Actual Deviation <sup>1</sup>	0.04
	Tolerance Check	Yes
	$(d < c)$	$(0.04 \text{ in} < 0.54 \text{ in})$

<sup>1</sup>  $(\text{Nominal O.D.} - \text{Minimum O.D.})/2 = (74.00 - 73.92)/2 = 0.04.$

Table 2.10.5-5 Material Properties for Buckling Analysis Input

Parameter <sup>1</sup>	Temperature (°F)		
	70	338	353
SA-240, Type 304 Stainless Steel			
E (psi)	$28.3 \times 10^6$	$26.7 \times 10^6$	$26.7 \times 10^6$
S <sub>y</sub> (psi)	$30.0 \times 10^3$	$22.0 \times 10^3$	$21.7 \times 10^3$
SA-240, Type XM-19 Stainless Steel			
E (psi)	$28.3 \times 10^6$	$26.7 \times 10^6$	$26.7 \times 10^6$
S <sub>y</sub> (psi)	$55.0 \times 10^3$	$42.6 \times 10^3$	$42.2 \times 10^3$

1 Section 2.3.2.

Table 2.10.5-6 Upper Bound Buckling Stresses

Load Condition		Temperature (°F)		
		70	338	353
SA-240, Type 304 Stainless Steel				
Elastic, Upper Bound Compressive Stress	Normal	15,000	11,320	10,960
$S_0$ or $S_\phi$ (psi)	Accident	22,390	16,900	16,343
Elastic, Upper Bound In-Plane Shear Stress	Normal	9,000	6,795	6,580
$S_{\phi 0}$ (psi)	Accident	13,434	10,140	9,806
(SA-240, Type XM-19 Stainless Steel)				
Elastic, Upper Bound Compressive Stress	Normal	27,500	21,800	21,300
$S_0$ or $S_\phi$ (psi)	Accident	41,040	32,550	31,790
Elastic, Upper Bound In-Plane Shear Stress	Normal	16,500	13,080	12,780
$S_{\phi 0}$ (psi)	Accident	24,620	19,530	19,070

Table 2.10.5-7 Theoretical Elastic Buckling Stress Values (Temperature Independent Form)

Elastic Buckling Stress	Inner Shell	Load Description
$S_{\phi eL}$	0.025035E	axial
$S_{\theta eL} = S_{reL}$	0.001841E	hoop, without end pressure
$S_{heL}$	0.001795E	hoop, with end pressure
$S_{\phi \theta eL}$	0.00661E	shear

Table 2.10.5-8 Theoretical Elastic Buckling Stresses for Selected Temperatures (SA-240, Type 304 and SA-240, Type XM-19 Stainless Steel)

Parameter	Theoretical Elastic Buckling Stress (psi)		
		Transition Section	Inner Shell
Modulus of Elasticity (E) at Temperature (T)	$E = 28.3 \times 10^6$ $T = 70^\circ\text{F}$	$E = 26.7 \times 10^6$ $T = 338^\circ\text{F}$	$E = 26.7 \times 10^6$ $T = 353^\circ\text{F}$
$S_{\phi eL}$	708,490	669,186	668,435
$S_{\theta eL} = S_{reL}$	52,100	49,213	49,155
$S_{heL}$	50,800	47,980	47,927
$S_{\phi \theta eL}$	187,060	176,685	176,487

## 2.10.6 Scale Model Test Program for the NAC-STC

### 2.10.6.1 Introduction

This section provides a detailed description of the Scale Model Test Program, which was carried out as confirmatory support of the analysis and licensing effort for the design qualification of the directly loaded fuel configuration of the NAC-STC cask. The analyses presented elsewhere in this report demonstrate that the directly loaded fuel configuration of the NAC-STC cask design meets all of the requirements for use in the packaging and transportation of radioactive material (10 CFR 71), PWR spent fuel. The test results presented in this appendix confirm those analyses and provide additional confidence that the cask design provides for the safe transport of spent nuclear fuel. The scale model test program for the directly loaded fuel configuration of the NAC-STC included: (1) quarter-scale model drop tests and (2) eighth-scale model impact limiter quasi-static compression tests. These tests were performed using the redwood and balsa wood impact limiters (redwood impact limiter[s]) described in Licensing Drawings 423-209 and 423-210 and scale model impact limiter Drawings 423-248 and 423-249.

This report revision incorporates the drawings and analyses that demonstrate the design qualification of the canistered configuration of the NAC-STC for Yankee Class fuel or GTCC waste. The cask body is unchanged. The directly loaded fuel basket is replaced by a similar tube and disk design basket structure enclosed in a welded canister. The Yankee-MPC canistered configuration of the NAC-STC includes spacers in the cask cavity that are designed to position the loaded canister such that the package center-of-gravity location is identical to that of the package containing directly loaded fuel. The total weight of the cavity contents for the Yankee-MPC fuel or GTCC waste configuration is just slightly less than that for the directly loaded fuel configuration, 55,590 or 54,271 pounds versus 56,000 pounds. Based on the location of the packaging center-of-gravity and on the cavity contents weight considerations, it is concluded that the confirmatory scale model drop tests and the resulting impact limiter qualification are valid for the Yankee-MPC canistered configuration and for the directly loaded fuel configuration. The scale model tests are not applicable to the Connecticut Yankee MPC (CY-MPC) canistered fuel or GTCC waste configurations since these configurations have a higher contents weight (67,195 pounds) than the scale model test weight (56,000 pounds). The CY-MPC configurations must be transported using the balsa wood impact limiter design (balsa wood impact limiter[s]) shown in Drawings 423-257 and 423-258.

#### 2.10.6.2 Purpose

The purpose of the Scale Model Test Program was to provide confirmatory support for the structural design analyses for the NAC-STC. The test program verified the structural adequacy of the NAC-STC cask packaging in: (1) the performance of its containment function, (2) the performance of the impact limiters, (3) reacting dynamic impact loadings, and (4) resisting puncture by a pin.

#### 2.10.6.3 Discussion

Scale model testing is an accurate means of confirming a proposed packaging design. The packaging comprises the fuel basket, cask body, closure lids, and the redwood impact limiters. The method of performing scale model testing for nonlinear behavior is well accepted. For this application quarter-scale and eighth-scale models were employed. In either case, when the dimensions are scaled, the weight will be adjusted by the (scale)<sup>3</sup> and the material properties and drop heights will remain the same as for the full-scale cask. This permits the material employed in the licensed full-scale cask to be used in the scale model testing.

Two types of tests are used in this program, static and dynamic. The tests to confirm the impact limiter design were a combination of eighth-scale model quasi-static compression tests and a quarter-scale model 30-foot drop tests. The packaging design was confirmed by performing 30-foot drop tests and one-meter pin puncture tests using a quarter-scale model that included the fuel basket, fuel assemblies, cask body, lids and impact limiters.

In the overall testing program, the testing of the impact limiter design precedes the quarter-scale testing of the entire package. The impact limiters are the critical component in limiting the impact loads imposed on the cask. Scale model impact limiters were tested as separate components before testing the scale model package assembly. Therefore, the description of the eighth-scale model impact limiter compression tests is presented first, followed by the description of the quarter-scale model drop tests, along with the development of the design changes brought about by the drop tests.

##### 2.10.6.3.1 Scale Model Redwood Impact Limiter Compression Tests

The function of the impact limiter is to limit the maximum acceleration experienced by the cask, regardless of the orientation of the cask. This is accomplished by using an energy absorbing



crushable material which exhibits a minimum degree of rebound once the cask has come to rest. In the NAC-STC redwood impact limiter design, redwood and balsa wood are used as the energy absorbing materials. Measurement of the acceleration resulting from the crushing of the redwood/balsa wood can be accomplished by two means:

- 1) use of accelerometers to record the accelerations in a dynamic drop test, or
- 2) measuring the force to crush the impact limiter in the same orientation as the cask would impact the unyielding surface.

In evaluating the impact limiter to determine the deceleration to be experienced by the cask, the latter method is preferred because although the acceleration time histories record the maximum acceleration experienced by the cask as a result of the impact limiter crushing, significant uncertainties may be introduced. The acceleration records may contain high frequency signals which can come from a number of sources: the cable transmitting the accelerometer output to storage, rattling of the model fuel assemblies, or high frequency shell modes. None of these relate to the performance of the impact limiter itself. The static test, in principle, is easier to reproduce and the data acquisition is simpler and is not affected by other transient events during the test. Static testing produces a number of useful results: the acceleration, which is the ratio of the crush force to the model mass; the absorbed energy, which is the area under the force-deformation curve; the crush strain; and the behavior of the impact limiter during crushing.

Static compression tests were performed to simulate an end impact, a corner impact, and a side impact using eighth-scale model impact limiters. The eighth-scale models used redwood/balsa wood as the energy absorbing materials, just as in the full-scale design. The impact limiter shells used in the eighth-scale model tests consisted of 0.031-inch thick stainless steel. The full-scale impact limiter design uses 0.25-inch thick stainless steel shells. Drawings of the eighth-scale model impact limiter are presented in Section 2.10.6.7.

The design of the NAC-STC redwood impact limiter was revised during the quarter-scale drop tests program. The final impact limiter design constrains the redwood during the side and shallow angle oblique drop tests. The eighth-scale model impact limiters represented the redesigned configuration.

The eighth-scale model redwood impact limiter compression tests demonstrated that:

- 1) The NAC-STC redwood impact limiter, as designed, does not generate deceleration loads larger than those used in the design analyses, and
- 2) The crush stroke does not exceed the acceptance criteria (the cask body does not come into contact with the impact plane).

#### 2.10.6.3.2 Quarter-Scale Model Drop Tests

The objective of the quarter-scale model drop tests was to confirm the design of the NAC-STC packaging. An important feature of the quarter-scale model is its accuracy in reflecting containment and structural features of the full-scale design. The quarter-scale model packaging was an exact replica of the full-scale design with two exceptions: (1) o-rings in the inner and outer lids were not scaled; and (2) the neutron shield was not modeled, but the weight of the neutron shield was modeled by steel blocks welded to the outer shell. All aspects of the model can be used to reflect the strains, accelerations, and impact limiter crush strokes of the full-scale design. With respect to containment, the model represents the geometrical arrangement and materials used in the full scale design. However, the o-ring dimensions and the leak rate cannot be scaled, which means that the pressure measurements can only be used to indicate the condition of the seals and the adjacent seating surfaces.

The drawings of the detailed quarter-scale model components of the body of the NAC-STC, which were fabricated for use in this test program, are presented in Section 2.10.6.6. The details of the quarter-scale model are described in Section 2.10.6.5.1 (see Figures 2.10.6-1 thru 2.10.6-3).

The test plan called for a series of tests to be conducted at the Winfrith Technology Centre drop test facility, which is located in the United Kingdom. These tests would confirm the NAC-STC design for the nine-meter (30-foot) drop condition and the one-meter (40-inch) drop pin puncture condition. The tests included:

- 1) Nine-meter (30-foot) top end drop
- 2) Nine-meter (30-foot) top corner drop (24 degrees from the vertical)
- 3) Nine-meter (30-foot) side drop
- 4) Nine-meter (30-foot) bottom end oblique drop (75 degrees from the vertical) to maximize the slapdown effect on the top end)

- 5) One-meter (40-inch) pin puncture drop at the cask axial mid-point
- 6) One-meter (40-inch) pin puncture at the center of the outer lid

The test plan included performing a pretest metrology inspection and a post-test metrology inspection to confirm the adequacy of the design. The initial scale-model design used impact limiters with aluminum shells.

For test number 1, the nine-meter (30-foot) top end drop, the aluminum impact limiter shells posed no problems and the cask was shown to meet the acceptance criteria described in Section 2.10.6.5.2 (see Figure 2.10.6-4). The end drop test is not reperformed using scale-model impact limiters with stainless steel shells because the model cask body penetrates into the model impact limiter for the end drop orientation and the effect of the impact limiter shell on this event is negligible. The cask remained upright and no damage was indicated to have occurred to the cask or its components.

For test number 2, the nine-meter (30-foot) top corner drop, it was observed that the accelerations were appropriate, but the limiters did not remain attached to the cask. Testing proceeded to test number 3, which was the nine-meter (30-foot) side drop. The results of test number 3 clearly indicated the inadequacy of the aluminum shell welds to maintain the integrity of the impact limiter shell. It was observed in the high speed films that the redwood was ejected from the limiter at a rate commensurate with the impact speed. As the side drop progressed, the steel blocks representing the neutron shield weight impacted the surface and were displaced into the outer shell of the cask body (see Figure 2.10.6-5). As a result, the inner shell was compressed against the fuel basket. Additionally, the top forging was slightly distorted and the internal pressure was released, even though the lids remained firmly attached to the cask body.

The cask body and basket were submitted to the metrology laboratory for inspection and repair. Hydraulic rams were employed to remove the indentations in the inner shell in conjunction with a machining operation to bring the model back to specifications (see Figures 2.10.6-6 and 2.10.6-7). The first three tests are identified as Test numbers 1, 2 and 3 of Phase 1. While the

indentations due to the steel blocks were on the order of 0.06 to 0.13 inch deep, the maximum strain obtained from the gauges was 0.0018 inch/inch, which would not significantly strain-harden the stainless steel.

The nine-meter (30-foot) side drop (Test No. 3 of Phase 1) demonstrated the integrity of the basket design. Decelerations of about 1200 g were imposed on the basket disks. Outside of the local deformation due to the steel blocks, the basket support disk number 6, which was located opposite the impacted block, was not deformed (see Figure 2.10.6-8). The center basket disk showed no damage. This represents a load factor of 5 over the basket design. Moreover, no out-of-plane or in-plane buckling was observed.

Once the metrology inspection had been completed, and the repairs were made to the model cask body, pin puncture tests were conducted. Since the pin puncture tests were bracketed by before and after metrology inspections, it was determined that the pin puncture tests would be identified as Phase 2 tests. During the performance of these tests, however, the 24-inch long pin deformed excessively, to the extent that maximum damage was not inflicted on the cask body or the outer lid. Therefore, it was determined that the pin puncture tests would be reperformed using an 8-inch tall pin, as specified by regulatory requirements.

Prior to resuming testing, the impact limiter aluminum shell design was replaced with a stainless steel design. This initiated Phase 3 tests, which were planned to include a side drop, an oblique end drop, a top corner drop and two pin puncture tests. Thus, the Phase 3 tests are identified as:

- 1) Test No. 1 of Phase 3: nine-meter (30-foot) side drop
- 2) Test No. 2 of Phase 3: nine-meter (30-foot) 75° oblique bottom end drop
- 3) Test No. 3 of Phase 3: nine-meter (30-foot) top corner drop (24°)
- 4) Test No. 4 of Phase 3: nine-meter (30-foot) 75° oblique top end drop (added during the test sequence)

- 5) Test No. 5 of Phase 3 : one-meter (40-inch) drop cask mid-point pin puncture
- 6) Test No. 6 of Phase 3 : one-meter (40-inch) drop outer lid center pin puncture

The results of the nine-meter (30-foot) top corner drop indicated that the NAC-STC cask model did maintain pressure, and no damage occurred to the fuel basket or the cask body.

For the nine-meter (30-foot) side and oblique drops, the tests indicated a weakness in the impact limiter design. Even with the improved stainless steel shell to contain the redwood, it was observed that the redwood in the side impact region that overlaps the side of the cask was reorienting itself during the crushing action for the side drop impact and the oblique drop slapdown impact. The "overlap" region is that segment of redwood which brings the cask to rest for a side drop impact or an oblique drop slapdown impact. As a result, the redwood effective crush strength was lower than the design values, and the crush stroke was greater than calculated. One of the elements of the acceptance criteria is to ensure that the neutron shield does not come into contact with the impact surface. The full-scale stroke extrapolated from these tests would permit the neutron shield to come into contact with the impact plane. The design analyses do not take into account any impact loading on the neutron shield, so contact with the impact surface is not acceptable. However, neither the top corner drop test, nor the pin puncture drop tests, are affected by the redwood in the overlap region, so those tests are valid. The pin puncture tests at the cask mid-point and at the center of the outer lid were performed with an 8-inch tall puncture pin per regulatory requirements, but without impact limiters on the package model. Additional weight was added in the model cask cavity to obtain the correct scaled mass of the package model. Inspection of the model and the puncture pin after each test revealed: slight deformation of the puncture pin; the outer shell incurred significant local deformation, but was not punctured; essentially no damage occurred to the outer lid; and only a very slight indentation occurred on the inside diameter of the inner shell at its axial midpoint.

After reviewing the unsatisfactory performance of the upper impact limiter in Test Nos. 1 and 2 of Phase 3, Test No. 4, a nine-meter (30-foot), 75° top oblique drop, was added to the test plan to assess the performance of the lower impact limiter (without trunnion cutouts) for a slapdown impact. No significant difference in behavior or crush characteristics was noted, so the trunnion cutouts are negligible.

At the conclusion of the Phase 3 tests, the satisfactory testing results were summarized as follows:

- 1) Test No. 1 of Phase 1 satisfactorily verified the packaging design for the nine-meter (30-foot) end drop, since the impact limiter shell material has no significant effect on the end drop decelerations.
- 2) Test No. 3 of Phase 3 satisfactorily verified the packaging design for the nine-meter (30-foot) top corner drop (see Figure 2.10.6-9).
- 3) Test No. 5 and Test No. 6 of Phase 3 satisfactorily verified the packaging design for the pin puncture events. The scaled eight-inch long puncture pin deformed slightly for both orientations of the cask. The degree of deformation was not significant (see Figures 2.10.6-10 and 2.10.6-11) and the pin length satisfied regulatory requirements, so these tests are valid.

A design revision of the NAC-STC impact limiters was developed to better constrain the redwood. Quarter-scale sections of the impact limiter, both with and without the modifications, were tested by quasi-static compression. It was observed that the modification was sufficient to correct previous deficiencies, and that the modification did not significantly affect the crushing of the impact limiter for an end impact or a corner impact.

Prior to initiating the next phase of testing, the inner shell of the model cask body was repaired to remove the pin puncture indentation. This would ensure that the cask model was representative of the full-scale cask body.

Phase 4 required that only the nine-meter (30-foot) bottom oblique and side drop tests be conducted. The nine-meter (30-foot) bottom oblique (top slapdown) drop test was conducted first, since it was expected that the slapdown effect would be maximum for the top impact limiter due to the cutout regions for the trunnions. The cutouts for the trunnions actually reduced, only slightly, the amount of redwood available for crushing.

Test Nos. 1 and 2 of Phase 4 demonstrated that the modified impact limiter design prevents the neutron shield from coming into contact with the impact surface. By defining the margin of safety to be based on the crush stroke and the distance of the crush plane to the edge of the neutron shield, the modified design of the NAC-STC impact limiter allowed a margin of safety of +0.33 for the most severe conditions. Additionally, the measured decelerations indicate that the maximum values are less than those employed for the design analyses of the NAC-STC.

For each of the tests, the pressure and temperature were measured and recorded before and after the test. In all valid tests, closure lid seal integrity was maintained. For the outer lid pin puncture (Test No. 6 of Phase 3), the cavity pressure valve was cracked, but after replacement of the valve, and prior to lid removal, the cask satisfactorily maintained pressure.

In Test Nos. 1 and 2 of Phase 4, diametral measurements indicated that no permanent deformation had been imposed on the cask body. While some of the strain gauges indicated some type of permanent deformation, the level was negligible, when it was compared to the industry accepted value of 0.2 percent strain for material yielding.

It is concluded that the adequacy of the full-scale NAC-STC packaging design is confirmed by the quarter-scale model drop tests.

#### 2.10.6.4 Eighth-Scale Redwood Impact Limiter Compression Tests

A series of quasi-static compression tests were performed with scale model redwood/balsa wood impact limiters to demonstrate that:

1. Force-Deformation curves are as predicted by the RBCUBED computer program.
2. Energy storage (rebound) in the crushed redwood/balsa wood impact limiters is negligible.
3. The impact limiter and cask body geometry effectively causes the impact limiter to stay in position on the cask.

#### 2.10.6.4.1 Force-Deformation Curves for the End, Corner, and Side Impact Orientations

Eighth-scale model impact limiter compression tests were conducted for the end, corner, and side orientations of the cask. These tests were performed using the modified NAC-STC impact limiter design. As indicated previously, the modification has a negligible effect on the crushing of the impact limiter in the end impact and corner impact orientations.

Eighth-scale tests were performed with both aluminum alloy and stainless steel impact limiter shells. The aluminum alloy shells split along the weld seams and came apart as compressive load was applied. The Type 304 stainless steel shells remained ductile and did not split along the weld seams. A full penetration weld was necessary to insure adequate joining of the pieces of the stainless steel shells. The stainless steel shells have a higher weight than the aluminum shells, so initial testing of the quarter-scale model in the nine-meter (30-foot) drops was performed with aluminum alloy impact limiter shells in an effort to reduce the overall cask weight. The weld failures experienced with the aluminum alloy impact limiter shells in the drop tests showed that stainless steel impact limiter shells were, in fact, required. The stainless steel impact limiter shells tested in the eighth-scale quasi-static testing were adopted for the final impact limiter shell design.

Eighth-scale model lower impact limiters were used in the force-deformation compression tests for the NAC-STC impact limiter design. This is primarily because the trunnion cutouts in an eighth-scale model upper impact limiter are extremely difficult to fabricate using the scaled shell thickness. Also, previous analyses, scale model compression tests, and scale model drop tests have all demonstrated that the trunnion cutout regions of the upper impact limiter do not significantly affect the energy absorption capability of the impact limiter.



The eighth-scale model impact limiters were crushed quasi-statically in a tensile test machine which can also apply compressive loads. The tensile test machine capacity limited the maximum size of the test impact limiter to one-eighth scale.

The eighth-scale model impact limiters were not attached mechanically to the cask-shaped test fixtures. Duct tape was used to hold the model impact limiter in place while the compressive test load was applied. The tape relaxed as successively higher loads were applied, demonstrating that the impact limiter geometry produces net crush forces which press the impact limiter against the cask body, regardless of the impact angle.

The force-deformation curve is measured by compressing the model impact limiter and recording the deflections and loads applied to the limiter. The energy storage, or rebound, of the model impact limiter is shown by the load-deformation curve as the test machine is unloaded slowly. The model impact limiter presses against the test machine heads and applies a load proportional to the elastically stored energy. This extra energy component can be restored to a cask in a multiple-impact, oblique drop "slapdown" scenario. The eighth-scale model impact limiter compression tests showed that a maximum of 8.2 percent of the absorbed energy may be stored during crushing and later released.

While each model impact limiter tested was being compressed, two calibrated linear variable differential transformers (LVDT) mechanically attached to test fixtures provided data to an X - Y recorder, which plotted crush force versus deformation. Deformation of the model impact limiter proceeded well into the compression lock-up range of the redwood. As the compression load on the model impact limiter was decreased after the test was stopped, force and deflection continued to be monitored, revealing the amount of elastically stored energy. Based on the results of the quasi-static tests, the force-deformation curve and the energy absorption capacity (area under the curve) of each model impact limiter is presented in Figures 2.10.6-12, 2.10.6-13, and 2.10.6-14. The static force for each data point is multiplied by 1.06, a static to dynamic scaling factor, enabling a direct comparison with the RBCUBED computed values. The dynamic scaling factor is determined from Figure 9 of NUREG/CR-0322, which is based on Sandia National Laboratory

tests. Figures 2.10.6-12, 2.10.6-13 and 2.10.6-14 show for comparison the dynamically scaled forces and the RBCUBED computed values. These figures also show the maximum compression forces that occur for each of the impact orientations.

For the end impact case, the impact limiter compression forces from the quasi-static test are higher than those calculated by the RBCUBED analyses using the maximum tolerance cold temperature crush strength and the minimum tolerance hot temperature crush strength properties of redwood. This difference in compression forces can be attributed to the additional forces on the cask due to the redwood material's resistance to shearing along the periphery of the "backed" area of the cask. The calculated equivalent deceleration force of the full-scale cask, based on the quasi-static eighth-scale model impact limiter test is 54.8 g for the end impact case. This force is greater than the 44.6 g end drop deceleration force obtained from the RBCUBED analysis using the maximum tolerance cold temperature crush strength of redwood, but less than the 56.1 g deceleration force obtained from the RBCUBED analysis using the minimum tolerance hot temperature crush strength of redwood. The higher deceleration force obtained using the minimum tolerance hot temperature crush strength of redwood is a result of the larger deformation and the partial lock-up of the redwood that occurs before the cask is stopped. Based on the area under the dynamically scaled force-deformation curve presented in Figure 2.10.6-12 for the end impact case, all of the energy of a one-eighth scale model of the NAC-STC for a 30-foot drop is absorbed when the impact limiter deformation reaches 1.58 inches (1.63 inches from the static force-deformation curve), which extrapolates to a 12.6-inch deformation for the full-scale NAC-STC impact limiter, or 42 percent of the depth of the impact limiter. The dynamic force-deformation curve for the eighth-scale model impact limiter for the end impact case is extrapolated to full-scale and presented in Figures 2.10.7-5 and 2.10.7-8 for comparison with the RBCUBED calculated force-deformation curves for the NAC-STC impact limiters.

For the corner impact case, the calculated equivalent deceleration force of the full-scale cask, based on the quasi-static eighth-scale model impact limiter test, is 32.6 g. This compares with the 44.0 g deceleration force calculated by the RBCUBED analysis using the maximum tolerance cold temperature crush strength of redwood, and with the 49.3 g deceleration force calculated using the minimum tolerance hot temperature crush strength of redwood. Based on the area under the dynamically-scaled force-deformation curve presented in Figure 2.10.6-13 for the corner impact case, all of the energy of a one-eighth scale model of the NAC-STC for a 30-foot drop is absorbed when the impact limiter deformation reaches 3.22 inches (3.30 inches for the static force-deformation curve), which extrapolates to a 25.76-inch deformation for the full-scale NAC-STC impact limiter, or 70 percent of the depth of the impact limiter. The dynamic force-deformation curve for the eighth-scale model impact limiter for the corner impact case is extrapolated to full-scale and presented in Figures 2.10.7-6 and 2.10.7-9 for comparison with the RBCUBED calculated force-deformation curves for the NAC-STC impact limiters.

For the side impact case, the calculated equivalent deceleration force for the full-scale cask, based on the quasi-static eighth-scale model impact limiter test, is 45.6 g. This force compares with the 51.7 g deceleration force from the RBCUBED analysis using the maximum tolerance cold temperature crush strength of redwood and with the 51.3 g deceleration force using the minimum tolerance hot temperature crush strength of redwood.

Based on the area under the dynamically-scaled force-deformation curve presented in Figure 2.10.6-14 for the side impact case, all of the energy of a one-eighth scale model of the NAC-STC for a 30-foot drop is absorbed when the impact limiter deformation reaches 1.64 inches (1.70 inches for the static force-deformation curve), which extrapolates to a 13.12-inch deformation for the full-scale NAC-STC impact limiter, or 71 percent of the depth of the impact limiter. The dynamic force-deformation curve for the eighth-scale model impact limiter for the side impact case is extrapolated to full-scale and presented in Figures 2.10.7-8 and 2.10.7-11 for comparison with the RBCUBED calculated force-deformation curves for the NAC-STC impact limiters.

Since the force-deformation curves obtained from the quasi-static compression tests are enveloped and reasonably approximated by those force-deformation curves calculated by the RBCUBED program, the NAC-STC transport impact limiters are designed based on RBCUBED analysis runs.

#### 2.10.6.4.2 Conclusion

The results of the eighth-scale model NAC-STC impact limiter quasi-static compression tests clearly demonstrate that the NAC-STC impact limiter design provides the energy absorption capacity to decelerate the cask to a stop for a 30-foot drop accident for the various impact orientations, while maintaining maximum compression forces that are less than the cask design values.

Table 2.10.6-1 shows: (1) the maximum side impact deceleration values determined by RBCUBED using the redwood cold crush strength plus 10 percent, and the hot crush strength minus 10 percent; (2) the deceleration value extrapolated from the eighth-scale quasi-static compression test results as documented above; (3) the actual deceleration value measured during the final quarter-scale model side drop test; and (4) the value used for design calculations. The maximum calculated side impact deceleration determined for the modified impact limiter is within 12 percent of the average value predicted by RBCUBED, and is within 11 percent of the deceleration value measured in the quarter-scale drop test. Therefore, it is concluded that the methodology used above adequately characterizes the structural behavior of the final design of the impact limiter for side impacts, and that the value of maximum side impact deceleration used in the design calculations (55g) is conservative.

#### 2.10.6.5 Quarter-Scale Model Drop Tests

##### 2.10.6.5.1 Model Description

The model of the body of the NAC-STC cask, which was used in the Drop Test Program, was a quarter-scale duplication of the full-scale cask in all aspects, except as described in subsequent paragraphs of this section. The model was fabricated of Type 304 stainless steel inner and outer shells, top and bottom forgings, and inner closure lid; the port covers and the outer closure lid

were Type 17-4PH stainless steel; the gamma shield was Chemical Lead per ASTM B29. The impact limiters were fabricated of redwood and balsa wood. Initially they were enclosed in 6061-T6 aluminum alloy shells, which have subsequently been changed to Type 304 stainless steel. Additionally, the attachment design was changed to include sixteen retaining rods and to allow more flexibility of these retaining rods during an impact loading, which eliminated direct shear failure.

The NAC-STC quarter-scale model lead gamma shield forms an annulus 0.925 inch thick and 40.25 inches long. The lead was enclosed between the 0.375-inch thick, 17.75-inch inside diameter inner shell, and the 0.665-inch thick, 21.68-inch outside diameter outer shell. The ends of the inner shell include 3.00-inch long by 0.505-inch thick transition regions. The bottom forging of the quarter-scale model cask is 1.55 inches thick. The bottom also includes a 0.50-inch thick, 19.77-inch diameter NS-4-FR neutron shielding disk enclosed by a 1.36-inch thick bottom plate. The upper end forging is 4.59 inches thick with an interior that is machined to accept the two closure lids. The main body of the inner closure lid is 2.25 inches thick and 19.750 inches in diameter. A 0.75-inch thick, 1.385-inch wide integral outer rim on the top of the inner lid encloses a 0.50-inch thick layer of NS-4-FR neutron shielding material and a 0.25-inch thick, Type 304 stainless steel coverplate. A bypass port was included in the model inner lid to ensure that the cavity pressure reached the outer lid o-rings for all of the quarter-scale model tests. This bypass port does not exist in the full-scale inner lid design. The model outer lid is 1.313 inches thick and 20.380 inches in diameter. There was a 12.50-inch diameter, 0.015-inch deep recess in the bottom surface of the outer lid to reduce the area that must be polished as a sealing surface. The 42 bolts for the model inner lid are 3/8-24 UNF x 2-1/2 inches long socket head cap screws; the 36 bolts for the model outer lid are 1/4-28 UNF x 1-5/8 inches long socket head cap screws. These bolts were selected to provide a tensile stress area equal to  $(1/4)^2$  times that of the full-scale closure bolts. Since the impact load factor on the model is four times that applied to the full-scale cask, the proper scaled bolt stress results. The port cover is a 0.72-inch diameter piston-type cylinder with an integral 0.25-inch thick, 1.130-inch diameter coverplate. The model impact limiters are quarter-scale replicas of the full-scale impact limiters with 22.3 pound-per-cubic-foot (average) redwood and 7 to 10 pound-per-cubic-foot (average) balsa wood energy-absorption materials. These model impact limiters produce the properly scaled (4 x full-scale) impact loads on the model cask. The wood material section pie-shapes, joints, and bonds of the scale model impact limiters duplicate those of the full-scale impact limiters. The redwood and balsa wood

materials of the model impact limiters used in the Phase 1 testing were enclosed in 0.12-inch thick, 6061-T6 aluminum alloy shells. For the Phase 3 and Phase 4 testing, the impact limiter shells were changed to 0.062-inch thick Type 304 stainless steel. For the Phase 4 tests, the model impact limiters included modifications to correct deficiencies identified earlier in the test program. Impact limiters were not used for the Phase 2 puncture tests.

The model impact limiters had an outside diameter of 31.0 inches and an overall length of 11.2 inches. The inner cup has an inside diameter of 21.9 inches and a depth of 3.0 inches. The model upper impact limiter has four 2.9-inches wide, 1.6-inch long, 0.9-inch deep cutouts for the lifting trunnions. The model impact limiters are attached to the end surfaces of the cask model with threaded retaining rods and nuts through the ends of the limiters. The model fuel load consisted of 26 steel bars simulating the scaled size and weight of the tubes and fuel assemblies. These "dummy" fuel assemblies fit within an exact quarter-scale model of the fuel basket.

The inner shell, end forging, and the inner lid establish a model cask cavity that is 41.25 inches in length and 17.75 inches in diameter. The weight of the quarter-scale model cask with impact limiters and cavity load is 3884 pounds (approximately 0.5 percent lighter than the scaled design weight).

Three differences do exist between the quarter-scale model cask body and the full-scale cask body: (1) the model does not include the neutron shield; the weight of the neutron shield is simulated on the model by segmented steel bars welded on the exterior surface of the outer shell; the use of segmented weights to simulate the neutron shield prevents the weights from contributing to the strength of the cask, and neglects the stiffening/strengthening effect of the neutron shield shell on the cask body; (2) the inner and outer shells of the model are entirely Type 304 stainless steel, with a yield strength of  $S_y = 30$  ksi and an ultimate strength of  $S_u = 75$  ksi, while the full-scale cask contains Type XM-19 stainless steel inner shell rings at each end of the Type 304 stainless steel inner shell; for Type XM-19 stainless steel,  $S_y = 55$  ksi and  $S_u = 100$  ksi; and (3) the model includes a recessed outer lid that is bolted to the inner lid with the upper impact limiter bolted to the outer lid. The final design of the NAC-STC includes separate inner and outer lids that each bolt directly to the top forging of the cask body. The inner lid and its outer o-ring are defined to be the primary containment boundary. The upper impact limiter attachment to the outer lid remains unchanged.

In the redesigned closure system: (1) inner lid - remains essentially identical to the quarter-scale model, except that it no longer has bolt holes for the outer lid bolts; (2) inner lid bolts - the size and number are unchanged, but the material, SB-637 N07718 ( $S_u = 185$  ksi and  $S_y = 150$  ksi), is considerably stronger than that in the quarter-scale model ( $S_u = 130$  ksi and  $S_y = 85$  ksi); (3) outer lid - material and effective thickness are unchanged, while the diameter is increased and includes a flange with bolt holes; (4) outer lid bolts - the material, size, and number remain unchanged, but the diameter of the bolt circle is increased to accommodate bolting through the flange directly to the top forging; (5) top forging - 2.56 inches shorter, but the thickness has increased from 2.47 inches to 3.79 inches; and (6) inner and outer lid bolt torques - remain unchanged, so the bolt torques specified for the quarter-scale model inner and outer lid bolts are appropriate. Since the redesigned outer lid protects the inner lid (primary containment boundary) and the ring stiffness of the top forging is significantly increased, while the basic configuration of the closure system is unchanged, the quarter-scale model conservatively represents the structural characteristics of the closure region of the full-scale cask.

Based on the foregoing discussion of the significant differences between the quarter-scale model cask body and the full-scale cask body, it is concluded that the NAC-STC quarter-scale model is a conservative, representative replica of the full-scale model.

#### 2.10.6.5.2 Acceptance Criteria for Model Performance

The acceptance criteria for the packaging components is established for the cask body and the impact limiters.

The acceptance criteria for the cask body performance is that cavity pressure be maintained and that the fuel remain in a subcritical configuration. For the cask body this requires that:

- 1) Permanent deformation must not be observed in the metrology results for the lids and their mating sealing surfaces.

- 2) Strains in the cask body must not exceed the 0.2 percent offset for determining material yield strength.
- 3) The pressure test must indicate that there was no loss of pressure during the test.
- 4) The fuel basket must not exhibit permanent deformation after the tests.
- 5) The inner and outer lid bolts must not exhibit permanent deformation after the tests.

The function of the impact limiter is to limit the deceleration of the cask body and components during a cask drop event. Then, the impact limiter acceptance criteria requires that:

- 1) The crush stroke be limited to prevent an impact of the cask body on the impact surface.
- 2) The accelerations be limited to those used in the design analyses (also verified by the static compression tests).
- 3) The impact limiters remain attached to the cask body and in position after the impact event.

#### 2.10.6.5.3 Equipment and Instrumentation for the Drop Tests

All drop tests were performed at the Winfrith Technology Centre located in the United Kingdom. The facility, which is an IAEA approved drop test facility, had the capacity to lift the model package to a drop height of 9 meters and had an appropriate unyielding impact surface. The target consisted of a 70 metric ton concrete mass and a 10 foot by 12.5 foot rectangular, 75 mm thick steel plate at the impact surface. Lifting and dropping the model was achieved through a single point suspension system (attaching the cask to the crane hook at a single point) in conjunction with an electromagnetic release. This release mechanism allowed the free fall of the package to be initiated in an unimpeded fashion with minimum perturbation to the angular position of the model.



To assess the model performance against the acceptance criteria, a set of basic data was required to be collected throughout each test. This consisted of:

- 1) Metrology data - to assess the permanent deformation of the cask body, including the closure lids and the seating area for them. Also included is fuel basket deformation data to determine the response of the basket during the drop.
- 2) Pressure and temperature data - to assess the retention of pressure by the cask primary containment boundary. The temperature data is needed to correlate pressure changes with an increase or decrease in the temperature while the test is conducted.
- 3) Strain data - to determine the maximum amount of strain that occurs in the cask body.
- 4) Acceleration data - to determine the maximum accelerations to which the cask was subjected.
- 5) Impact limiter deformation data - to evaluate the behavior of the impact limiters, the crush stroke for each orientation, and the condition of the limiter attachment to the cask body after each test.
- 6) High speed photography - to review and assess the actual angle of impact and the behavior of the cask body and impact limiters during the impact.

A wide range of additional equipment and instrumentation was employed to determine the measurements or capture the test data during the impact event.

1) Cask Body and Fuel Basket Metrology Data

Measurements before the tests and after the test series were performed in a metrology lab, which could determine the measurements within a tolerance of  $\pm 0.001$  inch for all dimensions except the inner diameters in the lower portion of the model cask cavity. Comparison of these sets of measurements permits determination of the presence of any permanent deformation of the diameter of the cask, seating area for the lids, or in the lids themselves.

Certain key dimensions for the fuel basket center support disk (Disk No. 12) were also measured using a metrology bench which was capable of determining the position of a point on a support disk to within 0.001 inch and the out-of-plane position of the disk to within 0.001 inch. After each test, the basket was field inspected to assess any change in the surfaces of the basket support disks.

Definitions of the measurement locations for the cask body and the support disk measurements made by the metrology laboratory are shown in Figures 2.10.6-15 and 2.10.6-16.

2) Pressure and Temperature Data

Through a pressure port located near the cask midpoint (for model only; not in full-scale design), the cask cavity was pressurized to 30 (+2/-0) psi. The pressure in the cask cavity was measured before and after each test. To assist in correlating the pressure change with a change in the cask temperature, the temperature of the cask body was also obtained by Chromel/Constantan thermocouples attached to the cask exterior near the pressure port used to pressurize the cavity.

### 3) Strain Data

Strain time-histories were recorded for each of the 30-foot drops for the locations shown in Figure 2.10.6-17. Ninety-degree tee-rosettes were mounted on the cask body for all of the drop tests. One gauge of each tee-rosette was positioned in the axial direction and another in the circumferential direction. This allowed the axial and the hoop stresses to be monitored. Later in the testing program, the 90-degree tee-rosettes were exchanged at two of the locations for rosettes with three gauges at 45-degree orientations, which allowed the shear stresses to be determined at the surface. All gauges had at least a 50 kHz response time to ensure that the transient strains could be accurately recorded.

Real time recording was accomplished by a system of strain amplifiers, signal conditioners and a magnetic recording unit to store the data. Strain gauge data was only taken for the 30-foot drop tests. It was concluded that the strain gauge data was not needed for the pin puncture drops.

The strains are converted to axial and hoop stresses by the following expressions:

$$\sigma_a = \frac{E}{1 - \nu^2} (\epsilon_a + \nu \epsilon_h) \text{ (axial stress, psi)}$$

$$\sigma_h = \frac{E}{1 - \nu^2} (\epsilon_h + \nu \epsilon_a) \text{ (hoop stress, psi)}$$

where

$E$  = Modulus of elasticity = 28.3E+6 psi

$\nu$  = 0.3

$\epsilon_a$  = Axial strain

$\epsilon_h$  = Hoop strain

The maximum stress is computed by taking the strain components at the same time point from the strain gauge traces. The time points from each trace (one for the hoop strain gauge and one for the axial strain gauge) are selected to determine a conservative value for the stress.

#### 4) Acceleration Data

Two single-axis accelerometers were mounted on the cask body for each of the 30-foot drop tests. The location and orientation for each test is shown in Figure 2.10.6-18. The directions were altered for each individual test to ensure that the vertical deceleration was measured.

Each accelerometer could measure accelerations up to 20,000 g with an accuracy of 1 percent per 2,000 g. For this application, in which an acceleration level of 300 g was expected, the accuracy was  $\pm 0.5$  g. The frequency response of the accelerometer was from 2 Hz to 15,000 Hz, which would envelope the frequency of the system.

All accelerometer data was conditioned and stored on magnetic media for later processing, which included filtering and integrating to obtain the impact velocities. Acceleration data was only taken for the 30-foot drop tests. It was concluded that the accelerometer data was not needed for the pin puncture drop tests.

#### 5) Limiter Deformation Data

After each test, the limiters were inspected to determine the amount of deformation that had occurred and to determine the condition of the attachment rods and nuts. Photographs of the deformed limiters were taken to record the post-test condition of the limiters.

#### 6) High Speed Photography

Two high speed cameras were used to record the behavior of the quarter-scale model as it impacted the target surface. For the top end drop, both cameras

were operated at 500frames/sec and the cameras were positioned at 90 degrees apart (side and end views). For the final top corner drop, side drop, and oblique slapdown drop, one camera was positioned to capture the overall motion of the cask at 500 frames/sec and the other camera was set to obtain a close up view of the crushing of the impact limiter at 1000 frames/sec.

#### 2.10.6.5.4 Drop Test Sequence

This section describes the test procedures that were used each time the scale model cask was tested. Winfrith personnel were responsible for the model cask preparation; they performed all tasks related to instrumentation and the actual sequence leading up to the drop.

1. Cask Preparation (Winfrith Personnel)
  - A. Install the model fuel basket assembly and model fuel assemblies.
  - B. Install the model cask inner lid using a new metallic o-ring. The by-pass port plug in the model inner lid has been removed to ensure that the outer lid o-rings will be subjected to the cask cavity pressure.
  - C. Torque the 42 model inner lid bolts to 400 ( $\pm 10$ ) inch-pounds.
  - D. Install the model outer lid using new TFE o-rings. The TFE o-rings are inspected for defects prior to installation.
  - E. Torque the 36 model outer lid bolts to 80 ( $\pm 5$ ) inch-pounds.
  - F. Verify the model outer lid seals by pressurizing the model cask cavity to 30 (+2/-0) psig. Observe the cavity pressure over a 10 minute period to ensure leak tightness.

- G. Attach the model upper and lower impact limiters to the model cask.

Note: For pin puncture drop tests, the basket and fuel assemblies were replaced with equal weight material. Impact limiters were not installed for the pin puncture tests.

2. Performing the Drop Test (Winfrith Personnel)

- A. Check umbilical cord connection to data recorders.
- B. Ensure the safety of cask release assembly prior to lift and the correct angle of orientation of the cask.
- C. Final check to ascertain if all systems are ready for the drop.
- D. Turn on the recorders for the strain gauges and accelerometers.
- E. Initiate the countdown in preparation for the drop.
- F. Start high speed (500 or 1000 frames/second) photography and normal speed photography.
- G. When the countdown reaches zero, energize the cask release mechanism. When the cask release mechanism is energized, the assembly restraining the cask allows the cask to initiate its fall unimpeded.
- H. Record post-test condition of the model cask body and impact limiters and perform leak test.
- I. Continue test sequence as described in this Section.

#### 2.10.6.5.5 Detailed Test Results

Data obtained from the tests consists of both qualitative information with respect to observations about the cask body and the impact limiters, as well as quantitative data obtained by measurements.

For each of the 30-foot drop tests, the data to be presented for each test consists of:

- 1) Maximum calculated stress for the locations monitored (based on strain measurements), and its location
- 2) Maximum permanent strain for the locations monitored, and its location (and the strain time-histories for this location)
- 3) Maximum filtered accelerations (and the acceleration time-histories)
- 4) Impact limiter deformation and attachment hardware condition (and sketches showing the deformation)
- 5) Pressure in the cask cavity, measured before and after the test
- 6) Observations of the impact limiter and cask body behavior

For the pin puncture tests, the data to be presented for each test consists of the pressure measurements and the measurement of the localized deformation due to the pin impact.

Since the model was repaired after the side drop (Test No. 3 of Phase 1), there are four sets of metrology data.

- 1) Pretest measurements of the cask body and basket.

- 2) Post-test measurements after the side drop test using the redwood limiter with the aluminum shell (Test No. 3 of Phase 1) and prior to the repair of the cask body.
- 3) Pretest measurements prior to resuming the tests.
- 4) Post-test measurements after the completion of the Phase 4 drop tests.

Conclusions about the cask body for the top corner drop, side drop and the oblique drop slapdown tests can only be drawn from metrology data sets (3) and (4).

Metrology data sets (1) and (2) can only be used to evaluate the nature of the damage incurred because of the malfunction of the impact limiters. Conclusions about the top end drop can be drawn by considering the strain data and the observations of the basket obtained in the top end drop.

#### 2.10.6.5.6 Thirty-Foot Top End Drop Using Impact Limiters with Aluminum Shells - Test No. 1 of Phase 1

This was the first drop test to be performed of the four phases of tests using the quarter-scale cask model. The impact limiters used the aluminum shell design, which weighs less than the stainless steel shell design that was used in later tests. The cask model at the time of the top end drop was within 0.5 percent of the design weight of 3906 pounds ( $250,000/4^3$ ).

##### 2.10.6.5.6.1 Impact Limiter Deformation and Attachment Data

The impact limiters used in the top end drop had aluminum shells. Essentially all of the crushing occurred within the backed region of the impact limiter. A sketch of the final shape of the impact limiter is shown in Figure 2.10.6-19. Based on viewing the high speed film and the final position of the cask body, the deviation of the cask centerline from the vertical was minimal. The maximum crush for the end drop is summarized in Table 2.10.6-2. The crush deformation was 2.11 inches, corresponding to a crush strain of 23 percent.



#### 2.10.6.5.6.2 Strain Gauge Data

Strain gauge time-histories were obtained for each data channel. The traces shown in Figures 2.10.6-20 and 2.10.6-21 are the axial and hoop direction strains at Location 9. Location 9 corresponds to the instrumented location at which the maximum stress of 8.6 ksi occurs. The hoop strain component was found to be extremely small. All three gauge locations near the top showed similar behavior in the axial and the hoop direction. Some of the strain gauges showed a permanent set of 10 to 15 microstrains, which corresponds to a maximum permanent strain of 0.0015 percent. Since the normal stresses are so low, this offset is not attributed to any yielding of the material. Additionally, only one out of three axial gauges near the top end exhibited this result.

#### 2.10.6.5.6.3 Accelerometer Data

Two accelerometers were mounted 180 degrees apart at the top end of the cask model. The maximum acceleration obtained from a 1000 Hz filtering of the accelerometer trace was 247 g, which corresponds to a full-scale acceleration of 62 g. The accelerometer trace for the top end drop is shown in Figure 2.10.6-22. The cyclic peaks in the accelerometer trace are the first longitudinal vibrational mode of the cask shell.

The filter frequency was computed by considering the first longitudinal vibrational mode,  $f_1$ , of the model. This was determined by using the expression from Blevins for a lump mass attached to a cantilevered beam,

$$f_1 = \frac{\lambda}{(2)(n)(L)} \left( \frac{E}{\mu} \right)^{0.5}$$

$$B = \frac{(\mu)(A)(L)}{M}$$

where:

- $L$  = Effective length of shell =  $161/4 = 40.25$  inches
- $E$  = Modulus of elasticity =  $28.3 \times 10^6$  psi
- $\mu$  = Mass density =  $0.288/386.4 = .0007453$  lb/in<sup>3</sup>
- $M$  = Total mass =  $250,000/[(64)(386.4)] = 1.118$  lb/in<sup>3</sup>
- $A$  = Cross sectional area of shells =  $210.5$  in<sup>2</sup>

Substituting,

$$B = 5.648$$

and  $l$  must satisfy  $B \cot(\lambda) = (\lambda)$

$\lambda = 1.35$  satisfies this expression

Substituting for  $f_1$  leads to  $f_1 = 868$  Hz.

Using 1000 Hz for the cut off frequency for the filter is acceptable and is conservative.

#### 2.10.6.5.6.4 Pressure Measurements

The pressure measured after the test showed a slight increase, which would correspond to the small increase in the cask body temperature. Since the temperature data cannot be expanded to determine the temperature of the cavity gas, an accurate calculation of the corresponding increase in the pressure cannot be made. The pressure measurements indicate that there was no loss of pressure.

#### 2.10.6.5.6.5 Test Observations

After the top end drop test, the basket was removed from the cask body to inspect for deformations. In removing the fuel basket, it was observed that the basket was removed without any interference and that no deformation had occurred in the fuel basket or in the dummy fuel assemblies. This indicates the following:

- 1) Out of plane buckling due to the vertical deceleration loads did not occur.
- 2) Buckling of the inner shell due to lead slump did not occur.

As evidenced by the nearly uniform crush of the impact limiter and the data from the two axial accelerometers, the load on the lead was essentially uniform around the model circumference. Thus, yielding of the inner shell at one location on the circumference would have precipitated yielding of the larger shell around the entire circumference. There was no evidence of yielding of any model component: lead, basket, lids, or bolts.

#### **2.10.6.5.7     Thirty-Foot Side Drop Using Impact Limiters with Aluminum Shells - Test 3 of Phase 1**

The third test in the first phase of testing was the 30-foot side drop test, which used impact limiters with aluminum shells. In this test, it was demonstrated that aluminum welds are inadequate to maintain the integrity of the impact limiter. The impact limiter shells split open and did not constrain the redwood. Thus, neither the model's deceleration, nor the impact limiter's crush stroke, remained within acceptable limits. Consequently, the model cask body struck the impact surface, producing a large impact force.

The most significant benefit from this test was the clear demonstration of the strength of the fuel basket design.

##### **2.10.6.5.7.1     Impact Limiter Deformation and Attachment Data**

The high speed film showed that the welds along the edges of the limiters failed immediately upon impact, which allowed the four steel blocks (180 degree location in Figure 2.10.6-17) at the lower edge of the cask to strike the impact surface. The force to decelerate the cask model was concentrated at the four steel blocks. The energy was absorbed by the local deformation of the model cask body shells and the model fuel basket. Based on the high-speed film, the rebound of the cask body was small, indicating that essentially all of the energy was absorbed in the

initial impact. As a result of the localized loading on the cask body shells, the top forging, which serves as the seat for the lids, was deformed and the internal cavity pressure was not maintained. However, the lids remained firmly attached to the cask body during and after the impact. This test served to describe the behavior of the cask body in a guillotine-type impact without a neutron shield.

#### 2.10.6.5.7.2 Strain Gauge Data

Strain gauge data was recorded at nine locations. The permanent strains are listed in Table 2.10.6-3. Since both the hoop and axial directions indicate a permanent strain, an equivalent plastic strain ( $e_{eq}$ ) is computed for the directions recorded. The  $e_{eq}$  is based on the Von Mises and Prandtl-Ruess Flow Rule material representation for material yielding. The  $e_{eq}$  is used to assess the amount of work-hardening to which the material was subjected. The maximum value found was 1811 microstrains, or 0.18 percent, at the midpoint of the cask at the point nearest the impact plane. The strain gauges at locations 3 and 9 were approximately 0.25 inches from the edge of the blocks which were displaced into the outer shell. This implies that the strain gauges were able to reflect the maximum strains generated by the impact.

#### 2.10.6.5.7.3 Accelerometer Data

The maximum accelerations recorded were 996 g and 1190 g for accelerometers Nos. 1 and 2, respectively. The trace corresponding to the top end location is shown in Figure 2.10.6-23. The first six or seven milliseconds correspond to the crushing of the redwood, after which the large increase in the deceleration is due to the steel blocks striking the impact surface.

#### 2.10.6.5.7.4 Metrology Data

After this side drop test, the cask was inspected by the metrology laboratory to obtain measurements for the locations shown in Figure 2.10.6-15. The pretest data (prior to Test 1 of Phase 1) and the post test data (after Test 3 of Phase 1) are shown for selected diametral dimensions in Table 2.10.6-4 for the cask body. The

radial deflection was greatest at the lid end of the cask. The inner radius was decreased by 0.126 inches at the 0-180 diameter, which corresponds to the point of impact.

The impact also caused out-of-round deformation of the cask at the other measured locations by approximately 0.06 inch to 0.09 inch on a radius.

The inner and outer lids were inspected for out-of-plane deformation, and the measurement of the out-of-plane dimensions showed that no deformation had occurred during the Phase 1 tests.

The deformation of the model cask body required that the fuel basket be partially disassembled in the cask cavity in order to remove the basket after the side drop test. Support disks Nos. 6 and 12 were submitted to the metrology laboratory for measurements. Support disk No. 6 was the disk loaded by the steel blocks, and support disk No. 12 was the disk at the axial center of the basket. For support disk No. 12, the out-of-plane measurement was 0.001 inch, which is the sensitivity limit of the equipment. For support disk No. 6, a pretest metrology inspection had not been performed. However, the maximum variation in the Z direction (i.e., in the direction perpendicular to the plane of the disk) was 0.004 inch. Figure 2.10.6-8 shows the final shape of support disk No. 6. The impact of the steel blocks into the cask body and basket resulted in the lateral movement of the lower four fuel assembly positions by 0.19 inch. The impact also caused the bottom of support disk No. 6 to be deformed as seen in Figure 2.10.6-24. The pretest metrology data for support disk No. 12 and the post-test metrology data for support disk Nos 6 and 12 are presented in Tables 2.10.6-5 through 2.10.6-7.

The greatest significance of the metrology data is that the center support disk did not experience plastic deformation and that none of the support disks exhibited any out-of-plane buckling. The deformation of the fuel basket near the steel block is not classified as buckling deformation, but rather deformation imposed by the impact of the steel blocks.

#### 2.10.6.5.7.5 Cask Body Repairs

Before proceeding with further testing, the following repairs were performed:

- 1) The inner radius of the cask inner shell was returned to drawing specification by using a hydraulic jack with a cylindrical seating surface to push the inner shell radially outward (see Figure 2.10.6-6).
- 2) The damaged basket was replaced with a new basket.
- 3) The seating surfaces for the lids were machined to return them to drawing specifications.

Since the inner shell was subjected to some small degree of work-hardening, the yield strength was changed slightly. The change in the yield strength is estimated by the product of the tangent modulus ( $E_t$ ) and the  $\epsilon_{eq}$  strain. From NUREG/CR-0481, for Type 304 stainless steel,  $E_t$  is 370,000 psi. Using 0.18 percent from Section 2.10.6.5.7.2, the yield strength is increased by 700 psi. The 700 psi change corresponds to a change of about 2 percent for Type 304 stainless steel at 70°F. This change is considered to be insignificant.

#### 2.10.6.5.8 Thirty-Foot Top Corner Drop Using Impact Limiter with Stainless Steel Shells - Test 3 of Phase 3

As a result of the first phase of testing, it was determined that obtaining the designed impact limiter performance required the use of a stainless steel impact limiter shell to enclose the redwood. A top corner drop (Test No. 2 of Phase 1) was initially performed with an aluminum impact limiter shell. The test was reperformed with impact limiters with stainless steel shells. Note, the impact limiters used for this top corner drop had been previously used in a side drop test (Test No. 1 of Phase 2), so they were oriented on the model such that the impact energy was absorbed by the undamaged portion of the model impact limiters. This impact limiter did include the later modification to constrain the redwood. Since the redwood in the overlap region did not get crushed in the corner drop, design

modifications located in that region would not have had any significant effect on the performance of the impact limiter in the corner drop. The top corner drop test was satisfactory.

For the top corner drop test, the cask axial centerline was oriented 24 degrees from the vertical. This corresponded to the center of gravity of the cask being over the edge of the impact limiter.

#### **2.10.6.5.8.1 Impact Limiter Deformation and Attachment Data**

The high speed film and the shape of the crushed impact limiter indicated that a small amount of impact limiter rotation occurred during the top corner drop. As the crushing was initiated, a force couple was applied to the impact limiter by the crushing force at the edge of the impact limiter and by a force due to the edge of the cask bottom moving into the impact limiter. This force couple resulted in rotation of the impact limiter away from the cask bottom, which produced the appearance of two crush faces on the bottom of the impact limiter. Initially, the crushed surface of the bottom of the impact limiter was at a 24 degree angle with respect to the uncrushed portion of the limiter (corresponding to the corner drop angle). During the impact, the impact limiter shifted slightly and the angle became smaller.

The maximum permissible deformation was assumed to be the distance from the edge of the redwood at the corner of the limiter to the edge of the limiter nearest the edge of the cask bottom. This was to ensure that the cask corner did not impact the unyielding surface.

The crush stroke for the corner drop was significantly larger than that for the end drop, since the crush area for the corner drop initially started out as a point and increased to the maximum area of 350 square inches (see Figure 2.10.6-25). For the end drop, the crush area remained a constant value of 477 square inches. The decreased crush area and crush force in the corner drop resulted in a much larger crush stroke.

#### 2.10.6.5.8.2 Strain Gauge Data

Strain data was recorded for all locations, but during the post processing, the data for location Nos. 5 thru 9 was inadvertently destroyed. Listed below are the maximum axial strains for location Nos. 1 thru 4 for the top end drop and the top corner drop.

Strain Gauge <u>Location</u>	Maximum Axial Strain Magnitude (microstrains)	
	<u>Top End Drop</u>	<u>Top Corner Drop</u>
1	85	56
2	53	63
3	61	57
4	90	50

The data confirms that the top end drop axial load envelopes that of the top corner drop, except for a spurious reading at location No. 2, which is near the bottom of the model cask and away from the point of impact. The maximum stress computed for the data obtained in the top end drop, 8.6 ksi, thus, envelopes the maximum stress which occurs in the top corner drop.

#### 2.10.6.5.8.3 Accelerometer Data

The accelerometer trace for the vertical acceleration of the top corner drop is shown in Figure 2.10.6-26. The maximum acceleration is listed in Table 2.10.6-8 as 127 g. The trace reflects the gradual increase of the impact limiter crushing area. As the impact limiter crush area increases, the deceleration force also increases. Since the dynamic modes of deformation are similar to those for the end drop, the cut off frequency used for the top end drop is applicable for the top corner drop.

For information purposes, the data for this test was also filtered at 4000 Hz to demonstrate the effects of using higher filter frequencies. The result is that spurious peaks are introduced into the signal.



In comparing the top corner drop to the top end drop, the top corner drop produces significantly lower accelerations. There are two reasons for this. The total crush area for the top end drop was 477 square inches, while the top corner drop utilized 27 percent less area (350 square inches). Additionally, the top corner drop does not subject the redwood to a uniform strain, but rather the crush strain varies from a maximum value to zero.

The top end drop impact force clearly envelopes that of the top corner drop.

#### 2.10.6.5.8.4 Pressure Measurements

The cavity pressure measured after the top corner drop test showed a decrease of 0.2 percent, which results from the 1.5°F decrease measured for the cask body temperature. The pressure measurements indicate that the cavity pressure was maintained during the test.

#### 2.10.6.5.8.5 Test Observations

The lids, lid bolts, basket and fuel assemblies were removed and no damage to any component was observed.

#### 2.10.6.5.9 One-Meter Pin Puncture Drops - Tests 5 and 6 of Phase 3

The purpose of the pin puncture drops is to confirm the ability of the cask design to withstand a pin puncture load in the potentially most damaging orientation. The fuel basket was removed to ensure that the cask shells would not receive any support from the fuel basket during the pin puncture tests. Bags of lead weights were placed in the model cask cavity to replace the weight of the components that were removed.

Two pin puncture tests are performed:

- 1) Pin puncture at the axial midpoint of the cask
- 2) Pin puncture at the center of the outer lid

The data of interest to confirm the design are the pressure measurements and any changes in the dimensions of the containment boundary components.

#### 2.10.6.5.8.4 Pressure Measurements

The pressure measurements are summarized in Table 2.10.6-9 for each of the pin puncture drops.

The pressure drop observed for the cask mid-point pin puncture event corresponds to the observed temperature drop. In the cask outer lid pin puncture event, the cavity pressure valve cracked, which allowed the cavity pressure to decrease. The cask was refitted with another valve and the cask was repressurized to 3.1997 bar.

At the end of 10 minutes the pressure was still at 3.1995 bar, indicating that the closure lid system had performed satisfactorily. The cavity pressure valve in the model is not a part of the full-scale NAC-STC design, and serves only as a convenient fixture to pressurize the model cavity.

#### 2.10.6.5.9.2 Metrology Data

After the two pin puncture tests, the cask body was submitted to metrology for inspection. The results are summarized in Table 2.10.6-9. The cask mid-point pin puncture resulted in an indentation of 0.33 inch in the outer shell. This did not result in penetration of the outer shell (see Figure 2.10.6-10). The test, however, did result in deformation of the pin itself, but the effect of the deformation of the 8-inch long pin is considered to be negligible.

For the outer lid pin puncture test, the pin was found to have impacted at a location 2.53 inches away from the true center. This corresponds to approximately 10 percent of the diameter, and would produce essentially the same result as if it were at the exact center. The metrology data indicates no permanent deformation of the outer lid for the pin puncture condition at the off-center location. A pin puncture at the center would not be expected to result in permanent deformation of the closure lids, either. Some minor scraping of the outer surface of the outer lid was noted.

**2.10.6.5.10 Thirty-Foot Bottom Oblique Drop (Top End Slapdown) using Modified Impact Limiters with Stainless Steel Shells - Test No. 1 of Phase 4**

As a result of the side and oblique drop tests performed in Phase 3, it was determined that the redwood in the overlap region of the impact limiter was not maintaining its original position and orientation. A design modification was added to the overlap region of the impact limiter to prevent the redwood in that region from changing its orientation during the side impact. The first test to be conducted in Phase 4 was the bottom oblique drop, since it was observed that the slapdown effect on the upper impact limiter would produce the most critical crush stroke. In this test, the bottom of the cask impacts first causing the top end of the cask to rotate (and slapdown). For a shallow angle oblique impact (near side impact), the slapdown impact usually will result in a higher acceleration than for a side drop due to the angular momentum of the rotating cask.

**2.10.6.5.10.1 Impact Limiter Deformation Data**

The impact limiter shells were Type 304 stainless steel. The high speed film verified that the model orientation angle was 75 degrees from the vertical. The maximum crush occurred in the top limiter, which was subjected to the slapdown effect. It is required that the maximum crush stroke be limited so as to prevent the neutron shield from coming into contact with the impact surface. For the quarter-scale model this maximum crush stroke distance is 3.22 inches. In the top end slapdown, the maximum crush stroke was 2.41 inches (see Table 2.10.6-10). The deformed upper impact limiter is shown in Figure 2.10.6-27 and the measured impact limiter deformations are shown in Figure 2.10.6-28. The impact limiters remained attached to the cask body (see Figure 2.10.6-29).

**2.10.6.5.10.2 Strain Gauge Data**

The maximum stress occurred at the top end at the 180 degree location which is location No. 9. The strain gauge time histories are shown in Figure 2.10.6.30 and Figure 2.10.6-31 for the axial and hoop strains at location No. 9. While some permanent strain was recorded, the level was significantly less than 0.2 percent.

### 2.10.6.5.10.3 Accelerometer Data

The maximum acceleration occurred at the top end of the cask (approximately a 10 percent increase over that at the lower end). The peak acceleration value was 225 g, using a filter frequency of 750 Hz. The acceleration time histories are shown in Figures 2.10.6-32 and 2.10.6-33. The top end accelerometer trace shows a delay of the impact, since the cask was rotating after the impact of the lower limiter. The filter frequency was computed by treating the cask body as a beam, but including a factor to reflect the presence of shear in the beam. The filter frequency was used to reduce the effect of higher frequency signals, which inflate the acceleration levels recorded by instrumentation. Using Blevins, Table 8-15, case # 1, the frequency is given by:

#### Bending Mode/Shear Beam

$$f_s = \frac{\lambda_1}{2\pi\ell} \left( \frac{kG}{\mu} \right)^{0.5} \quad (\text{Blevins, Table 8-15, Case \#1})$$

$$\lambda_1 = \pi$$

$$k = \frac{6(1+\nu) \left[ 1 + \left( \frac{20.35}{21.68} \right)^2 \right]^2}{(7+6\nu) \left[ 1 + \left( \frac{20.35}{21.68} \right)^2 \right]^2 + (20+12\nu) \left( \frac{20.35}{21.68} \right)^2} = 0.5293$$

$$\ell = 48.24 \text{ in}$$

$$\mu = \frac{0.288}{386.4} = 0.000745$$

$$G = 11.1 \times 10^6 \text{ psi}$$

$$f_s = 920 \text{ Hz}$$

Bending Mode/Beam Curvature

$$f_b = \frac{\lambda_1^2}{2\pi\ell^2} \left( \frac{EI}{m} \right)^{0.5} \text{ (Blevins, Table 8-1, Case \#1)}$$

$$\lambda_1 = 4.73$$

$$\ell = 48.24 \text{ in}$$

$$m = 0.21$$

$$E = 28.3 \times 10^6 \text{ psi}$$

$$I = 38,817 \text{ in}^4$$

$$f_b = 3500 \text{ Hz}$$

Combined Mode Frequency

$$\frac{1}{f_c} = \frac{1}{f_s} + \frac{1}{f_b} = \frac{1}{920} + \frac{1}{3500} \text{ (Blevins, page 175)}$$

$$f_c = 729 \text{ Hz}$$

2.10.6.5.10.4 Pressure Measurements

The pressure measured before and after the test remained constant to within the accuracy of the instrumentation. The pressure measurements indicated that no loss of pressure occurred during the test.

2.10.6.5.10.5 Test Observations

The metrology data summarized in Table 2.10.6-11 indicates that for a measurement tolerance of 0.01 inch, none of the diametral dimensions changed. In the process of removing the basket it was observed that the basket was removed without resistance.

#### **2.10.6.5.11 Thirty-Foot Side Drop - Test No. 2 of Phase 4**

Upon completing the oblique drop, the side drop was performed for Phase 4. It should be noted that the limiter from the oblique drop test was reused by rotating the limiter 180 degrees. In the slapdown test, the loading was not uniform, as it was in the case of the side drop. In the oblique drop, the loading tends to be concentrated towards the slapdown end. In the side drop the loading tended to be uniformly distributed over the length of the cask and, thus, equally to each impact limiter.

##### **2.10.6.5.11.1 Impact Limiter Deformation Data**

The high speed film verified that the cask was horizontal as it approached the impact surface. The maximum crush is summarized in Table 2.10.6-12. The condition of the cask model and limiters following the side drop is shown in Figures 2.10.6-34 and 2.10.6-35. The measured impact limiter deformations are shown in Figure 2.10.6-36. In this test, the amount of stroke was nearly the same for both the top and bottom impact limiters. The criteria for the impact limiter performance during the side drop is the same as that for the oblique drop: a clearance must remain between the neutron shield and the impact surface. The crush data does reflect that a clearance will exist between the neutron shield and the impact plane after the side drop condition.

##### **2.10.6.5.11.2 Strain Gauge Data**

The maximum strains and stresses occurred at the 180 degree location of the cask midpoint for the side drop. In fact, the stresses were larger for the side drop than those for the oblique drop, even though the oblique drop deceleration was 10 percent larger. The strain gauge time-histories are shown in Figures 2.10.6-37 and 2.10.6-38.

#### 2.10.6.5.11.3 Accelerometer Data

The accelerometers indicated that the magnitude of the measured accelerations on each end of the cask were nearly the same. This concurs with the crush stroke data. The accelerometer traces are shown in Figures 2.10.6-39 and 2.10.6-40.

#### 2.10.6.5.11.4 Pressure Measurements

The pressure, as measured before and after the test, remained constant to within the accuracy of the instrumentation. The pressure measurements indicated that no loss of pressure occurred during the test.

#### 2.10.6.5.11.5 Test Observations

The metrology data, summarized in Table 2.10.6-11, indicates that for a measurement tolerance of 0.01 inch, none of the diametral dimensions changed. In the process of removing the basket, it was observed that the basket was removed without resistance and no deformations had occurred.

#### 2.10.6.6 NAC-STC Quarter-Scale Model Drawings

423-019, Sheets 1 thru 4	Cask Body-Scale Model, NAC-STC Cask, SAR
423-020	Inner Lid-Scale Model, NAC-STC Cask, SAR
423-023	Model Fuel Assembly, NAC-STC Cask, SAR
423-025	Basket Spacer-Scale Model, NAC-STC Cask, SAR
423-026	Outer Lid-Scale Model, NAC-STC Cask, SAR
423-027	Port Cover-Scale Model, NAC-STC Cask, SAR

423-028	Cask Body Assembly-Scale Model, NAC-STC Cask, SAR
423-029	Instrument Fixture-Scale Model, NAC-STC Cask, SAR
423-248	Upper Limiter-Scale Model, NAC-STC Cask, SAR
423-249	Lower Limiter-Scale Model, NAC-STC Cask, SAR
423-050	26 Element Basket-Scale Model, NAC-STC Cask, SAR
423-098	Model Assembly-Scale Model, NAC-STC Cask, SAR

2.10.6.7     NAC-STC Eighth-Scale Model Drawings

423-236	Impact Limiter, Assy-1/8 Scale Model, Lower, NAC-STC Cask
---------	---





**FIGURE WITHHELD AS SENSITIVE UNCLASSIFIED INFORMATION**

NUCLEAR ASSURANCE CORPORATION <small>WILSONVILLE, OREGON 97158</small>			
CASK BODY-SCALE MODEL, NAC-STC CASK			
PROJECT	423	SECTION PACKAGE	DRAWING 019
SCALE 1/2	WEIGHT 2,449 lbs	IN 2 OF 4	REV 14

FIGURE WITHHELD AS SENSITIVE UNCLASSIFIED  
INFORMATION

NUCLEAR ASSURANCE CORPORATION <small>NUCLEAR POWER PLANTS</small>			
CASK BODY--SCALE MODEL, NAC-STC CASK			
Product	423	System Product	019
Scale 1/2 Model	Power 2449	Rev	3 of 4
		Page	14

FIGURE WITHHELD AS SENSITIVE UNCLASSIFIED  
INFORMATION

NUCLEAR ASSURANCE CORPORATION <small>PROVIDING SERVICE SINCE 1966</small>			
CASK BODY--SCALE MODEL, NAC--STC CASK			
Model	423	Scale Factor	019
Scale 1/2	1000	See 4 or 4	14

FIGURE WITHHELD AS SENSITIVE UNCLASSIFIED  
INFORMATION

[illegible]

**FIGURE WITHHELD AS SENSITIVE UNCLASSIFIED INFORMATION**

07	08	09	10	11	12	13	14	15	16	17	18	19	20	21	22	23	24	25	26	27	28	29	30	31	32	33	34	35	36	37	38	39	40	41	42	43	44	45	46	47	48	49	50	51	52	53	54	55	56	57	58	59	60	61	62	63	64	65	66	67	68	69	70	71	72	73	74	75	76	77	78	79	80	81	82	83	84	85	86	87	88	89	90	91	92	93	94	95	96	97	98	99	100																																																																																																																																																																																																																																																																																																																																																																																																																																																																																																																																																																																																																																																																																																																																																																																																																																																																														
1										LOAD										D18 CARBON STL										COLD FINISHED										2 1/2 SQUARE BAR																																																																																																																																																																																																																																																																																																																																																																																																																																																																																																																																																																																																																																																																																																																																																																																																																																																																																																																																			
07										08										09										10										11										12										13										14										15										16										17										18										19										20										21										22										23										24										25										26										27										28										29										30										31										32										33										34										35										36										37										38										39										40										41										42										43										44										45										46										47										48										49										50										51										52										53										54										55										56										57										58										59										60										61										62										63										64										65										66										67										68										69										70										71										72										73										74										75										76										77										78										79										80										81										82										83										84										85										86										87										88										89										90										91										92										93										94										95										96										97										98										99										100									
07										08										09										10										11										12										13										14										15										16										17										18										19										20										21										22										23										24										25										26										27										28										29										30										31										32										33										34										35										36										37										38										39										40										41										42										43										44										45										46										47										48										49										50										51										52										53										54										55										56										57										58										59										60										61										62										63										64										65										66										67										68										69										70										71										72										73										74										75										76										77										78										79										80										81										82										83										84										85										86										87										88										89										90										91										92										93										94										95										96										97										98										99										100									
07										08										09										10										11										12										13										14										15										16										17										18										19										20										21										22										23										24										25										26										27										28										29										30										31										32										33										34										35										36										37										38										39										40										41										42										43										44										45										46										47										48										49										50										51										52										53										54										55										56										57										58										59										60										61										62										63										64										65										66										67										68										69										70										71										72										73										74										75										76										77										78										79										80										81										82										83										84										85										86										87																																																																																																																																											

FIGURE WITHHELD AS SENSITIVE UNCLASSIFIED INFORMATION

ARMY			ARMY			ARMY			③			NUCLEAR ASSURANCE CORPORATION		
SECURITY												BASKET SPACER— SCALE MODEL, STC		
TYPE	DESCRIPTION	TELEPHONE			GROUP			DATE						
□	PLACEMENT	3 PLACE DEC.	REL.	2 PLACE DEC.	REL.	1 PLACE DEC.	REL.	1/10/43						
□	PRODUCTION	3-15	2-15	3-15	2-15	3-15	2-15	2/1/43						
□	ANALYSIS	3-15	2-15	3-15	2-15	3-15	2-15	2/1/43						
□	PERFORMANCE	3-15	2-15	3-15	2-15	3-15	2-15	2/1/43						
□	PARALLELISM	3-15	2-15	3-15	2-15	3-15	2-15	2/1/43						
□	CONCENTRICITY	3-15	2-15	3-15	2-15	3-15	2-15	2/1/43						
□	SIZE POSITION	3-15	2-15	3-15	2-15	3-15	2-15	2/1/43						
PROJECT 423									SCHEMATIC		DRAWING 025		REV 3	
SHEET 1/1									EXPLAN		ON 1 OF 1			





**FIGURE WITHHELD AS SENSITIVE UNCLASSIFIED INFORMATION**

[illegible]

**FIGURE WITHHELD AS SENSITIVE UNCLASSIFIED INFORMATION**

ARMY ARMY ARMY			11			NUCLEAR ASSURANCE CORPORATION DEFENSE NUCLEAR GROUP		
QUANTITY								
TYPE	DESIGNATION	TELEPHONE UNLESS OTHERWISE SPECIFIED	GROUP	NAME	DATE	CASK BODY ASSEMBLY- SCALE MODEL, NAC-STC CASK		
PLACEMENT	3 PLACE DES. REL. TO VAX DES. REL.	GROUP	NAME	DATE				
TRANSFORMER	GROUP 3	GROUP 3	NAME	DATE				
WINDLIFT	GROUP 12	GROUP 12	NAME	DATE				
APPROPRIATE	1 PLACE DES. (A) REL. TO VAX DES. REL.	GROUP	NAME	DATE				
TRANSFORMER	GROUP 12	GROUP 12	NAME	DATE				
CONCENTRATION	SCALE GROUP 12	GROUP 12	NAME	DATE				
SCALE POSITION	TYPE OF DRAWING: ENGINEERING	GROUP 12	NAME	DATE				
PROJECT 423						DESIGN PACKAGE	DRAWING 028	REV 11
SCALE 1/2						EXEMPT CHART	ON 1 of 1	

**FIGURE WITHHELD AS SENSITIVE UNCLASSIFIED INFORMATION**

[illegible]

**FIGURE  
WITHHELD AS  
SENSITIVE  
UNCLASSIFIED  
INFORMATION**

[illegible]



FIGURE WITHHELD AS SENSITIVE UNCLASSIFIED  
INFORMATION

[illegible]



**FIGURE  
WITHHELD AS  
SENSITIVE  
UNCLASSIFIED  
INFORMATION**

[illegible]



Figure 2.10.6-1 Quarter-Scale Model Package Assembly - Ready for Cavity Pressure Test

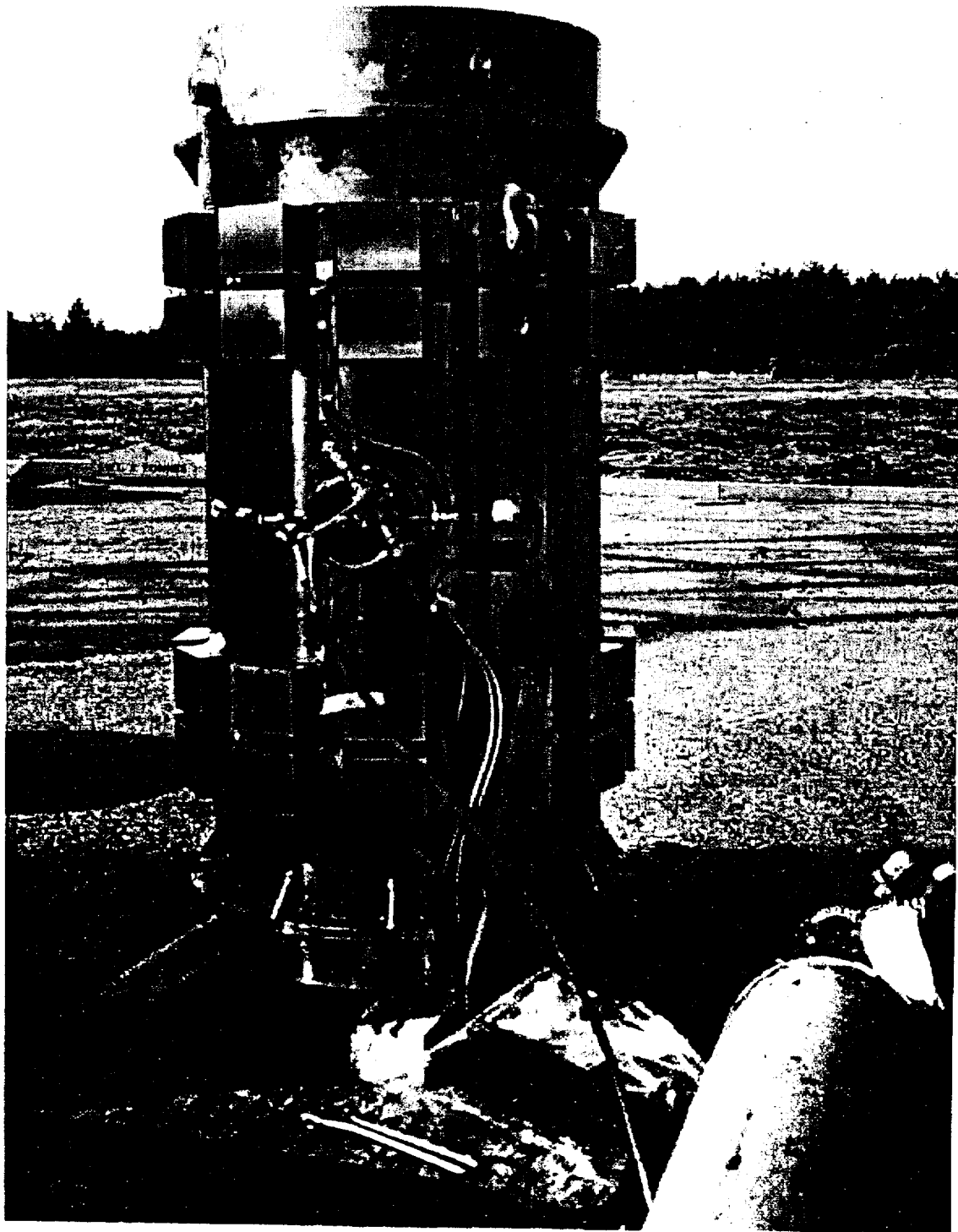


Figure 2.10.6-2 Assembly of Cask - Inner Lid Fitted



Figure 2.10.6-3 Assembly of Cask - Fuel Pin Assemblies Located in Basket

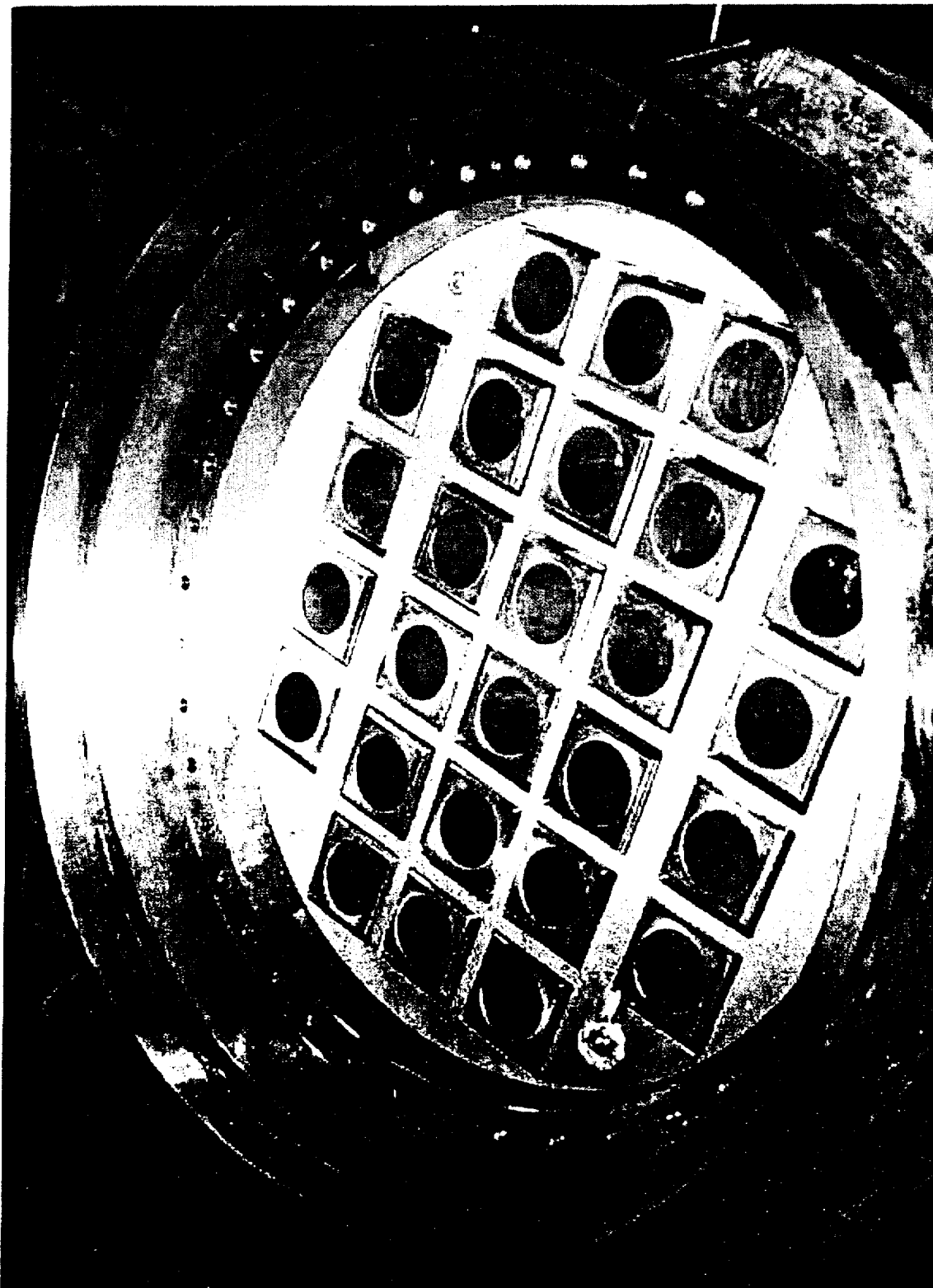


Figure 2.10.6-4 Top End Drop - Cask Penetration into Impact Limiter

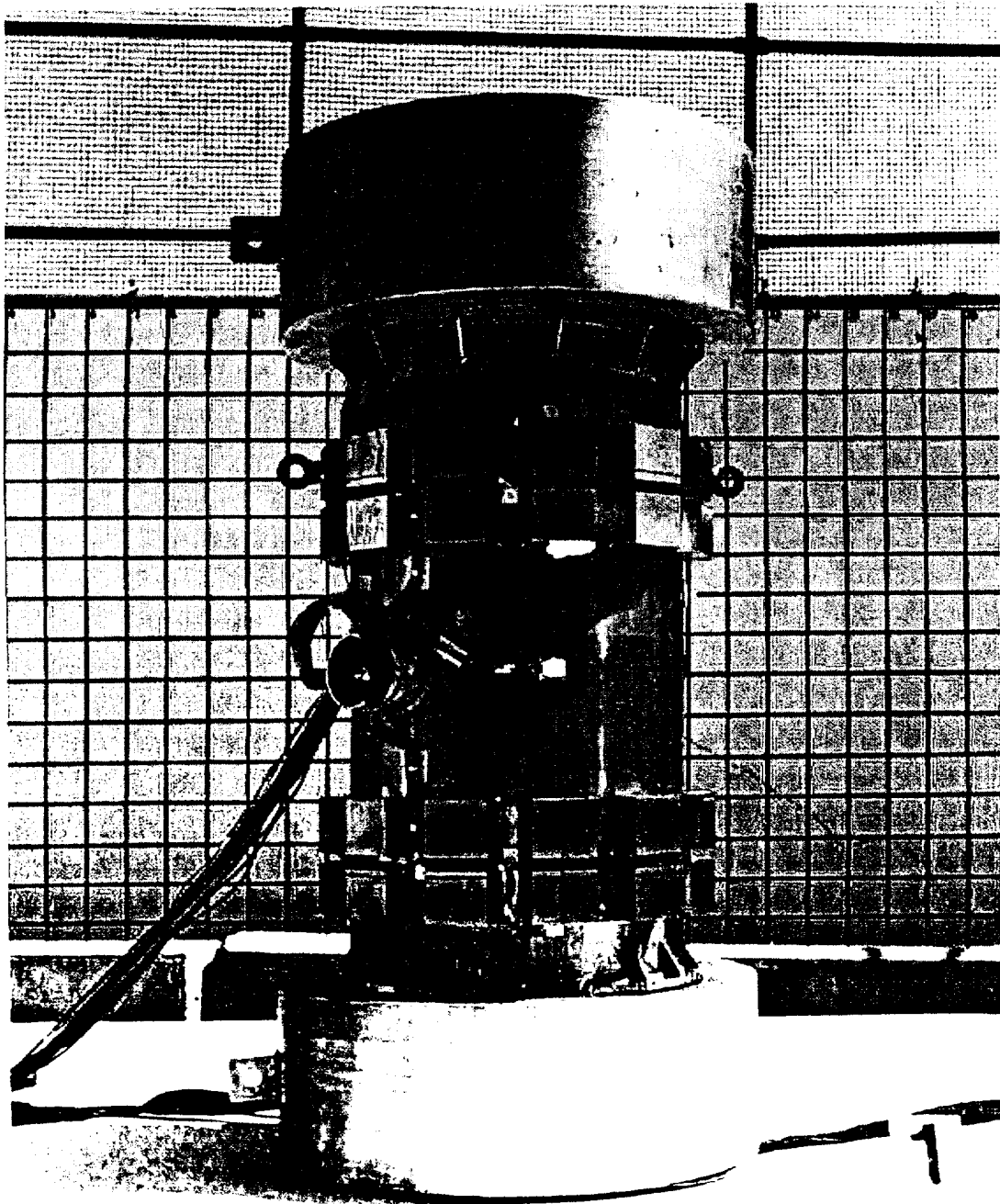


Figure 2.10.6-5 Side Drop - Detail of Shield Block Impact Near Bottom End

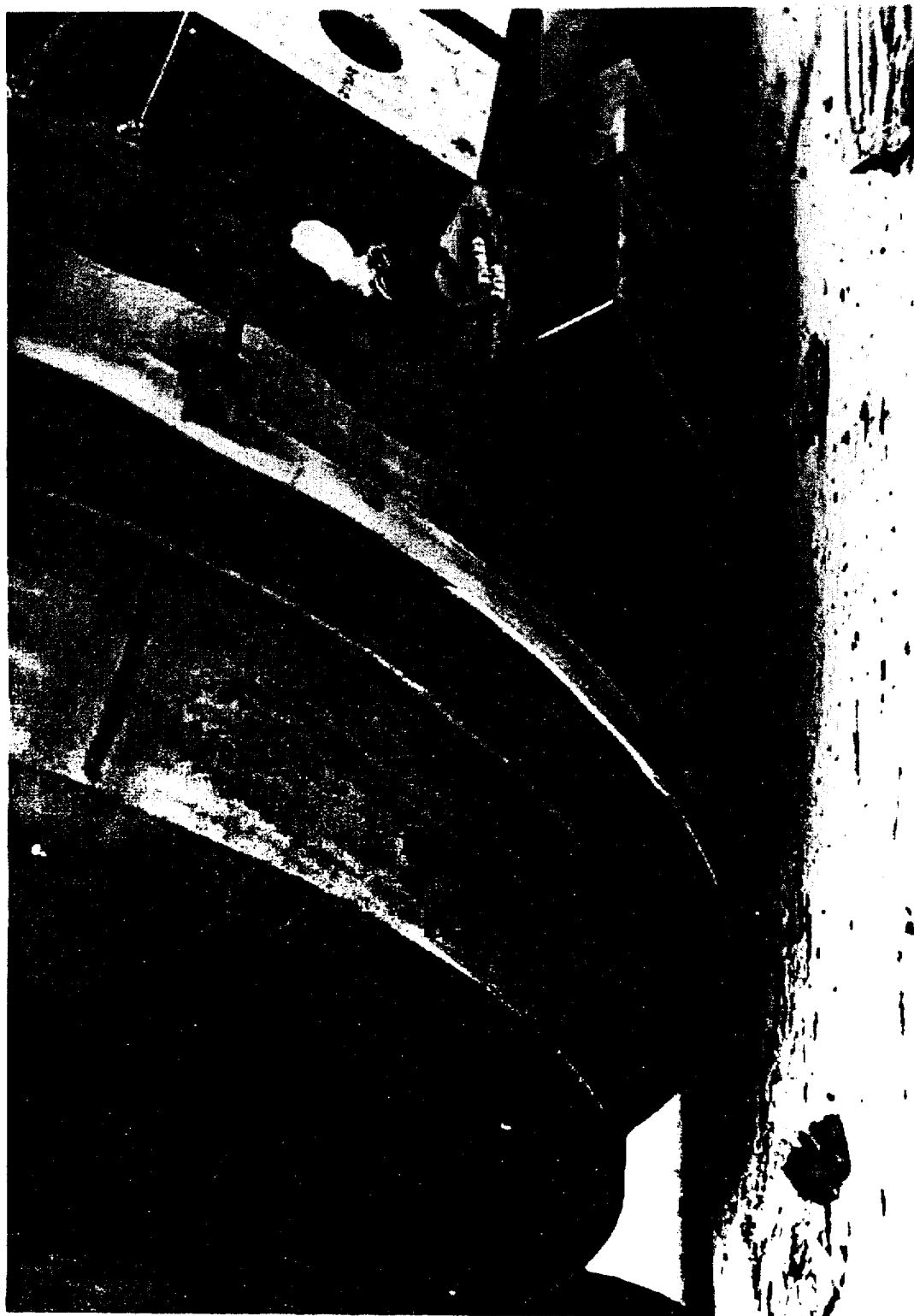


Figure 2.10.6-6 Repairs to Cask - 50 Metric Ton Hydraulic Press

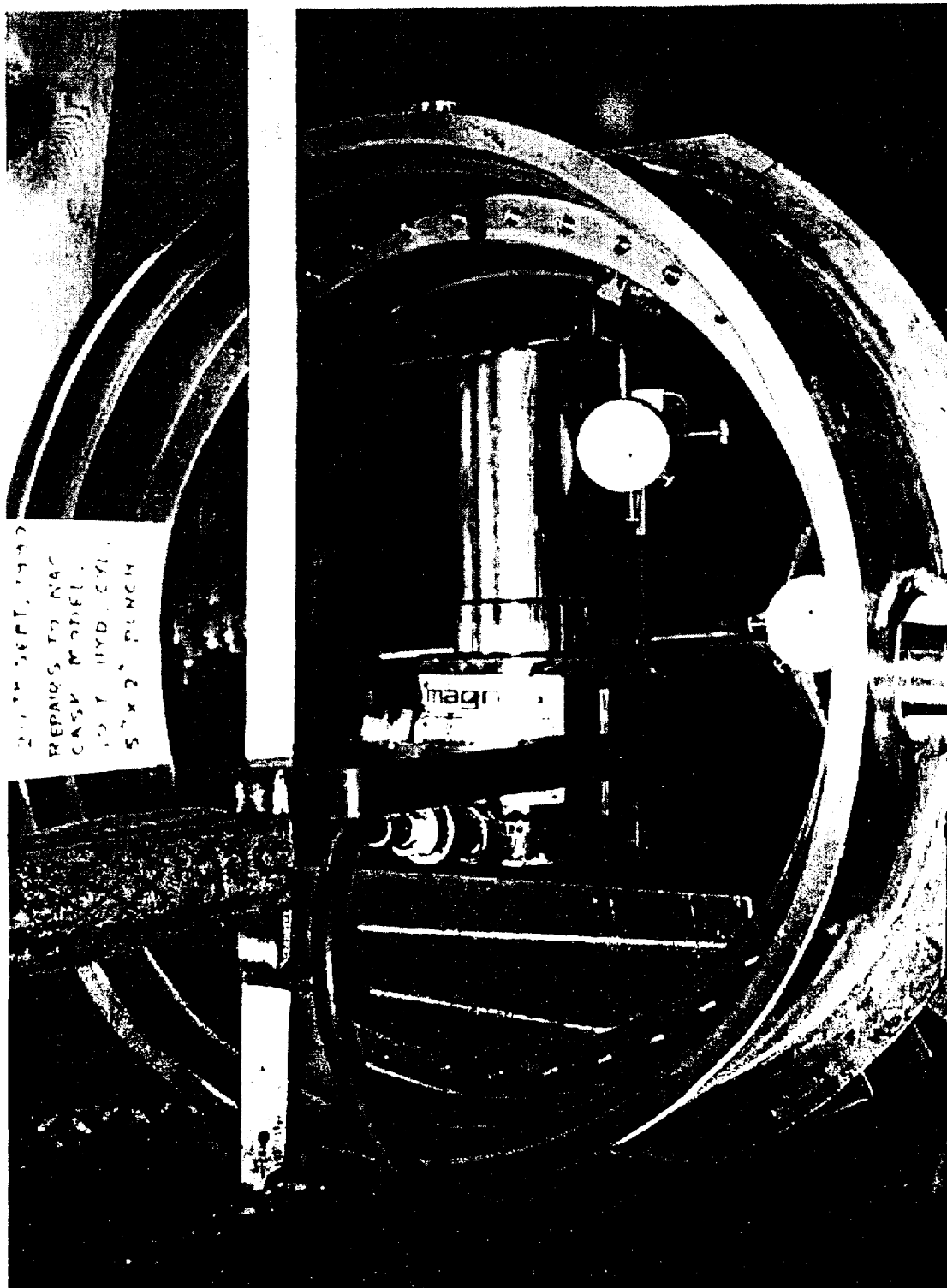


Figure 2.10.6-7 Repairs to Cask - Local Over Pressing

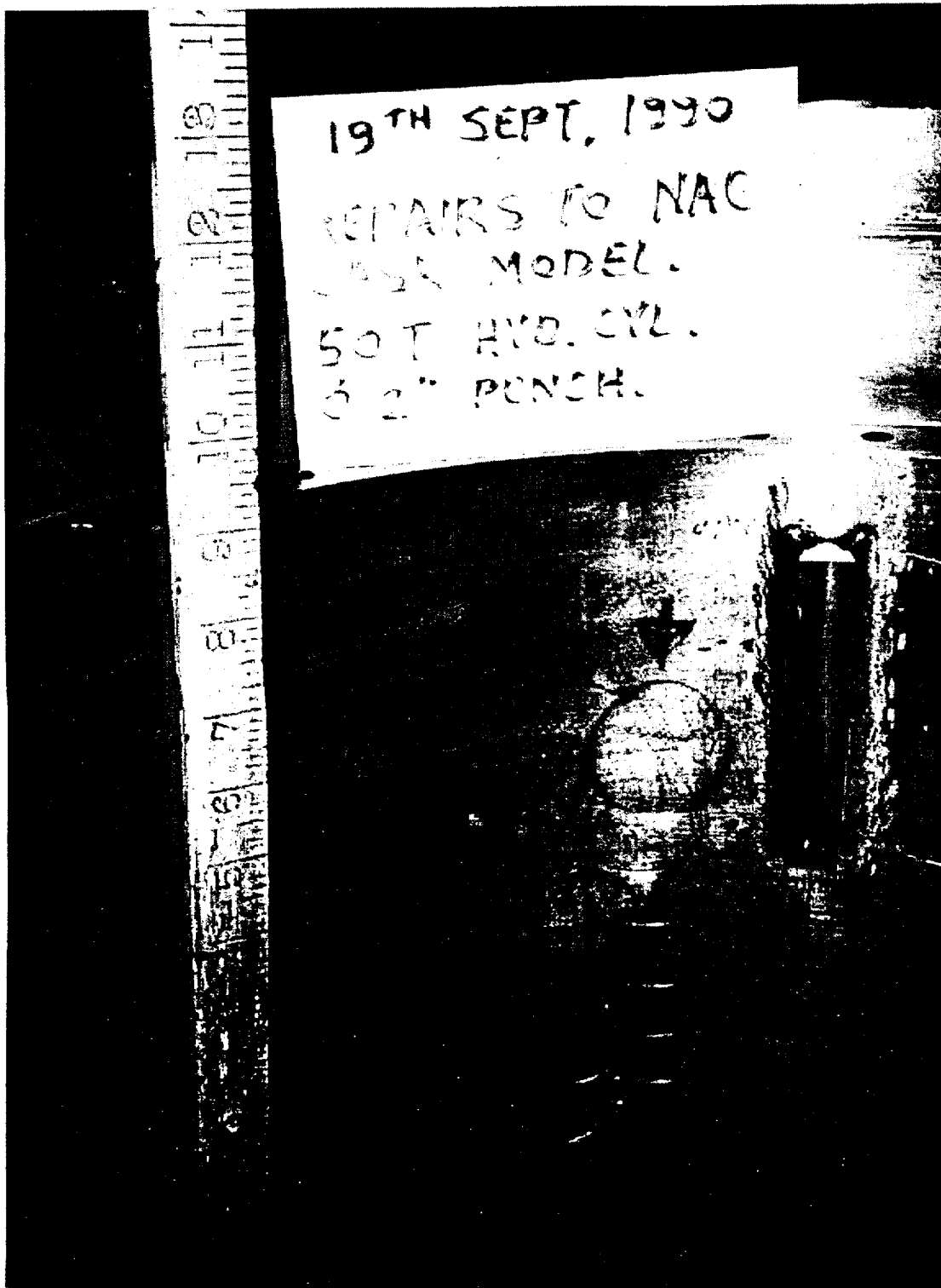


Figure 2.10.6-8 Detail of Distortion to Basket Disk No. 6 - Side Drop

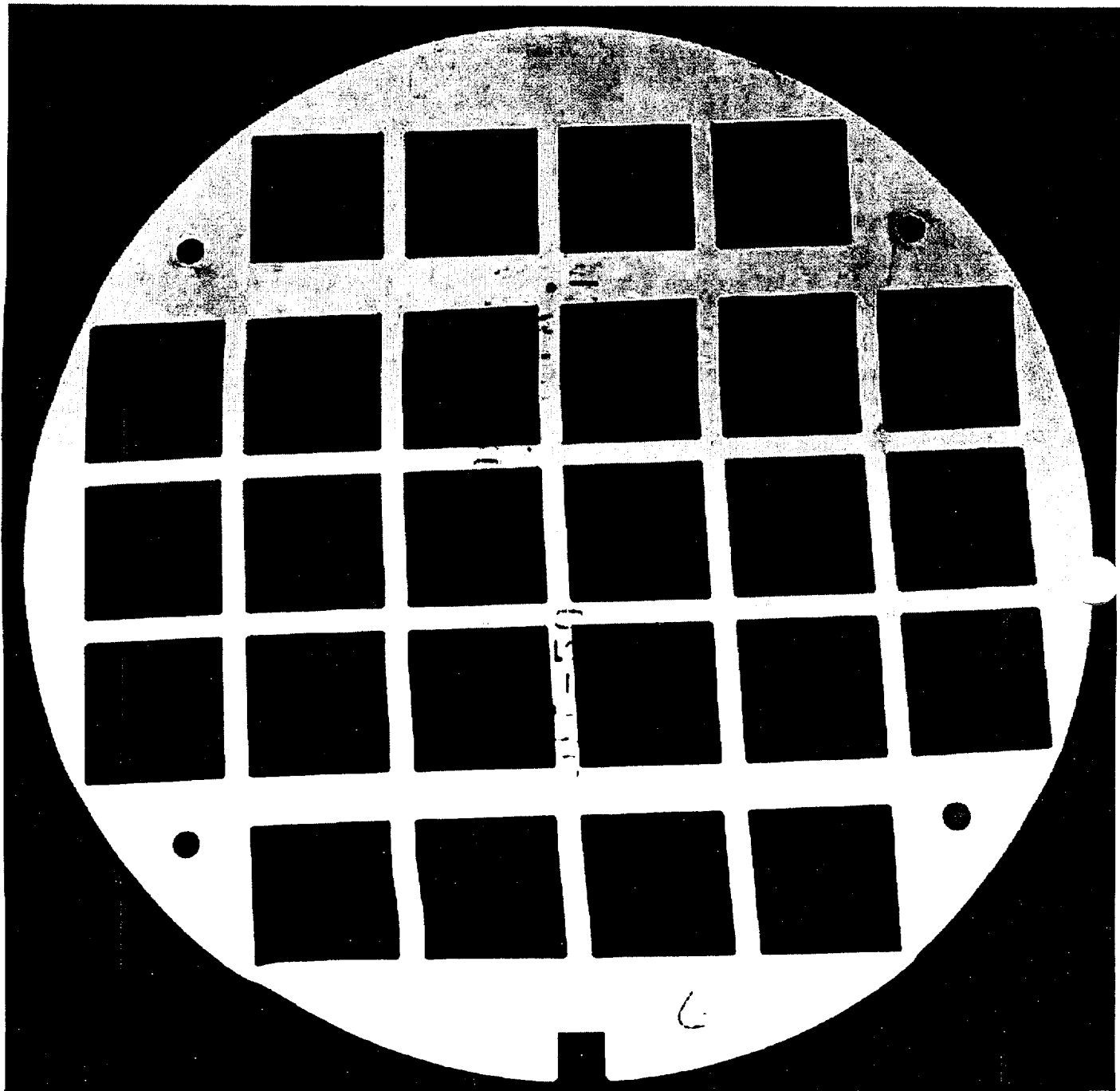




Figure 2.10.6-9 Deformation of Upper Impact Limiter - Top Corner Drop



Figure 2.10.6-10 Cask Midpoint Pin Puncture - Outer Shell Deformation

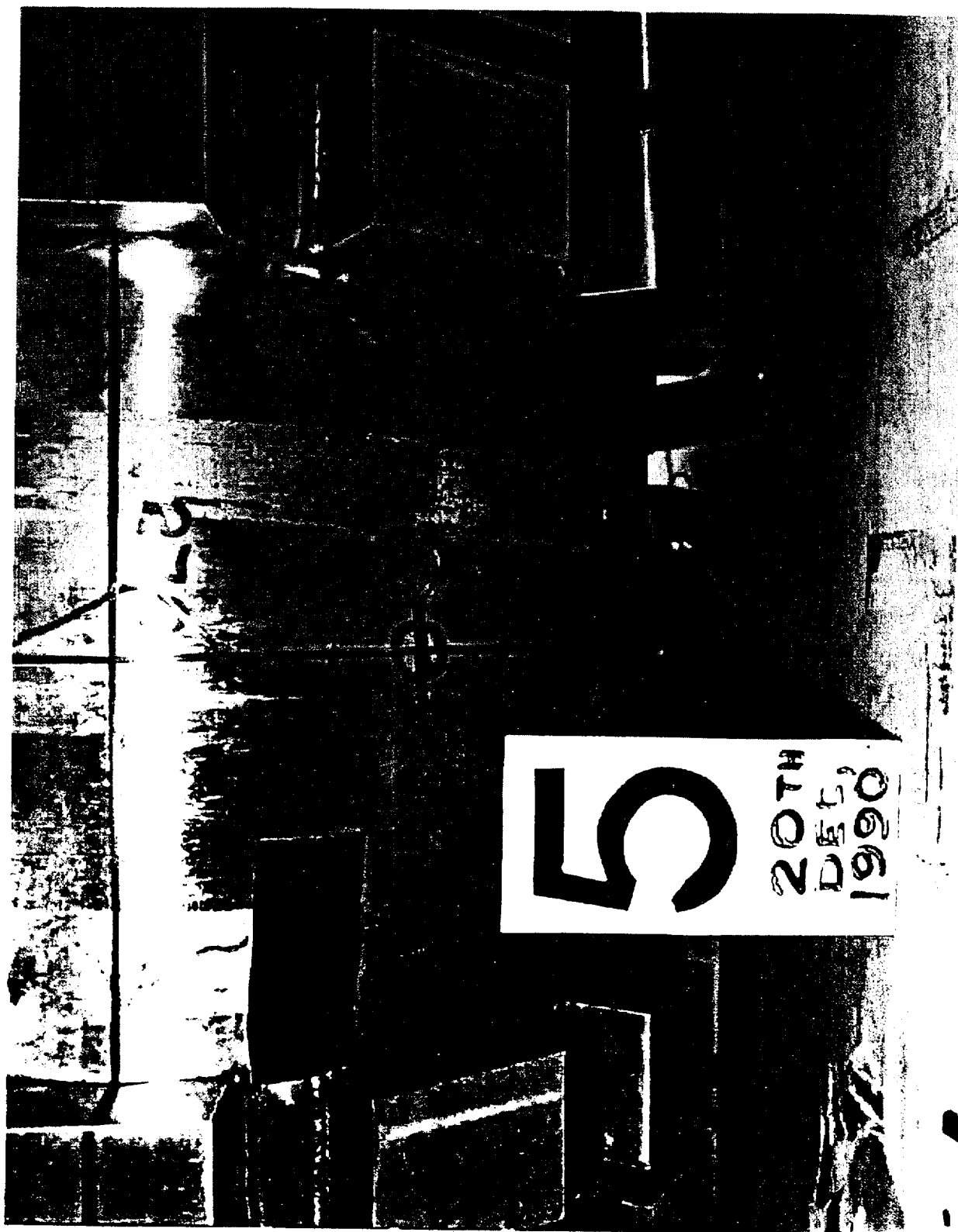


Figure 2.10.6-11 Center of Outer Lid Pin Puncture - Distortion of Punch

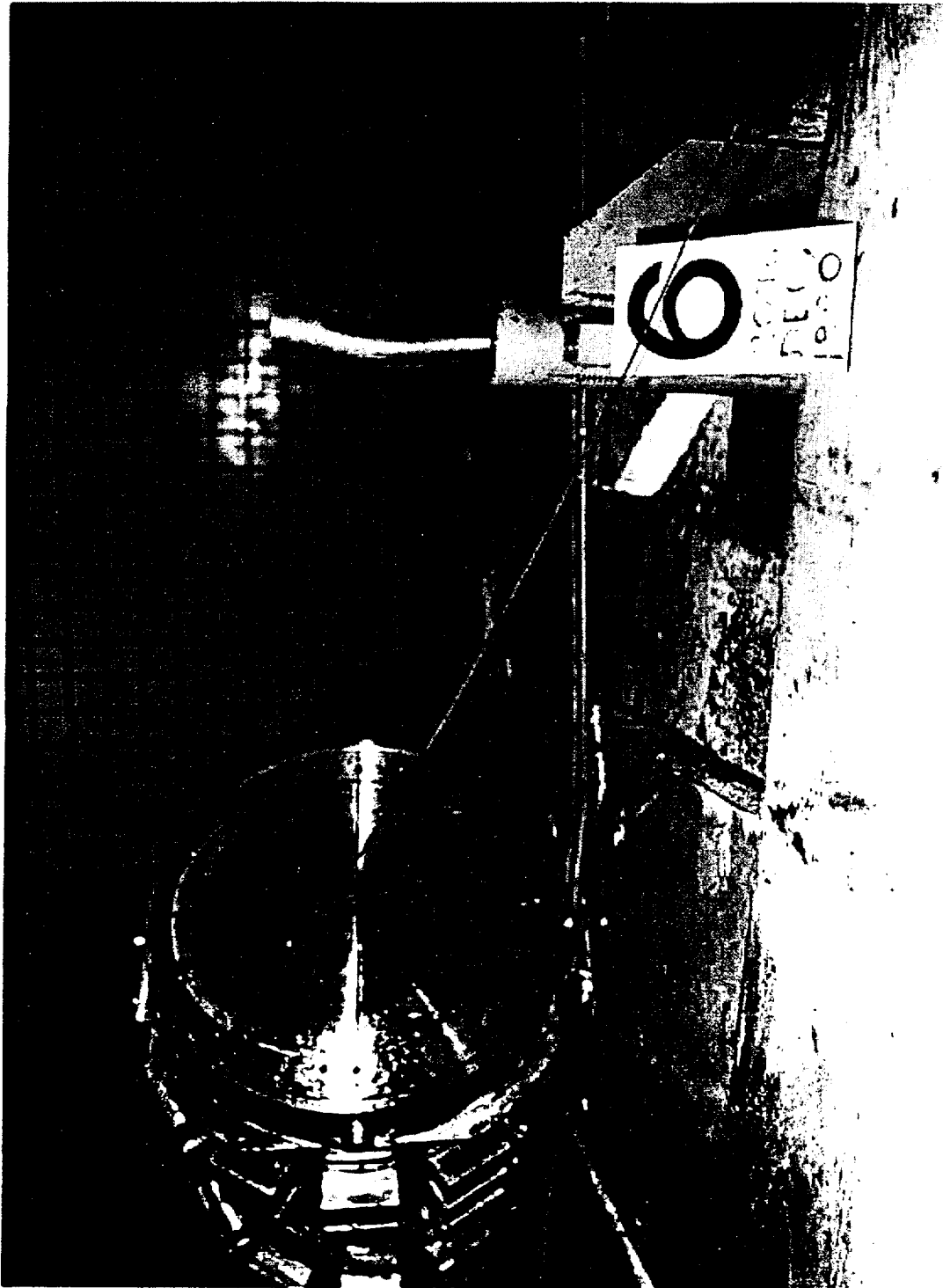


Figure 2.10.6-12      Quasi-Static Force-Deflection Curve, Eighth-Scale Model Impact Limiter -  
End (0-Degree) Impact

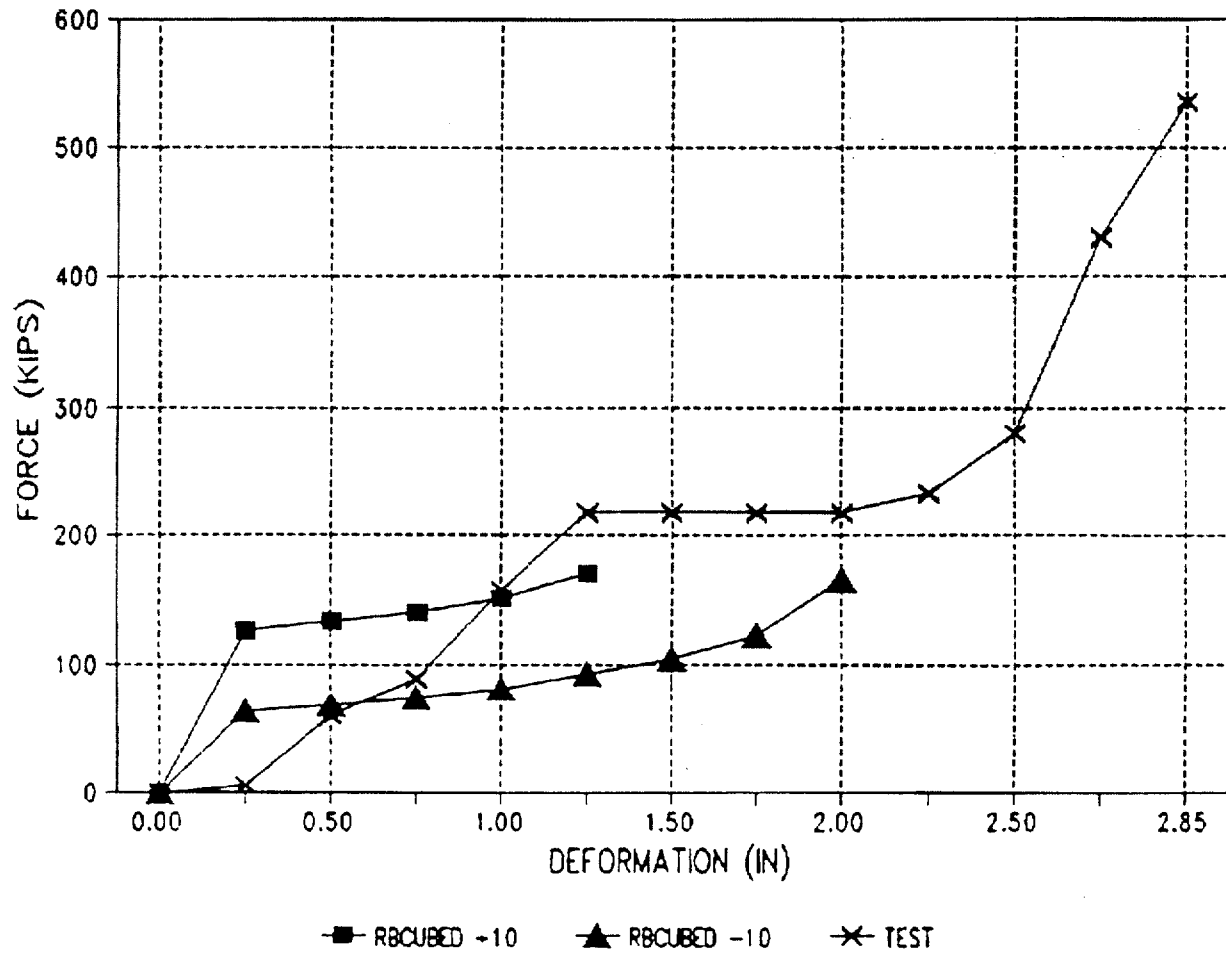


Figure 2.10.6-13      Quasi-Static Force-Deflection Curve, Eighth-Scale Model Impact Limiter -  
Corner (24-Degree) Impact

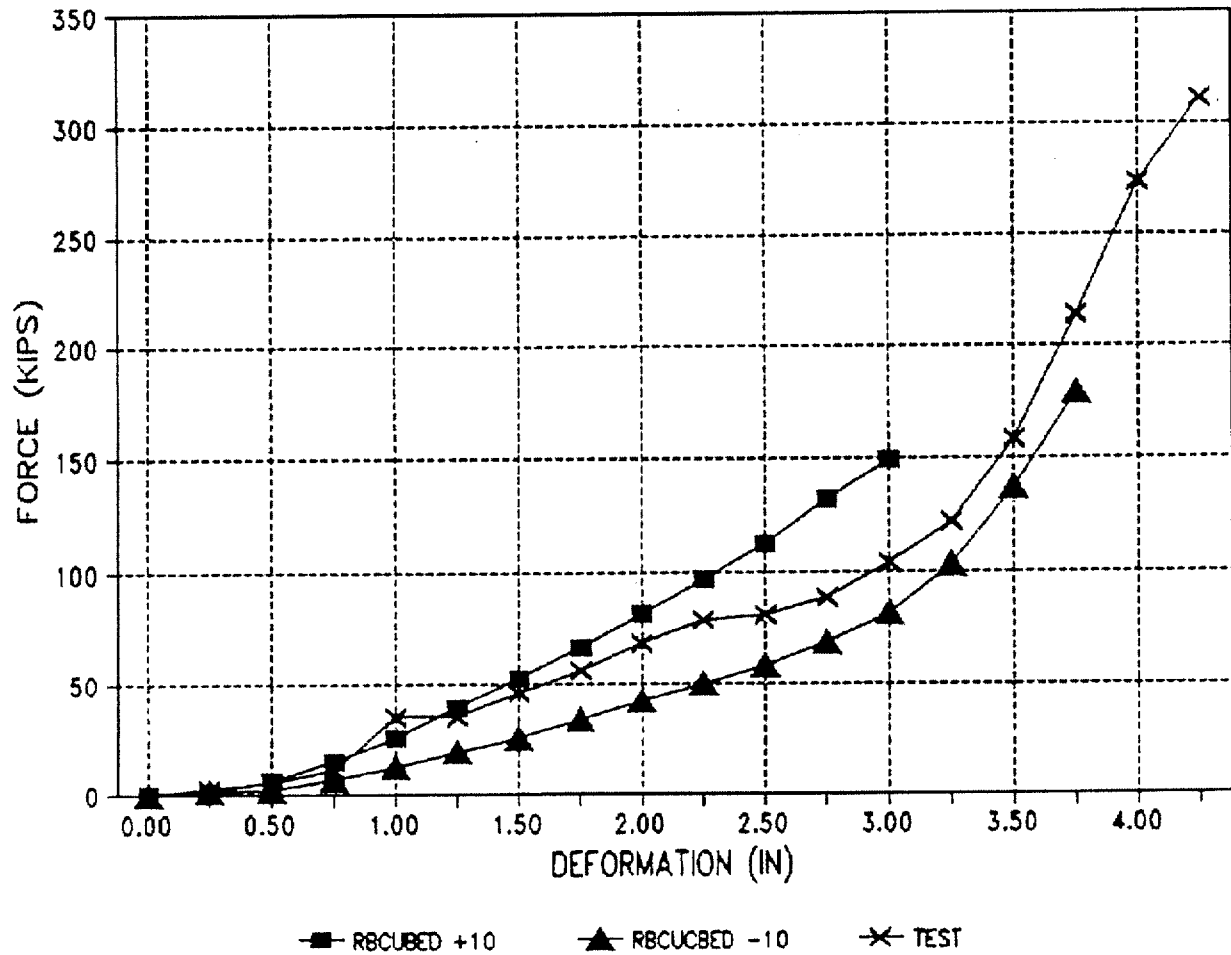


Figure 2.10.6-14 Force-Deformation Curve, Eighth-Scale Model Impact Limiter - Side (90-Degree) Impact

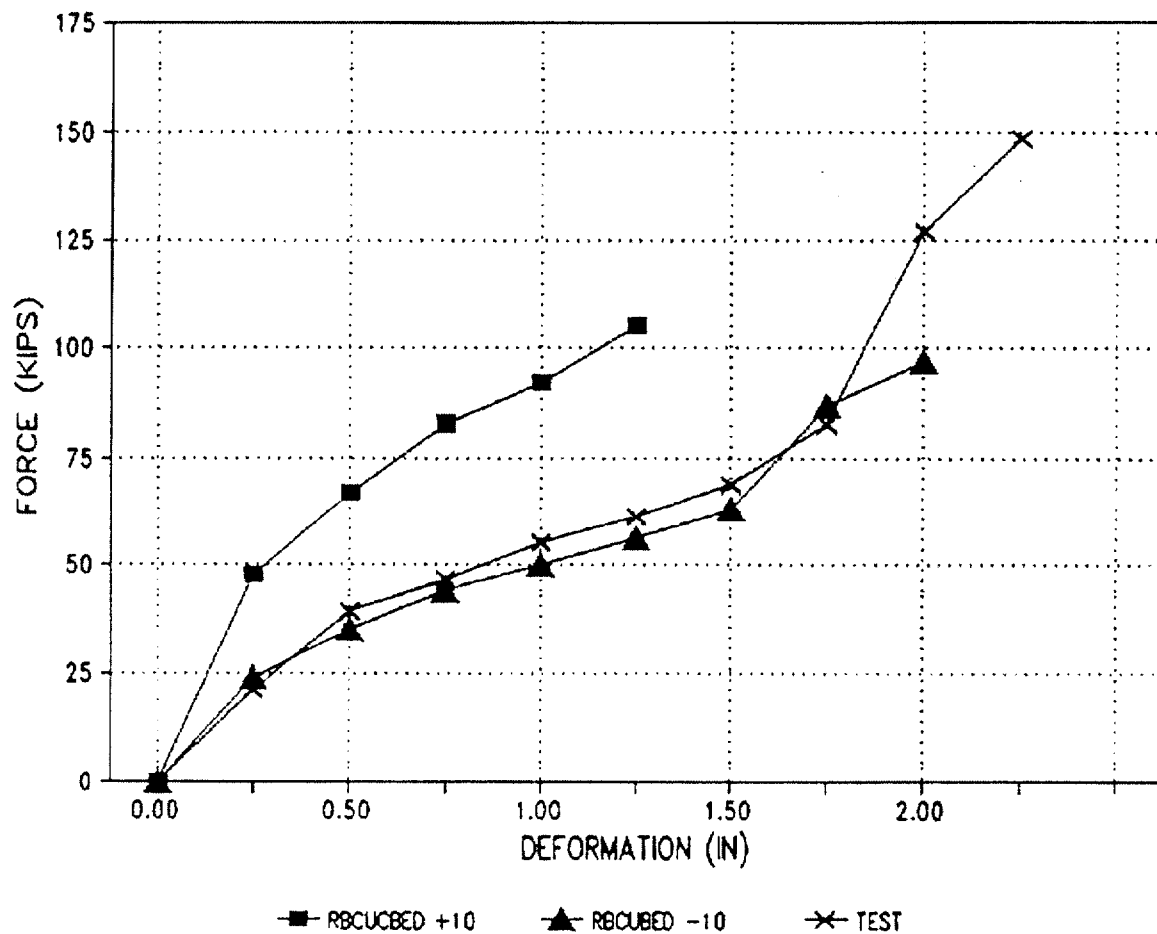


Figure 2.10.6-15 Location of Cask Body Metrology Measurements - Quarter-Scale Model

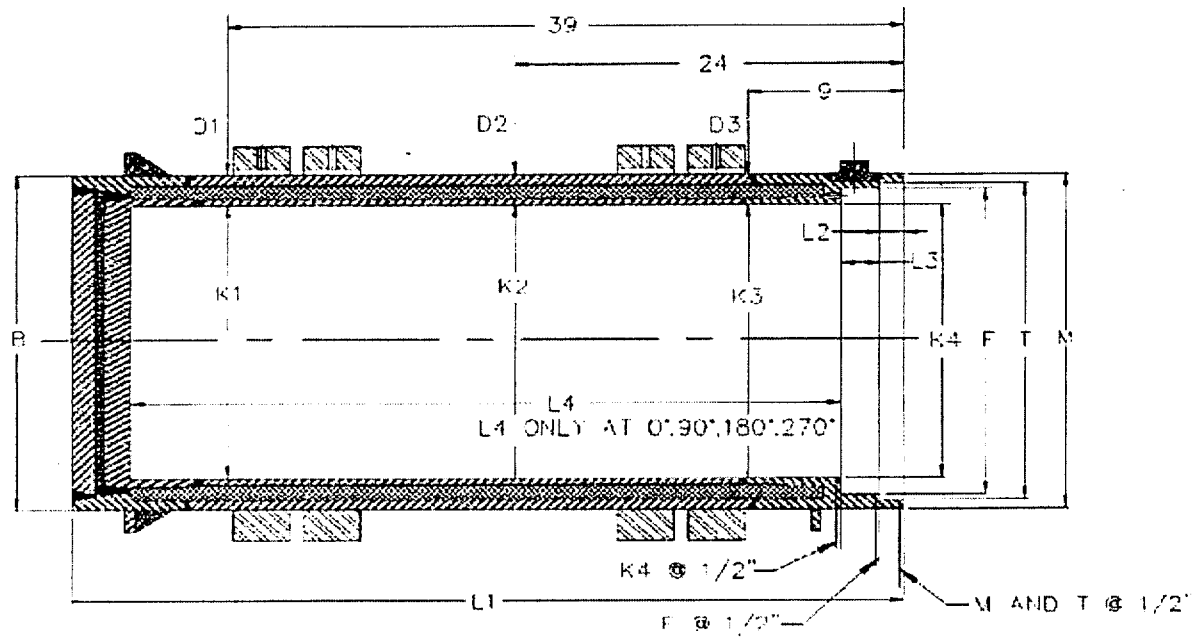


Figure 2.10.6-16 Location of Basket Support Disk Metrology Measurements - Quarter-Scale Model

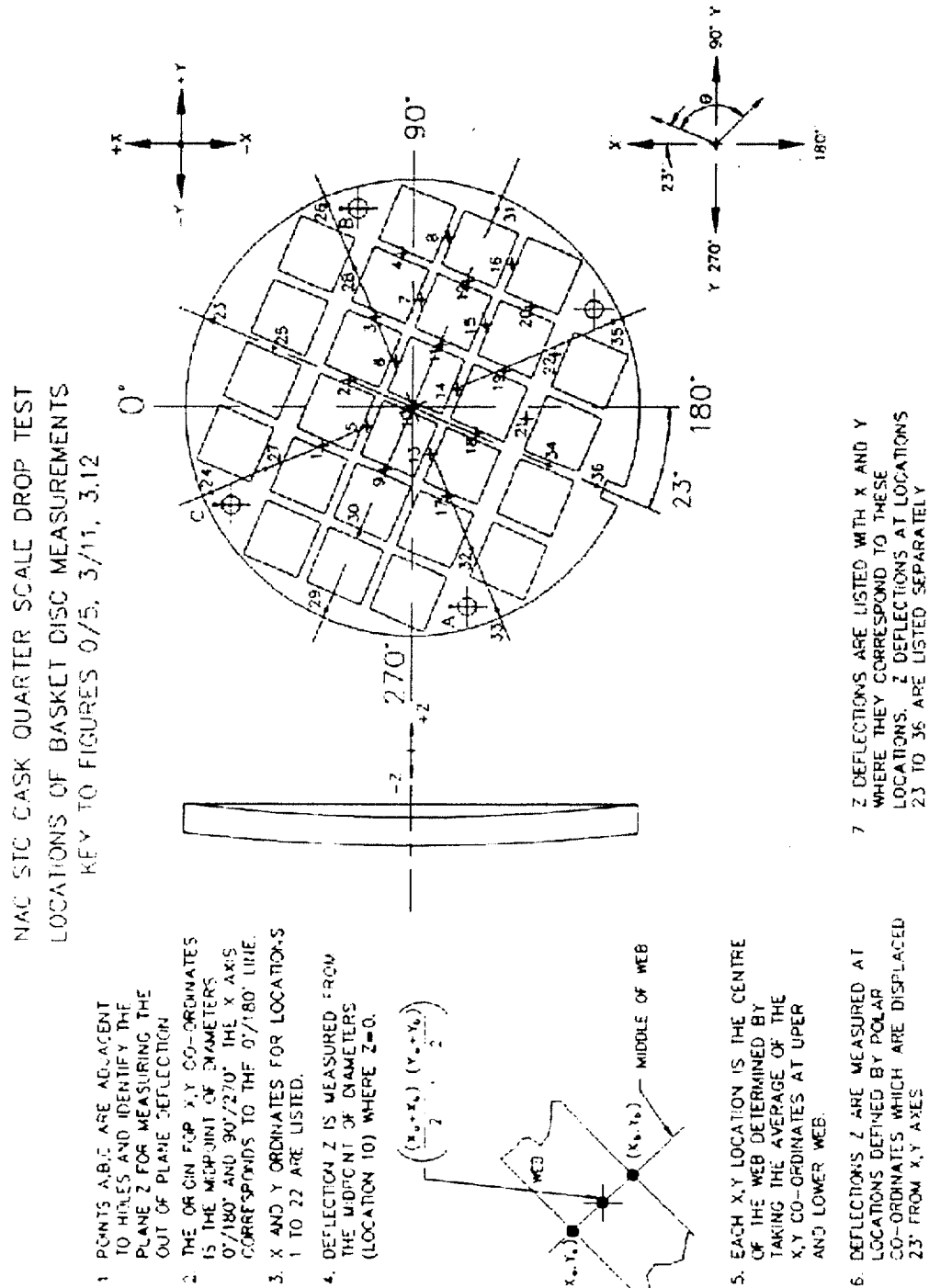




Figure 2.10.6-17 Strain Gauge Locations - Quarter-Scale Model

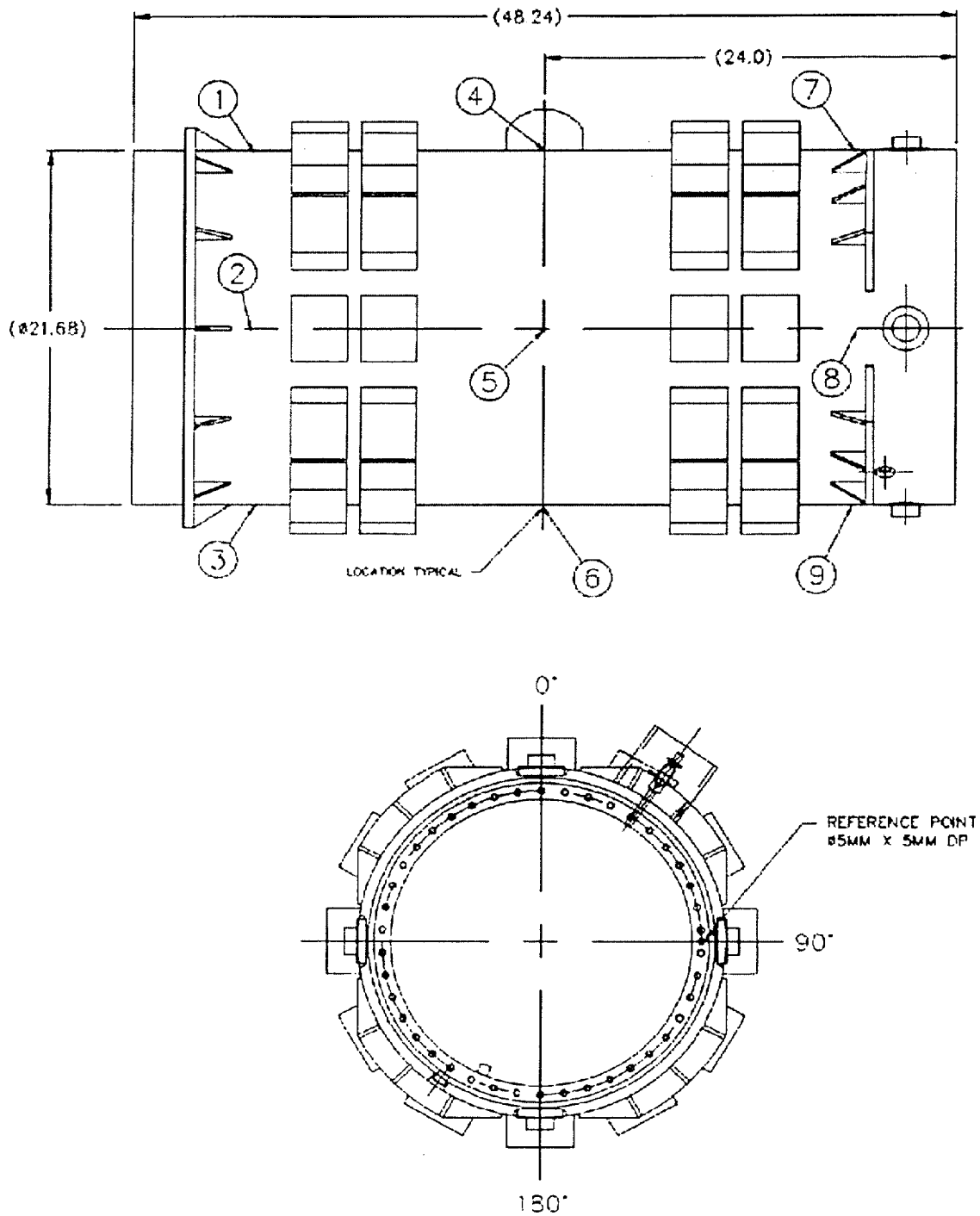


Figure 2.10.6-18 Accelerometer Locations - Quarter-Scale Model

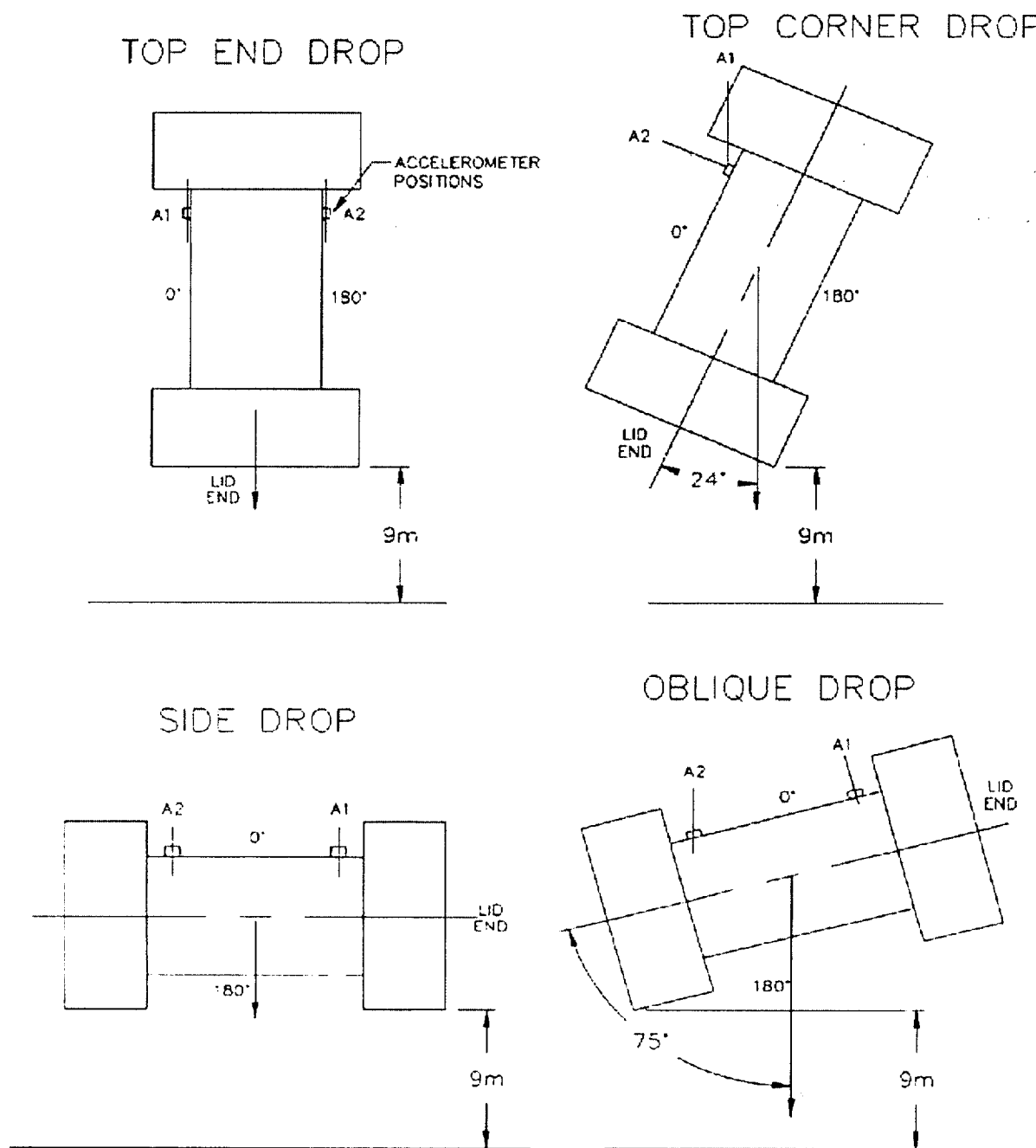


Figure 2.10.6-19      Top End Drop (Test No. 1 of Phase 1) - Upper Impact Limiter  
Deformation (Using Impact Limiters With Aluminum Shells)

**FIGURE WITHHELD AS SENSITIVE  
UNCLASSIFIED INFORMATION**

Figure 2.10.6-20 Top End Drop (Test No. 1 of Phase 1) Strain Data - Gauge S9.1 (Axial)  
(Using Impact Limiters With Aluminum Shells)

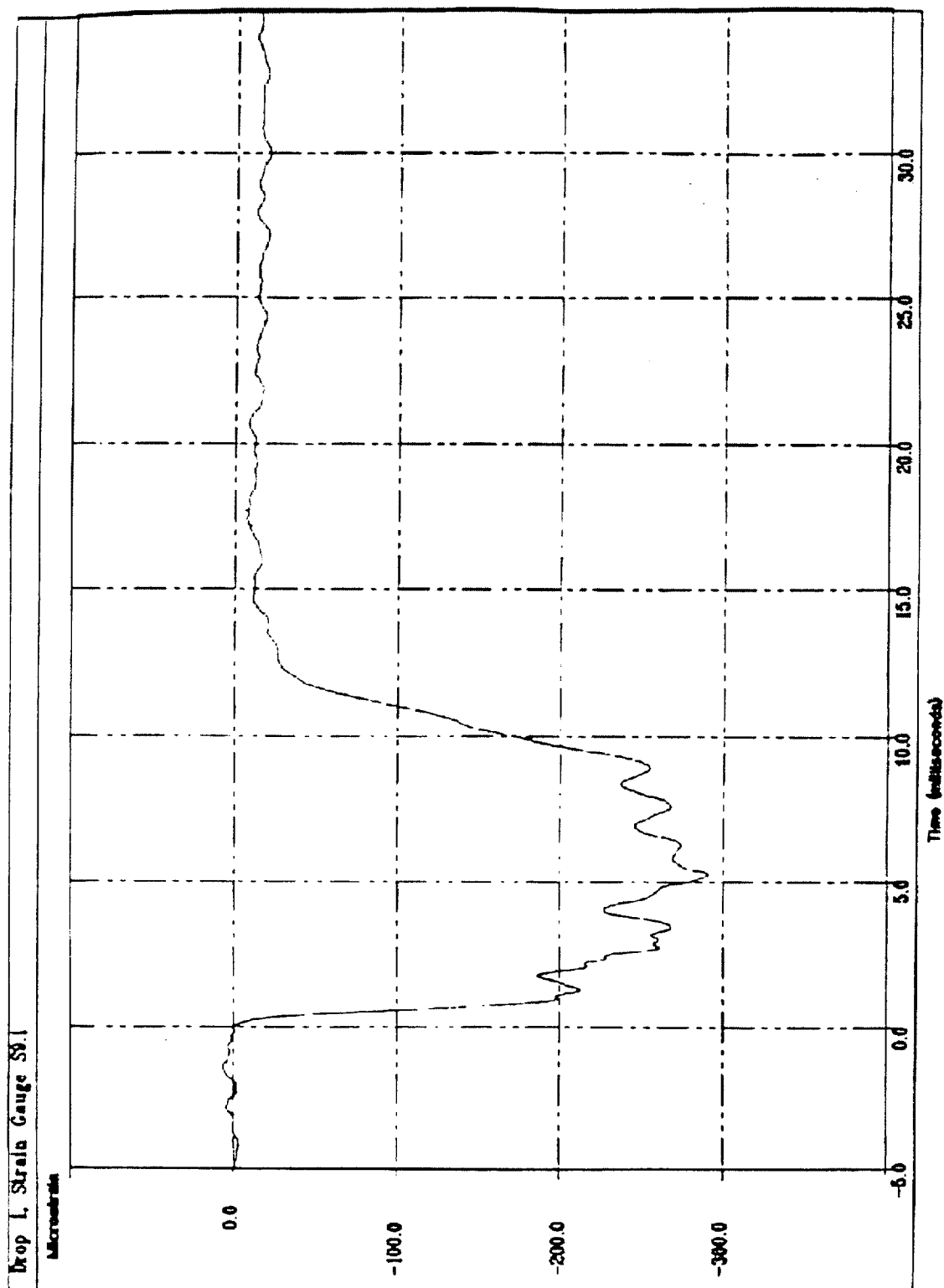


Figure 2.10.6-21 Top End Drop (Test No. 1 of Phase 1) Strain Data - Gauge S9.2 (Hoop)  
(Using Impact Limiters With Aluminum Shells)

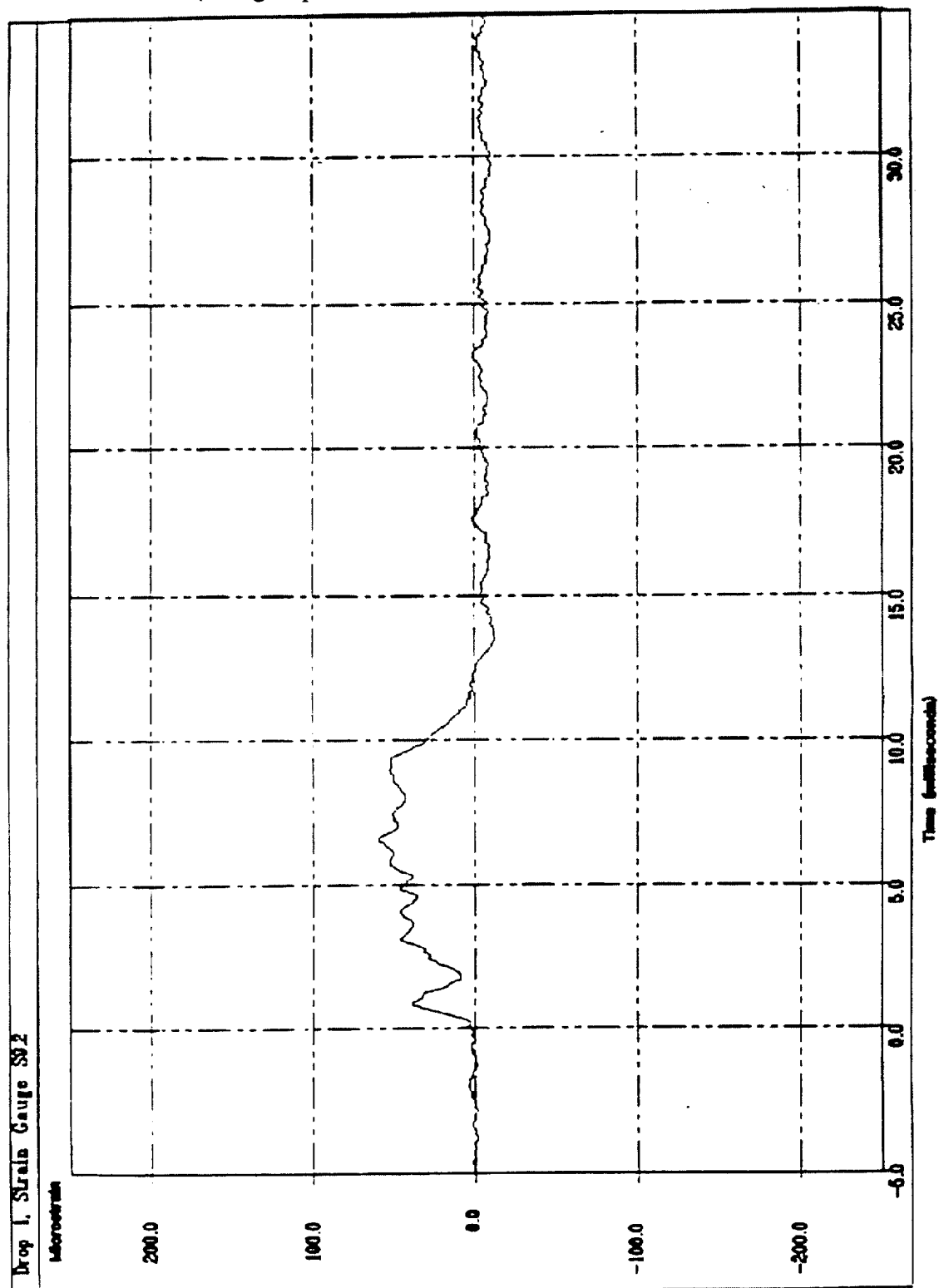


Figure 2.10.6-22 Top End Drop (Test No. 1 of Phase 1) Accelerometer Data - A2 (1 kHz Filter) (Using Impact Limiters With Aluminum Shells)

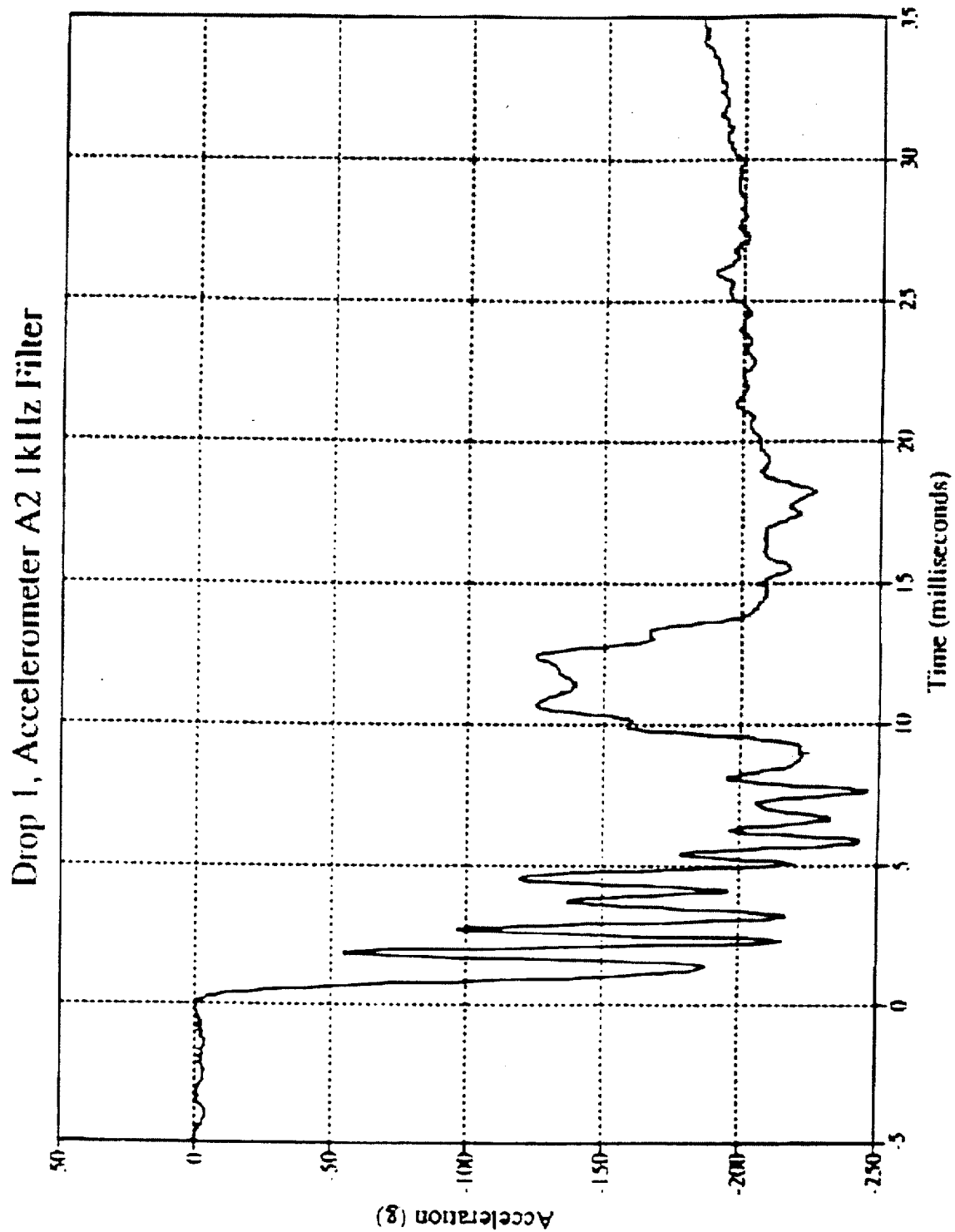


Figure 2.10.6-23 Side Drop Test (Test No. 3 of Phase 1) Accelerometer Data - A2 (Using Impact Limiters With Aluminum Shells)

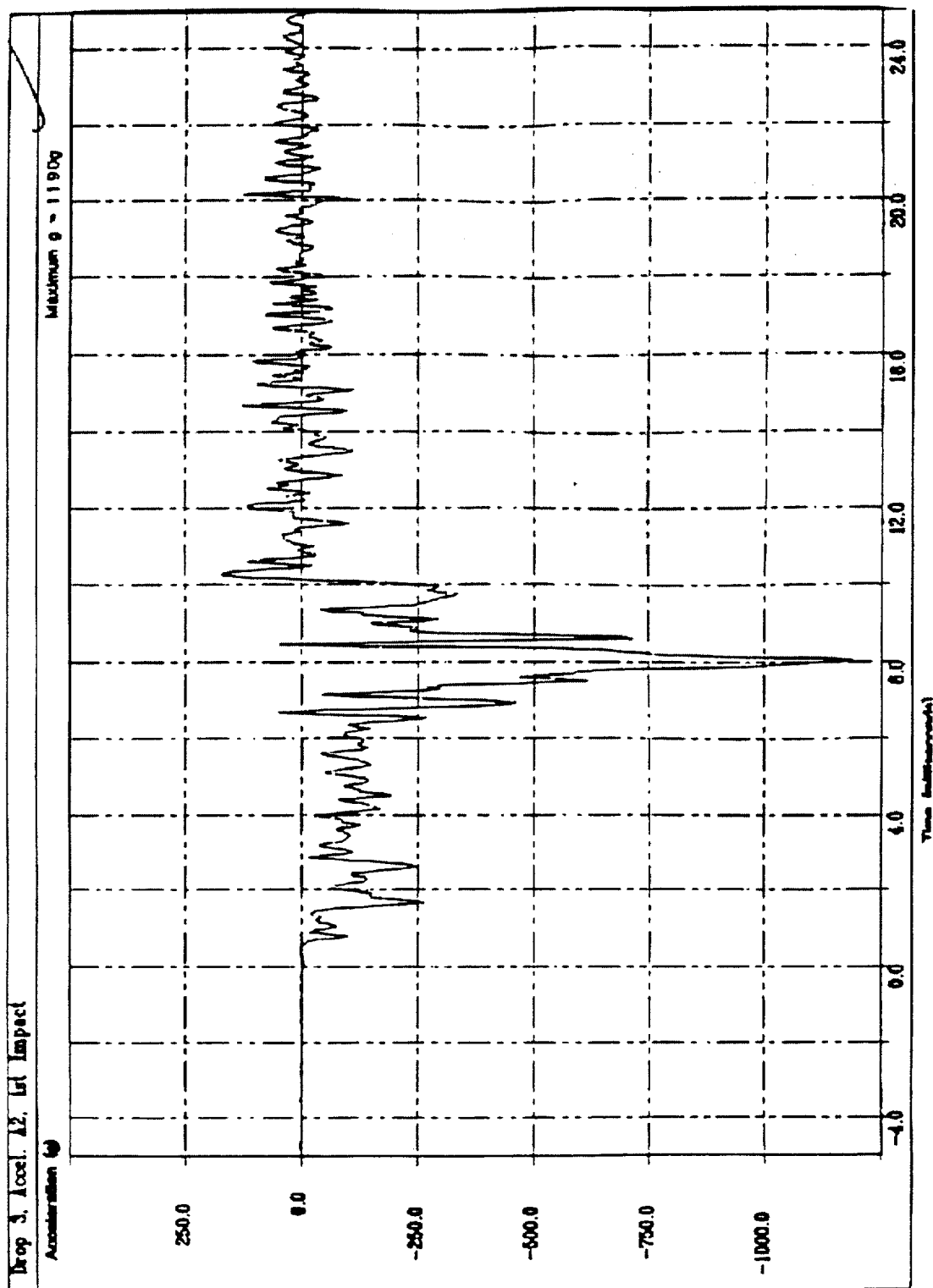


Figure 2.10.6-24 Side Drop Test (Test No. 3 of Phase 1) - Deformation of Support Disk No. 6 (Using Impact Limiters With Aluminum Shells)

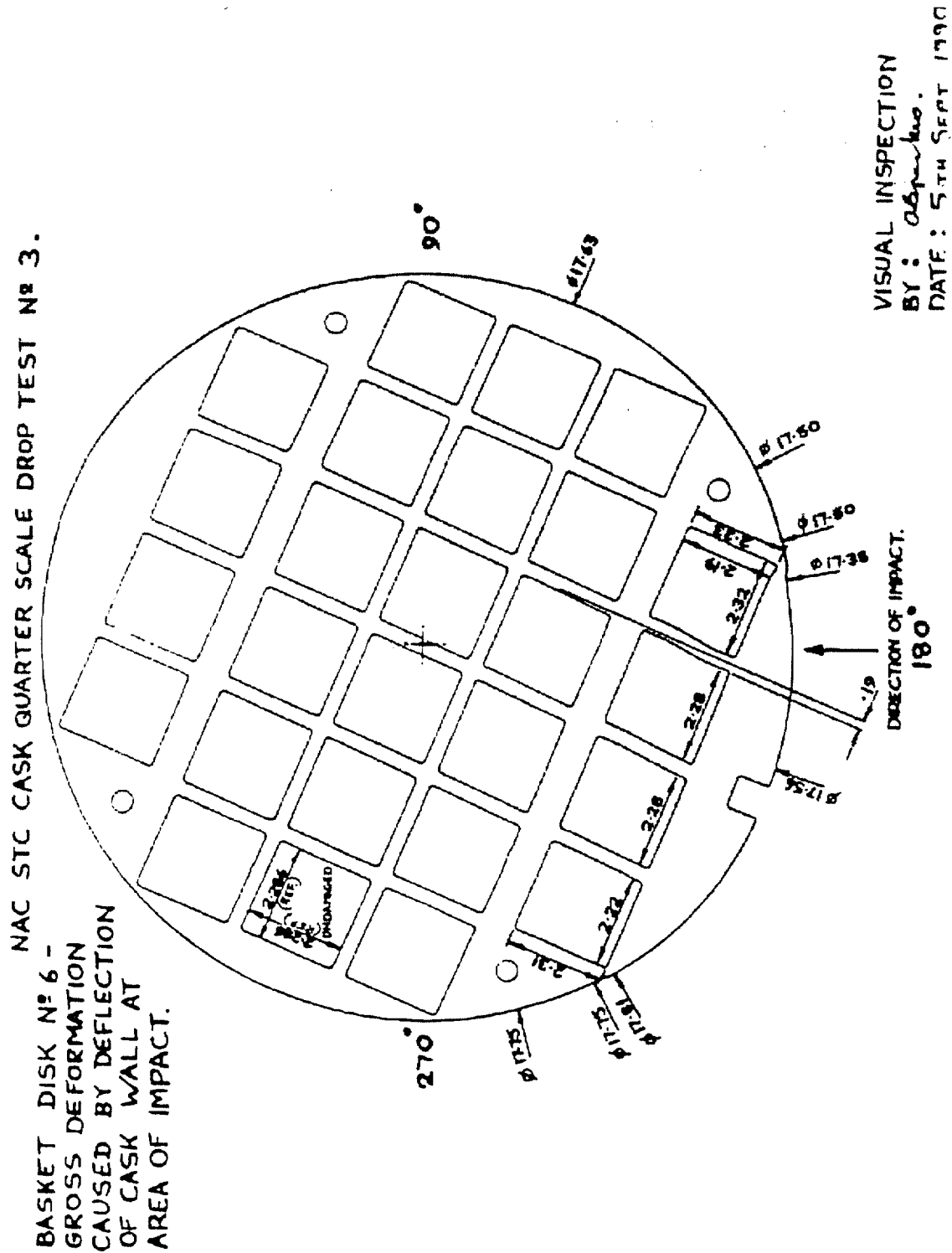




Figure 2.10.6-25 Top Corner Drop Test (Test No. 3 of Phase 3) - Impact Limiter Deformations

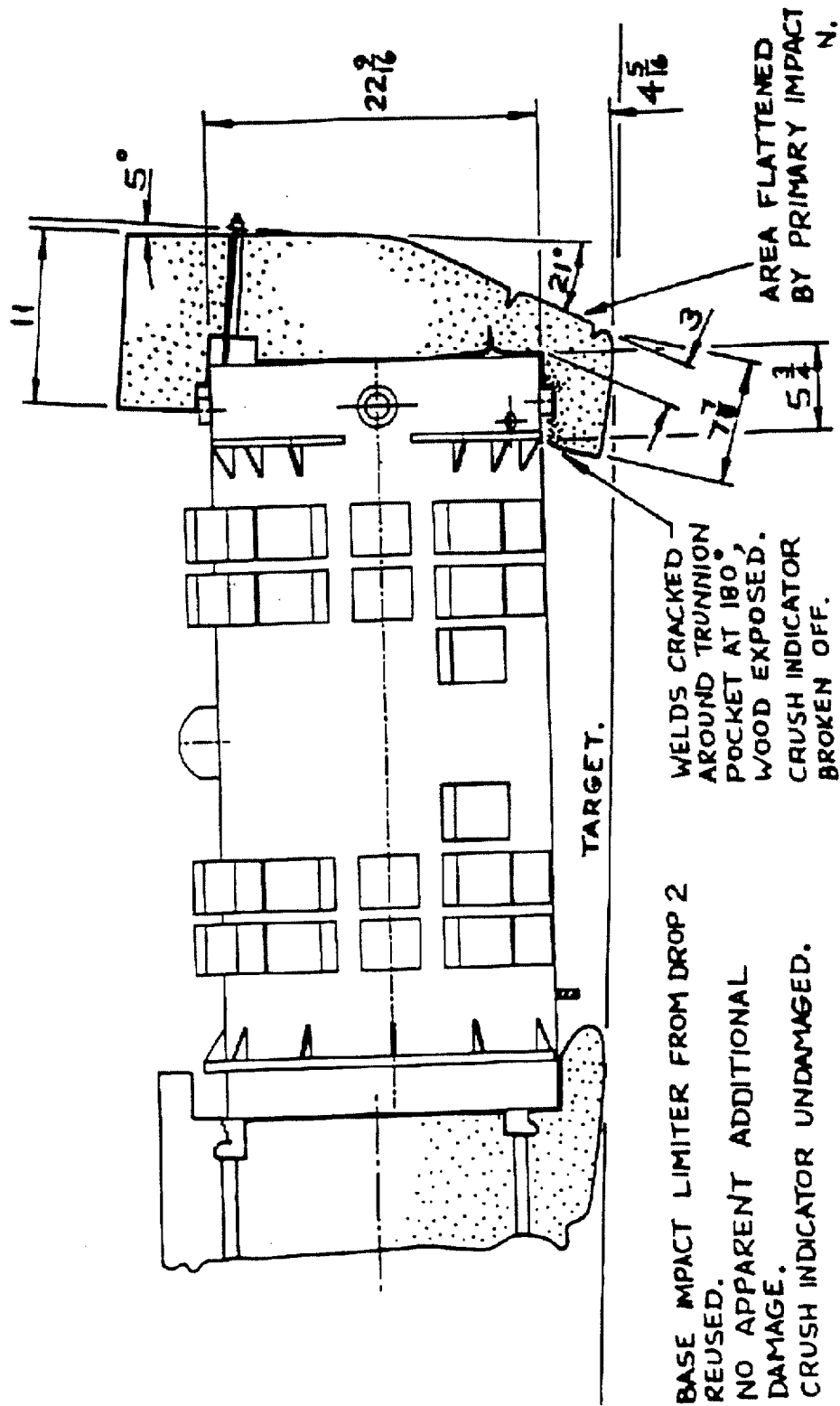


Figure 2.10.6-26 Top Corner Drop Test (Test No. 3 of Phase 3) Accelerometer Data - A1

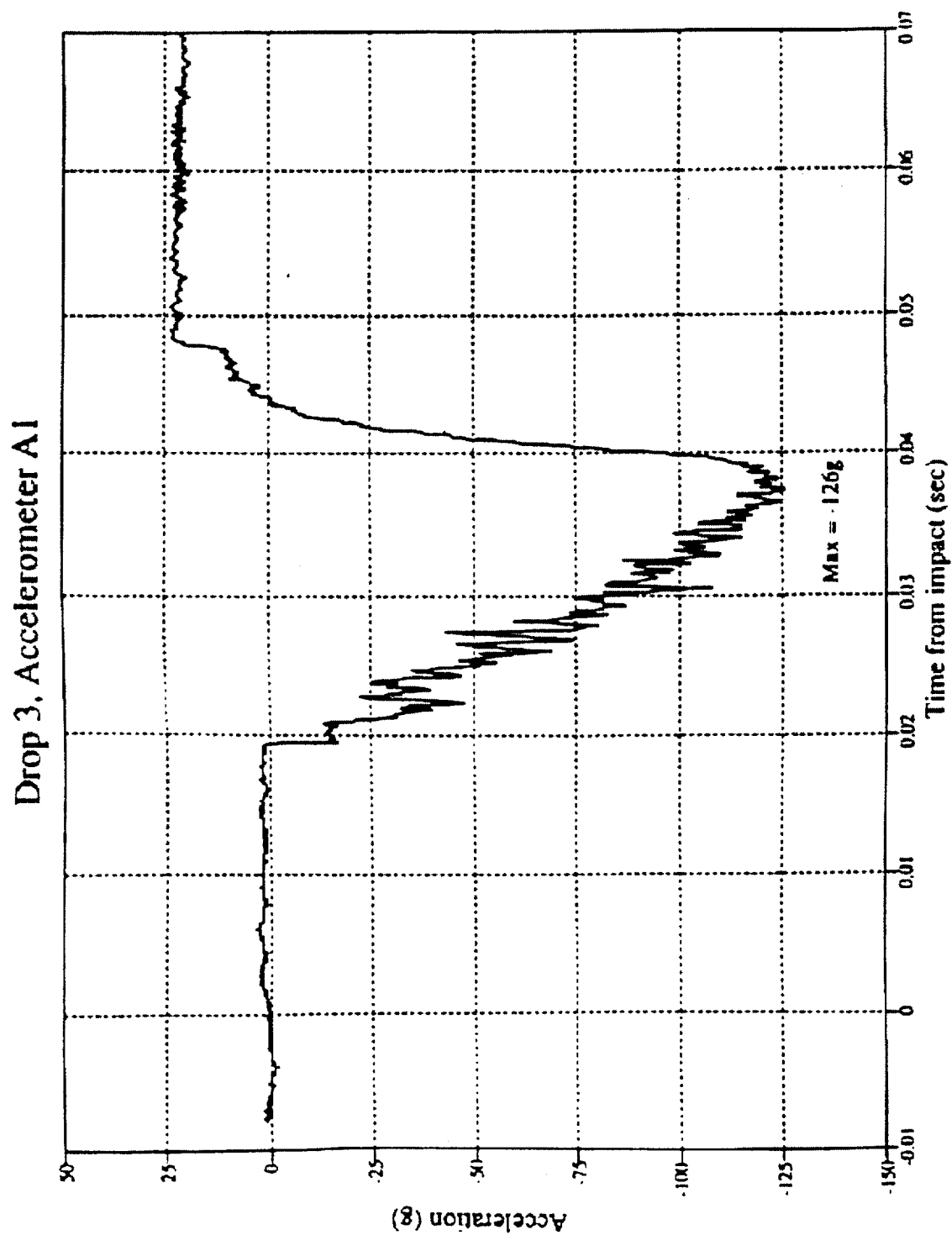


Figure 2.10.6-27 Bottom Oblique Drop Test (Test No. 1 of Phase 4) - Distorted Area of Upper Impact Limiter



Figure 2.10.6-28      Bottom Oblique Drop Test (Test No. 1 of Phase 4) - Impact Limiter  
Deformations

**FIGURE WITHHELD AS SENSITIVE  
UNCLASSIFIED INFORMATION**

Figure 2.10.6-29 Bottom Oblique Drop Test (Test No. 1 of Phase 4) - Impact Limiter Attachment Rods Post-Test Condition

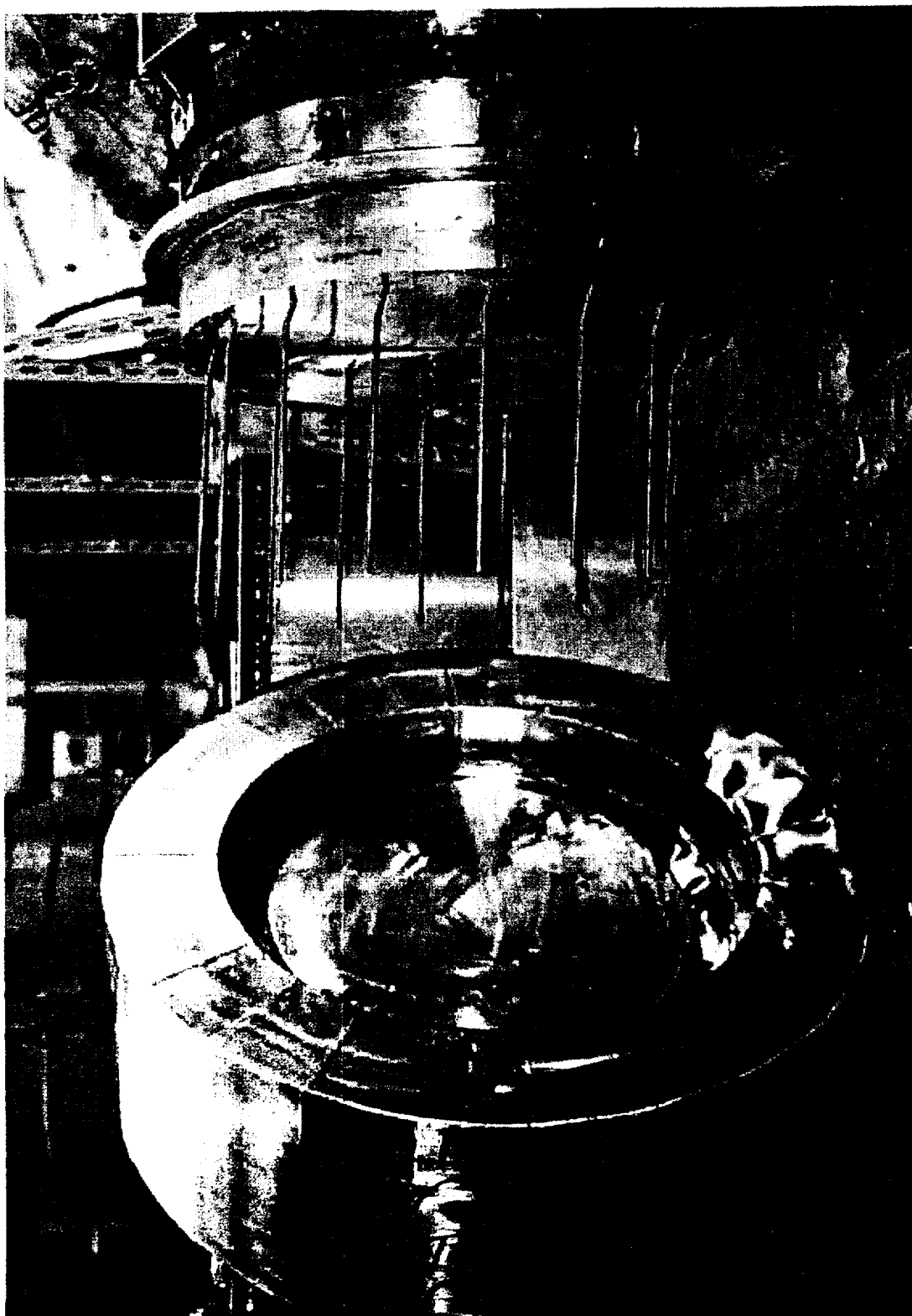


Figure 2.10.6-30 Bottom Oblique Drop Test (Test No. 1 of Phase 4) Strain Data - Gauge S9.1 (Axial)

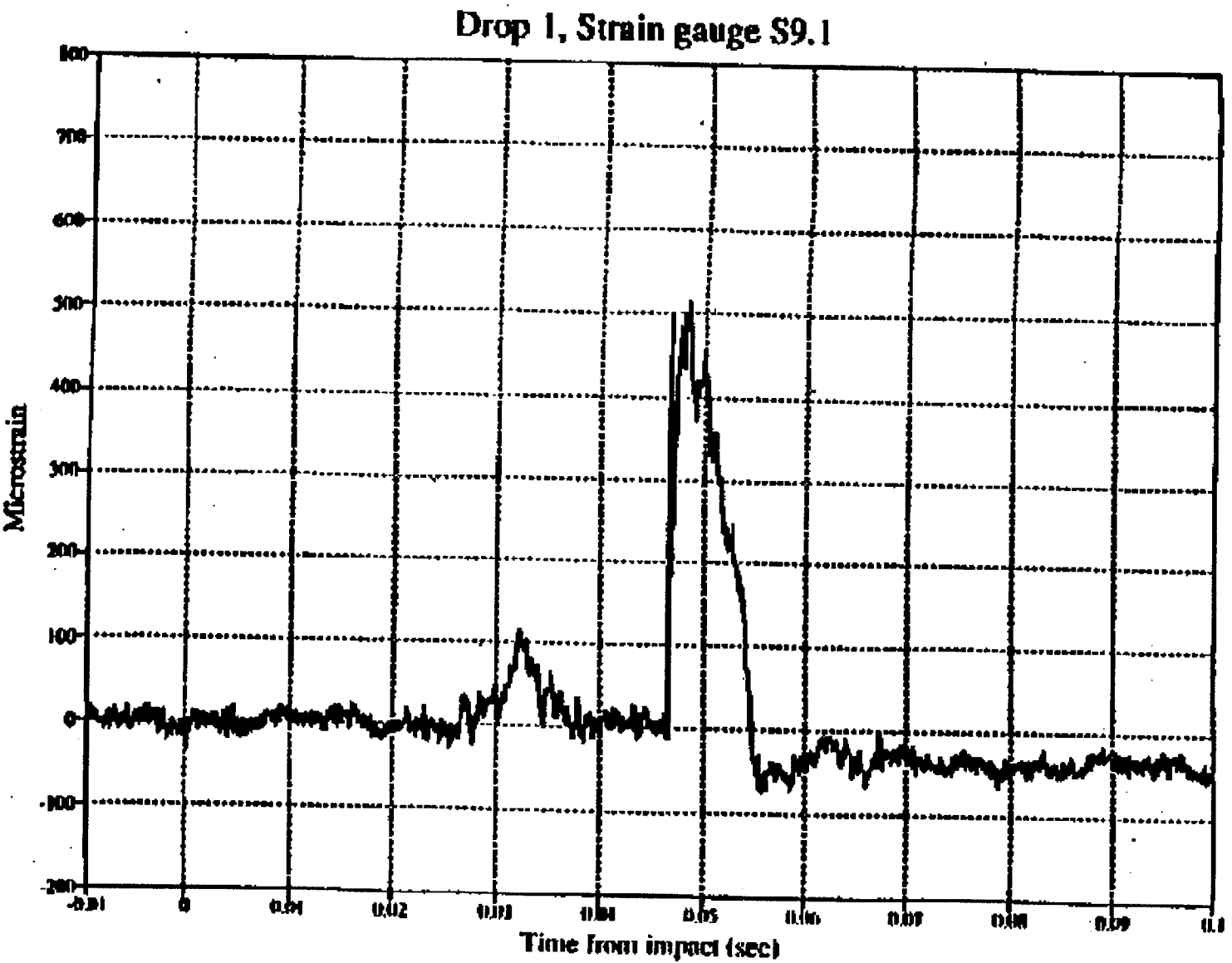


Figure 2.10.6-31 Bottom Oblique Drop Test (Test No. 1 of Phase 4) Strain Data - Gauge S9.2 (Hoop)

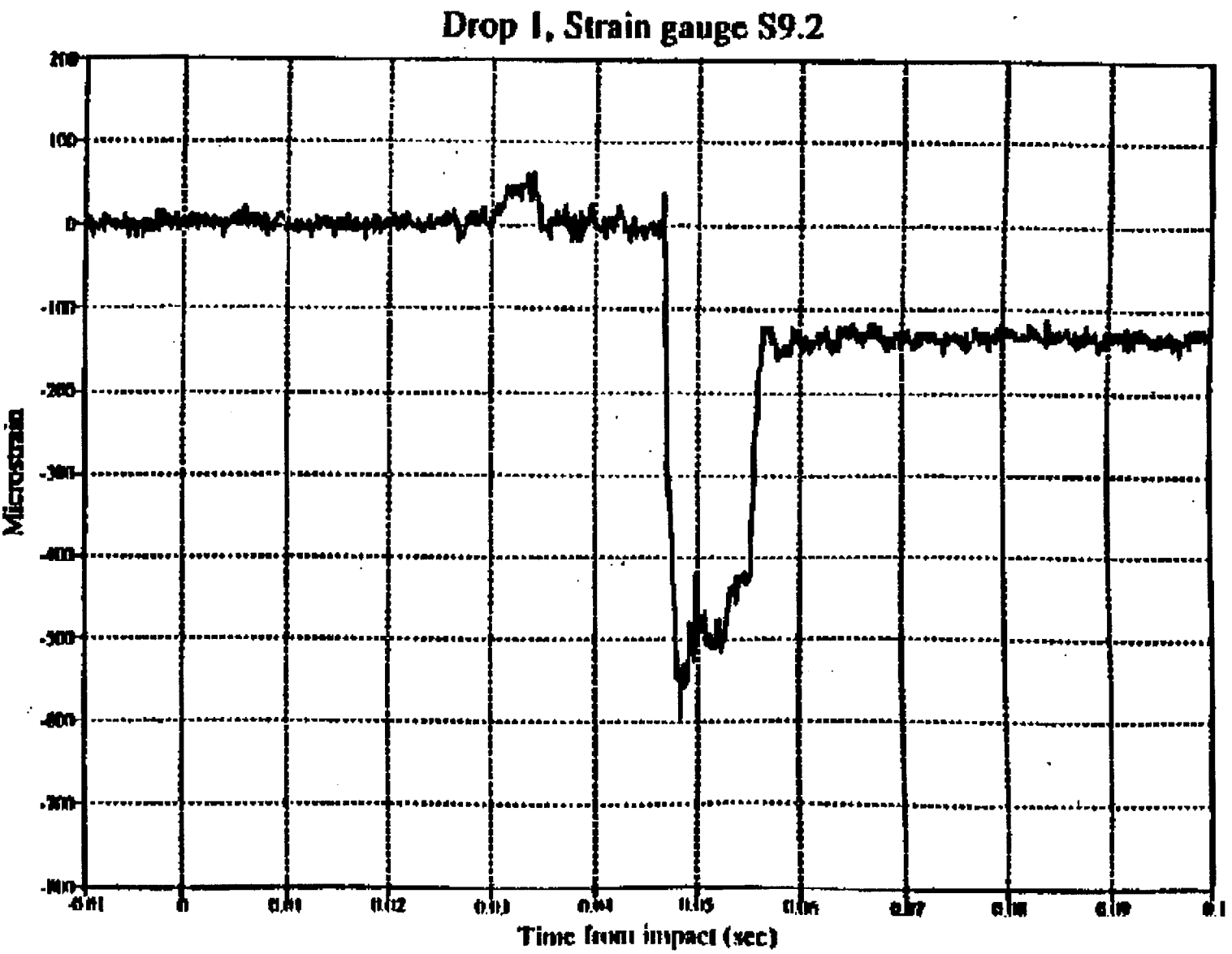


Figure 2.10.6-32 Bottom Oblique Drop Test (Test No. 1 of Phase 4) Accelerometer Data -  
AI (750 Hz Filter)

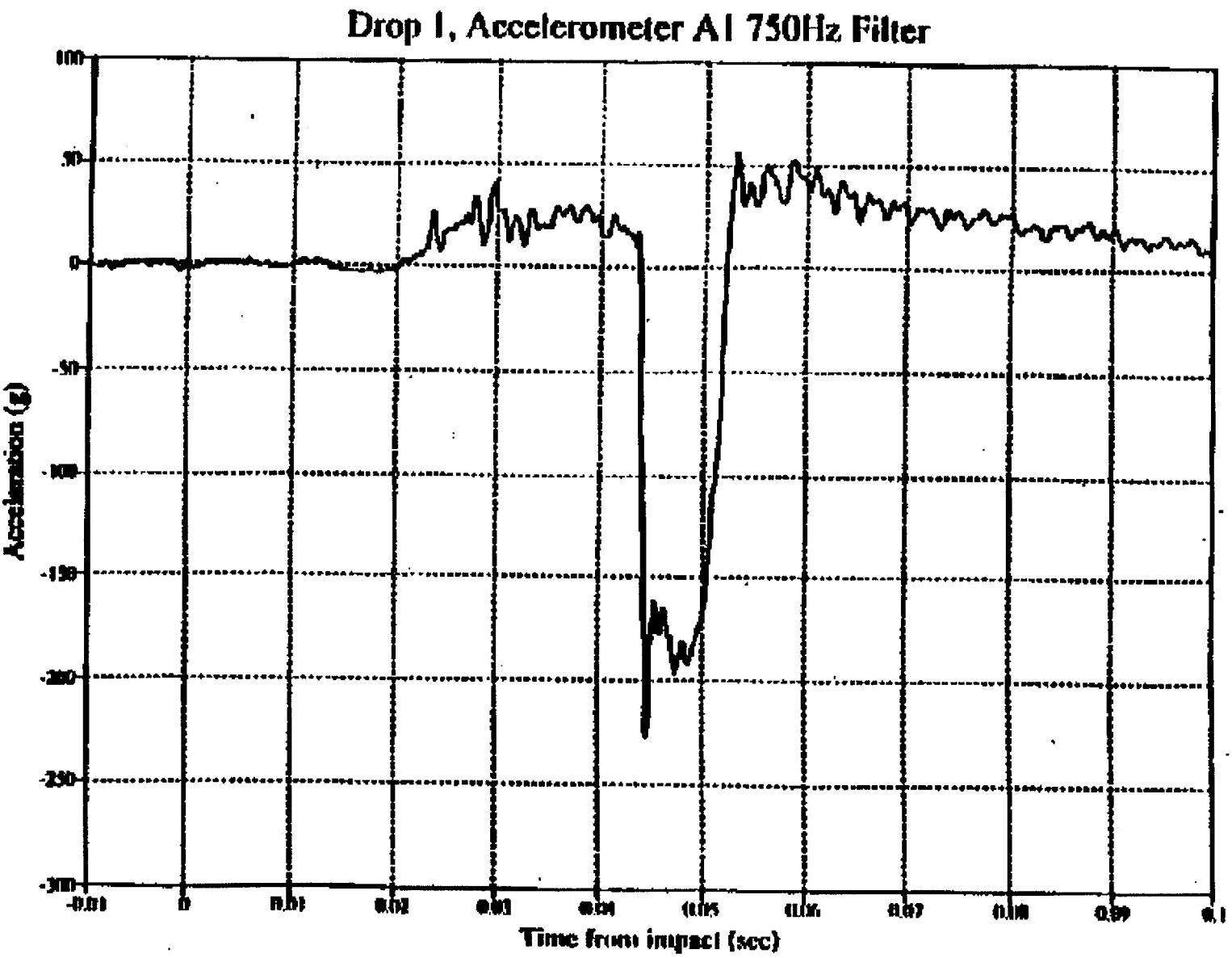




Figure 2.10.6-33 Bottom Oblique Drop Test (Test No. 1 of Phase 4) Accelerometer Data - A2 (750 Hz Filter)

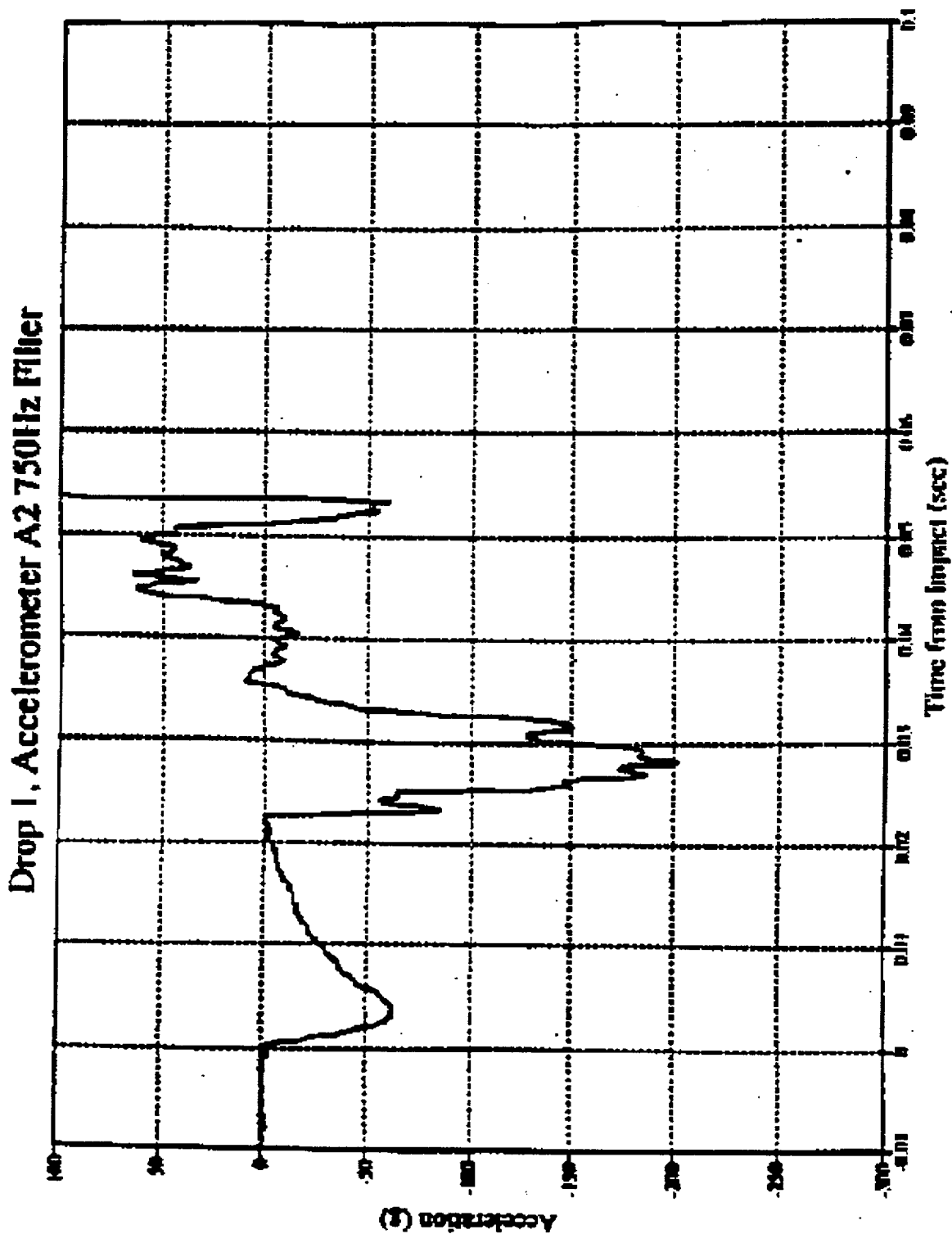


Figure 2.10.6-34 Side Drop Test (Test No. 2 of Phase 4) - Package Immediately After the Drop Test

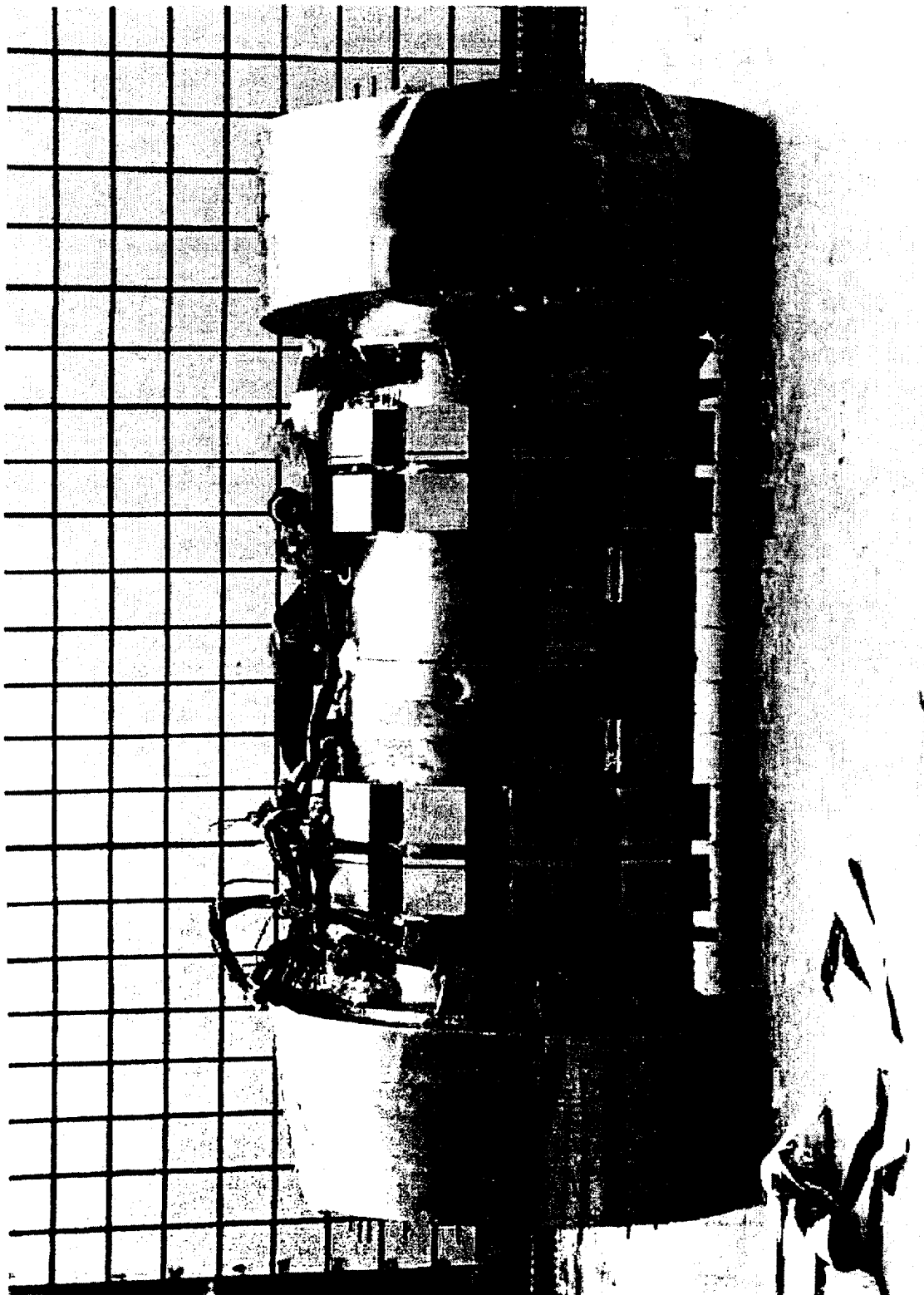


Figure 2.10.6-35 Side Drop Test (Test No. 2 of Phase 4) - Deformed Base Impact Limiter  
After Removal



Figure 2.10.6-36      Side Drop Test (Test No. 2 of Phase 4) - Impact Limiter Deformations

**FIGURE WITHHELD AS SENSITIVE  
UNCLASSIFIED INFORMATION**

Figure 2.10.6-37 Side Drop Test (Test No. 2 of Phase 4) Strain Data - Gauge S9.1 (Axial)

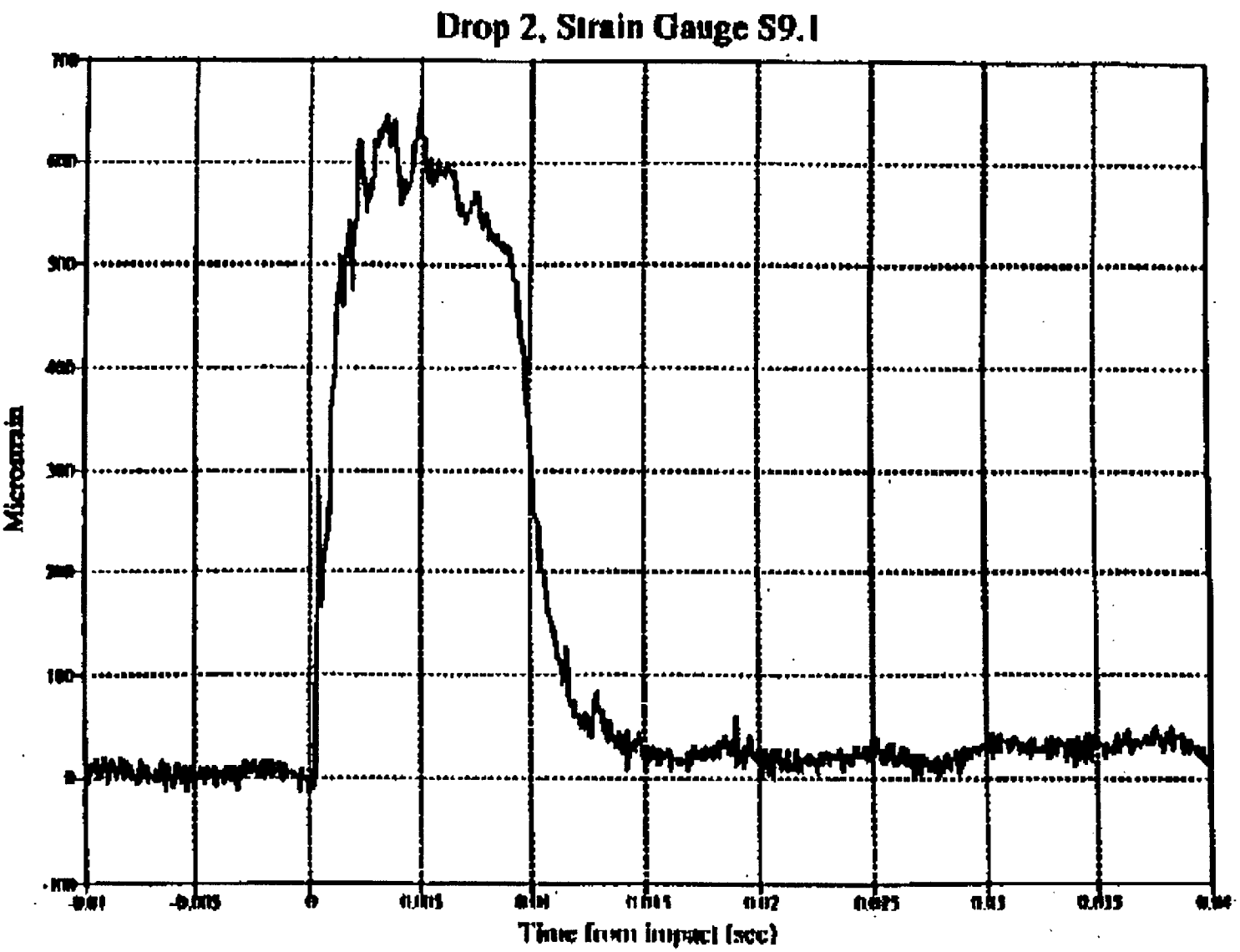


Figure 2.10.6-38

Side Drop Test (Test No. 2 of Phase 4) Strain Data - Gauge S9.2 (Hoop)

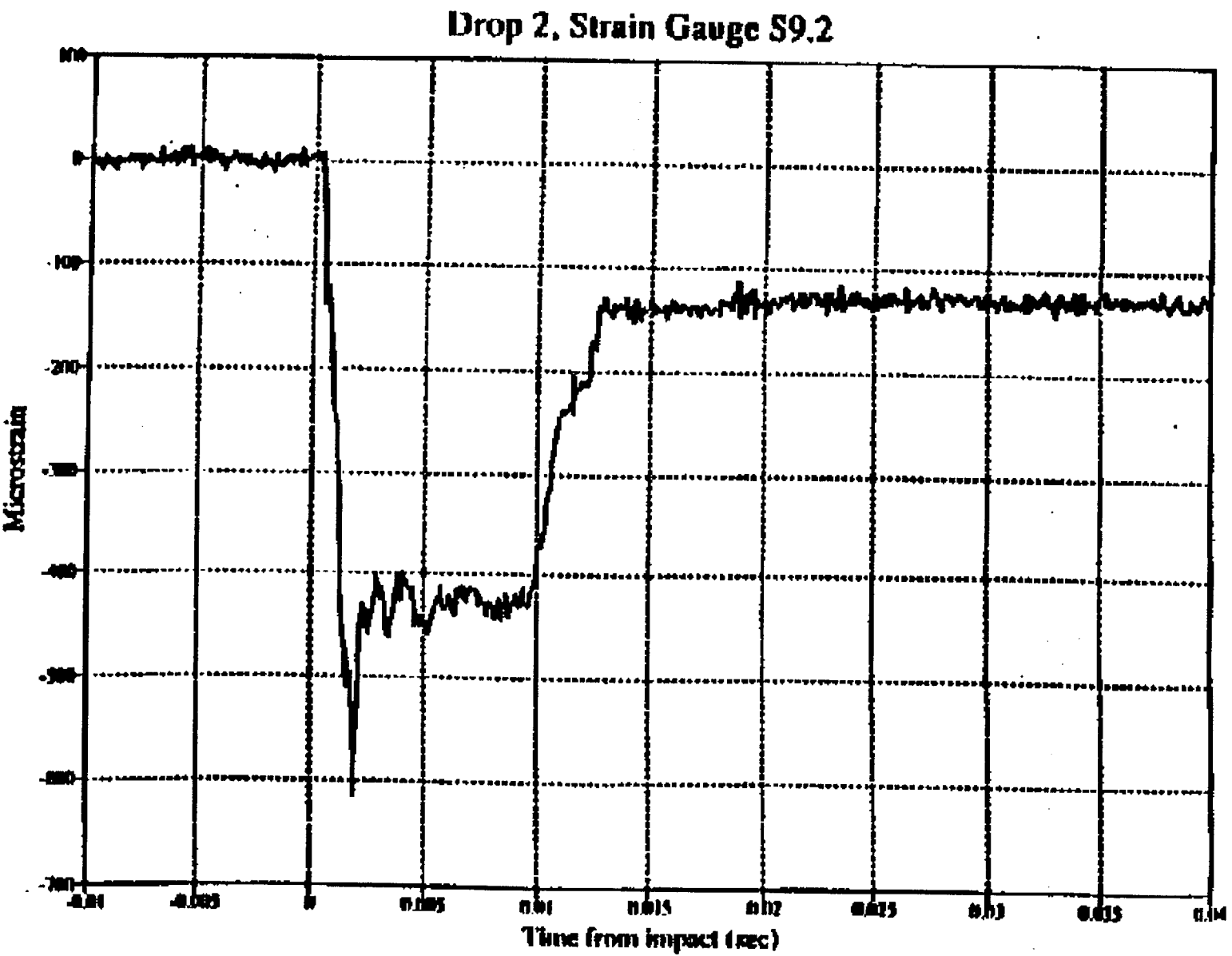


Figure 2.10.6-39 Side Drop Test (Test No. 2 of Phase 4) Accelerometer Data - A1 (1 KHz Filter)

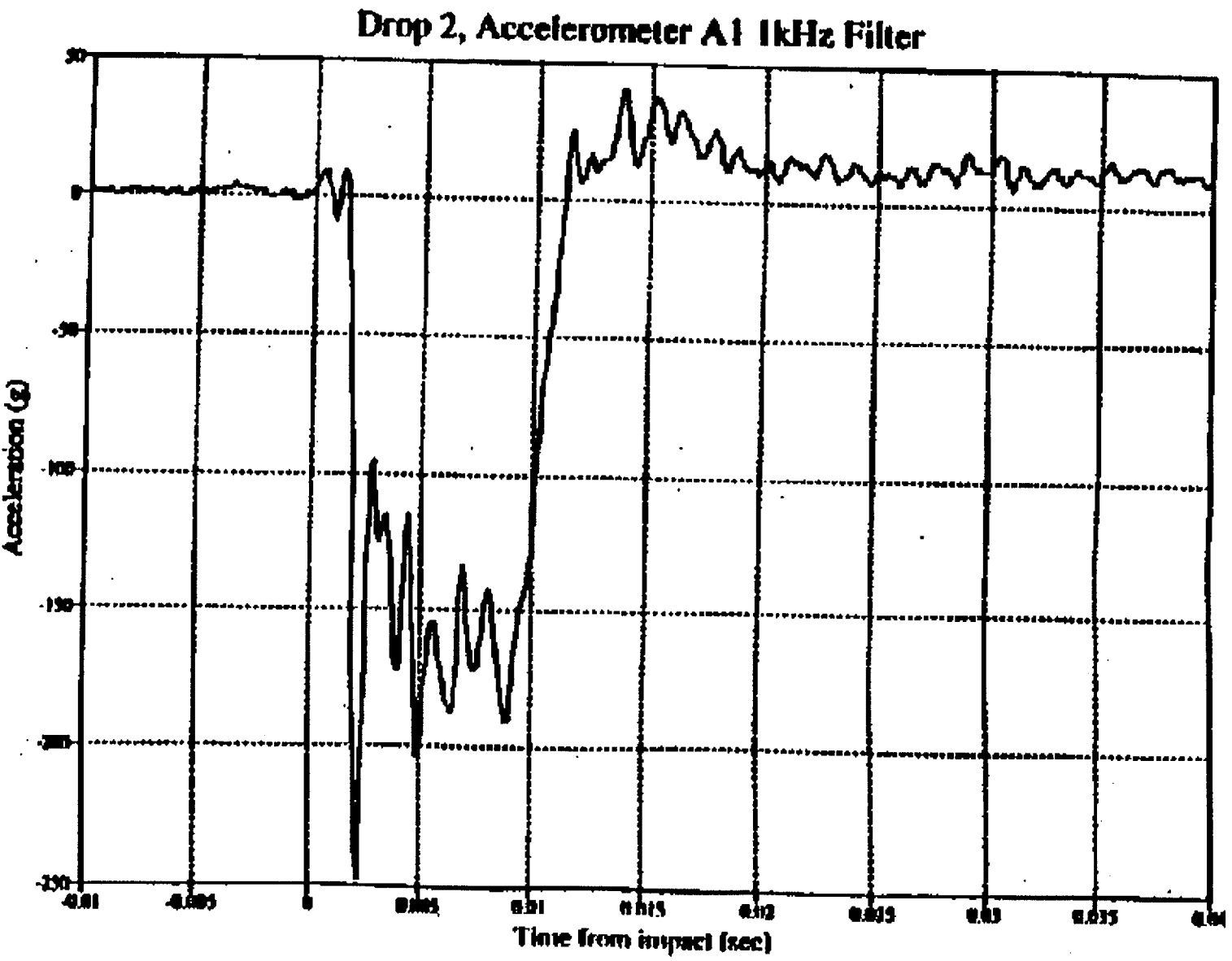


Figure 2.10.6-40 Side Drop Test (Test No. 2 of Phase 4) Accelerometer Data - A2 (750 Hz Filter)

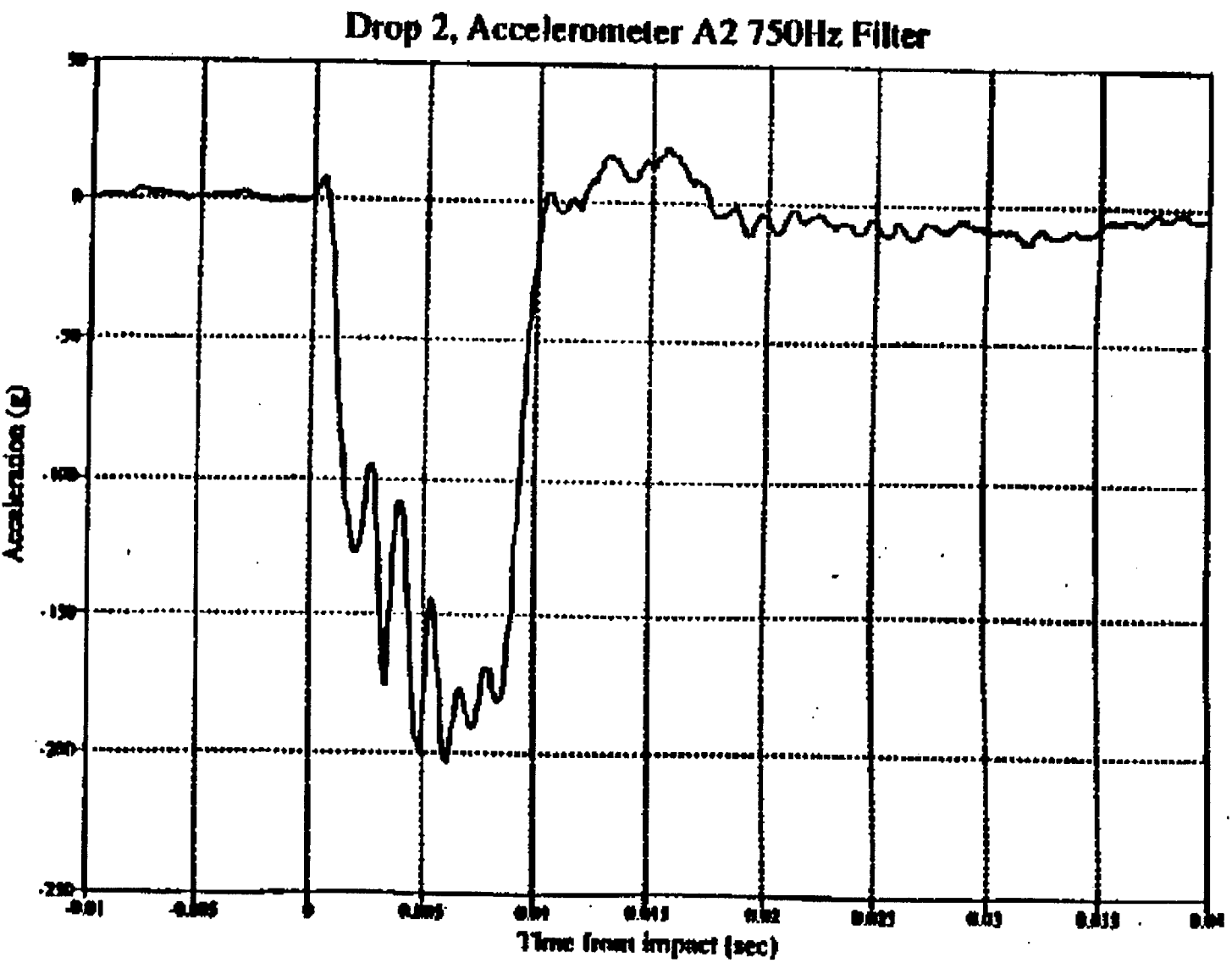




Table 2.10.6-1 Comparison of Full-Scale Deceleration Values for 30-Foot Drop Impacts

Drop Orientation	30-Foot Drop Deceleration (g)				
	RBCUBED <sup>1</sup> (Cold)	RBCUBED <sup>1</sup> (Hot)	Quasi-Static <sup>2</sup> Test	Drop <sup>3</sup> Test	Design <sup>4</sup>
End (0°)	44.6	56.1	54.8	55.6	56.1
Corner (24°)	44.0	49.3	32.6	29.2	55.0
Oblique (75°)	29.9	24.0	-	53.8	55.0
Side (90°)	51.7	51.3	45.6	51.3	55.0

<sup>1</sup> Impact g-loads calculated by RBCUBED (NAC's proprietary Impact Limiter Analysis Program).

<sup>2</sup> Extrapolated from eighth-scale model impact limiter quasi-static compression tests. Details are provided in Section 2.10.6.4.

<sup>3</sup> Extrapolated from quarter-scale model 30-foot drop test results. Details are provided in Section 2.10.6.5.

<sup>4</sup> Design g-load values used in the cask and fuel basket analyses.

Table 2.10.6-2      Top End Drop - Test Data (Test No. 1 of Phase 1)

CASK BODY DATA

Maximum Stress (ksi) and Location	8.6	@ Location 9
--------------------------------------	-----	--------------

Maximum Hoop strain (microstrain) and Location	80	@ Location 9
---	----	--------------

Maximum Acceleration (g) at Location 1 1,000 Hz filter	217
---	-----

Maximum Acceleration (g) at Location 2 1,000 Hz filter	247
---	-----

Pretest Cavity Conditions

Pressure (bar)	3.276
----------------	-------

Temperature (C)	93.6
-----------------	------

Post-Test Cavity Pressure (bar)

Pressure (bar)	3.283
----------------	-------

Temperature (C)	94.6
-----------------	------

IMPACT LIMITER DATA

Maximum Crush Stroke (inches)

Top limiter	2.11
-------------	------

Bottom Limiter	-
----------------	---

Crush strain	23%
--------------	-----

Table 2.10.6-3 Permanent Strains Side Drop Test Using Impact Limiters With Aluminum Shells (Test No. 3 of Phase 1)

Location	Axial Plastic Strain (microstrain)	Hoop Plastic Strain (microstrain)	Equivalent Plastic Strain (microstrain)
1	-113	16	122
2	-48	-170	152
3	387	-1279	1510
4	-216	162	328
5	1121	-431	1388
6	601	-1434	1811
7	-145	-83	126
8	-78	-295	265
	-284	338	381
9	500	-963	1288

Table 2.10.6-4 Cask Body and Outer Lid Pretest/Post-Test Metrology Data for Phase 1 Testing

Note: The Points of measurements are identified in Figure 2.10.6-15.

PRETEST METROLOGY MEASUREMENTS FOR THE CASK BODY

<u>Angle</u>	<u>K1</u>	<u>K2</u>	<u>K3</u>	<u>K4</u>	<u>D1</u>	<u>D2</u>	<u>D3</u>
0°/180°	17.746	17.752	17.746	17.680	21.657	21.686	21.671
45°/225°	17.739	17.745	17.742	17.716	21.680	Not Made	21.669
90°/270°	17.731	17.730	17.729	17.673	21.691	21.700	21.663
135°/315°	17.752	17.764	17.746	17.717	21.691	21.700	21.655

POST-TEST METROLOGY MEASUREMENTS FOR THE CASK BODY

<u>Angle</u>	<u>K1</u>	<u>K2</u>	<u>K3</u>	<u>K4</u>	<u>D1</u>	<u>D2</u>	<u>D3</u>
0°/180°	17.601	17.605	17.494	17.664	21.585	21.541	21.398
45°/225°	17.814	17.823	17.869	17.751	21.763	Not Made	21.805
90°/270°	17.759	17.827	17.779	17.705	21.720	21.796	21.712
135°/315°	17.780	17.731	17.765	17.698	21.727	21.660	21.689

Table 2.10.6-5 Fuel Basket Support Disk No. 12 Pretest Metrology Data for Phase 1 Testing

Note: The points of measurement are identified in Figure 2.10.6-16.

NAC STC CASK QUARTER SCALE DROP TEST.  
PRE-TEST BASKET DISC MEASUREMENTS - DISC N° 12.

WIDTH OF MED POSITION 1	WIDTH OF MED POSITION 12	POSITION No 1	POSITION No 9	POSITION No 10	DISC PT	θ	R	Z
ACTUAL 0.3732	ACTUAL 0.3732	ACTUAL 0.3732 ACTUAL 0.3732 ACTUAL 0.3732	ACTUAL 0.3732 ACTUAL 0.3732 ACTUAL 0.3732	ACTUAL 0.3732 ACTUAL 0.3732 ACTUAL 0.3732	23	0	8-40	-0.0057
WIDTH OF MED POSITION 2	WIDTH OF MED POSITION 13	ACTUAL 0.3732	ACTUAL 0.3732	ACTUAL 0.3732	28	315	8-40	0.0013
ACTUAL 0.3732	ACTUAL 0.3732	ACTUAL 0.3732	ACTUAL 0.3732	ACTUAL 0.3732	25	0	5-60	-0.0071
WIDTH OF MED POSITION 3	WIDTH OF MED POSITION 14	ACTUAL 0.3732	ACTUAL 0.3732	ACTUAL 0.3732	26	45	8-40	-0.0002
ACTUAL 0.3732	ACTUAL 0.3732	ACTUAL 0.3732	ACTUAL 0.3732	ACTUAL 0.3732	27	315	6-00	-0.0028
WIDTH OF MED POSITION 4	WIDTH OF MED POSITION 15	ACTUAL 0.3732	ACTUAL 0.3732	ACTUAL 0.3732	28	45	6-00	0.0004
ACTUAL 0.3732	ACTUAL 0.3732	ACTUAL 0.3732	ACTUAL 0.3732	ACTUAL 0.3732	29	270	8-40	0.0014
WIDTH OF MED POSITION 5	WIDTH OF MED POSITION 16	ACTUAL 0.3732	ACTUAL 0.3732	ACTUAL 0.3732	30	270	5-32	-0.0028
ACTUAL 0.3732	ACTUAL 0.3732	ACTUAL 0.3732	ACTUAL 0.3732	ACTUAL 0.3732	31	90	8-40	0.0270
WIDTH OF MED POSITION 6	WIDTH OF MED POSITION 17	ACTUAL 0.3732	ACTUAL 0.3732	ACTUAL 0.3732	32	270	6-00	0.0021
ACTUAL 0.3732	ACTUAL 0.3732	ACTUAL 0.3732	ACTUAL 0.3732	ACTUAL 0.3732	33	225	8-40	0.0053
WIDTH OF MED POSITION 7	WIDTH OF MED POSITION 18	ACTUAL 0.3732	ACTUAL 0.3732	ACTUAL 0.3732	34	200	5-60	0.0131
ACTUAL 0.3732	ACTUAL 0.3732	ACTUAL 0.3732	ACTUAL 0.3732	ACTUAL 0.3732	35	135	8-40	0.0347
WIDTH OF MED POSITION 8	WIDTH OF MED POSITION 19	ACTUAL 0.3732	ACTUAL 0.3732	ACTUAL 0.3732	36	180	8-00	0.0211
ACTUAL 0.3732	ACTUAL 0.3732	ACTUAL 0.3732	ACTUAL 0.3732	ACTUAL 0.3732	13	285	1-86	0.0005
WIDTH OF MED POSITION 9	WIDTH OF MED POSITION 20	ACTUAL 0.3732	ACTUAL 0.3732	ACTUAL 0.3732	FOR LOCATION OF EACH POSITION SEE FIGURE 0/4.			
ACTUAL 0.3732	ACTUAL 0.3732	ACTUAL 0.3732	ACTUAL 0.3732	ACTUAL 0.3732				
WIDTH OF MED POSITION 10	WIDTH OF MED POSITION 21	ACTUAL 0.3732	ACTUAL 0.3732	ACTUAL 0.3732	INSPECTION DATE: 1st AUG, 1990 BY: D. STEWART ALL DIMS. IN INCHES.			
ACTUAL 0.3732	ACTUAL 0.3732	ACTUAL 0.3732	ACTUAL 0.3732	ACTUAL 0.3732				
WIDTH OF MED POSITION 11	WIDTH OF MED POSITION 22	ACTUAL 0.3732	ACTUAL 0.3732	ACTUAL 0.3732				
ACTUAL 0.3732	ACTUAL 0.3732	ACTUAL 0.3732	ACTUAL 0.3732	ACTUAL 0.3732				

Table 2.10.6-6 Fuel Basket Support Disk No. 6 Post-Test Metrology Data for Phase 1 Test 3

Note: The points of measurement are identified in Figure 2.10.6-16.

NAC STC CASK QUARTER SCALE DROP TEST.  
POST-TEST BASKET DISC MEASUREMENTS - DISC NO 6.

POINT NO	θ	R	Z
23	0	0.40	0.012
24	315	0.40	0.001
25	0	0.40	0.000
26	45	0.40	0.000
27	315	0.40	0.004
28	45	0.40	0.000
29	270	0.40	0.000
30	270	0.32	0.000
31	30	0.40	0.002
32	270	0.40	0.000
33	315	0.40	0.000
34	180	0.40	0.004
35	135	0.40	0.004
36	180	0.40	0.007
37	225	0.40	0.002

POSITION NO 1	POSITION NO 2	POSITION NO 3	POSITION NO 18
AXIS X ACTUAL -0.000	AXIS X ACTUAL -0.000	AXIS X ACTUAL -0.000	AXIS X ACTUAL -0.000
AXIS Y ACTUAL -0.000	AXIS Y ACTUAL -0.000	AXIS Y ACTUAL -0.000	AXIS Y ACTUAL -0.000
AXIS Z ACTUAL 0.000	AXIS Z ACTUAL 0.000	AXIS Z ACTUAL 0.000	AXIS Z ACTUAL 0.000
POSITION NO 4	POSITION NO 5	POSITION NO 6	POSITION NO 19
AXIS X ACTUAL -0.000	AXIS X ACTUAL -0.000	AXIS X ACTUAL -0.000	AXIS X ACTUAL -0.000
AXIS Y ACTUAL -0.000	AXIS Y ACTUAL -0.000	AXIS Y ACTUAL -0.000	AXIS Y ACTUAL -0.000
AXIS Z ACTUAL 0.000	AXIS Z ACTUAL 0.000	AXIS Z ACTUAL 0.000	AXIS Z ACTUAL 0.000
POSITION NO 7	POSITION NO 8	POSITION NO 9	POSITION NO 20
AXIS X ACTUAL -0.000	AXIS X ACTUAL -0.000	AXIS X ACTUAL -0.000	AXIS X ACTUAL -0.000
AXIS Y ACTUAL -0.000	AXIS Y ACTUAL -0.000	AXIS Y ACTUAL -0.000	AXIS Y ACTUAL -0.000
AXIS Z ACTUAL 0.000	AXIS Z ACTUAL 0.000	AXIS Z ACTUAL 0.000	AXIS Z ACTUAL 0.000
POSITION NO 10	POSITION NO 11	POSITION NO 12	POSITION NO 21
AXIS X ACTUAL -0.000	AXIS X ACTUAL -0.000	AXIS X ACTUAL -0.000	AXIS X ACTUAL -0.000
AXIS Y ACTUAL -0.000	AXIS Y ACTUAL -0.000	AXIS Y ACTUAL -0.000	AXIS Y ACTUAL -0.000
AXIS Z ACTUAL 0.000	AXIS Z ACTUAL 0.000	AXIS Z ACTUAL 0.000	AXIS Z ACTUAL 0.000
POSITION NO 13	POSITION NO 14	POSITION NO 15	POSITION NO 22
AXIS X ACTUAL -0.000	AXIS X ACTUAL -0.000	AXIS X ACTUAL -0.000	AXIS X ACTUAL -0.000
AXIS Y ACTUAL -0.000	AXIS Y ACTUAL -0.000	AXIS Y ACTUAL -0.000	AXIS Y ACTUAL -0.000
AXIS Z ACTUAL 0.000	AXIS Z ACTUAL 0.000	AXIS Z ACTUAL 0.000	AXIS Z ACTUAL 0.000
POSITION NO 16	POSITION NO 17	POSITION NO 18	POSITION NO 23
AXIS X ACTUAL -0.000	AXIS X ACTUAL -0.000	AXIS X ACTUAL -0.000	AXIS X ACTUAL -0.000
AXIS Y ACTUAL -0.000	AXIS Y ACTUAL -0.000	AXIS Y ACTUAL -0.000	AXIS Y ACTUAL -0.000
AXIS Z ACTUAL 0.000	AXIS Z ACTUAL 0.000	AXIS Z ACTUAL 0.000	AXIS Z ACTUAL 0.000
POSITION NO 19	POSITION NO 20	POSITION NO 21	POSITION NO 24
AXIS X ACTUAL -0.000	AXIS X ACTUAL -0.000	AXIS X ACTUAL -0.000	AXIS X ACTUAL -0.000
AXIS Y ACTUAL -0.000	AXIS Y ACTUAL -0.000	AXIS Y ACTUAL -0.000	AXIS Y ACTUAL -0.000
AXIS Z ACTUAL 0.000	AXIS Z ACTUAL 0.000	AXIS Z ACTUAL 0.000	AXIS Z ACTUAL 0.000
POSITION NO 22	POSITION NO 23	POSITION NO 24	POSITION NO 25
AXIS X ACTUAL -0.000	AXIS X ACTUAL -0.000	AXIS X ACTUAL -0.000	AXIS X ACTUAL -0.000
AXIS Y ACTUAL -0.000	AXIS Y ACTUAL -0.000	AXIS Y ACTUAL -0.000	AXIS Y ACTUAL -0.000
AXIS Z ACTUAL 0.000	AXIS Z ACTUAL 0.000	AXIS Z ACTUAL 0.000	AXIS Z ACTUAL 0.000

WIDTH OF WEB POSITION 1	WIDTH OF WEB POSITION 18
ACTUAL 0.375	ACTUAL 0.375
WIDTH OF WEB POSITION 2	WIDTH OF WEB POSITION 19
ACTUAL 0.375	ACTUAL 0.375
WIDTH OF WEB POSITION 3	WIDTH OF WEB POSITION 20
ACTUAL 0.375	ACTUAL 0.375
WIDTH OF WEB POSITION 4	WIDTH OF WEB POSITION 21
ACTUAL 0.375	ACTUAL 0.375
WIDTH OF WEB POSITION 5	WIDTH OF WEB POSITION 22
ACTUAL 0.375	ACTUAL 0.375
WIDTH OF WEB POSITION 6	WIDTH OF WEB POSITION 23
ACTUAL 0.375	ACTUAL 0.375
WIDTH OF WEB POSITION 7	WIDTH OF WEB POSITION 24
ACTUAL 0.375	ACTUAL 0.375
WIDTH OF WEB POSITION 8	WIDTH OF WEB POSITION 25
ACTUAL 0.375	ACTUAL 0.375
WIDTH OF WEB POSITION 9	WIDTH OF WEB POSITION 26
ACTUAL 0.375	ACTUAL 0.375
WIDTH OF WEB POSITION 10	WIDTH OF WEB POSITION 27
ACTUAL 0.375	ACTUAL 0.375
WIDTH OF WEB POSITION 11	WIDTH OF WEB POSITION 28
ACTUAL 0.375	ACTUAL 0.375

FOR LOCATION OF EACH POSITION SEE FIGURE Q/4.	INSPECTION DATES: 30th AUG 1993 BY: B STEWART ALL DIMS IN INCHES
---	---

Note: The points of measurement are identified in Figure 2.10.6-16.

NAC ETC CASK QUARTER SCALE DROP TEST.  
POST-TEST BASKET DISC MEASUREMENTS - DISC # 12.

2.10.6-89

Table 2.10.6-8 Top Corner Drop - Test Data (Test No. 3 of Phase 3)

CASK BODY DATA

Maximum Stress (ksi) and Location	3.8	@ Location 9
--------------------------------------	-----	--------------

Maximum Hoop strain (microstrain) and Location	-
---	---

Maximum Vertical Acceleration (g) 4,000 Hz filter	127
--	-----

Maximum Cask lateral Acceleration (g) 4,000 Hz filter	107
--	-----

Pretest Cavity Conditions

Pressure (bar)	3.2114
Temperature (C)	46.8

Post-Test Cavity Pressure (bar)

Pressure (bar)	3.2045
Temperature (C)	45.3

IMPACT LIMITER DATA

Maximum Crush Stroke

Top limiter	6.4
Bottom Limiter	-

Maximum design stroke (inches)	9.07
--------------------------------	------



Table 2.10.6-9 Pin Puncture Drop Tests (Test Nos. 5 and 6 of Phase 3)

Pressure/Temperature Measurements

	Cask Body Midpoint	Location of Pin Impact	Outer Lid Center
Pretest			
pressure (bar)	3.0070		3.1397
temperature (F)	53.1		45.0
Post-test			
pressure	3.0020		<sup>1</sup>
temperature	45.9		

Metrology Data

Cask Midpoint Pin Puncture

Outer Diameter of Outer shell at pin puncture (inches)	21.30
Outer Diameter of Outer Shell at 5.62 inches from pin (inches) <sup>2</sup>	21.63
Inner Diameter of Inner Shell at pin puncture (inches)	17.509
Inner Diameter of Inner Shell at 5.62 inches from pin (inches) <sup>2</sup>	17.701

Cask Outer Lid Pin Puncture

Maximum out of plane measurement (inches)	
pretest	0.005
post-test	0.007

<sup>1</sup> The cavity valve was broken during the test.

<sup>2</sup> The 5.62 inches is measured in an axial direction parallel to the centerline of the cask body.

Table 2.10.6-10 Bottom Oblique Drop - Test Data (Test No. 1 of Phase 4)

CASK BODY DATA

Maximum Axial Stress (ksi) and Location	+10.41 @ Location 9
Maximum Hoop Stress (ksi) and Location	-12.49 @ Location 9
Maximum Permanent strain (microstrain) and Location	135 @ Location 9
Maximum Top End Acceleration (g)	225
Maximum Bottom End Acceleration (g)	205
Pretest Cavity Conditions	
Pressure (bar)	3.1903
Temperature (F)	47.8
Post-Test Cavity Pressure (bar)	
Pressure (bar)	3.1905
Temperature (F)	47.7

IMPACT LIMITER DATA

Maximum Crush Stroke (inches)	
Top limiter	2.41
Bottom Limiter	1.22
Maximum Permissible stroke (inches)	
Top limiter	3.22
Bottom limiter	3.22

Table 2.10.6-11 Cask Body and Outer Lid Pretest/Post-test Metrology Data for Phase 4 Testing

Pretest Metrology Data<sup>1</sup>

Angle	K1	K2	K3	K4	M	Ka
0°/180°	17.696	17.692	17.856	17.712	21.638	
30°/210°		17.730	17.720	17.716		17.732
90°/270°	17.742	17.778	17.732	17.666	21.619	
120°/300°		17.708	17.721	17.687		17.705

Post-test Metrology Data for the Oblique Drop (Test No. 1 of Phase 4)

Angle	K1	K2	K3	K4	M
0°/180°	17.694	17.692	17.857	17.705	21.618
90°/270°	17.743	17.787	17.741	17.675	21.614

Post-test Metrology Data for the Side Drop (Test No. 2 of Phase 4)

Angle	K1	K2	K3	K4	M
0°/180°	17.702	17.693	17.851	17.704	21.626
90°/270°	17.743	17.779	17.742	17.675	21.614

<sup>1</sup> Definition of dimensions and locations are shown in Figure 2.10.6-15.

Table 2.10.6-12      Side Drop - Test Data (Test No. 2 of Phase 4)

CASK BODY DATA

Maximum Axial Stress (ksi) and Location	+29.5 @ Location 6
Maximum Hoop Stress (ksi) and Location	+17.5 @ Location 6
Maximum Permanent strain (microstrain) and Location	135 @ Location 9
Maximum Top End Acceleration (g)	204
Maximum Bottom End Acceleration (g)	208
Pretest Cavity Conditions	
Pressure (bar)	3.1540
Temperature (F)	49.1
Post-Test Cavity Pressure (bar)	
Pressure (bar)	3.1526
Temperature (F)	49.1

IMPACT LIMITER DATA

Maximum Crush Stroke (inches)	
Top limiter	2.04
Bottom Limiter	2.16
Maximum Permissible stroke (inches)	
Top limiter	3.22
Bottom limiter	3.22

2.10.7 Redwood Impact Limiter Force-Deflection Curves and Data - Directly Loaded Fuel Configuration

As discussed in Section 2.10.6.1 and throughout this report, the center-of-gravity location and the cavity contents weight for the Yankee-MPC configuration of the NAC-STC are essentially identical to those of the directly loaded fuel configuration. Therefore, this evaluation is applicable to both contents configurations of the NAC-STC with the redwood and balsa wood impact limiters (referred to as the redwood impact limiter[s]) described in License Drawings 423-209 and 423-210 and in Section 2.6.7.4.1. The evaluation is not applicable to the balsa wood impact limiter described in License Drawings 423-257 and 423-258 and Section 2.6.7.4.2, used with the CY-MPC configuration. The two impact limiter configurations are described in Section 1.2.1.2.6.

2.10.7.1 Potential Energy and Cask Drop Impact Motion

It is stated in 10 CFR 71 that analyses must show that a spent-fuel shipping cask is capable of sustaining a normal condition test (a 1-foot free drop) followed by a hypothetical accident test (a 30-foot free drop). This has been interpreted to mean that impact limiters must be designed to absorb, or dissipate, the potential energy of the cask, if dropped in any orientation from 30 feet onto an unyielding surface. The cask would not be operated after the occurrence of a 1-foot drop until the impact limiter(s) had been replaced/repared.

The distance through which the cask free falls is measured from the nearest point on the cask (either impact limiter) to the unyielding surface. This ensures that the center of gravity will translate a minimum of 30 feet before an impact limiter contacts the unyielding surface. Additionally, it is assumed that the cask will always seek a stable orientation on both impact limiters after contacting the unyielding surface. After an end drop, for example, it is assumed that the cask tips over and reaches a stable horizontal orientation. When at rest horizontally on the unyielding surface (a datum surface), the cask is considered to have zero potential energy.

Potential energy is calculated by multiplying the weight of the cask by the height of the center of gravity of the cask above the datum surface. The design weight of the cask, contents and impact limiters is 250,000 pounds. For these analyses, the NAC-STC is considered to be symmetric about the three major axes; therefore, the center of gravity is at the midpoint of the longitudinal centerline of the cask. The center of gravity is a datum point at which all of the mass (weight) of the cask is considered to be located.

#### 2.10.7.1.1 Translational Motion - Side Drop

Figure 2.10.7-1 shows the cask in the horizontal or side drop position. When released in this orientation from 30 feet (360 in), the cask has  $9.00 \times 10^7$  inch-pounds of potential energy. As shown by the heavy dashed lines in Figure 2.10.7-1, the cask translates in the vertical direction and impacts on an unyielding surface. The deceleration forces that are created by crushing the impact limiters oppose the translational motion of the cask. Impact limiter crushing continues until all of the potential energy of the cask is absorbed, thereby decelerating the cask to rest. Both impact limiters crush simultaneously in a side drop; therefore, the cask is in a stable orientation following a side drop event.

In a side drop, the cask experiences only translational motion in the vertical direction. Ignoring the energy stored elastically in the impact limiter during deceleration, the dissipated energy equals the initial potential energy of the cask. During the side drop, both impact limiters are simultaneously engaged in decelerating the cask; therefore, each impact limiter absorbs the amount of energy shown in Table 2.10.7-1 and labeled E1--"Energy absorbed by the first limiter."

#### 2.10.7.1.2 Translational and End-Rotational Motion - End Drop

Figure 2.10.7-2 shows the cask in the end drop position. End drops are drop angles that range between 0 degrees (end drop) and 24 degrees (corner drop) and characteristically show translational and end-rotational motion. As in a side drop, a cask in the end drop position translates through a vertical distance of 30 feet and decelerates as a result of an impact on the unyielding surface. Deceleration forces acting on the end of the cask are symmetric and uniform for a flat end drop; therefore, the cask remains vertical during deceleration and after the cask has come to rest. The energy absorbed by one impact limiter, while decelerating the cask during an end impact, equals the initial potential energy of the cask. Considering the package center of gravity to be at the longitudinal midpoint and ignoring deformation, the center of gravity is 128.48 inches above the datum surface for an end impact. The cask comes to rest in the vertical position on the crushed impact limiter.

#### 2.10.7.1.3 Translational, End-Rotational, Mid-Point Rotational Motion - Oblique Drops

Figure 2.10.7-3 shows the cask in an oblique drop orientation. Oblique drops are drop angles that range between the corner drop and the side drop. After its fall is initiated, the cask translates through a vertical distance of 30 feet and impacts on the unyielding surface. The impact limiter, which contacts the unyielding surface first, crushes as it decelerates the leading end of the cask, bringing its velocity to zero. Energy absorbed by the leading impact limiter (E1) decelerates the leading end of the cask to rest. The cask now rotates or pivots on the stopped leading end. However, the energy absorbed by the first impact limiter is less than the initial energy of the cask, leaving the energy remaining (ER) to be absorbed by the second impact limiter.

Simultaneously during deceleration of the leading end of the cask, two other actions are taking place. First, the trailing, or free, end of the cask rotates around the stopped end of the cask and continues to accelerate due to gravity. Second, a component of the deceleration force causes a torque perpendicular to the longitudinal axis of the cask, resulting in the cask beginning to rotate around the center of gravity. Both "actions" contribute to the total amount of energy that must be absorbed by the second impact limiter.

During deceleration of the leading end of the cask, the trailing end continues to accelerate while translating vertically because no deceleration force is applied to it. Newton's first law, "Every body persists in its state of rest or of uniform motion in a straight line unless it is compelled to change that state by forces impressed on it..." (Resnick, page 75), requires the cask's trailing end to continue to translate vertically and to be accelerated by gravity until the second impact limiter contacts the unyielding surface. However, because the cask body is rigid, when the leading end of the cask stops, the trailing end of the cask continues translating and the cask begins to pivot on the crushed leading impact limiter. This continues until the second impact limiter contacts the unyielding surface and generates significant deceleration forces as it is crushed.

The second action, occurring while the leading end of the cask is decelerating, is a vector component of the deceleration force at the leading end of the cask, which causes the cask to rotate around its center of gravity. The deceleration force is always perpendicular to the unyielding surface. Depending on the cask angle, the deceleration force can be vectorially broken down into a force component parallel to, and a force component perpendicular to, the cask longitudinal axis. The perpendicular force component acts at a distance of approximately half of the cask length from the cask center of gravity. A torque, equivalent to the perpendicular force

component multiplied by half of the cask length attempts to “spin” the cask around the center of gravity. The spin or rotational velocity can also be thought of as rotational kinetic energy that must be absorbed by the second impact limiter. A detailed explanation of the torque and rotational kinetic energy is presented in the following paragraphs.

Finally, the third component of energy that must be absorbed by the second impact limiter is the energy stored elastically in the first impact limiter. The elastically stored energy produces a force perpendicular to the unyielding surface that augments the rotational velocity of the cask and tends to “lift” the lower end of the cask, which is at rest.

Oblique drops have four distinct quantities of energy that need to be absorbed to bring the cask to rest in a stable, horizontal orientation. These quantities are:

1. Potential energy (E1) absorbed by the impact limiter, which impacts on the unyielding surface first and brings the translational velocity of the leading end of the cask to zero.
2. Potential energy remaining (ER) after the first impact.
3. Potential energy (EP) of the cask by virtue of the height of its center of gravity above the unyielding surface after the first impact.
4. Rotational kinetic energy of the cask produced by the deceleration force and the elastically stored energy (ES), which results from the initial impact of the leading end of the cask.

The total amount of energy (ET) to be dissipated after a cask drop is calculated as:

$$ET = E1 + ER + EP + ES$$

where:

E1 = energy absorbed during the first impact  
ER = remaining energy after the first impact  
EP = rotational potential energy  
ES = elastically stored energy



The sum of the last three terms equals the energy absorbed by the second impact limiter (secondary impact). Terms E1, ER and EP can be calculated; however, testing the redwood and balsa wood in an impact limiter configuration was necessary to determine ES.

The impact limiter evaluation in Section 2.6.7.4 outlines an analysis of the NAC STC impact forces developed during the 30-foot hypothetical accident free drop. That analysis addresses the maximum force imparted to the cask through one impact limiter, resulting from the initial impact with the unyielding surface for various cask orientation angles. The following discussion addresses the primary impact loads (first impact limiter) on the cask structure. It also addresses the adequacy of the second impact limiter to absorb, for an oblique cask orientation, the remaining energy during the secondary impact on the unyielding surface. The geometry of the NAC-STC package is shown in Figure 2.10.7-4.

Based on 30-foot drop testing of a quarter-scale model of the NAC-STC, the secondary impact phenomenon has been reviewed. It has been concluded that elastically stored "rebound" energy (5 to 10 percent of the primary impact energy) may be restored to the cask in such a manner as to cause the leading end of the cask to lift from the ground several inches during the secondary impact (slapdown). Thus, the rebound energy must be dissipated by the second impact limiter.

Table 2.10.7-1 shows that at impact angles of 60 degrees and 75 degrees, the energy dissipated in the impact limiter during the secondary impact (E2) is greater than the energy dissipated in one impact limiter in a side impact, so that the cask "slaps down". This is because the residual drop energy not absorbed in the first impact (energy transformed to rotational energy), impact limiter rebound energy (elastic rebound), and potential energy converted to kinetic energy as the cask rotates to the second impact, all combine to exceed the energy absorbed by one limiter in a pure side drop orientation. Results of the model impact limiter tests show that the impact limiters do have sufficient energy absorption capacity to absorb the energy of the 60-degree and 75-degree oblique secondary impacts.

The calculation of E1 in the proprietary NAC impact limiter analysis program, RBCUBED (Section 2.10.1.2), is performed by solving the equations of motion for the cask. These equations are based on the force developed by the impact limiter as it crushes. The impact limiter force is equal to the crush strength of the redwood and balsa wood multiplied by the "backed" crush area. The RBCUBED program calculates this area as a function of the impact angle and crush depth, using a system of solid geometry subroutines developed by Oak Ridge National Laboratories as

part of the MORSE shielding code. These crush area calculations have been verified by manual calculation of crush area using graphical drafting techniques for several impact angles and crush depths. The accuracy of the area calculation may be shown by inspection of the model impact limiter results presented in Figures 2.10.6-12 through 2.10.6-14, which show that the RBCUBED force (the crush area times the crush strength) accurately tracks the measured force.

The impact limiter force is normal to the unyielding surface and is applied to the cask body, as shown in Figure 2.10.7-3. The cask's weight continues to accelerate the cask downward as the impact limiter decelerates, producing a crush force (FD), which decelerates the cask. During the initial contact of an impact limiter with the unyielding surface, the cask weight causes the net force to accelerate the cask downward until the crush area (footprint) becomes large enough to overcome the cask weight and produce a net deceleration.

The net force applied to the cask produces a force and deceleration parallel to the cask's longitudinal axis as well as a force and angular acceleration perpendicular to the longitudinal axis, as shown in Figure 2.10.7-3. The parallel force component acts on the cask center of mass to slow the cask down, but the perpendicular component transforms translational kinetic energy from the drop into rotational energy that must be absorbed in the secondary impact.

The calculations to determine the energy to be dissipated for each drop angle shown in Table 2.10.7-1 include the potential energy resulting from the cask tipping over to a horizontal position and elastically stored rebound energy from the first impact.

The cask and impact limiters are considered to be a mass (m). When the mass drops from rest, a distance (h), it is accelerated uniformly by gravity (g). Because the mass is not acted upon by any forces while free falling, it will remain in the same orientation that it had when it was released. The change in potential energy equals the change in kinetic energy. The vertical velocity of the mass at the time of contact with the unyielding surface is calculated as:

$$V_i = (2gh)^{0.5}$$

where:

- $V_i$  = vertical velocity of cask (ft/sec) at time of impact ( $t = 0$  sec)
- $g$  = the gravitational constant (ft/sec<sup>2</sup>)
- $h$  = the drop height (ft)

The cask may impact at any angle ( $0^\circ$  to  $90^\circ$ ). In the case of impact orientations from an end drop through a corner drop, the cask could be expected to remain upright after the total energy of the first impact is absorbed; as a result, the center of gravity does not have a moment arm, which would provide a rotational moment about the cask base, causing the cask to tip over. However, the calculated energy shown in Table 2.10.7-1 does include the energy of the tipover for conservatism for the corner drop impact. Ignoring elastically stored energy, the total energy that must be absorbed to bring the cask to rest for a corner impact is:

$$E_T = mg(h + H)$$

where:

$E_T$  = total energy to be absorbed (in-lbf)

$m$  = mass of the cask and limiters (lbm)

$g$  = acceleration due to gravity (ft/sec<sup>2</sup>)

$h$  = height of drop (ft)

$$H = \frac{(L/2)}{\cos \left[ \tan^{-1} \left( \frac{D/2}{L/2} \right) \right]} \left[ \cos |q| - \tan^{-1} \left( \frac{D/2}{L/2} \right) \right] - (D/2)$$

For oblique drops within the range from corner drop to side drop, the total energy absorbed is greater than that for the end to corner range, if one ignores cask tipover and elastically stored energy. Cask impact angles greater than 75 degrees are considered to be side drops because the leading impact limiter stops the cask as the trailing impact limiter begins to absorb energy.

In oblique drops, the center of gravity will fall a distance greater than the drop height,  $h$ . The additional distance the center of gravity must fall is  $L/2 (\cos q)$  (Figure 2.10.7-3), where  $L$  is the length of the cask body. Therefore, the total energy that must be absorbed to bring the cask to rest for impact orientations in the range from a corner drop to a side drop is again:

$$E_T = mg(h + H)$$

The total energy to be absorbed is greatest for the corner impact because the cask center of gravity must travel through the greatest distance from the initial impact position to the horizontal position. The total energy absorption capacity required is determined by summing  $E_1$  and  $E_2$  for each drop angle.

For cask impact orientations beyond a corner drop, the center of gravity of the cask is unsupported. The net crush force is applied at one end of the cask, resulting in a torque (T), possibly causing rotation of the cask about its center of gravity. As the cask is translating vertically while decelerating, it is also rotating around the end that is crushing. The cask is also attempting to rotate around the center of gravity due to the torque applied to the decelerating end of the cask by the perpendicular component ( $F_{d\perp}$ ) of the crush force. The applied torque is:

$$\begin{aligned} T &= F_{d\perp} \frac{L}{2} \\ &= F_d \sin\theta \frac{L}{2} \end{aligned}$$

where:

$$\begin{aligned} T &= \text{torque (in-lb)} \\ L &= \text{cask length (in)} \\ F_d &= \text{deceleration force (lb)} \end{aligned}$$

The impulse equation for an applied torque is:

$$T\Delta t = I\Delta\omega$$

where:

$$\begin{aligned} \Delta t &= \text{increment of time (sec)} \\ I &= \text{moment of inertia of a cylinder (cask) about its center of gravity} \\ &= \frac{mL^2}{12} \\ \Delta\omega &= \text{change in angular velocity (rad/sec)} \end{aligned}$$

The angular velocity is equal to the rotational velocity change ( $\Delta V_t$ ) divided by the radius:

$$\Delta\omega = \frac{\Delta V_t}{L/2}$$

Substituting for Dw in the impulse equation:

$$T\Delta t = \frac{I\Delta V_t}{L/2}$$

Substituting and solving for  $\Delta V_t$ :

$$\Delta V_t = \frac{F_d \sin\theta \Delta t L^2}{4I}$$

Substituting the formula for I for a cylinder yields:

$$\Delta V_t = \frac{F_d \sin\theta \Delta t 3g}{W_T}$$

Note that the same result for  $\Delta V_t$  is obtained by regarding the cask as rotating about one end.

This change in transverse velocity is subtracted from the transverse component of the initial velocity to determine the transverse velocity of the cask at the beginning of the next deformation step ( $\delta'$ ). When the sum of the transverse velocity changes equals the initial velocity, the leading end of the cask has been stopped along an axis normal to the longitudinal axis of the cask.

#### 2.10.7.2 Conversion of Potential Energy to Kinetic Energy

Just prior to a drop, the cask is at rest in a given orientation. The uniform gravitational force constantly acts on the cask and accelerates the cask at a constant rate. Gravitational acceleration (g) equals 32.2 feet/second/second. No other forces act on the cask during a drop; therefore, the cask acquires no additional energy during a drop. Uniform forces acting on the cask will not change the orientation of the cask while it is falling. Since energy can't be created or destroyed, the initial potential energy of the cask is converted to kinetic energy. To calculate the velocity at the time the impact limiter contacts the unyielding surface, conservation of energy is used as follows:

$$PE = KE$$

or

$$mgh = \frac{1}{2} mv^2$$

Solving for v:

$$v = (2gh)^{0.5}$$

The initial velocity (at the time crushing begins) is only a function of drop height. For a drop height of 30 feet, the velocity of the cask at the time that the leading impact limiter contacts the unyielding surface is 44.0 feet/second.

The correlation between potential energy and kinetic energy is the foundation on which the computer program RBCUBED is based. Translational velocity (translational kinetic energy), which the cask attains while free falling or while pivoting on end (oblique drop), is a direct function of the initial potential energy of the cask. Rotational velocity (rotational kinetic energy) results during an oblique drop while the leading end of the cask is decelerated; elastically stored energy is a small, calculable quantity of energy. When the total energy absorbed is equal to the sum of the potential energy dissipated during the initial impact, the rotational kinetic energy, and the elastically stored energy of the cask, then the cask is at rest.

#### 2.10.7.3 Deceleration Forces and Energy Absorption Calculation

The following quotation describes how an impact limiter works: "...the kinetic energy of a body in motion is equal to the work it can do in being brought to rest..." (Resnick, page 75). The source of kinetic energy in a cask was established in Section 2.10.7.2. The work done by the force crushing the impact limiter is the magnitude of that force multiplied by the distance (deformation) through which the crush occurs. The units of work are inch-pounds.

The NAC-STC cask redwood impact limiters are right cylindrical stainless steel shells filled with redwood and balsa wood. The wood is used to dissipate the kinetic energy of the cask, and is crushed when a nominal force per unit area is applied to the impact limiter. The redwood and balsa wood show nominal crush strength in the plane that is parallel to the grain direction. The redwood and balsa wood are specified and tested to ensure that the crush strength is within design criteria tolerances. Wedges of wood are bonded together to form a solid cupped cylinder with uniform properties around its circumference. A thin stainless steel shell is welded around each impact limiter to prevent cosmetic, contamination, or decomposition damage.

The wood impact limiter crushes because it is trapped between the cask and the unyielding surface. The initial energy (PE) of the cask will have an equivalent amount of kinetic energy (KE) just before the impact limiter contacts the unyielding surface. When the impact limiter contacts the unyielding surface, it immediately comes to rest; however, the cask continues to move into the impact limiter until it is opposed by a force vector. To explain the work done in stopping the cask, an illustrative example of an end drop is presented:

The cask weighing 250,000 pounds, is assumed to have been dropped 8.8 inches;  $PE = KE = 2.2 \times 10^6$  inch-pounds. The velocity of the cask when the impact limiter contacts the unyielding surface is 6.87 feet/second (82.5 in/sec).

The cask is a rigid structure and each end has an area of approximately 5904 square inches. Nominal crush strength of the redwood is 6240 psi. The cask is rigid and isolates, or "backs", the wood; the backed wood effectively stops the cask. The force required to crush the backed wood is  $36.84 \times 10^6$  pounds. When the backed wood crushes 0.05 inch,  $1.84 \times 10^6$  inch-pounds of work is performed:

$$\begin{aligned} W &= (F)(d) \\ &= 1.84 \times 10^6 \text{ in-lb} \end{aligned}$$

where:

$$\begin{aligned} F &= 36.84 \times 10^6 \text{ lb} \\ d &= 0.05 \text{ in} \end{aligned}$$

Using the definition of work and Newton's second law,  $F = ma$ , yields the following derivation:

$$W = \frac{1}{2}mv^2 - \frac{1}{2}mv_0^2$$

where:

$$\begin{aligned} W &= \text{work performed on a particle, in-lb (work performed on the} \\ &\quad \text{cask by the wood is negative)} \\ m &= \text{mass of the cask (weight of the cask divided by the} \\ &\quad \text{gravitational constant } 32.2 \text{ ft/sec}^2), \text{ lbf-sec}^2/\text{ft} \\ v &= \text{velocity of the cask after the work is performed, ft/sec} \\ v_0 &= \text{initial velocity of the cask, ft/sec} \end{aligned}$$

Solving for the velocity after an incremental amount of work has been performed:

$$v = \sqrt{\frac{2W}{m} + v_o^2}$$

Substituting for  $W$ ,  $m$ ,  $v_o$  and adjusting for correct units, the cask velocity after the first crush increment is 2.77 feet/second. Repeating this analysis for another 0.05-inch increment shows that after another fraction of a crush increment, the cask is stopped.

In summary, the force (a vector quantity) that is created by crushing the wood opposes the cask's velocity, which is also a vector quantity. Crushing an incremental amount of wood is a finite quantity of work performed on the cask, decreasing the cask's velocity and kinetic energy. Once the kinetic energy is completely dissipated, the cask velocity equals zero.

RBCUBED, the impact limiter computer program used to design the redwood impact limiters, functions in exactly the same way as the illustrative example. Cask geometry and weight, drop angle, crush increment, wood crush strengths, wood lock-up stroke and wood geometry are entered into the program. RBCUBED calculates an initial velocity (as the limiter touches the unyielding surface), a backed area engaged in crushing, a crush force, the energy absorbed for a crush increment, the elapsed crush time and the cask velocity at the end of the crush increment. The computation cycle is repeated until all the kinetic energy is absorbed and the end of the cask is stopped.

RBCUBED calculates the energy dissipation necessary to stop the translational motion of the end of the cask that first contacts the unyielding surface (both limiters in the side drop). In Table 2.10.7-1, the energy dissipated while reducing the translational velocity of the first end to contact the unyielding surface is the energy absorbed by the first limiter ( $E_1$ ). If  $E_1$  is less than the initial kinetic energy of the cask, the difference is reported by RBCUBED as "remaining energy," and shown in Table 2.10.7-1 as energy remaining after first impact (ER).

In oblique drops, at the instant the translational velocity of the first end to contact the unyielding surface is zero, the cask is in position 2 in Figure 2.10.7-3. (Rotation of the cask around its mid-point is addressed in Section 2.10.7.2.) The center of gravity of the cask has a calculable potential energy, which is the energy that increases the velocity of the cask as it pivots on the crushed



("first") impact limiter. In Table 2.10.7-1, the potential energy, which equals the velocity gain as the cask pivots on end, is the potential energy of the cask after the first impact (EP).

The redwood and balsa wood dissipate energy while crushing, but elastically store a small amount of the total energy dissipated. The quantity of elastically stored energy was determined by quasi-static testing of scale model impact limiters (Section 2.10.7.5). The quantity of stored energy ranged between 8.2 percent (side drop) to 7.2 percent (end drop) of the total energy dissipated by the impact limiters tested. As stated above, once the first end of the cask is stopped, the stored energy is released. The force, which the stored energy creates, tends to augment the torque attempting to cause the cask to spin around the center of gravity. This analysis has conservatively ignored the cask spinning and assumes that the energy is absorbed by the second impact limiter. In Table 2.10.7-1, the elastically stored energy (conservatively considered to be 8.2 percent of the total energy dissipated by the leading impact limiter) is the energy stored in the leading impact limiter and absorbed in the second impact limiter while in the side drop orientation (ES).

In summary, the translational velocity of the leading end of the package is reduced to zero by absorbing an amount of energy (E1). The cask will pivot over and absorb--the remaining potential energy (ER), the potential energy resulting from the rotation to a horizontal orientation (EP), and the elastically stored energy (ES)--all in the second impact limiter in the side drop orientation. Table 2.10.7-1 shows that the four components of energy are absorbed by both impact limiters for impact angles from 0 to 90 degrees.

#### 2.10.7.4 RBCUBED Calculated Force-Deflection Graphs

Figures 2.10.7-5 through 2.10.7-11 show the deceleration force as a function of crush depth, calculated using RBCUBED for the full-scale cask impact limiters. Each curve is for either the upper or lower impact limiter, showing the plus and minus tolerance energy absorption profile. Quasi-static tests of eighth-scale model impact limiters further substantiate the RBCUBED calculated values, as described in Section 2.10.6.4. Table 2.10.7-2 provides a comparison of the maximum deceleration values obtained from: (1) the eighth-scale model impact limiter compression tests; (2) RBCUBED impact limiter analysis program; (3) the quarter-scale model drop tests; and (4) the NAC-STC design criteria.

Figure 2.10.7-1 Side Drop

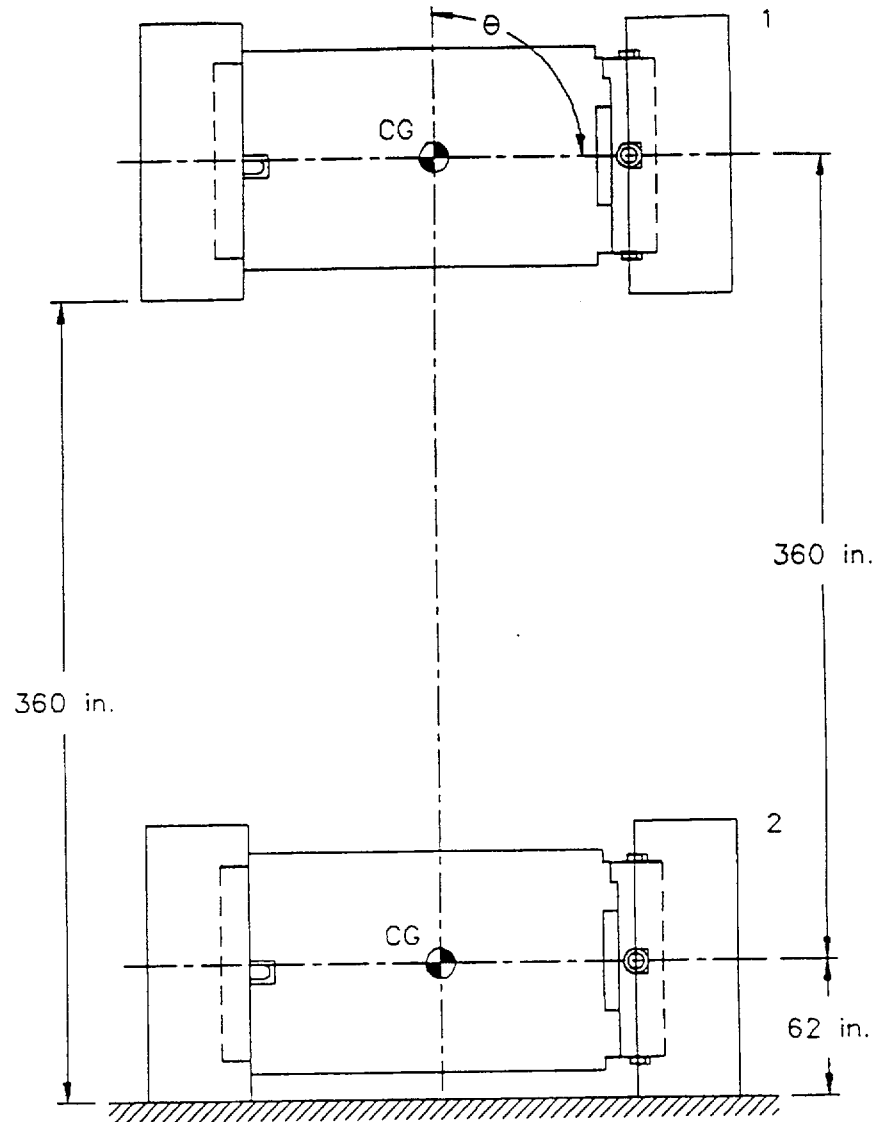


Figure 2.10.7-2 End Drop

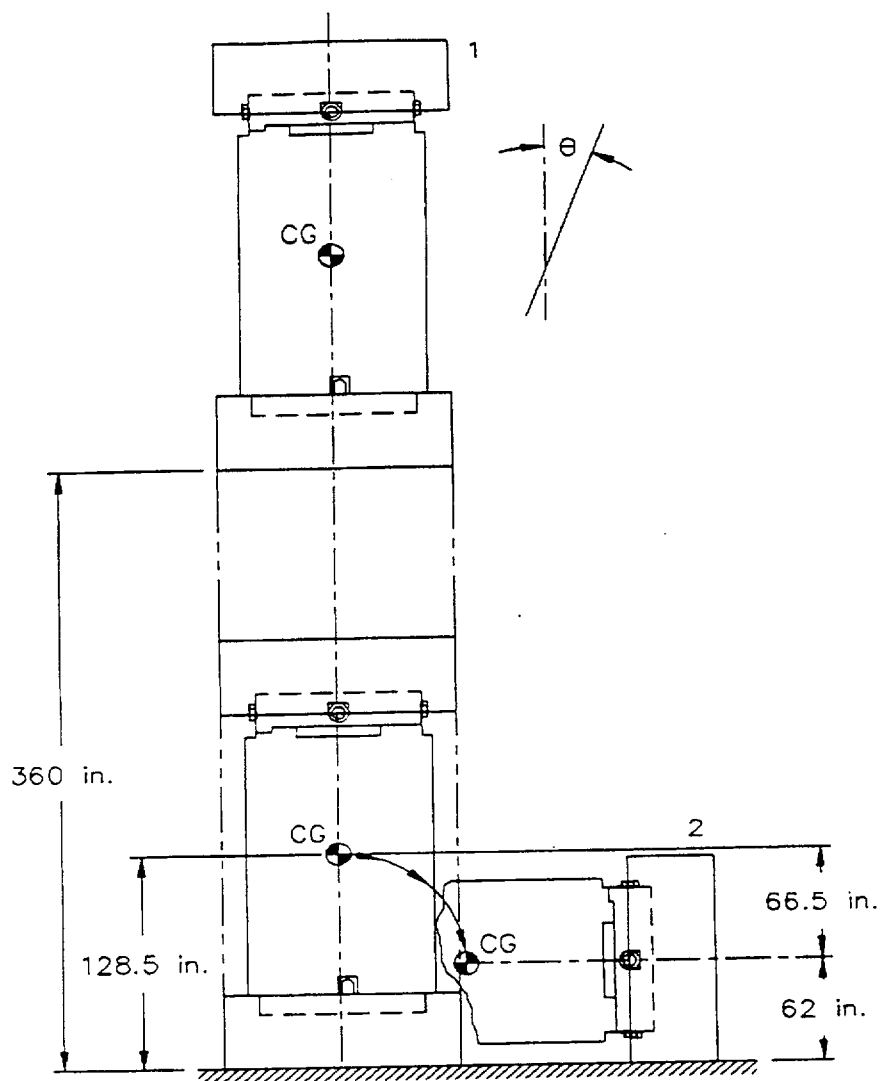


Figure 2.10.7-3 Oblique Drop

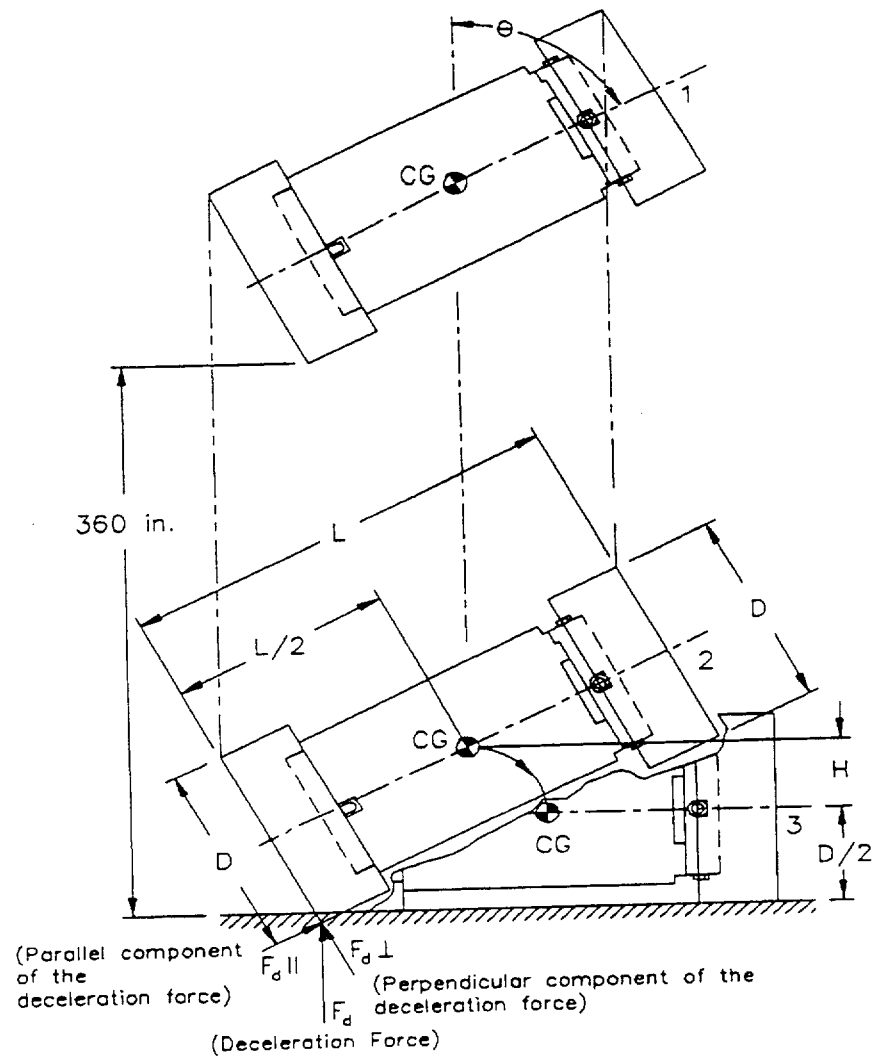


Figure 2.10.7-4 Cask Slapdown Geometry

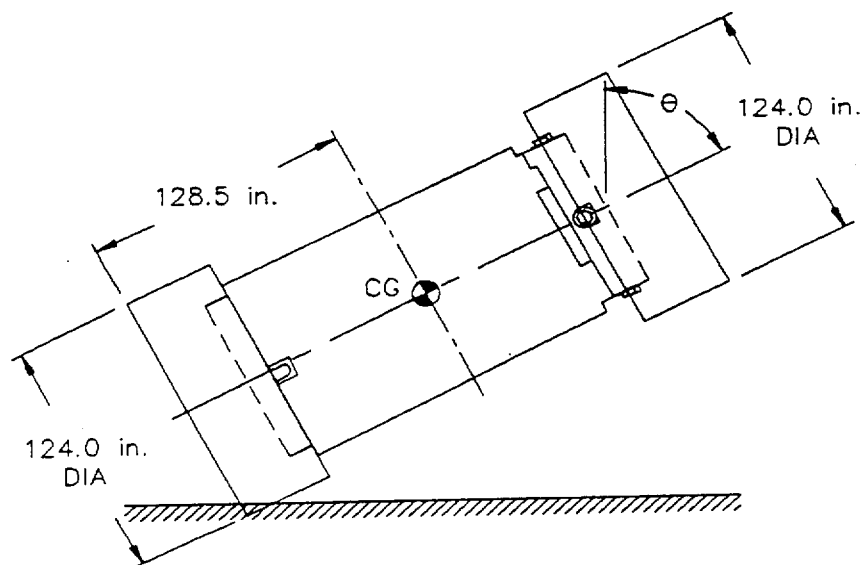


Figure 2.10.7-5 Force-Deformation Curve - Lower Redwood Impact Limiter (Bottom End Impact, 0 Degrees)

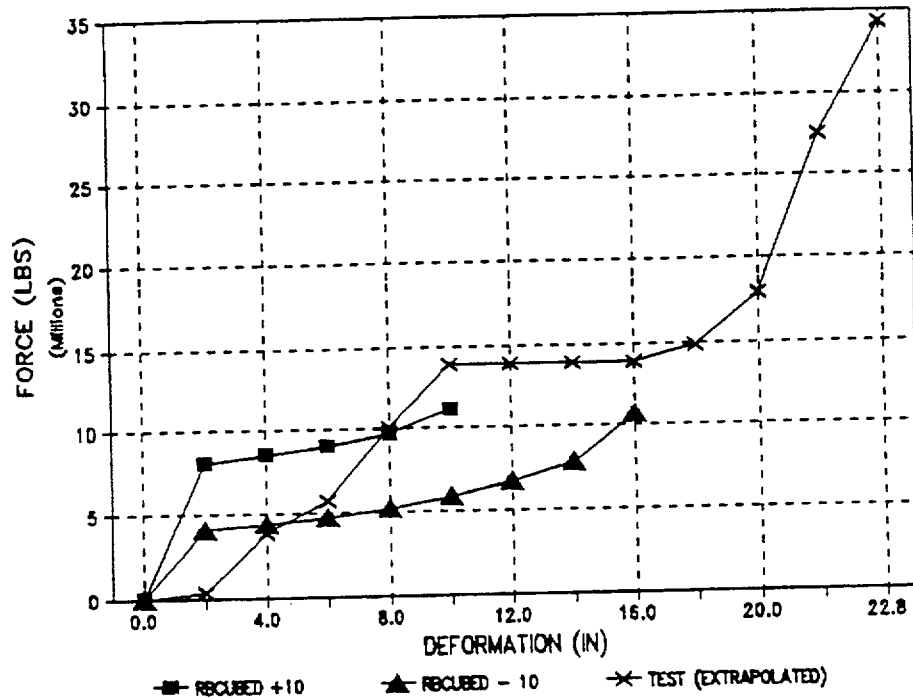


Figure 2.10.7-6 Force-Deformation Curve - Lower Redwood Impact Limiter (Bottom Corner Impact, 24 Degrees)

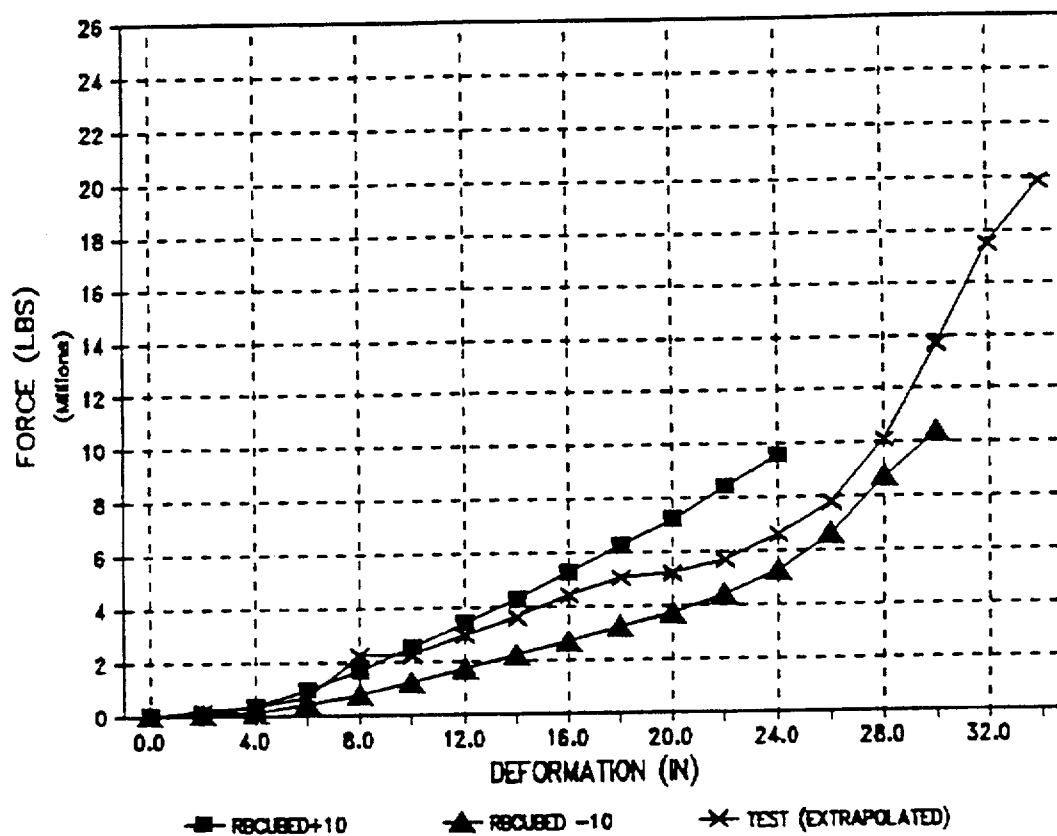


Figure 2.10.7-7 Force-Deformation Curve - Lower Redwood Impact Limiter (Bottom Oblique Impact, 75 Degrees)

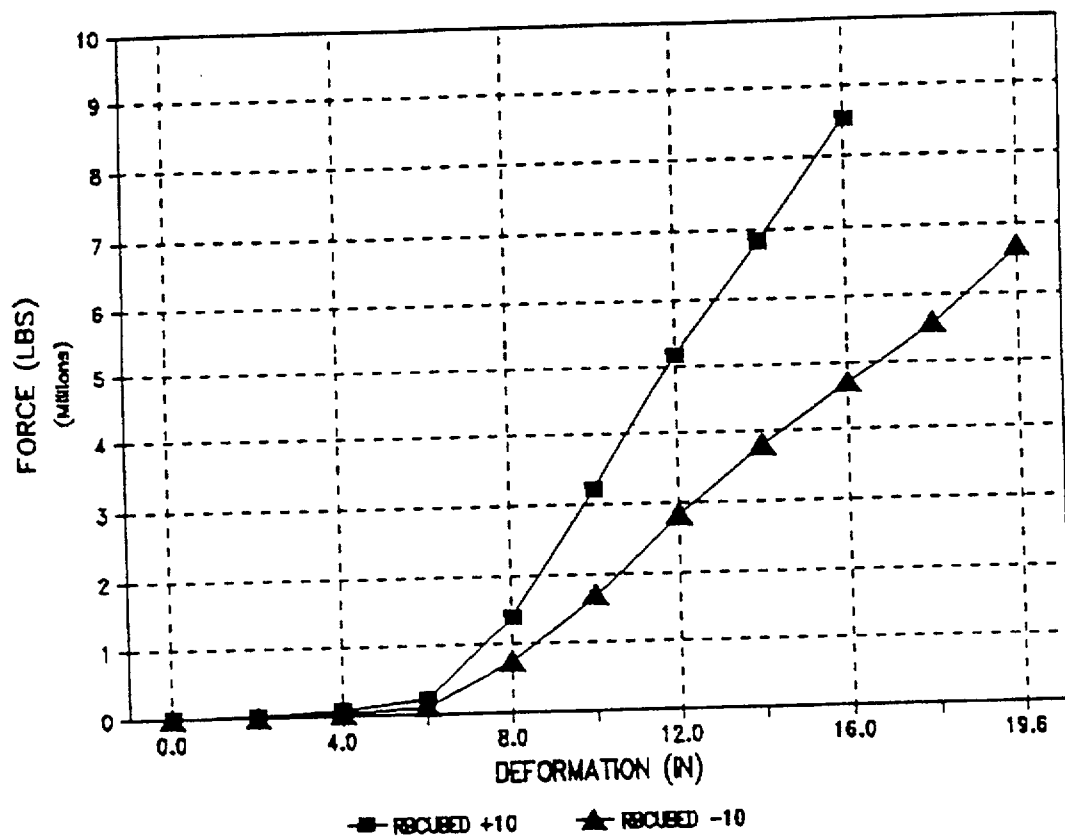




Figure 2.10.7-8 Force-Deformation Curve - Upper Redwood Impact Limiter (Top End Impact, 0 Degrees)

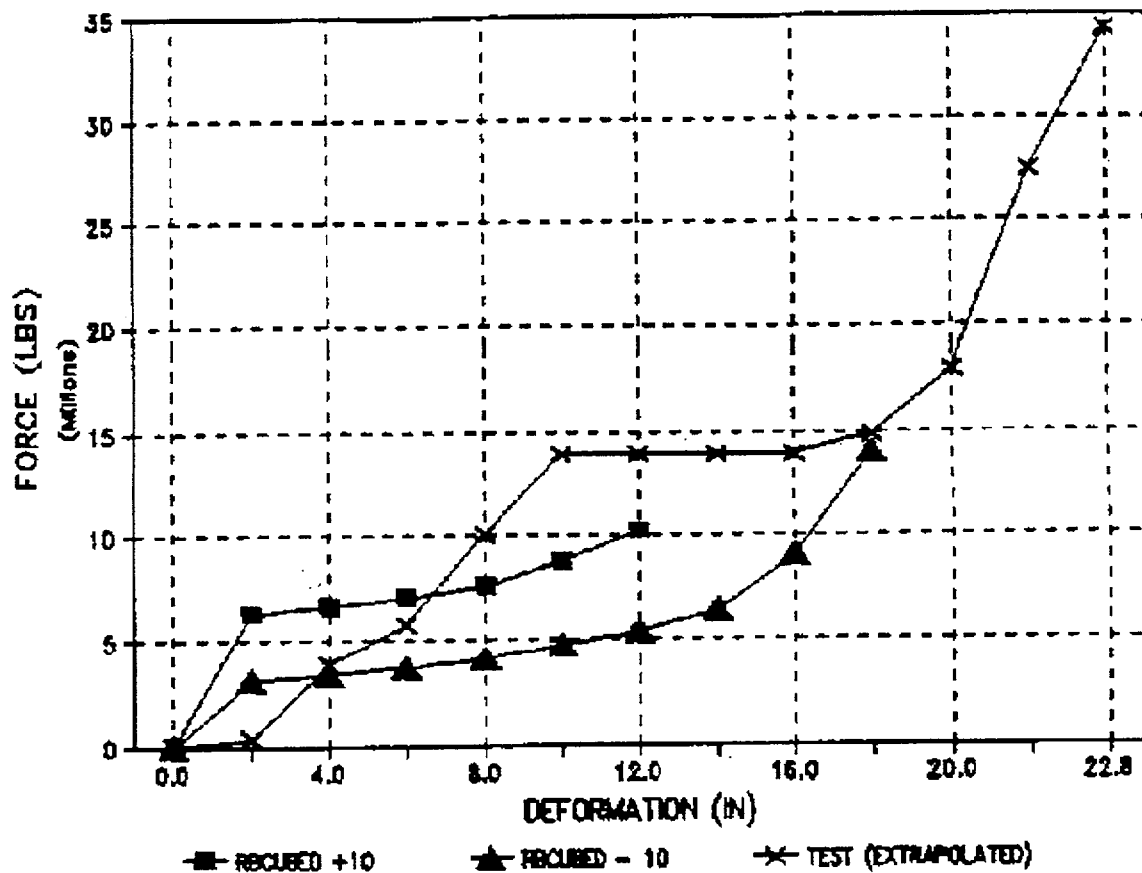


Figure 2.10.7-9 Force-Deformation Curve - Upper Redwood Impact Limiter (Top Corner Impact, 24 Degrees)

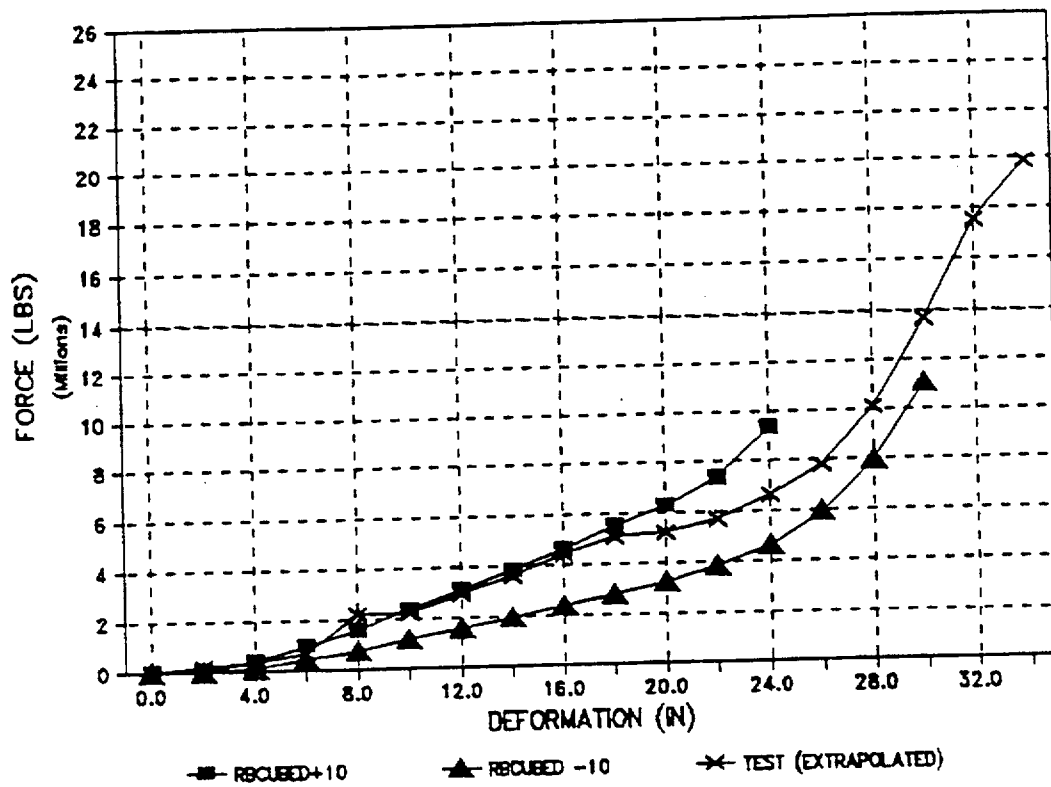


Figure 2.10.7-10 Force-Deformation Curve - Upper Redwood Impact Limiter (Top Oblique Impact, 75 Degrees)

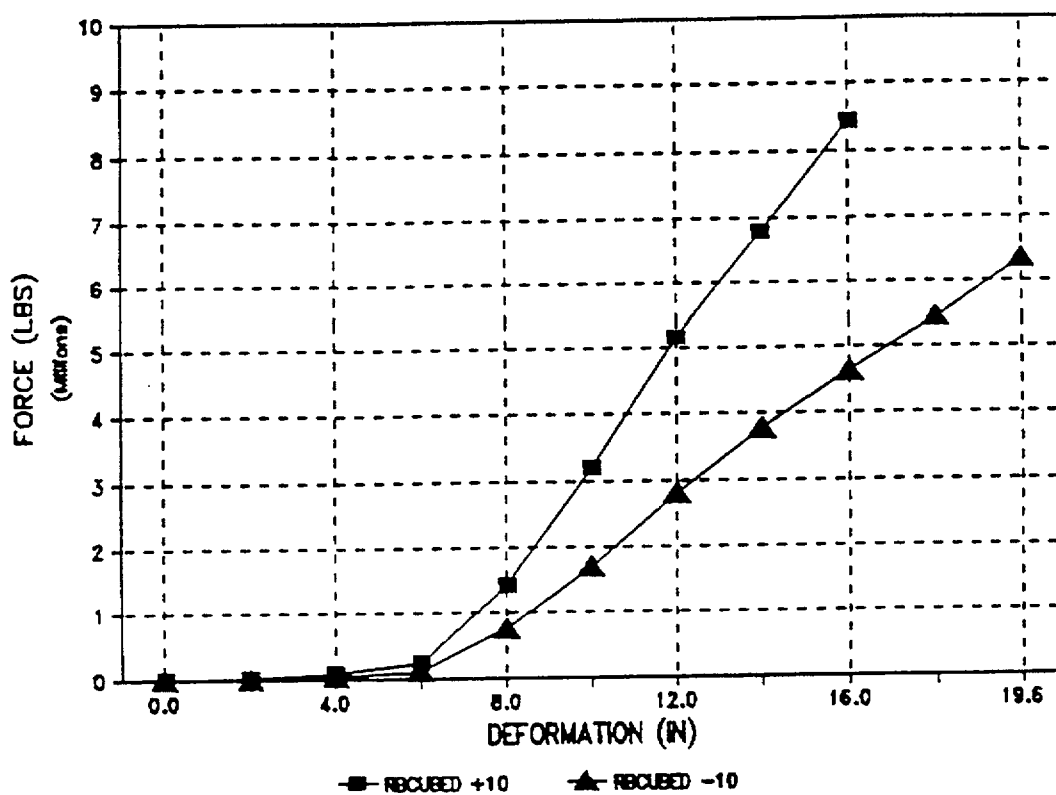


Figure 2.10.7-11 Redwood Impact Limiter Force-Deformation Curve - Side Impact  
(90 Degrees)

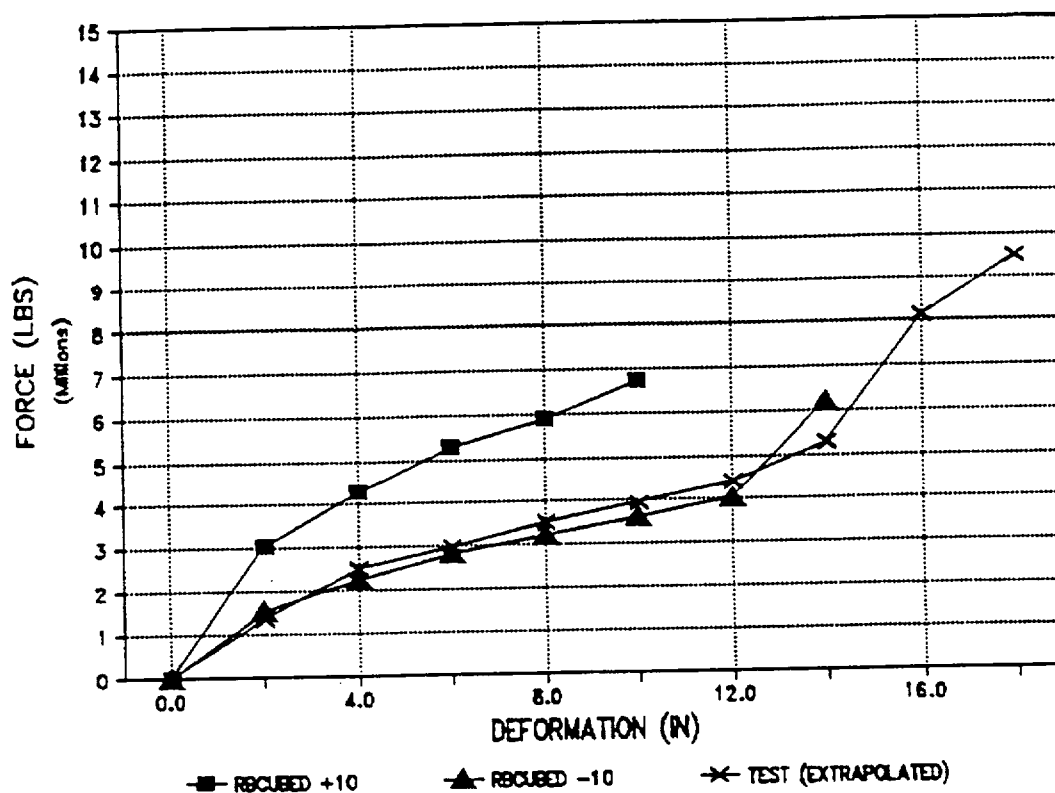


Table 2.10.7-1 Determination of Maximum Energy Remaining for Secondary Impact – Full-Scale Redwood Impact Limiter

DROP ANGLE	24°	30°	45°	60°	75°
<sup>1</sup> E1 Energy absorbed by first limiter (in-lb)	$9.15 \times 10^7$	$8.66 \times 10^7$	$7.49 \times 10^7$	$5.94 \times 10^7$	$4.38 \times 10^7$
<sup>1</sup> ER Energy remaining after first impact (in-lb)	$3.99 \times 10^6$	$8.02 \times 10^6$	$1.93 \times 10^7$	$3.21 \times 10^7$	$4.66 \times 10^7$
<sup>2</sup> EP Potential energy of cask after first impact (in-lb)	$2.02 \times 10^7$	$2.01 \times 10^7$	$1.82 \times 10^7$	$1.40 \times 10^7$	$0.78 \times 10^7$
<sup>3</sup> ES Energy stored in first limiter; absorbed in second limiter in side drop orientation (in-lb)	$7.51 \times 10^6$ (8.2%)	$7.10 \times 10^6$ (8.2%)	$6.14 \times 10^6$ (8.2%)	$4.87 \times 10^6$ (8.2%)	$3.59 \times 10^6$ (8.2%)
E2 Secondary impact total of ER + EP+ ES (in-lb)	$3.17 \times 10^7$	$3.52 \times 10^7$	$4.36 \times 10^7$	$5.10 \times 10^7$	$5.80 \times 10^7$
<sup>4</sup> E <sub>max</sub> - Side Drop Maximum energy absorption capability of impact limiter in side drop orientation(in-lb)	$6.35 \times 10^7$	$6.35 \times 10^7$	$6.35 \times 10^7$	$6.35 \times 10^7$	$6.35 \times 10^7$
Energy Absorption Margin of Safety	+1.01	+0.80	+0.45	+0.24	+0.09

<sup>1</sup> From RBCUBED impact limiter analysis.

<sup>2</sup> Calculated based on Figure 2.10.7-2.

<sup>3</sup> Estimated springback based on quasi-static compression tests.

<sup>4</sup> Extrapolated from quasi-static compression tests.

Table 2.10.7-2 Comparison of Full-Scale Deceleration Values for 30-Foot Drop Impacts

Drop Orientation	30-Foot Drop Deceleration (g)				
	RBCUBED <sup>1</sup> (Cold)	RBCUBED <sup>1</sup> (Hot)	Quasi-Static <sup>2</sup> Test	Drop Test <sup>3</sup>	Design <sup>4</sup>
End (0°)	44.6	56.1	54.8	55.6	56.1
Corner (24°)	44.0	49.3	32.6	29.2	55.0
Oblique (75°)	29.9	24.0	-	53.8	55.0
Side (90°)	51.7	51.3	45.6	51.3	55.0

- 1 Impact g-loads calculated by RBCUBED (NAC's proprietary Impact Limiter Analysis Program).
- 2 Extrapolated from eighth-scale model impact limiter quasi-static compression tests. Details are provided in Section 2.10.6.4.
- 3 Extrapolated from quarter-scale model 30-foot drop test results. Details are provided in Section 2.10.6.5.
- 4 Design g-load values used in the cask and fuel basket analyses.

## 2.10.8      Bolts - Closure Lids (Stress Evaluations)

This section presents the analytical methods, assumptions, and detailed example calculations for the evaluation of the stresses in the inner and the outer lid bolts for selected impact orientations. This evaluation is applicable for both the directly loaded fuel and the canistered fuel configurations of the NAC-STC. The bounding load condition for the NAC-STC inner lid bolt evaluation is the combined weight of the loaded Yankee-MPC, canister spacers and inner lid multiplied by the acceleration factors applicable to the redwood impact limiter as summarized in Tables 2.6.7.4.1-1 through 2.6.7.4.1-3. Although the loaded CY-MPC canister is heavier, the lower impact factor developed by the balsa impact limiters (See Tables 2.6.7.4.2-1 and 2.6.7.4.2-2) results in a lower impact load for the inner lid bolts. For these configurations, the end-drop impact load for the Yankee-MPC is  $(66,690 \times 56.1g =) 3.74 \times 10^6$  lb. and for the CY-MPC it is  $(77,885 \times 42.4g =) 3.3 \times 10^6$  lbs. The bounding weight for the outer lid bolts evaluation is the combined weight of the redwood impact limiter and the outer lid.

The detailed analyses of the inner and outer lid bolts consider impact orientations at 5-degree intervals from 0-degrees to 90-degrees. The structural analyses of the inner lid bolts and the outer lid bolts for the normal conditions of transport and the hypothetical accident conditions are presented in Sections 2.6.7.5 and 2.7.1.6, respectively. Tables 2.6.7.5-1 and 2.6.7.5-2 summarize the inner lid bolt stresses for the normal conditions of transport "hot" 1-foot drop and the "cold" 1-foot drop, respectively. Tables 2.6.7.5-3 and 2.6.7.5-4 summarize the outer lid bolt stresses for the normal conditions of transport "hot" 1-foot drop and the "cold" 1-foot drop, respectively. Tables 2.7.1.6-2 through 2.7.1.6-5 summarize the corresponding "hot" and "cold" 30-foot drop accident condition stresses for the inner lid bolts and outer lid bolts. The inner lid bolts and the outer lid bolts are evaluated for the Thermal (fire) accident condition in Section 2.7.3.4.

### 2.10.8.1      Analysis Approach

The inner and outer lid bolt stress analyses for normal transport and hypothetical accident conditions consider the impact loads, pressure loads, thermal loads and bolt preloads. Each summary table of bolt stresses is preceded with an explicit listing of relevant geometry, mechanical properties and constant loading data (bolt torque, pressure, etc.) taken directly from Sections 2.1, 2.2, 2.3 and the license drawings in Section 1.3.2.

The NAC-STC inner and outer lid bolts are evaluated for the hypothetical accident free drop condition in the following example calculations. Impact loads are expressed in g acceleration loads as summarized in Tables 2.6.7.4.1-1 through 2.6.7.4.1-3 for the redwood impact limiters and Tables 2.6.7.4.2-1 and 2.6.7.4.2-2 for the balsa impact limiters. The "hot" condition temperature of the lid bolts impact for the evaluations is conservatively defined as 270°F for this example calculation. The "cold" condition temperature of the inner lid bolts is -20°F, per regulatory requirements. Allowable stress limits and material properties for the lid bolts are taken at 270°F and at room temperature (70°F) for the "hot" and the "cold" conditions, respectively. The allowable bolt tensile stress is taken as the material yield strength,  $S_y$ , at operating temperature as defined in Tables 2.1.2-1 and 2.1.2-2. For conservatism, external energy absorber reaction forces, which resist separation of the cask lid and body, are completely neglected in all calculations.

An explanatory discussion of bolt stress analysis is found in Section 2.10.8.2. Table 2.7.1.6-2 contains the results of the bolt stress analysis. An example calculation is included with each note to verify the accuracy of the tabular calculation.

The analysis methodology, allowables and basic assumptions used are consistent with conventional design/analysis codes, such as "AISC Manual of Steel Construction," 8th Edition, and "ASME Boiler and Pressure Vessel Code," Section III, Appendix F, Paragraph F-1335, but this analysis is more conservative. Specifically, this analysis includes stresses associated with the bolt preloads. Conventional design/analysis codes consider only externally applied loads and ignore preloads.

Like the methodology given in the "ASME Boiler and Pressure Vessel Code," Appendix F, Paragraph F-1335, this analysis uses nominal tensile and shear stresses based on the tabulated stress area of the bolts. It should be noted that the elliptic interaction equations of Paragraph F-1335.2 of the "ASME Boiler and Pressure Vessel Code" and the approach used here give nearly identical results when adjustments in loadings are made to account for the differing treatment of preload tension (This approach conservatively includes preloads, whereas the code approach ignores preloads).

#### 2.10.8.2      Inner Lid Closure Bolt Analyses

All numerical examples pertain to the evaluation of the inner lid bolts of the NAC-STC with the Yankee-MPC canistered fuel under hypothetical accident conditions (Table 2.7.1.6-2).



spacer multiplied by the g-load associated with a 30-foot drop accident condition; and (4) the differential thermal expansion between the inner lid material and the bolt.

The required bolt preload to offset the combined static and dynamic loads is determined by:

$$F_b = F_s + F_a$$

where:

$$\begin{aligned} F_b &= \text{calculated required bolt preload} \\ F_s &= \text{total static load} \\ F_a &= \text{total dynamic (impact) load} \end{aligned}$$

The cask lid closure bolt preload necessary to offset static loads is:

$$\begin{aligned} F_s &= F_{\text{press}} + F_{\text{or1}} + F_{\text{or2}} \\ &= 4,578 \text{ lb} + 2,208 \text{ lb} + 2,250 \text{ lb} \\ &= 9,036 \text{ lb} \end{aligned}$$

where:

$$\begin{aligned} F_s &= \text{total static load per bolt (lb)} \\ F_{\text{press}} &= \text{internal pressure force per bolt (lb)} \end{aligned}$$

$$\left( \frac{PA}{N_b} \right) = \left( 45.3 \text{ psig} \times \frac{(73.51 \text{ in.})^2 \pi}{4} \right) \div 42 \text{ bolts} = 4,578 \text{ lb}$$

where:

$$\begin{aligned} P &= \text{internal cask lid pressure} = 45.3 \text{ psi} \\ A &= \text{area (in.}^2\text{) of the cask lid at the O-rings, based on 73.51 in. diameter} \\ N_b &= \text{number of cask lid closure bolts} \\ F_{\text{or1}} &= \text{inner O-ring compression force per bolt (lb)} \end{aligned}$$

$$F_{\text{or1}} = \frac{\pi(D_f)(D_{\text{imor}})(P_c)}{N_b} = \frac{\pi(1.0)(72.00)(410)}{42} = 2,208 \text{ lb}$$

where:

$$\begin{aligned} D_{\text{imor}} &= \text{diameter of inner (metal) O-ring} = 72.00 \text{ in (71.89 in. actual)} \\ D_f &= \text{design factor of Type 321 material} = 1.0 \\ P_c &= \text{inner O-ring compression force} = 410 \text{ lb/in} \\ N_b &= \text{number of bolts} = 42 \\ F_{\text{or2}} &= \text{outer O-ring compression force per bolt (lb)} \end{aligned}$$

$$F_{or2} = \frac{\pi(D_f)(D_{o_{omor}})(P_c)}{N_b} = \frac{\pi(1.0)(73.36)(410)}{42} = 2,250 \text{ lb}$$

where:

$D_{omor}$  = diameter of outer (metal) O-ring = 73.36 in  
 $P_c$  = outer O-ring compression force = 410 lb/in  
 $N_b$  = number of bolts = 42

The end impact load ( $F_a$ ) based on the cask inner lid most severe loading orientation (end impact), is calculated as:

$$F_a = \frac{P_a}{N_b} = \frac{3,741,309}{42} = 89,079 \quad [\text{Equation 1}]$$

$$P_a = (W_a \times g) \cos\theta = (66,690 \text{ lb} \times 56.1g) \cos(0^\circ) = 3,741,309 \text{ lb}$$

where:

$W_a$  = wt. of the loaded canister + canister spacer + inner lid = 66,690 lb  
 $g$  = drop g-load = 56.1g  
 $\theta$  = drop angle (from cask axis) =  $0^\circ$   
 $N_b$  = number of bolts = 42

Therefore, the calculated required preload per bolt,  $F_b$ , is:

$$F_b = F_s + F_a = 9,036 \text{ lb} + 89,079 \text{ lb} = 98,115 \text{ lb}$$

The total torque ( $T$ ) to develop the required axial bolt preload ( $F_b$ ) is:

$$\begin{aligned} T &= \left[ \left( \frac{d_m}{2d} \right) \left( \frac{\tan\lambda + \mu \sec\alpha}{1 - \mu \tan\lambda \sec\alpha} \right) + 0.625\mu \right] (F_b)(d) \\ &= \left[ \left( \frac{1.4375}{3.0} \right) \left( \frac{\tan\lambda + 0.15 \sec 30}{1 - (0.15)(\tan\lambda) \sec 30} \right) + 0.625(0.15) \right] (112,340)(1.5) \\ &= 28,036 \text{ in.-lb, or } 28,036/12 = 2,336 \text{ ft-lb} \end{aligned}$$

where:

$T$  = applied torque in inch-pounds  
 $F$  = preload force in pounds  
 $d$  = bolt diameter = 1.50 in  
 $d_m$  = mean diameter of threads =  $d - p/2 = 1.4375$  in  
 $\alpha$  = one-half the thread angle =  $30^\circ$   
 $\mu$  = coefficient of friction = 0.15  
 $n$  = threads/inch  
 $\tan \lambda$  =  $1 / (\pi d_m n)$

The design minimum torque is  $2,540 - 200 \text{ ft-lb} = 2,340 \text{ ft-lb}$

$$T_{\text{design}} > T_{\text{required}} = 2,340 \text{ ft-lb} > 2,336 \text{ ft-lb}.$$

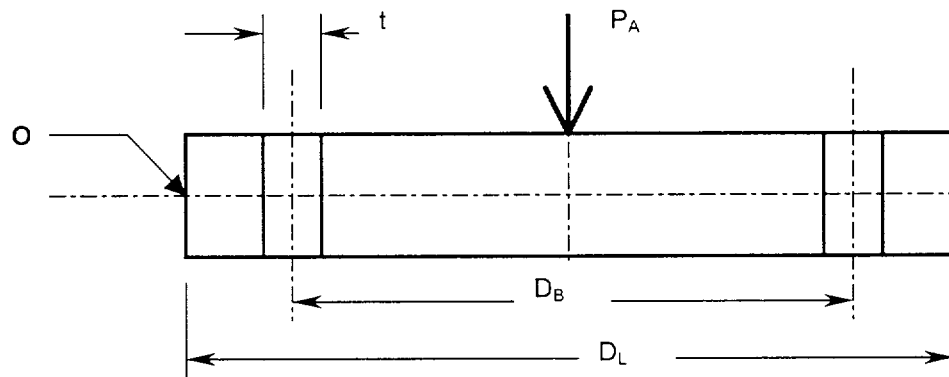
Therefore, the design torque is adequate.

The following calculations of bolt stresses are presented in order to verify the values in Table 2.7.1.6-2. The inner lid bolts will be evaluated for the end drop ( $0^\circ$ ), oblique drop ( $5^\circ$ ), corner drop ( $24^\circ$ ), and side drop ( $90^\circ$ ). The calculation summarized in this section is for the hypothetical accident condition (30-ft drop), which bounds the normal operating condition (1-ft drop).

Bolt stress is evaluated by combining the stress from the maximum design installation torque (nominal torque + tolerance) with the maximum static and inertial loads generated by the highest hypothetical accident condition acceleration. The calculated stress is compared to the allowable criteria specified in Table 2.1.2-1.

#### Derivation of Bolt Stresses - Pivoting Lid Assumed

The derivation of this relationship for tensile bolt stresses assumes the lid pivots about the outer edge of the lid, point "O". The bolts are approximated as a thin, circular ring with a thickness equivalent to  $(\text{total bolt area}) = (\text{ring area})$ .



Inner Lid Section

$$R_B = \text{bolt circle radius} = D_B/2 = 37.655 \text{ in}$$

$$R_L = \text{lid radius} = D_L/2 = 39.5 \text{ in}$$

Equivalent ring thickness is found as:

$$t = A/(\pi D_B) = 0.2649 \text{ in}$$

where:

$$A = (42 \text{ bolts})(1.492 \text{ in}^2/\text{bolt}) = 62.66 \text{ in}^2$$

The moment of inertia of the bolt ring about point "O" is:

$$I_o = \pi R_B^3 t + A R_L^2 = 142,204 \text{ in}^4$$

The applied bending moment about point "O" resulting from the impact force,  $P_A$ , is:

$$M = P_A R_L$$

Thus, the bolt stress is found as:

$$f_a = Mc/I = \frac{[(P_A R_L)(R_L + R_B)]}{\pi R_B^3 t + A R_L^2}$$

or

$$F_A = f_a A_b = P_A [R_L(R_L + R_B)/I_o] A_b \quad [\text{Equation 2}]$$

In this analysis, considering impacts from vertical (end) impacts through side impacts, the two bolt tension relations, equations [1] and [2], must transition from one to the other at some orientation angle. Both conservatively neglect reaction forces from external energy absorbers. This neglect is extraordinarily conservative for near vertical impacts, but becomes more realistic as the package approaches side impact orientations. Specifically, the center of pressure of the external energy absorber reaction force on the lid moves from the center of the lid towards the impacting corner of the package as the impact orientation moves from near vertical to near horizontal.

For conservatism, this transition from an end relation, [Equation 1], for bolt force to an oblique relation, [Equation 2], is assumed to occur reasonably close to vertical; hence, only the 0-degree case uses the uniform force assumption.

2.10.8.2.2 Top End Drop (0°)

The total applied external load is:

$$\begin{aligned} P &= F_s (\text{static}) + F_a (\text{impact}) \\ &= 9,036 + 89,079 \\ &= 98,115 \text{ lb} \end{aligned}$$

where:

$$\begin{aligned} F_s &= \text{total static load} = 9,036 \text{ lb} \\ F_a &= \text{total dynamic load resulting from impact} = 89,079 \text{ lb} \end{aligned}$$

The net bolt load is:

$$\begin{aligned} F_b &= K_b P / (K_b + K_m) + F_i (\text{preload}) + F_t (\text{thermal}) \\ &= 7,656 + 115,066 + 13,703 = 136,425 \text{ lb} \end{aligned}$$

where:

$$\begin{aligned} K_b &= \text{bolt stiffness} \\ &= A_b E_b / L \\ &= 4.57 \times 10^6 \text{ lb/in} \end{aligned}$$

where:

$$\begin{aligned} A_b &= 1.492 \text{ in}^2 \\ E_b &= 28.0 \times 10^6 \\ L &= \text{total bolt length} - \frac{1}{2} \text{ bolt head thickness} - \frac{1}{2} \text{ engagement length} \\ &= 9.14 \text{ in} \\ K_m &= \text{lid stiffness} \\ &= A_L E_{\text{lid}} / L_g \\ &= 5.40 \times 10^7 \text{ lb/in} \end{aligned}$$

where:

$$\begin{aligned} A_L &= \text{an assumed cross-sectional area equal to a thick-walled cylinder with an inner diameter equal to the nominal bolt diameter and an outer diameter equal to three times the nominal bolt diameter (Shigley).} \\ &= \pi/4(9d^2 - d^2) = 2\pi d^2 \\ &= 14.14 \text{ in}^2 \end{aligned}$$

and:

$$\begin{aligned} E_{lid} &= 27.2 \times 10^6 \text{ psi} \\ L_g &= \text{grip length} = 7.12 \text{ in} \\ F_{\text{thermal}} &= \text{bolt differential thermal expansion load} \\ &= A_b \Delta T [\alpha_l - \alpha_b] E_b \text{ (conservatively assume } E_1 = E_2) \\ &= 13,703 \text{ lb} \end{aligned}$$

where:

$$\begin{aligned} \Delta T &= 270^\circ\text{F} - 70^\circ\text{F} = 200^\circ\text{F} \\ \alpha_l &= 8.94 \times 10^{-6} \text{ in/in/}^\circ\text{F} \\ \alpha_b &= 7.30 \times 10^{-6} \text{ in/in/}^\circ\text{F} \\ E_b &= 28.0 \times 10^6 \text{ psi} \end{aligned}$$

The shear stress in the bolt = 0 because the impact is at  $0^\circ$  with respect to the bolt axis.

The direct tensile stress in the bolt is:

$$f_b = F_b/A_b = 136,425 \text{ lb}/1.492 \text{ in}^2 = 91,437 \text{ psi}$$

where:

$$A_b = 1.492 \text{ in.}^2, \text{ the bolt tensile area}$$

The margin of safety (MS) is:

$$MS = \frac{S_y}{f_b} - 1 = \frac{141,700}{91,437} - 1 = +.55$$

#### 2.10.8.2.3 Oblique Drop (5°)

The impact force (tension) on the bolts is:

$$\begin{aligned} F_A &= P_A [R_L(R_L + R_B)/I_o] A_B \\ &= 116,201 \text{ lb} \end{aligned}$$

where:

$$\begin{aligned} P_A &= (n_g)(W_A)(\cos 5^\circ) \\ &= (54.7)(66,690)(\cos 5^\circ) \\ &= 3,634,061 \text{ lb} \\ R_L &= \text{lid radius,} \\ &= 39.5 \text{ in} \\ R_B &= \text{bolt circle radius,} \\ &= 37.655 \text{ in} \\ I_o &= \text{bolt circle moment of inertia} = \pi R_B^3 t + A_b N_b R_L^2 \\ &= \pi (37.655^3)(0.2649) + (1.492)(42)(39.5^2) \\ &= 142,204 \text{ in.}^4 \\ t &= \text{equivalent ring thickness,} \\ &= A_b N_b / (2\pi R_B) = (1.492)(42) / [(2\pi)(37.655)] \\ &= 0.2649 \text{ in} \\ A_B &= \text{bolt stress area} \\ &= 1.492 \text{ in}^2 \end{aligned}$$

The total applied external load is:

$$\begin{aligned} P &= f_s(\text{static}) + F_A(\text{impact}) \\ &= 9,036 + 116,201 \\ &= 125,237 \text{ lb} \end{aligned}$$

where:

$f_s$  = total static load

$F_A$  = total dynamic load resulting from impact

The net bolt tensile load is:

$$\begin{aligned} F_b &= K_b P / (K_b + K_m) + F_i \text{ (preload)} + F_t \text{ (thermal)} \\ &= 9,772 + 115,066 + 13,703 = 138,541 \text{ lb} \end{aligned}$$

The shear force in each bolt is:

$$\begin{aligned} F_L &= n_g W_L \sin \theta / N_b \\ &= (54.7)(10,690)(\sin 5^\circ) / 42 \\ &= 1,213 \text{ lb} \end{aligned}$$

where:

$n_g$  = impact acceleration based on impact force

$W_L$  = weight acting in lateral direction = 10,690 lb

$N_b$  = 42, number of bolts

The direct tension stress ( $f_b$ ) in the bolt is:

$$\begin{aligned} f_b &= F_b / A_b \\ &= 138,541 / 1.492 \\ &= 92,856 \text{ psi} \end{aligned}$$

The shear stress ( $f_v$ ) in the bolt is:

$$\begin{aligned} f_v &= F_L / A_b \\ &= 1,213 / 1.492 \\ &= 813 \text{ psi} \end{aligned}$$



The principal stresses are calculated as:

$$\begin{aligned}\sigma_1, \sigma_2 &= \frac{f_b}{2} \pm \sqrt{\left(\frac{f_b}{2}\right)^2 + f_v^2} \\ \sigma_1, \sigma_2 &= \frac{92,856}{2} \pm \sqrt{\left(\frac{92,856}{2}\right)^2 + 813^2} \\ &= 92,863 \text{ psi}; -7 \text{ psi}\end{aligned}$$

The stress intensity (SI) is:

$$SI = |\sigma_1 - \sigma_2| = 92,870 \text{ psi}$$

The margin of safety (MS) is:

$$MS = \frac{S_y}{SI} - 1 = \frac{141,700}{92,870} - 1 = +0.53$$

#### 2.10.8.2.4 Corner Drop (24°)

The impact force (tension) on the bolts is:

$$\begin{aligned}F_A &= P_A[R_L(R_L + R_B)/I_0] A_B \\ &= 96,041 \text{ lb}\end{aligned}$$

where:

$$\begin{aligned}P_A &= (n_g)(W_A)(\cos 24^\circ) \\ &= (49.3)(77,885)(\cos 24^\circ) \\ &= 3,003,570 \text{ lb}\end{aligned}$$

The total applied external load is:

$$\begin{aligned}P &= F_s (\text{static}) + F_A (\text{impact}) \\ &= 9,036 + 96,041 \\ &= 105,077 \text{ lb}\end{aligned}$$

where:

$F_s$  = total static load

$F_A$  = total dynamic load resulting from impact

The net bolt load is:

$$\begin{aligned} F_b &= K_b P / (K_b + K_m) + F_i \text{ (preload)} + F_t \text{ (thermal)} \\ &= 8,199 + 115,066 + 13,703 = 136,968 \text{ lb} \end{aligned}$$

The shear force in each bolt is:

$$\begin{aligned} F_L &= n_g W_L \sin \theta / N_b \\ &= (49.3)(10,690)(\sin 24^\circ) / 42 \\ &= 5,104 \text{ lb} \end{aligned}$$

where:

$n_g$  = impact acceleration based on impact force

$W_L$  = 10,690, weight acting in lateral direction

$N_b$  = 42

The direct tension stress in the bolt is:

$$\begin{aligned} f_b &= F_b / A_b \\ &= 136,968 / 1.492 \\ &= 91,801 \text{ psi} \end{aligned}$$

The shear stress in the bolt is:

$$\begin{aligned} f_v &= F_L / A_b \\ &= 5,104 / 1.492 \\ &= 3,421 \text{ psi} \end{aligned}$$

The principal stresses are calculated as:

$$\sigma_1, \sigma_2 = \frac{f_b}{2} \pm \sqrt{\left(\frac{f_b}{2}\right)^2 + f_v^2}$$
$$\sigma_1, \sigma_2 = \frac{91,801}{2} \pm \sqrt{\left(\frac{91,801}{2}\right)^2 + 3,421^2}$$
$$= 91,929 \text{ psi}; -127 \text{ psi}$$

The stress intensity (SI) is:

$$SI = |\sigma_1 - \sigma_2| = 92,056 \text{ psi}$$

The margin of safety (MS) is:

$$MS = \frac{S_y}{SI} - 1 = \frac{141,700}{92,056} - 1 = +0.54$$

#### 2.10.8.2.5 Side Drop (90°)

$$F_b = K_b f_s / (K_b + K_m) + F_i (\text{preload}) + F_t (\text{thermal})$$
$$= 705 + 115,066 + 13,703 = 129,474 \text{ lb}$$

The direct tension stress in the bolt is:

$$f_b = F_b / A_b$$
$$= 129,474 / 1.492$$
$$= 86,779 \text{ psi}$$

The shear force ( $F_L$ ) in each bolt is:

$$F_L = (10,690)(51.3)/42 = 13,057 \text{ lb}$$
$$f_s = 8,308$$
$$f_v = 8,751 \text{ psi}$$

The principal stresses are calculated as:

$$\sigma_1, \sigma_2 = \frac{f_b}{2} \pm \sqrt{\left(\frac{f_b}{2}\right)^2 + f_v^2}$$
$$\sigma_1, \sigma_2 = \frac{86,799}{2} \pm \sqrt{\left(\frac{86,799}{2}\right)^2 + 8,751^2}$$
$$= 87,653 \text{ psi}; -874 \text{ psi}$$

The stress intensity (SI) is:

$$SI = |\sigma_1 - \sigma_2| = 88,526 \text{ psi}$$

The margin of safety (MS) is:

$$MS = \frac{S_y}{SI} - 1 = \frac{141,700}{88,526} - 1 = +0.60$$

#### 2.10.8.3 Outer Lid Closure Bolt Analyses

All numerical examples pertain to the evaluation of the NAC-STC outer lid bolts under hypothetical accident conditions (Table 2.7.1.6-4).

##### 2.10.8.3.1 Outer Lid Bolt Preload

In selecting a preload for the outer lid cask closure bolts, the following loading factors are considered: (1) an internal pressure force on the closure lid of 7.35 psig; (2) the O-ring compression force; and (3) the inertial weight of the outer cask lid and impact limiter due to the 30-foot accident drop condition; and (4) the differential thermal expansion between the outer lid material and the bolt. Based on these loading conditions, an installation torque was selected to be 550±50 foot-pounds.

The required bolt preload to offset the combined static and dynamic loads is determined by:

$$F_b = F_s + F_A$$

where:

$F_b$  = calculated required bolt preload

$F_s$  = total static load

$F_A$  = total dynamic (impact) load

The cask lid closure bolt preload necessary to offset static loads is:

$$\begin{aligned} F_s &= F_{\text{pressure}} + F_{\text{O-ring}} \\ &= 38,635 \text{ lb} + 105,221 \text{ lb} \\ &= 143,856/36 = 3,996 \text{ lb/bolt; conservatively, use 4,000 lb/bolt} \end{aligned}$$

where:

$F_s$  = total static load (lb)

$F_{\text{press}}$  = internal pressure force (lb)

$$= (P)(\pi / 4)(D_{\text{or}})^2 = \left[ (7.35 \text{ psig}) \times \frac{\pi (81.69 \text{ in.})^2}{4} \right] = 38,635 \text{ lb}$$

$P$  = internal cask lid pressure = 7.35 psig

$D_{\text{or}}$  = cask outer lid O-ring diameter of 81.69 in.

$F_{\text{O-ring}}$  = O-ring compression force per bolt (lb),

$$= \pi(D_{\text{or}})(P)_c = \pi(81.69 \text{ in.})(410 \text{ lb/in}) = 105,221 \text{ lb}$$

where:

$D_{\text{or}}$  = diameter of (metal) O-ring = 81.69 in.

$P_c$  = O-ring compression force = 410 lb/in

The inertial (dynamic) load ( $F_a$ ) based on the cask's most severe loading orientation (end impact), is calculated as follows:

$$\begin{aligned} F_a &= \text{end impact bolt force} \\ &= \frac{P_a}{N_b} = \frac{952,859}{36} = 26,468 \text{ lb/bolt} \end{aligned}$$

where:

$$P_a = (W_a \times g) \cos \theta = (16,985 \times 56.1) \cos 0^\circ = 952,859 \text{ lb}$$

$$W_a = \text{outer lid (8,120) + impact limiter (8,865) weight} = 16,985 \text{ lb}$$

$$g = \text{end drop g-load} = 56.1 \text{ g}$$

$$\theta = \text{drop angle (from cask axis)} = 0^\circ$$

The impact limiter weight used, 8,865 lbs, is conservative because it considers the weight of the redwood impact limiter, which is heavier than the balsa wood impact limiter specified for the CY-MPC configuration.

Therefore, the calculated required tensile preload per bolt,  $F_b$ , is:

$$\begin{aligned} F_b &= F_s + F_a \\ &= 4,000 \text{ lb} + 26,468 \text{ lb} = 30,468 \text{ lb} \end{aligned}$$

The total torque (T) to develop the required tensile bolt preload ( $F_b$ ) is:

$$T = \left[ \left( \frac{d_m}{2d} \right) \left( \frac{\tan \lambda + \mu \sec \alpha}{1 - \mu \tan \lambda \sec \alpha} \right) + 0.625 \mu \right] (F)(d) = 5,960 \text{ in. lb, or } 5,960/12 = 497 \text{ ft-lb.}$$

The minimum design torque is  $550 - 50 \text{ ft-lb} = 500 \text{ ft-lb} > 497 \text{ ft-lb}$ . Therefore, the design installation torque is adequate.

#### 2.10.8.3.2 Top End Drop (0°)

The total applied external load is:

$$\begin{aligned} P &= F_s (\text{static}) + F_A (\text{impact}) \\ &= 4000 + 26,468 \\ &= 30,468 \text{ lb} \end{aligned}$$

where:

$$F_s = \text{total static load} = 4000 \text{ lb}$$

$$F_A = \text{total dynamic load resulting from impact} = 26,468 \text{ lb}$$

The net bolt load is:

$$\begin{aligned} F_b &= K_b P / (K_b + K_m) + F_i \text{ (preload)} + F_t \text{ (thermal)} \\ &= 2,267 + 36,810 + 0 = 39,077 \text{ lb} \end{aligned}$$

where:

$$\begin{aligned} K_b &= \text{bolt stiffness} \\ &= A_b E_b / L \\ &= 5.49 \times 10^6 \text{ lb/in} \end{aligned}$$

where:

$$\begin{aligned} A_b &= 0.606 \text{ in}^2 \\ E_b &= 27.2 \times 10^6 \\ L &= \text{total bolt length} - \frac{1}{2} \text{bolt head thickness} - \frac{1}{2} \text{engagement length} \\ &= 3.0 \text{ in} \\ K_m &= \text{lid stiffness} \\ &= A_L E_l / L_g \\ &= 6.83 \times 10^7 \text{ lb/in} \end{aligned}$$

where:

$$\begin{aligned} A_L &= \text{an assumed cross-sectional area equal to a thick-walled cylinder with} \\ &\quad \text{an inner diameter equal to the nominal bolt diameter and an outer} \\ &\quad \text{diameter equal to three times the nominal bolt diameter (Shigley).} \\ &= \pi/4(9d^2 - d^2) = 2\pi d^2 \\ &= 6.28 \text{ in}^2 \end{aligned}$$

and,

$$\begin{aligned} E_l &= 27.2 \times 10^6 \text{ psi} \\ L_g &= \text{grip length} = 2.5 \text{ in} \\ F_{\text{thermal}} &= \text{bolt differential thermal expansion load} = 0 \text{ because the bolt and the} \\ &\quad \text{lid are made of the same material.} \end{aligned}$$

The shear stress in the bolt = 0 because the impact is at 0° with respect to the bolt axis.

The direct tensile stress in the bolt is:

$$f_b = F_b/A_b = 39,077 \text{ lb}/0.606 \text{ in.}^2 = 64,483 \text{ psi}$$

where:

$$A_b = 0.606 \text{ in.}^2, \text{ the bolt tensile area}$$

The margin of safety (MS) is:

$$MS = \frac{S_y}{f_b} - 1 = \frac{94,200}{64,483} - 1 = +0.46$$

#### 2.10.8.3.3 Oblique Drop (5°)

The impact force (tension) on the bolts is:

$$\begin{aligned} F_A &= P_A[R_L(R_L + R_B)/I_o] A_B \\ &= 34,463 \text{ lb} \end{aligned}$$

where:

$$\begin{aligned} P_A &= (n_g)(W_a)(\cos 5^\circ) \\ &= (54.7)(16,985)(\cos 5^\circ) \\ &= 925,544 \text{ lb} \end{aligned}$$

$$\begin{aligned} R_L &= \text{lid radius,} \\ &= 43.35 \text{ in} \end{aligned}$$

$$\begin{aligned} R_B &= \text{bolt circle radius,} \\ &= 41.85 \text{ in} \end{aligned}$$

$$\begin{aligned} I_o &= \text{bolt circle moment of inertia} = \pi R_B^3 t + A_b N_b R_L^2 \\ &= \pi (41.85^3)(0.083) + (0.606)(36)(43.35^2) \\ &= 60,109 \text{ in}^4 \end{aligned}$$

$$t = \text{equivalent ring thickness,}$$



$$\begin{aligned} &= A_b N_b / (2\pi R_B) = (0.606)(36) / [(2\pi)(41.85)] \\ &= 0.083 \text{ in} \\ A_B &= \text{bolt stress area} \\ &= 0.606 \text{ in}^2 \end{aligned}$$

The total applied external load is:

$$\begin{aligned} P &= f_s (\text{static}) + F_A (\text{impact}) \\ &= 4,000 + 34,463 \\ &= 38,463 \text{ lb} \end{aligned}$$

where:

$$\begin{aligned} f_s &= \text{total static load} \\ F_A &= \text{total dynamic load resulting from impact} \end{aligned}$$

The net bolt tensile load is:

$$\begin{aligned} F_b &= K_b P / (K_b + K_m) + F_i (\text{preload}) + F_t (\text{thermal}) \\ &= 2,862 + 36,810 + 0 = 39,672 \text{ lb} \end{aligned}$$

The shear force in each bolt is:

$$\begin{aligned} F_L &= n_g W_L \sin\theta / N_b \\ &= (54.7)(8,120)(\sin 5^\circ) / 36 \\ &= 1,075 \text{ lb} \end{aligned}$$

where:

$$\begin{aligned} n_g &= \text{impact acceleration based on impact force} \\ W_L &= \text{weight acting in lateral direction} = 8,120 \text{ lb} \\ N_b &= 36 \end{aligned}$$

The direct tension stress in the bolt is:

$$\begin{aligned}f_b &= F_b/A_b \\&= 39,672/0.606 \\&= 65,465 \text{ psi}\end{aligned}$$

The shear stress in the bolt is:

$$\begin{aligned}f_v &= F_L/A_b \\&= 1,075/0.606 \\&= 1,774 \text{ psi}\end{aligned}$$

The principal stresses are calculated as:

$$\begin{aligned}\sigma_1, \sigma_2 &= f_b/2 \pm \sqrt{[(f_b/2)^2 + f_v^2]} \\&= 65,465/2 \pm \sqrt{[(65,465/2)^2 + (1,774)^2]} \\&= 65,513 \text{ psi}; -48 \text{ psi}\end{aligned}$$

The stress intensity (SI) is:

$$SI = |\sigma_1 - \sigma_2| = 65,561 \text{ psi}$$

The margin of safety (MS) is:

$$\begin{aligned}MS &= (S_y / SI) - 1 \\&= (94,200/65,561) - 1 = +0.44\end{aligned}$$

#### 2.10.8.3.4 Corner Drop (24°)

The impact force (tension) on the bolts is:

$$\begin{aligned}F_A &= P_A[R_L(R_L + R_B)/I_o] A_B \\&= 28,484 \text{ lb}\end{aligned}$$

where:

$$\begin{aligned} P_A &= (n_g)(W_A)(\cos 24^\circ) \\ &= (49.3)(16,985)(\cos 24^\circ) \\ &= 764,967 \text{ lb} \end{aligned}$$

The total applied external load is:

$$\begin{aligned} P &= F_s (\text{static}) + F_A (\text{impact}) \\ &= 4,000 + 28,484 \\ &= 32,484 \text{ lb} \end{aligned}$$

where:

$$\begin{aligned} F_s &= \text{total static load} \\ F_A &= \text{total dynamic load resulting from impact} \end{aligned}$$

The net bolt load is:

$$\begin{aligned} F_b &= K_b P / (K_b + K_m) + F_i (\text{preload}) + F_t (\text{thermal}) \\ &= 2,417 + 36,810 + 0 = 39,277 \text{ lb} \end{aligned}$$

The shear force in each bolt is:

$$\begin{aligned} F_L &= n_g W_L \sin \theta / N_b \\ &= (49.3)(8120)(\sin 24^\circ) / 36 \\ &= 4,523 \text{ lb} \end{aligned}$$

where:

$$\begin{aligned} n_g &= \text{impact acceleration based on impact force} \\ W_L &= 8,120 \text{ lb, weight acting in lateral direction} \\ N_b &= 36 \end{aligned}$$

The direct tension stress in the bolt is:

$$\begin{aligned}f_b &= F_b/A_b \\&= 39,277/0.606 \\&= 64,731 \text{ psi}\end{aligned}$$

The shear stress in the bolt is:

$$\begin{aligned}f_v &= F_L/A_b \\&= 4,523/0.606 \\&= 7,464 \text{ psi}\end{aligned}$$

The principal stresses are calculated as:

$$\begin{aligned}\sigma_1, \sigma_2 &= f_b/2 \pm \sqrt{[(f_b/2)^2 + f_v^2]} \\&= 64,731/2 \pm \sqrt{[(64,731/2)^2 + (7,464)^2]} \\&= 65,581 \text{ psi; } -850 \text{ psi}\end{aligned}$$

The stress intensity (SI) is:

$$\begin{aligned}SI &= |\sigma_1 - \sigma_2| \\&= 66,431 \text{ psi}\end{aligned}$$

The margin of safety (MS) is:

$$\begin{aligned}MS &= (S_y / SI) - 1 \\&= (94,200/66,431) - 1 = +0.42\end{aligned}$$

#### 2.10.8.3.5 Side Drop (90°)

$$\begin{aligned}F_b &= K_b f_s / (K_b + K_m) + F_i \text{ (preload)} + F_t \text{ (thermal)} \\&= 298 + 36,810 + 0 = 37,108 \text{ lb}\end{aligned}$$

The shear force in each bolt is:

$$F_L = (8,120)(51.3)/36 = 11,571 \text{ lb}$$

$$f_s = 4,000$$

$$f_b = 37,108/0.606 = 61,234 \text{ psi}$$

$$f_v = 11661/0.606 = 19,094 \text{ psi}$$

The principal stresses are calculated as:

$$\begin{aligned}\sigma_1, \sigma_2 &= f_b/2 \pm \sqrt{[(f_b/2)^2 + f_v^2]} \\ &= 61,234/2 \pm \sqrt{[(61,234/2)^2 + (19,094)^2]} \\ &= 66,700; -5,466 \text{ psi}\end{aligned}$$

The stress intensity (SI) is:

$$\begin{aligned}\text{SI} &= |\sigma_1 - \sigma_2| \\ &= 72,166 \text{ psi}\end{aligned}$$

The margin of safety (MS) is:

$$\begin{aligned}\text{MS} &= (S_y / \text{SI}) - 1 \\ &= (94,200/72,166) - 1 = +0.31\end{aligned}$$

**THIS PAGE INTENTIONALLY LEFT BLANK**

#### 2.10.9      Lead Slump Evaluation

The objective of this lead slump evaluation is to determine the effect of varying the value of the modulus of elasticity of lead used in the 30-foot end drop impact analysis of the NAC-STC at normal operating temperature on: (1) the calculated lead slump distance; and (2) the magnitude of the calculated stresses in the inner and outer shells. A secondary objective of this lead slump evaluation is to verify that the inner and outer shell stresses presented in Section 2.7.1 for the 30-foot drop analyses are conservative (Note: Section 2.7.1 analyses used the modulus of elasticity of lead that reflected a perfectly elastic material throughout the loading event. The lead slump evaluation presented in this section uses the secant modulus, a minimum value of the modulus of elasticity of lead.).

The NAC-STC cask shell is a composite of a 3.70-inch thick lead sandwiched between a 1.50-inch thick stainless steel inner shell and a 2.65-inch thick stainless steel outer shell.

The detailed analysis that follows considers the secant modulus of elasticity of lead to be 27.75 ksi. This value represents a conservative estimate of the strain rate dependent dynamic modulus of elasticity (Evans).

A coefficient of friction of 0.5 is used at the contact surfaces between the stainless steel shells and the lead shielding. According to the Standard Handbook For Mechanical Engineers (Baumeister), the static friction coefficient between lead and steel is 0.95 for dry surface contact and 0.5 for greasy surface contact. Therefore, the 0.5 friction coefficient value adopted for the lead slump evaluation is very conservative.

A uniform temperature of 300°F is conservatively applied to the model. Under normal operating conditions, the temperature spectrum with respect to the longitudinal axis of the composite shell varies from a maximum of 331°F to a minimum of 200°F. The thermal analysis results presented in Section 3.4 define the location of the maximum temperature of the composite shell at the mid-section of the longitudinal axis, with the temperature decreasing at locations away from the mid-section.

This lead slump analysis of the 30-foot end drop impact considers a cask total weight of 250 kips with the maximum deceleration of 56.1 g. Total force at impact is  $14.025 \times 10^6$  pounds.

#### 2.10.9.1 Methodology/Finite Element Analysis

An ANSYS two-dimensional axisymmetric finite element model was constructed using 2-D isoparametric elements (STIF42), 2-D gap elements (STIF12), and general mass elements (STIF21). The model geometry includes the inner and outer stainless steel shells, neutron shield, lead shielding and the inner and outer lids. The impact limiters were not explicitly modeled. Impact limiter weight was accounted for in the model by discrete lump masses using ANSYS general lump mass elements (STIF21). See Figures 2.10.9-1 and 2.10.9-2 for the finite element model plots.

The weight of the internal contents of the cask, i.e the fuel basket, fuel, and basket spacer, is applied as a pressure load amplified by 56.1 g on the cask model. The total weight of the cask is applied as a 56.1-g impact load to simulate the 30-foot end drop accident. Component stresses--longitudinal,  $S_y$ , and circumferential,  $S_z$ --are calculated and tabulated for representative locations on the cask body.

Gap elements were introduced at the contact surfaces between the lead shielding and the inner and outer shells. The initial boundary conditions for this evaluation assume that the lead is in contact with both the inner and the outer shells. Gap element stiffness was set to  $5.0 \times 10^6$  based on elementary classical evaluation of stiffness between the composite shells as detailed in Section 2.6.12.2. As mentioned earlier, a conservative value of 0.5 was used as the coefficient of static friction between the lead and the stainless steel shells. Introduction of a coefficient of friction into the gap elements creates a highly nonlinear problem. To facilitate solution convergence of the ANSYS impact analyses, radial displacement boundary conditions were defined between the contacting surfaces. The nonlinear gap elements were modeled with a contact interference value of 0.001 inch at both the inner and the outer lead/stainless steel contact surfaces.



As previously stated, the analysis approach presented in this section considers a 0.001-inch contact interference at both the inner and the outer lead/stainless steel interface surfaces so that the analytical program, ANSYS, can obtain a converged solution. Thus, there is considered to be no gap present at either interface surface for the normal operating temperature condition at the time the 30-foot end drop accident occurs. There are 121 gap elements spaced at 1.3417-inch intervals modeled on each side of the lead annulus. The normal force at each gap element is approximately 3727 pounds/inch/radian due to the 0.001-inch contact interference modeled at the interface surfaces. (The friction force is  $0.5 \times$  the normal force). Then, considering both interface surfaces, the total normal force applied in the finite element model is 7454 pounds/inch/radian. An axisymmetric finite element model evaluation of the differential thermal expansion of the lead and stainless steel shells calculated a gap of 0.0271 inch at the lead/outer shell interface at normal operating temperature and a contact interference at the lead/inner shell interface, which produces a normal force of 14,296 pounds/inch/radian. Therefore, the total interface force modeled in this analysis is conservatively low by a factor of  $14,296/7454 = 1.9$ . Then, the impact lead pressures and resulting inner and outer shell stresses that are calculated by ANSYS in this evaluation are conservative.

#### 2.10.9.2      Analysis Result

##### 2.10.9.2.1    Lead Slump

Figure 2.10.9-3 shows the longitudinal displaced shape due to the 30-foot end drop hypothetical accident condition, corresponding to a deceleration value of 56.1 g, with respect to the full cask weight of 250 kips. The displacement plots show the maximum lead shielding longitudinal settlement is 0.15037 inch at the top. The lead settlement decreases downwards to a value of 0.008354 inch near the bottom of the cask. The deformed shape of the lead shielding after impact clearly concludes that there is no appreciable slump other than a localized maximum compression of 0.15037 inch after the 30-foot end drop hypothetical accident condition.

#### 2.10.9.2.2 Stress Evaluation

Drop tests were carried out on a quarter-scale model of the NAC-STC. The quarter-scale model outer shell was instrumented with three groups of strain gauges, each group consisting of three 90-degree, two-element, rosette type gauges. The strain gauge groups were located longitudinally on the model at 9 inches, 24 inches, and 39 inches from the bottom outer surface of the cask body model. In each group of strain gauges, a 90-degree, two-element, rosette type gauge was located circumferentially at 0°, 90°, and 180° with one element oriented in the cask body axial direction and one element oriented in the circumferential direction. These strain gauges were used to measure strains at each of the above locations on the cask outer shell during impact. Corresponding longitudinal and circumferential component stresses at each location were then calculated based on the generalized Hook's law as follows:

$$Ee_{ij} = [(1+n)s_{ij} - nd_{ij}s_{kk}]$$

where:

- n = Poisson's ratio
- e = Strain (in)
- s = Stress (psi)
- E = Elastic Modulus
- d = Kronecker Delta ; 1 when  $i \neq j$ ; 0 otherwise

Finite element component stresses and von Mises stresses at similar location to the test strain gauge locations are listed in Tables 2.10.9-1 and 2.10.9-2 for the outer and inner shells, respectively. Figure 2.10.9-4 shows the node locations used in this stress summary. Table 2.10.9-3 provides a comparison of the stresses at selected locations on the outer shell, corresponding to the locations where strain gauges were positioned for the drop tests. The stresses are determined by four different methods, including: (1) SCANS dynamic analysis, using a lead modulus of 2280 ksi, (2) 30-foot end drop test using a quarter-scale cask model, (3) ANSYS analysis using a lead modulus value of 27.0 ksi with the consideration of friction between

the lead and surrounding steel shells, and (4) ANSYS analysis using a lead modulus value of 2280 ksi without the consideration of friction between the lead and the steel shells.

The comparison provided by Table 2.10.9-3 illustrates that the stress evaluations performed using the two different lead modulus values, together with the different considerations of friction, result in similar stress results. The stress results from the ANSYS analysis which uses a lead modulus of 2280 ksi, without friction, are more consistent with the drop test results than the results obtained from the ANSYS analysis using the lead modulus of 27.0 ksi. Therefore, the analysis results documented in Section 2.7, which were performed using a lead modulus of 2280 ksi, are accurate, and adequately represent the behavior of the NAC-STC.

#### 2.10.9.3 Conclusion

A structural analysis using the strain dependent secant modulus of elasticity for lead shows that there is negligible lead slump after the 30-foot end drop hypothetical accident condition. These analytical results closely agree with test results from the quarter-scale model drop test and the elastic analysis results based on Young's modulus for lead used in the analyses of Section 2.7. The NAC-STC cask is, therefore, adequately designed.

Figure 2.10.9-1      Lead Slump - Cask 2D Model Element Plot

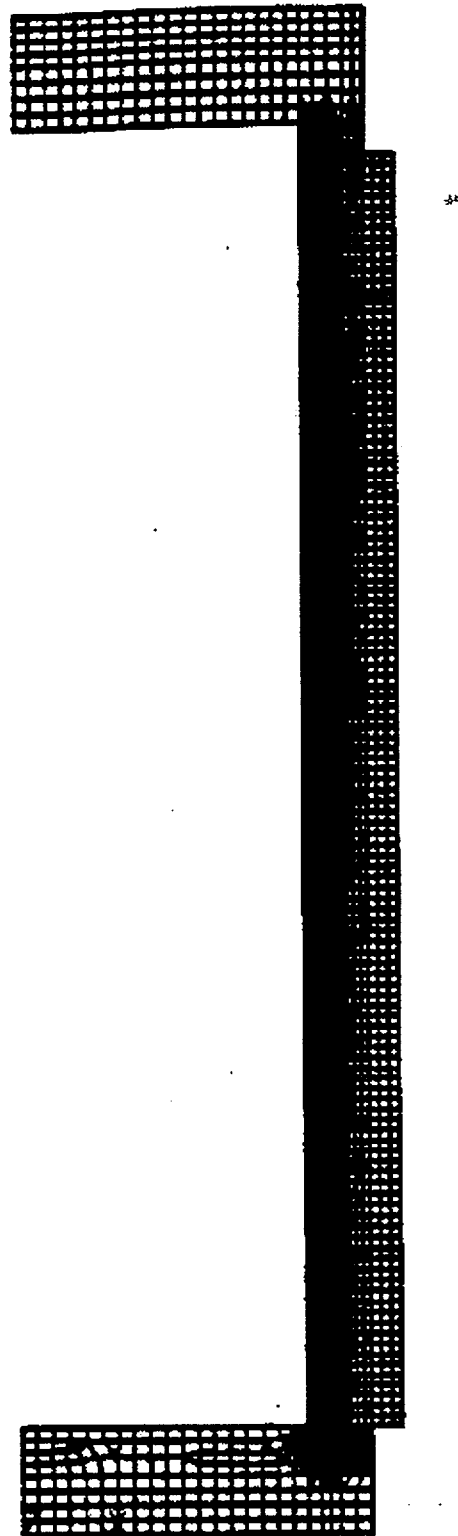


Figure 2.10.9-2 Lead Slump - Gap Element Plot

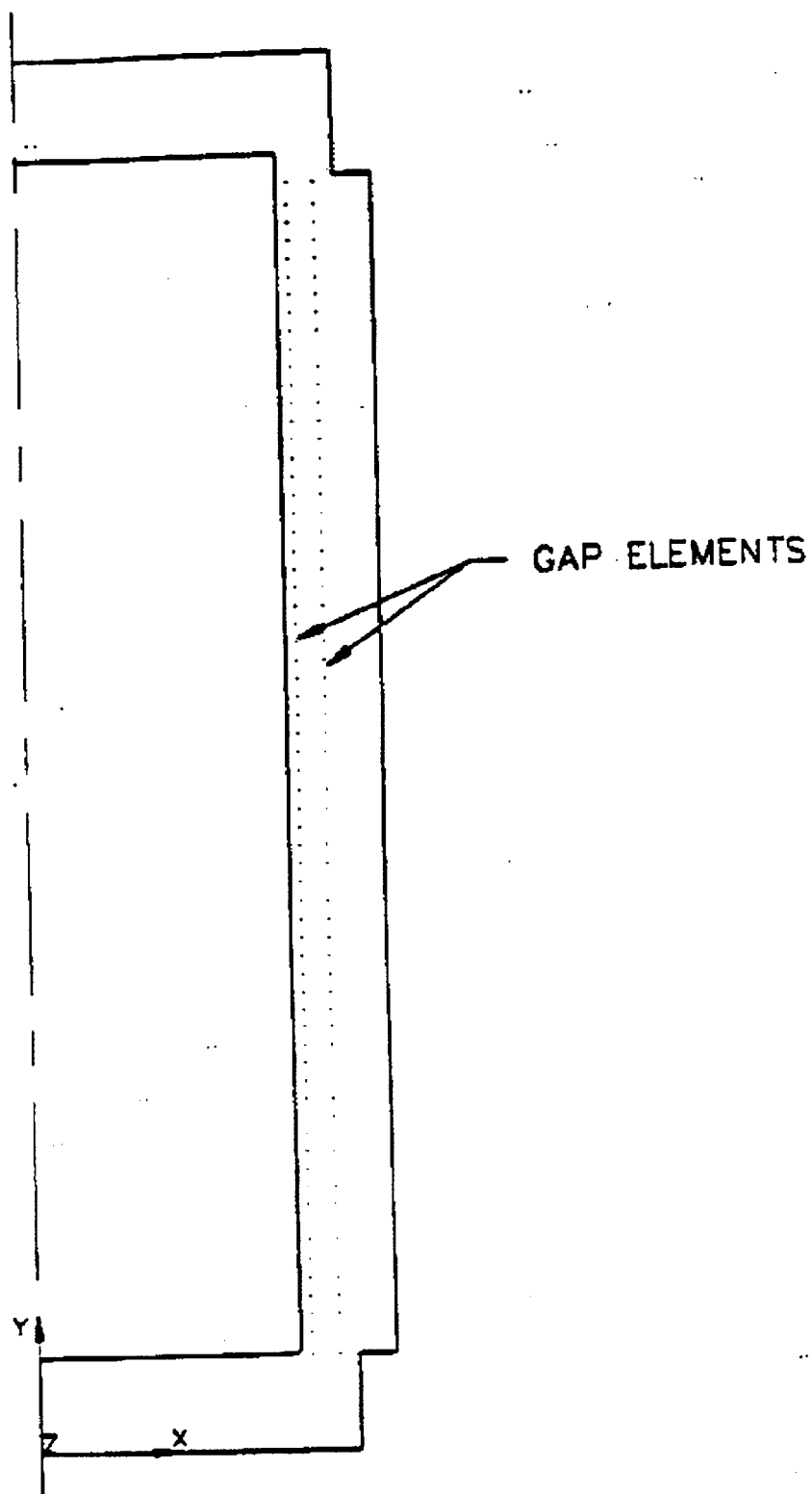


Figure 2.10.9-3      Lead Slump Displacement

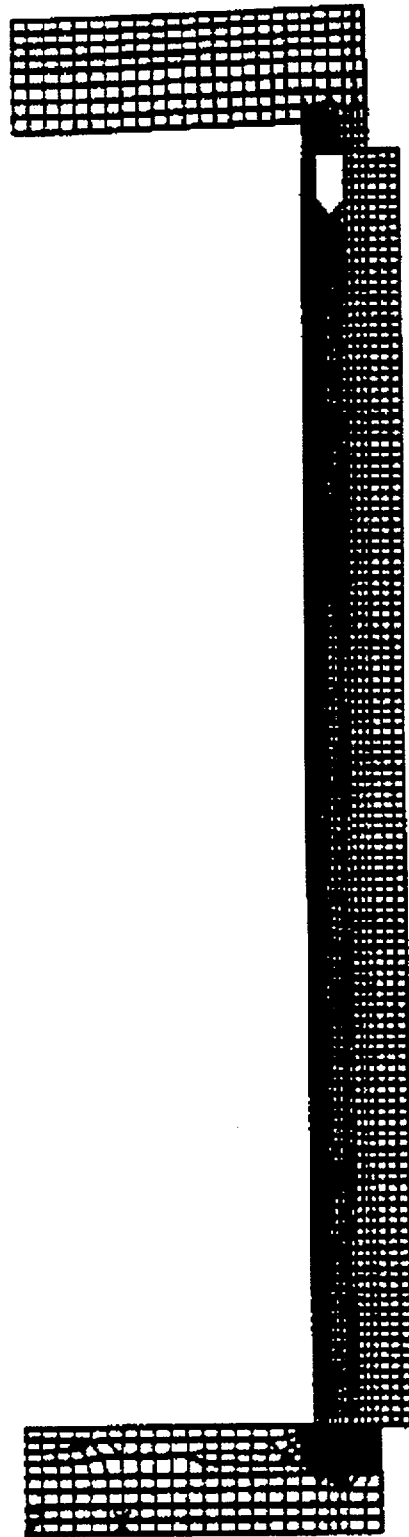


Figure 2.10.9-4 Location of Node Points Used in Stress Summary

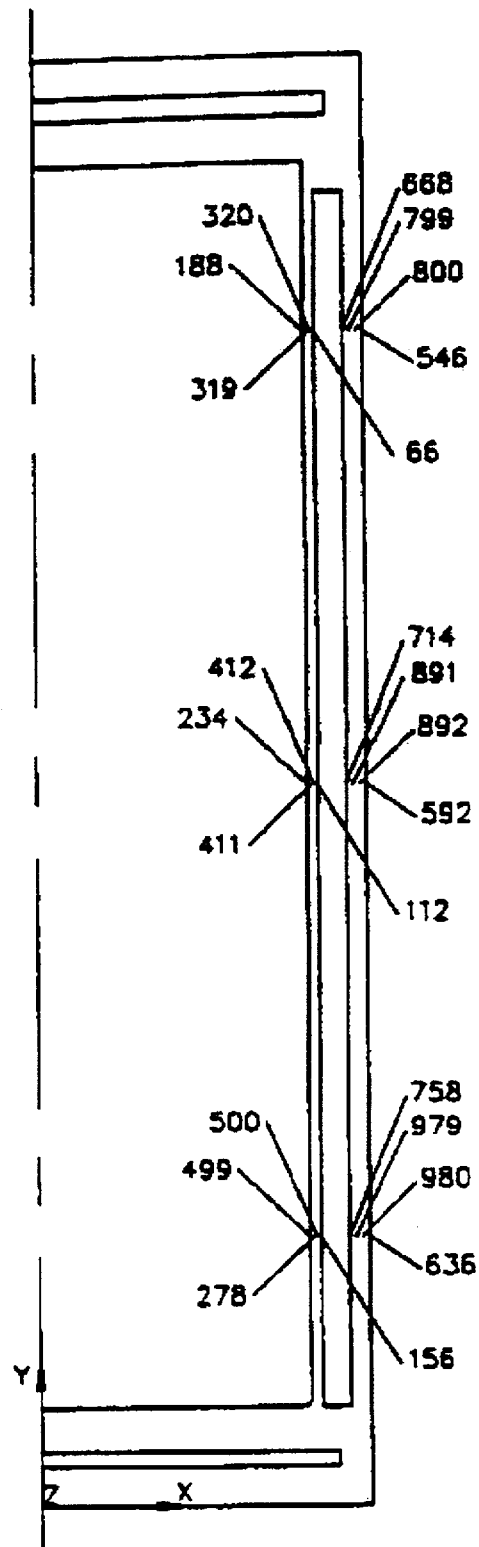


Table 2.10.9-1 Summary of 30-Foot End Drop Stress Results on the Outer Shell of the NAC-STC (ANSYS)

Longitudinal Location (in)	Node #	S <sub>x</sub>	S <sub>y</sub>	S <sub>z</sub> (psi)	S <sub>xy</sub>	SIG <sub>E</sub>
156.96	758	1.65	-5510.60	106.49	-22.20	5565.54
	979	0.00	-5668.74	67.06	-18.06	5702.62
	980	0.32	-5588.86	87.10	-23.41	5633.22
	636	1.65	-5510.60	106.49	-22.20	5565.54
96	714	0.0	-4100.67	3.39	-2.04	4102.37
	891	0.0	-4100.68	3.32	-4.02	4102.39
	892	0.13	-4100.69	3.25	-7.93	4102.41
	592	0.19	-4100.70	3.19	-9.74	4102.42
36	668	-0.93	-2338.39	177.04	-2.40	2431.34
	799	1.64	-2452.86	141.99	-4.20	2527.61
	800	2.46	-2564.15	108.36	-7.36	2621.20
	546	3.38	-2676.15	75.50	-8.63	2716.35

Note: See Figure 2.10.9-4 for locations of node numbers listed above S<sub>x</sub>, S<sub>y</sub>, S<sub>z</sub>, S<sub>xy</sub> and SIG<sub>E</sub> are the radial, longitudinal, circumferential, shear and von Mises stresses, respectively.



Table 2.10.9-2 Summary of 30-Foot End Drop Stress Results on the Inner Shell of the NAC-STC (ANSYS)

Longitudinal Location (in)	Node #	S <sub>x</sub>	S <sub>y</sub>	S <sub>z</sub> (psi)	S <sub>xy</sub>	SIG <sub>E</sub>
156.96	278	-0.2	-7146.9	-2176.69	-7.52	345.33
	499	-30.20	-7145.84	-2146.40	-14.70	6329.15
	500	-59.05	-7144.69	-2117.33	-28.83	6313.94
	156	-86.71	-7143.51	-2089.40	-35.48	6299.59
96	234	00.00	-4422.21	-1571.61	-5.43	3883.04
	411	-21.79	-4422.31	-1549.98	-10.67	3870.15
	412	-42.63	-4422.34	-1529.22	-21.10	3858.09
	112	-62.61	-4422.30	-1509.27	-26.07	3846.70
36	188	1.02	-2091.81	-1073.98	-4.24	1812.99
	319	-13.52	-2055.79	-1049.27	-7.91	1769.07
	320	-27.17	-2021.25	-1025.65	-14.42	1727.38
	66	-40.38	-1985.03	-1002.32	-17.12	1684.70

Note: See Figure 2.10.9-4 for location of node numbers listed above. S<sub>x</sub>, S<sub>y</sub>, S<sub>z</sub>, S<sub>xy</sub> and SIG<sub>E</sub> are the radial, longitudinal, circumferential, shear and von Mises stresses, respectively.

Table 2.10.9-3 Comparison of Outer Shell Stresses for 30-Foot End Drop

Location <sup>1</sup>			Stress (ksi)			
Longitudinal (inch)	Circumferential (degree)		SCANS <sup>3</sup> (51.4g)	Drop Test (55.6g)	ANSYS <sup>4</sup> (56.1g)	ANSYS <sup>5</sup> (56.1g)
156.96	0	$S_z$	-7.17	-8.27	-5.67	-6.0
		$S_t$	1.88	1.68	0.10	1.1
	90	$S_z$	-7.17	-5.66	-5.67	-6.0
		$S_t$	1.88	1.04	0.10	1.1
	180	$S_z$	-7.17	-5.88	-5.67	-6.0
		$S_t$	1.88	2.01	0.10	1.1
96.0	0	$S_z$	-5.0	-4.74	-4.10	-3.2
		$S_t$	1.28	1.76	0.0	0.0
	90	$S_z$	-5.0	-4.54	-4.10	-3.2
		$S_t$	1.28	1.42	0.0	0.0
	180	$S_z$	-5.0	-3.95	-4.10	-3.2
		$S_t$	1.28	1.71	0.0	0.0
36.0	0	$S_z$	-2.7	-1.86	-2.68	-1.9
		$S_t$	0.35	1.42	0.20	0.3
	90	$S_z$	-2.7	-1.79	-2.68	-1.9
		$S_t$	0.35	1.49	0.20	0.3
	180	$S_z$	-2.7	-1.67	-2.68	-1.9
		$S_t$	0.35	1.56	0.20	0.3

- Locations where the strain gauges were positioned for the NAC-STC drop tests. Longitudinal location is measured from the cask bottom; circumferential location is the angular position on the cask circumference. (Note that the 0-degree circumferential location for the analyses is the 180 degrees circumferential location for the specification of gauge location.
- $S_z$  (longitudinal) and  $S_t$  (circumferential) are normal stresses.
- Lead modulus 2280 ksi was used in the SCANS dynamic evaluation.
- Lead modulus 27.75 ksi with friction was used in the ANSYS non-linear evaluation.
- Lead modulus 2280 ksi was used in the ANSYS impact evaluation in Section 2.10.4, Table 2.10.4-14.

2.10.10      Assessment of the Effect of the Revised Temperature Distribution on Structural Qualification

Finite element structural analysis of the directly loaded fuel configuration of the cask for normal and accident condition loads had been completed based on temperature distributions obtained using analytical thermal boundaries different than those currently documented in the heat transfer analyses in Chapter 3. Therefore, an evaluation of the effect of the revised temperature distribution on the cask structural qualification is performed to evaluate the adequacy of the previously completed structural analyses. The following discussion presents the methodology, and data evaluation used to investigate the dependence of the structural analyses on the temperature distribution in the cask. From this evaluation it is concluded that the structural analyses are conservative and that the calculated stress intensity values are higher than those that would be obtained using the revised thermal distribution. Therefore, revision of the structural analyses of the cask to reflect the revised temperature distributions is not required. Note: Separate thermal analyses have been performed for the canistered fuel configuration of the NAC-STC (refer to Chapter 3).

2.10.10.1      Evaluation Methodology

The cask temperature distribution influences the structural analyses through temperature dependent material properties and through induced secondary stress resulting from temperature gradients. These parameters are expressed as a function of temperature in the following generalized relationship for calculating temperature induced stress in structural members:

$$S = C E_{(T)} \alpha_{(T)} \Delta T$$

where

S = thermal induced stress

C = problem configuration constant

$E_{(T)}$  = temperature dependent modulus of elasticity

$\alpha_{(T)}$  = temperature dependent coefficient of thermal expansion  
 $\Delta T$  = temperature difference between two points in the structure  
(through the thickness of the component or between adjacent components).

The problem configuration constant is not dependent on the temperature distribution in a structure and will not have an effect on the stress results obtained for a constant cask geometry subjected to different heat transfer results. Therefore, C, the problem configuration constant does not enter into the following evaluation.

The modulus of elasticity,  $E_{(T)}$ , is a temperature dependent material property which produces a direct proportional response in the resultant stress. However, it is important to note that this material property is temperature dependent and that its value has an inverse relationship with temperature for all cask component materials presented in Section 2.3. As the temperature increases the modulus of elasticity becomes smaller. Therefore, as the average temperature of the cask components change, the component stress will change as an inverse relationship. It is also important to note that the modulus of elasticity is the only temperature dependent material property that effects primary stress results.

The coefficient of thermal expansion,  $\alpha_{(T)}$ , is also a temperature dependent material property that, unlike the modulus of elasticity, increases with temperature. Influence of the coefficient of thermal expansion on the resultant stress components is only included as a stress component in combination with the temperature difference between adjacent points in the structure,  $\Delta T$ . Therefore, to obtain an assessment of the influence of the coefficient of thermal expansion on the resultant stress values it must be evaluated in combination with the respective temperature difference between two adjacent points. Thus, the combined function ( $\alpha_{(T)} \Delta T$ ) is a temperature dependent set influencing this evaluation.

From the above general equation, secondary temperature dependent stress is directly dependent on the difference in temperature,  $\Delta T$ , between adjacent points in the cask. Boundary conditions used in the heat transfer analysis have a significant influence on the actual temperatures

throughout the cask. Therefore, to perform an assessment of the influence of these different parameters on the completed structural analyses, the cask component average temperatures and temperature gradients resulting from the original and revised heat transfer analyses are summarized for the different cask components.

In addition to the temperature effects on the stress results, as discussed above, allowable stress limits are based on temperature dependent yield and ultimate material strengths. Material strength for each structural component in the cask has an inverse relationship with temperature as shown in the material property tables presented in Section 2.3. Therefore, in addition to evaluating the effect of the change in temperature on the resultant stress intensity for both the normal and accident condition loadings, the influence of temperature on the allowable stress values is performed for comprehensive assessment of the revised heat transfer analysis on the structural qualification of the NAC-STC.

#### 2.10.10.2 Temperature Dependent Stress Results

Tables 2.10.10-1 and 2.10.10-2 present the comparison of the temperature results between the original heat transfer analysis that was used in the structural qualification to the revised heat transfer analysis that is documented in Chapter 3. The original heat transfer analysis represented boundary conditions: (1) without the gap between the basket and inner shell wall; (2) without the influence of the attached impact limiters; and (3) with surface convection based on a vertical circular cylinder. The original heat transfer analysis results were obtained from a two-dimensional finite difference model analyzed using HEATING5 (Turner). The revised heat transfer analysis represents boundary conditions: (1) with the gap between the basket and inner shell wall; (2) with the influence of both installed impact limiters; (3) with convection based on a horizontal circular cylinder; (4) with air as the cavity gas; and (5) with the revised fuel tube design. The revised heat transfer analysis results have been obtained from a three-dimensional finite element model analyzed using ANSYS.

The following observations and conclusions are made from a review of the data presented in Tables 2.10.10-1 and 2.10.10-2.

1. The average temperature of the cask components enclosed by the impact limiters increased significantly. The average temperature for the inner lid increased approximately 50EF, and the bottom plate and forging increased approximately 210EF and 250EF, respectively.
2. As noted in Section 2.10.10.1, the modulus of elasticity is a temperature dependent material property that reduces in value as the temperature increases. The evaluation of the change in stress resulting from the effect of modulus of elasticity is performed by calculating the ratio of the material property values for the component having the greatest change in average temperature. Therefore, for the bottom forging this calculation is:

$$\frac{E_{(T-\text{Revised})}}{E_{(T-\text{Original})}} = \frac{E_{(425)}}{E_{(150)}} = \frac{26.33 \times 10^6 \text{ psi}}{27.9 \times 10^6 \text{ psi}} = 0.94$$

Based on this calculation for the cask component having the greatest increase in temperature, it is concluded that the change in the modulus of elasticity resulting from the revised heat transfer analysis will lower the stress results to as much as 94 percent of the stress calculated using the temperature from the original heat transfer analysis. Therefore, the current structural qualification as influenced by the modulus of elasticity is conservative.

3. Temperature gradients are small through the thickness of the individual components. Therefore, evaluating the influence of the change in temperature on stress results produced from the combined coefficient of thermal expansion and temperature gradient is performed for both the top and bottom of the cask relative to the shell. The temperature gradients are defined in Table 2.10.10-2.

To compare the structural influence of the differential thermal expansion of the inner shell and forging ends using previous thermal analysis with the differential expansion using the revised thermal analysis, the general expression is:

$$\frac{(\alpha_{(T)} \Delta T)_{\text{Revised}}}{(\alpha_{(T)} \Delta T)_{\text{Original}}}$$

where  $\Delta T = (\text{average temperature of forging}) - (\text{average temperature of inner shell})$

For the bottom of the cask, this expression becomes:

$$\frac{(\alpha_{(425)} \Delta T)}{(\alpha_{(150)} \Delta T)} = \frac{(9.24 \times 10^{-6} \times 53)}{(8.67 \times 10^{-6} \times 153)} = 0.37$$

For the top of the cask, this expression becomes:

$$\frac{(\alpha_{(225)} \Delta T)}{(\alpha_{(200)} \Delta T)} = \frac{(8.85 \times 10^{-6} \times 88)}{(8.79 \times 10^{-6} \times 113)} = 0.78$$

This calculation shows that the effect of the revised heat transfer analysis on stress resulting from the difference in average temperature between adjacent cask components will be less than that produced from the original heat transfer analysis. Therefore, that portion of the secondary stress results, which are produced from the coefficient of thermal expansion and temperature gradients in the cask structural qualification are conservative.

4. In addition to the above direct stress component effects, the allowable stress limits are influenced by the maximum component temperature. The following is a comparison of the revised and original temperature dependent material yield strength for the cask component experiencing the greatest change in temperature (the bottom plate of the cask). This comparison is representative of the revised temperature influence on the allowable stress values (independent of the specific evaluation), which are a function of  $S_m$ ,  $S_y$ , or  $S_u$ .

$$\frac{S_{y(350)}}{S_{y(150)}} = \frac{21.6}{26.2} = 0.83$$

Based on this evaluation it is concluded that the allowable stress limits for both normal and accident condition structural evaluations for the revised heat transfer results may be as much as 20 percent less than stress allowable based on the original heat transfer analysis. Therefore, allowable stress and margins of safety are revised throughout the structural qualification based on the temperature results from the revised heat transfer analysis.

5. Further evaluation of the effect of the temperature increase throughout the cask considers the enclosed non-structural members of the cask, i.e., the chemical lead gamma shield and the BISCO NS4FR neutron shield.

The average temperature of the lead gamma shield has effectively not changed over the average temperature of the lead defined from the original heat transfer analysis and used in the finite element structural analyses of the cask. This result represents the combined influence of including gaps and reducing the heat load. These changes tend to cancel each other. Therefore, it is concluded that the influence of the revised temperature in the cask shell wall has no impact on the structural qualification of the NAC-STC cask.

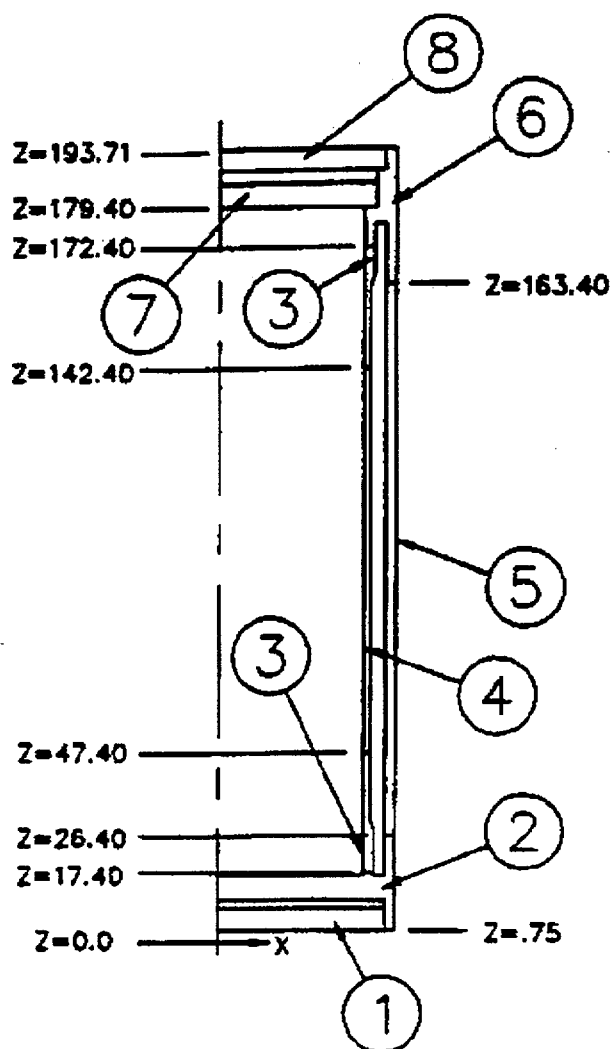
The most significant increase in a cask component temperature is in the bottom where heat loss has been significantly reduced by the modeling of the bottom impact limiter. Although this has reduced temperature gradients in this region, the temperature of the bottom neutron shield has increased to 403EF. The neutron shield will be sized such that no stress will be induced into the cask structure from thermal expansion of the neutron shield. Additionally, off-gas from the neutron shield material between the inner lid top plate and the inner lid, and between the bottom plate and bottom forging will not be released. Considering the neutron shield cavity in both cask ends to be completely filled with off-gas experiencing temperature increases from 70EF to their respective steady state temperatures will result in an induced stress of 3200 psi in the inner lid top plate and 240 psi in the bottom. These stress levels are insignificant with respect to the structural qualification of the cask and have been neglected.



2.10.10.3      Conclusions - Revised Temperature Distribution Evaluation

From the above evaluation it is seen that each of the different temperature parameters will have a positive margin of safety impact on the current structural analyses. The evaluation of the influence of the modulus of elasticity effect shows that the current set of stress results are conservative. The evaluation of the influence of the coefficient of thermal expansion in combination with the thermal gradients between the cask components shows a 20 to 80 percent conservatism for the interaction between the cask shell and the cask ends. In addition to the conservative changes in stresses, adjusting the allowable stress values to those representative of the maximum component temperature based on the revised thermal conditions provides qualification of conservative structural analyses. Therefore, it is concluded from this evaluation that the detailed finite element analyses performed for normal and accident condition loads using the original temperature distributions are conservative. Revisions to the structural qualification of the cask resulting from the revised heat transfer analyses are limited to changes in the allowable stress and the margins of safety in the stress summary tables in Section 2.10.4.

Figure 2.10.10-1 Identification Applicable to Temperature Summary



- 1 - Bottom Plate
- 2 - Bottom Forging and  
Bottom Ring Forging
- 3 - Transition Shell
- 4 - Inner Shell
- 5 - Outer Shell
- 6 - Top Forging
- 7 - Inner Lid
- 8 - Outer Lid

Figure 2.10.10-2      Component Wall Gradient Locations

**FIGURE WITHHELD AS SENSITIVE  
UNCLASSIFIED INFORMATION**

Table 2.10.10-1 Comparison of Cask Component Temperatures (Directly Loaded Fuel Configuration)

		Wall <sup>2</sup> Gradient Location	Original 2D Heat Transfer Analysis			Revised 3D Heat Transfer Analysis <sup>3</sup>		
			Maximum Temp. (°F)	Average Temp. (°F)	Wall Grad. °F/in	Maximum Temp. (°F)	Average Temp. (°F)	Wall Grad. °F/in
Component <sup>1</sup> I.D.	Description							
1	Bottom Plate	B	140	124	2.57	350	319	0.48
2	Bottom forging	A	165	158	2.65	418	329	2.57
3	Upper Transition Shell	P	247	225	1.3	255	224	1.06
3	Lower Transition Shell	H	222	171	1.3	300	282	1.0
4	Inner Shell	L	351	311	2.11	311	276	3.73
5	Outer Shell	M	324	250	2.83	286	254	2.90
6	Top Forging	T	217	198	0.82	211	188	0.62
7	Inner Lid	W	181	180	0.66	223	175	0.18
8	Outer Lid	X	180	174	1.33	178	159	0.43

<sup>1</sup> Refer to Figure 2.10.10-1 for component definitions.

<sup>2</sup> Refer to Figure 2.10.10-2 for wall gradient locations.

<sup>3</sup> The temperature reported below corresponds to the condition of a heat load of 22.1 kW, solar insolation, 100°F ambient condition with air in the cask cavity.

Table 2.10.10-2 Comparison of Cask Component Average Temperature Difference  
(Directly Loaded Fuel Configuration)

Component I.D.	Description	Original 2D Heat Transfer Analysis		Revised 3D Heat Transfer Analysis	
		Average Temp. °F	Temperature Difference (4-2 or 4-6)	Average Temp. °F	Temperature Difference (4-2 or 4-6)
2	Bottom Forging	158		329	
4-2			153		53
4	Inner Shell	311		276	
4-6			113		88
6	Top Forging	198		188	

**THIS PAGE INTENTIONALLY LEFT BLANK**

#### 2.10.11 Sensitivity Studies of the Yankee-MPC Canistered Fuel Basket Analysis

This section presents the results of various sensitivity studies and provides supplemental data for the Yankee-MPC canistered fuel basket support disk evaluation. Section 2.10.11.1 presents the justification of considering the 0° and 45° basket drop orientations as bounding cases for the support disk side drop evaluations. Section 2.10.11.2 shows that the stress results of the support disk evaluation are not sensitive to the value of the gap stiffness used in the support disk side drop models. Section 2.10.11.3 demonstrates that the finite element mesh used for the disk ligaments is adequate to determine maximum stress of the ligaments. The CY-MPC fuel baskets are very similar in design to the Yankee-MPC fuel basket, differing primarily in the overall length dimension.

##### 2.10.11.1 Yankee-MPC Fuel Basket Drop Orientation

As described in Section 2.6.14.1, three basket drop angles, 0°, 22.9° and 45° (shown in Figure 2.10.11-1) are considered in the support disk evaluation for the side drop condition. The angles 22.9° and 45° are selected because a minimal ligament between the corner of the fuel assembly slot and the disk outer radius occurs at these orientations. This section shows that the worst case stress occurs in the 45° drop orientation, and that the 0° and 45° drop orientations are the bounding cases for the support disk evaluation.

As shown in Figure 2.10.11-2, a finite element model for the support disk is generated using the ANSYS program to perform analyses for six-side impact cases:

Case No.	Side Impact Acceleration (g)	Basket Drop Orientation (Degree)
1	20	0
2	20	22.9
3	20	45
4	55	0
5	55	22.9
6	55	45

The model consists of a support disk and a section of the canister shell, as shown in Figure 2.10.11-2. ANSYS SHELL63 elements are used to model the disk and canister. The disk ligaments are modeled using the same number of elements and mesh ratio as those in the three dimensional support disk side drop models described in Section 2.6.14.2. As shown in Figure

Figure 2.10.11-2 ANSYS Model for the Yankee-MPC Fuel Basket Support Disk

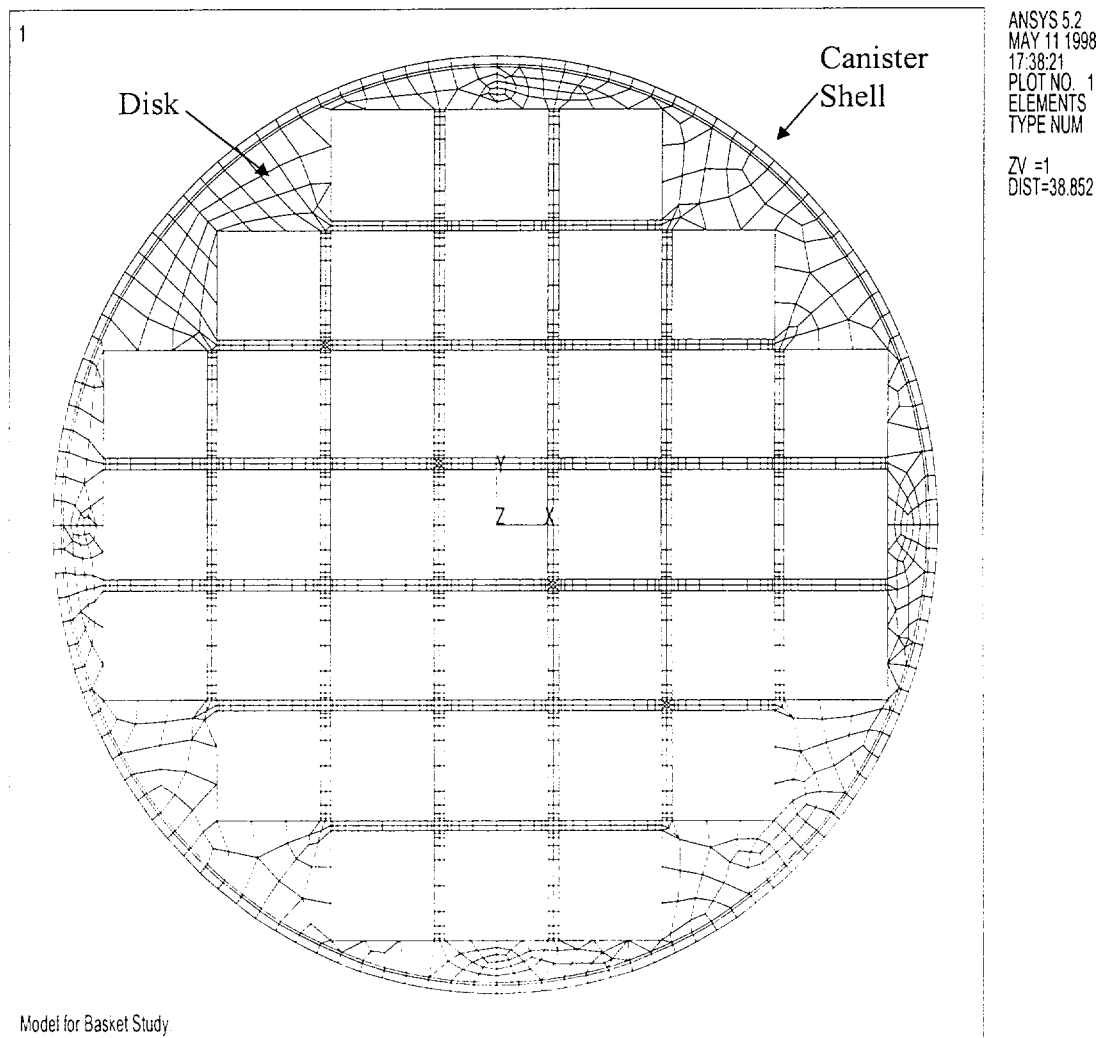




Figure 2.10.11-3 ANSYS Model for the Yankee-MPC Fuel Basket Support Disk (Detail)

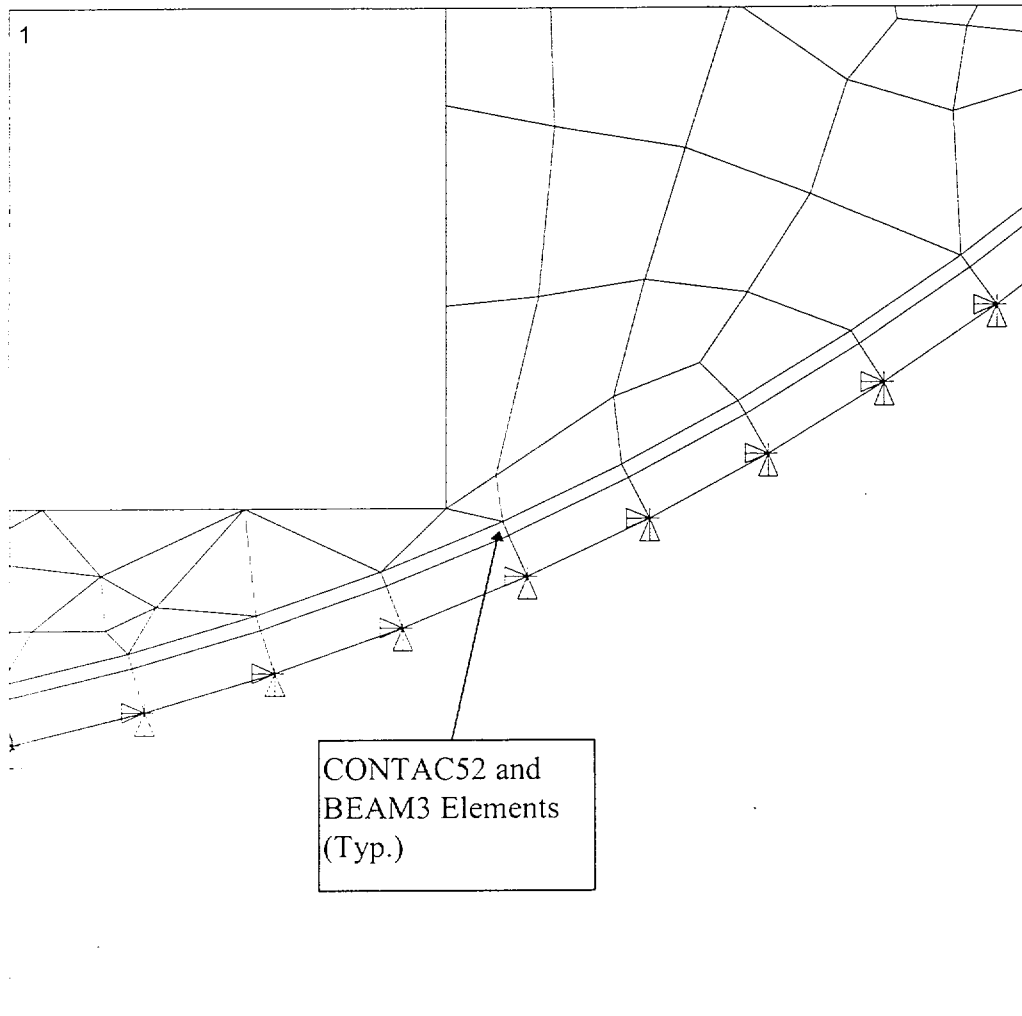


Figure 2.10.11-4 ANSYS Models for Yankee-MPC Support Disk Ligament Mesh

